15096

A CYCLIC ELECTRODIALYSIS PROCESS

Investigation of Closed Systems

by

DIETER BASS

Dipl. Ing., Universitaet Fridericiana Zu Karlsruhe, 1968

A THESIS SUBMITTED IN PARTIAL FULFILMENT OF

THE REQUIREMENTS FOR THE DEGREE OF

DOCTOR OF PHILOSOPHY

in the Department

of

CHEMICAL ENGINEERING

We accept this thesis as conforming to the

required standard

THE UNIVERSITY OF BRITISH COLUMBIA

December, 1972

In presenting this thesis in partial fulfilment of the requirements for an advanced degree at the University of British Columbia, I agree that the Library shall make it freely available for reference and study. I further agree that permission for extensive copying of this thesis for scholarly purposes may be granted by the Head of my Department or by his representatives. It is understood that copying or publication of this thesis for financial gain shall not be allowed without my written permission.

Department of Chemical Engineering

The University of British Columbia
Vancouver 8, Canada

Date April 13, 73

ABSTRACT

The cyclic electrodialysis process combines two concepts. The idea of flow reversal from parametric pumping is applied to an electrically driven absorption-desorption process operating with a stack of three-layer, ion-selective membranes.

The cyclic process was investigated for the demineralization of aqueous NaCl solutions in a closed system.

The standard parametric pumping operation was found to be generally very inefficient because of the finite rates of mass transfer. Flow pauses after each polarity reversal substantially improved both the rate and the limit of separation.

Two designs of the electrodialysis cell were studied. Ten system parameters were analysed on a simple bench scale cell. Final separations were limited by large axial dispersion and ranged between 1 and 40. A second electrodialysis cell consisted of up to eight single stages (15 [cm] channel length) which were usually operated in series hydraulically and in parallel electrically. Final separation factors ranged between 2 and ~6000.

Large separation factors were achieved for long channels, long pause times, and high applied potentials. The initial rate of

separation appeared to be a maximum for a channel length of approximately one meter and pause times of about ten seconds. During the first few cycles the separation factor could be approximated by an exponential function of time.

The potential of the process for continuous separation in open systems was demonstrated.

Models of the closed systems are presented and are used to discuss the experimental results.

TABLE OF CONTENTS

	Page
ABSTRACT	ii
LIST OF TABLES	x
LIST OF FIGURES	xiii
ACKNOWLEDGEMENTS	xxiii
Chapter	
1 INTRODUCTION AND SCOPE	1
2 PROCESS PRINCIPLES	4
2.1 Electrodialysis	4
2.1.1 Origin of separation	5
2.1.2 Membrane selectivity	8
2.1.3 Transport processes through ion selective membranes	12
2.1.4 Multicell electrodialyzer and its applications	14
2.1.5 Concentration polarization and other problems in steady-state electrodialysis	16
2.1.6 Current reversal techniques	21
2.2 Parametric pumping, heatless adsorption and similar cyclic separation processes	24

Chapter		Page
	2.2.1 Parametric pumping	25
	2.2.2 Other cyclic operations	33
3	EFFECT OF FINITE MASS TRANSFER RATES ON PARAMETRIC PUMPING AND PURE PAUSE OPERATION	37
	3.1 General	37
	3.2 Constant, Uniformly Distributed Rates of Mass Transfer	39
	3.2.1 Parametric pumping operation	41
	3.2.2 Pure pause operation	51
	3.3 Concentration Dependent Rates of Mass Transfer	52
	3.3.1 Pure pause operation	54
	3.3.2 Parametric pumping operation	56
	3.3.3 Comparison of pause and parametric pumping operations	56
	3.4 Summary	60
	3.5 Comment on an Equilibrium Model with Instantaneous Displacement	61
4	THE CYCLIC ELECTRODIALYSIS PROCESS - OPERATION AND APPARATUS	65
	4.1 Description of the Batch Operation	65
	4.2 The First Bench Module	68
	4.2.1 Electrodialyser No. 1 (ED1)	71
	4.2.2 Membrane spacer stacks	75
	4.2.3 Process flow	83
	4.2.4 Timing and switch boxes	84
	4.2.5 Rinse loop	88
	4.2.6 Measuring and recording	88

Chapter		Page
	4.3 The Mini Pilot Plant Module	90
	4.3.1 Electrodialyser No. 2 (EDII)	90
	4.3.2 Rinse distribution system.	98
	4.3.3 Current and voltage measurements . . .	98
5	EXPERIMENTAL RESULTS AND DISCUSSION.	101
	5.1 Data Collection	102
	5.2 Main Survey Tables.	104
	5.3 The First Electrodialysis Cell (EDI).	108
	5.3.1 Parameters	108
	5.3.2 Effect of applied voltage.	109
	5.3.3 Effect of pause time	120
	5.3.4 Effect of superficial velocity	128
	5.3.5 Effect of displaced volume	135
	5.3.6 Effect of dead volumes	141
	5.3.7 Effect of initial concentration. . . .	147
	5.3.8 Effect of internal flow distribution and axial dispersion	151
	5.3.9 Effect of external mixing in brine reservoir.	159
	5.3.10 Effect of capacity cell thickness. . .	164
	5.3.11 Effect of thickness and hydrodynamic properties of spacer screens.	165
	5.3.12 Comment on pH-changes.	167
	5.3.13 Comment on current efficiencies. . . .	167
	5.3.14 Comment on true limits and on reproducibility of batch runs.	170

Chapter | Page

5.4 Summary of Experience Gained on First Electrodialysis Cell. 173

5.5 The Second Electrodialysis Cell (EDII). . . . 175

5.5.1 Data reduction and presentation. . . . 176

5.5.2 Effect of channel length 178

5.5.3 Effect of pause time 194

5.5.4 Effect of applied voltage. 205

5.5.5 Effect of initial concentration. . . . 205

5.5.6 Effect of displaced volume 211

5.5.7 Effect of dead volumes 221

5.5.8 Effect of superficial velocity 221

5.5.9 Reproducibility. 226

5.5.10 Comment on the material balance for the solute 229

5.5.11 Comment on the performance of individual stages. 231

5.5.12 Experimental test of the constant rate model 239

5.5.13 Comment on the effect of end mixing 241

5.5.14 Production of 90% demineralized solution 243

5.6 Summary of Results and Experience on the Second ED Module 247

6 MATHEMATICAL MODELS. 250

6.1 Spacer Model. 250

6.1.1 Model equations. 252

6.1.2 Considerations related to cyclic process operations 261

Chapter Page

6.1.3 Solutions 262

6.1.4 Backward Difference scheme with Gauss-Seidel iteration 264

6.1.5 Results of computer simulations. . . . 269

6.1.5.1 Accuracy and convergence. . . 269

6.1.5.2 Effect of operating parameters. 270

6.1.5.3 Comparison with experimental results 271

6.1.6 Concluding comments on the spacer model 278

6.2 Rate Model. 279

7 CONCLUSIONS AND RECOMMENDATIONS. 280

NOMENCLATURE. 284

REFERENCES. 289

APPENDICES

A DETAIL DRAWINGS, PICTURES OF THE MODULES AND MANUFACTURING PROCEDURES 295

A.1 ELECTRODIALYZER NO. 1. 296

A.2 ELECTRODIALYZER NO. 2. 302

A.3 MANUFACTURING PROCEDURE FOR MEMBRANE-SPACER FRAME 305

B MATHEMATICAL DERIVATIONS 308

B.1 DERIVATION OF CONCENTRATION TRANSIENTS FOR CONSTANT, UNIFORMLY DISTRIBUTED RATES OF MASS TRANSFER. PARAMETRIC PUMPING OPERATION. 309

B.2 DERIVATION OF CONCENTRATION TRANSIENTS FOR CONCENTRATION DEPENDENT RATES OF MASS TRANSFER - PURE PAUSE OPERATION 313

B.3 RATE THEORY OF PARAMETRIC PUMPING. 318

APPENDICES

		Page
B.4	MULTIPLE STEP DISPLACEMENT MODEL (STOP-GO ALGORITHM)	325
B.5	DERIVATION OF CONCENTRATION TRANSIENTS FOR EQUILIBRIUM CONTROLLED PURE PAUSE OPERATION	330
C	COMPUTER PROGRAMS	336
C.1	EVALUATION OF EDI EXPERIMENTS	337
C.2	EVALUATION OF EDII EXPERIMENTS	378
C.3	SPACER MODEL	408

LIST OF TABLES

Table		Page
1	Computer Simulations of Pure Pause, Parametric Pumping, and Multiple Step Displacement Operations for Concentration Dependent Mass Transfer Rates.	59
2	Electrodialyser No. 1 (EDI)	75
3	Properties of Neosepta Membranes.	76
4	Stack Pack Versions Used in First ED Cell	79
5	Piston Pump Specifications.	84
6	Conductivity and NaCl Concentration Ranges of Beckman Conductivity Cells CEL-VDJ Corresponding to a 0-10 [mV] D.C. Signal from a Beckman Solu-meter RA5.	89
7	Electrodialyser No. 2 (EDII).	97
8	Compilation of Experiments on EDI-S1-8.	107
9	Compilation of Experiments on EDI-S2-15	
10	Compilation of Experiments on EDI-S2-16	
11	Compilation of Experiments on EDI-S3-12	
12	Compilation of Experiments on EDI-S3-13	
13	Compilation of Experiments on EDII-S1-8	

Table		Page
14	Effect of Applied Voltage ($\Delta\Phi$) on EDI-S1-8.	116
15	Effect of Applied Voltage ($\Delta\Phi$) on EDI-S2-15	
16	Effect of Applied Voltage ($\Delta\Phi$) on EDI-S3-12 and EDI-S3-13	
17	Effect of Pause Time (τ) on EDI-S2-15 and EDI-S2-16	122
18	Effect on Pause Time (τ) on EDI-S3-12	
19	Effect of Pause Time (τ) on EDI-S3-13	
20	Effect of Superficial Velocity (v) on EDI-S1-8	131
21	Effect of Superficial Velocity (v) on EDI-S2-16, EDI-S3-12	
22	Effect of Superficial Velocity (v) on EDI-S3-13.	
23	Effect of Displaced Volume (δ) on EDI-S1-8, EDI-S2-15 and EDI-S3-13	137
24	Effect of Dead Volumes (δ_B/δ_T) on EDI-S2-15, EDI-S3-12 and EDI-S3-13	142
25	Effect of Initial Concentration (c_0) on EDI-S3-12 and EDI-S3-13	148
26	Step Response Experiments on EDI-S1-8	157
27	Step Response Experiments on EDI-S3-12 Runs #1-14.	157
28	Step Response Experiments on EDI-S3-12 Runs #15-24	158

Table		Page
29	Step Response Experiments on EDI-S3-13.	158
30	Effect of End Mixing on EDI-S3-12	162
31	Effect of Capacity Cell Thickness on Electrodialyzer No. 1	166
32	pH-Changes in Some EDI-S3-12 Runs	167
33	Results of Step-Response Tests on Second ED Cells	180
34	Effect of Channel Length (MS) on Second Electrodialyzer.	184
35	Effect of Pause Time (τ) on Second Electrodialyzer	196
36	Effect of Applied Voltage ($\Delta\Phi$) on Second Electrodialyzer.	206
37	Effect of Initial Concentration (c_0) on Second Electrodialyzer	212
38	Effect of Displaced Volume (δ) on Second Electrodialyzer.	217
39	Effect of Superficial Velocity (v) on Second Electrodialyzer.	223
40	Spacer Model No. I, Effect of Layer Thickness	272
41	Spacer Model No. I, Effect of Fourier Number.	273
42	Spacer Model No.I, Effect of Applied Potential	274

LIST OF FIGURES

Figure		Page
1	The electrodialysis principle.	6
2	Transport processes across an anion-selective membrane	13
3	Multicell electrodialysis stack (schematic).	13
4	Concentration polarization of an ion-selective membrane	18
5	Thermal parametric pumping	18
6	Characteristics of batch separation via equilibrium theory of parametric pumping	30
7	Concentration transients for equilibrium theory of parametric pumping (according to Pigford, 1969a).	32
8	Heatless adsorption air drying system, used by Skarstrom (1959)	34
9	Cyclic zone adsorption (proposed by Pigford, 1969b).	35
10	Electrodialysis systems with constant, uniformly distributed rates of mass transfer . .	40
11	Concentration profiles during the first cycle of a cyclic electrodialysis process operated in parametric pumping mode under conditions of equal, constant, and uniformly distributed rates of mass transfer	43

Figure		Page
12	Product concentration transients for cyclic electrodialysis process operated in parametric pumping mode under conditions of equal, constant, and uniformly distributed rates of mass transfer.	44
13	Product concentration transients for cyclic electrodialysis process operated in parametric pumping mode under conditions of unequal, constant, and uniformly distributed rates of mass transfer	45
14	Development of standing waves in a parametric pumping operation under conditions of equal, constant and uniformly distributed rates of mass transfer when variables are switched one-quarter cycle out of phase.	47
15	Product concentration transients for cyclic electrodialysis process operated in parametric pumping mode under conditions of equal, constant and uniformly distributed rates of mass transfer, when periodic variables are switched one-quarter cycle out of phase	48
16	Average top and bottom product transients for phase shift operation of a constant rate controlled parametric pump	50
17	Lateral concentration profile and co-ordinate systems in flow channel and triple membrane. . .	50
18	Effect of the number of segments (N) on the product concentration transients for concentration dependent rates of mass transfer ($a_1 = a_2 = 0.01$ sec^{-1}, T=20 sec, ρ=1.0, δ=1.0). . .	58
19	Product concentration transients for equilibrium controlled pure pause operation.	63
20	Batch operation of cyclic electrodialysis process.	66

Figure		Page
21	Time variation of applied potential (a) and flow rate (b) for cyclic electrodialysis process	66
22	Block diagram of experimental testing station. . .	69
23	First electrodialysis cell EDI (exploded view, schematic)	72
24	Electrodialyser No. 1.	80,81,82
25	Glass fibre spacer screen.	78
26	Floating lid expansion tank.	85
27	Automatic switching arrangement for cyclic electrodialysis process.	85
28	Piston Pump Drive. Electric circuit for motor reversal	87
29	Clamping arrangement of eight stages in mini pilot plant module.	91
30	Schematic assembly of one stage of the second electrodialyzer	87
31	Integrated membrane-spacer frame for electrodialyzer No. 2. Parts and assembly	93
32	Electrodialyser No. 2. Electrode end frames of a single stage	94
33	Process flows through second electrodialysis cell (schematic).	96
34	Current monitoring circuit	99
35	EDI-S2-15/#15. Traces of current and probe voltage recording during the first five cycles	111

Figure		Page
36	Stack voltage vs. electrode voltage for first ED cell.	112
37	EDI-S1-8/#36. Example of concentration transients in parametric pumping operation when mass transfer rates are constant.	113
38	EDI-S2-15/#9. Example of concentration transients in parametric pumping operation when mass transfer rate is concentration dependent.	113
39	Effect of applied voltage on final concentrations, separation factor, and current. Second stack experiments in no-pause operation. EDI-S2-15/#7,8,9,10,17	117
40	Effect of applied voltage on final product concentrations for third stack experiments. EDI-S3-12/#17,18,19,1-2 and EDI-S3-13/#6,7,11,8,22,9	118
41	Effect of applied voltage on final separation factor for third stack experiments. EDI-S3-12/#17,18,19,1-2 and EDI-S3-13/#6,7,11,8,22,9	119
42	Effect of pause time (τ) on separation factor for second and third stack experiments	123
43	Effect of pause time on final reservoir concentrations for third stack experiments. EDI-S3-12/#24,18,21,22,23 and EDI-S3-13/#10,11,7,12,2,13,1,14	124
44	Effect of pause time (τ) on final separation factor for third stack experiments. EDI-S3-12/#24,18,21,22,23 and EDI-S3-13/#10,11,7,12,2,13,1,14.	124
45	Dialysate-concentration-transient of EDI-S3-12/#6-0	125
46	Effect of pause time (τ) on concentration transients of third stack experiments.	126

Figure		Page
47	Contrasting pause and no-pause operation for third stack experiments. EDI-S3-13/#21,32	127
48	Effect of superficial velocity (v) on final reservoir concentrations for pause and no-pause operation. EDI-S3-13/#15,3,16,25,17,32,18,31 and EDI-S3-13/#20,19,21	132
49	Effect of superficial velocity (v) on final separation factors for pause and no-pause operation. EDI-S3-13/#15,3,16,25,17,32,18,31 and EDI-S3-13/#20,19,21	132
50	Effect of superficial velocity (v) on concentration transients for no-pause operation. EDI-S3-13.	133
51	Effect of superficial velocity (v) on concentration transients for pause operation. EDI-S3-13.	134
52	Effect of displaced volume (δ) on final reservoir concentrations for pause operation. EDI-S3-13/#4,3,2,12,5.	138
53	Effect of displaced volume (δ) on final separation factor for pause operation. EDI-S3-13/#4,3,2,12,5	138
54	Effect of displaced volume (δ) on concentration transients for pause operation. EDI-S3-13.	139
55	Effect of displaced volume (δ) on real time transients for no-pause operation.	140
56	Effect of dead volumes (δ_B/δ_T) on concentration transients. EDI-S2-15.	143
57	Effect of dead volumes (δ_B/δ_T) on concentration transients. EDI-S3-13.	144

Figure		Page
58	Effect of dead volumes (δ_B/δ_T) on salting factor transients. EDI-S2-15.	146
59	Effect of initial concentration (c_0) on dialysate concentration transients. EDI-S3-12.	149
60	Effect of initial concentration (c_0) on concentration transients. EDI-S3-13	150
61	Effect of initial concentration (c_0) on concentration transients. EDI-S3-13	150
62	Internal mixing. Effect of number of effective mixing stages (m) on response to step change in feed concentration: (a) response function $\bar{x}(\bar{t})$; (b) slope ($\dot{\bar{x}}(\bar{t})$) of response curve (dimensionless).	155
63	Maximum slope ($\dot{\bar{x}}$) vs. number of mixing stages (m)	156
64	Step response of second stack versions (schematic).	156
65	Effect of internal dispersion. Transients of separation factor and dialysate product concentration for second stack versions.	160
66	Qualitative model of the concentration profiles in a cyclic electrodialysis process in pause time operation with internal dispersion and well mixed end reservoirs.	163
67	Uniqueness and reproducibility of final separation factor for second stack experiments.	171
68	Uniqueness of final separation factor for second stack experiments	172
69	Dimensionless slope of step response curves for second ED cell as function of the number of electrodialysis stages	179

Figure		Page
70	Effect of channel length (MS) on separation factor transients	185
71	Effect of channel length (MS) on concentration transients	186
72	Effect of channel length (MS) on current distribution	187
73	Effect of channel length (MS) on separation factor transients	188
74	Effect of channel length (MS) on current distribution	189
75	Effect of channel length (MS) on separation factor transients	190
76	Effect of channel length (MS) on concentration transients	191
77	Effect of channel length (MS) on current distribution	192
78	Effect of channel length (MS) on initial rate of separation (a)	193
79	Effect of pause time (τ) on separation factor transients	197
80	Effect of pause time (τ) on concentration transients	198
81	Effect of pause time (τ) on current distribution	199
82	Effect of pause time (τ) on separation factor transients	200
83	Effect of pause time (τ) on current distribution	201

Figure		Page
84	Effect of pause time (τ) on separation factor transients.	202
85	Effect of pause time (τ) on concentration transients.	203
86	Effect of pause time (τ) on initial rate of separation (a).	204
87	Effect of applied voltage ($\Delta\Phi$) on separation factor transients	207
88	Effect of applied voltage ($\Delta\Phi$) on separation factor transients	208
89	Effect of applied voltage ($\Delta\Phi$) on separation factor transients	209
90	Effect of applied voltage ($\Delta\Phi$) on initial rate of separation (a)	210
91	Effect of initial concentration (c_0) on separation factor transients.	213
92	Effect of initial concentration (c_0) on separation factor transients.	214
93	Effect of initial concentration (c_0) on separation factor transients.	215
94	Effect of displaced volume (δ) on separation factor transients	218
95	Effect of displaced volume (δ) on separation factor transients	219
96	Effect of displaced volume (δ) on separation factor transients	220
97	Effect of dead volumes (δ_B/δ_T) on concentration transients	222

Figure		Page
98	Effect of superficial velocity (v) on separation factor transients	224
99	Effect of superficial velocity (v) on separation factor transients	225
100	Reproducibility of second stack experiments.	227
101	Reproducibility of second stack experiments.	228
102	Overvoltage-current curves of the electrodialysis stages.	232
103	Time-space distribution of current at limiting conditions.	236
104	Time-space distribution of probe voltage at limiting conditions	237
105	Influence of phase shift (γ) on transients for constant rate operation.	240
106	Effect of end mixing on concentration transients	242
107	Concentration transients of top and bottom reservoir concentrations during production run #3 compared to batch run #26 (low concentration)	245
108	Concentration transients of top and bottom reservoir concentrations during production run #5 compared to batch run #6 (high concentration)	246
109	Derivation of the spacer model equations	253
110	Effect of width ratio (δ) on separation factor transients predicted by Spacer Model	275

Figure		Page
111	Comparison of computer simulation with experimental results on runs #22,23,24 (first stack).	276
112	Comparison of computer simulation with experimental run #36 (first stack)	277

ACKNOWLEDGEMENT

I wish to thank Dr. D.W. Thompson, under whose direction this work was conducted, for his helpful guidance and encouragement throughout this investigation.

I also wish to thank the faculty and staff of the Chemical Engineering Department of the University of British Columbia.

I am indebted to the University of British Columbia, the National Research Council, and Environment Canada for financial support.

I would like to express my gratitude to my wife Jacqueline for her continual support and forebearance throughout these years.

Chapter 1

INTRODUCTION AND SCOPE

Electrodialysis has achieved only partial success in brackish water demineralization despite many theoretical advantages it offers over other desalting processes. The problem areas in electrodialysis practise are fouling and scale formation on the membranes and the rather complex design of the multicompartment electrodialysis cell.

Periodic current interruptions and/or reversals have been employed in standard electrodialysis stacks to reduce polarization effects and deposition of particulates on the membranes. Lacey (1965) invented an electrosorption stack of much simpler construction than conventional electrodialysis stacks. In this apparatus salt is absorbed by, or desorbed from, the stack depending on the direction of the electric current. The process resembles packed bed adsorption/desorption or ion exchange systems.

Wilhelm *et al.* (1966) investigated a temperature cycled adsorption-desorption process in which the direction of the fluid flow was reversed synchronously with the temperature

switching. This process, known as parametric pumping, has recently attracted a great deal of attention because very large separations were experimentally obtained for one system.

The concept of this work is to combine cyclic electrosorption-desorption with the flow reversal employed in the temperature cycled parametric pump.

The purpose of this study is to analyze the potential of a cyclic electrodialysis process for large separations, to develop suitable modules for experimental tests, and to investigate systematically the effect of process variables on the performance of closed systems.

The material of this thesis has been arranged in three main parts:

The second chapter reviews the principles which are combined in the cyclic electrodialysis process, and the third chapter presents some basic considerations of the controlling steps and contrasts the standard cyclic process (parametric pumping) with a new cyclic operation (pure pause mode).

In the fourth chapter details of the laboratory apparatus are given, and the fifth chapter presents and discusses experimental results.

A mathematical model of the standard cyclic operation of the electrodialysis stacks is developed in the sixth chapter, which also includes a numerical solution of the model equations, and compares computer simulations with experimental results.

Conclusions and recommendations, based on the results of this work, are contained in the seventh chapter.

Chapter 2

PROCESS PRINCIPLES

This section reviews the basic process principles which are combined in the cyclic electrodialysis process.

2.1 Electrodialysis

Electrodialysis is a unit operation for separations in an ionic solution. Along with other membrane processes electrodialysis belongs to the class of "selective transport methods" (Shaffer and Mintz, 1966).

Since electrodialysis gained commercial status some fifteen years ago, a large number of publications have appeared on fundamental aspects, membrane phenomena, potential applications, process technology, and process economics. Wilson's monograph (1960) is the only major work entirely devoted to the field. Chapters on electrodialysis are included in books dealing with desalination processes, e.g. Spiegler (1962,1966), Sporn (1966), Popkin (1968); or with membrane processes, e.g. Rickles (1967), Lacey (1972).

In this work the term electrodialysis is used in the conventional sense, i.e. related to solute-solvent separations, although it is not restricted to such processes as discussed below.

2.1.1 Origin of separation.

Consider the system in Figure 1 in which an electrolytic cell is divided into two compartments by an ion-selective membrane. Anode and cathode are connected to a power source (not shown in Figure 1) which maintains a constant electric potential difference between the electrodes. Suppose the applied potential difference (or voltage) is large enough so that current flows through the cell, which is filled with electrolyte solution of a simple salt such as sodium chloride (NaCl).

The current is transported by anions and cations according to their transport numbers. The sum of these transport numbers is unity in the solution and in the membrane,

$$\underset{\text{solution}}{\nu_+ + \nu_-} = \underset{\text{membrane}}{\bar{\nu}_+ + \bar{\nu}_-} = 1 \qquad (1)$$

but the transport numbers of the ionic species is not necessarily equal in the two phases.

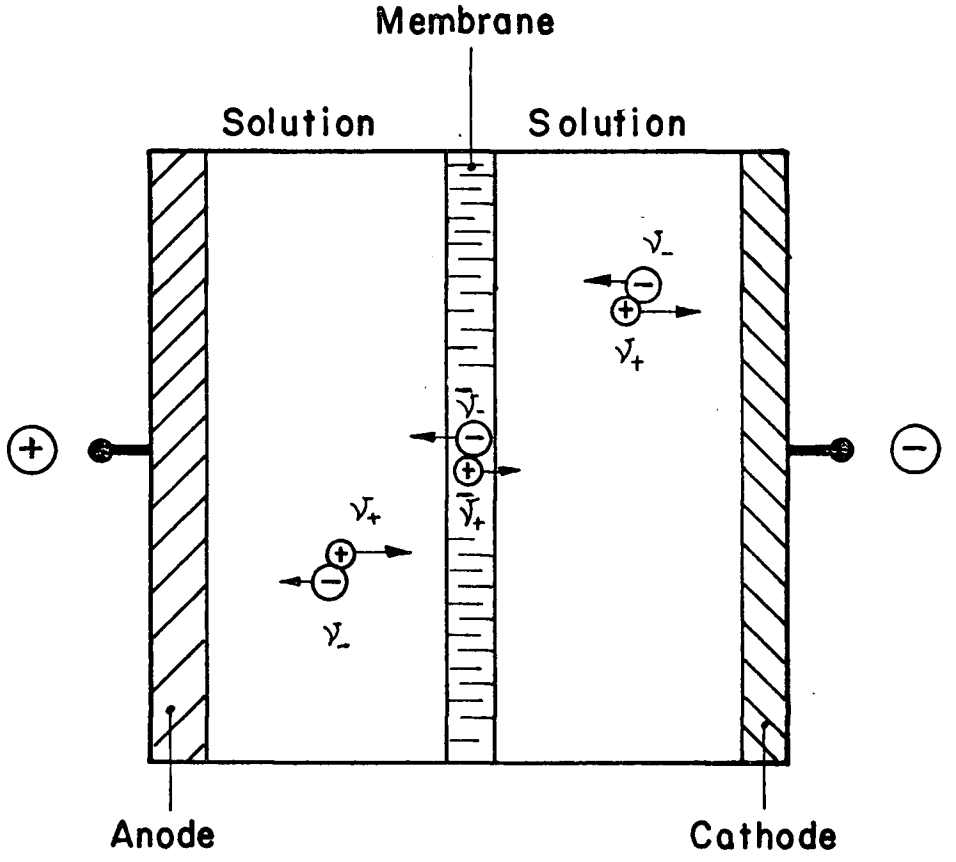

Figure 1. The electrodialysis principle.

If $\bar{\nu}_- > \nu_-$ the membrane is said to be anion selective. This means that the number of anions which carry current is larger in the membrane than in the solution.

The number of moles of anions (n_-) which are selectively transferred through an anionic membrane by electrolysis is proportional to the number of Coulombs and the difference in transport numbers ($\bar{\nu}_- - \nu_-$). The number of Coulombs is given by the time integral of the current (I)

$$\int_0^{t_1} I(t)dt$$

Thus

$$n_- = \frac{\bar{\nu}_- - \nu_-}{z_- F} \int_0^{t_1} I(t)dt \quad , \qquad (2)$$

where z_- is the valence of the anions, and F is Faraday's constant.

Because of the condition of electroneutrality, the number of moles of cations (n_+) which are rejected by the membrane is identical for equivalent ions ($z_- = z_+ = z$). The molar concentration change (Δc) of the solution with volume (V) is given as

$$\Delta c = \frac{\bar{\nu}_- - \nu_-}{z\ F V} \int_0^{t_1} I(t)dt \qquad (3)$$

The two solution-membrane interfaces experience concentration changes which are of identical magnitude but of opposite sign. The side facing the cathode is depleted and the side facing the anode is enriched.

Enrichment and depletion are inverted at a cation selective membrane, which is characterized by the inequality $\bar{\nu}_+ > \nu_+$.

The concentration changes are carried into the membrane and solution bodies by diffusional and/or convective mass transport. Demineralized solvent (dialysate) and enriched solution (brine) may, therefore, be withdrawn from opposite sides of the membrane.

The separation of solute and solvent originates, therefore, from a difference in transport number of ionic species in membrane and solution. This difference is called selectivity, and is the subject of the following section.

2.1.2 Membrane selectivity.

Commercially available membranes are almost exclusively of the resinous ion-exchange type. The selectivity is

achieved by incorporating a large number of fixed ionic groups in a matrix of inert material.*

The presence of a high concentration of fixed ionic groups has an exclusion effect on ions with the same sign as these groups.

According to the Gibbs-Donnan principle, equilibrium between solution and membrane phase means equality of the chemical potentials of the solute. For a fully ionized salt and neglecting osmotic pressure terms, one has

$$a_+^{\alpha_+} \cdot a_-^{\alpha_-} = \bar{a}_+^{\alpha_+} \cdot \bar{a}_-^{\alpha-} \tag{4}$$

where the a's denote ion activities and the α's stoichiometric coefficients.

In simplified form, when activities are replaced by concentrations and assuming equivalent ions equation (4) reduces to

$$\bar{c}_+ \cdot \bar{c}_- = c_+ \cdot c_- \tag{5}$$

---

*An excellent summary of preparative methods found in the patent literature is given by Placek (1970).

In an anion selective membrane in which anionic groups of concentration X are present, the electroneutrality condition has the form

$$\bar{c}_- = X + \bar{c}_+ \tag{6}$$

The ionic concentrations in the solution are identical to the solute concentration (c) because of the assumption of equivalent anions and cations:

$$c = c_+ = c_- \tag{7}$$

Combining (5), (6) and (7) one finds

$$\bar{c}_+ \cdot (X + \bar{c}_+) = c^2 \quad . \tag{8}$$

Dividing both sides by the fixed ion concentration yields equation (9)

$$\bar{c}_+ \cdot \left(1 + \frac{\bar{c}_+}{X}\right) = \frac{c^2}{X} \tag{9}$$

which may be approximated for dilute solutions ($\bar{c}_+ << X$) by

$$\bar{c}_+ \approx \frac{c^2}{X} \tag{10}$$

Equation (10) shows that the cation concentration in an anion selective membrane varies as the square of the

solution concentration and may be kept very small by increasing the number of fixed ionic groups (X) in the membrane.

The contribution of cations to the current flow is accordingly small, since the flux of cations ($\vec{j}_+$) along an electric potential gradient (grad(Φ)) is

$$\vec{j}_+ = - \bar{u}_+ \cdot \bar{c}_+ \cdot \bar{z}_+ \cdot \text{grad}(\Phi) \qquad (11)$$

where $\bar{u}_+$ is the mobility of the cations in the membrane.

It must be kept in mind that equation (11) is written as the isolated ion flux due to a potential gradient. The presence of concentration and pressure gradients as well as the migration of other species results in very complicated actual dependences. It is beyond the scope of this work to account for the various treatments of these aspects. Guides to the published literature may be found in Wilson's (1960) or in Helfferich's (1962) books.

Also, most of the results reported are limited to steady-state conditions and it is difficult or impossible to project those results to unsteady-state situations which dominate the present process.

The selectivity of the membranes is often characterized by a quantity called permselectivity (P) which is defined (Wilson, 1960), as

$$P = \frac{\bar{\nu}_{\pm} - \nu_{\pm}}{1 - \nu_{\pm}} \qquad (12)$$

where positive subscripts refer to cation selective membranes and negative signs to anion selective ones.

> *The permselectivity therefore expresses the increase in transport number over the value in free solution as a fraction of the maximum possible increase, i.e. the increase that would be observed in the case of an ideally selective membrane* (Wilson, 1960).

2.1.3 Transport processes through ion-selective membranes.

The various transport processes which occur simultaneously through ion-selective membranes are briefly catalogued in this section. Figure 2 illustrates these processes for an anion selective membrane during electrodialytic separation. It also shows the lateral concentration profile.

a) Gegen-ion transport: The membrane exhibits a preference for some ions (gegen-ions) and discriminates against others (co-ions). Ideally the total current is carried by gegen-ions alone.

b) Co-ion transport: Any co-ion participation in the current flow uses energy but yields no separation.

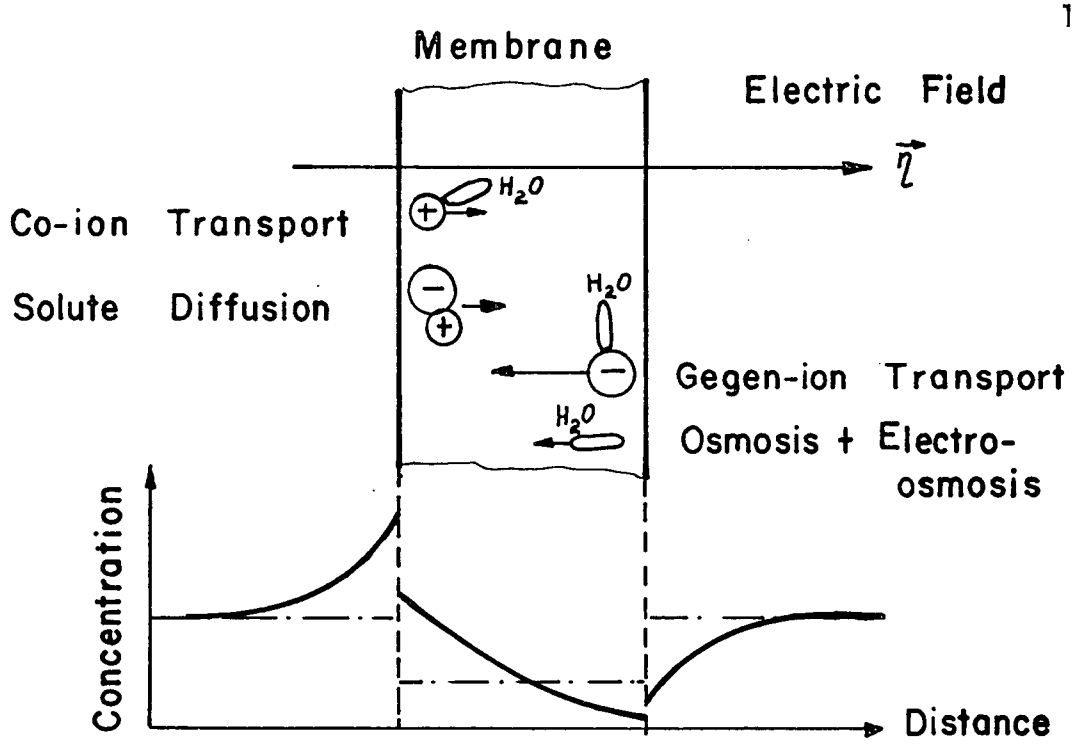

Figure 2. Transport processes across an anion-selective membrane.

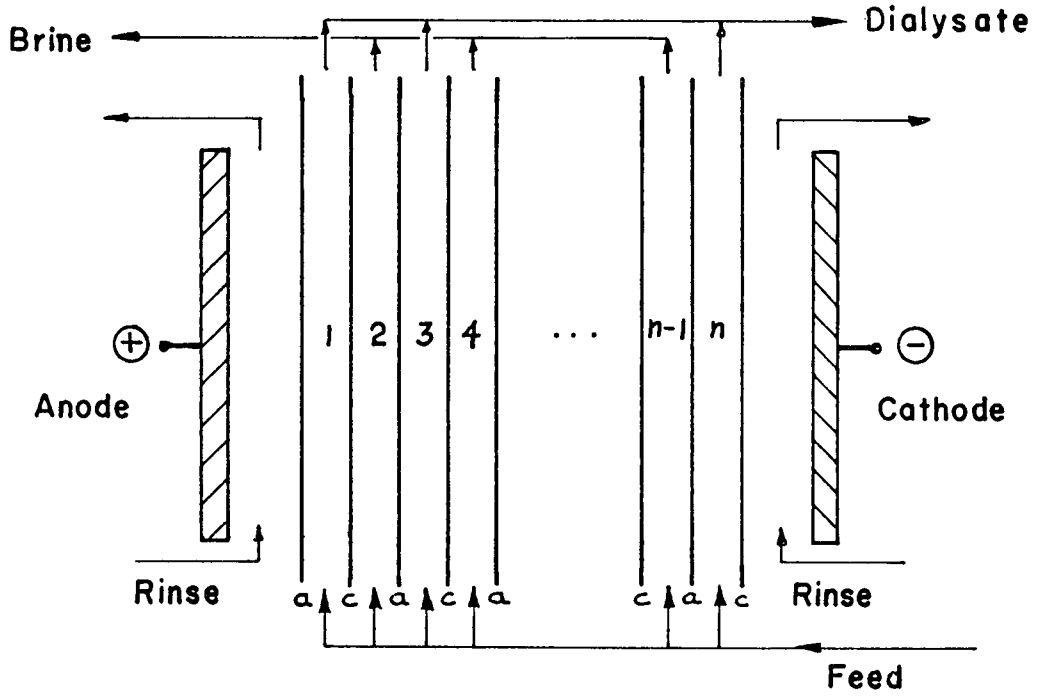

Figure 3. Multicell electrodialysis stack (schematic).

c) Solute diffusion: A concentration gradient develops inside the membrane as a result of the concentration changes. Solute diffuses back along this gradient.

d) Solvent transfer due to ion solvation usually dilutes the enriched interface, but this depends upon the effective number of solvent molecules attached to each ionic species and the actual degree of selectivity of the membrane.

e) Electro-osmosis: Solvent in the membrane experiences frictional forces imparted by the moving ions.

f) Osmosis: The difference in solvent activities in the adjoining solutions forces solvent through the membrane. Osmotic effects reduce the extent of separation.

Wilson (1960) presented a detailed discussion of these effects and Schlögel (1964) wrote an excellent monograph on membrane transport phenomena in general (i.e. not restricted to ion-selective membranes).

2.1.4 Multicell electrodialyzer and its applications.

The multicell electrodialyzer which is presently used was proposed by Meyer and Strauss (1940).* Figure 3 is a

*In this discussion the electrode reactions have been disregarded because they provide merely a link between electronic and electrolytic current transport in electrodialysis systems. The energy requirements to maintain the electrode reactions are only a small fraction of the total energy input in a multicell arrangement.

sketch of such a multicell arrangement. A number of parallel channels (1,2,3,•••,n) is formed by an array of interleaved cation (c) and anion (a) selective membranes. This stack is placed between flat electrodes. Feed solution flows upward through the stack, becomes depleted in one set of channels (1,3,5,•••,Figure 3), and enriched in another set (2,4,6,•••, Figure 3). Dialysate and brine have to be collected and drawn off separately. Electrode reaction products are removed by independent rinse streams (Figure 3).

It is not essential to have both anion and cation selective membranes in the stack.

In the transport depletion process neutral, or non-selective, membranes replace the anionic ones in the stack, see e.g. Kollsman (1959), Lacey (1962), Lang *et al.* (1968), Huffman (1969).

Only one kind of selective membranes form the stack of the electrodecantation process. Feed is introduced at an intermediate location to the flow channels. Separation is achieved by density induced convection, see Frilette (1957), Kollsman (1958), Bier (1959), Friedlander and Rickles (1965).

Electrodialysis is conventionally applied to separate solutes from solvent. The membranes discriminate also between ions of different charge and size but of the same sign. Based on this membrane property, purification processes have

been proposed for mixed electrolyte solutions by Dewey and Gilliland (1956), and several others (Wilson, 1960).

On a commercial scale, table salt is produced from sea water in Japan by a process in which monovalent ions (above all NaCl) are selectively extracted and concentrated by electrodialysis (Tsunoda, 1965; Yamane, 1969).

Exchange reactions in the electrolytic state is another field of application (Wilson, 1960: Cohan, 1965).

Electrodialysis competes with other membrane processes and conventional separation techniques in water desalination and pollution control. It is attractive whenever problems with minor impurities (less than 10,000 ppm) arise (Friedlander, 1966).

2.1.5 Concentration polarization and other problems in steady-state electrodialysis.

The difference in transport numbers between membranes and solution causes local depletion and enrichment of solute at the interfaces, and lateral concentration gradients develop in the vicinity of the membranes. Stirring of the bulk solution may limit these concentration gradients to diffusion controlled layers. If the concept of a Nernst layer is adopted, the steady-state condition for the solute flux at an

anion selective membrane corresponds to

$$\frac{\overline{\nu}_- - \nu_-}{z\,F}\, i = \frac{D}{\delta}(c'_m - c_0) = \frac{D}{\delta}(c_0 - c''_m) \qquad (13)$$

see Figure 4 and compare with equation (3)

where	i	current density	[ampere/cm^2]
	D	diffusion coefficient	[cm^2/sec]
	δ	Nernst film thickness	[cm]
	c_0	bulk concentration	[g-moles/litre]
	c'_m, c''_m	solution concentrations at the membrane surface	[g-moles/litre]

If the layer thickness is controlled by the flow conditions alone, a limiting case exists when c'_m becomes zero. The corresponding limiting current density $(i)_{lim}$ is

$$-(i)_{lim} = \frac{zF\,D}{\delta \cdot (\overline{\nu}_- - \nu_-)} \cdot c_0 \qquad (14)$$

In aqueous solutions, no true limit exists because hydroxyl or hydrogen ions will take part in the ionic transfer at very low concentrations of solute. This is usually referred to as water splitting.

Effects of concentration polarization of the membranes on the electrodialysis process are always undesirable:

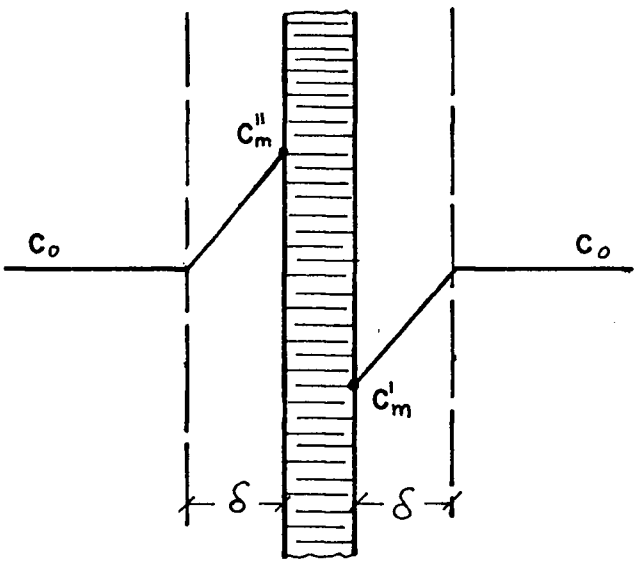

Figure 4. Concentration polarization of an ion-selective membrane.

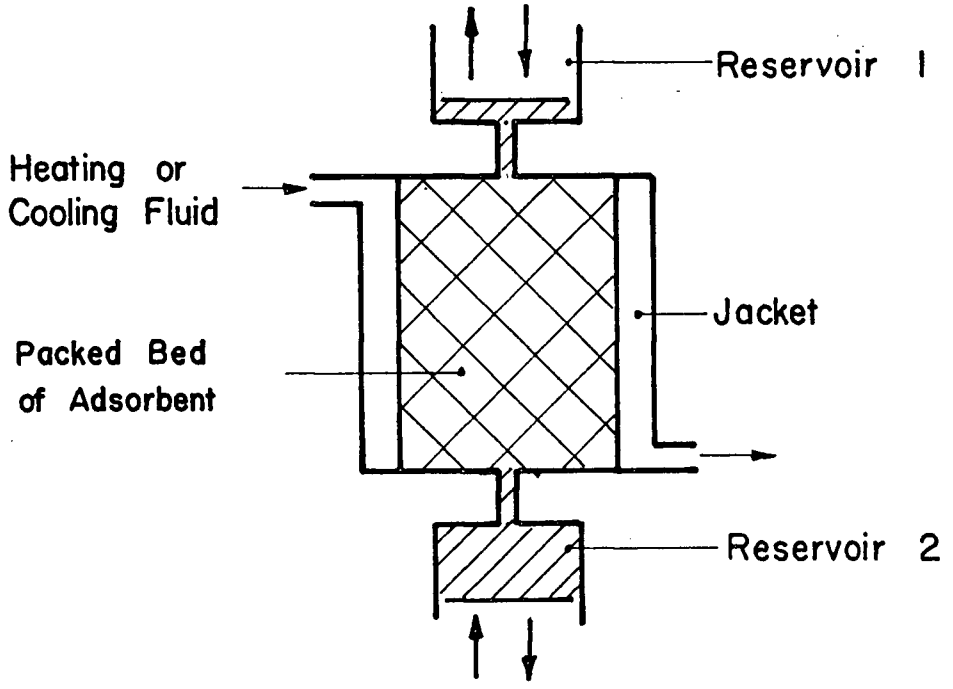

Figure 5. Thermal parametric pumping.

a) The mass transfer rates are limited. This requires larger membrane areas.

b) If the current density is close to the limiting one, water splitting reduces the current efficiency and possibly the pH of the product.

c) The stack resistance is increased.*

d) The Donnan potential (Helfferich, 1962) is increased and the effective stack voltage is therefore reduced.†

The early work on this phenomenon was summarized by Wilson (1960). The more recent literature may be divided in the following three classes:

1. Fundamental aspects of the concentration polarization phenomena, Cook (1961,1965); Mandersloot (1965); Spiegler (1971); Forgacs (1972).

2. Theoretical prediction of the effective stack resistance mainly based upon solutions of the flow field in the channels, Belfort (1968); Sonin (1968); Solan (1969,1971); Pnueli (1970); Mas (1970), and an experimental study of the hydrodynamic conditions existing in actual ED stacks (Belfort, 1972).

---

*Compared to horizontal concentration profiles across the films.

†See equation (24), page 53 for details.

3. Engineering studies using mass transfer correlations to characterize individual stack performances, e.g. Rosenberg (1957); Cowan (1959); Weiner (1964); Mandersloot (1965); Kitamoto (1970,1971); Sata (1969); Yamane (1969a).

Concentration polarization is often linked with other problems in actual electrodialysis practise.

Scale formation. Supersaturation and local pH changes may cause some components of the feed water to precipitate at the membrane surface. In particular Calcium and Magnesium Bicarbonates and Sulphates may form deposits in the concentrate channels of the stack (Matz, 1965).

Fouling is caused by suspended solids present in many waters. These particles deposit and accumulate on the membrane surface, thus increasing the stack resistance. Korngold (1970) presented a comprehensive experimental study of the fouling behaviour of ten commercial anion selective membranes. It has been observed that fouling is apparently restricted to anionic membranes, mainly because precipitation of organic matter occurs often under acidic conditions (Kressman, 1969; Cook, 1965; Solt, 1965).

Poisoning is defined as a reaction of ionic species with the fixed ionic groups of the membrane matrix. There seems to be

a close relation to the fouling mechanism and it is experimentally difficult to distinguish between both. Kobus (1972) reported cases of soap poisoning in which anionic membranes eventually became cation selective after complete poisoning. These membranes did not only lose their selective properties but also showed an increase in resistivity.

Other problems in practical ED operation may be summarized as follows (Matz, 1965; Wilson, 1960; Furukawa, 1968; Tsunoda, 1965; Calvit, 1965):

(i) Electrical leakage through manifold distributors.

(ii) Hydraulic and electrical leakage due to gasketting difficulties.

(iii) Irregular flow distribution between channels, and areas of stagnation in individual channels.

(iv) Alignment difficulties and plastic deformation of sealant as well as of the membranes.

The latter problems are basically mechanical and design difficulties which are related to the complicated construction of conventional electrodialysis equipment.

2.1.6 Current reversal techniques.

Current reversal has been proposed as a measure to reduce scale formation, fouling and poisoning and is employed in two forms (Matz, 1965).

Reversed polarity. At periodic intervals (usually several hours) the electrode polarity is reversed, either for a short time during which the effluents are usually discarded, or in a regular cycle with continuous production. The latter operating method requires interchange piping for brine and dialysate. Matz states that many plants are partially successful in extending the periods between dismantling of the stacks when operated in this mode.

Pulsed current. The usual current direction is periodically interrupted by short current pulses with inverted polarity. The cycle periods are in the order of several seconds, with counterpulses lasting fractions of a second only (Matz, 1962). The basic idea of this technique is to frequently disturb the concentration layers, since it has been found that scale forming precipitates as well as fouling colloids require some induction period before permanent deposition occurs (Spiegler, 1961; Korngold, 1970). Tests of this method in Webster, South Dakota, showed some success in scale reduction at the price of a moderate reduction in current efficiency (Calvit, 1965).

Electrosorption-desorption. Lacey (1965,1968) conceived and investigated a process which is based on the reversed polarity technique. The standard electrodialysis stack was converted

into an absorption stack, which contained only one set of flow channels. The channels were separated by three-layer sheets which consisted of an anion and a cation selective membrane and a non-selective inner layer or core. These composite sheets were sealed along the four edges.

They served as temporary storage compartments for solute during one polarity of the applied electric potential. Feed solution, which flowed continuously through the channels, became demineralized and was drawn off as dialysate product for the duration of this absorption part of the cyclic operation.

The polarity was reversed before the compartments reached a state of saturation, i.e. before their storage capacity was filled. Subsequent regeneration of the membrane compartments enriched the feed solution, and the resulting brine efflux was usually rejected. Cycle times ranged between 15 minutes and one hour.

This stack modification has some interesting consequences:

First, the process is no longer continuous in nature but resembles more a fixed bed adsorption system operating with an electrochemical potential driving force. Dialysate and brine are produced successively in a single set of channels instead of simultaneously in adjacent channels as in a conventional multicell electrodialyzer.

Second, the stack is much simpler in design. It has less leakprone distribution manifolds, a smaller number of channels, and improved membrane utilization factors since the membranes are not used to separate brine and dialysate and may therefore be as small as the active interior of the stack.

Third, the regeneration step usually requires additional energy, the cost of which must be balanced against savings resulting from the simplified cell design.

2.2 Parametric Pumping, Heatless Adsorption and Similar Cyclic Separation Processes

The term parametric pumping was introduced by Wilhelm (1966) for a temperature cycled adsorption-desorption process with reversing flow direction. Skarstrom (1959) had used a similar process, before, to dry air in a pressure cycled operation which Alexis (1967) called heatless adsorption and employed to upgrade hydrogen. Wilhelm and his co-workers investigated temperature cycled adsorption of liquids both theoretically and experimentally: Wilhelm and Sweed (1968), Wilhelm *et al.* (1968), Sweed and Wilhelm (1969), Rolke and Wilhelm (1969). This system has also been studied by Wakao *et al.* (1968), Pigford *et al.* (1969), Aris (1969), Horn and Lin (1969), Harris (1970), Baker III (1970), Gregory and

Sweed (1970), Rhee and Amundson (1970), Sweed and Gregory (1971), Chen and Hill (1971), Chen *et al.* (1972), Butts *et al.* (1972). Temperature cycled gas adsorption has been investigated by Jenczewski and Myers (1968,1971) and Patrick *et al.* (1972). Sabadell and Sweed (1970) showed the applicability of the parametric pumping principle to pH cycled packed bed adsorption. Heatless adsorption was revived by Eluard (1970), Batta (1971), and Shendelman and Mitchell (1972).

Although Sweed (1971) presented an excellent review on parametric pumping up to the year 1970 inclusive, the basic concept and Pigford *et al.'s* (1969) equilibrium model are briefly introduced in the next section. Heatless adsorption and some other cyclic separation processes are subsequently related to parametric pumping.

2.2.1 Parametric pumping.

Consider the closed system in Figure 5. It consists of a jacketed tubular column and two end reservoirs. The column is packed with a bed of adsorbent, the temperature of which is controlled by the temperature of the jacket fluid. The mixture to be separated is contained in the bottom reservoir No. 2 and in the void spaces of the column. The system is a closed one, i.e. there is neither feed of fresh solution nor removal of products. This situation is

analoguous to the familiar total reflux operation of a distillation column, and it will, therefore, be referred to as total reflux mode.

Most workers describe a parapump cycle of the total reflux system, shown in Figure 5, as a sequence of these steps:

(i) Displace upward through a heated bed.

(ii) Displace downward through a cooled bed.

Initially the bed is usually hot, the concentration is uniform, and solution and adsorbent are everywhere in equilibrium. If the coupled cycling of bed temperature and fluid displacement is carried out, the average concentration of the effluents from top and bottom reservoirs will change as function of the number of cycles (transients).

During the first upward displacement, the concentrations remain at their initial equilibrium values. After this displacement is complete, the temperature is lowered and the flow moves downward. Solute redistributes between the phases and solution which is depleted in adsorbate emerges from the bottom end of the column.

The second cycle begins by reversing the flow direction and raising the temperature to the initial level. If conditions are properly chosen, the top effluent will be enriched in adsorbate, and the bottom effluent will be even further depleted during this second cycle.

Very large concentration differences between top and bottom effluents have been experimentally achieved for repetetive cycling by Wilhelm (1968a) for a toluene-heptane-silica gel system. The separation factor (ns) which has been defined as the ratio of the average effluent concentrations, top compared to bottom, increased beyond 10^5 in this system.

Favourable conditions for temperature cycled parametric pumping of liquids in packed bed adsorption columns are:

1. Large temperature changes and temperature sensitive adsorption isotherms.
2. Packing with large adsorption capacity.
3. No breakthrough of concentration fronts.
4. Equilibrium between solution and adsorbent.
5. Large heat transfer coefficients.
6. Minimal axial dispersion.
7. Synchronous switching of bed temperature and fluid displacement.

Pigford *et al.* (1969a) developed a simple model which must be regarded as limiting case for parametric pumping separations. This "equilibrium model" has the advantage that it describes the concentration transients in closed mathematical form. It has, therefore, been used extensively to simulate batch, semicontinuous and continuous systems (Gregory, 1970; Chen, 1970,1972; Butts, 1972; Shendelman, 1972). However, Gregory (1970) showed that this model is usually inadequate to describe experimental results quantitatively.

The following assumptions characterize the equilibrium theory:

(a) instantaneous interphase equilibration, i.e. no mass transfer resistance,

(b) linear equilibrium isotherms,

(c) no axial dispersion,

(d) instantaneous temperature changes.

Upon close inspection of these assumptions, one sees that they account for conditions 4, 5, and 6 above. The remaining conditions may be externally set by the experimenter.

For square wave displacement of one void volume combined with a synchronous temperature square wave, the mass conservation equation (for a slice of thickness dz)

$$v \frac{\partial c_f}{\partial z} + \frac{\partial c_f}{\partial t} + \frac{(1-\varepsilon)}{\varepsilon} \cdot \frac{\partial c_s}{\partial t} = 0 \qquad (15)$$

where

v	constant interstitial velocity	[cm/sec]
c_f	fluid concentration	[g-moles solute/ cm^3 solution]
c_s	solid concentration	[g-moles solute/ cm^3 solid]
z	direction of flow	[cm]
t	time	[sec]
ε	fractional void volume of the packing	

becomes

$$(1 + m) \frac{\partial c_f}{\partial t} + v \frac{\partial c_f}{\partial z} = 0 \qquad (16)$$

Here

$$c_s = M \cdot c_f \qquad (17)$$

M = linear equilibrium constant

and

$$m = \frac{1-\varepsilon}{\varepsilon} M$$

The hyperbolic differential equation (16) may be solved by the method of characteristics for each half cycle (Acrivos, 1956). The characteristics in the (z,t) plane are straight lines. Since c_f remains constant along any characteristic,

$$\frac{dz}{dt} = \frac{v}{1 + m} \qquad (18)$$

The movement of concentration waves in the bed may be displayed graphically. The analytical solutions are thus based on keeping track of concentration bands as they travel through the bed.

Figure 6 is a hypothetical example of a closed system. The bed length is shown as ordinate against the number of cycles. The lines have slopes

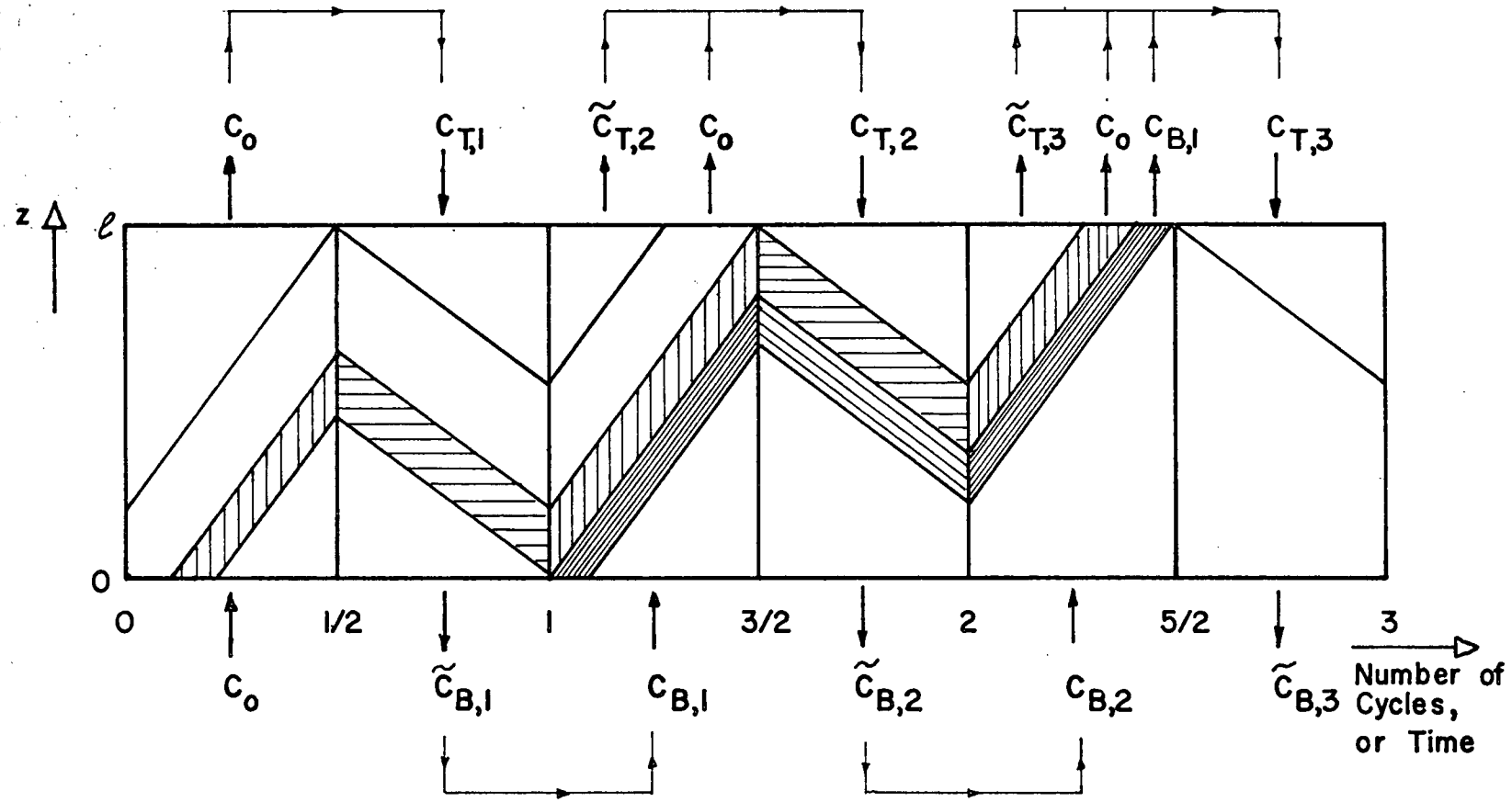

Figure 6: Characteristics of batch separation via equilibrium theory of parametric pumping.

$$\frac{v}{1 + m_{HOT}}$$ during first half cycles,

and

$$\frac{-v}{1 + m_{COLD}}$$ during second half cycles.

Since $m_{HOT} < m_{COLD}$, the net motion of the bands is upward. The top or bottom effluent concentration is a mixture of bands which originate in known concentrations of preceding cycles. A band which travels from bottom to top emerges with the same concentration it had when it entered. After an initial start-up period the bands no longer depend on the initial concentration.

Aris (1969) has shown that a pair of difference equations always exists, which completely describe average top and bottom product concentrations as functions of the number of cycles. Gregory (1970) extended the analysis to allow for dead volumes in the top and bottom reservoirs and displacements of less than one void volume.

The common result of these analytical solutions is the prediction that the concentration at the bottom of the column tends to that of pure solvent as the number of cycles increases. Figure 7 is a plot of the normalized top and bottom concentration transients according to Pigford *et al.*'s equations for $m_{HOT} = 0.2\overline{27}$ and $m_{COLD} = 0.5$.

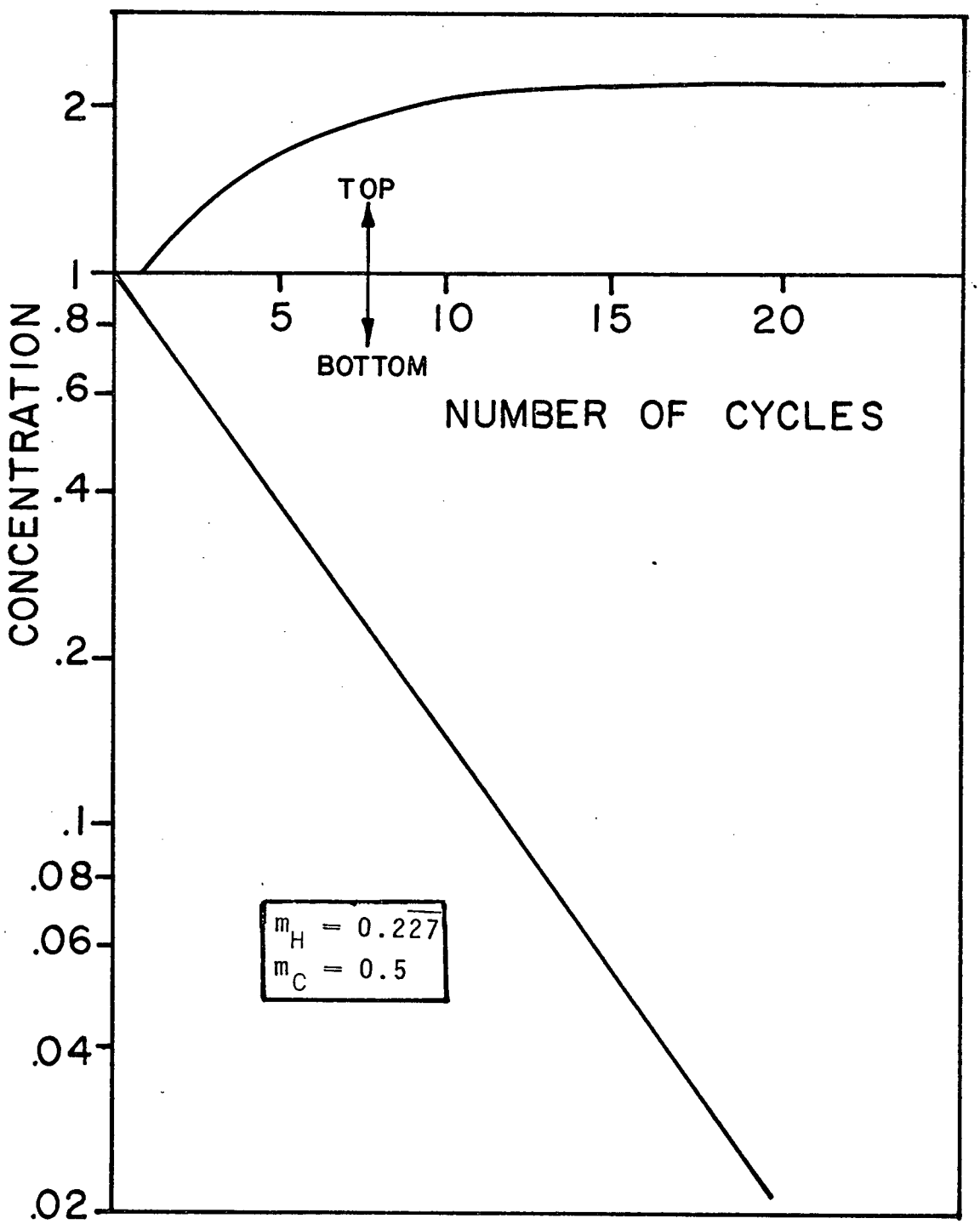

Figure 7. Concentration transients for equilibrium theory of parametric pumping (according to Pigford, 1969a).

In reality dispersive effects and finite mass and heat transfer rates limit the separation, as also may non-linear equilibrium isotherms (Rhee and Amundson, 1970).

Wilhelm and his co-workers developed models which take some or all of those non-idealities into account (Wilhelm, 1966; Wilhelm and Sweed, 1968; Wilhelm *et al.*, 1968; Sweed and Wilhelm, 1969; Rolke and Wilhelm, 1969; Sweed and Gregory, 1971). Their numerical solutions agreed quite well with experimental results.

2.2.2 Other cyclic operations.

Heatless adsorption, the original cyclic adsorption system, works on the pressure dependence of the gas adsorption equilibrium. The system is much more attractive from a practical point of view because pressure changes may be initiated almost instantly compared to the slow heating and cooling in thermally forced systems.

Skarstrom's (1959) double column arrangement is illustrated in Figure 8.

When column A adsorbs under high pressure, column B is backwashed under low pressure with a purge stream of dry air. Very high purifications are achieved when the volumetric purge flow rate exceeds the feed flow rate. Shendelman (1972) obtained similar results for a system

CO_2 in He, as did Alexis (1967) with the system H_2 in hydrocarbons, and Batta (1971) with O_2 in air.

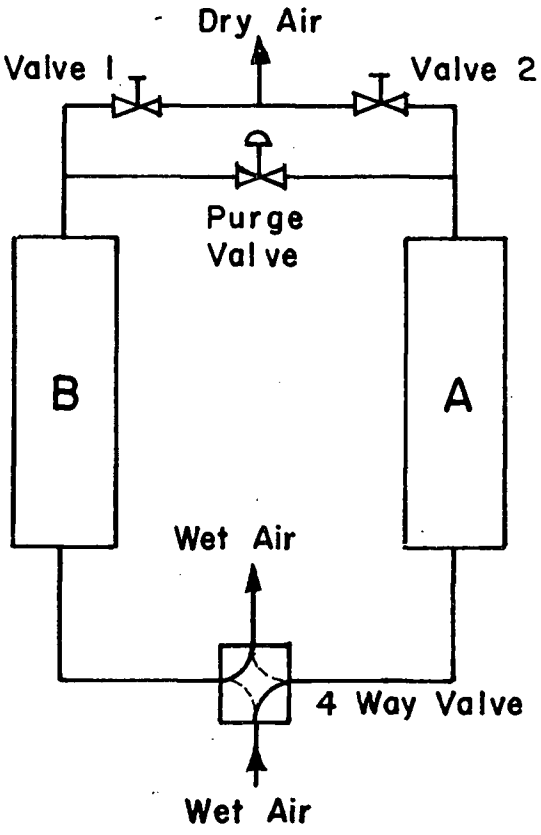

Figure 8: Heatless adsorption air drying system, used by Skarstrom (1959).

Heatless adsorption must be considered a one-cycle operation which resembles more a conventional chromatographic separation or a fixed bed ion exchange than a parametric pump. The regeneration step for each column is a counter

current backwashing with a purge stream from the other column's product. This is the only reflux in the system.

Cyclic zone adsorption — Cyclic zone adsorption was devised by Pigford *et al.* (1969b). The system, which is shown in Figure 9, consists of two temperature cycled adsorption columns. The temperature cycles of the columns are one-half cycle out of phase, i.e. one adsorbs (cold) while the other one desorbs (hot) and vice versa. A four-way valve is switched synchronously with the temperature of the beds.

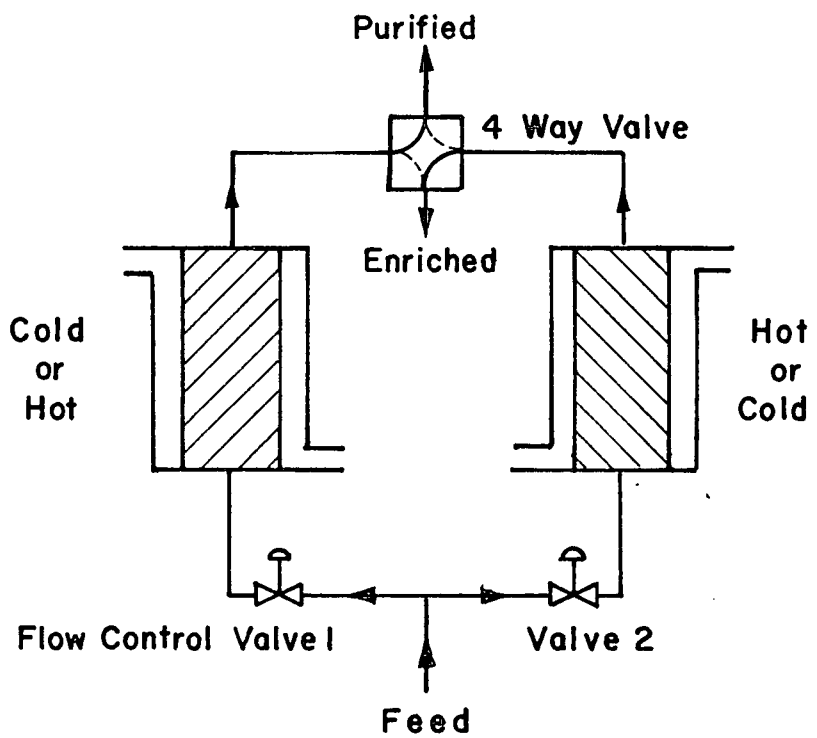

Figure 9. Cyclic zone adsorption (proposed by Pigford, 1969b).

Obviously, the twin columns may be considered as two independent separators which have been synchronized in such a way as to achieve 'continuous production of two streams of different concentrations, one higher and one lower than that of the feed' (Pigford, *et al.*, 1969b). There is no reflux between the columns, which are regenerated using feed solution in co-current flow.

Electrosorption-desorption (Lacey, 1965,1968) — The electrosorption process, described in Section 2.1.6, is also a one-cycle separation process without reflux. It is analoguous to a single column cyclic zone adsorber, which alternately produces enriched and depleted solution.

Chapter 3

EFFECT OF FINITE MASS TRANSFER RATES ON PARAMETRIC PUMPING AND PURE PAUSE OPERATION

3.1 General

The equilibrium theory of parametric pumping illustrates the process principle with great simplicity. Although the analytical solutions provided by this theory agree qualitatively with experimental results on some adsorption separation systems, the equations are not suitable for designing real systems (Gregory and Sweed, 1970). In particular the equilibrium theory neglects all rate processes. Rolke and Wilhelm (1969) attributed the small separations obtained on a NaCl/mixed ion exchange resin system for water demineralization to slow rates of intraparticle mass transfer.

An electrodialysis process may be operated with comparatively high mass transfer rates at concentrations far removed from equilibrium and may therefore be better represented by a rate model than by the equilibrium theory.

Two very simple but physically reasonable rate models will be investigated theoretically. The basic assumption

of these models is that the equilibrium condition may be neglected. In other words, if the two phases were in stationary contact for an indefinite period of time, the adsorbate would be transferred completely into one of the phases.

It is further assumed that axial dispersion is negligible, that the fluid is incompressible and has constant density, that no lateral concentration gradients exist or develop, and that the fluid velocity changes in a stepwise manner and remains constant during the time intervals between steps.

Using the same notation as in Section 2.1, the mass balance equation for a horizontal slice of thickness dz is again

$$\frac{\partial c_f}{\partial t} + v \frac{\partial c_f}{\partial z} + \rho \frac{\partial c_s}{\partial t} = 0 \qquad (15)$$

where $\rho = \frac{1-\varepsilon}{\varepsilon}$ = volume ratio.

Two simple rate laws will be considered:

a) Constant and uniformly distributed interphase mass transfer rates.

b) Mass transfer rates which are proportional to the concentration in one of the phases.

These rate laws are investigated for two operational modes:

I. Continuous displacement or parametric pumping: both variables (e.g. fluid displacement and electric potential) are continuously "on" at all times.

(i) potential "on" — upward displacement,

(ii) potential "on" in reverse polarity — downward displacement.

2. Exchange-displace or pure pause: when one variable is "on" the other is "off" and vice versa. In particular the simplest periodic form of this mode. is considered here, which consists of four steps.

(i) potential "on" — no flow,

(ii) potential "off" — upward displacement,

(iii) potential "on" in reverse polarity — no flow,

(iv) potential "off" — downward displacement.

A closed system in which one void volume is displaced will be the basis of the subsequent analysis.

3.2 Constant, Uniformly Distributed Rates of Mass Transfer

There are two electrodialysis systems which would obey such rate laws. Figure 10 is a sketch of the physical arrangements. The stacks are supposed to be sorption stacks composed of perfect ion-selective membranes.

In the meandering flow version (Figure 10.a) the fluid is introduced into one of the outer channels. The effluent from this first channel flows to the adjacent channel, etc. until it has reached the last channel in the stack. The electrodes are connected to a regulated constant current power supply. The channels should be short to eliminate

unequal potential distributions due to resistance changes in the solution.

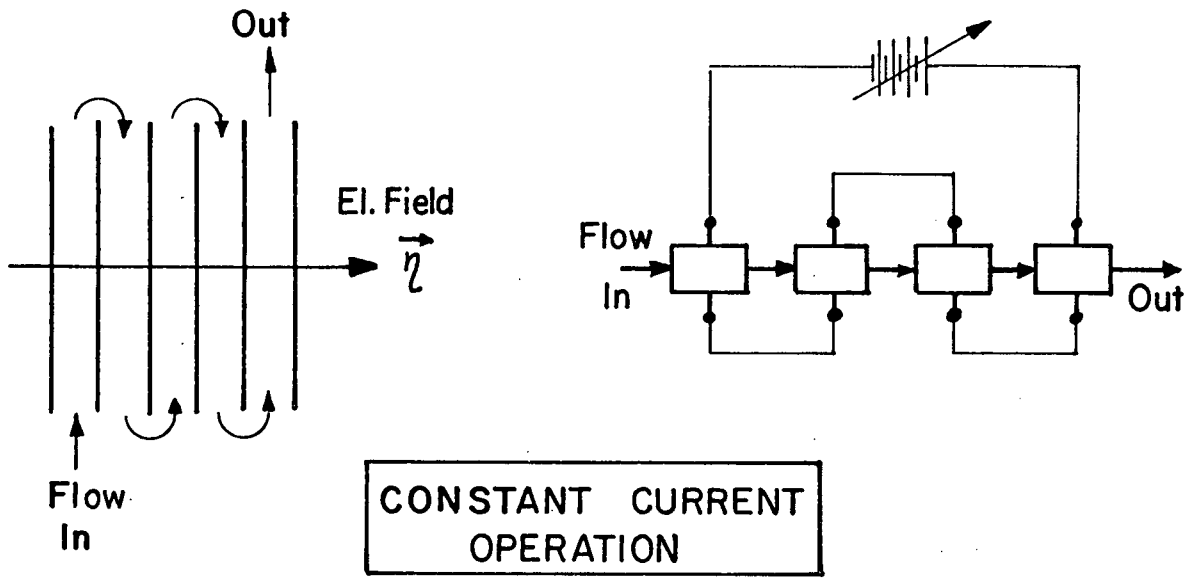

Figure 10: Electrodialysis systems with constant, uniformly distributed rates or mass transfer.

The meandering current version is basically a segmented or staged electrodialysis cell, the stages of which are connected in series electrically as well as hydraulically. Again, the D.C. power supply is operated in constant current mode, and the stages should be short.

Both devices allow an external control of the mass transfer rates, or

$$\frac{dc_f}{dt} = -\rho \frac{dc_s}{dt} = K = \text{constant} \qquad (19)$$

Obviously equation (19) will break down as one of the concentrations approaches zero, since the applied potential must then increase beyond all bounds. Since the equation can predict negative concentrations it must be used with caution.

3.2.1 Parametric pumping operation.

If the rate constants are of equal magnitude but of opposite sign during the two half cycles of a parametric pumping operation, one has

$$\left.\begin{aligned} \frac{d\,c_f}{dt} &= -\rho \frac{dc_s}{dt} = -K \quad \text{for dilution} \\ \frac{d\,c_f}{dt} &= -\rho \frac{dc_s}{dt} = K \quad \text{for enrichment} \end{aligned}\right\} \qquad (20)$$

The solution of this system of differential equations is trivial. Suppose the initial condition is $c_f(t=0) = c_0$, $c_s(t=0) = c_0$. The effluent concentration during the first (demineralization) half cycle is

$$c_f(t) = c_0 - Kt$$

The average product concentration $C_{T,1}$ becomes

$$c_{T,1} = \frac{1}{T/2} \int_0^{T/2} c_f(t)dt = c_0 - K \cdot \frac{T}{4}$$

where T = cycle period ($T < 2c_0/K$, for non-negative values of $c_f(t)$).

If the polarity of the electric potential and the direction of the fluid displacement are simultaneously switched it is straightforward to show that the average bottom product concentration during the next part cycle is

$$c_{B,1} = c_0$$

During the next demineralization the top product concentration is

$$c_{T,2} = c_0 - K \cdot \frac{T}{4}$$

which is identical to $c_{T,1}$. Final conditions are therefore reached within the first cycle. Figure 11 illustrates the internal and product concentration profiles initially (Figure 11.a), after the first half cycle (Figure 11.b), and after the second half cycle (Figure 11.c).

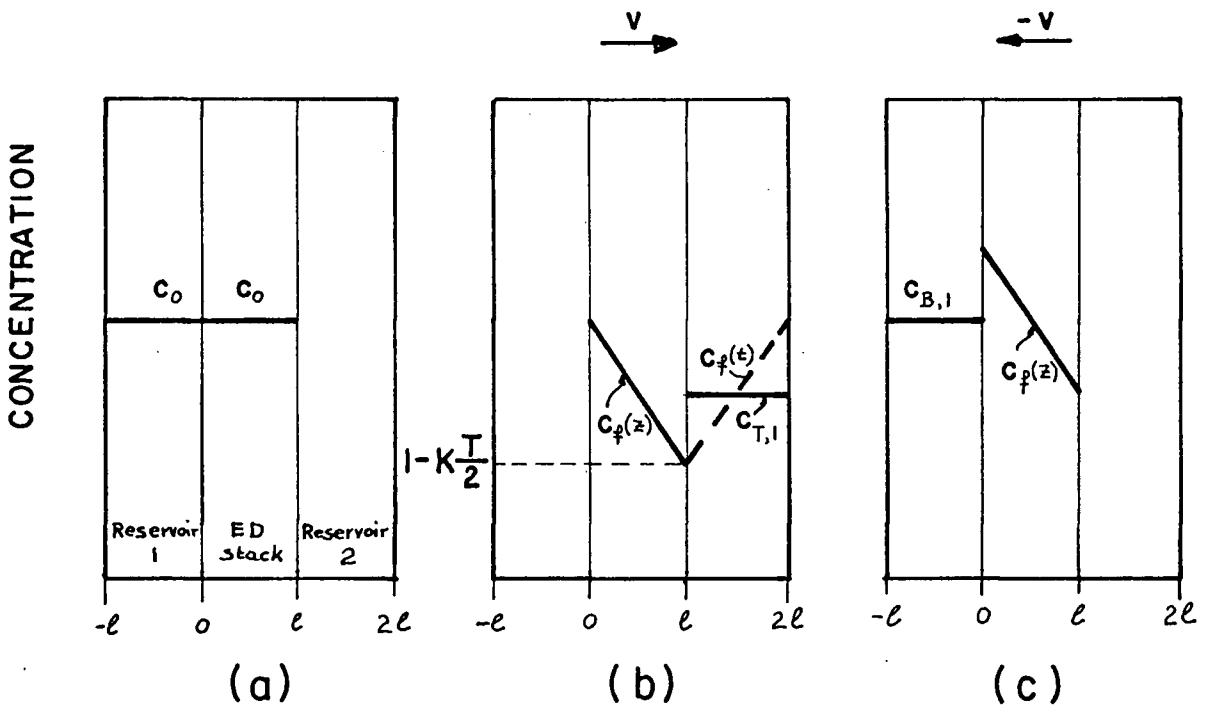

Figure 11: Concentration profiles during the first cycle of a cyclic electrodialysis process operated in parametric pumping mode under conditions of equal, constant, and uniformly distributed rates of mass transfer.

For simplicity it is assumed that the end reservoirs are packed with inert material having the same void volume as the separator.

A plot of the average top and bottom product concentration transients is shown in Figure 12. The initial decrease in top product concentration is clearly a result of the starting conditions.

If the more general case of unequal rate constants is considered, the resulting product concentrations are

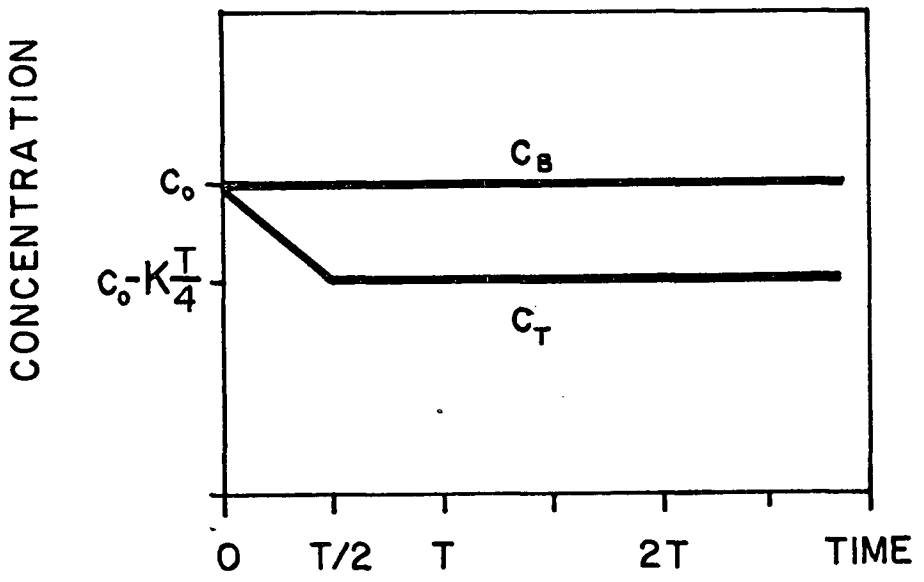

Figure 12: Product concentration transients for cyclic electrodialysis process operated in parametric pumping mode under conditions of equal, constant, and uniformly distributed rates of mass transfer.

shown in Figure 13. Here it is assumed, that K_1 applies for demineralization and K_2 for enrichment, see also equation (20). Although the concentrations show further changes after the first cycle, these changes cannot be considered as true separation because top and bottom product transients remain parallel. Concentrations continue to change due to redistribution of solute between solution and sorption

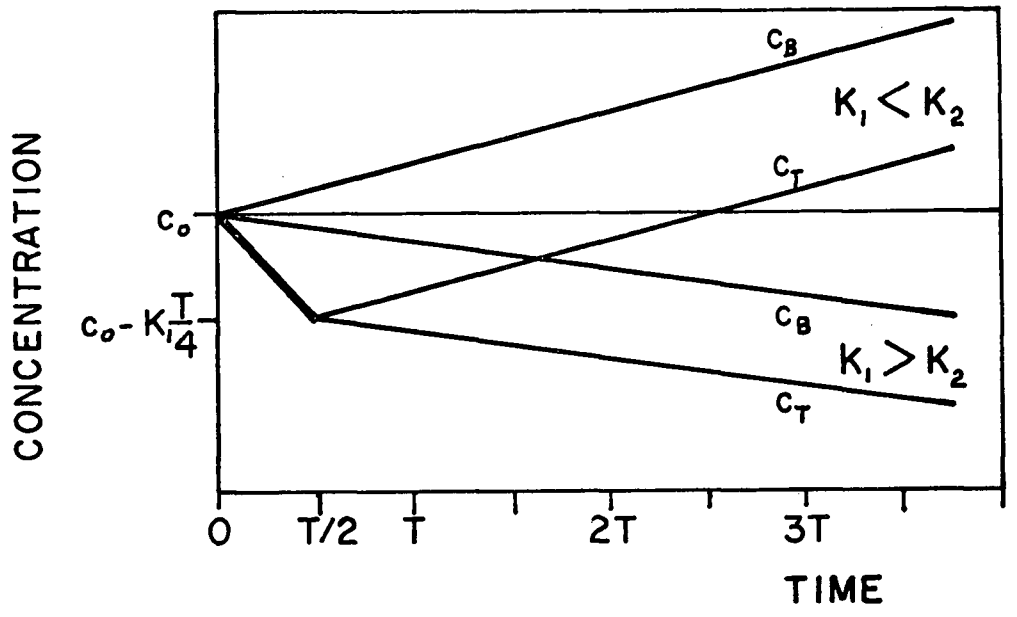

Figure 13: Product concentration transients for cyclic electrodialysis process operated in parametric pumping mode under conditions of unequal, constant, and uniformly distributed rates of mass transfer.

membranes. Obviously, the model will break down if one of the concentrations reaches zero. These physical restrictions of the model are discussed above.

Up to this point standard parametric pumping seems to have no separation potential when used in a system controlled by a constant transfer rate. This is in contrast to

experimental results on a thermal parapump system which is operated close to equilibrium, see Wilhelm and Sweed (1968).

It was found that maximum separation was achieved when the two control variables were switched simultaneously. The equilibrium theory substantiated this finding theoretically, see Pigford *et al.* (1969a). In their work no separation occurred if temperature and displacement were switched one quarter cycle out of phase.

This behaviour is inverted when the system is controlled by constant transfer rates. In this case maximum separation is obtained when the electric polarity is switched one quarter cycle out of phase to the flow reversal.

Figure 14 illustrates the consecutive action for two cycles in steps of one-half cycle from the start. It is assumed that the rate constants are equal ($K_1 = K_2$), and that the effluent remain unmixed in the end reservoirs.* For convenience it is, again, assumed that the reservoirs are packed with inert material having the same void volume as the separator. The abscissa in Figure 14 is, therefore, divided into three sections:

$$-\ell \leq z < 0 \qquad \text{for the bottom reservoir}$$
$$0 \leq z \leq \ell \qquad \text{for the separator}$$
$$\ell < z \leq 2\ell \qquad \text{for the top reservoir}$$

*This assumption does not affect the values of the average top and bottom effluent concentrations.

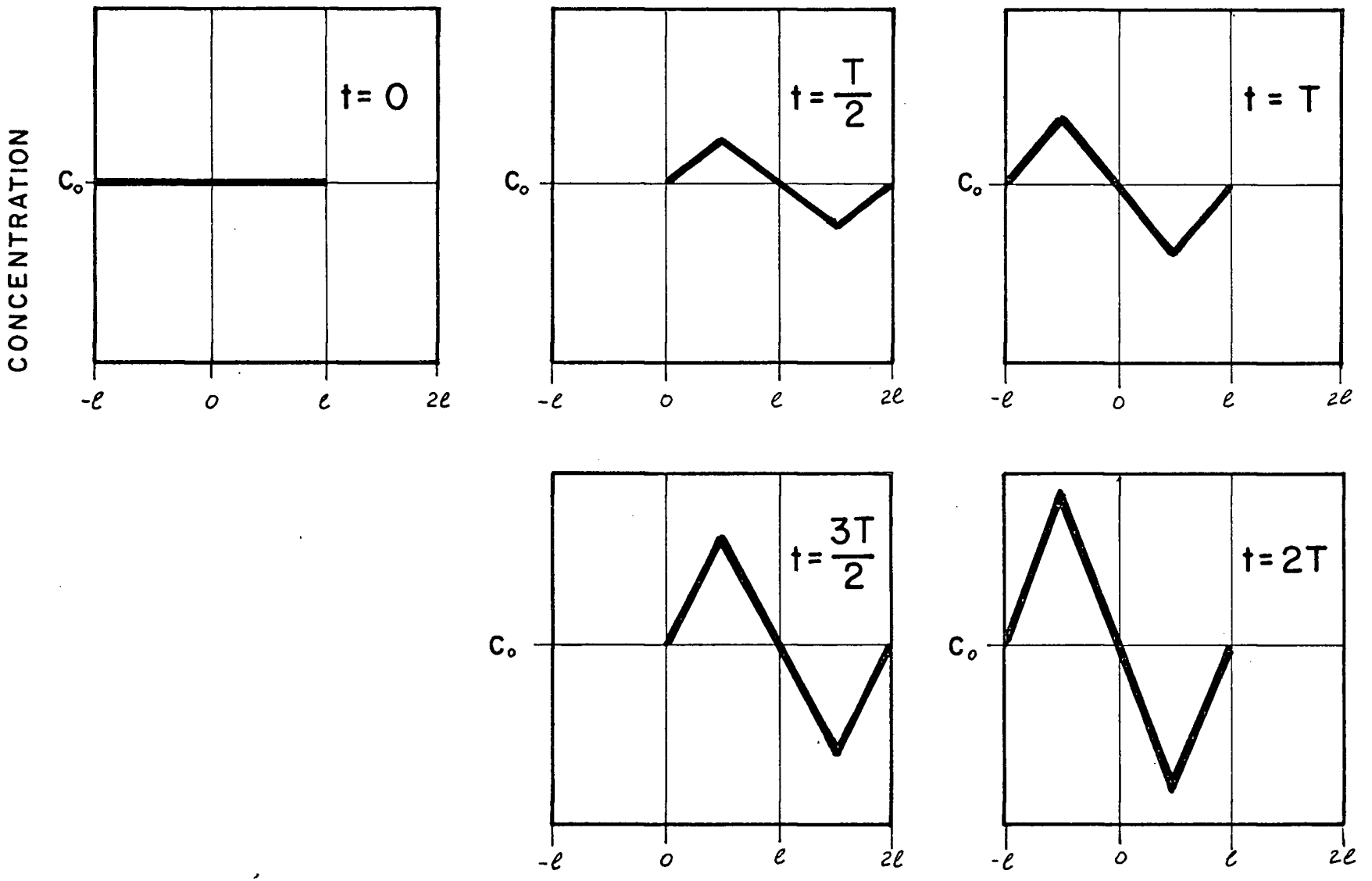

Figure 14: Development of standing waves in a parametric pumping operation under conditions of equal, constant, and uniformly distributed rates of mass transfer if variables are switched 1/4 cycle out of phase.

A symmetric standing wave of increasing amplitude is generated as a result of the periodic forcing. The average product transients (see Figure 15) are straight lines.

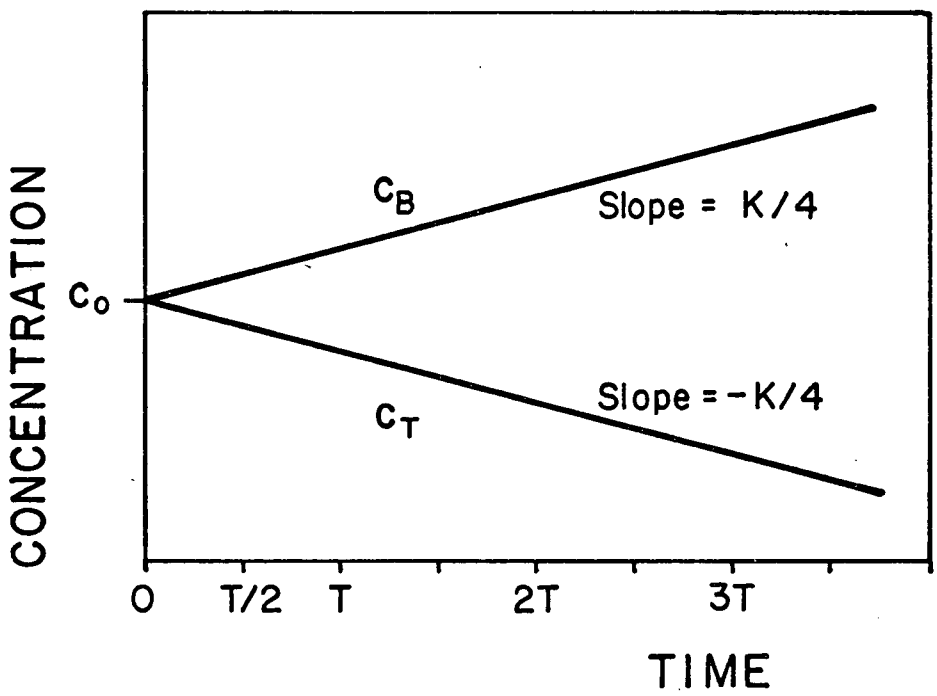

Figure 15: Product concentration transients for cyclic electrodialysis process operated in parametric pumping mode under conditions of equal, constant, and uniformly distributed rates of mass transfer, when periodic variables are switched one quarter out of phase.

The general case of unequal rate constants and any phase shift γ is summarized in the following equations for the average top and bottom product transients ($0 \leq \gamma \leq \frac{T}{4}$), which are derived in Appendix B.1.

$$c_T = c_0 - K_1\frac{T}{4} + (K_2 + K_1)\frac{\gamma^2}{T} + \left(\frac{K_2-K_1}{4} - \frac{K_2+K_1}{2}\frac{\gamma}{T}\right)\left(t - \frac{T}{2}\right)$$

where

$$t = \frac{T}{2}\ ,\ \frac{3T}{2}\ ,\ \frac{5T}{2}\ ,\ \cdots$$

and

$$c_B = c_0 + \left(\frac{K_2-K_1}{4} + \frac{K_2+K_1}{2}\frac{\gamma}{T}\right) t$$

where

$$t = T\ ,\ 2T\ ,\ 3T\ ,\ \cdots \qquad (21)$$

The transients are straight lines. Figure 16 is a plot for three values of $\gamma = 0,\ T/8,\ T/4$, assuming $K_2 > K_1$.

The important results of this section are summarized as follows:

1. Constant, uniformly distributed rates of mass transfer lead to generally poor separations in a parametric pumping operation.

2. The influence of the phase relationship for these rate laws is opposite to the equilibrium theory of parametric pumping.

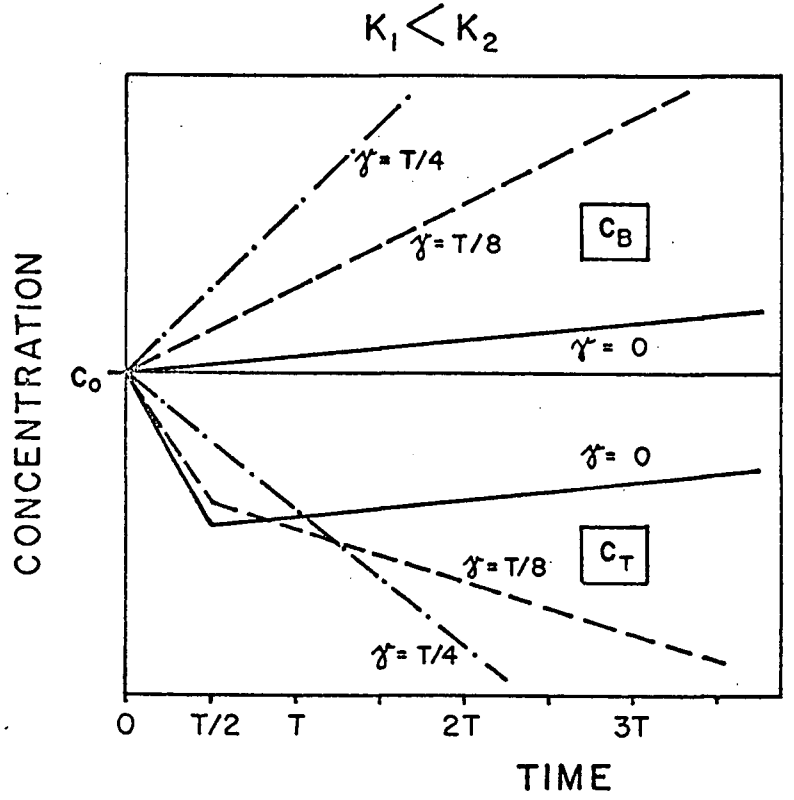

Figure 16. Average top and bottom product transients for phase shift operation of a constant rate controlled parametric pump.

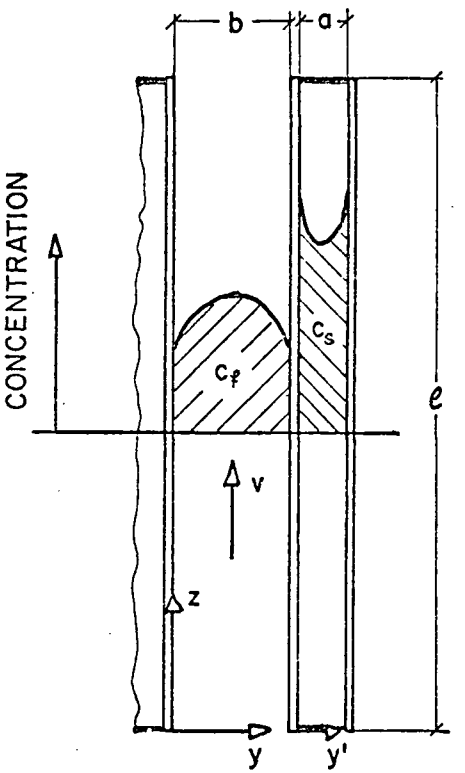

Figure 17: Lateral concentration profile and co-ordinate systems in flow channel and triple membrane.

3. Analytical solutions for the average product concentrations as functions of the cycle time have been derived. These transients are straight lines.

4. The break in the top product transient reflects the influence of the initial concentration distribution.

3.2.2 Pure pause operation.

The mass transfer rates in the model systems of Figure 10 do not depend on flow conditions, rather they are externally controlled. It may, therefore, be assumed that the rate constants K_1 and K_2 are equal for pure pause and parametric pumping operation, although this will not be valid for other systems.

The solutions of the model equations (13) are very simple in this case. The transients of the product concentrations obey the relations

$$\left.\begin{aligned} c_T &= c_0 - \left[\frac{K_1}{2} - (K_2+K_1)\frac{\gamma}{T}\right]\left(t+\frac{T}{2}\right) \quad \text{for } t = \frac{T}{2}, \frac{3T}{2}, \frac{5T}{2}, \cdots \\ \text{and} \\ c_B &= c_0 + \left[\frac{K_2}{2} - (K_2+K_1)\frac{\gamma}{T}\right] t \qquad \text{for } t = T, 2T, 3T, \cdots \end{aligned}\right\} \quad (22)$$

where again the phase shift is defined in the interval

$$0 \leq \gamma \leq \frac{T}{4}$$

i.e. the switching of the potential leads the flow switching by γ.

One can recognize that maximum separation is obtained by simultaneously switching the two variables. In this case the product transients have twice the slope of a parametric pump with one-quarter cycle phase shift (see Figure 15, and equation 21).

3.3 Concentration Dependent Rates of Mass Transfer

While it might be possible to operate a constant rate electrodialysis process, this is not very practical. In conventional electrodialysis a constant electric potential is usually applied to the electrodes. The local current density (i) is then a function of the concentrations along the current path.

For perfectly selective membranes in steady state the concept of the Donnan potential may be adopted, see Helfferich (1962). The current density (i) is then the ratio of the effective stack voltage and the total resistance per unit membrane area

$$i = \frac{(\Delta\Phi)_{eff}}{R_{tot}} = \frac{\Delta\Phi - \Delta\Phi_{Don}}{R_f + R_s + R_m} \qquad (23)$$

Figure 17 illustrates the co-ordinate system and the lateral concentration profile in the smallest unit of an electrosorption stack: a flow channel and an adjacent three-layer membrane, see also Section 2.1.6. The applied potential ($\Delta\Phi$) is diminished by the Donnan potential ($\Delta\Phi_{Don}$).

$$\Delta\Phi_{Don} = \frac{2RT}{zF}\ell n \left(\frac{c_s}{c_f}\right)_{\text{at membranes}} \tag{24}$$

The total resistance of the unit is the sum of the integral solution resistances, R_f and R_s.

$$\left.\begin{aligned} R_f &= \frac{RT}{2z^2F^2D} \cdot \int_0^b \frac{dy}{c_f(y)} \\ R_s &= \frac{RT}{2z^2F^2D} \cdot \int_0^a \frac{dy'}{c_s(y')} \end{aligned}\right\} \tag{25}$$

and the resistance of both membranes (R_m).

Substituting (24) and (25) into (23) gives

$$i = \frac{\Delta\Phi - \frac{2RT}{zF} \ell n \left(\frac{c_s}{c_f}\right)_{\text{at membranes}}}{\frac{RT}{2z^2F^2D}\left[\int_0^b \frac{dy}{c_f(y)} + \int_0^a \frac{dy'}{c_s(y')}\right] + R_m} \qquad (26)$$

The Donnan potential will usually be small compared to the applied potential. The current density is therefore mainly controlled by the lowest concentration in the current path. The concentration is low in the flow channels during depletion, and in the membrane core during enrichment. The rate laws subsequently assumed are based on these approximations:

$$\left.\begin{aligned} \rho \frac{\partial c_s}{\partial t} &= +a_1 c_f \quad \text{during dilution} \\ \frac{\partial c_s}{\partial t} &= -a_2 c_s \quad \text{during enrichment} \end{aligned}\right\} \qquad (27)$$

3.3.1 Pure pause operation.

The exchange-displace type of process operation is considered first, because it may be solved analytically. The details of this step-by-step calculation are referred to in Appendix B.2.

For one void volume displacement, without phase shift, the product concentration transients are

$$\left.\begin{aligned} \frac{c_T}{c_0} &= p^n \\ \frac{c_B}{c_0} &= 2+\rho - p^n - \rho q^n - q p^{n-1}(1-p) \sum_{\ell=0}^{n-1} \left(\frac{q}{p}\right)^{\ell} \end{aligned}\right\} \quad (28)$$

where

$p = \exp\ (-\ a_1 T/2)$

$q = \exp\ (-\ a_2 T/2)$

ρ = is as defined before .

In equation (28) the bottom product concentration decreases exponentially, whereas the top product concentration is limited by the overall mass balance.

The separation factor (ns) is here defined as the ratio of bottom and top product concentrations. This separation factor increases without limit as the number of cycles approaches infinity.

Although the product transients are of similar form to those for parametric pumping under equilibrium control, a fundamental difference exists. Equations (28) are functions of real time, whereas the equilibrium theory essentially excludes time from the mathematical solution.

3.3.2 Parametric pumping operation.

If equations (27) are substituted into the mass balance (15) the resulting partial differential equations may, in principle, be solved for any half cycle, see Appendix B.3.

A numerical solution to the problem was preferred here, however, since the number of terms in the finite series solution grows geometrically with the number of cycles. The numerical calculation scheme was identical to the STOP-GO algorithm, developed by Sweed and Wilhelm (1969).

In this scheme the continuous partial differential equations are approximated by a set of N ordinary differential equations (ODE) which are solved N times for a displacement of one void volume. A conceptual model of the algorithm and a FORTRAN IV program for computer simulations are described in Appendix B.4.

Incidentally, the case N=1 is equivalent to a pure pause operation, and the results of computer simulations are identical to numerical evaluations of equations (28).

3.3.3 Comparison of pause and parametric pumping operations.

In this section the results of a number of computer simulations for three values of N(N = 1,4,50) are compared.

Figure 18 shows the normalized concentration transients for $a_1 = a_2 = 0.01$ [sec^{-1}] , T = 20 [sec] , and $\rho = 1.0$ for one void volume displacement:

(i) N = 1 or pure pause operation shows unhindered and unlimited separation.

(ii) N = 4 represents an operation which consists of four pauses and four one-quarter displacements. The transients illustrate a gradual transition from pure pause to continuous displacement. A break in the top product transient after the first cycle may be recognized.

(iii) N = 50 or parametric pumping shows very little additional separation after the first cycle.
NOTE: The results for N = 100 are virtually identical.

Table 1 lists normalized top and bottom concentrations and the corresponding separation factor after 50 cycles for various parameter values. The results may be summarized as follows:

1. Best separation is always achieved with a pure pause operation.

2. Longer cycle periods generally improve the separation. This is equivalent to increasing the rate constants a_1 and a_2 by equal factors.

3. If the rate constant for enrichment is increased (equivalent to longer second half cycle) the separation is improved. However, the transients drift simultaneously toward higher concentrations for Run No. 11.

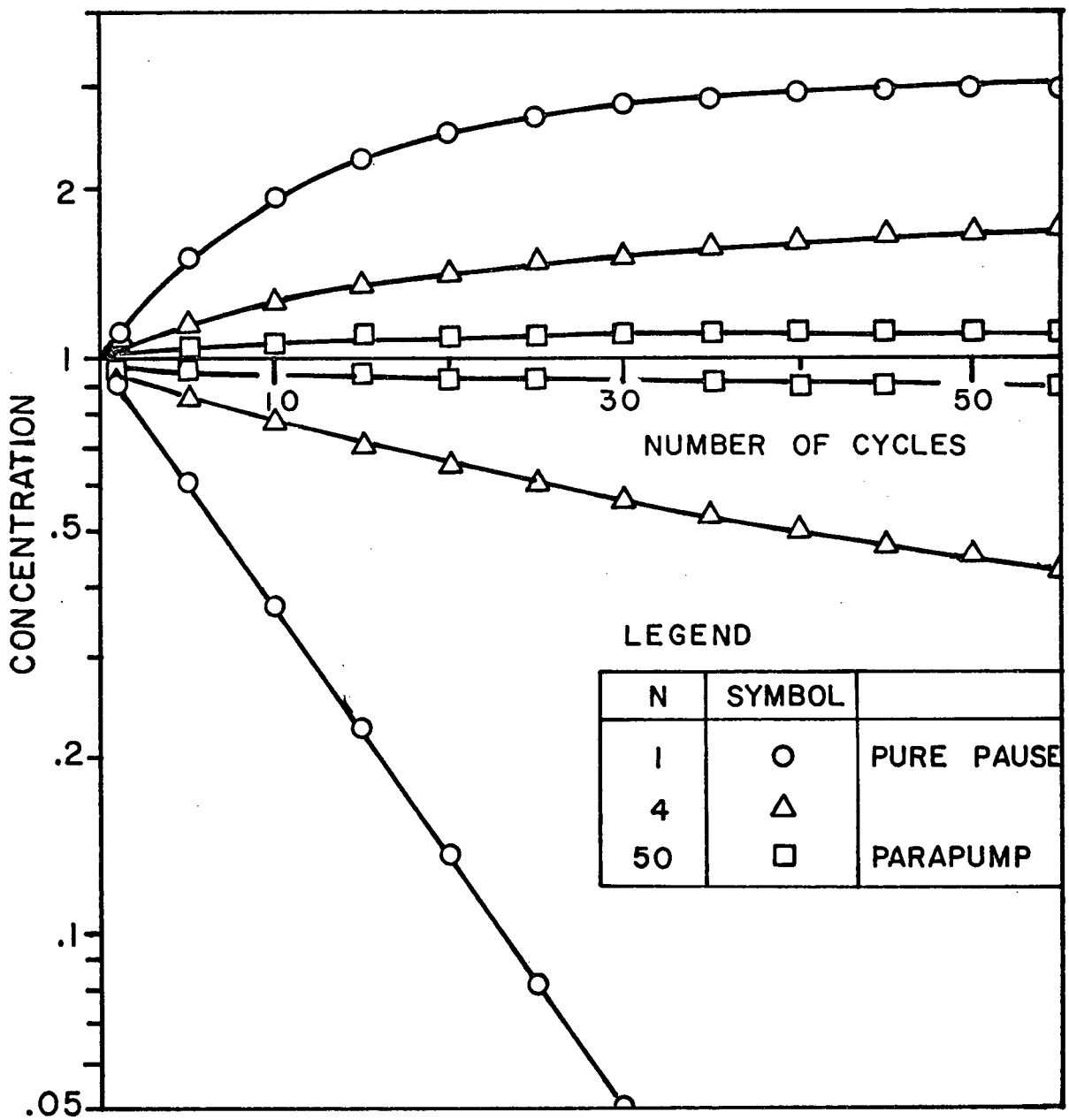

Figure 18: Effect of the number of segments on the product concentration transients for concentration dependent rates of mass transfer ($a_1 = a_2 = 0.01$ sec^{-1}, $T = 20$ sec, $\rho = 1.0$, $\delta = 1.0$).

Table 1

Computer Simulations of Pure Pause, Parametric Pumping, and Multiple Step Displacement Operations for Concentration Dependent Mass Transfer Rates

SIMULATION RUN NO.	RATE CONSTANTS		CYCLE PERIOD	VOLUME RATIO	DISPLACED VOLUME	NO. OF SEGMENTS	NO. OF CYCLES	CONCENTRATIONS		SEPARATION FACTOR
								BOTTOM	TOP	
	a_1	a_2	T	ρ	δ	N	nc	x_B	x_T	ns
[-]	[sec^{-1}]	[sec^{-1}]	[sec]	[-]	[-]	[-]	[-]	[-]	[-]	[-]
1	.01	.01	20	1	1	1	50	2.95	.0067	438.
2						4	50	1.66	.450	3.70
3						50	50	1.11	.894	1.24
4			40	1	1	1	50	3.00	.0000	66067.
5						4	50	1.87	.303	6.17
6						50	50	1.21	.806	1.50
7			80	1	1	4	50	2.04	.207	9.85
8				1	1	50	50	1.38	.661	2.08
9	.01	.02	20	1	1	1	50	2.99	.0067	443.
10						4	50	2.01	.488	4.11
11						50	50	1.36	1.04	1.30
12	.01	.01	20	1/2	1	1	50	2.46	.0067	365.
13						4	50	1.38	.378	3.66
14						50	50	.92	.747	1.24
15				1/4	1	1	50	2.21	.0067	328.
16						4	50	1.24	.342	3.63
17						50	50	.83	.672	1.24
18				1/2	1/2	2	50	3.64	.0067	540.
19						8	50	1.56	.328	4.77
20						100	50	.92	.710	1.29
21					1/4	4	50	4.56	.0067	677.
22						16	50	1.58	.328	4.83

4. A decrease in volume ratio (less adsorbent or thinner membrane core) reduces top and bottom product concentrations and may lead to a steady decline of bottom product concentration in parametric pumping operation (N=50).

5. If less than one void volume is displaced with the same cycle period the separation is improved.

   Note that $\delta = \frac{1}{2}$ requires $N = 2$ for pure pause operation, $\delta = \frac{1}{4}$ requires $N = 4$ etc.

3.4 Summary

In this chapter two simple laws for the rate of mass transfer in cyclic separation processes have been analyzed to determine their effect on the transient response of closed systems with continuous or pulse like displacement. The rate laws are physically well founded for an electrodialysis process and may be viewed as limiting conditions complementary to the local equilibrium concept.

It is shown that the standard parametric pumping operation is generally very inefficient for finite mass transfer rates if the influence of an equilibrium relationship is negligible. A pure pause operation overcomes much of these limitations and leads to unlimited separations.

It is also demonstrated that for constant and uniformly distributed mass transfer rates, the phase relation between the forced variables is contrary to that for the equilibrium theory of parametric pumping. The maximum

separation effect will be obtained if the phase shift amounts to one quarter of a total cycle. The separation in this case is, however, still small compared to a pure pause operation.

3.5 Comment on an Equilibrium Model with Instantaneous Displacement

At this point the question may be asked, what is the effect of a pure pause operation on an equilibrium controlled system? Is the instantaneous solute redistribution at the beginning of the half cycles the true separating mechanism? Or is it, also, necessary to displace the solution slowly enough that equilibrium is always maintained?

The derivation of the model equations is contained in Appendix B.5. The product concentrations as functions of the number of cycles are described by the following equations:

CASE 1: The stationary phase is initially unloaded or in the low equilibrium state. The first displacement is up without changing the equilibrium

$$\left.\begin{aligned} \frac{c_B}{c_0} &= 1 + \frac{\kappa - \lambda}{\kappa\lambda - 1}\left[1 - \left(\frac{1}{\kappa\lambda}\right)^{n-1}\right] \\ \text{and} \\ \frac{c_T}{c_0} &= \frac{\lambda}{\kappa} - \frac{1}{\kappa}\cdot\frac{\kappa - \lambda}{\kappa\lambda - 1}\left[1 - \left(\frac{1}{\kappa\lambda}\right)^{n-1}\right] \end{aligned}\right\} \quad (29)$$

where $\kappa = 1 + m_1$, and $\lambda = 1 + m_2$; m_1 & m_2 are defined in Section 2.2.1.

CASE 2: The stationary phase is initially loaded. First displacement is down without changing the equilibrium

$$\left.\begin{aligned} \frac{c_B^*}{c_0} &= \frac{\kappa}{\lambda} + \frac{1}{\lambda}\cdot\frac{\kappa - \lambda}{\kappa\lambda - 1}\left[1 - \left(\frac{1}{\kappa\lambda}\right)^{n-1}\right] \\ \text{and} \\ \frac{c_T^*}{c_0} &= 1 - \frac{\kappa - \lambda}{\kappa\lambda - 1}\left[1 - \left(\frac{1}{\kappa\lambda}\right)^{n-1}\right] \end{aligned}\right\} \quad (30)$$

Figure 19 illustrates the transients for $\kappa = 1.5$ and $\lambda = 1.25$.

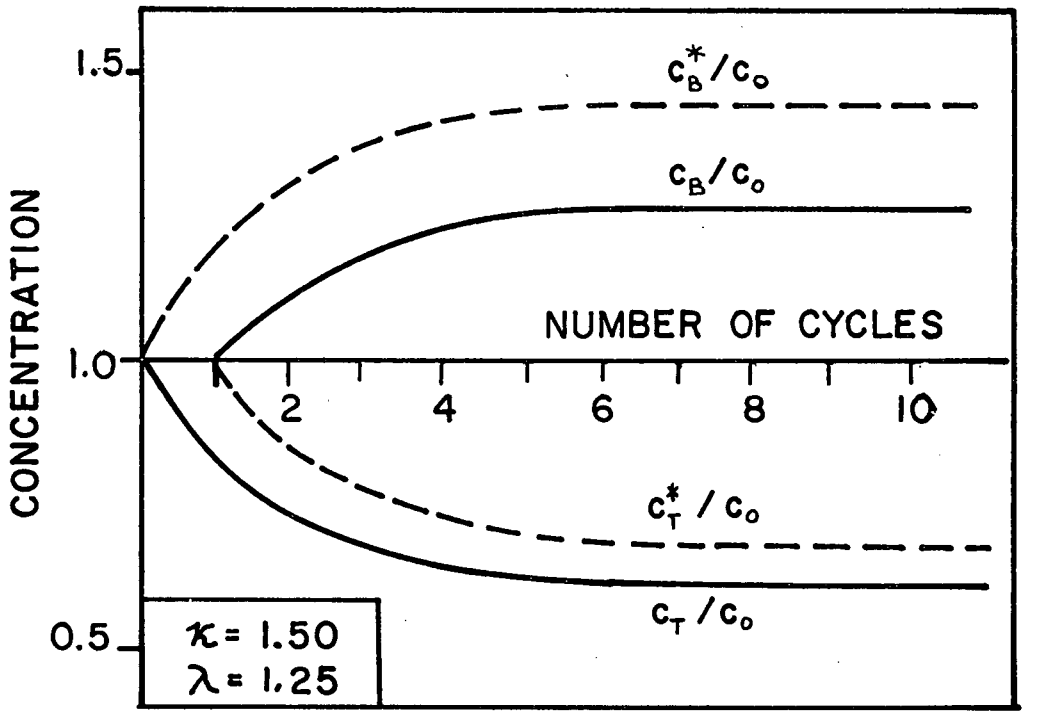

Figure 19: Product concentration transients for equilibrium controlled pure pause operation (or parametric pumping with instantaneous displacement).

It can be seen that limiting conditions are reached within a few cycles. The limiting separation factor for both cases is finite and identical:

$$\lim_{n\to\infty}(ns) = \lim_{n\to\infty}\left(\frac{c_B}{c_T}\right) = \frac{\kappa-1}{\lambda-1} = \frac{m_1}{m_2} \qquad (31)$$

The solute merely redistributes according to the two equilibrium states in such a manner that the adsorbent concentration asymptotically approaches a constant value. The time interval of active separation is comparatively short.

In answer to the above questions one can therefore deduce that, in the standard parametric pumping operation, finite flow rates are essential for successful separation when the system is controlled by equilibrium.

Another aspect of this model emerges if a combination of rate and equilibrium control is considered for a pure pause operation. Obviously the transient equations (29) or (30) constitute the maximum separation which can be obtained in such a system. For electrodialysis, however, where the ratio m_1/m_2 is usually extremely large, this limitation does not arise in practise.

Chapter 4

THE CYCLIC ELECTRODIALYSIS PROCESS - OPERATION AND APPARATUS

4.1 Description of Batch Operation

Figure 20 illustrates the four basic steps which constitute a single cycle. The electrodialysis (ED) cell is shown schematically as a rectangular box with a diagonal division indicating the membranes (a symbol which is found frequently for membrane separators). The composite sorption membranes are represented by a double-layer. Two reservoirs (circles in Figure 20) are connected to the ends of the ED cell. Partial shading of the circles indicates the liquid content of these reservoirs at different stages during the cycle.

The first half cycle is characterized by positive direction of the electric field ($\vec{n}$) (sign convention: anode left - cathode right). This will be referred to as positive polarity of the applied potential ($\Delta\phi$). The membranes are positioned in such a way that positive polarity is equivalent

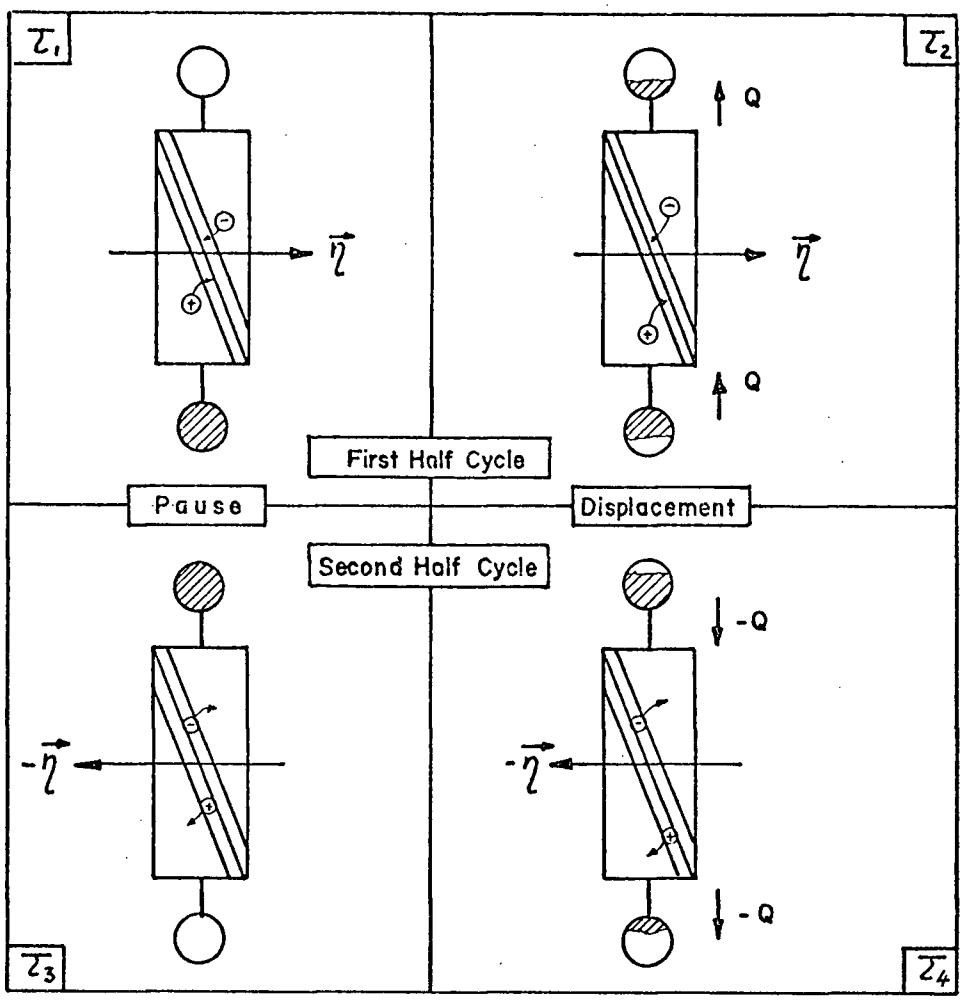

Figure 20. Batch operation of cyclic electrodialysis process.

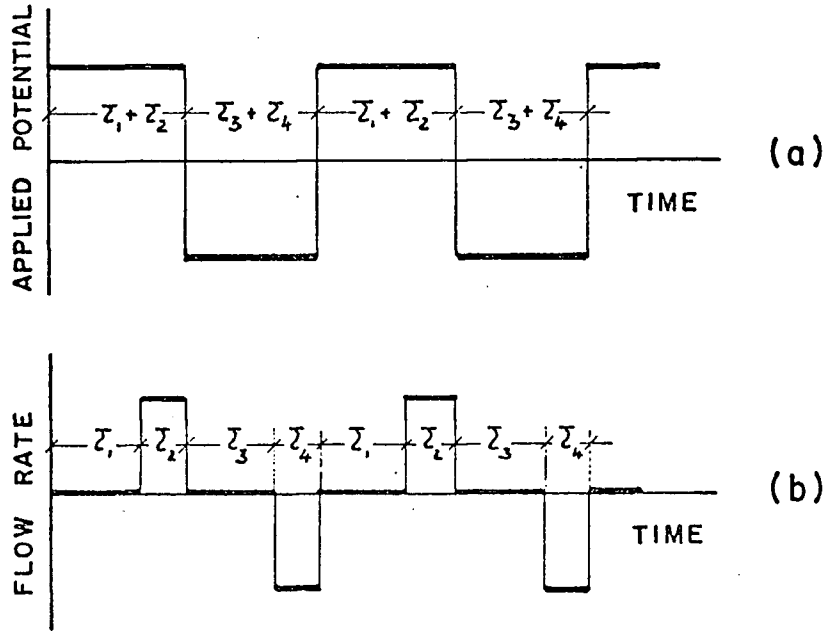

Figure 21. Time variation of applied potential (a) and flow rate (b) for cyclic electrodialysis process.

to solute uptake, i.e. the cationic membranes face the anode. The intrachannel solution becomes depleted during the entire first half cycle which consists of a "PAUSE" or no-flow interval (τ_1) followed by a "DISPLACEMENT" interval (τ_2). The fluid flows with rate (Q) from the lower to the upper reservoir.

The second half cycle begins with a polarity reversal ($-\vec{n}$) and simultaneously the flow stops for another "PAUSE" interval (τ_3). The intrachannel solution receives solute for the duration of this second half cycle, which is concluded by a "DISPLACEMENT" interval (τ_4). Solution is thus returned from the upper to the lower reservoir with flow rate ($-$ Q).

In this study the parameters $\Delta\phi$, Q , τ_i (i = 1, 2, 3, 4) are subject to the following conditions:

(i) The applied potential ($\Delta\phi$) changes in a square wave manner. At the beginning of every half cycle the sign is reversed but the magnitude is regulated to remain constant during the entire operation, Figure 21a.

(ii) The flow rate (Q) varies in a pulse like fashion. Positive pulses alternate with negative ones of the same magnitude and duration ($\tau_2 = \tau_4$) , see Figure 21b.

(iii) In most experiments the pause times are equal ($\tau_1 = \tau_3$) and because of (ii) this means symmetric half cycles.

(iv) Flow rate (Q) and displacement times ($\tau_2 = \tau_4$) are adjusted so that the total volume displaced ($Q \cdot \tau_2$) is equal or less than the solution volume initially contained in the lower reservoir. The ED cell remains completely filled with solution, therefore, but the displaced volume and any excess volumes in the reservoirs may vary from run to run. In Figure 20 no excess volumes (or dead volumes) are shown.

(v) The basic cycle is repeated in the same order for a finite number of times.

Starting conditions are always

(a) uniformly distributed concentrations.

(b) The first half cycle is a demineralizing one with upward displacement.

4.2 The First Bench Module

The experimental part of this work was performed on two ED cell versions, the first of which will be described in this section. Most of the auxilary equipment was identical for both modules. In order to avoid unnecessary repetitions, but at the same time retain the clarity of the presentation, the equipment will be shown as a block diagram. This block diagram is identical for both ED cell versions, see Figure 22.

The electrodialysis cell (ED) is connected to the process line, the rinse loop and the electric power.

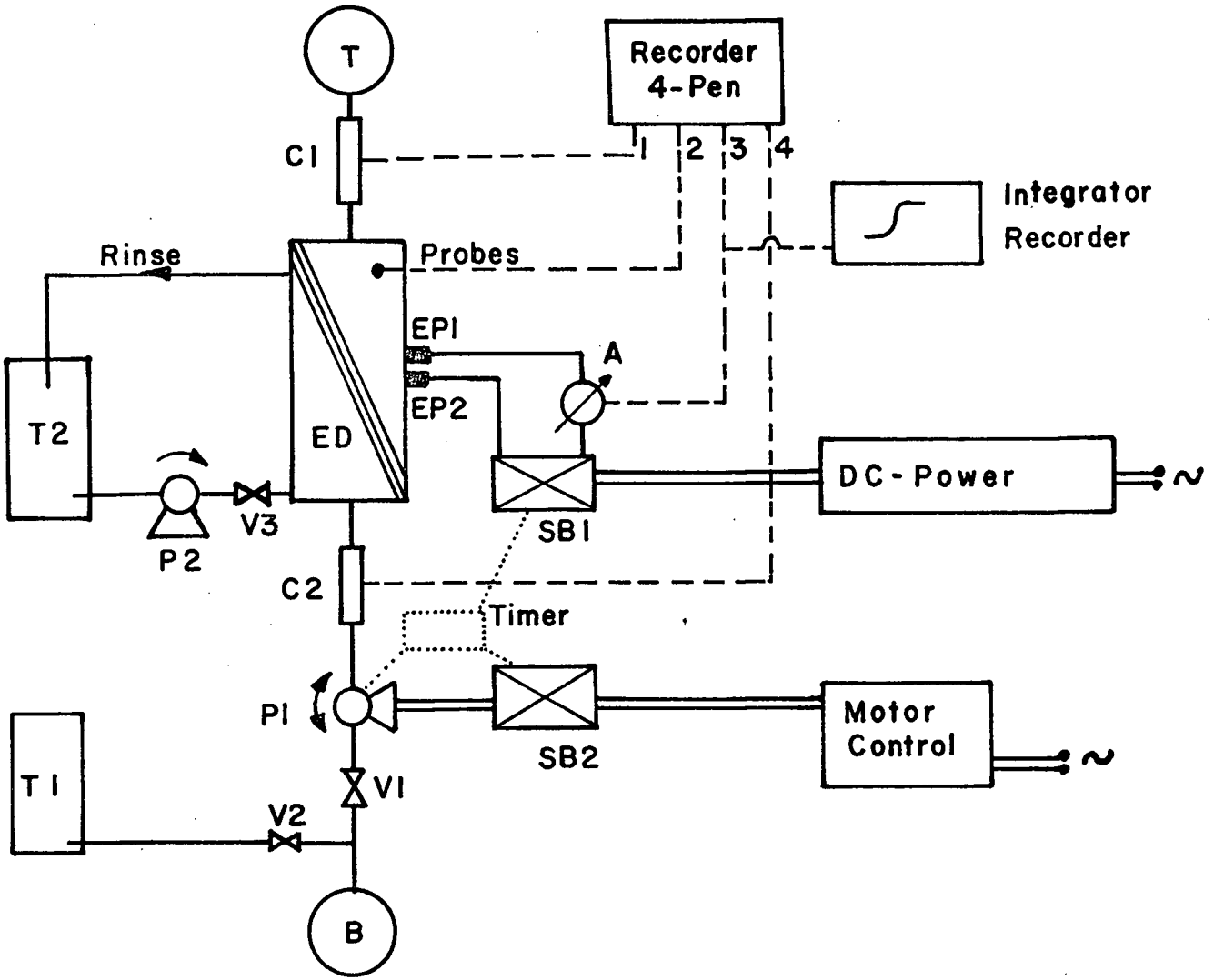

Figure 22. Block diagram of experimental testing station.

The rinse loop consists of tank T2, valve V3 and pump P2. The process line is open-ended and terminates in the top reservoir T above ED and in the bottom reservoir B below ED. In the same line are found the conductivity cells C1 and C2, pump P1, and valve V1, and a branch leading through valve V2 to tank T1 which contains the stock solution ($NaCl/H_2O$).

The DC power input may be traced from the electric binding posts EP1 and EP2, through the switch box SB1 to the regulated DC rectifier.

A second electric circuit indicates that the flow rate and the direction of flow delivered by the positive displacement pump P1 may be controlled by means of a motor controller and a switch box SB2.

A timer, which is triggered by P1, initiates the switching of SB1 and SB2.

Four signals are recorded simultaneously and continuously: The solution concentrations in the conductivity cells, the current input to the ED cell measured by shunt A, and the actual potential drop across the stack pack measured by reversible probe electrodes.

The current signal was integrated during some of the experiments to determine the average current consumption.

4.2.1 Electrodialyser No. 1 (EDI)

The primary objective of this first unit was to identify important parameters of the cyclic process and to study their effects qualitatively. Figure 23 shows an exploded view of EDI, reduced machine drawings are contained in Appendix A.1.

A constant thickness centre frame design was chosen for the following reasons:

1. Simple construction which is easy to manufacture.

2. No liquid distribution manifolds because flow is dispersed internally.

3. Only two seals required.

4. Membrane-spacer stack is a separate block, the overall size of which is determined by the centre frame opening. Thickness of sorption membranes and/or spacer screens may be varied within these limits.

The centre frame is made from a 1" Perspex plate. The opening in the centre is recessed at top and bottom to form two liquid distribution chambers in which distributor plates, each containing 32 x 0.032"ϕ holes, are mounted.

The process solution which flows through the centre frame is physically separated by two single membranes from the

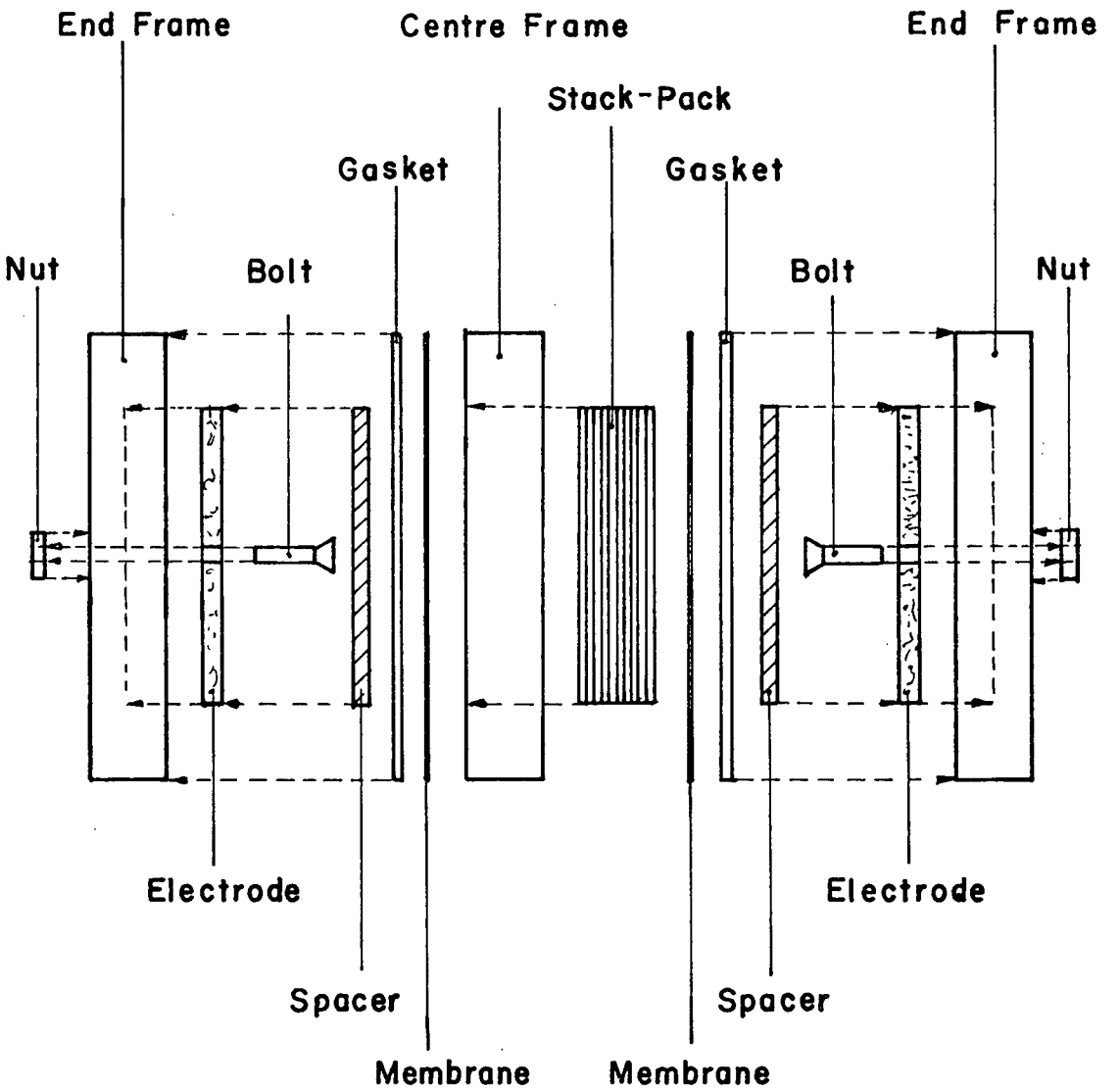

Figure 23. First electrodialysis cell EDI (exploded view, schematic).

electrode assemblies. Each of these assemblies consists of a 1" polyethylene plate, a flat graphite electrode, a graphite bolt with a nylon nut, a spacer screen, and a resilent silicon rubber gasket. Two rinse ports provide inlet and outlet of the wash solution. Detail drawings of the electrode end frame (see Appendix A.1) show how the rinse stream is distributed and collected.

Electrodes were cut from a graphite block of unknown origin and fitted in the resets provided in the polyethylene plates. Some unsuccessful experimenting with brass connectors led finally to the threaded graphite bolts shown in Figure 23. These had a conical head to provide a larger contact area with the counter-sunk electrode plates. Bolts and electrodes were sanded flat after assembly. Special Nylon nuts were made to tighten the bolts.

The electrodes were permanently set into the end blocks with a bed of silicon rubber.

The separating membranes were of the same kind as used in the stack (see below).

The whole assembly was held together by a clamping device which consisted of two rectangular frames (manufactured from 1" square pipes) and four tie rods (see detail drawing, Appendix A.1).

The probe electrodes were made from 1 [Ω/ft] silver wire. Four threads twisted into a single wire (10" long) were protected by a sleeve of SCOTCH tape except the ends. One end was soft soldered to a 1 x 2 [mm^2] silver plate (0.020" thick) and the point of contact was covered with contact cement. This probe was always inserted into the rinse compartment with the unprotected side of the plate facing the electrode and the covered side touching the separating membrane. The probes measured, therefore, the potential drop across the stack and the two separating membranes.

The main features of the first ED cell are summarized in the following Table 2.

4.2.2 Membrane-spacer stacks.

Three stack versions were tested in the course of this work by combining two types of spacer screens with two different sorption membranes.

The Sorption Membranes

Resinous ion exchange membranes were purchased from Tokuyama Soda, Japan. These were commercially used membranes. The manufacturer's specifications are given in Table 3.

Table 2

Electrodialyser No. I (EDI)

Design	Rigid Centre Frame Single Stage
Electrode Area	230 [cm^2]
Active Volume*	630 [cm^3]
Inherent Dead Volume**	40 [cm^3]
Membrane Utilization***	83 [%]
Rinse System	Single Pass
Gaskets	One on Each Electrode Frame
Materials	Centre Frame: Plexiglass Electrode Frame: L.D. P.E. Electrode: Graphite Terminal: Graphite Gaskets: Silicon Rubber

* refers to the space which will be filled with the membrane spacer stack

** calculated from the dimensions of the two flow distribution chambers

*** fraction of total membrane area exposed to circulating solution.

Table 3

Properties of NEOSEPTA Membranes,

from Yamane (1969)

Type		CL 25T cation selective	AV4-4T anion selective
Backing		PVC	PVC
Thickness	1)	0.15 - 0.17	0.15 - 0.17
Burst strength	2)	3 - 4	5 - 7
Ion exchange capacity	3)	1.8 - 2.0	1.5 - 2.0
Water content	4)	.30 - .40	.20 - .25
Electric resistance	5)	2.7 - 3.2	3.5 - 4.5
Transport number	6)	> .98	> .98

1) [mm]

2) [kg/cm^2]

3) [meg/gram dry membrane in Na-form, or Cl-form]

4) equilibrated with 0.5 N NaCl solution
[gramm H_2O/gram dry membrane in Na-form, or Cl-form]

5) equilibrated with 0.5 N NaCl solution at 25 [°C]
[Ω cm^2]

6) measured by electrodialysis in 0.5 N NaCl solution, current density 10 [m A/cm^2] at 25 [°C]

The sorption membranes, or "capacity cells," were made in two versions with a large core and with zero core. In the first case the core was 1/32" thick, consisting of a sturdy SPURLDITE frame, and a double layer of plastic coated

glass fibre screen (14/18 strands per inch, approx. 1/64" thick) fitted into the central opening of the frame. An anion and a cation selective membrane of the same size as the frame were placed on opposite sides and sealed around the four edges with SCOTCH tape. Care had to be taken to keep the membranes always moist because they not only shrink upon drying but may develop cracks. Also, it was desired to produce capacity cells in which no air bubbles were entrapped.

The membranes could be permanently cemented onto the frame using Eastman 910® adhesive (Armstrong Cork Co.) which was found to form a satisfactory bond between the damp membrane and SPURLDITE if both surfaces had been slightly sanded. Since the strengthening fabric of the membranes is PVC, the sanding procedure probably exposed the PVC filaments. This method was not used in the experimental cells since it seemed desirable to be able to inspect the capacity cell interior and to modify the core.

In the "zero" core version, the capacity cells consisted of the two membranes and the sealing tape. Again, the air pockets were completely removed before sealing.

The Spacers

Belfort and Guter (1968) investigated the flow pattern produced by various screens, and found that multiple

layers of net-like fabrics showed the least tendency to develop areas of stagnation.

The first spacer was made of four layers of the same glass fibre screen used for the first capacity cell core. The sketch below indicates the folding. SPURLDITE strips (10" x 1/4" x 1/32") strengthened the structure along the sides.

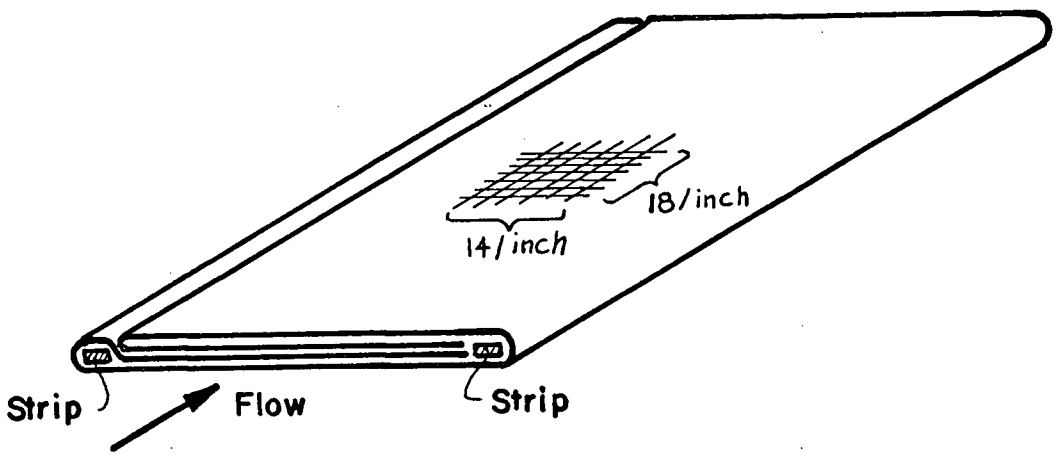

Figure 25: Glass fibre spacer screen.

The second spacer material was a conventional VEXAR® plastic net: L 12 (12/12 strands/inch, clear polypropylene) which was kindly supplied by DuPont DeNemours of Canada.

It was cut parallel to one strand direction and used as a single layer only. Thickness approx. 0.81 [mm]. The spacers are also shown in Figure 24a.

The following membrane spacer stacks were combined and investigated in this work:

Table 4

Stack Pack Versions Used in First ED Cell

Property \ Stack Version	1	2	3
No. of units	8	15 or 16	12 or 13
Spacer material	glass fibre	VEXAR® L12	glass fibre
Channel thickness [cm]	0.205	0.127 or 0.116	0.165 or 0.155
Membrane material	NEOSEPTA CL 25T & AV4T		
Capacity cell type	with core	no core	no core
Free flow volume [cm^2]	282	387 or 373	389 or 370

The stacks were assembled to form packs using two PVC clamps as shown in Figure 24b. These packs fitted into the centre frame opening and were inserted as one block according to Figure 24c.

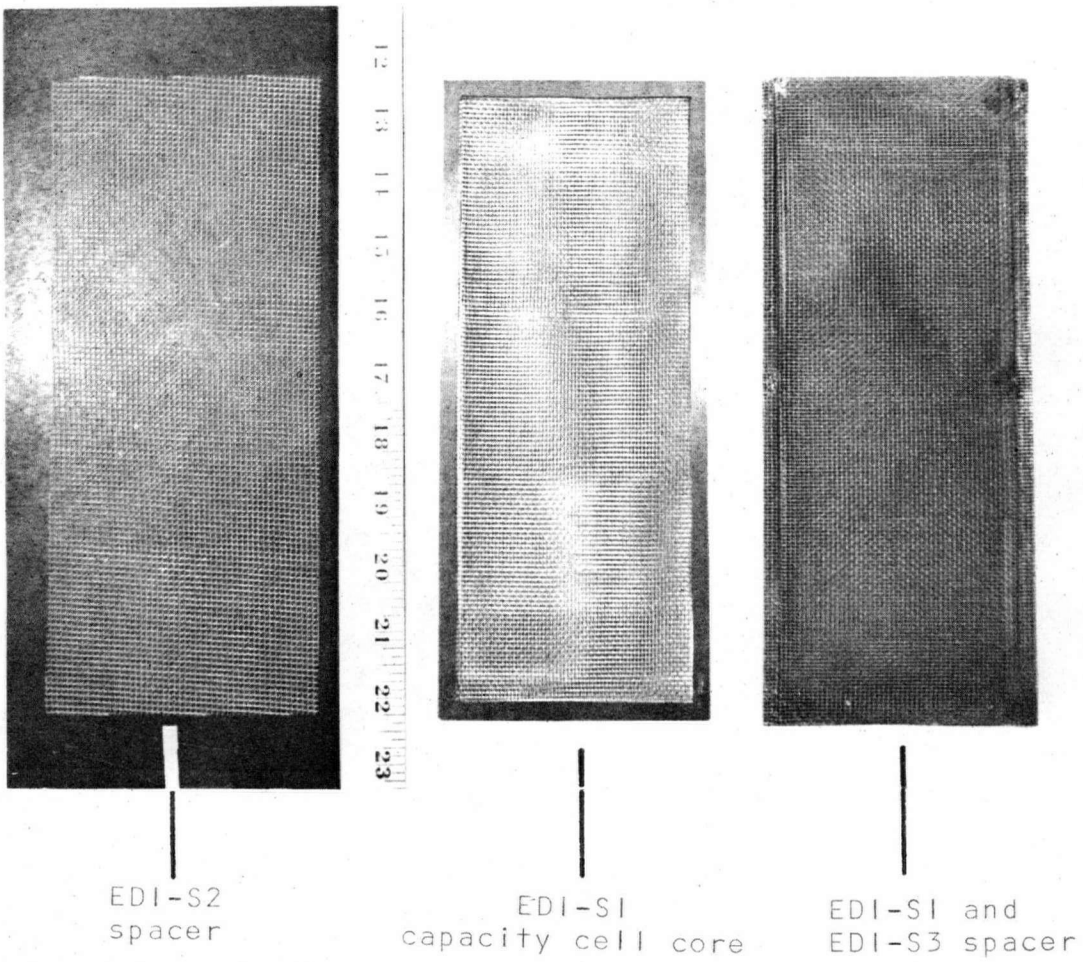

Figure 24. Electrodialyzer No. 1. (a) Spacer screens and capacity cell core (scale : inches).

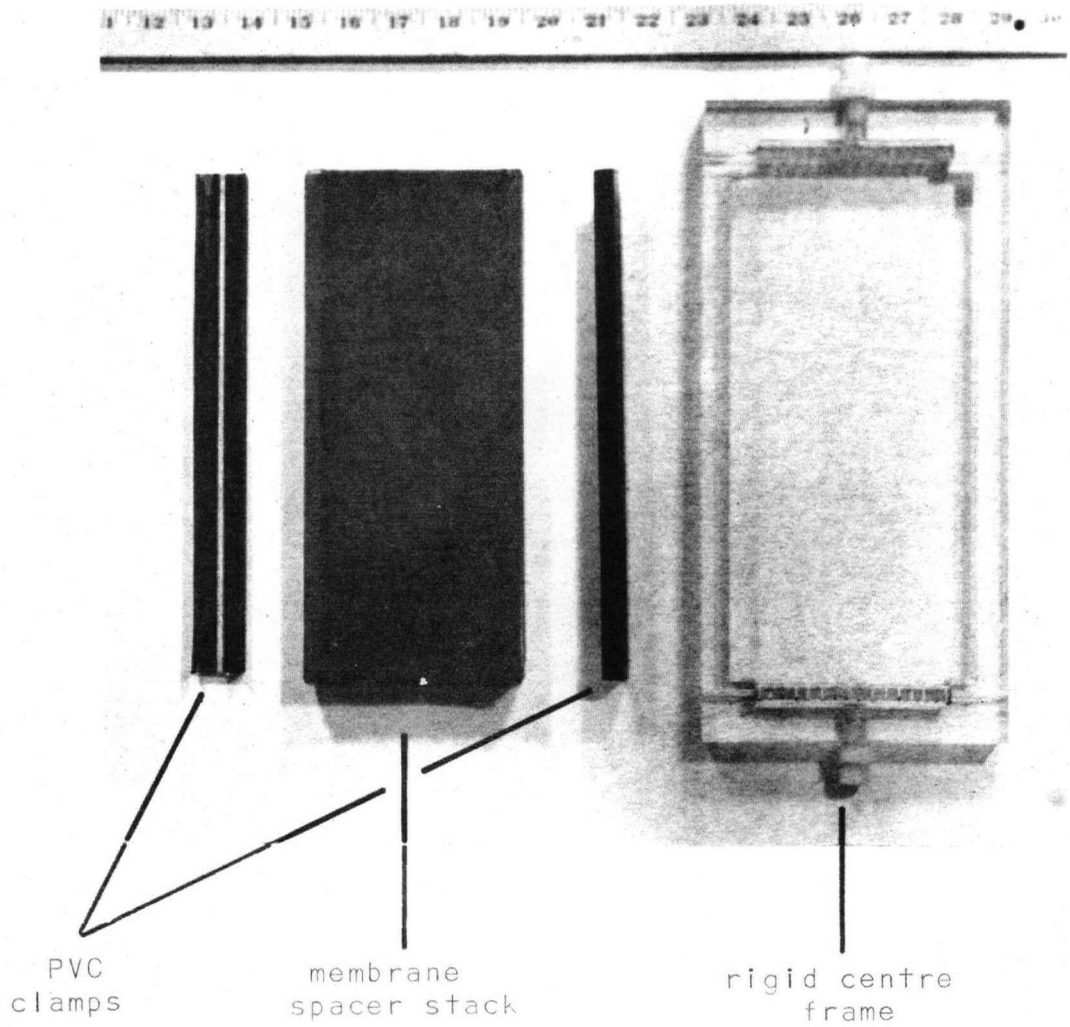

Figure 24. Electrodialyzer No. 1. (b) Stack-pack and rigid centre frame (scale : inches).

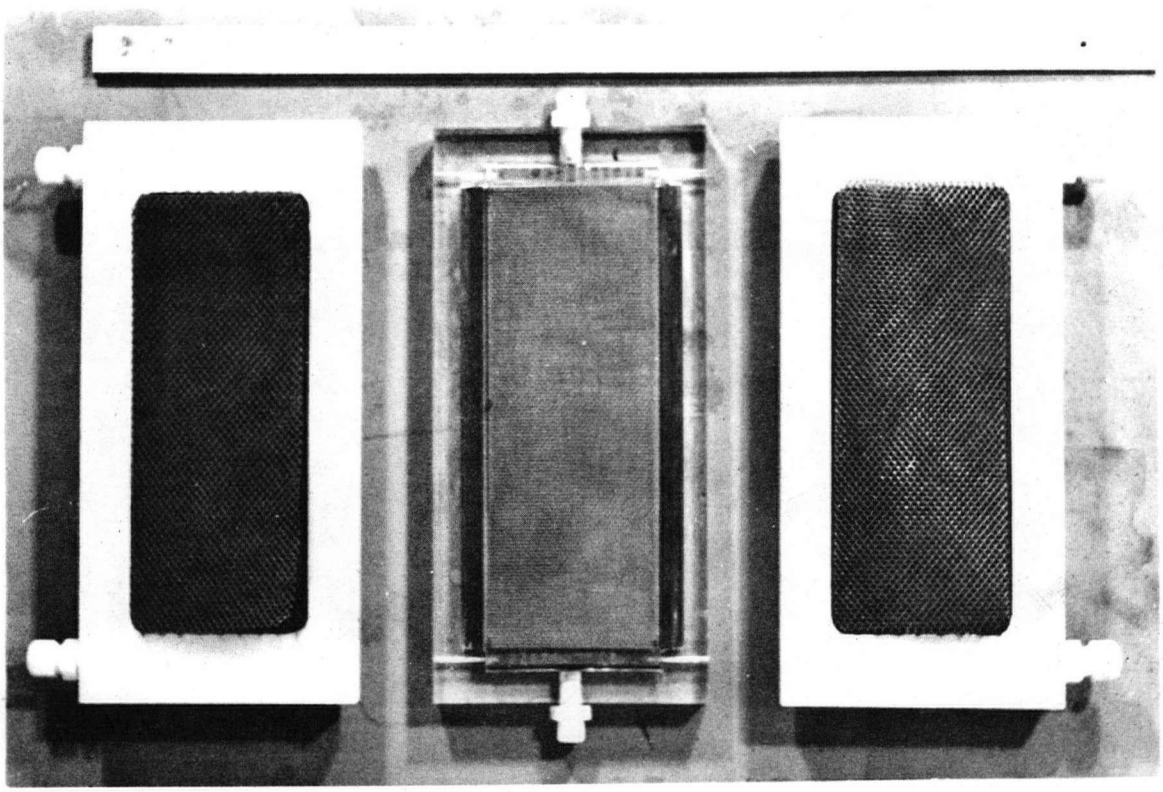

electrode end frame | centre frame with stack-pack | electrode end frame

Figure 24. Electrodialyzer No. I. (c) Cell ready for assembling (scale : inches).

4.2.3 Process flow.

It was planned that the volume of each displacement pulse would be of the same magnitude as the free flow volume of the electrodialyser. Since this was relatively small, a piston pump driven by a variable speed D.C. motor was feasible. The features of this combination are:

1. Positive displacement.
2. Pump body and end reservoir are one part.
3. Reversible with minimal time lag.
4. Short start-up time (i.e. square pulses).
5. No dead volume.
6. Accurate flow rate setting.
7. Piston displacement is natural trigger for timing.
8. May be modified to produce other than square pulses.
9. Simple construction, may be manufactured according to specifications in workshop.
10. Reliable because very little wear.

The reciprocating piston acted as an infusion-withdrawal pump. The pump was manufactured according to the specifications given in Table 5.

The cylinder of the piston pump formed the storage tank at one end of the process line. The opposite end of the

Table 5

Piston Pump Specifications

PUMP	PISTON FACE AREA [cm^2]	22.88
	MAXIMUM PISTON MOVEMENT [cm]	27.5
	DISPLACED VOLUME [cm^3]	0 to 630
	FLOW RATE [cm^3/sec]	2.5 to 75
DRIVE	1/4 hp DC MOTOR	
	SCR MOTOR CONTROL	BOSTON RADIOTROL E25
	REDUCTION GEAR RATIO	1/48
	PINION and RACK	

line was connected to a floating lid expansion tank which is shown in Figure 26.

4.2.4 Timing and switch boxes.

As mentioned in the previous section, the linear displacement of the piston is used to trigger timing and switching circuits. In the cyclic operation described in detail under 4.1 the natural control variable for switching is displaced volume and not time. However, the pause times are independent variables and separate timing devices have to be provided for these.

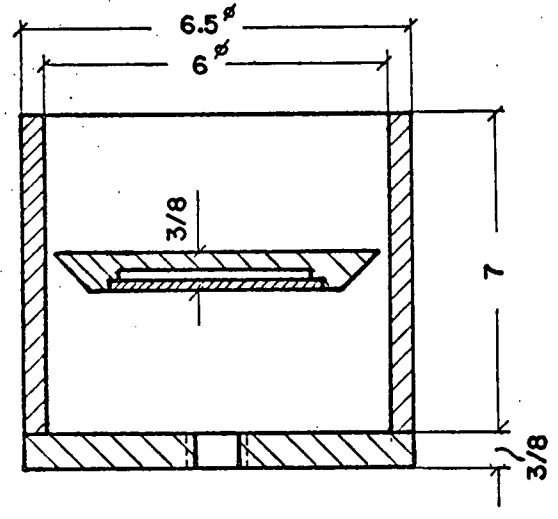

Figure 26. Floating lid expansion tank.

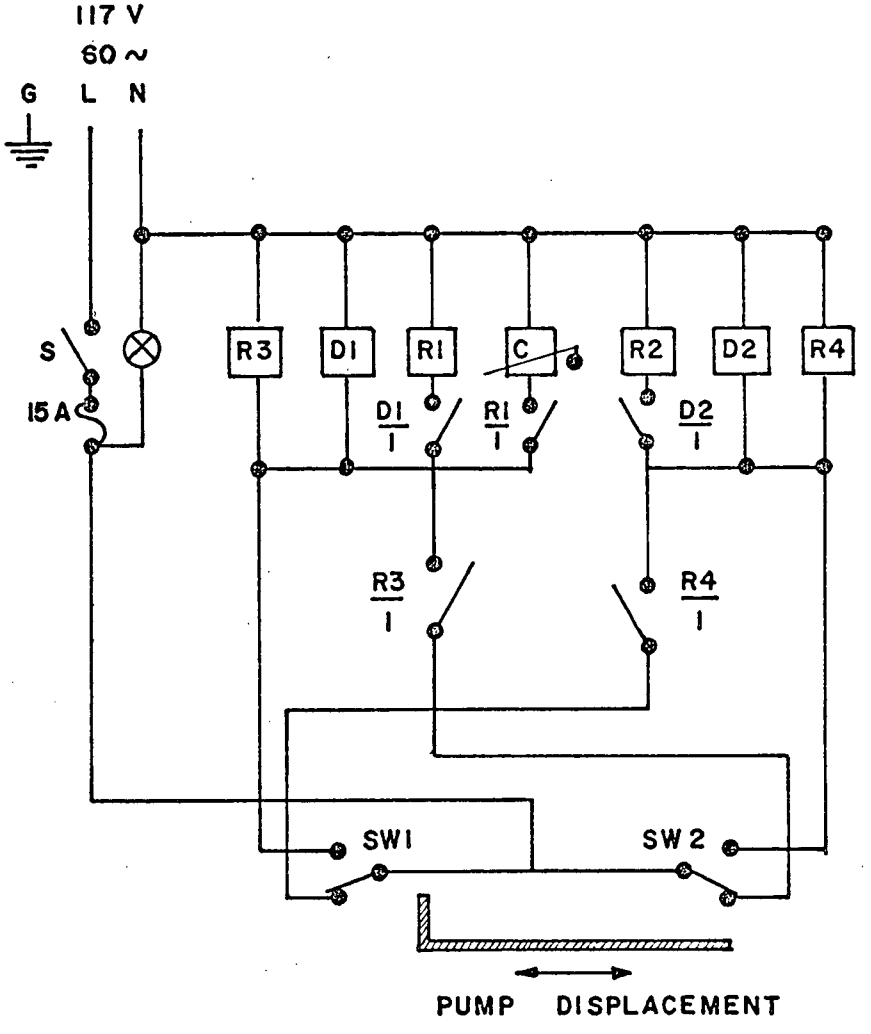

Figure 27. Automatic switching arrangement for cyclic electrodialysis process
S = switch, R = relay, D = time delay relay
C = electromechanical counter,
SW = micro switch.

Figure 27 shows how displaced volume and pause times are controlled: A cam is attached to the reciprocating rack which drives the piston. This cam operates microswitches SW1 and SW2 which are adjustably mounted.

Relays R1 and R2 are used to reverse the polarity of the motor armature (see Figure 28). Both are, however, delayed by solid state delayed relays D1 and D2 (Potter and Brumfield CDB38-70004, adjustable from 0.6 to 60 seconds).

Relays R3 and R4 control the polarity of the electric potential which is applied to the electrodialysis cell from a SORENSON DCRA 40-10A power supply. The relay circuit is identical to the one shown in Figure 28 except that the input comes from the DC power supply and the output goes to the cell.

When the piston is moving the circuits are self-holding using contacts R3/1 or R4/1.

An electromechanical counter C receives one inpulse every cycle by means of contact R1/1.

The switch boxes SB1 and SB2 in Figure 22 consist of the following components which are combined in one network:

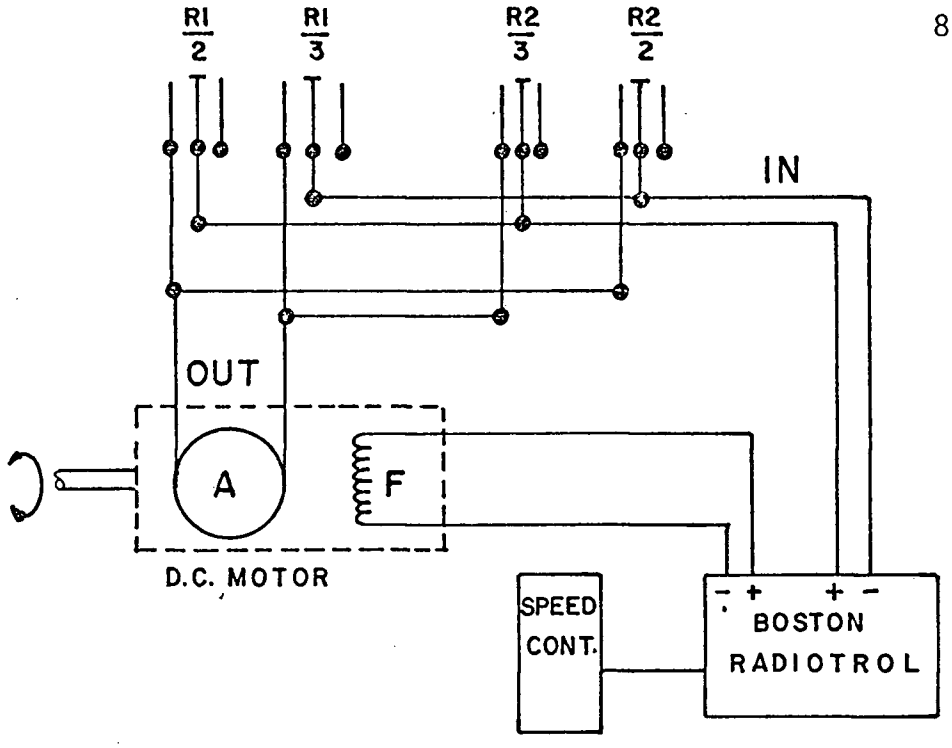

Figure 28. Piston Pump Drive. Electric circuit for motor reversal.

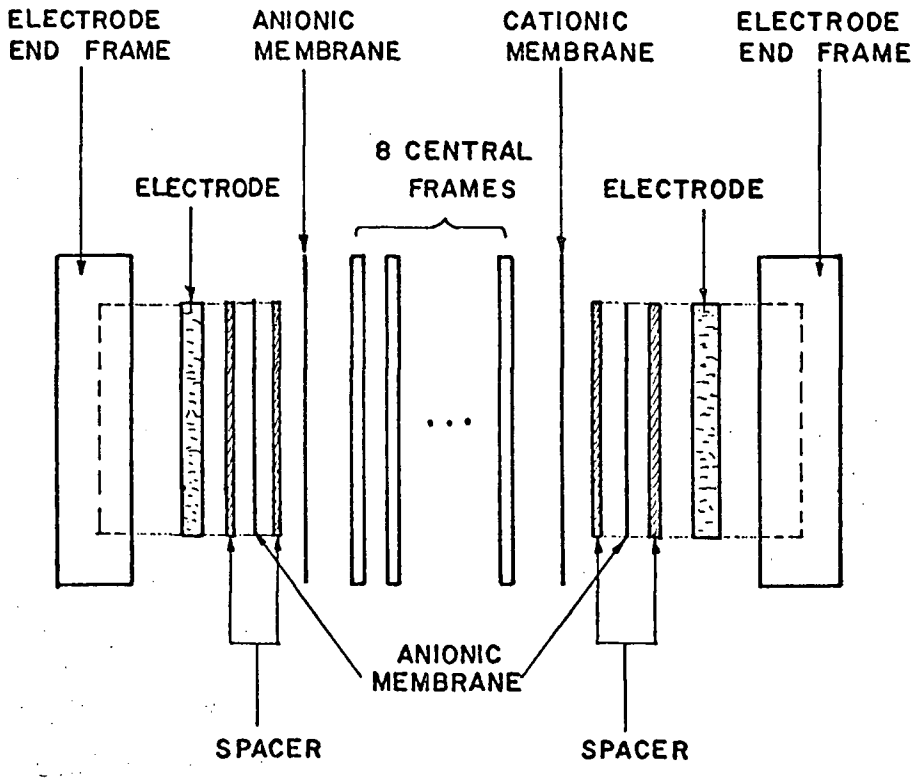

Figure 30. Schematic assembly of one stage of the second electrodialyzer.

SB1 : relays R3 and R4

SB2 : relays R1, R2, D1, D2

4.2.5 Rinse loop.

The electrode wash liquor was pumped by a peristaltic pump from a plastic tank through a flow splitter to the electrode end frames. It returned to the holding tank where the streams were remixed. Plastic tubing allowed the flow rates to each electrode to be balanced.

4.2.6 Measuring and recording.

Concentrations: Sodium chloride concentration was continuously measured conductometrically. Flow type conductivity cells (Beckman Instr., CEL-VDJ series) used with direct reading conductivity meters (Beckman Instr., Solu-Meter RA5) monitored the concentrations of the solution flows at both ends of the ED cell. Automatic temperature compensation was provided. A 0 to 10 [mV] D.C. output signal from the Solu-Meter allowed potentiometric recording of the concentration in the following ranges (see Table 6).

Table 6

Conductivity and NaCl Concentration Ranges of BECKMAN Conductivity Cells CEL-VDJ Corresponding to a 0-10[m V]D.C. signal from a BECKMAN Solu-Meter RA5

Cell Constant K [cm^{-1}]	Conductivity [micromhos/cm]	NaCl solution concentration [ppm]
5	0 - 2,500	0 - 1,300
20	0 - 10,000	0 - 5,480
50	0 - 25,000	0 - 15,370

The accuracy of the output signal is ±0.5% of full scale.

Current: The current was recorded as the potential drop across a Nichrome resistance wire (16 gauge). The shunt resistance varied according to the length of the wire. Prior to every experiment a D.C. current signal of known magnitude was calibrated to full scale of the recorder pen using the sliding scale vernier of the recorder (see below). Current was therefore measured directly and continuously.

Voltage: The preparation of probe electrodes has been described in detail in Section 4.2.1. The signal which was picked up by these probes represented the voltage drop across the stack. Continuous recording of this probe voltage

allowed the average stack potential to be determined. The local changes could be used to identify polarization effects.

Recorder: The above signals were traced by a WATANABE 4 pen recorder, model MC6-11S4H. All four pens utilized the full chart width of 25[cm].

pH: Samples for pH-checks were taken for some runs just prior to the experiment and immediately thereafter from both process and rinse stream and measured in the usual way.

4.3 The Mini Pilot Plant Module

The principle modification of this module compared to the first one consisted of a complete redesign of the electrodialysis cell. This necessitated modifications to the rinse loop as well as additions to current and voltage measuring systems.

4.3.1 Electrodialyser No. 2 (EDII)

Based on the experience with the first ED cell a staged electrodialyser was developed which consisted of eight equal stages, each composed of eight membrane-spacer frames and two electrode end frames.

The eight stages were mounted in a two level clamping device as illustrated in Figure 29. The stages were

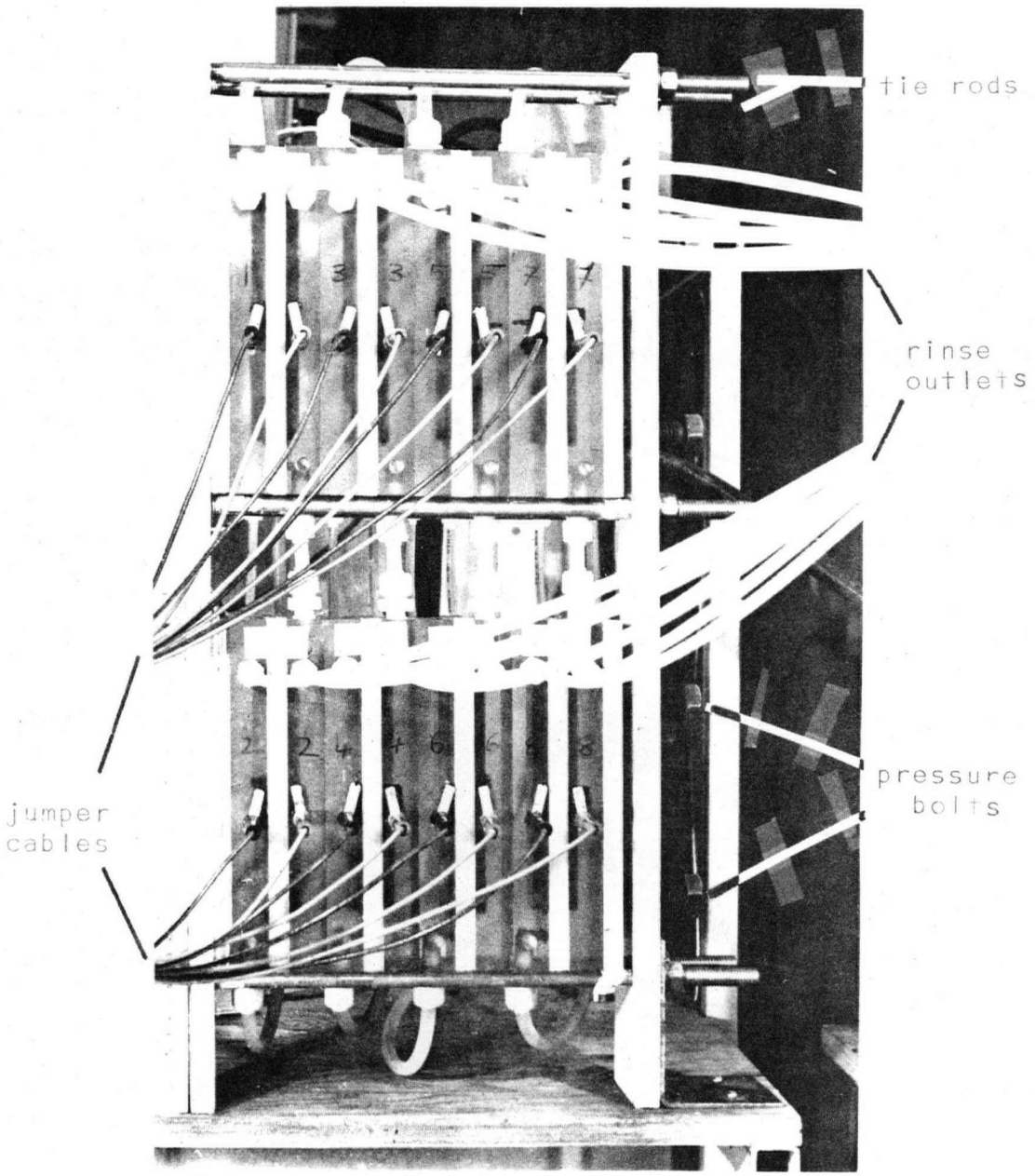

Figure 29. Clamping arrangement of eight stages in mini pilot plant module (scale : centimeters).

numbered from 1 to 8 starting from the dialysate end. The stages were always connected in series hydraulically and usually in parallel electrically. Less than eight stages could be operated on line by changing tube connections and disconnecting the idle stages from the electric power.

Each stage was a complete electrodialytic cell in itself. Apart from the location of rinse and process flow ports in the electrode end frames the stages were identical. In contrast to the first ED cell, which had a rigid centre frame to hold the membrane-spacer stack, the new design features a multiple-frame centre part. A schematic picture of the assembly is given in Figure 30, (page 87).

Each central frame consisted of three components which were permanently joined together, see Figure 31:

(i) An outer sealing frame (8-7/8" x 3" x 1/16") with keyshaped liquid distribution slots, made of low density polyethylene.

(ii) A triple membrane 6-3/8" x 1-3/4", composed of two ion exchange membranes (C100 and A100, cation and anion selective respectively, American Machine and Foundry Crop.) and a layer of Whatman filter paper No. 1.

(iii) A spacer screen 6-14/16" x 1-7/8" x 0.038" Vexar® TP23, 10 x 10 strands per inch, cut diagonally, made of clear polypropylene.

The membranes were heat sealed along both short sides. The long sides remained open to insert and to remove the filter paper.

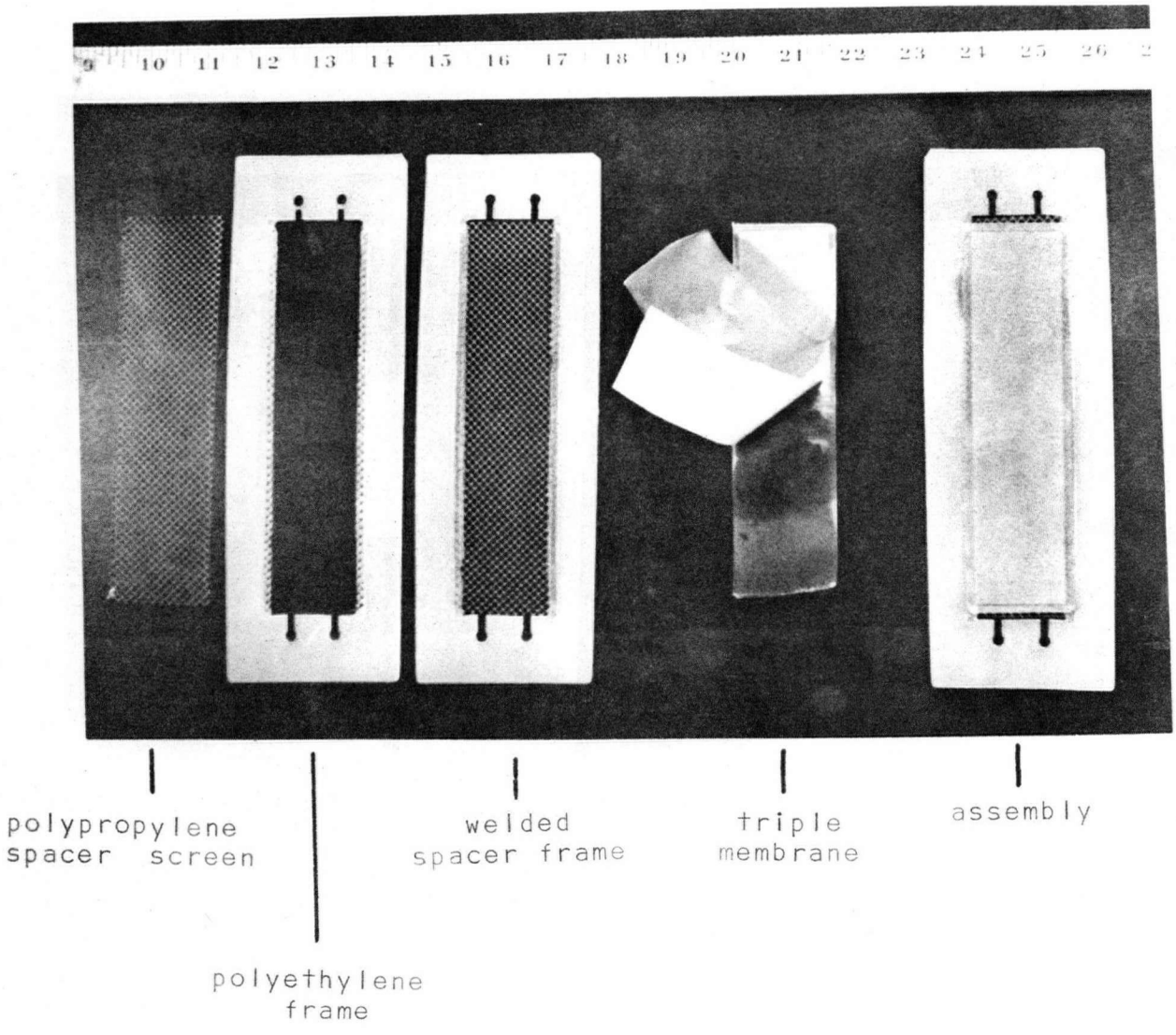

Figure 31. Integrated membrane-spacer frame for electrodialyzer No. 2. Parts and assembly (scale : inches).

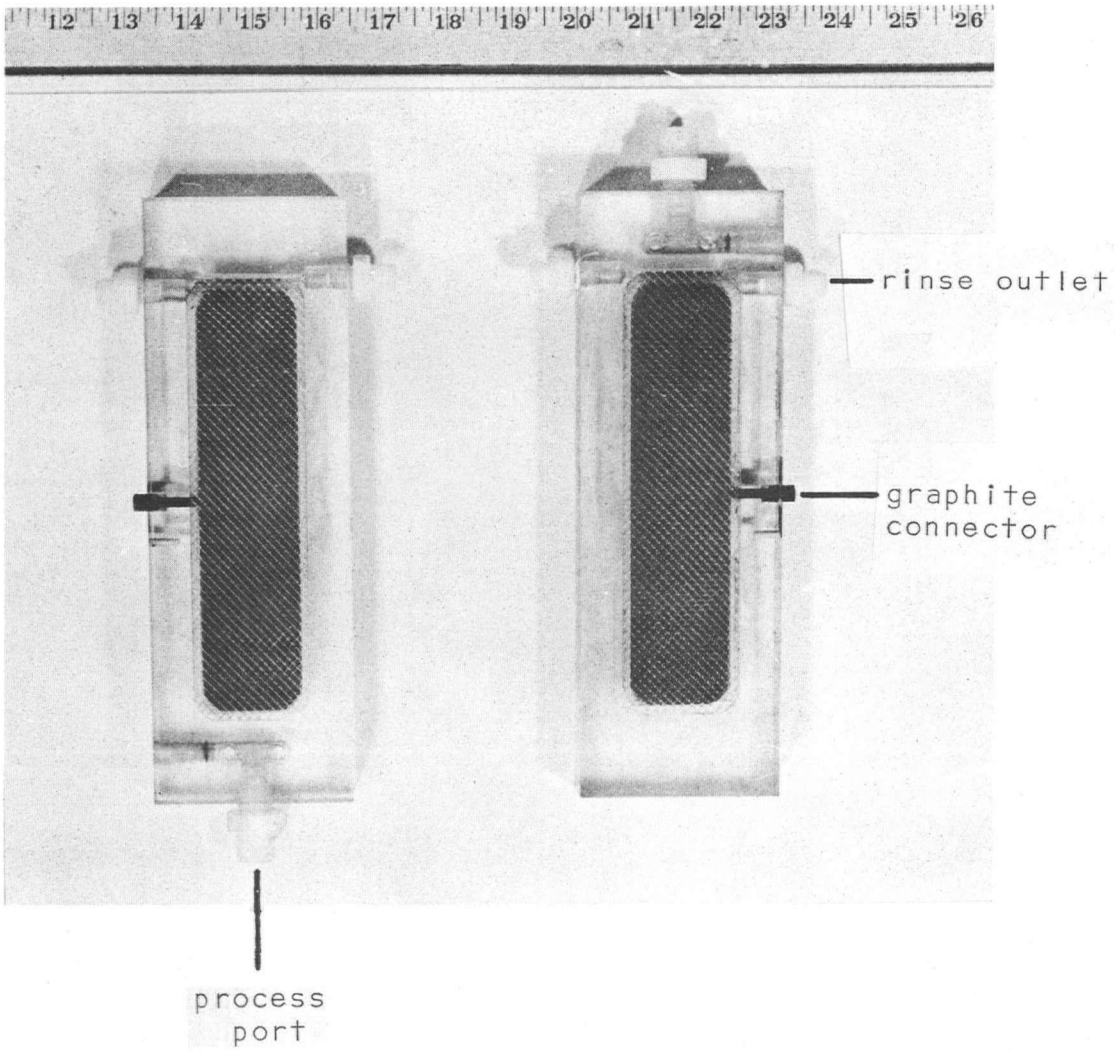

Figure 32. Electrodialyzer No. 2. Electrode end frames of a single stage (scale : inches).

The polypropylene spacer screen was pressed into the frame by means of a heated jig. Then the triple membrane was tagged at three corners to the frame using a heated bar. A more detailed description of the manufacturing procedure may be found in Appendix A.3. It should be noted that although approximately 20 different operations were necessary to produce one unit, all 64 membrane-spacer frames showed excellent similarity.

The electrode end frames had to fulfill the following tasks:

1. Hold the electrodes with their terminals.
2. Provide a rinse chamber.
3. Distribute (or collect) the process flow into (or from) the membrane stack.
4. Provide a sealing face.

Appendix A.2 shows how the end frame was designed to meet these demands, see also Figure 32.

The double pass rinse was an important characteristic of the construction.

The external pipe connections for the process solution were located in the electrode end frames. Figure 33 illustrates the internal flow distribution.

Hydraulic leaks between rinse and process stream could be avoided by O-ring seals as indicated in Figure 33.

These were the only gaskets in addition to the separating membranes, see also Figure 30, (page 87).

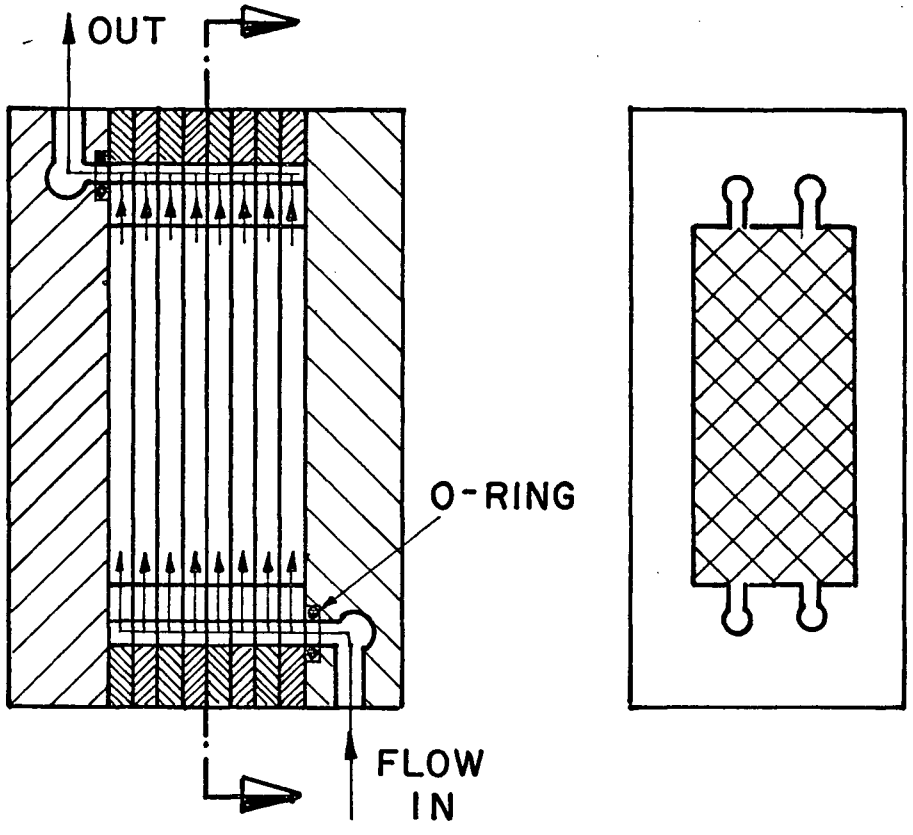

Figure 33: Process flow through second electrodialyser stage.

Table 7 summarizes the specifications of the second electrodialyser:

Table 7

Electrodialyser No. 2 (EDII)

Design	Multiple Frame Stack Eight Stages with Eight Frames Each
Membrane-Spacer Frame	Composite Pop-In Unit, 3 Parts Permanently Joined
Electrode Area*	60 [cm^2]
Active Void Volume*	50 [cm^3]
Inherent Dead Volume*	10 [cm^3]
Membrane Utilization**	97 [%]
Rinse System	Double Pass
Gaskets*	2 Separating Membranes 4 O-Rings for Process Flows
Materials	Stack Frame — Polyethylene Electrode Frame — Plexiglass Electrode — Graphite Terminal — Graphite

* per stage

** fraction of total membrane area available for ionic transfer.

4.3.2 Rinse distribution system.

The wash liquor (10,000 [ppm] aqueous NaCl solution) was pumped by a centrifugal pump (Cole Parmer, model MDX-3) from a two-gallon plastic tank through a distribution manifold and the 16 rinse compartments and returned to the holding tank. The flow rate was measured at $0.90\ ^{+0.06}_{-0.08}$ [litre/min] per compartment and did not require special control.

4.3.3 Current and voltage measurements.

Current consumption and stack voltage were measured individually for each stage. However, because of the limited number of pens, only one current and one voltage signal were recorded simultaneously.

Current

Shunts were prepared from NICHROME resistance wire (14 gauge), and integrated into the electrical manifold which distributed the D.C. power from switch box SB1 (see Figure 22) to the stages. The wiring is shown in Figure 34.

The shunt resistances were 50.0[mΩ] ± 1.5% for the currents to the individual stages and 25.0 mΩ for the total current.

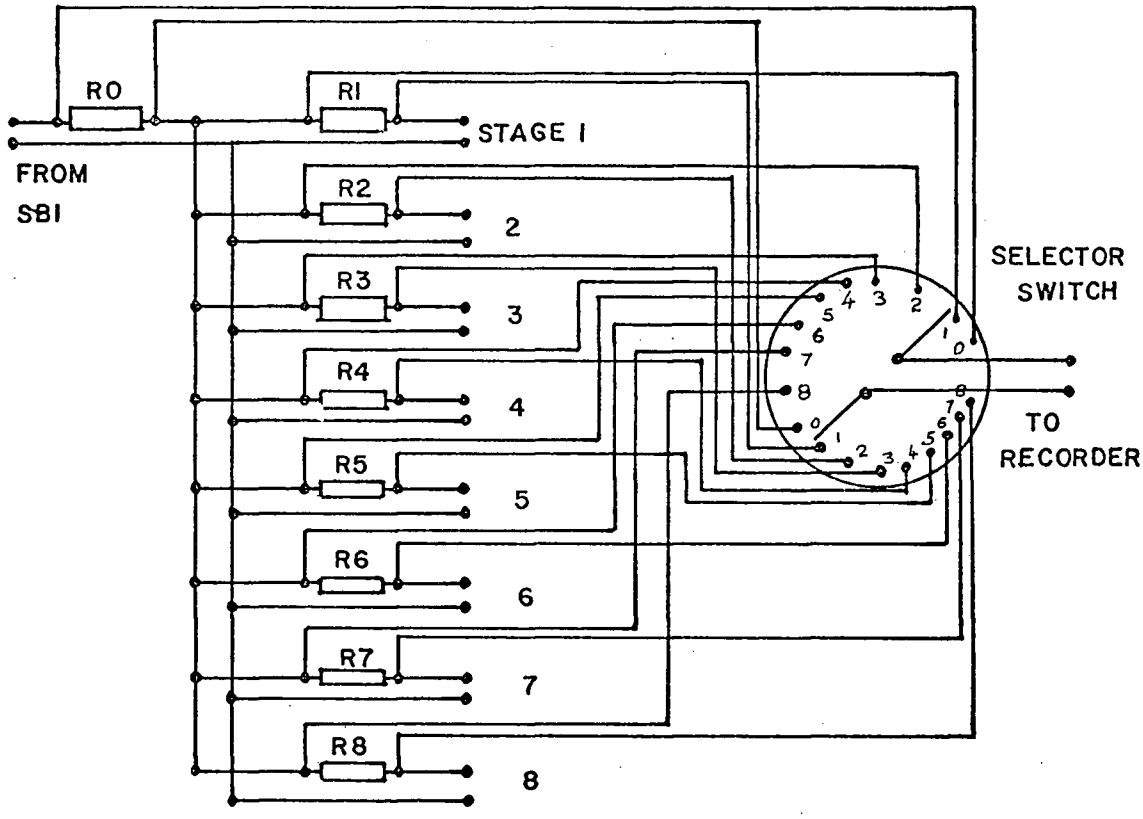

Figure 34. Current monitoring circuit.

Voltage

Probe electrodes were prepared from silver wire cable (8 leads of 1[Ω/ft] resistance wire) which was hammered into strips approximately 1/8" wide and 5/1000" thick. The strips were dip coated with waterproof contact cement (Canadian Industries Limited) and the coating was removed from one side of the tip which was located inside the stack. The probes were inserted between the separating membranes and the stack pack and sealed with self-setting silicon rubber gel.

A second selector switch was connected to the probes and to one recorder pen. The circuit is analoguous to the one shown in Figure 34.

Chapter 5

EXPERIMENTAL RESULTS AND DISCUSSION

In this chapter the experiments are compiled and correlated in three ways:

a. Survey tables for each stack contain the operating conditions and the limiting, steady-periodic state reached after a certain number of cylces.

b. Group tables and diagrams illustrate the effect of single variables under otherwise fixed conditions.

c. Individual tables and diagrams present a record of the transients for single test runs.

The collection of raw data during the course of a complete batch run will be described first, followed by details about the processing of these data into table form. Subsequently, a discussion of the variables will illustrate the main features of the process phenomena. In the concluding section of this chapter the application of these batch system results to the operation of a continuous system will be dicussed.

5.1 Data Collection

A complete batch run consisted of the following consecutive steps:

1. Fill rinse tank with 6 to 8 liters of fresh rinse liquor (NaCl in distilled water, varying concentration).
2. Fill system with process solution of desired concentration (NaCl in distilled water).
3. Start rinse pump.
4. Start piston pump to equilibrate sorption membranes with process solution.
5. Adjust check point of conductivity meters.
6. Calibrate resistance of current shunt using recorder pen (first ED cell only).
7. Select recorder pen ranges and chart speed.
8. Take pH samples of process and rinse solution.
9. Set operating conditions (pump displacement, dead volumes, pump speed, pause times, applied D.C. voltage).
10. Note down date, operating conditions, variable recorded by each pen and appropriate range, chart speed.
11. Check total cycle period with stop watch.
12. Turn counter back to zero, and
13. Close electric power circuit after completion of next foreward stroke of piston pump (the membrane arrangement and the electrode polarity is set to demineralize the solution during this first half cycle).

14. Record current and voltage signals for different stations by manipulating selector switches, and mark pen traces accordingly (second ED cell only).

15. Write down any observation related to experiment.

16. Change recorder pen ranges in order to utilise maximal chart width.

17. Terminate run when steady periodic state is reached by disconnecting power supply, and stopping piston pump in this order.

18. Read total number of cycles and note down.

19. Take pH samples of process and rinse streams, or equilibrate concentration of process solution to check mass balance for solute.

20. Test pH samples and note down results.

The recorder chart thus contained all the original information related to the test run. The following details were extracted from the chart.

a. Mean product concentrations in end reservoirs after each cycle. These were conveniently obtained as the reflux concentrations since both reservoirs were reasonably well mixed.

b. Mean current consumption for any half cycle. The local current transients were averaged either planimetrically or by an integrator recorder. The total current consumption of the second ED cell module was recorded continuously during the first cycles, and in a rotating sequence with the individual stages thereafter.

c. Mean stack voltage for each half cycle. This was evaluated planimetrically. Again, the stages were read in rotation for the second ED cell.

d. Local transients of current, voltage, and effluent concentrations contained additional information related to mass transfer mechanisms and internal concentration distributions.

5.2 Main Survey Tables

Current and concentration data were converted into proper units by means of calibration curves. The columns of the main survey tables are (see Tables 8 to 13):

1. Run number (#): The experiments on each stack were numbered chronologically and they are listed in this order. Two numbers separated by a dash (-) indicate a change in operating conditions during the run.

2. Initial concentration (c_0) in parts per million NaCl in distilled water.

3. Displaced volume (δ) as fraction of the free solution volume V_0 contained in the system between the conductivity cells.

4. Superficial velocity (v) in centimeters per second. This is based on the active void volume (V_a) of the

stack and the total length (ℓ) of the electrodes in flow direction.

$$v = \frac{Q}{V_a} \cdot \ell$$

where Q = volumetric flow rate delivered by piston pump.

5. Pause time (τ) in seconds. A single number is given when the pause times for first and second half cycle were equal. For unequal pause times the notation 10/5 stands for 10 sec during demineralization, 5 sec during enrichment.

6. Cycle period (T) in seconds. Since the flow rates Q were equal for both half cycles T is calculated as

$$T = 2 \frac{V_0 \cdot \delta}{Q} + \tau_T + \tau_B$$

where τ_T and τ_B are the pause times for demineralization and enrichment respectively.

7. Applied potential in volts ($\Delta\Phi$). The electrode voltage is given because this is the true independent variable.

8. Number of cycles (nc). The subsequent columns refer to conditions which exist after nc cycles from start-up.

9. Total current (I) in amperes. This base current is the arithmetic mean of the average current consumption for demineralizing and enriching half cycles.

10. Brine concentration (x_B) and

11. Dialysate concentration (x_T) both normalized with respect to the initial concentration c_0.

12. Separation factor (ns) defined as the ratio of brine (bottom product) to dialysate (top product) concentration

$$ns = \frac{x_B}{x_T}$$

13. This column contains comments on: The presence of dead volumes* δ_B and δ_T in brine and dialysate reservoir, respectively (δ_B and δ_T are given as fractions of the free solution volume V_0 (see item 3)), whether limiting conditions are reached or not, and the number of stages for the second ED cell.

The main survey tables of all successful experiments are presented on the following pages. Successful means not interrupted by mechanical, electrical, or human failure.

*Or excess volumes.

Table 8

Compilation of Experiments on EDI-S1-8

1	2	3	4	5	6	7	8	9	10	11	12	13
RUN NO.	CONCENTR. INITIAL	VOLUME DISPLACED	VELOCITY SUPERFICIAL	PAUSE TIME	CYCLE PERIOD	VOLTAGE APPLIED	CYCLE NO.	CURRENT TOTAL	CONCENTRATION		SEPARATION FACTOR	REMARKS
									BRINE	DIALYSATE		
#	c_0	δ	v	τ	T	$\Delta\Phi$	nc	I	x_B	x_T	n_s	L = limit reached NL = limit not reached δ_B/δ_T = dead volumes
[-]	[ppm]	[-]	[cm/sec]	[sec]	[sec]	[volt]	[-]	[ampere]	[-]	[-]	[-]	
1	1090	1.10	1.21	-	53.3	4	10	-	1.020	1.020	1.00	NL
2	1050	1.10	1.21	-	53.3	6	7	0.37	0.995	0.999	1.00	NL
3	1040	1.10	1.77	-	36.4	6	8	0.385	0.999	0.996	1.00	NL
4	1050	1.10	2.33	-	27.6	6	9	0.40	0.998	1.000	1.00	NL
5	1090	1.10	1.21	-	53.3	6	8	0.35	1.005	1.000	1.01	NL
6	1080	1.73	1.21	-	84.3	4	6	0.23	1.030	0.974	1.06	L
7	1090	1.73	1.21	-	84.3	6	9	0.37	1.020	0.938	1.09	L
8	1090	1.73	1.66	-	61.4	6	12	0.39	1.010	0.955	1.06	L
9	1080	1.73	2.62	-	39.0	6	10	0.41	1.010	0.972	1.04	L
10-0	1110	1.73	0.65	-	157.4	8	9	0.52	1.110	0.900	1.23	L
-1			1.21	-	84.3	8	16	0.57	1.020	0.928	1.10	NL
14	1020	1.00	1.21	-	50.2	6	7	0.32	0.969	0.983	0.99	NL
15-0	1020	1.00	1.21	-	50.2	6	9	0.32	0.970	0.997	0.97	L
-1			0.65	-	93.8		13	0.30	0.965	0.972	0.99	L
21	770	1.00	0.65	-	93.8	4*	7	-	0.950	1.000	0.95	NL
22	775	1.00	1.21	-	50.2	5*	10	-	0.955	1.010	0.95	L
23	760	1.00	1.21	-	50.2	5*	10	-	0.956	1.010	0.95	L
24	765	1.00	1.21	-	50.2	5*	10	-	0.962	1.020	0.95	L
29	850	0.42	2.33	-	8.7	11	40	1.00	1.10	0.969	1.13	L
30	700	1.75	1.77	-	57.1	7.55	10	-	1.03	0.973	1.06	L
31	710	1.00	1.77	-	34.3	7.55	13	0.35	0.99	1.00	0.99	L
32	720	1.00	1.77	-	34.3	12.5	6	0.55	0.95	0.97	0.98	L
33	710	1.00	2.33	-	26.1	12.5	10	0.60	0.965	0.985	0.98	L
34	700	1.00	2.89	-	21.0	12.5	9	0.65	0.975	0.99	0.985	L
35	700	1.00	1.21	-	50.2	12.5	9	0.55	0.96	0.96	1.00	L
36	700	1.00	0.65	-	93.8	12.5	8	0.50	1.04	0.935	1.11	L
37	720	1.00	0.65	-	93.8	5.0	5	0.20	1.02	0.98	1.05	L
38	725	1.80	1.21	-	87.3	15.0	6	0.60	1.02	0.862	1.19	L
39	710	1.80	1.21	-	87.3	20.0	5	0.75	1.07	0.86	1.25	L
40	760	1.00	1.21	-	50.2	6.0	8	0.28	0.986	0.995	0.991	L
41	760	1.00	1.21	-	50.2	10.0	7	0.44	0.956	0.975	0.980	L
42	760	1.00	1.21	-	50.2	20.0	7	0.78	0.972	0.954	1.02	L

*Probe voltage, hand regulated.

Table 9

Compilation of Experiments on EDI-S2-15

1	2	3	4	5	6	7	8	9	10	11	12	13
RUN NO.	CONCENTR. INITIAL	VOLUME DISPLACED	VELOCITY SUPERFICIAL	PAUSE TIME	CYCLE PERIOD	VOLTAGE APPLIED	CYCLE NO.	CURRENT TOTAL	CONCENTRATION		SEPARATION FACTOR	REMARKS
									BRINE	DIALYSATE		
#	c_0	δ	v	τ	T	$\Delta\Phi$	nc	I	x_B	x_T	n_s	L = limit reached NL = limit not reached δ_B/δ_T = dead volumes
[-]	[ppm]	[-]	[cm/sec]	[sec]	[sec]	[volt]	[-]	[ampere]	[-]	[-]	[-]	
1	930	0.95	1.29	0	35	4	10	0.23	1.00	0.990	1.01	L
2	890	0.95	0.47	20	137	10	8	0.30	1.45	0.580	2.50	NL
3	910	0.47	1.41	10	36	16	15	0.60	1.37	0.566	2.42	L, δ_B = .47
4	910	0.47	1.41	10	36	16	14	0.60	1.50	0.582	2.59	L
5-0	930	0.47	2.11	5	21	16	14	0.74	1.25	0.722	1.73	NL
-1				10	31		25	0.62	1.50	0.563	2.67	NL
6	990	1.00	2.23	10	42	20	14	0.75	1.23	0.641	1.92	L
7	940	1.00	0.88	0	55	8	10	0.40	1.01	0.935	1.08	L
8	950	1.00	0.88	0	55	16	10	0.70	1.01	0.858	1.18	L
9	970	1.00	0.88	0	55	24	10	0.85	1.07	0.801	1.33	L
10	960	1.00	0.88	0	55	32	10	1.00	1.14	0.750	1.52	L
11	960	1.00	2.23	5	32	32	14	1.25	1.29	0.631	2.05	L
12-0	940	1.00	2.23	5	32	32	10	1.25	1.31	0.623	2.10	L
-1				10	42		16	0.90	1.41	0.548	2.58	NL
13	930	1.00	2.23	10	42	16	10	0.65	1.28	0.671	1.91	L
14	980	1.00	2.23	15	52	16	10	0.60	1.32	0.607	2.17	NL
15	960	1.00	0.47	15	132	16	7	0.43	1.42	0.585	2.43	L
16	975	0.59	0.47	25	111	16	15	0.30	1.60	0.397	4.03	NL, δ_B = .35
17	1025	1.0	0.88	0	55	40	10	1.30	1.14	0.747	1.52	L
18	1010	1.0	1.70	14	56	40	7	1.15	1.54	0.561	2.75	L
19	1020	0.5	1.70	7	28	40	14	1.40	1.72	0.529	3.24	L
20	1040	0.5	1.70	7	28	40	15	1.28	1.50	0.463	3.24	NL, δ_B = .5
21	980	0.5	1.70	7	28	40	22	1.32	1.54	0.568	2.72	NL, $\delta_B=\delta_T=1.0$
22	1050	0.5	0.88	0	28	40	10	1.25	0.98	0.950	1.03	L, δ_B = 1.5
23	1020	1.0	1.70	0	29	32	10	1.44	1.00	0.888	1.13	NL
24	1020	0.25	1.70	3.5	14	40	65	1.72	1.42	0.468	3.02	NL, δ_B = .75
26	1020	1.0	0.47	15	132	24	8	0.48	1.51	0.582	2.60	L
27	1090	1.0	2.23	15	52	32	10	0.96	1.46	0.537	2.72	L
28-0	1070	1.0	2.23	5	32	32	4	1.38	1.25	0.719	1.74	NL
-1				10	42		7	1.18	1.37	0.615	2.23	NL
-2				15	52		11	1.00	1.45	0.540	2.69	NL
-3				5	32		18	1.30	1.28	0.644	1.99	L
29	1070	1.54	0.88	0	84	40	6	1.05	1.20	0.670	1.80	L
30-0	1010	0.5	1.77	7	28	16	21	0.80	1.27	0.621	2.05	L, δ_B = .5
-1				14	42		34	0.52	1.41	0.486	2.91	L
31	1030	0.59	0.47	25	111	16	13	0.36	1.55	0.449	3.45	L, δ_B = .4
32	1120	0.25	1.70	3.6	14	40	60	1.70	1.63	0.494	3.31	NL
33	1150	1.0	2.23	15	52	32	11	0.90	1.39	0.517	2.70	L

Table 10

Compilation of Experiments on EDI-S2-16

1	2	3	4	5	6	7	8	9	10	11	12	13
RUN NO.	CONCENTR. INITIAL	VOLUME DISPLACED	VELOCITY SUPERFICIAL	PAUSE TIME	CYCLE PERIOD	VOLTAGE APPLIED	CYCLE NO.	CURRENT TOTAL	CONCENTRATION		SEPARATION FACTOR	REMARKS
									BRINE	DIALYSATE		
#	c_0	δ	v	τ	T	$\Delta\Phi$	nc	I	x_B	x_T	ns	L = limit reached NL = limit not reached δ_B/δ_T = dead volumes
[-]	[ppm]	[-]	[cm/sec]	[sec]	[sec]	[volt]	[-]	[ampere]	[-]	[-]	[-]	
1	1100	1.00	2.32	15	52	32	10	0.84	1.47	0.484	3.04	L
2	1070	1.00	0.92	15	85	32	9	0.71	1.55	0.476	3.25	L
3-0	1175	0.61	0.92	15	52	32	14	0.70	1.88	0.341	5.52	NL
-1				25	72		20	0.60	2.04	0.274	7.46	L
4	1220	0.61	0.92	25	72	32	14	0.70	2.11	0.278	7.58	L
5-0	1250	0.61	0.92	15	52	32	13	0.70	1.36	0.238	5.71	NL, δ_B = 1.84
-1				25	72		21	0.50	1.41	0.179	7.88	L, δ_B = 1.84
-2			0.49	25	111	32	40	0.40	1.46	0.158	9.24	L, δ_B = 1.84
-3			1.77	25	67	32	50	0.45	1.44	0.176	8.18	NL, δ_B = 1.84
-4			0.92	25	72	16	60	0.30	1.40	0.222	6.32	NL, δ_B = 1.84
6-0	1225	0.61	0.92	15	52	16	16	0.50	1.29	0.308	4.18	L, δ_B = 1.84
-1				25	72	16	22	0.40	1.32	0.250	5.28	L, δ_B = 1.84
-2				15	52	40	38	0.63	1.43	0.196	7.05	L, δ_B = 1.84
-3				25	72	40	45	0.52	1.41	0.142	10.10	L, δ_B = 1.84
7	1250	0.61	0.92	0	22	40	50	1.50	1.11	0.585	1.88	L, δ_B = 1.84
8-0	1240	0.61	0.92	0	22	32	30	1.41	1.10	0.714	1.54	L
-1				0	22	40	50	1.60	1.22	0.630	1.94	L
9-0	1200	1.00	0.92	0	53	40	15	1.26	1.31	0.589	2.22	L
-1			0.49		99	40	19	0.84	1.48	0.447	3.31	NL

Table 11

Compilation of Experiments on EDI-S3-12

1	2	3	4	5	6	7	8	9	10	11	12	13
RUN NO.	CONCENTR. INITIAL	VOLUME DISPLACED	VELOCITY SUPERFICIAL	PAUSE TIME	CYCLE PERIOD	VOLTAGE APPLIED	CYCLE NO.	CURRENT TOTAL	CONCENTRATION		SEPARATION FACTOR	REMARKS
									BRINE	DIALYSATE		
#	c_0	δ	v	τ	T	$\Delta\Phi$	nc	I	x_B	x_T	ns	L = limit reached NL = limit not reached δ_B/δ_T = dead volumes
[-]	[ppm]	[-]	[cm/sec]	[sec]	[sec]	[volt]	[-]	[ampere]	[-]	[-]	[-]	
1-0	1225	1.00	1.33	0	36	32	10	1.50	1.07	0.821	1.31	L
-1			0.92	0	52		18	1.35	1.18	0.705	1.67	L
-2				5	62		25	1.20	1.41	0.526	2.69	L
-3				15	82		30	1.00	1.56	0.411	3.81	L
-4			0.49	15	129		35	0.70	1.72	0.316	5.46	L
2-0	1220	0.59	0.92	15	62	32	20	0.90	2.04	0.265	7.72	L
-1				25	82		25	0.70	2.21	0.217	10.20	L
-2			0.49	25	111		31	0.62	2.32	0.175	13.28	L
3-0	1230	0.59	0.92	15	62	32	16	0.80	1.37	0.194	7.06	L, δ_B = 1.75
-1				25	82		24	0.60	1.43	0.136	10.52	L, δ_B = 1.75
-2			0.49	25	111		30	0.50	1.47	0.110	13.40	L, δ_B = 1.75
4-0	1245	0.59	0.92	15	62	32	16	0.90	2.03	0.259	7.85	L
-1				25	82		23	0.70	2.17	0.218	9.97	L
5-0	1280	0.59	0.92	25	82	32	16	0.75	2.12	0.237	8.98	NL
-1			0.49	25	111		20	0.70	2.21	0.217	10.19	NL
-2		0.47	0.49	25	96		28	0.65	2.33	0.091	25.70	L, δ_B = 0.12
-3		0.29	0.49	25	80		36	0.56	2.38	0.055	43.00	L, δ_B = 0.30
6-0	1280	0.29	1.33	10	31	32	50	0.65	1.36	0.131	10.41	L, δ_B = 2.06
-1			0.92	10	36		60	0.60	1.38	0.111	12.48	NL, δ_B = 2.06
-2			0.49	10	50		70	0.55	1.39	0.106	13.17	L, δ_B = 2.06
-3				20	70		80	0.45	1.43	0.083	17.14	L, δ_B = 2.06
-4		0.12	0.49	20	52		145	0.35	1.47	0.048	30.50	L, δ_B = 2.18
7	1280	0.59	0.49	20	100	32	15	0.85	2.09	0.222	9.38	NL
7a	1280	0.59	0.49	20	100	32	15	0.75	2.29	0.191	12.00	L, brine unmixed
8	1270	1.00	0.92	20	93	32	10	0.95	1.64	0.376	4.36	L
8a	1270	1.00	0.92	20	93	32	12	0.75	1.83	0.255	7.18	NL, brine unmixed
9-0	4800	1.00	0.92	0	53	16	5	3.10	—	0.922	—	L
-1				5	63		10	3.00	—	0.898	—	NL
-2				10	73		20	2.70	—	0.636	—	NL
-3				15	83		35	2.30	—	0.545	—	NL
10-0	4680	0.59	0.92	15	62	32	15	3.20	—	0.273	—	L
-1				25	82		20	2.80	2.00	0.205	10.00	L
11	4560	1.00	0.92	15	83	32	11	3.60	1.52	0.386	3.94	L
11a	4600	1.00	0.92	15	83	32	15	3.10	1.76	0.267	6.60	L, brine unmixed
12-0	4690	0.59	0.92	15	62	16	20	2.00	—	0.341	—	NL, δ_B = 1.75
-1			0.49	30	120	16	29	1.30	—	0.216	—	NL, δ_B = 1.75
-2						24	33	1.40	—	0.157	—	L, δ_B = 1.75
13	4830	1.00	0.92	15	83	16	10	2.20	1.30	0.533	2.44	L

CONTINUED

Table 11 (Continued)

1	2	3	4	5	6	7	8	9	10	11	12	13
RUN NO.	CONCENTR. INITIAL	VOLUME DISPLACED	VELOCITY SUPERFICIAL	PAUSE TIME	CYCLE PERIOD	VOLTAGE APPLIED	CYCLE NO.	CURRENT TOTAL	CONCENTRATION		SEPARATION FACTOR	REMARKS
									BRINE	DIALYSATE		
#	c_0	δ	v	τ	T	$\Delta\Phi$	nc	I	x_B	x	ns	L = limit reached NL = limit not reached δ_B/δ_T = dead volumes
[-]	[ppm]	[-]	[cm/sec]	[sec]	[sec]	[volt]	[-]	[ampere]	[-]	[-]	[-]	
14	5000	1.00	0.92	25	103	16	8	2.10	1.42	0.496	2.86	L
15	1000	1.00	1.32	5	46	20	18	0.95	1.29	0.588	2.19	L
16	980	1.00	1.32	5	46	20	18	0.90	1.27	0.598	2.12	L
17	1130	1.00	0.90	5	64	10	18	0.53	1.20	0.700	1.72	L
18	1080	1.00	0.90	5	64	20	18	0.84	1.32	0.578	2.28	L
19	1175	1.00	0.90	5	64	30	16	1.06	1.34	0.473	2.85	L
20	1160	0.25	0.90	20	54	30	50	0.75	2.67	0.211	12.64	L
21	1230	1.00	0.90	10	74	20	10	0.81	1.39	0.508	2.73	L
22	1200	1.00	0.90	15	84	20	17	0.74	1.49	0.486	3.04	L
23	1200	1.00	0.90	20	94	20	16	0.69	1.52	0.469	3.23	L
24	1170	1.00	0.90	0.6	55	20	15	1.09	1.14	0.703	1.62	L

Table 12

Compilation of Experiments on EDI-S3-13

1	2	3	4	5	6	7	8	9	10	11	12	13
RUN NO.	CONCENTR. INITIAL	VOLUME DISPLACED	VELOCITY SUPERFICIAL	PAUSE TIME	CYCLE PERIOD	VOLTAGE APPLIED	CYCLE NO.	CURRENT TOTAL	CONCENTRATION		SEPARATION FACTOR	REMARKS
									BRINE	DIALYSATE		
#	c_0	δ	v	τ	T	$\Delta\Phi$	nc	I	x_B	x_T	ns	L = limit reached NL = limit not reached δ_B/δ_T = dead volumes
[-]	[ppm]	[-]	[cm/sec]	[sec]	[sec]	[volt]	[-]	[ampere]	[-]	[-]	[-]	
1	1240	1	.90	20	93	22	19	.70	1.69	.349	4.85	L
2	1250	1	.95	10	71	22	18	.85	1.60	.398	4.03	L
3	1228	0.5	.95	10	45	22	36	.77	2.08	.278	7.46	NL
4	1240	0.25	.95	10	34	22	65	.73	2.34	.236	9.90	NL
5	1270	1.5	.95	10	96	22	10	.91	1.33	.531	2.50	L
6	1300	1	.95	5	61	10	17	.62	1.31	.603	2.18	L
7	1270	1	.95	5	61	22	17	1.00	1.52	.432	3.53	L
8	1260	1	.95	5	61	30	15	1.20	1.61	.389	4.15	L
9	1135	1	.95	5	61	40	22	1.28	1.77	.330	5.36	L
10	1045	1	.95	0.6	52	22	23	.99	1.28	.570	2.24	L
11	1250	1	.95	5	61	22	18	.96	1.52	.424	3.59	L
12	1282	1	.95	10	71	22	20	.87	1.61	.372	4.33	L
13	1205	1	.95	20	91	22	19	.69	1.71	.324	5.27	L
14	1125	0.5	.95	30	111	22	13	.50	1.79	.301	5.95	L
15	1265	0.5	.50	10	68	22	28	.62	2.14	.239	8.93	NL
16	1275	0.5	1.40	10	37	22	34	.80	2.08	.248	8.35	NL
17	1270	0.5	1.85	10	33	22	45	.79	2.10	.242	8.71	L
18	1180	0.5	2.36	10	30	22	45	.70	2.12	.240	8.83	L
19	1195	0.5	.50	0.6	50	22	50	.87	1.26	.540	2.33	L
20	1185	0.5	.27	0.6	90	22	45	.60	1.72	.350	4.91	L
21	1205	0.5	1.85	0.6	14	22	160	1.69	0.90	.856	1.05	NL
22	1205	1	.95	5	61	30	18	1.05	1.61	.375	4.29	L
24	1260	0.5	1.40	10/5	32	22	40	.91	2.03	.228	8.90	L
25	1250	0.5	1.40	10/10	37	22	35	.81	2.14	.228	9.35	NL
26	1260	0.5	1.40	10/10	37	10	40	.54	1.83	.344	5.33	L
27	1260	0.5	1.40	10/5	32	10	50	.65	1.65	.376	4.39	L
28	1210	1	1.40	10/5	49	10	20	.59	1.38	.535	2.59	NL
29	1270	1	1.40	10/10	54	10	16	.54	1.48	.515	2.86	L
30	1280	0.5	2.36	10/5	25	22	35	.92	2.01	.228	8.85	NL
31	1300	0.5	2.36	10/10	30	22	30	.80	2.16	.233	9.27	L
32	1290	0.5	1.85	10	33	22	30	.81	2.15	.230	9.33	L
33	1280	0.5	1.85	10	33	22	60	.77	2.05	.217	9.43	L, $\delta_B=\delta_T=0.5$
34	1200	0.5	1.85	10	33	22	70	.71	1.99	.235	8.44	NL, $\delta_B=\delta_T=1.0$
35	1200	0.5	1.85	10	33	22	40	.60	1.57	.171	9.16	L, $\delta_B=\delta_T=0.0$
36	1260	0.5	1.85	10	33	22	60	1.00	2.82	.326	8.66	NL, $\delta_B=\delta_T=1.0$
37	4640	1	0.95	5	61	10	15	1.65	1.15	.684	1.68	L
38	4500	0.5	0.95	5	35	10	40	1.73	1.25	.644	1.95	NL
39	4890	0.5	1.40	10	37	10	35	1.54	1.54	.462	3.33	NL
40	5560	0.5	1.40	10	37	15	34	2.44	1.70	.333	5.10	L
40a	5275	0.5	1.40	10	74	15	35	2.35	1.70	.330	5.14	L
41	5125	1	1.40	10	54	15	15	2.58	1.57	.495	3.18	L
42	5215	1	.16	0.6	285	5	15	0.60	1.27	.586	2.17	NL

Table 13

Compilation of Experiments on EDII-S1-8

1	2	3	4	5	6	7	8	9	10	11	12	13
RUN NO.	CONCENTR. INITIAL	VOLUME DISPLACED	VELOCITY SUPERFICIAL	PAUSE TIME	CYCLE PERIOD	VOLTAGE APPLIED	CYCLE NO.	CURRENT TOTAL	CONCENTRATION		SEPARATION FACTOR	REMARKS
									BRINE	DIALYSATE		
# [-]	c_0 [ppm]	δ [-]	v [cm/sec]	τ [sec]	T [sec]	$\Delta\Phi$ [volt]	nc [-]	I [ampere]	x_B [-]	x_T [-]	ns [-]	MS = No. of stages L = limit reached NL = limit not reached δ_B/δ_T = dead volumes
6	5700	2/3	5.4	10	40	10	40	5.6	2.51	0.011	224	NL
7	5700	2/3	5.4	0.6	50	10	30	3.8	1.48	0.507	3	L
8	5300	2/3	5.4	5	60	10	45	3.2	2.38	0.023	104	NL
9	5400	2/3	5.4	20	80	10	25	2.0	2.63	0.008	348	L
10	4800	2/3	5.4	5	50	10	46	4.1	2.35	0.026	91	NL
11	5300	1	5.4	5	68	10	26	4.6	1.91	0.159	12	L
12	4300	1/4	5.4	5	25	10	90	2.6	3.50	0.004	874	L
13	5100	2/3	5.4	5	50	5	55	2.0	1.87	0.219	9	L
14	5050	2/3	3.0	0.6	70	10	40	5.7	1.60	0.324	5	L
15	5400	2/3	1.6	0.6	129	10	20	5.5	1.75	0.155	11	L
16	5500	2/3	5.4	5	50	15	30	6.9	2.55	0.011	231	NL
17	5100	2/3	5.4	10	50	10	33	2.6	2.40	0.030	80	L, MS = 6
18	5300	2/3	5.4	10	39	10	30	1.7	2.27	0.072	32	NL, MS = 4
19	4900	2/3	5.4	10	29	10	40	0.9	2.13	0.130	16	L, MS = 2
20	5500	2/3	5.4	10	30	10	45	1.0	2.16	0.132	16	L, MS = 2
21	5200	2/3	5.4	10	59	15	34	3.4	2.69	0.004	648	L
22	2600	2/3	5.4	20	80	10	25	1.5	2.86	0.004	710	L
23	2650	2/3	5.4	10	61	10	30	2.1	2.68	0.019	143	L
24	2650	2/3	5.4	10	60	15	30	3.0	2.91	0.012	250	L
25	1250	2/3	5.4	0.6	40	10	45	2.4	2.32	0.068	34	L
26	1290	2/3	5.4	10	60	10	30	1.4	2.84	0.014	202	L
27	1250	2/3	5.4	20	80	10	30	1.1	3.18	0.009	362	L
28	1280	2/3	5.4	5	50	10	35	1.8	2.70	0.012	222	L
29	1260	1	5.4	10	79	10	16	1.8	2.19	0.029	74	L
30	1270	1	5.4	0.6	60	10	25	2.6	1.94	0.092	21	L
31	1220	2/3	5.4	0.6	41	15	34	3.4	2.49	0.024	103	L
32	1240	2/3	5.4	5	50	15	26	2.8	2.90	0.005	546	L
33	1200	2/3	5.4	10	59	15	25	2.0	3.17	0.001	3600	NL
34	1280	2/3	5.4	20	78	15	25	1.8	3.70	0.001	6100	NL
35	1220	2/3	5.4	5	50	5	35	1.1	2.34	0.054	43	NL
35a	1220	2/3	5.4	10	60	10	30	1.4	2.87	0.012	247	L
36	1250	2/3	5.4	10	60	5	40	0.8	2.57	0.026	99	L
37	1150	2/3	1.4	0.6	135	10	30	1.6	2.99	0.011	285	L
38	1250	2/3	3.0	0.6	71	10	40	2.2	2.46	0.021	118	L
39	1260	2/3	1.4	10	145	10	30	1.5	3.40	0.006	552	NL
40	1290	2/3	2.2	10	92	10	25	1.6	3.00	0.008	373	NL

CONTINUED

Table 13 (Continued)

1	2	3	4	5	6	7	8	9	10	11	12	13
RUN NO.	CONCENTR. INITIAL	VOLUME DISPLACED	VELOCITY SUPERFICIAL	PAUSE TIME	CYCLE PERIOD	VOLTAGE APPLIED	CYCLE NO.	CURRENT TOTAL	CONCENTRATION		SEPARATION FACTOR	REMARKS
									BRINE	DIALYSATE		
#	c_0	δ	v	τ	T	$\Delta\Phi$	nc	I	x_B	x_T	ns	MS = No. of stages L = limit reached NL = limit not reached δ_B/δ_T = dead volumes
[-]	[ppm]	[-]	[cm/sec]	[sec]	[sec]	[volt]	[-]	[ampere]	[-]	[-]	[-]	
41	1300	1/4	5.4	0.6	16	10	110	3.4	2.56	0.169	15	NL
42	1175	1/4	5.4	10	35	10	54	0.9	5.18	0.006	810	NL
43	1210	2/3	5.4	0.6	31	10	60	2.2	2.20	0.095	23	L, MS = 6
44	1225	2/3	5.4	10	50	10	26	1.0	2.74	0.022	122	NL, MS = 6
45	1275	2/3	5.4	10	40	10	34	0.7	2.67	0.040	66	L, MS = 4
46	1240	2/3	5.4	0.6	21	10	80	1.5	1.75	0.320	5	L, MS = 4
47	1225	2/3	5.4	10	21	10	50	0.4	2.61	0.095	28	L, MS = 2
48	1250	2/3	5.4	0.6	11	10	100	1.2	1.30	0.657	2	L, MS = 2
49	1270	2/3	5.4	20	80	10	40	1.2	3.46	0.008	452	NL
50	1290	2/3	2.2	10	91	10	20	1.5	3.31	0.013	262	NL
51	1280	2/3	5.4	10	40	10	110	0.6	3.19	0.051	63*	NL, MS = 4, $\delta_B = \delta_T = \frac{1}{2}$ unmixed
52	1250	2/3	5.4	10	40	10	60	0.6	2.30	0.040	58	NL, MS = 4, $\delta_B = \delta_T = \frac{1}{2}$
53	1280	2/3	5.4	10	40	10	55	0.6	2.70	0.072	38**	NL, MS = 4, $\delta_B = \delta_T = \frac{1}{2}$ unmixed

*CONCENTRATIONS MEASURED IN WELL MIXED END RESERVOIRS. TWO STAGES ON EACH END INACTIVE.

**CONCENTRATIONS MEASURED BETWEEN ACTIVE AND INACTIVE STAGES.

Tables 8 to 12 contain experimental results obtained with the first ED cell, Table 13 shows results from the second ED cell in batch mode.

The following type of abbreviation will be used subsequently:

EDI - S2 - 15/#5

This stands for the first electrodialyser (EDI), used with the second stack (S2) version, which contained fifteen (15) spacer-membrane units, and refers to run number five (#5).

5.3 The First Electrodialysis Cell (EDI)

5.3.1 Parameters.

The parameters which were studied on this first ED cell (EDI) may be divided into the following two groups:

Operating parameters:

1. Applied voltage $\Delta\Phi$
2. Pause time τ
3. Superficial velocity v
4. Displaced volume δ
5. Dead volume δ_B/δ_T
6. Initial concentration c_0

Design parameters:

7. Internal flow distribution and axial dispersion
8. External mixing in brine reservoir
9. Thickness of capacity cell core
10. Thickness and hydrodynamic properties of spacer screen.

All except two of these parameters are defined in preceding sections. Items 7. and 8. are discussed in full detail under 5.3.8 and 5.3.9, respectively.

Each of these ten parameters is analysed separately by forming groups of experiments in which the other parameters are constant. These groups are presented in tables which display the operating parameters and the final conditions at the end of each experiment in the same order as the main survey tables.

The transient response of the ED cell was evaluated for a series of systematic runs on the second and third stack versions. Appendix C.1 describes the computer calculations which were performed on the raw data for each cycle and lists tables of printout.

5.3.2 Effect of applied voltage.

The main survey tables list values of the constant voltage supplied by the regulated D.C. power source, since

this is the true independent variable. The voltage drop across the stack is primarily a function of this applied voltage but it varies systematically during the cyclic operation.

A typical example of these fluctuations is shown in Figure 35, which is a copy of the traces of probe voltage (potentiogram) and current (electrogram) recorded during the first five cycles of EDI - S2 - 15/#15. The polarity reversal of the electric potential is suppressed in the potentiogram but is indicated by positive and negative signs in the time fields below the curve. The following trends characterize the potentiogram:

a. Probe voltage is generally well below the electrode voltage due to the solution resistance of the rinse stream, the electrode overpotentials, and the resistances in the connectors.

b. Peaks result from each polarity reversal. The peaks reflect the battery effect of the membrane stack, and appear to be sharper when switching from positive to negative polarity than vice versa. This battery effect is most pronounced for capacity cells with "zero" core because of the very large concentration changes in those cells (DONNAN effect). However, the peaks are of moderate magnitude compared to the level of the applied potential. This indicates that the DONNAN potential has little influence.

c. The peaks decay within a few seconds. Subsequent changes of the probe voltage are antagonistic to the current changes, and must therefore be associated with the electrode reactions.

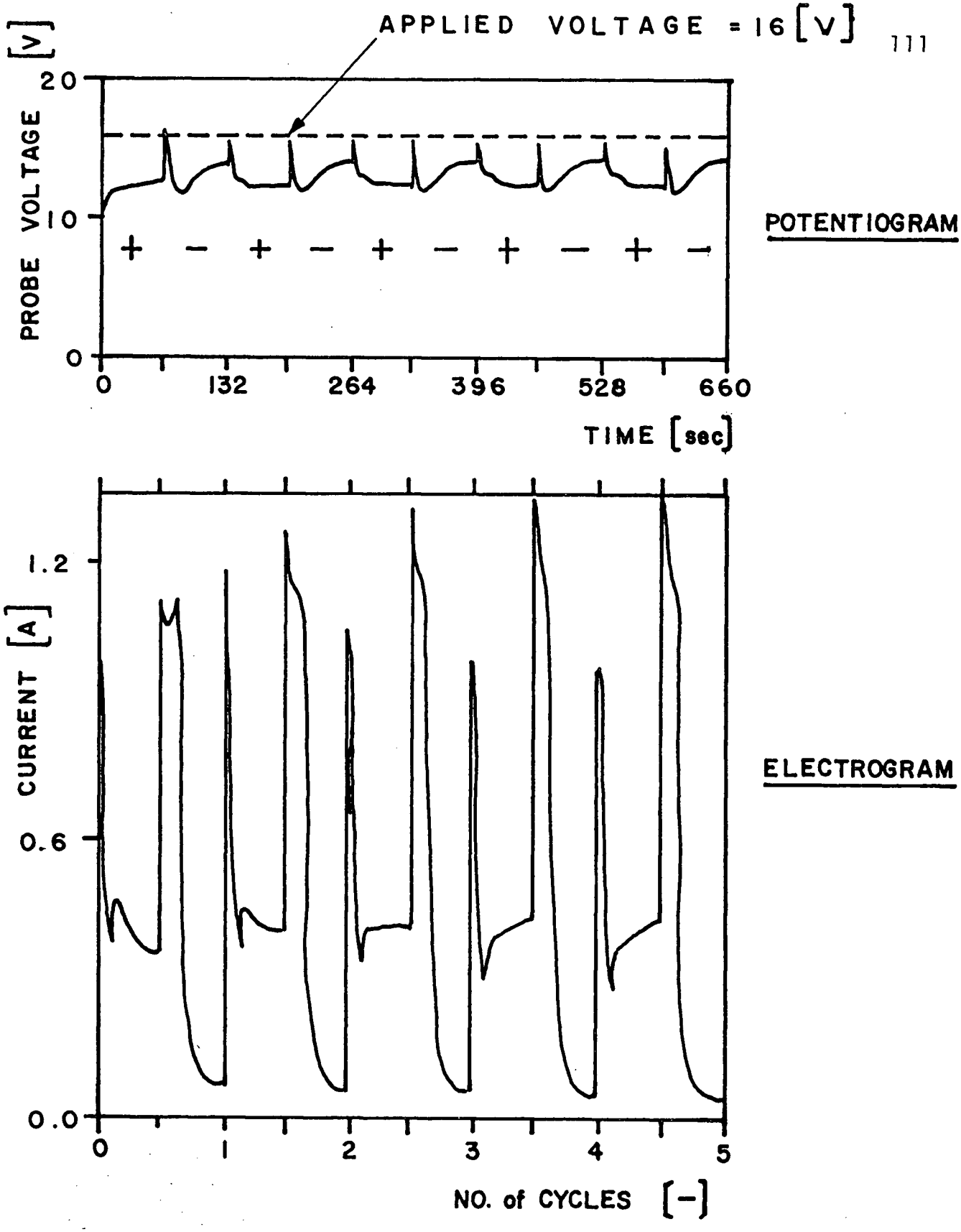

Figure 35. EDI-S2-15/#15. Traces of current and probe voltage recording during the first five cycles.

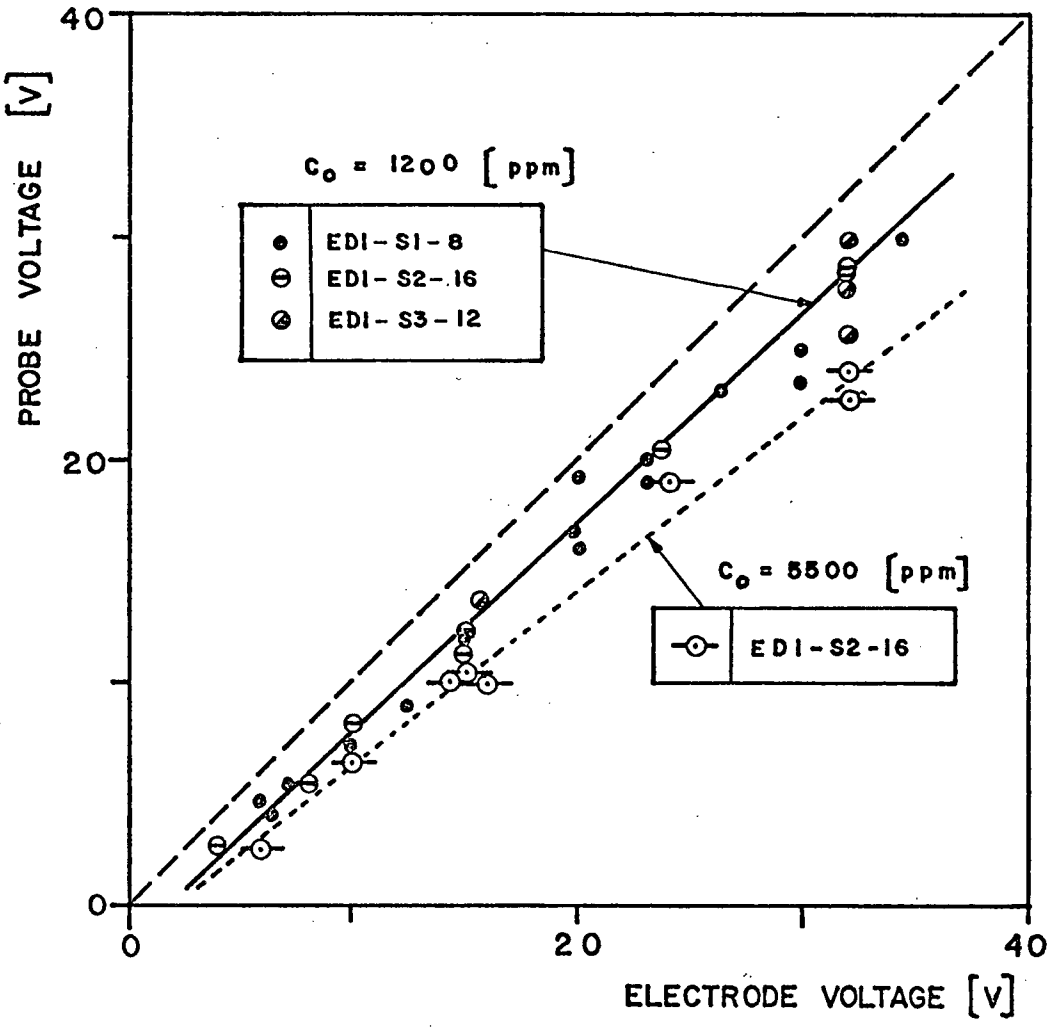

Figure 36. Probe voltage vs. electrode voltage for first ED cell.

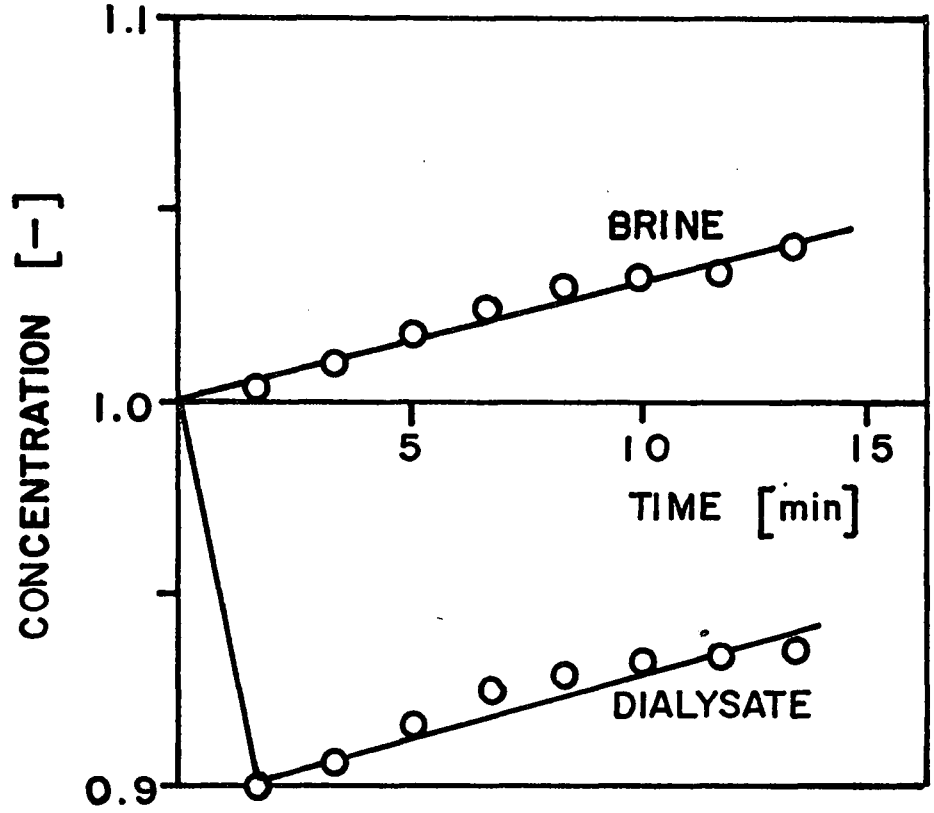

Figure 37. EDI-S1-8/#36. Example of concentration transients in parametric pumping operation when mass transfer rates are constant.

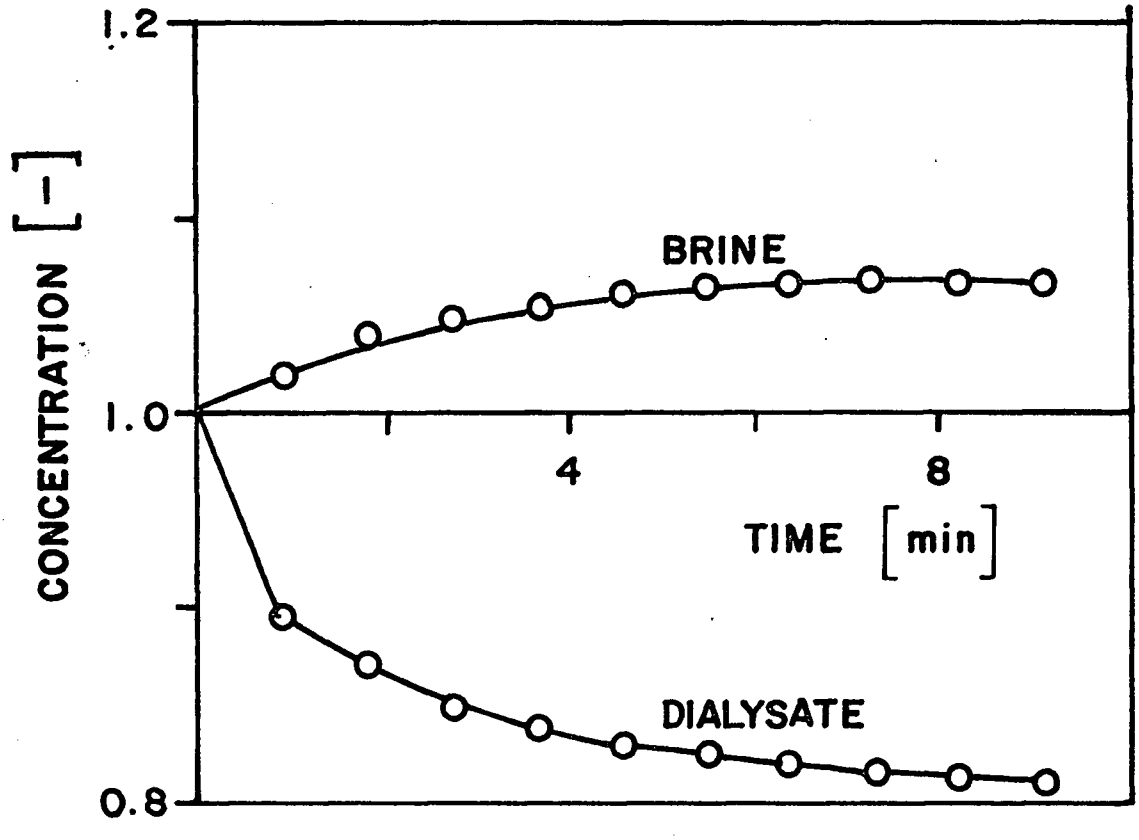

Figure 38. EDI-S2-15/#9. Example of concentration transients in parametric pumping operation when mass transfer rates are concentration dependent.

A plot of the mean probe voltage vs. applied voltage for all three membrane packs may be fitted by straight lines as illustrated in Figure 36. The points fall below the diagonal line and are divided in low concentration and high concentration runs.* The scatter of the points is caused by variations in process concentration, positioning of the probes, and by inaccuracies of the averaging method.

Tables 14, 15 and 16 show the effect of the applied voltage ($\Delta\Phi$) on final conditions for experiments with first, second, and third stack versions, respectively. The separation is generally improved for larger values of $\Delta\Phi$, and the current consumption increases simultaneously.

The improvements in separation with increasing potential depend on the values of the other parameters. The following trends may be identified.

1. Little or no improvement occurred for zero pause time, fast displacement, and large sorption capacity of the membranes (see Table 14). An inspection of the concentration transients shows all the characteristics of the model discussed in Section 3.2.1. Figure 37 is a typical example of the real time transients of the reservoir concentrations. The top reservoir concentration (dialysate) drops sharply for the first cycle, and both concentrations remain parallel and drift upward for subsequent cycles. Separation is thus completed

---

*See page 147.

after one cycle. The improvements which may be achieved by an increased potential are restricted to the first cycle, and therefore remain small.

The current consumption increased almost proportionally to the applied potential. In these experiments the concentrations changed very little compared to the initial concentration, i.e. the electric resistance of the stack stayed almost constant.

2. Small improvements were observed for zero pause time, slow displacement, and small sorption capacity of the membranes (see the first group in Table 15). Typical concentration transients of these experiments are shown in Figure 38. A break of the dialysate transient after the first cycle is clearly visible, but the separation is further increased during the next cycles. The shape of these curves agrees well with the model presented in Section 3.3.2.

Figure 39 illustrates directly the influence of the applied potential ($\Delta\Phi$) on final separation factor (ns), final reservoir concentrations (x_B and x_T), and final current (I).

The current consumption is seen to rise less than proportional to the applied potential up to approximately 32 [V]. This behaviour is attributed to the simultaneous increase in bottom

Table 14
Effect of Applied Voltage ($\Delta\Phi$) on EDI-S1-8

1	2	3	4	5	6	7	8	9	10	11	12	13
RUN NO.	CONCENTR. INITIAL	VOLUME DISPLACED	VELOCITY SUPERFICIAL	PAUSE TIME	CYCLE PERIOD	VOLTAGE APPLIED	CYCLE NO.	CURRENT TOTAL	CONCENTRATION		SEPARATION FACTOR	REMARKS
									BRINE	DIALYSATE		
#	c_0	δ	v	τ	T	$\Delta\Phi$	nc	I	x_B	x_T	ns	L = limit reached NL = limit not reached δ_B/δ_T = dead volumes
[-]	[ppm]	[-]	[cm/sec]	[sec]	[sec]	[volt]	[-]	[ampere]	[-]	[-]	[-]	
14	1020	1.00	1.21	-	50.2	6.0	7	0.32	0.969	0.983	0.99	NL
15-0	1020					6.0	9	0.32	0.970	0.997	0.97	L
40	760					6.0	8	0.28	0.986	0.995	0.99	L
41	760					10.0	7	0.44	0.956	0.975	0.98	L
35	700					12.5	9	0.55	0.960	0.960	1.00	L
42	750					20.0	7	0.78	0.972	0.954	1.02	L
6	1080	1.73	1.21	-	84.3	4.0	6	0.23	1.03	0.974	1.06	L
7	1090	1.73			84.3	6.0	9	0.37	1.02	0.938	1.09	L
38	725	1.80			87.3	15.0	6	0.60	1.02	0.862	1.19	L
39	710	1.80			87.3	20.0	5	0.75	1.07	0.860	1.25	L
37	720	1.00	0.65	-	93.8	5.0	5	0.20	1.02	0.980	1.05	L
15-1	1020					6.0	13	0.30	0.965	0.972	0.99	L
36	700					12.5	8	0.50	1.04	0.935	1.11	L
3	1040	1.10	1.77	-	36.4	6.0	8	0.39	0.999	0.996	1.00	NL
31	710	1.00			34.3	7.55	13	0.35	0.99	1.00	0.99	L
32	720	1.00			34.3	12.5	6	0.55	0.95	0.97	0.98	L

Table 15

Effect of Applied Voltage ($\Delta\Phi$) on EDI-S2-15

1	2	3	4	5	6	7	8	9	10	11	12	13
RUN NO.	CONCENTR. INITIAL	VOLUME DISPLACED	VELOCITY SUPERFICIAL	PAUSE TIME	CYCLE PERIOD	VOLTAGE APPLIED	CYCLE NO.	CURRENT TOTAL	CONCENTRATION		SEPARATION FACTOR	REMARKS
									BRINE	DIALYSATE		
# [-]	c_0 [ppm]	δ [-]	v [cm/sec]	τ [sec]	T [sec]	$\Delta\Phi$ [volt]	nc [-]	I [ampere]	x_B [-]	x_T [-]	ns [-]	L = limit reached NL = limit not reached δ_B/δ_T = dead volumes
7	940	1.00	0.88	0.0	55	8	10	0.40	1.01	0.935	1.08	L
8	950					16	10	0.70	1.01	0.858	1.18	L
9	970					24	10	0.85	1.07	0.801	1.33	L
10	960					32	10	1.00	1.14	0.750	1.52	L
17	1025					40	10	1.30	1.14	0.747	1.52	L
13	930	1.00	2.23	10	42	15	10	0.65	1.28	0.671	1.91	L
6	990					20	14	0.75	1.23	0.641	1.92	L
12-1	940					32	16	0.90	1.41	0.548	2.58	NL
14	980	1.00	2.23	15	52	15	10	0.60	1.32	0.607	2.17	NL
27	1090					32	10	0.96	1.46	0.537	2.72	L
28-2	1070					32	11	1.00	1.45	0.540	2.69	NL
33	1150					32	11	0.90	1.39	0.517	2.70	L
												EDI-S2-16
5-4	1250	0.61	0.92	25	72	16	60	0.30	1.40	0.222	6.32	NL, δ_B = 1.84
6-1	1225					16	22	0.40	1.32	0.250	5.28	L, δ_B = 1.84
5-1	1250					32	21	0.50	1.41	0.179	7.88	L, δ_B = 1.84
6-3	1225					40	45	0.52	1.41	0.142	10.10	L, δ_B = 1.84

Table 16

Effect of Applied Voltage ($\Delta\Phi$) on EDI-S3-12 and EDI-S3-13

1	2	3	4	5	6	7	8	9	10	11	12	13
RUN NO.	CONCENTR. INITIAL	VOLUME DISPLACED	VELOCITY SUPERFICIAL	PAUSE TIME	CYCLE PERIOD	VOLTAGE APPLIED	CYCLE NO.	CURRENT TOTAL	CONCENTRATION		SEPARATION FACTOR	REMARKS
									BRINE	DIALYSATE		
# [-]	c_0 [ppm]	δ [-]	v [cm/sec]	τ [sec]	T [sec]	$\Delta\Phi$ [volt]	nc [-]	I [ampere]	x_B [-]	x_T [-]	ns [-]	L = limit reached NL = limit not reached δ_B/δ_T = dead volumes
17	1130	1.00	.90	5	64	10	18	0.53	1.20	0.700	1.72	L
18	1080		.90		64	20	18	0.84	1.32	0.578	2.28	L
19	1175		.90		64	30	16	1.06	1.34	0.473	2.85	L
1-2	1225		.92		62	32	25	1.20	1.41	0.526	2.69	L
												EDI-S3-13
6	1300	1.00	.95	5	61	10	17	.62	1.31	0.603	2.18	L
7	1270					22	17	1.00	1.52	0.432	3.53	L
11	1250					22	18	.96	1.52	0.424	3.59	L
8	1260					30	15	1.20	1.61	0.389	4.15	L
22	1205					30	18	1.05	1.61	0.375	4.29	L
9	1135					40	22	1.28	1.77	0.330	5.36	L

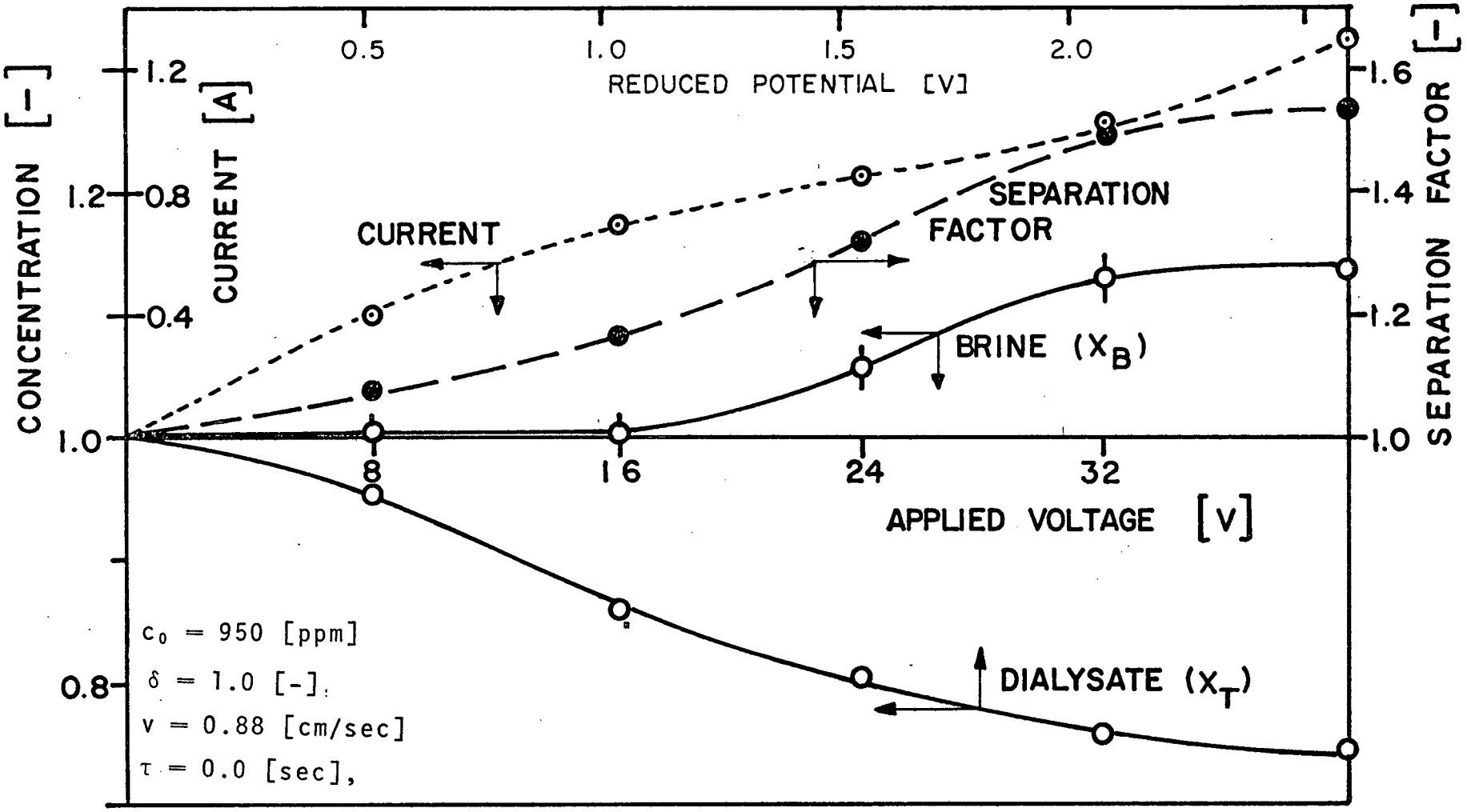

Figure 39. Effect of applied voltage on final concentrations, separation factor, and current. Second stack experiments in no-pause operation. EDI-S2-15/ #7,8,9,10,17.

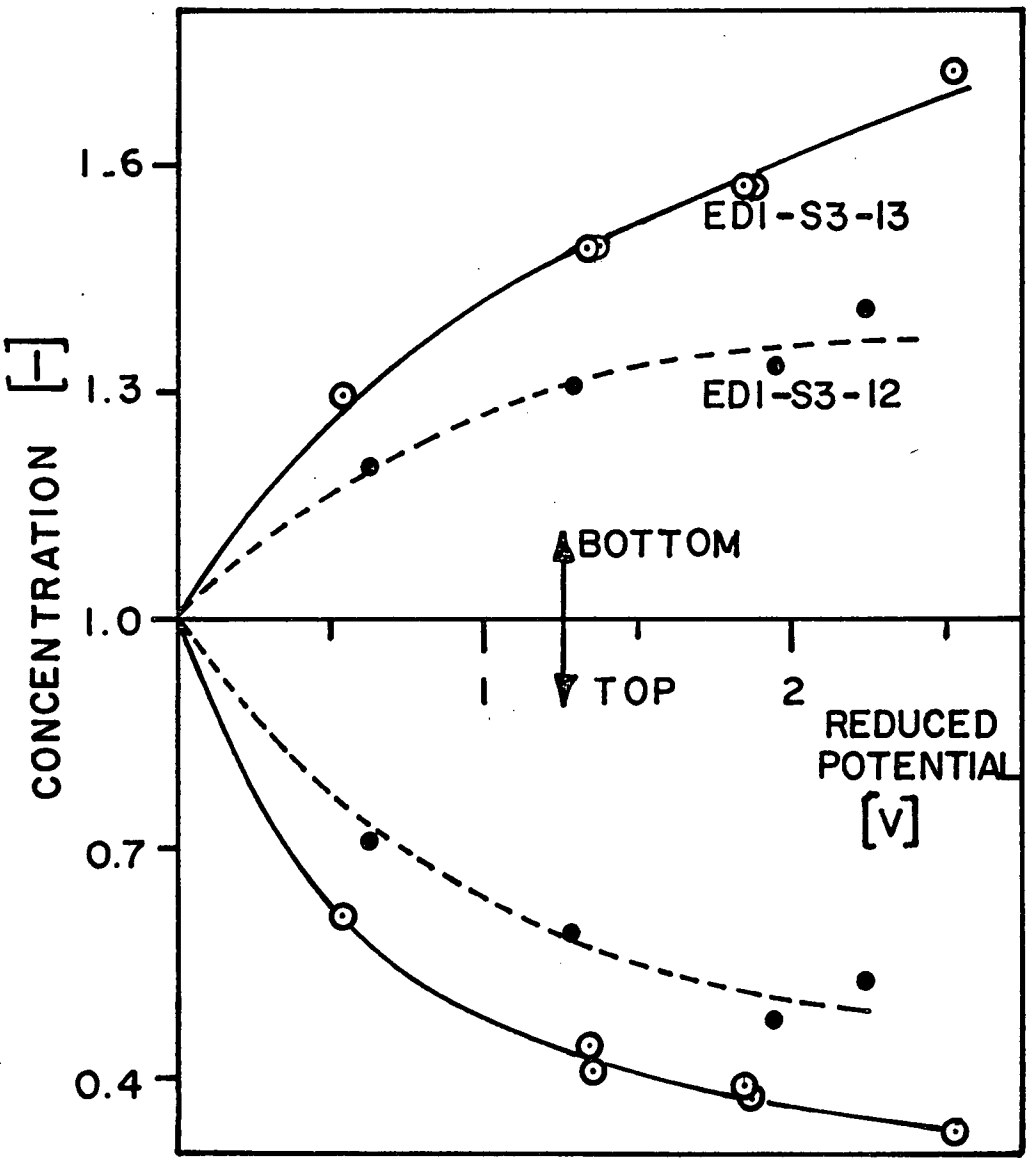

c_0 = 1200 [ppm], δ = 1.0 [-], v = 0.95 [cm/sec], τ = 5.0 [sec]

Figure 40. Effect of applied voltage on final product concentrations for third stack experiments. EDI-S3-12/#17,18,19,1-2 and EDI-S3-13/#6,7,11,8,22,9.

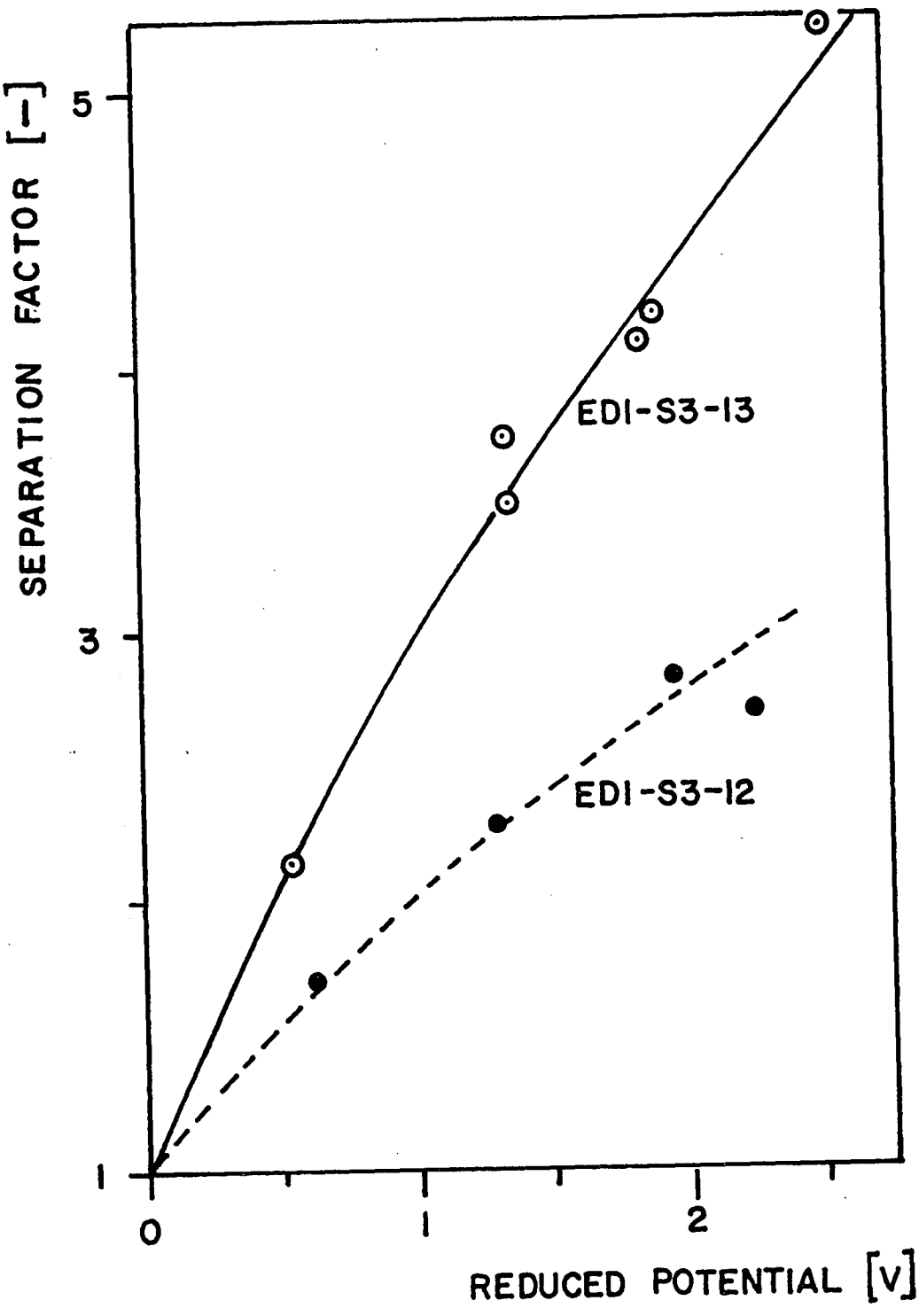

c_0 = 1200 [ppm], δ = 1.0 [-], v = 0.95 [cm/sec], τ = 5.0 [sec]

Figure 41. Effect of applied voltage on final separation factor for third stack experiments. EDI-S3-12/ #17,18,19,1-2 and EDI-S3-13/#6,7,11,8,22,9.

reservoir concentration, and reflects the changes in stack resistance due to partial removal of solute from the ED cell. The rise of the current with $\Delta\Phi$ is accelerated as the brine concentration stagnates between 32 and 40 [V].

3. Large improvements were recorded for pause time operations on the second and third stack version of the first ED cell (see Tables 15 and 16). The influence of the applied potential ($\Delta\Phi$) on final reservoir concentrations and final separation factor of the groups in Table 16 are shown in Figures 40 and 41 respectively.* The final current consumption increased less than proportional to the applied potential. This confirms the concept of an overall resistance increase within the stack for enhanced separation.

5.3.3 Effect of pause time.

The influence of equal pause times (τ) at the beginning of each half cycle was studied on the second and third stack versions. Table 17, 18, and 19 summarize the operating parameters and the final conditions reached in these experiments, and Figures 42, 43 and 44 directly display the effect of the pause time on final separation factors and final reservoir concentrations for several groups of experiments.

*The abscissa is the applied potential per number of flow channels. This reduced potential allows comparison between stacks containing different numbers of flow channels.

The results show that the separation is improved for prolonged pause times, and that better separation is always accompanied by reduced current consumption. There is some indication that the final separations will eventually reach limiting levels set by the amount of internal mixing, and the combined influences of molecular diffusion, DONNAN equilibrium, and capacity of the sorption membranes. Figure 45 shows the transient of the top reservoir concentration for EDI - S3 - 12/#6-0. The initial part of the curve is a fine example of the exponential decay predicted by the model in Section 3.3.1.* However, after twenty cycles the curve begins to asymptotically approach a finite limit set by dispersive effects which are discussed in Section 5.3.8.

The real time transients of the reservoir concentrations for the EDI - S3 - 13 group (see Table 19) are shown in Figure 46. Final conditions are reached after approximately 15 [min] in all experiments. The break in the transients of the top reservoir concentration disappears as the pause time is lengthened and the solution in the bottom reservoir accumulates more and more of the total solute.

---

*This model does not account for the mass transfer during displacement, which happened in the experiment due to the continuous application of the electric potential ($\Delta\Phi$). Since the displaced volume (δ) was small and the velocity of displacement was large, the ratio of pause time to residence time was also large. Sections 5.3.4 and 5.3.5 demonstrate that the material transferred during displacement contributes very little to the separation under such conditions.

Table 17

Effect of Pause Time (τ) on EDI-S2-15 and EDI-S2-16

1	2	3	4	5	6	7	8	9	10	11	12	13
RUN NO.	CONCENTR. INITIAL	VOLUME DISPLACED	VELOCITY SUPERFICIAL	PAUSE TIME	CYCLE PERIOD	VOLTAGE APPLIED	CYCLE NO.	CURRENT TOTAL	CONCENTRATION		SEPARATION FACTOR	REMARKS
									BRINE	DIALYSATE		
# [-]	c_0 [ppm]	δ [-]	v [cm/sec]	τ [sec]	T [sec]	$\Delta\Phi$ [volt]	nc [-]	I [ampere]	x_B [-]	x_T [-]	ns [-]	L = limit reached NL = limit not reached δ_B/δ_T = dead volumes
11	960	1.00	2.33	5	32	32	14	1.25	1.29	0.631	2.05	L
12-0	940			5	32		10	1.25	1.31	0.623	2.10	L
28-3	1070			5	32		18	1.30	1.28	0.644	1.99	L
27	1090			15	52		10	0.96	1.46	0.537	2.72	L
28-2	1070			15	52		11	1.00	1.45	0.540	2.69	NL
33	1150			15	52		11	0.90	1.33	0.517	2.70	L
												EDI-S2-16
8-0	1240	0.61	0.92	0	22	32	30	1.41	1.10	0.714	1.54	L
3-0	1175			15	52		14	0.70	1.88	0.341	5.52	NL
3-1	1175			25	72		20	0.60	2.04	0.274	7.46	L
4	1220			25	72		14	0.70	2.11	0.278	7.58	L
7	1250	0.61	0.92	0	22	40	50	1.50	1.11	0.567	1.96	L, δ_B = 1.84
6-2	1225			15	52		38	0.63	1.43	0.196	7.05	L, δ_B = 1.84
6-3	1225			25	72		45	0.52	1.41	0.142	10.10	L, δ_B = 1.84

Table 18

Effect of Pause Time (τ) on EDI-S3-12

1	2	3	4	5	6	7	8	9	10	11	12	13
RUN NO.	CONCENTR. INITIAL	VOLUME DISPLACED	VELOCITY SUPERFICIAL	PAUSE TIME	CYCLE PERIOD	VOLTAGE APPLIED	CYCLE NO.	CURRENT TOTAL	CONCENTRATION		SEPARATION FACTOR	REMARKS
									BRINE	DIALYSATE		
# [-]	c_0 [ppm]	δ [-]	v [cm/sec]	τ [sec]	T [sec]	$\Delta\Phi$ [volt]	nc [-]	I [ampere]	x_B [-]	x_T [-]	ns [-]	L = limit reached NL = limit not reached δ_B/δ_T = dead volumes
1-1	1225	1.00	0.92	0	52	32	18	1.35	1.18	0.705	1.67	L
1-2	1225			5	62		25	1.20	1.41	0.526	2.69	L
1-3	1225			15	82		30	1.00	1.56	0.411	3.89	L
8	1270			20	93		10	0.95	1.64	0.376	4.36	L
24	1170	1.00	0.90	0.6	55	20	15	1.09	1.14	0.703	1.62	L
18	1080			5	64		18	0.84	1.32	0.578	2.28	L
21	1230			10	74		20	0.81	1.39	0.508	2.73	L
22	1200			15	84		17	0.74	1.49	0.486	3.04	L
23	1200			20	94		16	0.69	1.52	0.469	3.23	L
9-0	4800	1.00	0.92	0	53	16	5	3.10	—	0.922	—	L
9-1				5	63		10	3.00	—	0.898	—	NL
9-2				10	73		20	2.70	—	0.636	—	NL
9-3				15	83		35	2.30	—	0.545	—	NL

Table 19

Effect of Pause Time (τ) on EDI-S3-13

1	2	3	4	5	6	7	8	9	10	11	12	13
RUN NO.	CONCENTR. INITIAL	VOLUME DISPLACED	VELOCITY SUPERFICIAL	PAUSE TIME	CYCLE PERIOD	VOLTAGE APPLIED	CYCLE NO.	CURRENT TOTAL	CONCENTRATION		SEPARATION FACTOR	REMARKS
									BRINE	DIALYSATE		
# [-]	c_0 [ppm]	δ [-]	v [cm/sec]	τ [sec]	T [sec]	$\Delta\Phi$ [volt]	nc [-]	I [ampere]	x_B [-]	x_T [-]	ns [-]	L = limit reached NL = limit not reached δ_B/δ_T = dead volumes
14	1045	1.00	0.95	0.6	52	22	23	0.99	1.28	0.570	2.24	L
11	1250			5	61		18	0.96	1.52	0.424	3.59	L
7	1270			5	61		17	1.00	1.52	0.432	3.53	L
12	1285			10	71		20	0.87	1.61	0.372	4.33	L
2	1250			10	71		18	0.85	1.60	0.398	4.03	L
13	1205			20	91		19	0.69	1.71	0.324	5.27	L
1	1240			20	91		19	0.70	1.69	0.349	4.85	L
14	1125			30	111		13	0.50	1.79	0.301	5.95	L
24	1260	0.50	1.40	10/5	32	22	40	0.91	2.03	0.228	8.90	L
16	1275			10/10	37		34	0.80	2.08	0.248	8.35	NL
25	1250			10/10	37		35	0.81	2.14	0.228	9.35	NL
27	1260	0.50	1.40	10/5	32	10	50	0.65	1.65	0.376	4.39	L
26	1260			10/10	37		40	0.54	1.83	0.344	5.33	L
30	1280	0.50	2.36	10/5	25	22	35	0.92	2.01	0.228	8.85	NL
31	1300			10/10	30		30	0.80	2.16	0.233	9.27	L
18	1180			10/10	30		45	0.70	2.12	0.240	8.83	L

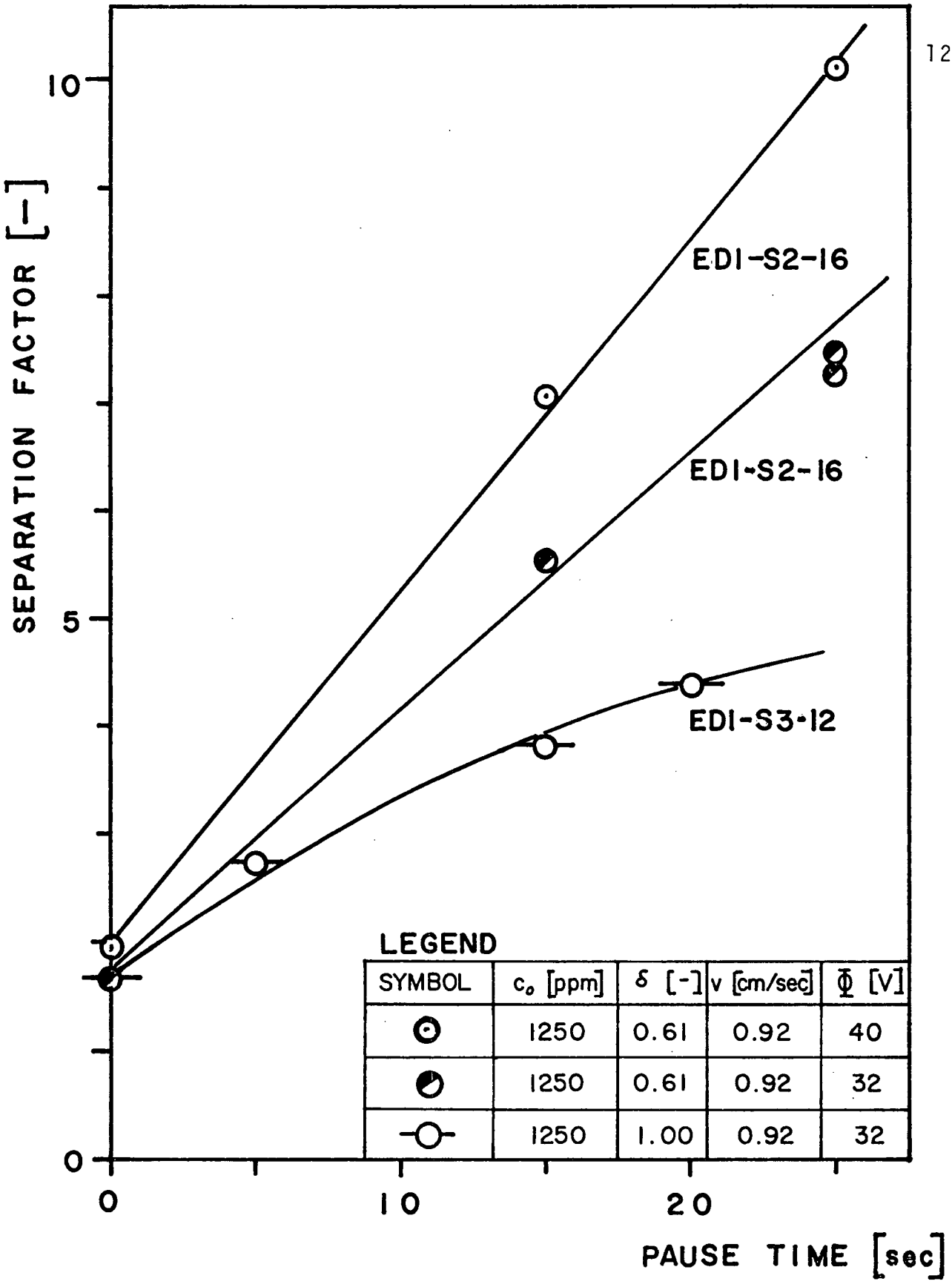

Figure 42. Effect of pause time (τ) on separation factor for second and third stack experiments.

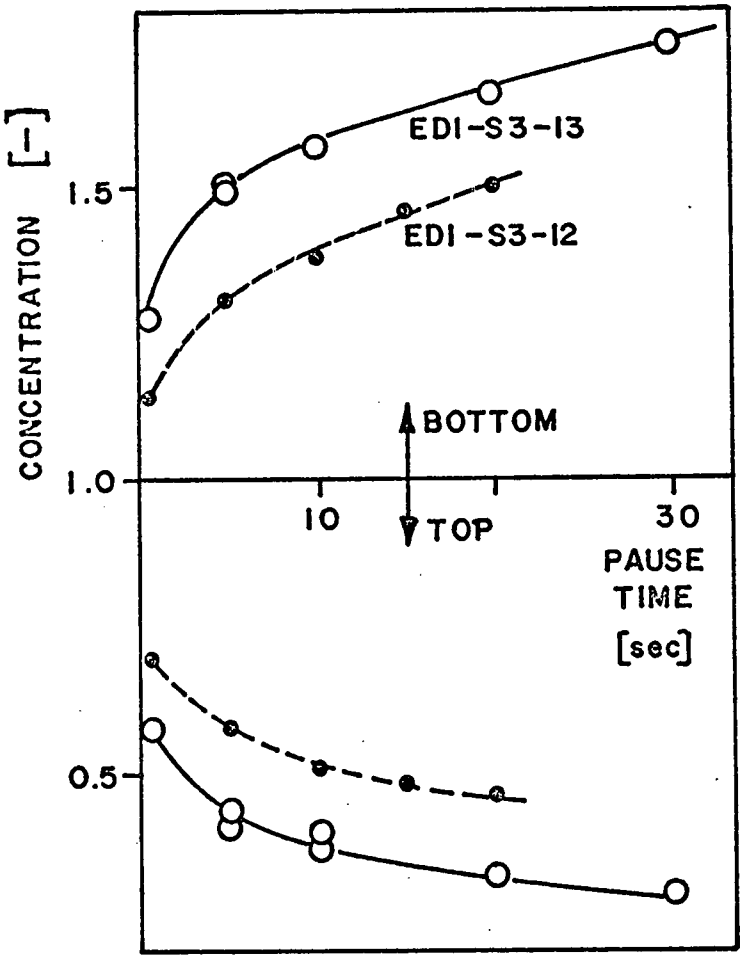

Figure 43.

Effect of pause time on final reservoir concentrations for third stack experiments. EDI-S3-12/#24,18,21,22,23 and EDI-S3-13/#10,11,7,12,2,13,1,14.

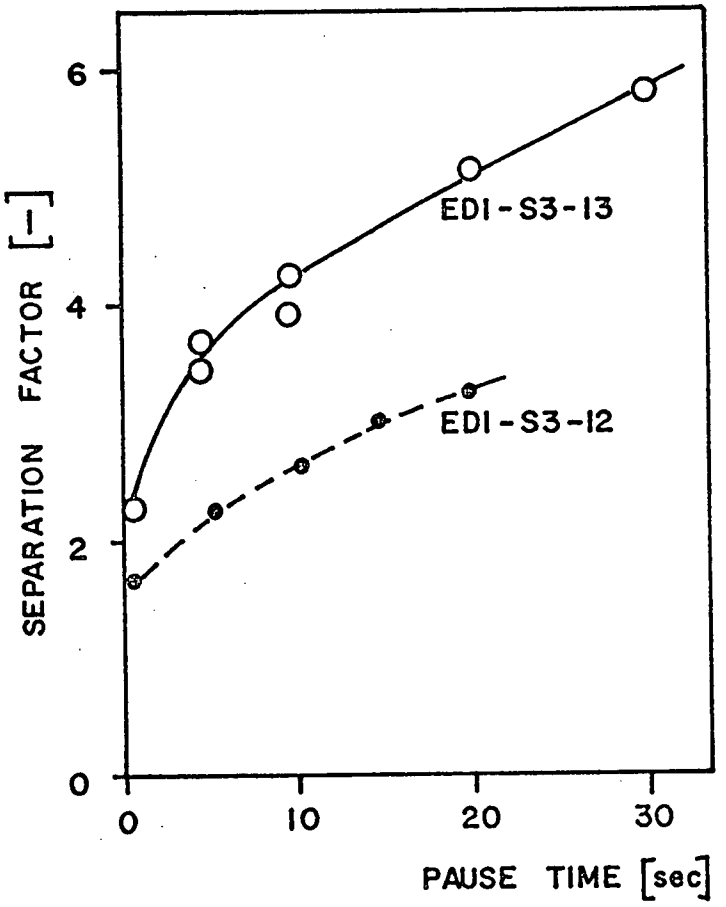

Figure 44.

Effect of pause time (τ) on final separation factor for third stack experiments. EDI-S3-12/#24,18,21,22,23 and EDI-S3-13/#10,11,7,12,2,13,1,14.

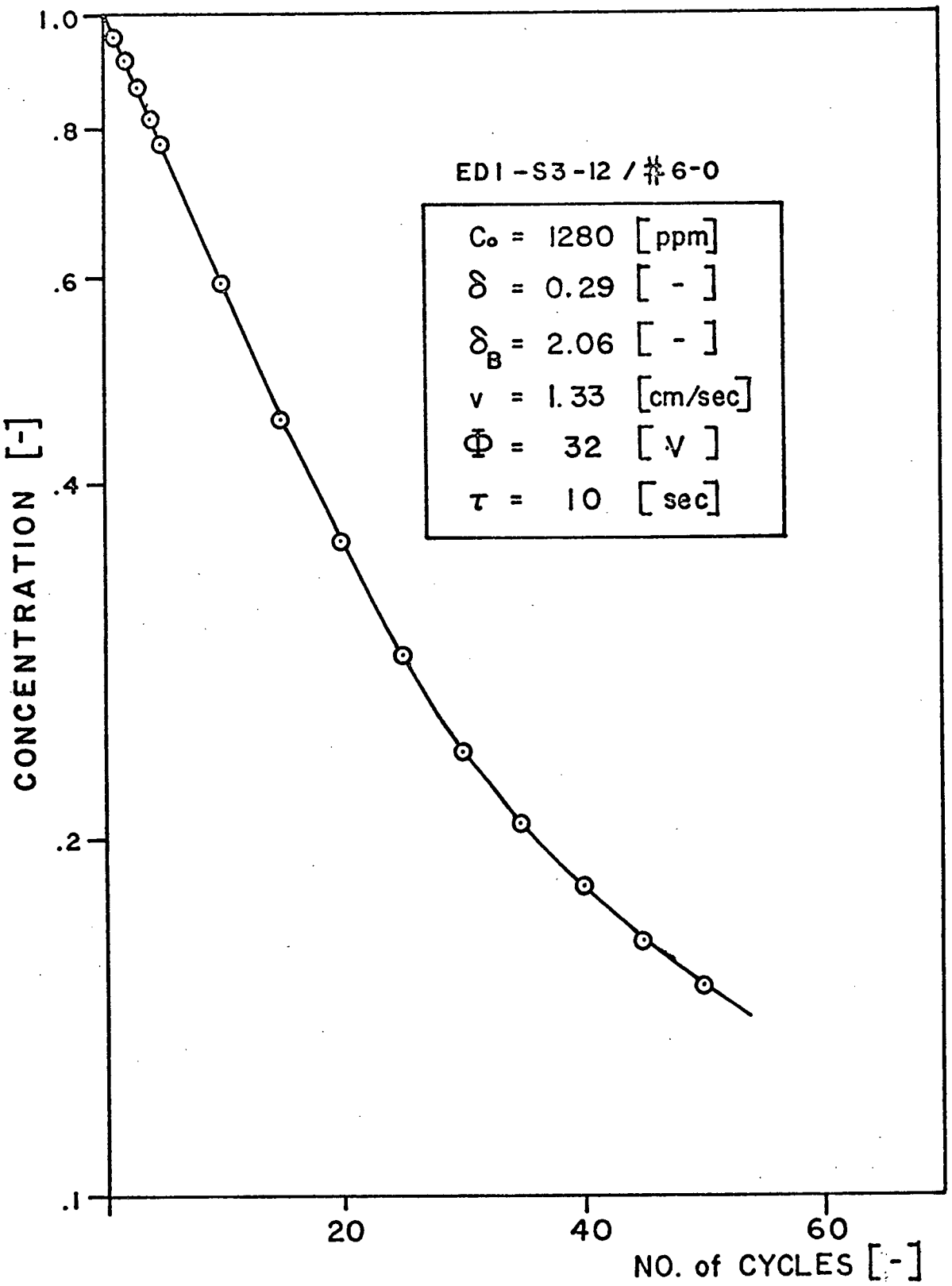

Figure 45. Dialysate-concentration-transient of EDI-S3-12/#6-0.

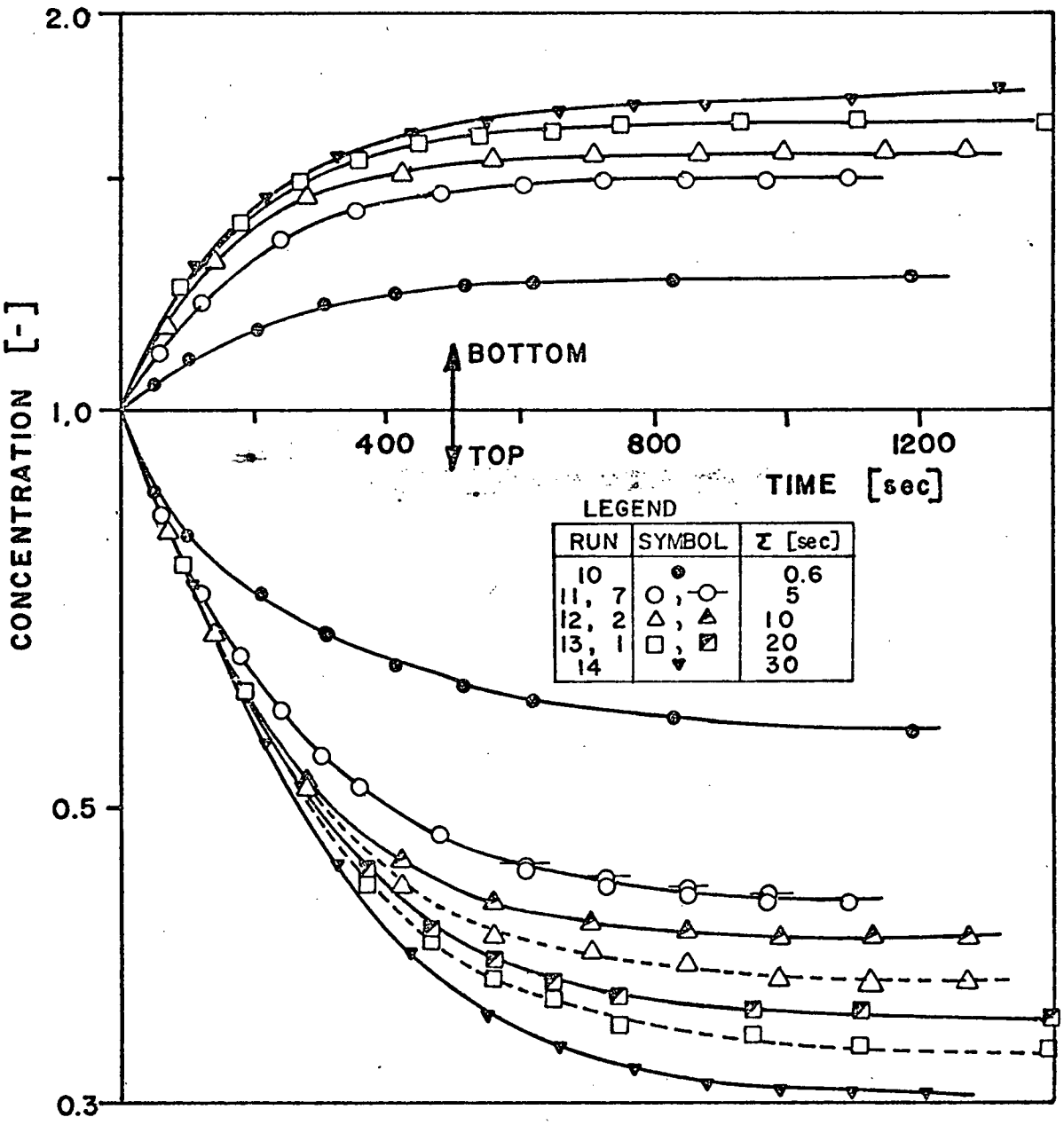

c_0 = 1200 [ppm] δ = 1.0 [-], v = 0.95 [cm/sec], $\Delta\Phi$ = 22 [V]

Figure 46. Effect of pause time (τ) on concentration transients of third stack experiments.

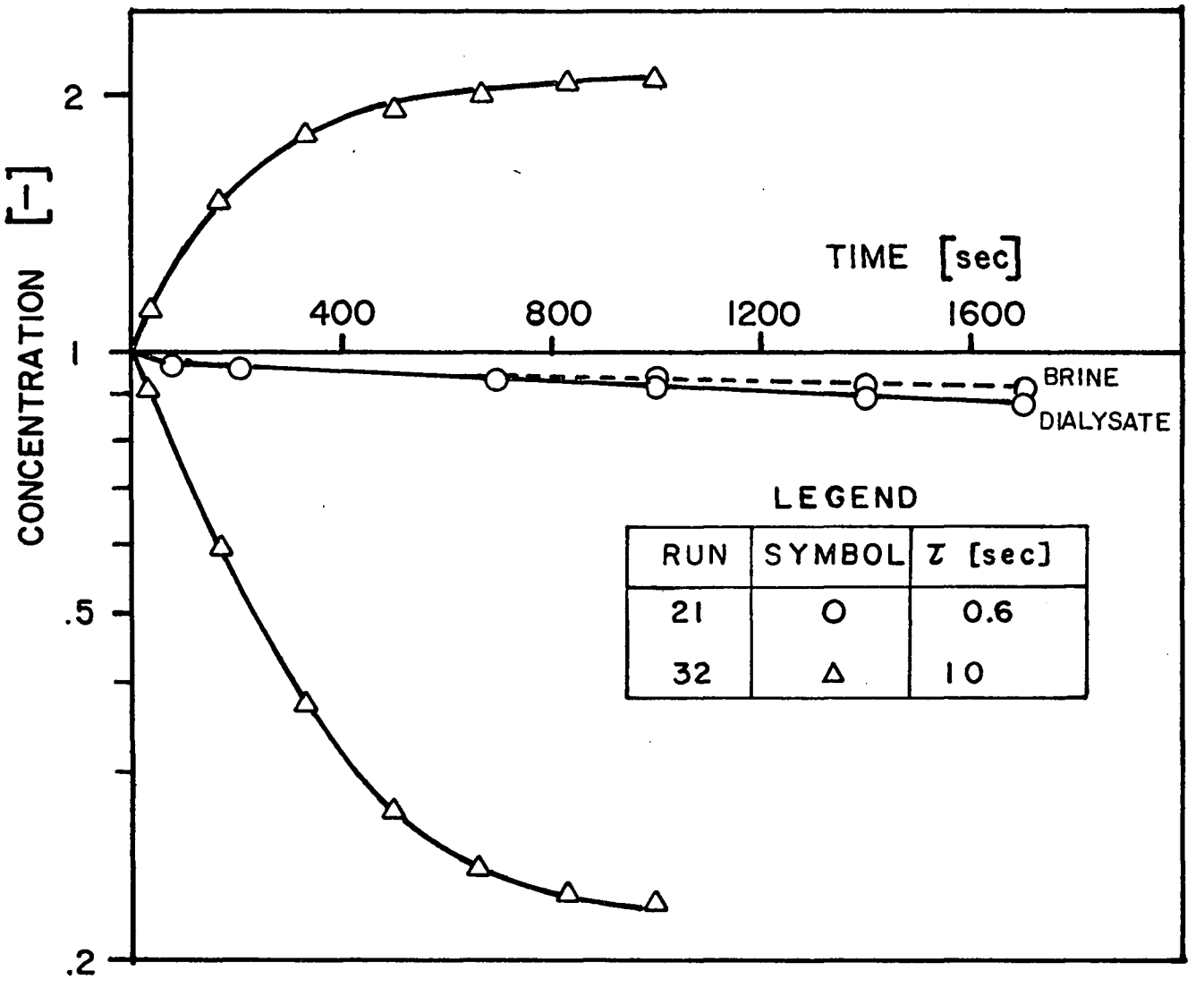

c_0 = 1250 [ppm], δ = 0.5 [-], v = 1.85 [cm/sec], $\Delta\Phi$ = 22 [V]

Figure 47. Contrasting pause and no-pause operation for third stack experiments. EDI-S3-13/#21,32.

Figure 47 contrasts the concentration transients of standard parametric pumping operation (no-pause) with pause operation (τ = 10 [sec]) under otherwise identical conditions. The latter are particularly favourable for the pause operation because they combine small displaced volume (δ = 0.5), fast displacement (v = 1.85 [cm/sec]), and moderate applied potential ($\Delta\Phi$ = 12.5 [V]).

The last group of Table 19 contains experiments with unequal pause times. In particular, the brine producing half cycle was shortened, since the current consumption during these periods became usually very small (see the electrogram in Figure 35). The pause times for these part cycles were halved without significant effects on the final conditions.

5.3.4 Effect of superficial velocity.

The superficial velocity (v) was varied for groups of experiments on all three stack versions. Operating parameters and final conditions are compiled in Table 20, 21 and 22 for first, second and third stack, respectively. The effect of the superficial velocity on final reservoir concentrations and final separation factors is graphically displayed in Figure 48 and 49, respectively, for the groups of Table 22. Figures 50 and 51 show the real time transients of the reservoir concentrations of these groups.

The results are quite different depending on the value of the pause time, and may be summarized as follows.

1. No-pause operation. Final separation is considerably improved for slow velocities of displacement. The improvement in separation is accompanied by reduced current consumption.

   This agrees with the models presented in Chapter 3. If the cycle period is prolonged by reducing the flow rate, the residence time will be proportionally increased, but at the same time the rate of mass transfer will be decreased according to some power function of v. Generally, in packed beds and in flow channels with turbulence promoters, the steady state transfer coefficients have been found to be proportional to v^n, where n = 0.5 to 0.8 (see e.g. Hicks, 1968; Yamane, 1969b; and Kitamoto *et al.*, 1971). It may be expected that the influence of the residence time is prevailing in the case of unsteady-state mass transfer in the electrodialysis system, too.

   The experiments with no-pause time confirm this train of thoughts, and Figure 50 illustrates

that a reduction in velocity leads to concentration transients which resemble those of pause operations.

2. Operations with moderate pause time. Final separation is virtually independent of superficial velocity. The rate at which this limit is approached may be improved by increasing the velocity. The increase in rate is at the expense of a higher current consumption.

The improved rate of separation is in complete accord with the concept that the pause time is the true cause of a successful cyclic operation of the electrodialysis process, at least in the parameter regime investigated.

The pause periods of the cyclic operation seem to be responsible for a certain amount of separation which is independent of the velocity. The displacement may, therefore, be implemented as fast as mechanically feasible or economically desirable.

Table 20
Effect of Superficial Velocity (v) on EDI-S1-8

1	2	3	4	5	6	7	8	9	10	11	12	13
RUN NO.	CONCENTR. INITIAL	VOLUME DISPLACED	VELOCITY SUPERFICIAL	PAUSE TIME	CYCLE PERIOD	VOLTAGE APPLIED	CYCLE NO.	CURRENT TOTAL	CONCENTRATION		SEPARATION FACTOR	REMARKS
									BRINE	DIALYSATE		
# [-]	c_0 [ppm]	δ [-]	v [cm/sec]	τ [sec]	T [sec]	$\Delta\Phi$ [volt]	nc [-]	I [ampere]	x_B [-]	x_T [-]	ns [-]	L = limit reached NL = limit not reached δ_B/δ_T = dead volumes
2	1050	1.10	1.21	-	53.3	6	7	0.37	0.995	0.999	1.00	NL
5	1090		1.21		53.3		8	0.35	1.005	1.000	1.01	NL
3	1040		1.77		36.4		8	0.39	0.999	0.996	1.00	NL
4	1050		2.33		27.6		9	0.40	0.998	1.000	1.00	NL
7	1090	1.73	1.21	-	84.3	6	9	0.37	1.02	0.938	1.09	L
8	1090		1.66		61.4		12	0.39	1.01	0.955	1.06	L
9	1080		2.62		39.0		10	0.41	1.01	0.972	1.04	L
36	700	1.00	0.65	-	93.8	12.5	8	0.50	1.04	0.935	1.11	L
35	700		1.21		50.2		9	0.55	0.96	0.96	1.00	L
32	720		1.77		34.3		6	0.55	0.95	0.97	0.98	L
33	710		2.33		26.1		10	0.60	0.965	0.985	0.98	L
34	700		2.89		21.0		9	0.65	0.975	0.990	0.985	L

Table 21

Effect of Superficial Velocity (v) on EDI-S2-16, EDI-S3-12

1	2	3	4	5	6	7	8	9	10	11	12	13
RUN NO.	CONCENTR. INITIAL	VOLUME DISPLACED	VELOCITY SUPERFICIAL	PAUSE TIME	CYCLE PERIOD	VOLTAGE APPLIED	CYCLE NO.	CURRENT TOTAL	CONCENTRATION		SEPARATION FACTOR	REMARKS
									BRINE	DIALYSATE		
# [-]	c_0 [ppm]	δ [-]	v [cm/sec]	τ [sec]	T [sec]	$\Delta\Phi$ [volt]	nc [-]	I [ampere]	x_B [-]	x_T [-]	ns [-]	L = limit reached NL = limit not reached δ_B/δ_T = dead volumes
5-2	1250	0.61	0.49	25	111	32	40	0.40	1.46	0.158	9.24	L, δ_B = 1.84
5-1			0.92		72		21	0.50	1.41	0.179	7.88	L, δ_B = 1.84
5-3			1.77		67		50	0.45	1.44	0.176	8.18	NL, δ_B = 1.84
												EDI-S3-12
6-2	1280	0.29	0.49	10	50	32	70	0.55	1.39	0.106	13.17	L, δ_B = 2.06
6-1			0.92		36		60	0.60	1.38	0.111	12.48	NL, δ_B = 2.06
6-0			1.83		31		50	0.65	1.36	0.131	10.41	L, δ_B = 2.06

Table 22

Effect of Superficial Velocity (v) on EDI-S3-13

1	2	3	4	5	6	7	8	9	10	11	12	13
RUN NO.	CONCENTR. INITIAL	VOLUME DISPLACED	VELOCITY SUPERFICIAL	PAUSE TIME	CYCLE PERIOD	VOLTAGE APPLIED	CYCLE NO.	CURRENT TOTAL	CONCENTRATION		SEPARATION FACTOR	REMARKS
									BRINE	DIALYSATE		
# [-]	c_0 [ppm]	δ [-]	v [cm/sec]	τ [sec]	T [sec]	$\Delta\Phi$ [volt]	nc [-]	I [ampere]	x_B [-]	x_T [-]	ns [-]	L = limit reached NL = limit not reached δ_B/δ_T = dead volumes
15	1265	0.50	0.50	10	68	22	28	0.62	2.14	0.239	8.93	NL
3	1228		0.95		45		36	0.77	2.08	0.278	7.46	NL
16	1275		1.40		37		34	0.80	2.08	0.248	8.35	NL
25	1250		1.40		37		35	0.81	2.14	0.228	9.35	NL
17	1270		1.85		33		45	0.79	2.10	0.242	8.71	L
32	1290		1.85		33		30	0.81	2.15	0.230	9.33	L
18	1180		2.36		30		45	0.70	2.12	0.240	8.83	L
31	1300		2.36		30		30	0.80	2.16	0.233	9.27	L
20	1185	0.50	0.27	0.6	90	22	45	0.60	1.72	0.350	4.91	L
19	1195		0.50		50		50	0.87	1.26	0.540	2.33	L
21	1205		1.85		14		160	1.69	0.90	0.856	1.05	NL

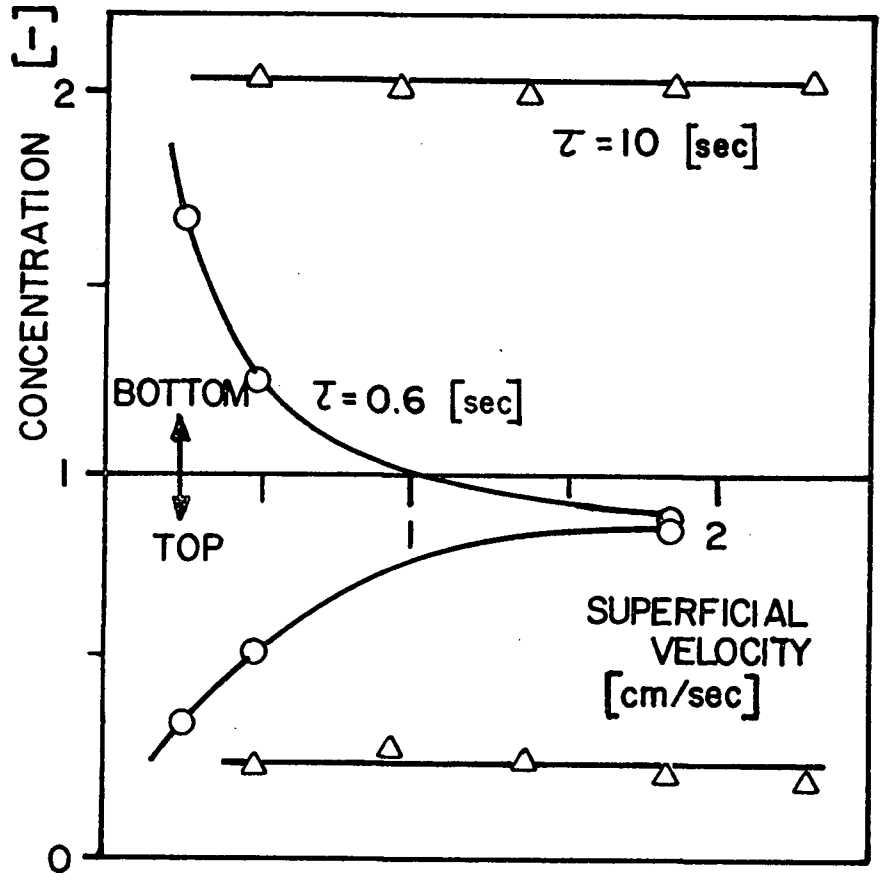

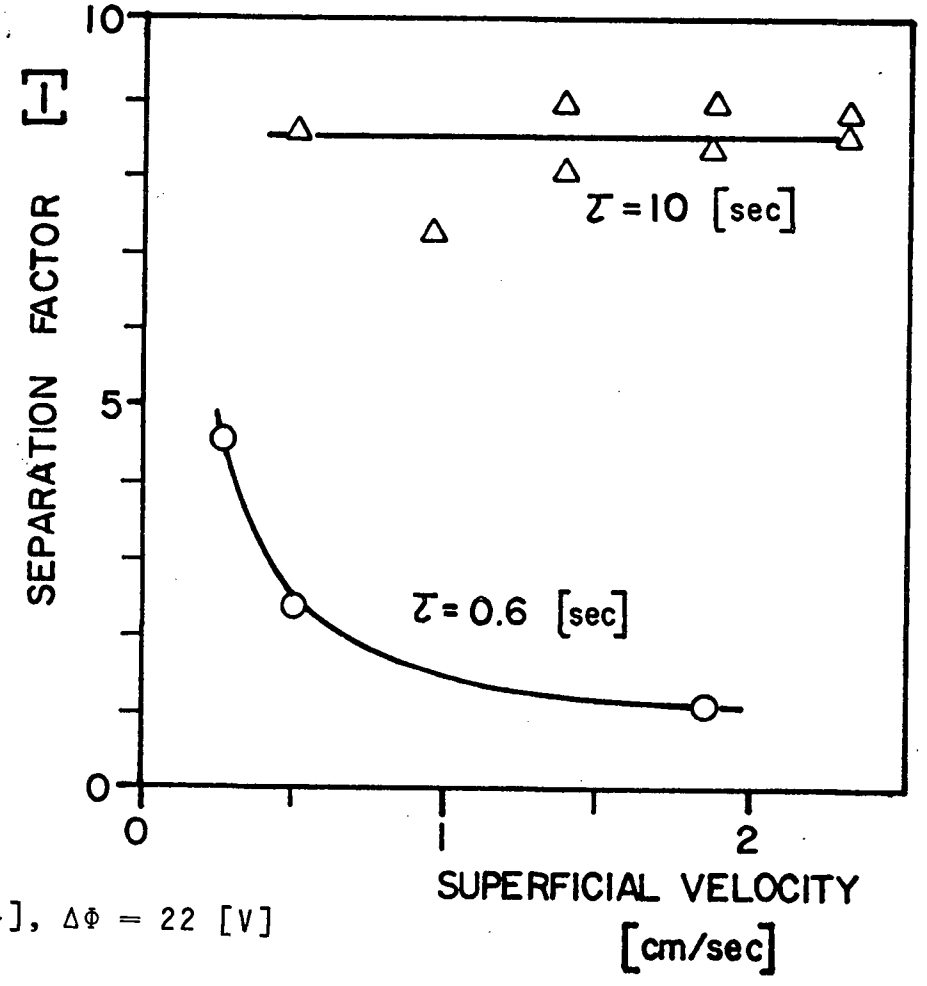

c_0 = 1250 [ppm], δ = 0.5 [-], $\Delta\Phi$ = 22 [V]

Figure 48.

Effect of superficial velocity (v) on final reservoir concentrations for pause and no-pause operation. EDI-S3-13/#15,3,16,25,17,32,18,31 and EDI-S3-13/#20,19,21.

Figure 49.

Effect of superficial velocity (v) on final separation factors for pause and no-pause operation. EDI-S3-13/#15,3,16,25,17,32,18,31 and EDI-S3-13/#20,19,21.

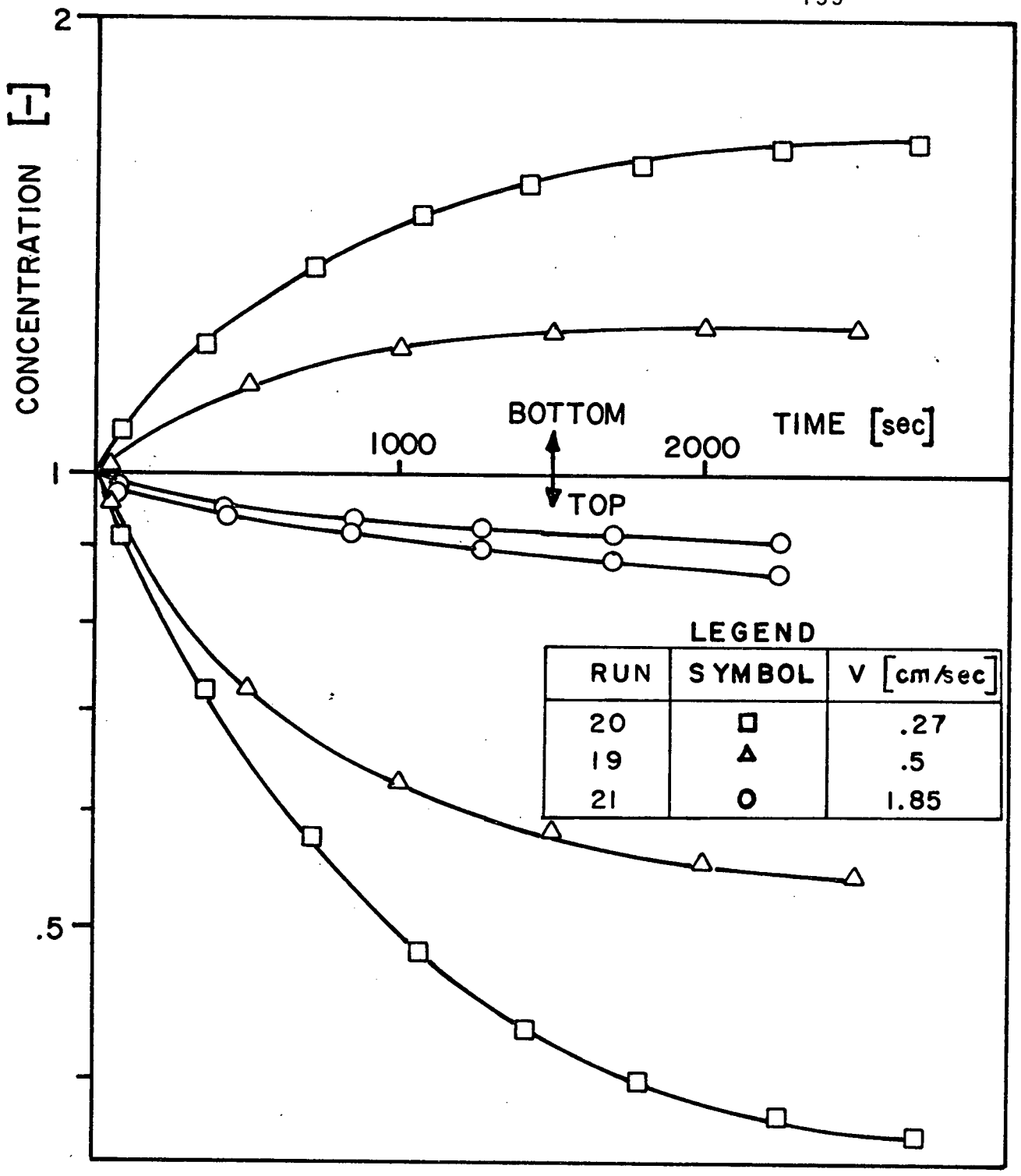

c_0 = 1250 [ppm], δ = 0.5 [-], τ = 0.60 [sec], $\Delta\Phi$ = 22 [V]

Figure 50. Effect of superficial velocity (v) on concentration transients for no-pause operation. EDI-S3-13.

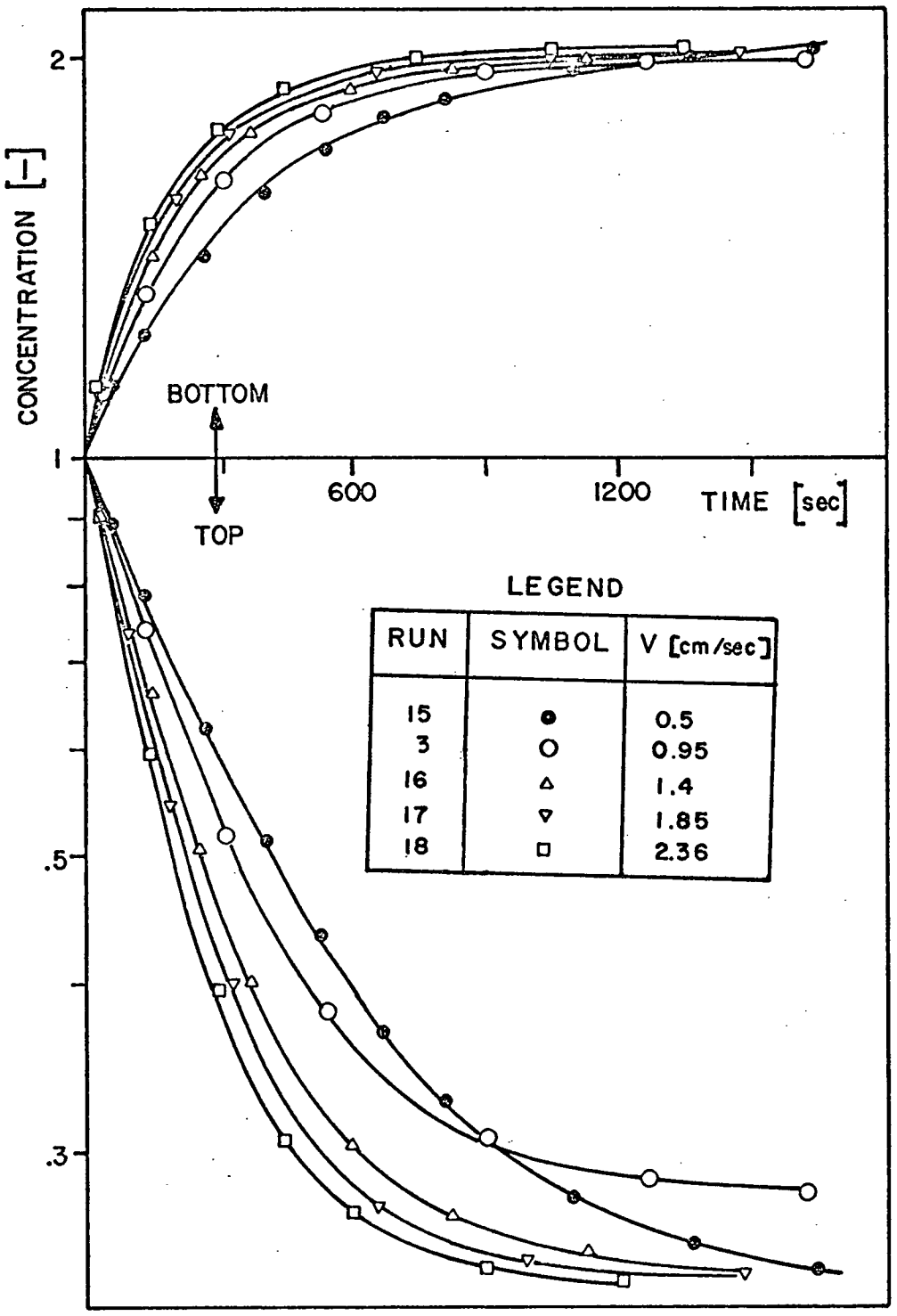

c_0 = 1250 [ppm], δ = 0.5 [-], τ = 10.0 [sec], $\Delta\Phi$ = 22 [V]

Figure 51. Effect of superficial velocity (v) on concentration transients for pause operation. EDI-S3-13.

5.3.5 Effect of displaced volume.

The displaced volume (δ) was varied in three groups of experiments. Table 23 summarizes operating parameters and final conditions. Figures 52 and 53 show, respectively, the effect of displaced volume on final reservoir concentrations and final separation factor for the group of experiments with 10 seconds pause time. The real time transients of top and bottom reservoir concentrations are illustrated in Figure 54 for the same group of experiments. Figure 55 shows analoguous real time transients for two experiments with no pause time.

Reducing the displaced volume (δ) has the following effects.

1. No-pause operation: The final separation is reduced. Most of the reduction occurs during the first cycle. The final current is unaffected.

2. Pause operation (τ = 10 [sec]): The final separation is improved. The rate of separation is slowed down. The final current is reduced.

These results agree with a model in which finite mass transfer rates are controlling, and may be explained as follows using this model.

1. For no-pause operation: Most of the separation occurs during the first cycle as shown in Chapter 3. The

local effluent concentration during the first half cycle decreases monotonically with time. The average effluent concentration therefore also decreases monotonically with time. Reducing the displaced volume shortens the duration of each half cycle. Thus, the mean value of the effluent concentration during the first half cycle is reduced. Since the overall concentration changes are generally small, the current consumption is unaffected.

2. For pause operation: Two limiting situations may be considered. When the displacement is very large the cycle time increases and the ratio of pause time to cycle time approaches zero. The initial influence of the pause time on the effluent concentration, therefore, gradually disappears. The other limit is obtained as the displaced volume approaches zero. In this case the system would be expected to respond more and more as to a pure pause operation, i.e. exponential decay of the dialysate concentration. The results confirm this trend. The limited final concentrations for finite displacement are caused by dispersion effects: When the displaced volume is large the concentration front emerges from the stack. The part of the front that emerges becomes completely dispersed in the well mixed dialysate reservoir. Similarly, during reversed flow, low concentrated solution breaks through into the well mixed brine reservoir and becomes completely dispersed

Table 23

Effect of Displaced Volume (δ) on EDI-S1-8, EDI-S2-15 and EDI-S3-13

1	2	3	4	5	6	7	8	9	10	11	12	13
RUN NO.	CONCENTR. INITIAL	VOLUME DISPLACED	VELOCITY SUPERFICIAL	PAUSE TIME	CYCLE PERIOD	VOLTAGE APPLIED	CYCLE NO.	CURRENT TOTAL	CONCENTRATION		SEPARATION FACTOR	REMARKS
									BRINE	DIALYSATE		
ℓ [-]	c_0 [ppm]	δ [-]	v [cm/sec]	τ [sec]	T [sec]	$\Delta\Phi$ [volt]	nc [-]	I [ampere]	x_B [-]	x_T [-]	ns [-]	L = limit reached NL = limit not reached δ_B/δ_T = dead volumes
14	1020	1.00	1.21	-	50.2	6	7	0.32	0.969	0.983	0.99	NL
15-0	1020	1.00			50.2		9	0.32	0.970	0.997	0.97	L
40	760	1.00			50.2		8	0.28	0.986	0.995	0.99	L
2	1050	1.10			53.3		7	0.37	0.995	0.999	1.00	NL
5	1090	1.10			53.3		8	0.35	1.005	1.000	1.01	NL
7	1090	1.73			84.3		9	0.37	1.02	0.938	1.09	L
												EDI-S2-15
22	1050	0.50	0.88	0	28	40	10	1.25	0.98	0.95	1.03	L, δ_B = 1.5
17	1025	1.00			55		10	1.30	1.14	0.747	1.52	L
29	1070	1.54			84		6	1.05	1.20	0.670	1.80	L
												EDI-S3-13
4	1240	0.25	0.95	10	34	22	65	0.73	2.34	0.236	9.90	NL
3	1230	0.50			45		36	0.77	1.99	0.278	7.15	NL
2	1250	1.00			71		18	0.85	1.56	0.398	3.93	L
12	1280	1.00			71		20	0.87	1.57	0.372	4.22	L
5	1270	1.50			96		10	0.91	1.31	0.531	2.46	L

c_0 = 1250 [ppm], v = 0.95 [cm/sec], τ = 10 [sec], $\Delta\Phi$ = 22 [V]

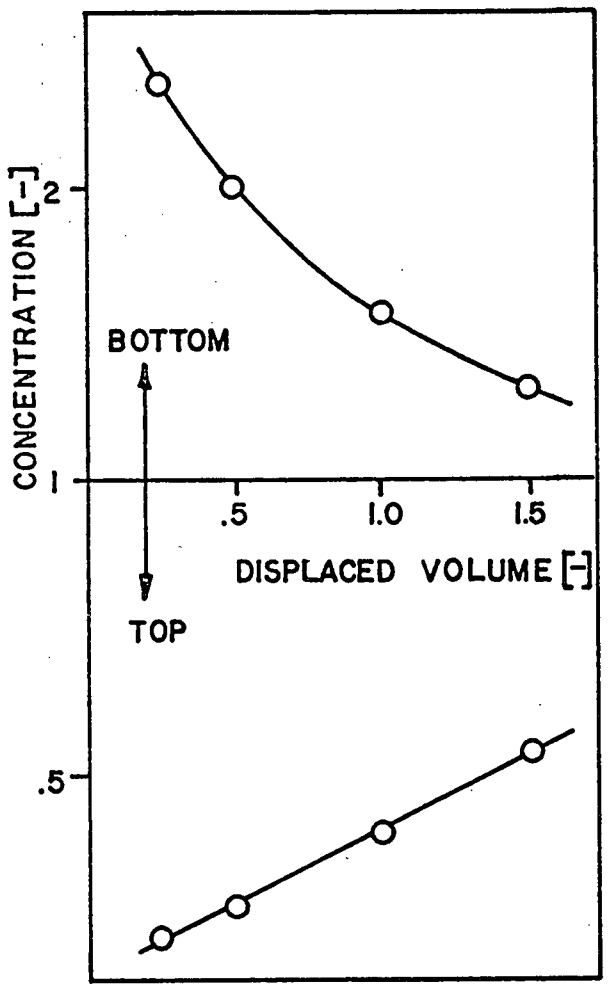

Figure 52.

Effect of displaced volume (δ) on final reservoir concentrations for pause operation. EDI-S3-13/#4,3,2,12,5.

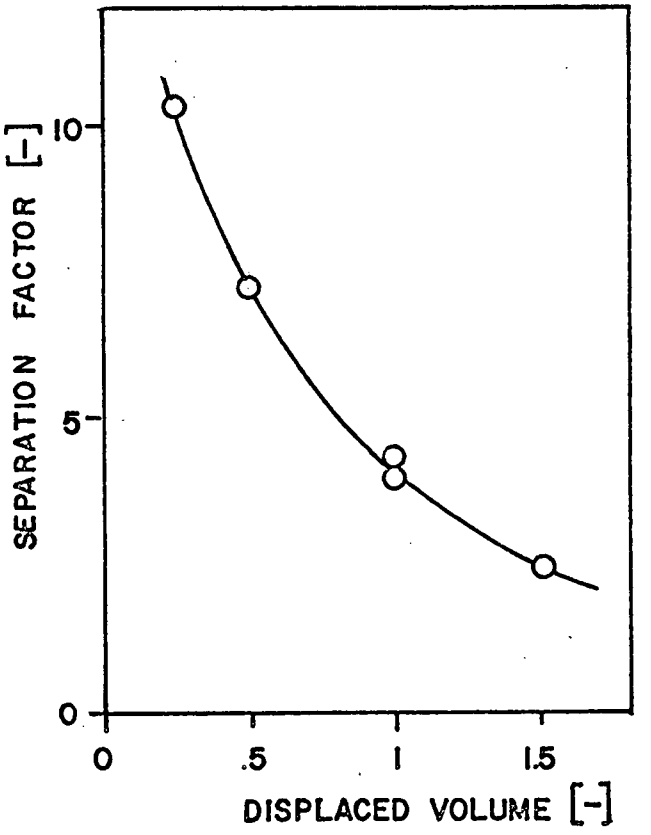

Figure 53.

Effect of displaced volume (δ) on final separation factor for pause operation. EDI-S3-13/#4,3,2,12,5.

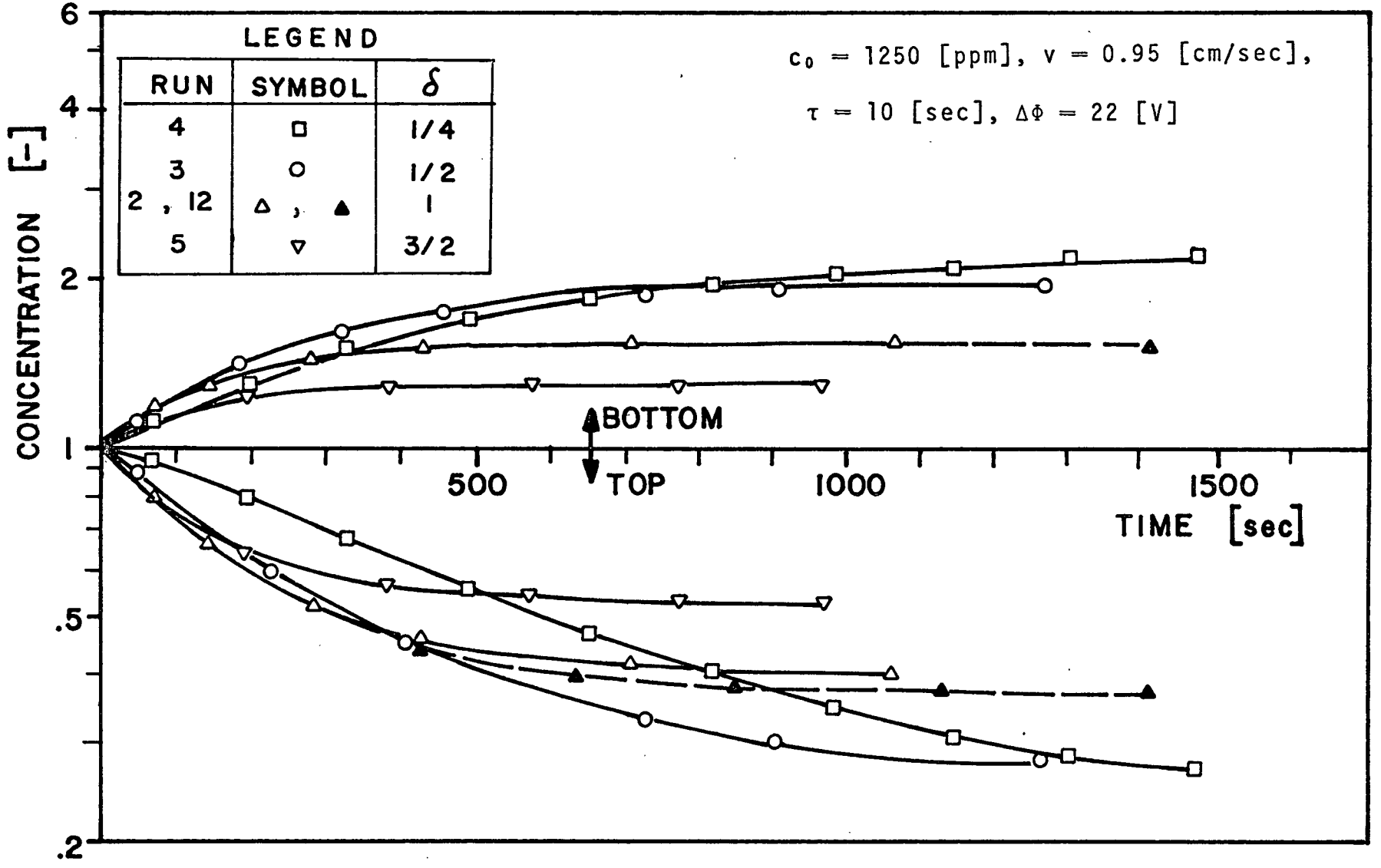

Figure 54. Effect of displaced volume (δ) on concentration transients for pause operation. EDI-S3-13.

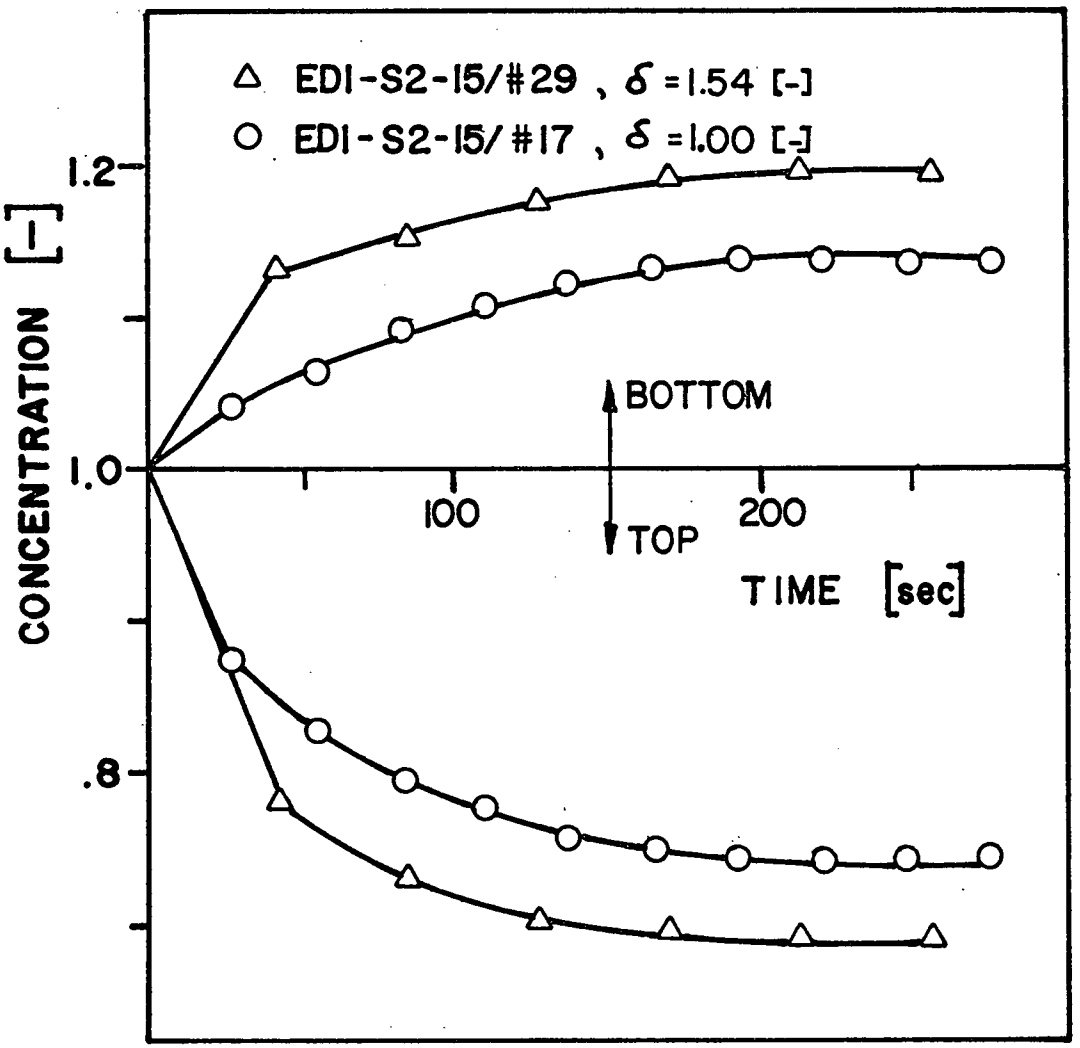

c_0 = 1050 [ppm], v = 0.88 [cm/sec], τ = 0.0 [sec], $\Delta\Phi$ = 40 [V]

Figure 55. Effect of displaced volume (δ) on real time transients for no-pause operation.

therein. When the displaced volume is small enough to prevent breakthrough, dispersion is restricted to mixing, bypassing and channeling in the stack. These internal dispersion effects are always present and will be discussed in detail under 5.3.7.

5.3.6 Effect of dead volumes.

The experiments with variable dead volumes* in the end reservoirs are grouped in Table 24. These results, together with the real time transients of the product concentrations for the first group (see Figure 56) and the third group (see Figure 57) of Table 24 may be summarized as follows:

1. The presence of dead volumes does not influence the final separation factor.

2. If the dead volumes are equal the final product concentrations are unchanged. The rate of separation is slowed down, however, as the dead volumes in each reservoir are increased.

3. Experiments with equal total dead volume but unequal dead volumes in the reservoirs show that the final concentrations are lower and the current consumption much smaller when $\delta_B > \delta_T$, and vice versa when $\delta_B < \delta_T$. This confirms the concept of a developing concentration wave, which

*Or excess volumes.

Table 24

Effect of Dead Volumes (δ_B/δ_T) on EDI-S2-15, EDI-S3-12 and EDI-S3-13

1	2	3	4	5	6	7	8	9	10	11	12	13
RUN NO.	CONCENTR. INITIAL	VOLUME DISPLACED	VELOCITY SUPERFICIAL	PAUSE TIME	CYCLE PERIOD	VOLTAGE APPLIED	CYCLE NO.	CURRENT TOTAL	CONCENTRATION		SEPARATION FACTOR	REMARKS
									BRINE	DIALYSATE		
# [-]	c_0 [ppm]	δ [-]	v [cm/sec]	τ [sec]	T [sec]	$\Delta\Phi$ [volt]	nc [-]	I [ampere]	x_B [-]	x_T [-]	ns [-]	L = limit reached NL = limit not reached δ_B/δ_T = dead volumes
19	1020	0.5	1.70	7	28	40	14	1.40	1.72	0.529	3.24	L, δ_B = 0.0, δ_T = 0.0
20	1040						15	1.30	1.50	0.463	3.24	L, δ_B = 0.5, δ_T = 0.0
21	980						22	1.35	1.54	0.568	2.72	NL, δ_B = 1.0, δ_T = 1.0
												EDI-S3-12
2-0	1220	0.59	0.92	15	62	32	20	0.90	2.04	0.265	7.72	L
-1				25	82		25	0.70	2.21	0.217	10.20	L
-2			0.49	25	111		31	0.62	2.32	0.175	13.28	L
3-0	1230		0.92	15	62		16	0.80	1.37	0.194	7.06	L, δ_B = 1.75, δ_T = 0.0
-1				25	82		24	0.60	1.43	0.136	10.52	L, δ_B = 1.75, δ_T = 0.0
-2			0.49	25	111		30	0.50	1.47	0.110	13.40	L, δ_B = 1.75, δ_T = 0.0
												EDI-S3-13
32	1290	0.5	1.85	10	33	22	30	0.81	2.15	0.230	9.33	L, δ_B = 0.0, δ_T = 0.0
33	1280						60	0.77	2.05	0.217	9.43	L, δ_B = 0.5, δ_T = 0.5
34	1200						70	0.71	1.99	0.235	8.44	NL, δ_B = 1.0, δ_T = 1.0
35	1200						40	0.60	1.57	0.171	9.16	L, δ_B = 1.0, δ_T = 0.0
36	1260						60	1.00	2.82	0.326	8.66	NL, δ_B = 0.0, δ_T = 1.0

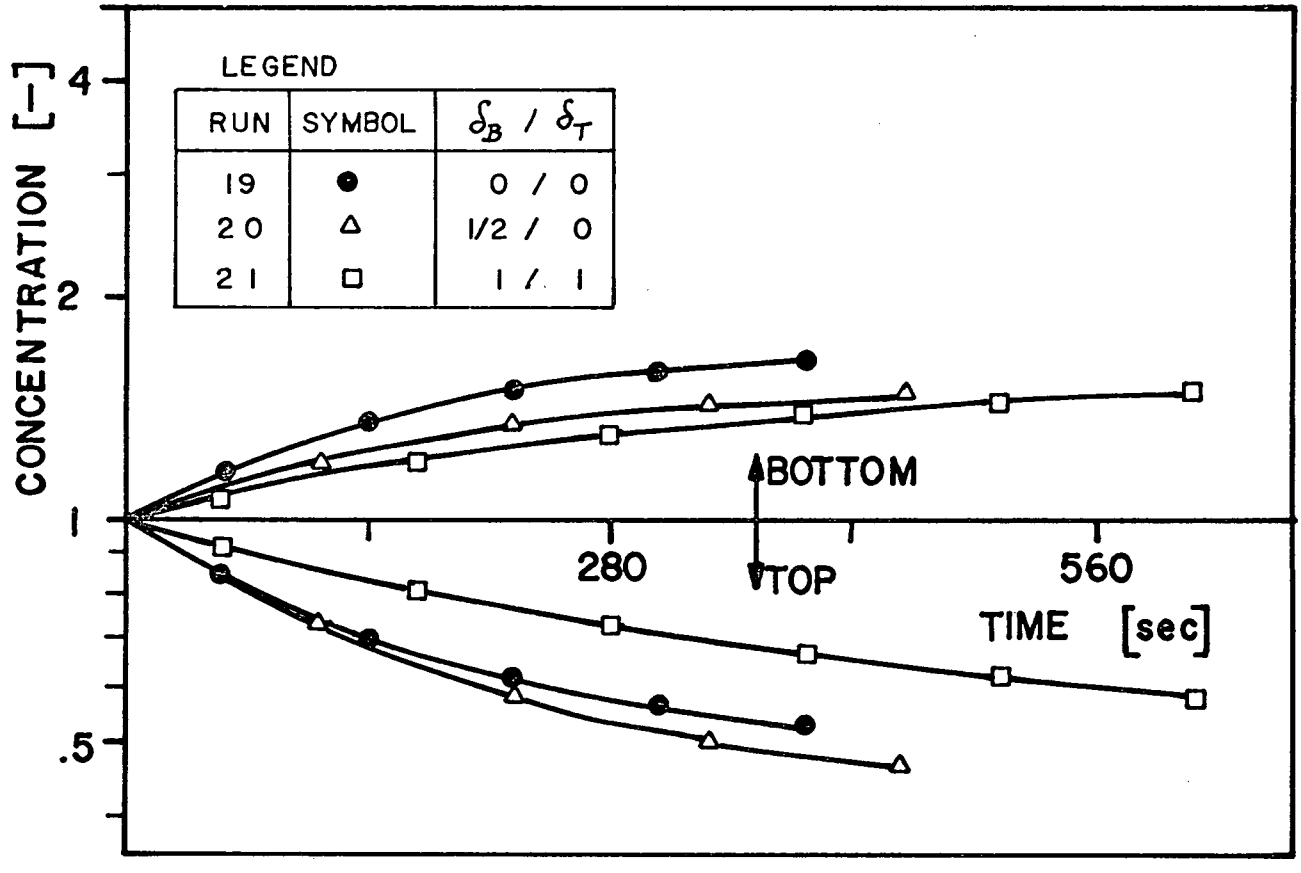

c_0 = 1000 [ppm], δ = 0.5 [-], v = 1.70 [cm/sec], τ = 7.0 [sec], $\Delta\Phi$ = 40 [V]

Figure 56. Effect of dead volumes (δ_B/δ_T) on concentration transients. EDI-S2-15.

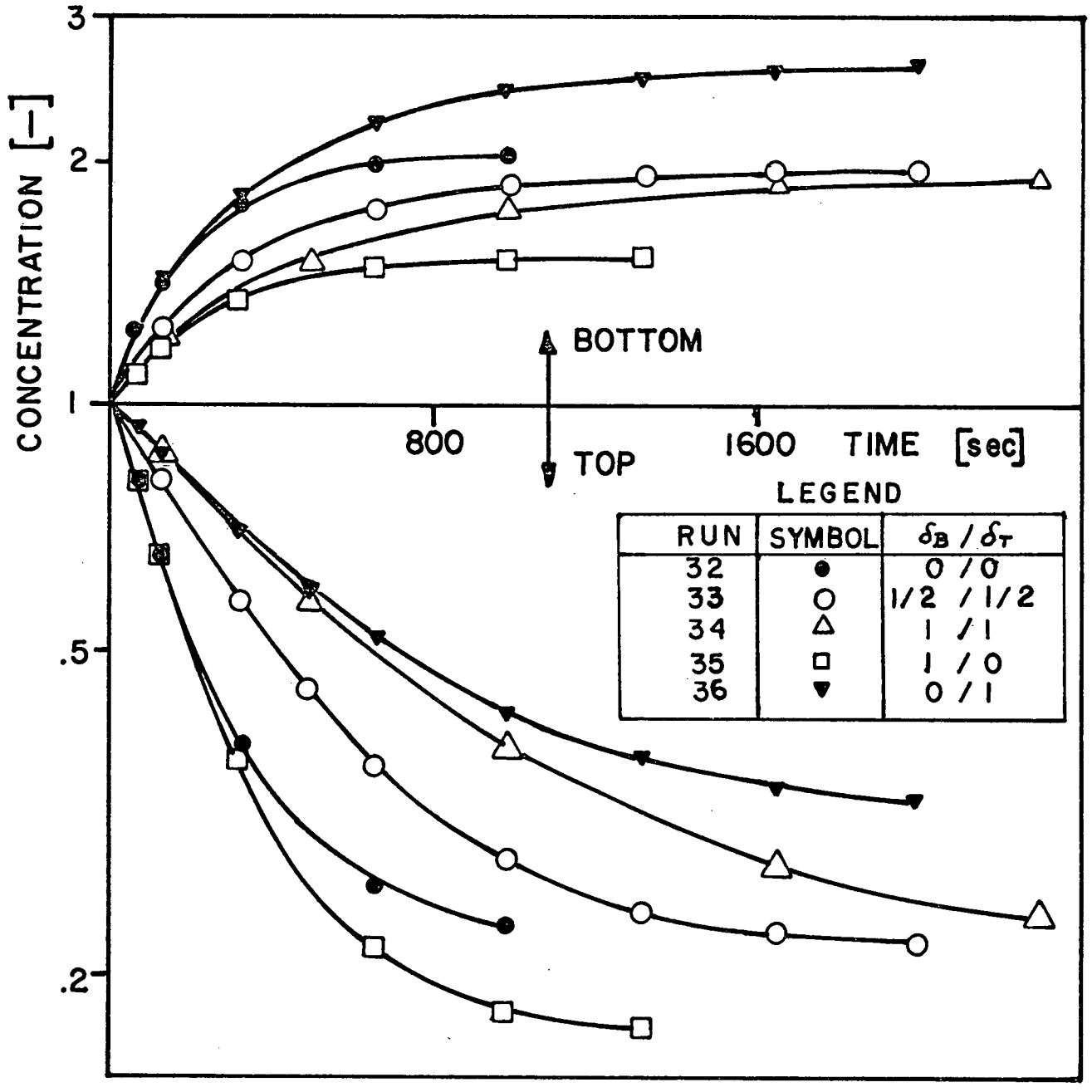

c_0 = 1250 [ppm], δ = 0.5 [-], v = 1.85 [cm/sec], τ = 10.0 [sec], $\Delta\Phi$ = 22 [V]

Figure 57. Effect of dead volumes (δ_B/δ_T) on concentration transients. EDI-S3-13.

is pushed out into the brine reservoir. A large reservoir volume means a small concentration change. Since the front reenters the electrodialyzer during every odd half cycle, the current consumption is smaller if the front has a low concentration.

4. A "salting factor" may be defined as the amount of solute added to the brine product and a "desalting factor" as the amount removed from the dialysate product. The factors are normalized with respect to the initial solute concentration and the displaced volume:

$$P_D = \frac{(c_T - c_0)(\delta v_0 + v_T)}{c_0\ \delta v_0} = \left(x_T - 1\right)\left(1 + \frac{v_T}{\delta v_0}\right) = \left(x_T - 1\right)\left(1 + \frac{\delta_T}{\delta}\right)$$

$$P_S = \frac{(c_B - c_0)(\delta v_0 + v_B)}{c_0\ \delta v_0} = \left(x_B - 1\right)\left(1 + \frac{\delta_B}{\delta}\right)$$

A plot of these factors as functions of real time shows that the device could be used as a continuous solute pump. If the reservoir volumes were infinite and well mixed, a constant amount of salt would be removed from one reservoir and added to the opposite one during each cycle (see Figure 58).

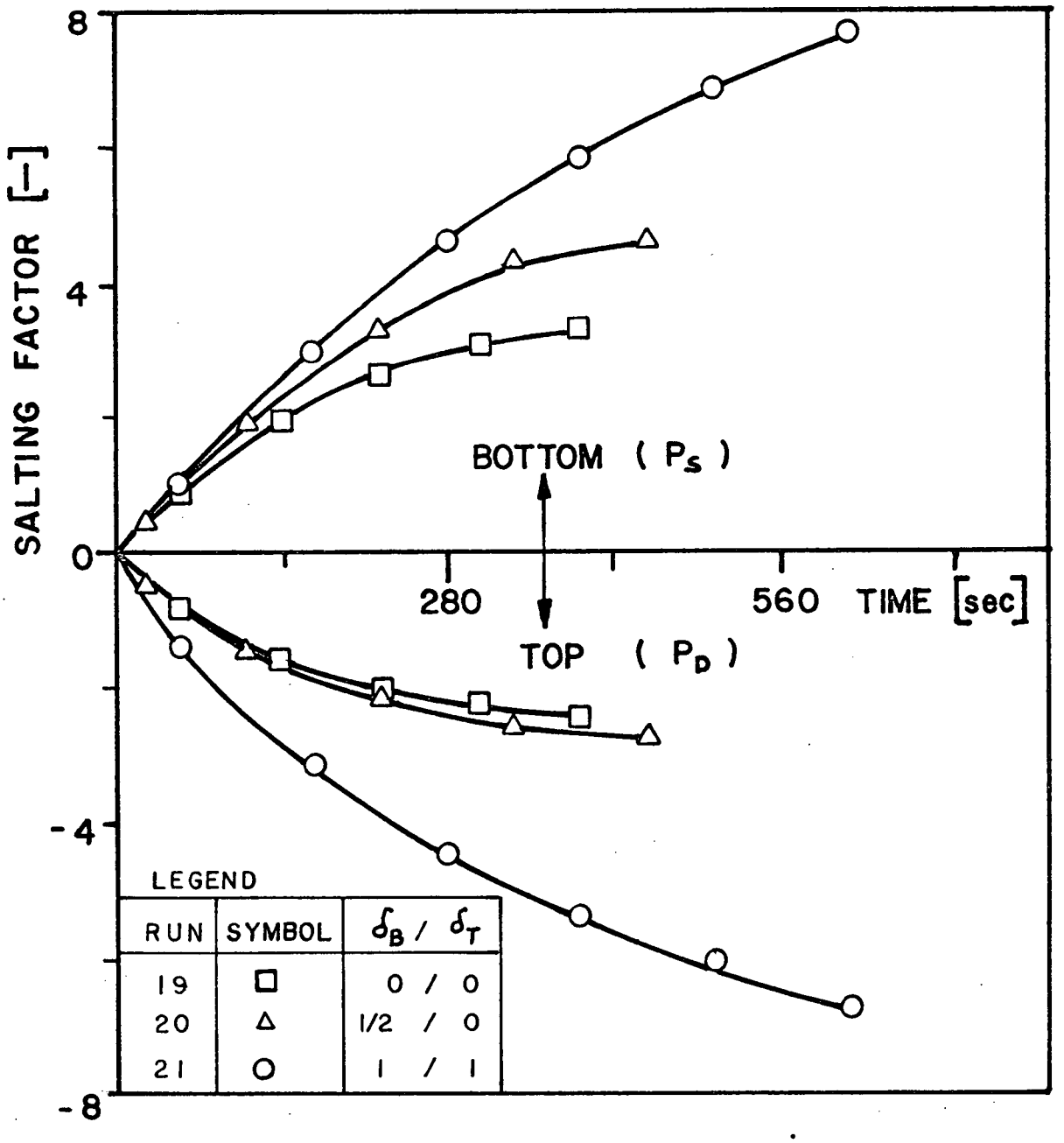

$c_0 = 1250$ [ppm], $\delta = 0.5$ [-], $v = 1.85$ [cm/sec], $\tau = 10.0$ [sec], $\Delta\Phi = 22$ [V]

Figure 58. Effect of dead volumes (δ_B/δ_T) on salting factor transients. EDI-S2-15.

5.3.7 Effect of initial concentration.

The initial concentration (c_0) was changed from ~ 1250 ppm to ~ 5000 ppm $NaCl/H_2O$ in three groups of experiments (see Table 25). At the same time the concentration of the rinse solution was increased from 2,000 to 10,000 ppm in order to maintain the same ratio between the resistances of the two solutions. In all cases the higher c_0 had a retarding effect on the transients (see Figure 59,60,61). The limiting separation factor was reduced for the EDI-S3-13 runs which had shorter pause times and a smaller applied voltage than the EDI-S2-12 group.

The reasons for this behaviour are:

1. The higher concentration requires proportionally larger mass transfer rates to achieve the same separation. The overpotentials which are necessary to maintain the increased electrode current densities reduce the effective stack voltage (see also Figure 36).

2. The specific conductivity of ion exchange membranes is more or less independent of the solution concentration in the range investigated (D'Alessandro, 1971). This constant resistance term reduces the current density (compare with equation (23), Section 3.3.

If the pause times are long or the voltage high, these effects are less pronounced (Figure 59).

Table 25

Effect of Initial Concentration (c_0) on EDI-S3-12 and EDI-S3-13

1	2	3	4	5	6	7	8	9	10	11	12	13
RUN NO.	CONCENTR. INITIAL	VOLUME DISPLACED	VELOCITY SUPERFICIAL	PAUSE TIME	CYCLE PERIOD	VOLTAGE APPLIED	CYCLE NO.	CURRENT TOTAL	CONCENTRATION		SEPARATION FACTOR	REMARKS
									BRINE	DIALYSATE		
# [-]	c_0 [ppm]	δ [-]	v [cm/sec]	τ [sec]	T [sec]	$\Delta\Phi$ [volt]	nc [-]	I [ampere]	x_B [-]	x_T [-]	ns [-]	L = limit reached NL = limit not reached δ_B/δ_T = dead volumes
4-0	1245	0.59	0.92	15	62	32	16	0.90	2.03	0.259	7.85	L
-1				25	82		23	0.70	2.17	0.218	9.97	L
10-0	4680			15	62		15	3.20	—	0.273	—	L
-1				25	82		20	2.80	2.00	0.205	10.00	L
												EDI-S3-13
6	1300	1.00	0.95	5	61	10	17	0.62	1.31	0.603	2.18	L
37	4640						15	1.65	1.15	0.684	1.68	L
26	1260	0.50	1.40	10	37	10	40	0.54	1.83	0.344	5.33	L
39	4890						35	1.54	1.54	0.462	3.33	NL

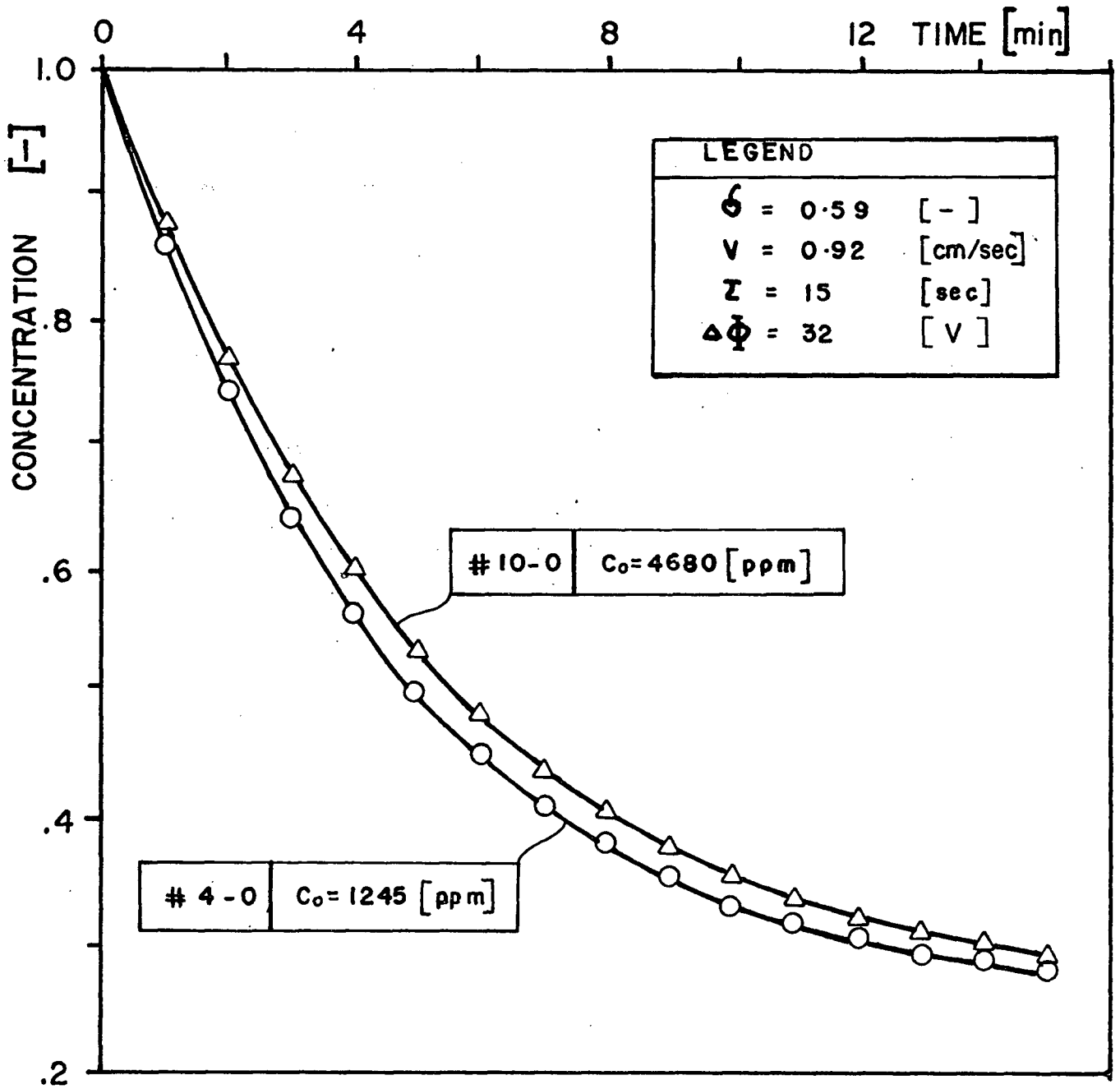

Figure 59. Effect of initial concentration (c_0) on dialysate concentration transients. EDI-S3-12.

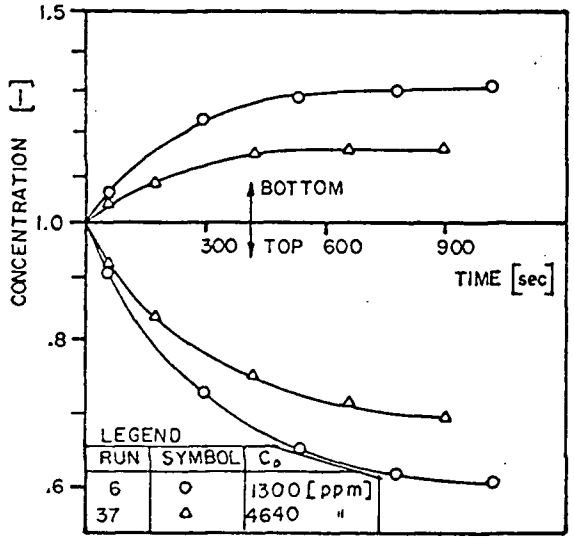

δ = 1.0 [-], v = 0.95 [cm/sec], τ = 5.0 [sec], Δφ = 10 [V]

Figure 60. Effect of initial concentration (c_0) on concentration transients. EDI-S3-13.

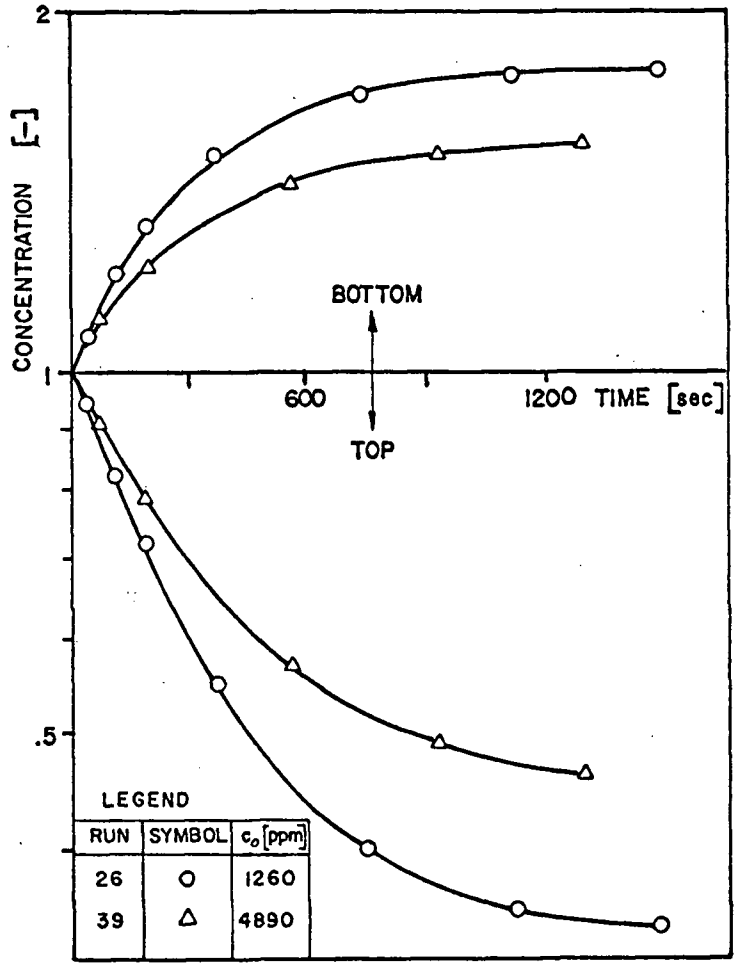

δ = 0.5 [-], v = 1.40 [cm/sec], τ = 10.0 [sec], Δφ = 10 [V]

Figure 61. Effect of initial concentration (c_0) on concentration transients. EDI-S3-13.

5.3.8 Effect of internal flow distribution and axial dispersion.

The flow distribution and longitudinal mixing were measured using a step response method. Flow systems with axial dispersion have often been simulated by models based on distributions of residence times. The concept has been discussed by Danckwerts (1953) who also measured the axial diffusion coefficient by a method which involved the response function of a system to a step change in concentration at the inlet. Kramers and Alberda (1953) proposed a mixing cell model and measured the axial mixing by a frequency response method, which was also employed by McHenry and Wilhelm (1957). Aris (1957) showed that the mixing cell model and the continuous model using an axial diffusion coefficient coincide for more than about 25 mixing cells. The mixing cell concept was further advanced by Young (1957), Epstein (1958), and many others. Young (1957), in particular, gives an analytical expression for the effluent response of m equal mixing tanks to a step change of the inlet concentration.

The equation may be modified to account for the inherent dead volumes of the first ED cell design. If these dead volumes are assumed to be well mixed, the normalized effluent concentration is a function of time according to equation (32).

$$\bar{x} = \left(1 - \frac{1}{r - \frac{1}{m}} + \frac{\bar{t}}{r}\right)\left(\frac{r}{r - \frac{1}{m}}\right)^{m} \exp\left(-\frac{\bar{t}}{r}\right) +$$

(32)

$$+ \exp(-m\bar{t}) \sum_{j=0}^{m-1} \frac{(m\bar{t})^{j}}{j!}\left[1 + (m - j)\left(\frac{r}{r - \frac{1}{m}}\right)^{m+1-j} - (m + 1 - j)\left(\frac{r}{r - \frac{1}{m}}\right)^{m-j}\right]$$

where

$r = \frac{v_0 - v_a}{2\ v_a}$ $\qquad$ $v_0 - v_a$ = inherent dead volume

v_a = active stack void volume

$\bar{t} = \frac{t\ Q}{v_a}$ $\qquad$ t = time

Q = flow rate

$\bar{x} = \frac{c - c_1}{c_0 - c_1}$ $\qquad$ c_0 = initial concentration

c_1 = final concentration.

This function was evaluated using a digital computer. The results for $r = 0.04$ are shown in Figure 62. The upper part of the diagram illustrates the function (32), the lower part is the first derivative of (32) w.r.t. time $\bar{t}$. Figure 63 shows the dependence of the maximum slope ($\dot{x}$) on m for two values of r. The curves go through a minimum at $m = 2$,

increase monotonically for larger m, and approach a finite limit which is given by

$$\lim_{m\to\infty} |(\dot{x})| = \frac{1}{r \cdot e}$$

According to equation (32) the response should be independent of the flow rate, the direction of flow, and whether the step is an increase or a decrease in concentration.[+]

The results for tests on the first and third stack versions are presented in Table 26 to 29. The sign of the slopes indicates response to an increasing (+) or a decreasing (-) step. $\bar{t}^*$ is the time at which the maximum slope occurred, and $\bar{x}^*$ the corresponding concentration.

The response curves of the second stack versions could not be evaluated in the same way, since pronounced by-passing was observed. Typical response curves are sketched in Figure 64. The concentration in experiments with EDI-S2-15 decreased very soon after the step had entered the stack, passed through a plateau, and descended finally toward the inlet concentration. Another spacer plus sorption membrane added to the same pack almost eliminated the plateau, but the shape of the curve was not of the F type predicted by a

---

[+]The step response method may be utilized to measure the void volume between the conductivity detectors.

mixing cell model. This may be due to a nonuniform flow distribution.

The spacer screens consisted of a single layer of plastic netting cut parallel to one strand. The solution flowed therefore in many parallel groves rather than through a random packing. The flow rates through the groves varied because the spacing was not controlled accurately.

The response curves of EDI-S1-8 stack most closely resembled those predicted by a mixing cell model (see Table 26). The mean value of the maximum slopes was $\dot{x} = 1.27$ and occurred after $\bar{t}^* = 0.965$. This corresponded to 10 effective mixing stages (see Figure 63).

The third stack was tested with 12 and 13 spacers plus sorption membranes. By-passing (or channelling) was noticed for the former and is manifested in the high value of $\bar{t}^* = 1.11$. The addition of another unit increased the value of the slope from $\dot{x} = 1.26$ to $\dot{x} = 1.42$ and shortened the time lapse to $\bar{t}^* = 1.01$.[+] The effective number of mixing stages is m = 12 or 13, see Figure 63.

The third stack comprised the same spacer screens as the first one. The increased m is a result of the more flexible capacity cells. They distribute the areal compression from the electrode end frames more evenly than the

---

[+]All values averaged.

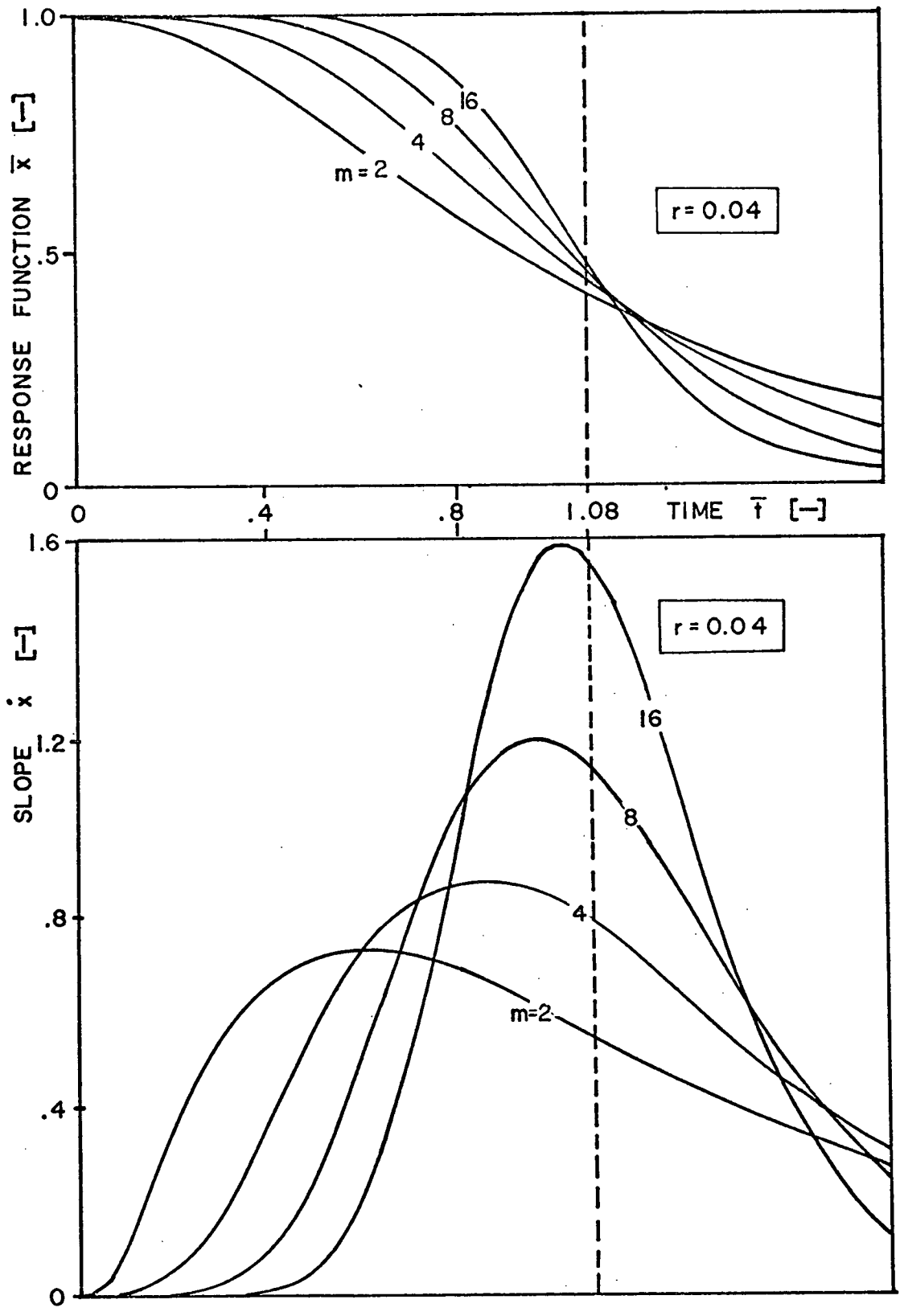

Figure 62. Internal mixing. Effect of number of effective mixing stages (m) on response to step change in feed concentration: (a) response function $\bar{x}(\bar{t})$; (b) slope ($\dot{x}(\bar{t})$) of response curve (dimensionless).

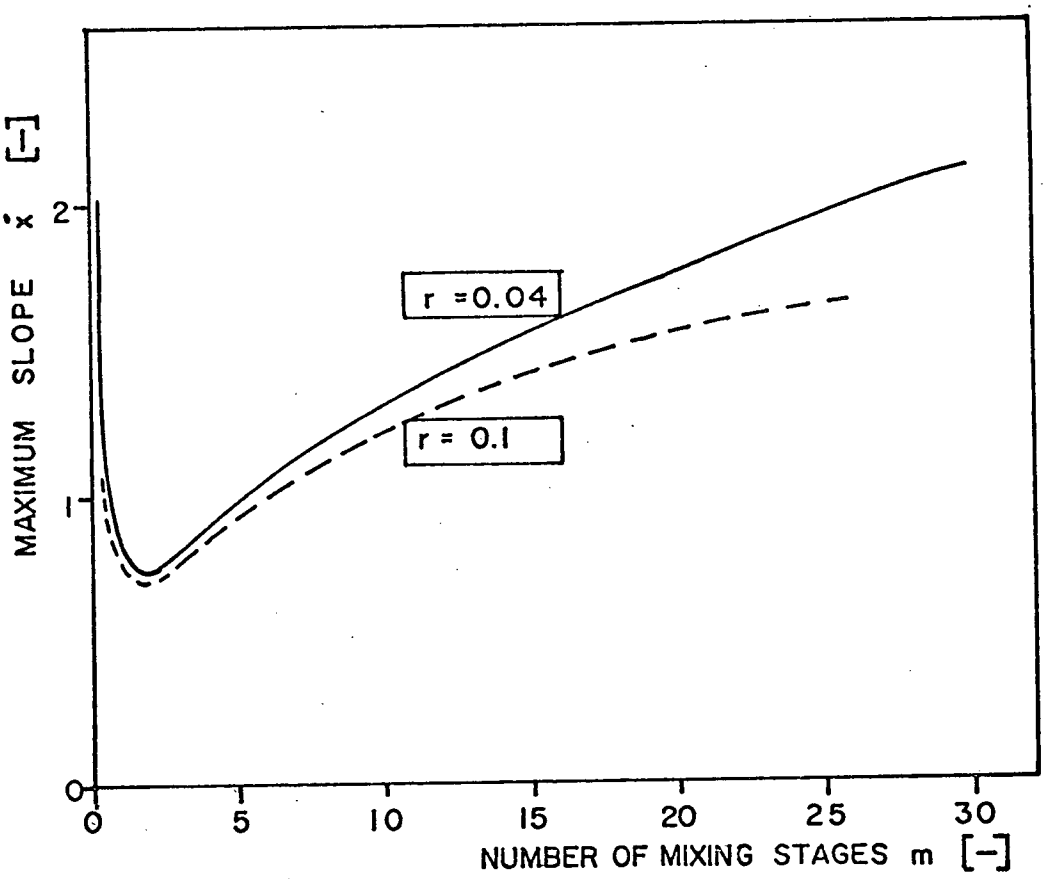

Figure 63. Maximum slope ($\dot{x}$) vs. number of mixing stages (m).

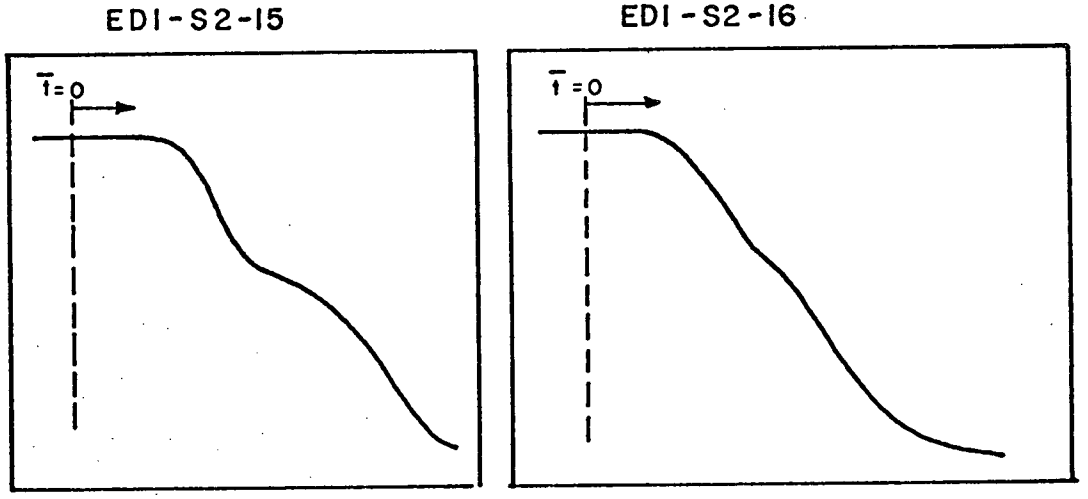

Figure 64. Step response of second stack versions (schematic).

Table 26

Step Response Experiments on EDI-SI-8

Flow Rate Q [cm^3/sec]	Displacement Up/Down [-]	Maximum Slope $\dot{\bar{x}}$ [-]	Time $\bar{t}^*$ [-]	Concentration $\bar{x}^*$ [-]
14.1	Down	-1.27	0.856	0.517
14.1	Up	-1.26	0.960	0.564
14.1	Down	+1.21	1.11	0.423
20.8	Up	-1.38	1.03	0.549
20.8	Down	-1.24	1.02	0.570

Table 27

Step Response Experiments on EDI-S3-12

Runs #1-14

Flow Rate Q [cm^3/sec]	Displacement Up/Down [-]	Maximum Slope $\dot{\bar{x}}$ [-]	Time $\bar{t}^*$ [-]	Concentration $\bar{x}^*$ [-]
14.1	Up	-1.12	1.19	-
14.1	Down	+1.07	1.21	-
20.8	Up	-1.09	1.20	-
20.8	Down	+1.14	1.17	-

Table 28

Step Response Experiments on EDI-S3-12

Runs #15-24

Flow Rate Q [cm^3/sec]	Displacement Up/Down [-]	Maximum Slope $\dot{\bar{x}}$ [-]	Time $\bar{t}^*$ [-]	Concentration $\bar{x}^*$ [-]
7.03	Down	-1.174	1.181	0.592
7.03	Up	+1.210	1.031	0.469
7.03	Down	+1.057	1.159	0.426
7.03	Up	-1.210	1.054	0.570
14.1	Down	-1.148	1.204	0.497
14.1	Up	+1.275	1.024	0.518
14.1	Down	+1.123	1.148	0.512
14.1	Up	-1.131	1.125	0.512
28.3	Down	-1.349	1.155	0.520
28.3	Up	+1.336	1.058	0.568
28.3	Down	+1.227	1.005	0.600
28.3	Up	-1.249	1.155	0.506

Table 29

Step Response Experiments on EDI-S3-13

Flow Rate Q [cm^3/sec]	Displacement Up/Down [-]	Maximum Slope $\dot{\bar{x}}$ [-]	Time $\bar{t}^*$ [-]	Concentration $\bar{x}^*$ [-]
7.03	Down	-1.259	1.049	.604
7.03	Up	+1.416	0.940	.336
7.03	Down	+1.326	1.005	.393
7.03	Up	-1.351	1.020	.596
14.1	Down	-1.468	1.086	.591
14.1	Up	+1.598	0.978	.388
14.1	Down	+1.327	1.032	.340
14.1	Up	-1.427	1.032	.639
28.3	Down	-1.429	0.974	.623
28.3	Up	+1.743	0.967	.451
28.3	Down	+1.374	1.029	.371
28.3	Up	-1.324	1.008	.640

combination of sturdy frames and strengthened spacers present in the first stack. A comparison of the separation runs on the stacks shows that the versions with less axial dispersion, by-passing, channelling, etc. achieved much better separation factors, see Figures 40,41; 44,45; 65.

The internal dispersion effects are, therefore, mainly responsible for the finite separation limit of pause operations. Figure 51 presents further evidence in favour of this interpretation of the results, since the limiting conditions are shown to be independent of the flow rate.

5.3.9 Effect of external mixing in brine reservoir.

Three pairs of experiments were performed on the EDI-S3-12 stack to study the effect of mixing of the efflux concentration on the performance. The first run of each pair had the usual complete mixing of both reservoirs but in the second run the brine reservoir was replaced by a coil of 5/16" I.D. TYGON tubing (8 m long). Consequently, the mixing was reduced. The improvement in separation as well as in power requirement is evident from the results listed in Table 30. The pair #7-#7a shows the least improvement. This is due to the small displaced volume as explained subsequently.

A qualitative picture of the concentration profiles in the reservoirs and in the ED cell at limiting conditions

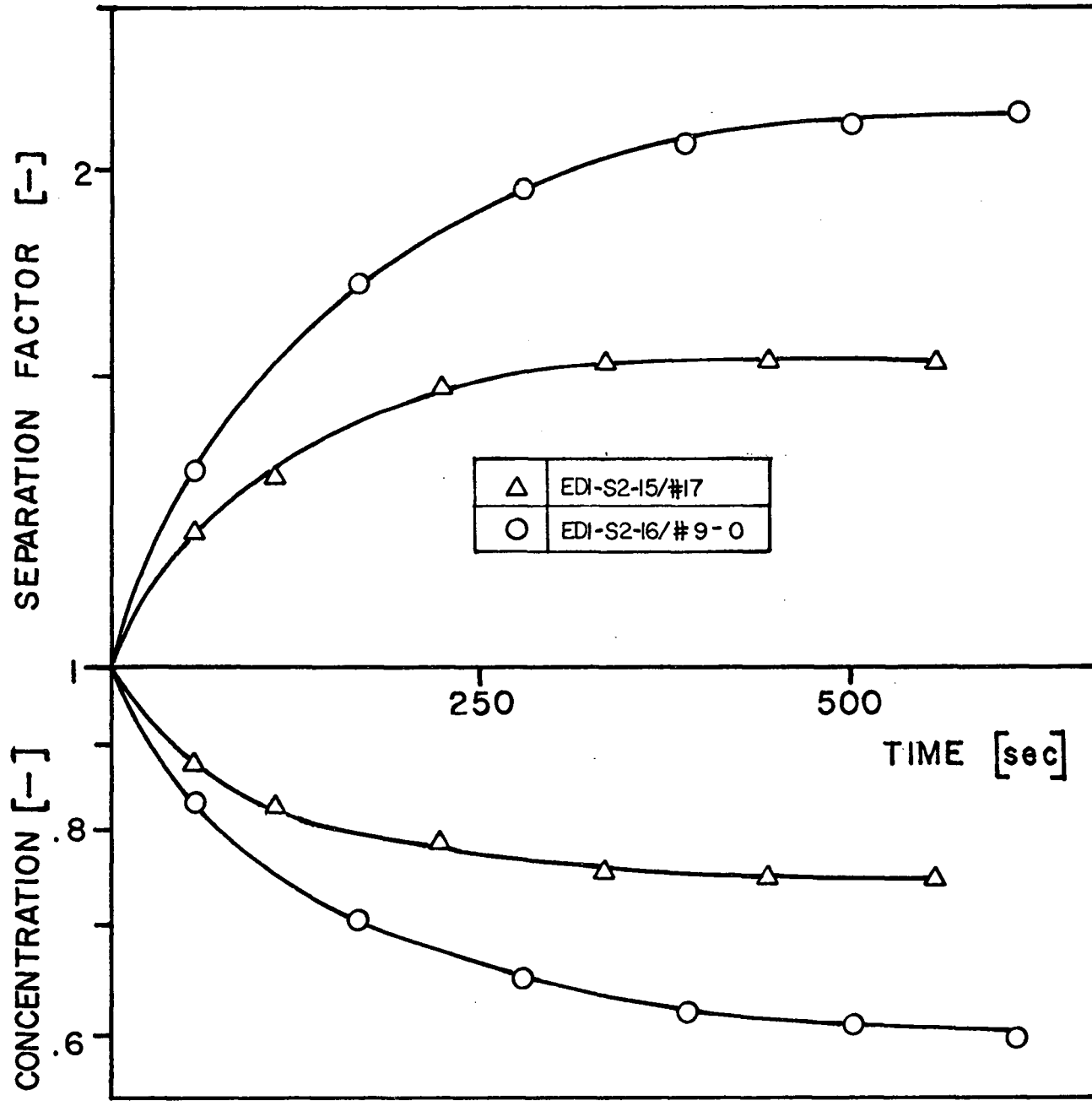

c_0 = 1100 [ppm], δ = 1.0 [-], v = 0.90 [cm/sec], τ = 0.00 [sec], $\Delta\Phi$ = 40 [V]

Figure 65. Effect of internal dispersion. Transients of separation factor and dialysate product concentration for second stack versions.

is presented in Figure 66, which is similarly constructed to Figures 11 and 14 , Section 3.2.1. It is assumed that the end reservoirs are well mixed after each displacement, and that the total void volume of the stack is displaced. The lines are followed through one cycle according to the operating sequence:

(0)	$t = 0$	The ED cell and the brine tank contain solution, the dialysate tank is empty. Dialyzation starts, flow is stopped.
(i)	$t = \tau$	At the end of the first pause time the internal concentration profile is lowered.
(ii)	$t = \frac{T}{2}$	The well mixed brine volume is flowed through the ED cell producing the dialysate profile (ii) which is then well mixed, i.e. the diagonally shaded areas above and below (iii) are equal.
(iii)	$t = \frac{T}{2} + \tau$	The internal profile is raised from (ii) to (iii) during the enriching pause time.
(iv)	$t = T$	The effluent profile (iv) in the brine tank is well mixed to yield (v). Since limiting conditions were assumed (v) coincides with (0) externally, and (iv) with (0) inside the ED cell, and the loop is thus closed.

The cross shaded areas indicate the current requirements to maintain the steady periodic concentration fronts. The dotted lines (with arrows) show the concentration changes of some volume elements as they reciprocate in the module.

Several effects may be explained by this model:

Table 30
Effect of End Mixing on EDI-S3-12

1	2	3	4	5	6	7	8	9	10	11	12	13
RUN NO.	CONCENTR. INITIAL	VOLUME DISPLACED	VELOCITY SUPERFICIAL	PAUSE TIME	CYCLE PERIOD	VOLTAGE APPLIED	CYCLE NO.	CURRENT TOTAL	CONCENTRATION		SEPARATION FACTOR	REMARKS
									BRINE	DIALYSATE		
# [-]	c_0 [ppm]	δ [-]	v [cm/sec]	τ [sec]	T [sec]	$\Delta\Phi$ [volt]	nc [-]	I [ampere]	x_B [-]	x_T [-]	ns [-]	L = limit reached NL = limit not reached δ_B/δ_T = dead volumes
7	1280	0.59	0.49	20	100	32	15	0.85	2.09	0.222	9.38	NL
7a	1280						15	0.75	2.29	0.191	12.00	L, brine unmixed
8	1270	1.00	0.92	20	93	32	10	0.95	1.64	0.376	4.36	L
8a	1270						12	0.75	1.83	0.255	7.18	NL, brine unmixed
11	4560	1.00	0.92	15	83	32	11	3.60	1.52	0.386	3.94	L
11a	4600						15	3.10	1.76	0.267	6.60	L, brine unmixed

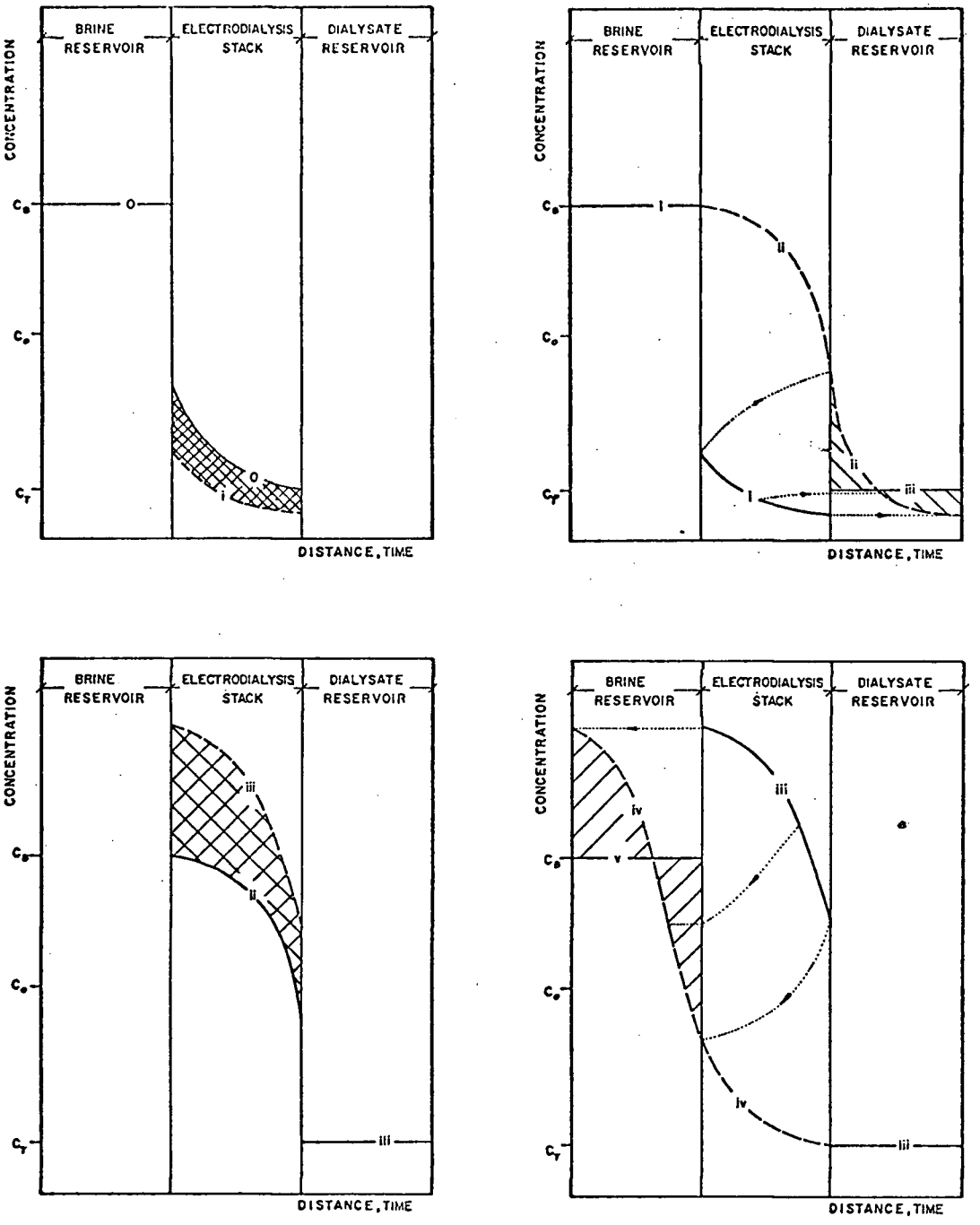

Figure 66. Qualitative model of the concentration profiles in a cyclic electrodialysis process in pause time operation with internal dispersion and well mixed end reservoirs.

1. A preservation of the efflux profile renders the internal dispersion less effective because the gradients are smoother, and the breakthrough occurs later.

2. Smaller displaced volumes also prevent a breakthrough of the fronts.

3. Current consumption is reduced if the high concentration peaks reside only for short time periods in the active ED cell, i.e. if the efflux peaks are preserved.

5.3.10 Effect of capacity cell thickness.

First and third stacks only differ in the construction of the capacity cells. However, a comparison of experiments under similar operating conditions is difficult for two reasons:

1. The effective thickness of the flow channels changed when the frames were removed from the capacity cells. This is probably a result of the increased flexibility of the cells.

2. The internal mixing of the stacks was found to be different (see Section 5.3.8).

The basis of comparison is therefore open to discussion. Only two pairs of experiments were selected from

the data, see Table 31. (Note, the applied voltage is reduced to the potential per spacer plus sorption membrane.) The runs were no-pause operations and were therefore rate limited. The actual value of the concentrations and of the separation factors should not be stressed because of the reasons given above. One fact emerges nevertheless quite clearly:

A reduction in the thickness of the capacity cell core increases the current consumption. This is quite important for a pause operation. The high rates of mass transfer increase the separation. Unfortunately, the importance of the pause times was not realized at the time experiments on the first stack were performed.

5.3.11 Effect of thickness and hydrodynamic properties of spacer screens.

The second and third stack versions were designed to study the effect of the spacer screen. The channel thickness was believed to have a similar effect to the thickness of the capacity cell. The step response measurements, Section 5.3.9, revealed however, that the internal dispersion is caused by different mechanisms for the two stacks, and it becomes very difficult to define a common basis for the runs.

Table 31

Effect of Capacity Cell Thickness on Electrodialyzer No. 1

1	2	3	4	5	6	7	8	9	10	11	12	13
RUN NO.	CONCENTR. INITIAL	VOLUME DISPLACED	VELOCITY SUPERFICIAL	PAUSE TIME	CYCLE PERIOD	VOLTAGE APPLIED	CYCLE NO.	CURRENT TOTAL	CONCENTRATION		SEPARATION FACTOR	REMARKS
									BRINE	DIALYSATE		
# [-]	c_0 [ppm]	δ [-]	v [cm/sec]	τ [sec]	T [sec]	$\Delta\Phi$ [volt]	nc [-]	I [ampere]	x_B [-]	x_T [-]	ns [-]	L = limit reached NL = limit not reached δ_B/δ_T = dead volumes
42	750	1.00	1.21	-	50.2	2.5	7	0.78	0.972	0.954	1.02	L, EDI-S1-8
1-0	1225	1.00	1.33	-	36	2.7	10	1.50	1.07	0.821	1.31	L, EDI-S3-12
36	700	1.00	0.65	-	94	1.56	8	0.50	1.04	0.935	1.11	L, EDI-S1-8
24	1170	1.00	0.90	-	55	1.66	15	1.09	1.14	0.703	1.62	L, EDI-S3-12

5.3.12 Comment on pH-changes.

At first the pH of process and rinse solutions was checked before and after each run. However, no significant changes occurred. The systematic pH sampling was, therefore, discontinued. Occasional later checks, especially for experiments with long pause times and high voltages, disclosed that the pH of the process solution becomes more acidic, but the rinse stream remains essentially unchanged. Typical results are listed below in Table 32.

Table 32

pH-Changes for some EDI-S3-12 Runs

pH / Run #	PROCESS		RINSE	
	before	*after*	*before*	*after*
11	6.3	5.6	7.6	7.7
13	6.4	6.35	7.5	7.6
14	6.3	5.8	7.5	7.5
22	6.6	6.35	7.5	7.5
23	6.35	6.18	7.4	7.5

5.3.13 Comment on current efficiency.

The change in current efficiency during the course of a number of experiments are listed in Table C.1.1 to C.1.66

(see Appendix C.1). Depending on the values of the operating parameters (see Tables 9 to 13), the current efficiencies start between 25 and 50% for the first cycle, decrease quite rapidly for subsequent cycles, and tend to zero as the separation approaches steady, periodic state.

When these results are compared to conventional, steady-state electrodialysis, batch and continuous systems may be distinguished.

(i) Most continuous systems require several stages for demineralizing the feed water to the specified product concentration. The electrodialysis test bed in Webster, South Dakota, operated with four stages, and demineralized 1600 ppm brackish water to 350 ppm product (Calvit and Sloan, 1965). The average current efficiency per stage decreased from 92 to 83% as the stream became progressively depleted. The overall current efficiency for removing 79% total dissolved solids was 90%.

(ii) The current efficiency in a batch recirculation system decreases in time similar to the present cyclic electrodialysis process. Mandersloot (1964) reported current efficiencies of 85% for 94% demineralization of 0.05N aqueous sodium chloride solution.

The reasons for much smaller current efficiencies for experiments on the first ED cell are as follows:

Nature of the cyclic operation: Suppose the current density is uniform and constant, one void volume is displaced, the membranes are perfectly selective, and the pause time is zero. In this case, the effluent concentration during the first half cycle decreases linearly in time. The current efficiency is exactly 50% since only one-half of the demineralized solution volume is recovered, the other half remains in the electrodialyzer. According to this model the current efficiencies of subsequent cycles are zero, since the effluent concentrations remain unchanged.

In reality, when operating with pause times, the current efficiencies decreased gradually as functions of the number of cycles. The displaced volume in most of these experiments was less than a void volume. This reduced the efficiency, as did the presence of dead volumes.

It was also found that the current consumption of the stack during displacement contributed very little to the separation. It may be more efficient to disconnect the electric power during displacements, or displace at very high flow rates.

Internal mixing results in dispersion of the concentration front. These dispersive effects must be balanced by electric energy input at steady periodic conditions, i.e. a larger and larger amount of the current is consumed to maintain the concentration wave as the separation progresses.

Channeling and/or unequal flow distribution causes nearly stagnant volume elements which become periodically demineralized and enriched but never emerge as products.

5.3.14 Comment on true limits and reproducibility of batch runs.

The operating conditions were changed during the course of some experiments in such a manner as to test the uniqueness of the final concentrations, see the tables in Appendix C.1 for runs:

#28 (EDI-S2-16)
#5,6,8,9 (EDI-S2-16)

Figure 67 shows the separation factor (ns) as a function of the number of cycles (nc) for runs #27 and #28 on EDI-S2-15, and Figure 68 is a similar plot for runs #8 and #9 on EDI-S2-16. Both figures demonstrate the reproducibility and the uniqueness of the final separation factor.

The reproducibility of the results was tested frequently throughout the experimental program and was found to be excellent in most cases. Tables 14, 15, 16, 17, 19, 22, 23 and Figures 40, 41, 43, 44, 46 may be referred to for a comparison of replicate experiments. However, the flow distribution and consequently the internal dispersion appeared to be different when the same stack was dismantled and reassembled. This influenced the reproducibility of separation runs.

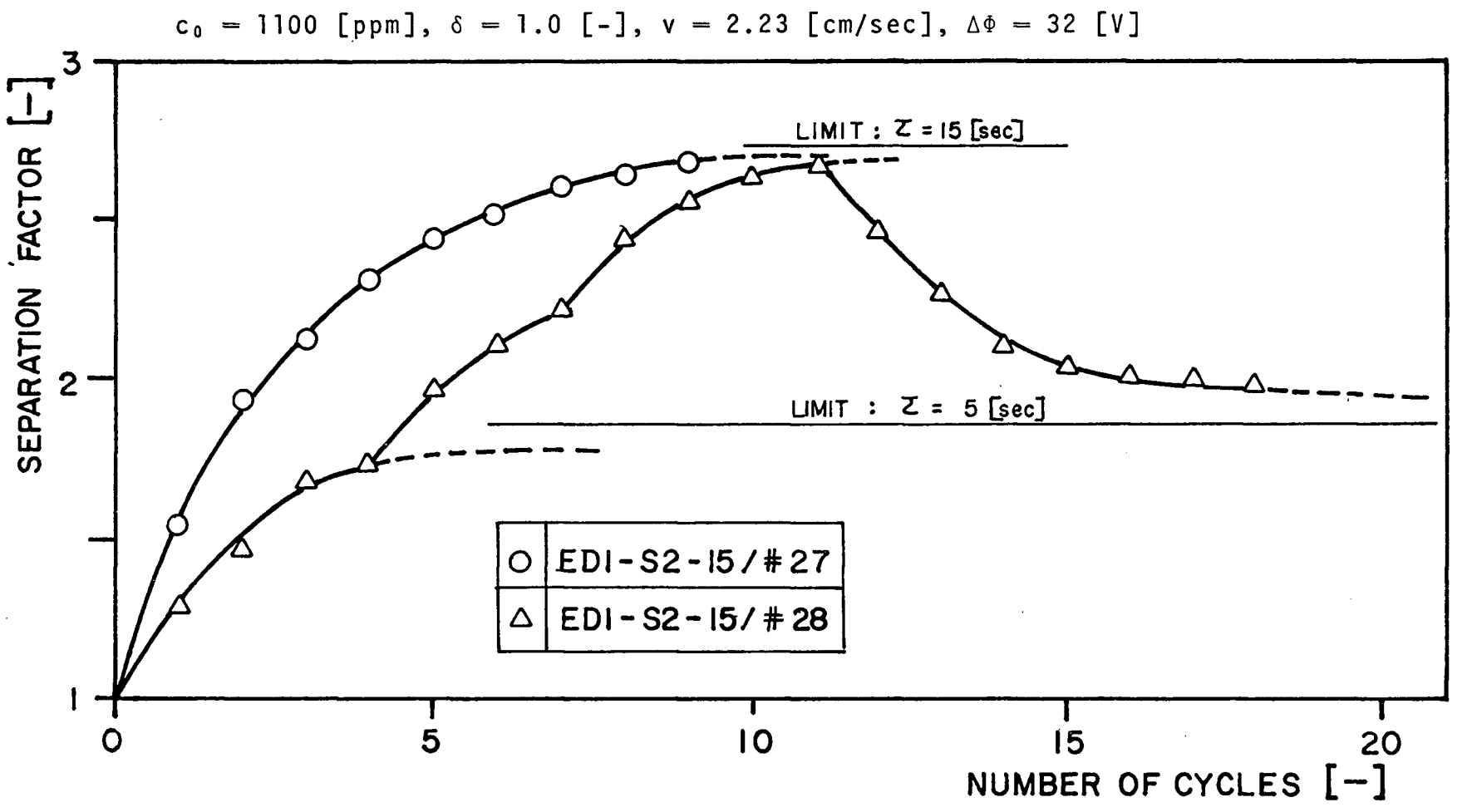

Figure 67. Uniqueness and reproducibility of final separation factor for second stack experiments.

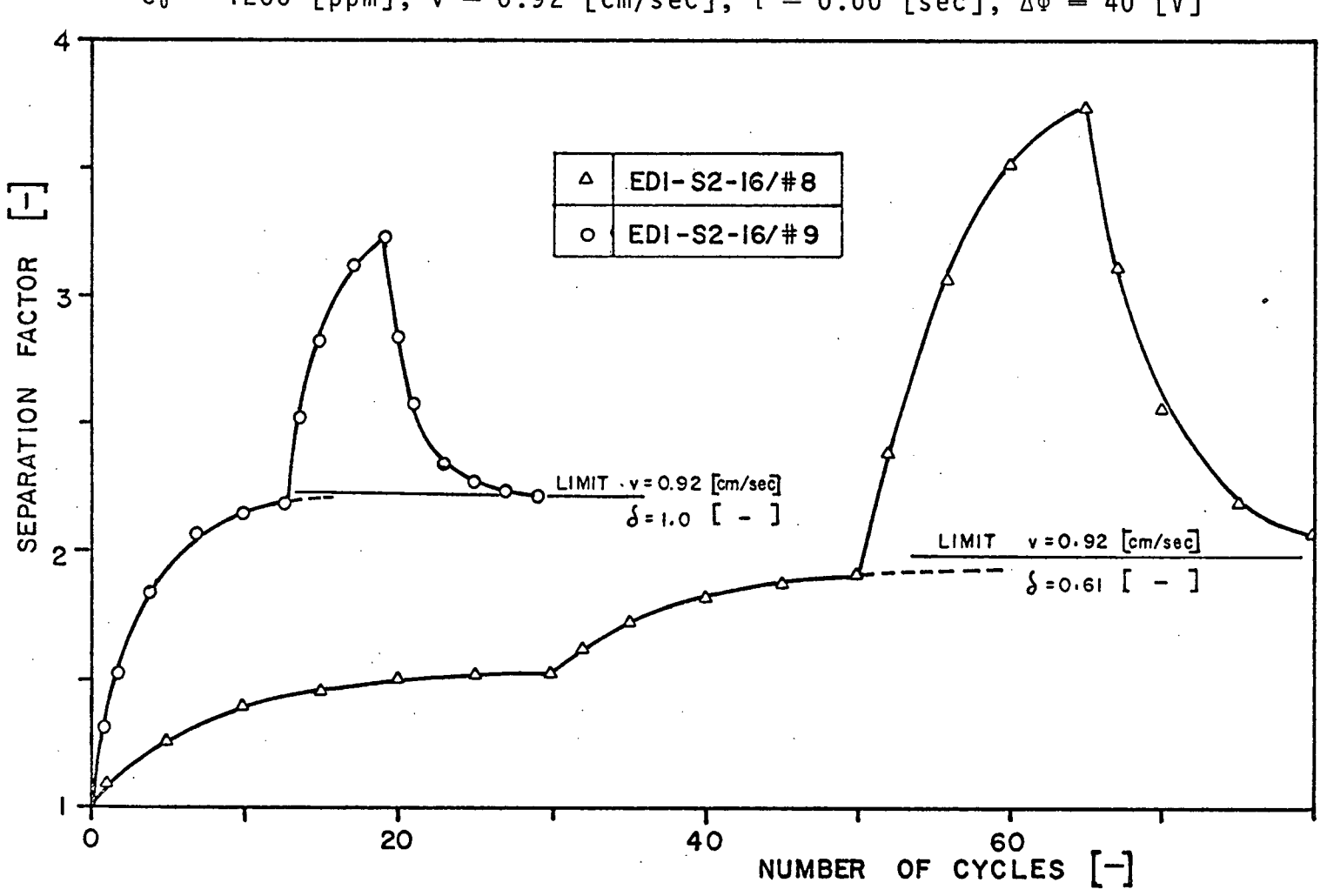

Figure 68. Uniqueness of final separation factor for second stack experiments.

5.4 Summary of Experience Gained on First ED Cell

The experimental work on the first ED cell had to meet several objectives:

a) Serve as preliminary investigation to explore the possibilities of applying cyclic operations to an electrosorption stack.

b) Test predictions of several simple theoretical models.

c) Screen operating and design parameters to determine their relative importance for such cyclic operations.

d) Provide a basis for understanding the phenomena involved in order to design an improved stack and ED module.

This program was successfully completed and produced the following results:

1. The cyclic ED process is almost entirely controlled by the rates of mass transfer across the membranes. Equilibrium plays only a subordinate role.

2. The standard parametric pumping operation is usually very inefficient under these circumstances. The concentration transients show that the main separation occurs during the first cycle, except for large applied voltages and/or long residence times.

3. The addition of a flow pause after each polarity reversal improves the separation factors by more than an order of magnitude.

4. Internal dispersion effects which include channelling and by-passing are the main cause for limited separation in a pause operation.

5. The applied voltage is the second important parameter.

6. The current consumption increases approximately proportional with the initial concentration at otherwise identical conditions. However, the separation factor is found to be slowed down and approaches lower limiting values.

7. Dead volumes in the end reservoirs delay the separation but do not alter the limit.

8. The displaced volume may be reduced to obtain better final separation.

9. External mixing reduces separation when internal mixing is also present.

10. The superficial velocity has a minor effect on separation in pause operations and may be increased to a level set by pumps or mechanical limitations.

5.5 The Second Electrodialysis Cell (EDII)

The results on the first ED cell were used to design a second module. The following objectives were pursued:

1. Design and produce new stack pack which
   - is simple in construction,
   - may be manufactured accurately,
   - is reliable in performance,
   - is readily assembled and disassembled,
   - allows the pack size to be increased or decreased,
   - may be used with the same auxilary equipment as the previous cell,
   - might be easily scaled up.

2. Design and produce new electrode end frames for this stack pack.

3. Investigate effect of channel length.

4. Study effect of operation parameters:
   - pause time
   - initial concentration
   - displaced volume
   - applied voltage
   - flow rate

5. Test theoretical model based on constant uniform rate of mass transfer.

The equipment and its features are described in Chapter 4.3, and the manufacturing procedures for stack units and electrode end frames are contained in Appendix A.3.

The length of the flow channels was adjustable since the new ED module consisted of eight identical stages. The stages were always connected in series hydraulically and usually in parallel electrically. In four runs an electric series connection was used to analyze uniform rates of mass transfer. In the latter case the D.C. power supply was operated in constant current mode, whereas the regular test series called for the more realistic constant voltage mode. These tests were performed on the full number of stages.

5.5.1 Data reduction and presentation.

The data obtained on the second ED module differed from those on the first one as explained in Section 5.2. This required different processing and modified presentation of the results.

The form of the main survey table is retained to allow easier comparison with the results on the first ED cell. Table 13 lists operating parameters and conditions at the end of experiments #6 to #53 in chronological order. It can be

seen that the final dialysate concentrations are often well below 1% of the initial concentration. The conductometric measuring system is not very accurate in this regime, see Section 4.2.6, and the table should, therefore, be used with caution.

Consequently, it is more meaningful to compare rates of separation instead of final conditions. For this purpose the concentration changes and the separation factors were evaluated as functions of time. The corresponding tables are described and contained in Appendix C.2.

From these evaluation tables transients of the separation factors are plotted in semi-logarithmic diagrams for groups of experiments in which a single parameter was varied. The initial rates of separation were determined from the graphs by drawing a straight line through the initial points. The initial rate of separation was approximated by

$$\frac{d\ \log(ns)}{dt} = a = \text{const.} \qquad (33)$$

Equation (33) is also the definition of the rate constant(a) which will be reported subsequently.

Complementary to the transients, additional information was compiled and grouped in tables for initial and final total current consumption, applied electrode voltage, mean current, and mean probe voltage in each stage (see

Appendix C.2). Operating conditions, initial rate of separation (a), initial and final total current, and the pH changes in process and rinse streams of the same groups of experiments are presented in tables 35 to 39.

5.5.2 Effect of channel length.

The effect of the channel length on internal dispersion was analyzed using the step response method previously described. The resulting F-diagrams did not suggest channelling or by-passing, and the fronts were much sharper than for the previous ED cell. The results of these response tests are listed in Table 33, and the dimensionless slope $\dot{x}$ of the curves is graphically displayed in Figure 69 as a function of the number of stages (L).

One can see that the shape of the curve is similar to the theoretical one shown in Figure 63. However, the graphical determination of the slopes is not only rather inaccurate but also subject to a certain personal touch. The finite limit of the slope for increasing number of stages is caused by mixing in the interconnecting pipes and in the liquid distribution systems in the stack. For more than 6 stages this limit is nearly reached. In other words, the flow in the channels may be considered to be piston flow, although there is still internal mixing in the system. (A

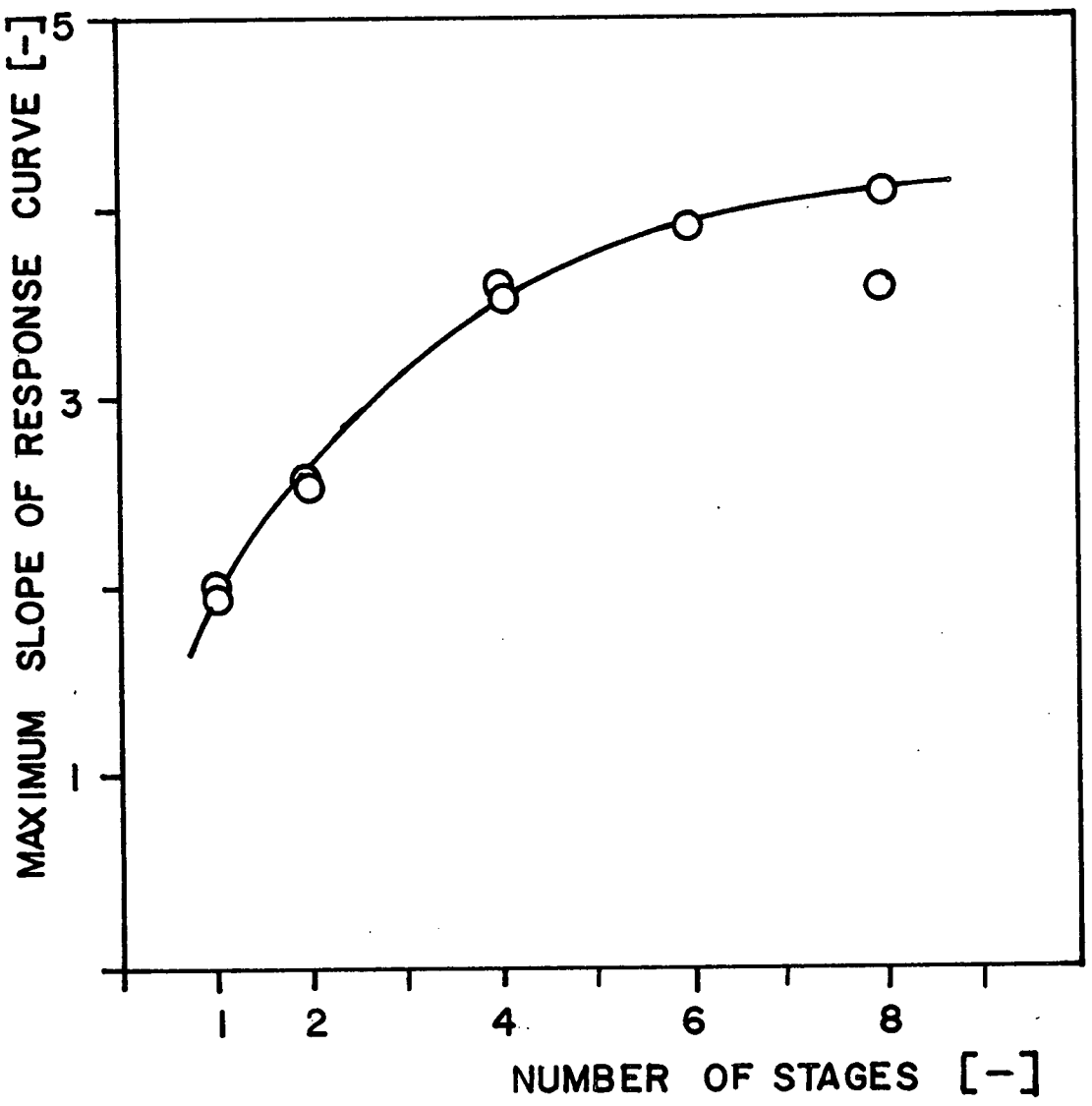

Figure 69. Dimensionless slope of step response curves for second ED cell as function of the number of electrodialysis stages.

Table 33

Results of Step-Response Tests on Second ED Cells

Stages in Series [-]	Flow Rate $\dot{Q}$ [cm^3/sec]	Time Lapse $\bar{t}^*$ [sec]	Maximum Slope $\dot{x}$ [-]	Concentration $\bar{x}^*$ [-]
#1	2.81 3.60	37.1 29.3	-1.95 -2.03	0.62 0.66
#5 & #6 #7 & #8	7.40 7.72	21.7 19.1	-2.56 -2.58	0.58 0.68
#5 to #8	14.3 14.1	20.2 19.8	-3.60 +3.60	0.61 0.55
#3 to #8	14.25	28.5	-3.90	0.66
#1 to #8	6.4 14.1	84.0 37.7	-3.50 -4.07	0.62 0.55

value of $\dot{x} \approx 4.0$ corresponds to at least 50 effective mixing stages.)

The effect of the channel length on separation was studied in three sets of experiments with 2, 4, 6, and 8 stages connected in series (see Table 34). The separation factor transients of the three groups are displayed in Figure 70, 73, and 75; the concentration transients of two groups are illustrated in Figure 71 and 76, and the local current consumptions at steady periodic conditions are plotted in

Figures 72, 74 and 77. Finally, in Figure 78, the rate constant (a) is plotted against the number of stages (MS). The results are:

1. A fourfold increase in channel length (from 31 cm to 124 cm) raises the final separation by at least one order of magnitude.

2. The initial transient of the separation factor may be approximated by an exponential function

$$ns = 10^{at}$$

3. The rate constant (a) increases with the channel length but appears to go through a maximum. For the high concentration group this maximum is at about MS = 5. The maxima for the other groups lie between MS = 6 and MS = 8.

4. If the pause time is increased (from τ = 0.6 to 10 [sec]) the rate constant vs. MS curve seems to be displaced to a higher level with no change in shape.

5. The concentration transients for the no-pause group show an improvement in separation with MS, which has some similarity to the effect of the pause time on the first ED cell.

page 182 does not exist

6. For the last group in Table 34 the rate constant appears to be less affected by MS. This group has a high concentration and a pause time of τ = 10 [sec]. The dialysate transients in Figure 76 show points of inflection, i.e. the amount of solute which is removed from this product stream is almost constant per cycle and does not decrease at a constant rate as predicted by the model in Section 3.3. It is believed that this behaviour reflects a saturation effect of the sorption membranes which is only noticeable at higher concentrations (for further details see Section 5.5.3).

7. The initial total current is approximately proportional to the channel length, as expected. The ratio of final to initial current does not depend on MS for the groups with τ = 10 [sec], but decreases in the no-pause case.

8. The local current distributions reflect the internal mass transfer rates averaged over one cycle at steady periodic conditions. They illustrate the concentration gradients which have developed. A large difference in current consumption between first and last stage is identical to large separation.

9. Most of the current distribution curves level off toward the bottom end (stage No. 8). This reflects the

Table 34

Effect of Channel Length (MS) on Second Electrodialyzer

RUN NO.	NO. OF STAGES	PAUSE TIME	INITIAL CONC.	APPLIED VOLTAGE	DISPL. VOLUME	SUPERF. VELOCITY	INITIAL RATE	TOTAL CURRENT		PROCESS pH		RINSE pH	
								INITIAL	FINAL	INITIAL	FINAL	INITIAL	FINAL
#	MS	τ	c_0	$\Delta\Phi$	δ	v	a						
[-]	[-]	[sec]	[ppm]	[volt]	[-]	[cm/sec]	[min^{-1}]	[ampere]	[ampere]	[-]	[-]	[-]	[-]
48	2	0.6	1250	10	2/3	5.4	.028	0.88	1.16	5.2	6.3	5.7	5.8
46	4		1240				.064	1.44	1.48	5.7	6.0	5.2	5.1
43	6		1210				.077	2.60	2.16	5.9	5.5	5.1	5.1
25	8		1250				.077	3.00	2.40	6.1	5.3	6.0	5.8
47	2	10	1225	10	2/3	5.4	.109	0.70	0.36	6.5	6.3	5.4	5.6
45	4		1275				.140	1.32	0.68	6.4	6.0	5.4	5.2
44	6		1225				.170	1.88	1.04	6.5	5.0	5.2	5.6
26	8		1290				.170	2.70	1.40	6.1	5.5	5.8	5.7
35a	8		1220				.170	2.60	1.40	7.2	6.3	5.2	5.6
19	2	10	4900	10	2/3	5.4	.087	1.45	0.88	-	-	-	-
20	2		5500				.087	1.75	1.00	5.3	5.2	5.9	6.1
18	4		5300				.096	3.00	1.72	-	-	-	-
17	6		5100				.096	4.70	2.60	-	-	-	-
6	8		5700				.086	5.60	3.20	-	-	-	-

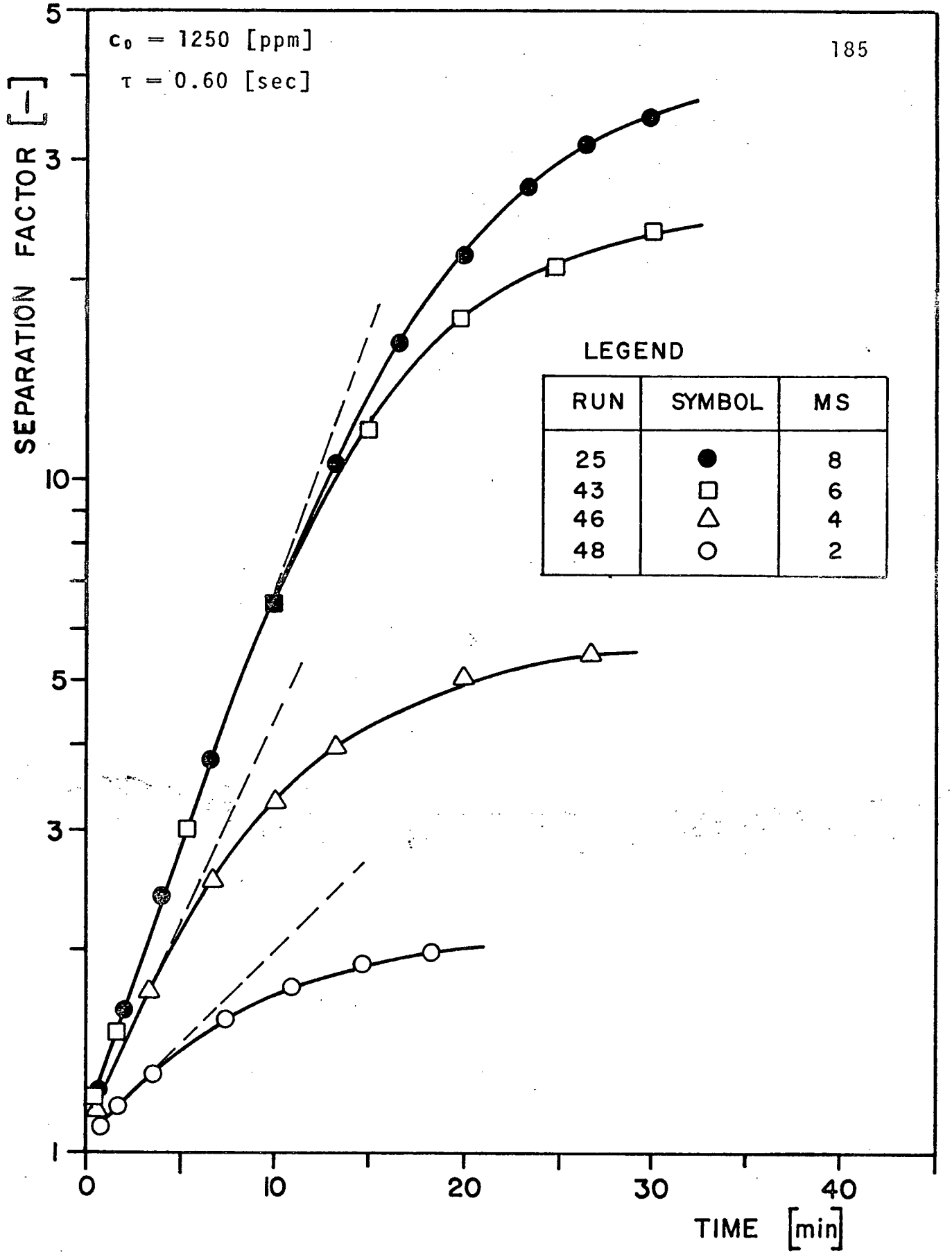

Figure 70. Effect of channel length (MS) on separation factor transients.

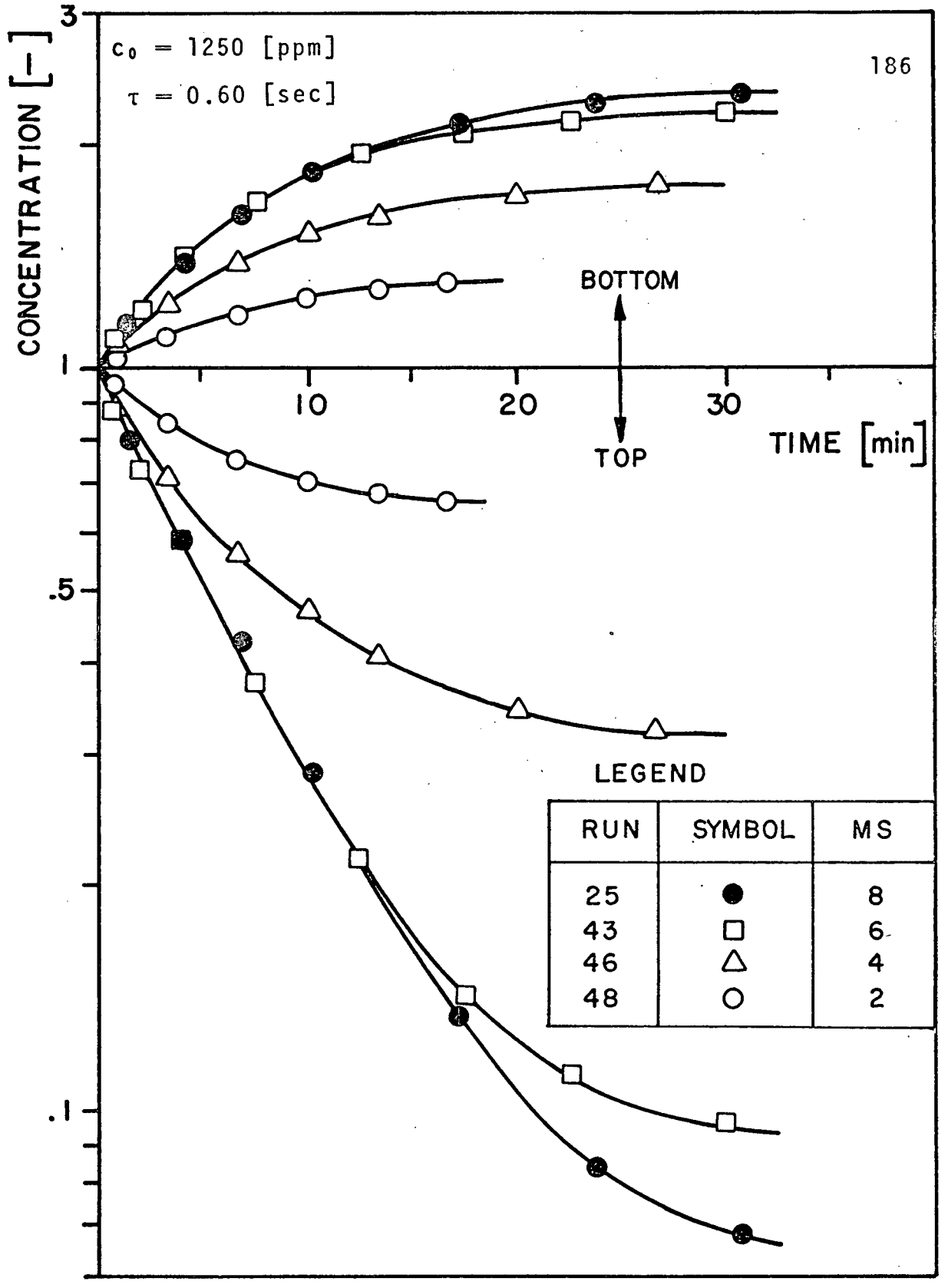

Figure 71. Effect of channel length (MS) on concentration transients.

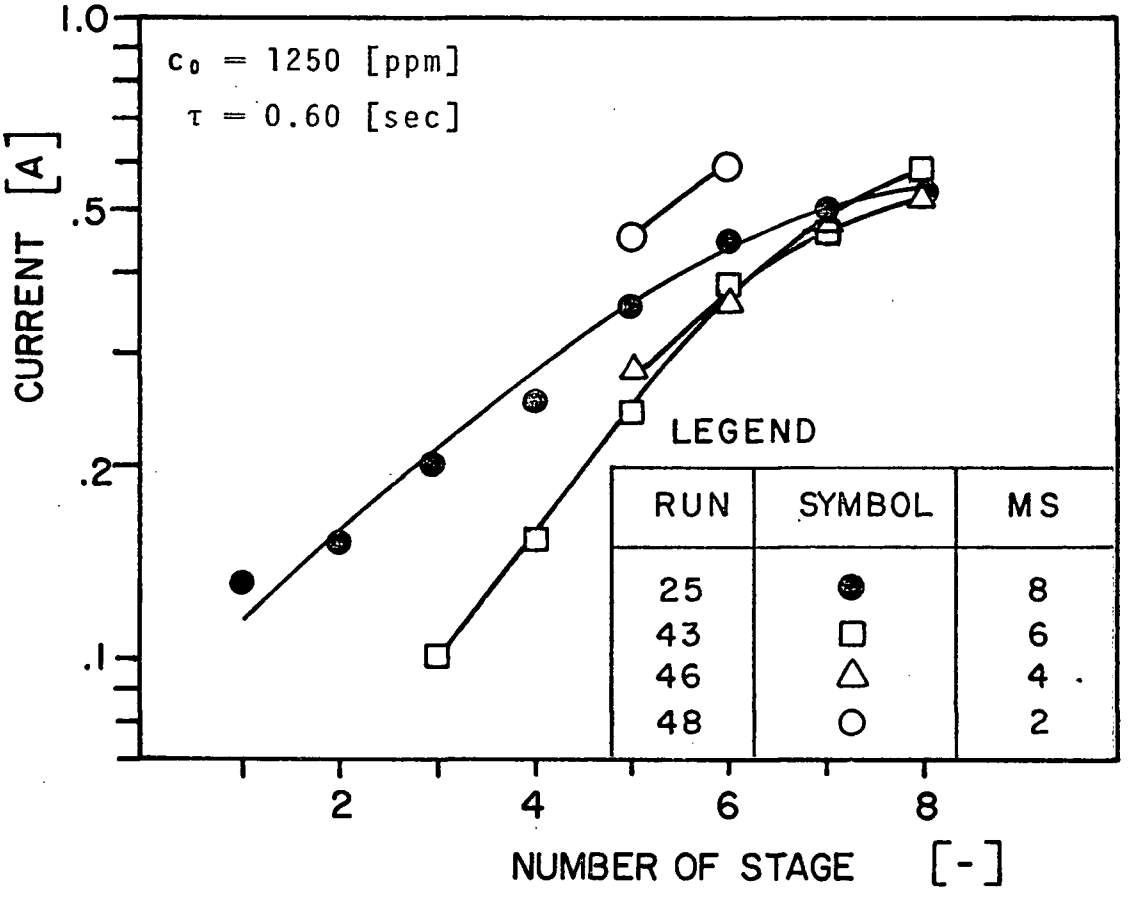

Figure 72. Effect of channel length (MS) on current distribution.

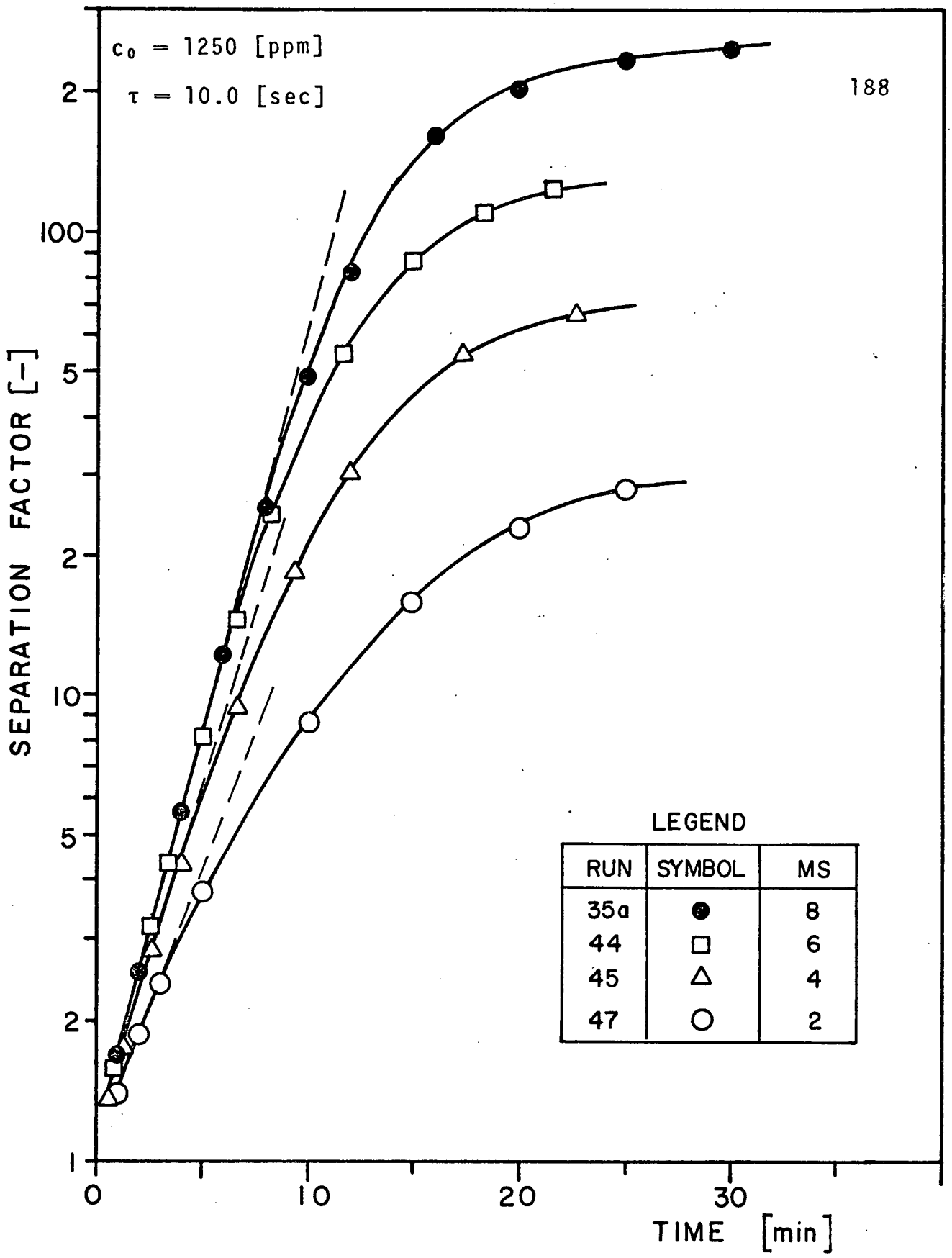

Figure 73. Effect of channel length (MS) on separation factor transients.

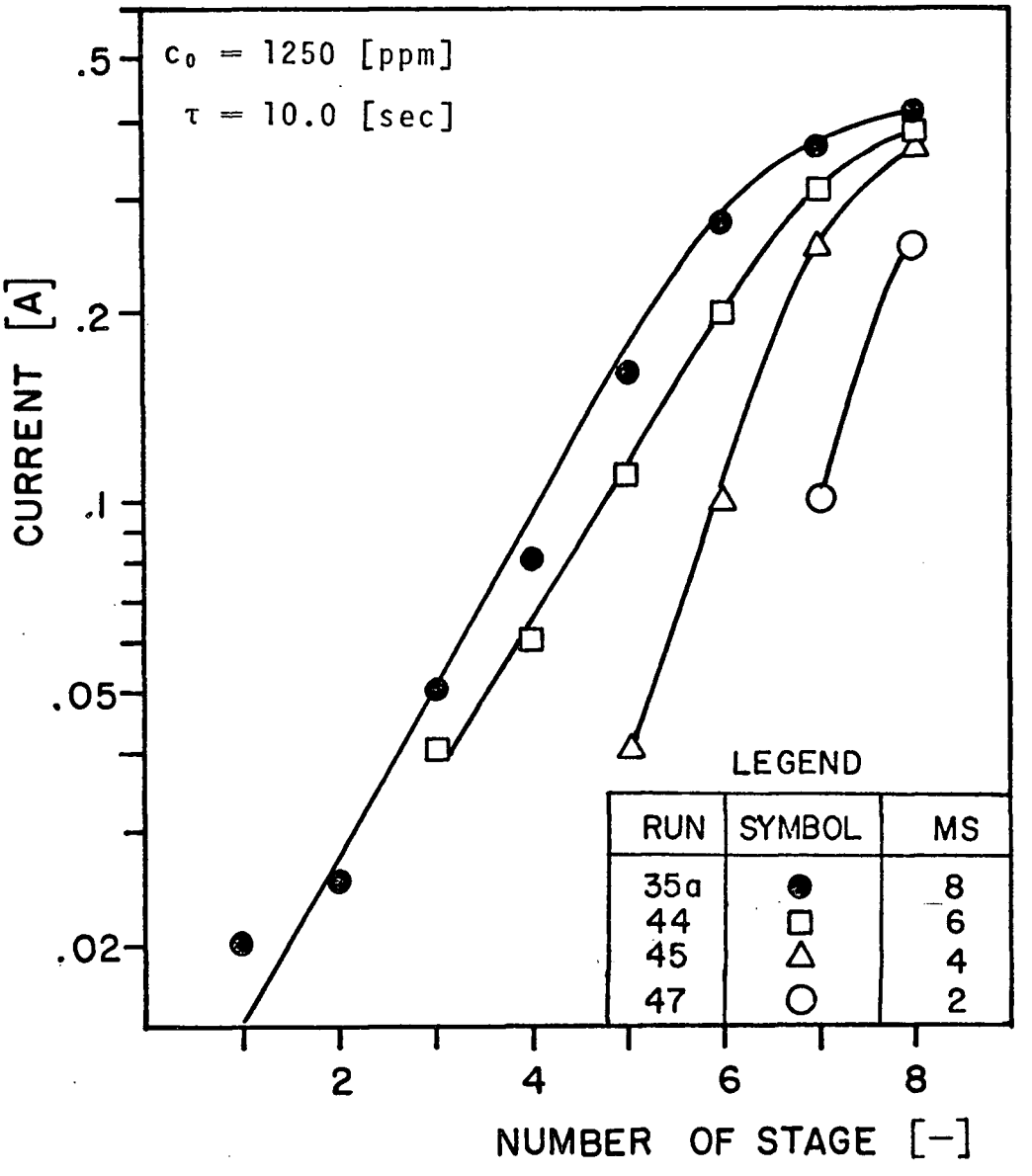

Figure 74. Effect of channel length (MS) on current distribution.

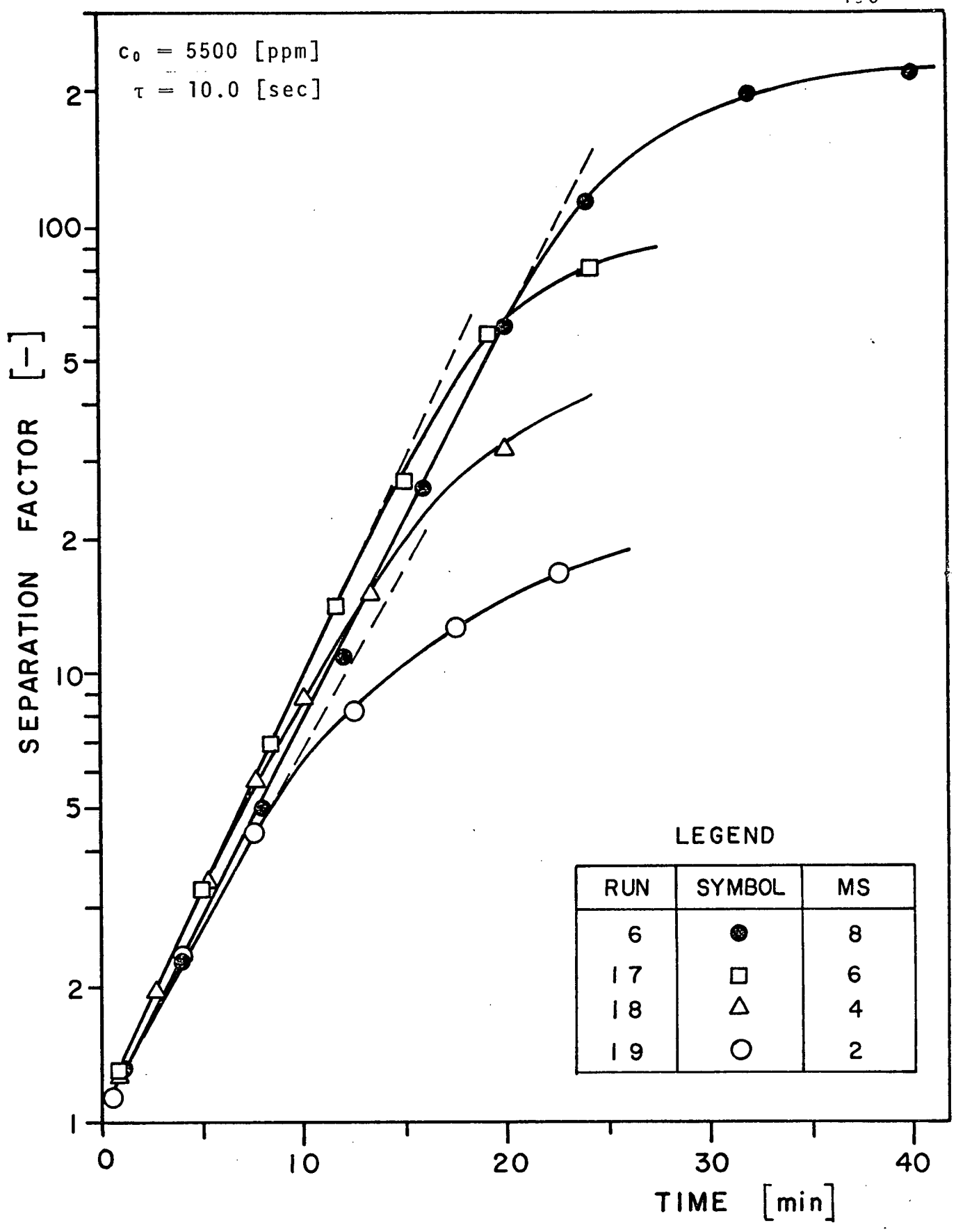

Figure 75. Effect of channel length (MS) on separation factor transients.

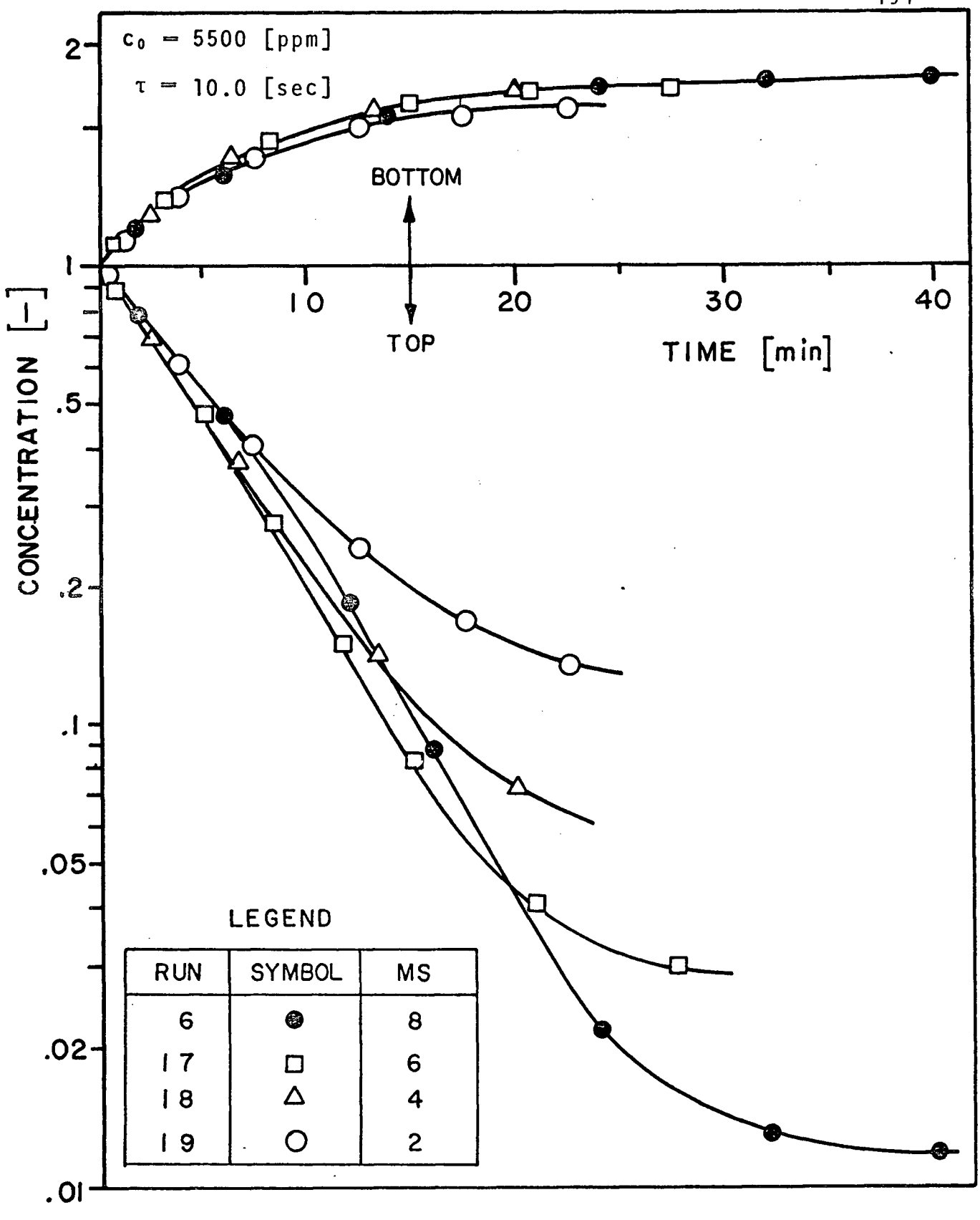

Figure 76. Effect of channel length (MS) on concentration transients.

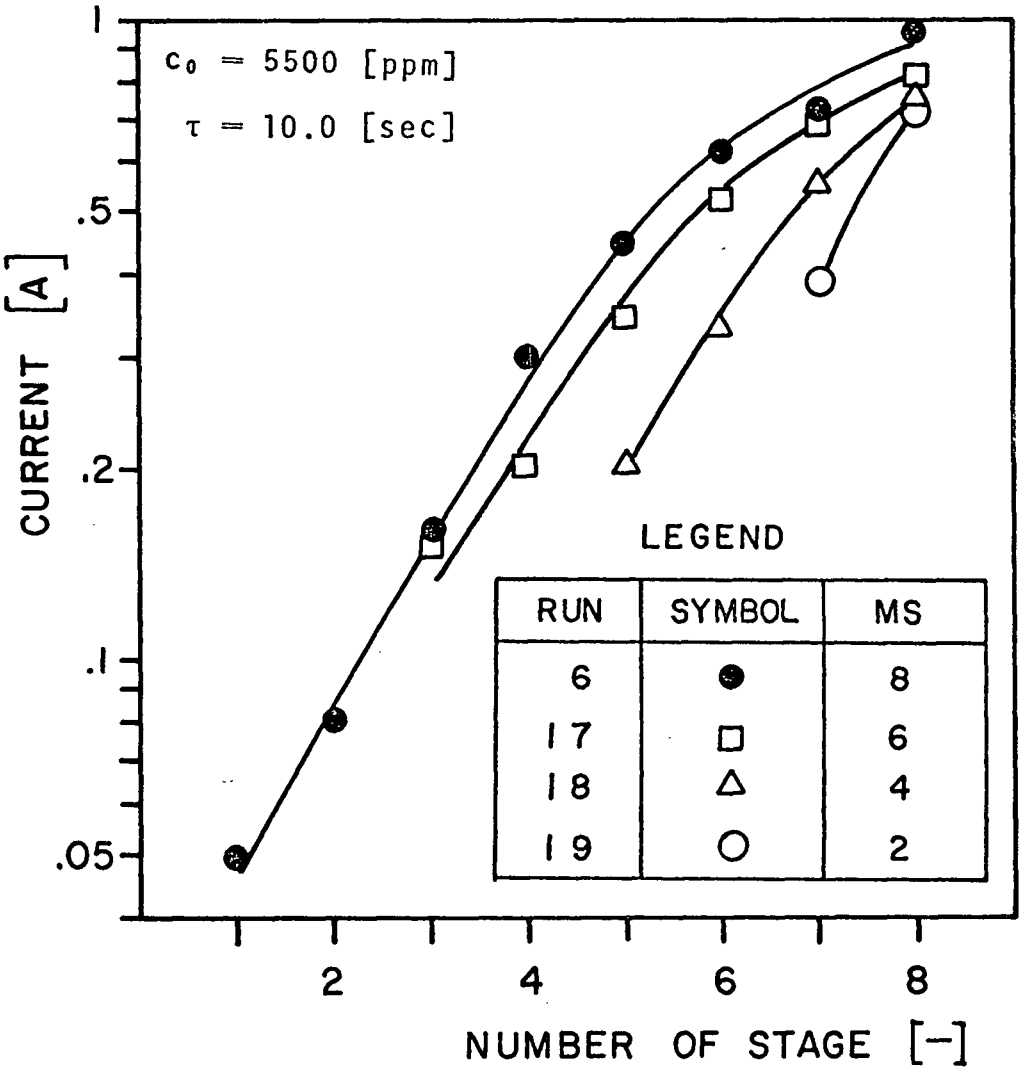

Figure 77. Effect of channel length (MS) on current distribution.

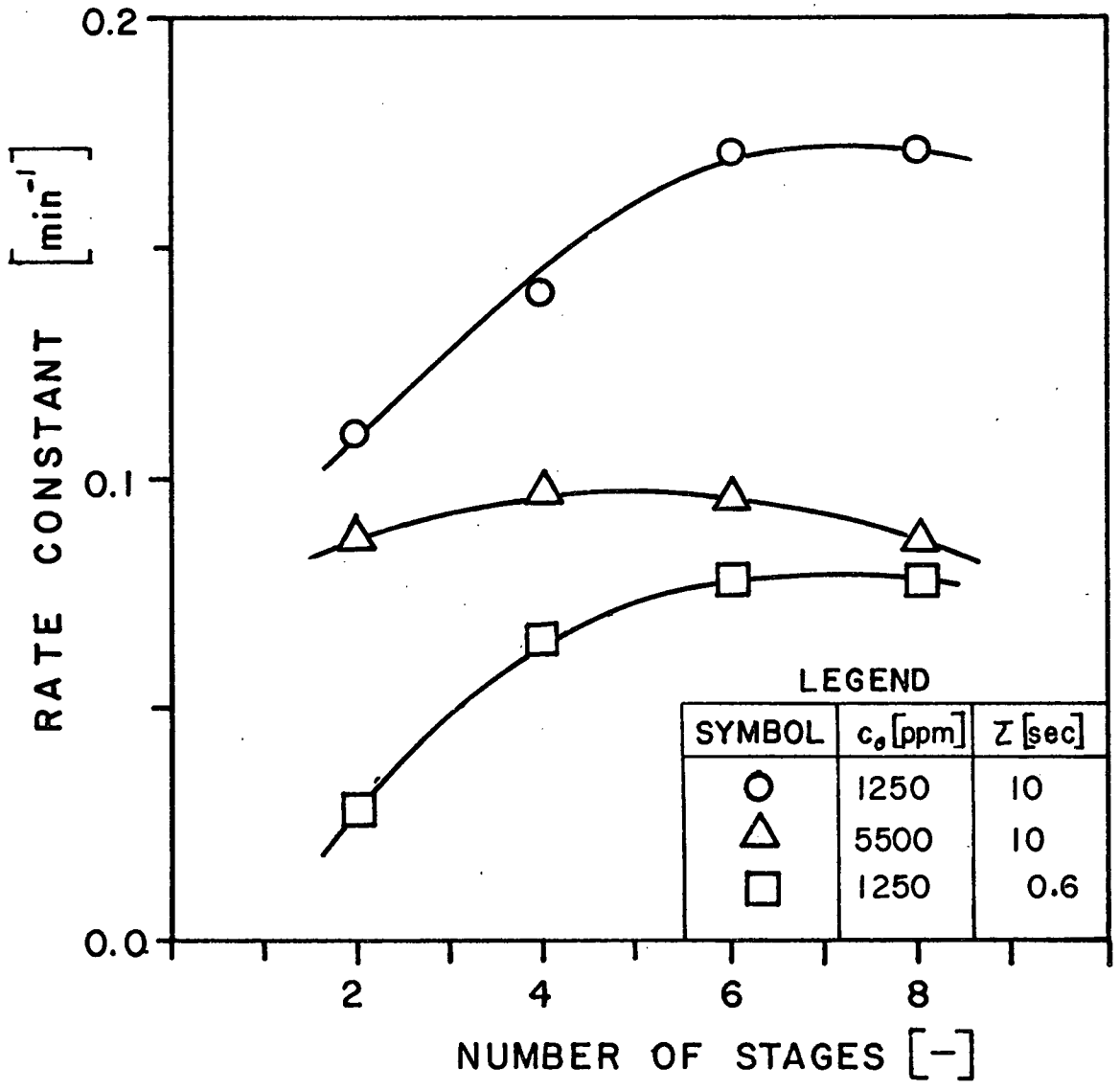

Figure 78. Effect of channel length (MS) on initial rate of separation (a).

penetration of the concentration front into the ED stack during a complete cycle. Also, one can see that the more successful separation results in larger currents at the bottom end of the channel, although some of this effect is obscured by the fact that the runs with shorter channels have less segments.

5.3.3 Effect of pause time.

The pause time (τ) was varied for three sets of experiments from 0.6 to 20 seconds, see Table 35. The separation factor transients are displayed in Figure 79, 82, 84; concentration transients in Figure 80, 85; current distributions in Figure 81, 82; and the effect of pause time on the rate constant (a) is plotted in Figure 86. The results are summarized as follows:

1. An increase in the pause time from 0.6 to 10 [sec] enhances the rate of separation as well as the final separation. The final dialysate concentration is at least an order of magnitude smaller than in no-pause operation.

2. Increasing of the pause time beyond 10 [sec] improves the separation for high concentration (c_0) but not for a low one. This coincides with a saturation effect, see Figure 80, which is similar to the one observed in the previous section (see also below).

3. The current distributions illustrate the transition from no-pause to pause operation. The concentration front is gradually built-up and pushed out of the electrodialyzer as τ increases.

4. The initial, total current decreases with increasing τ for the groups with low concentrations, but remains fairly constant for high concentration runs. The final current always decreases with τ.

Note on the saturation effect: If the concentration is large, the capacity cell core experiences drastic concentration changes. During absorption the increase may reach the level where the membranes become flooded with solute from within and gradually loose their ion selectivity. At the same time, the membrane polarization is much larger and the rate of absorption further reduced. A certain amount of solute has to be accumulated in the capacity cells before the effect becomes apparent.

At low initial concentrations the mass transfer rates are probably more controlled by high solution resistance than by polarization effects. Therefore the transients of the dialysate products decrease exponentially.

Table 35
Effect of Pause Time (τ) on Second Electrodialyzer

RUN NO.	NO. OF STAGES	PAUSE TIME	INITIAL CONC.	APPLIED VOLTAGE	DISPL. VOLUME	SUPERF. VELOCITY	INITIAL RATE	TOTAL CURRENT		PROCESS pH		RINSE pH	
								INITIAL	FINAL	INITIAL	FINAL	INITIAL	FINAL
#	MS	τ	c_0	$\Delta\Phi$	δ	v	a						
[-]	[-]	[sec]	[ppm]	[volt]	[-]	[cm/sec]	[min^{-1}]	[ampere]	[ampere]	[-]	[-]	[-]	[-]
7	8	0.6	5700	10	2/3	5.4	.018	5.6	5.6	-	-	-	-
8		5	5300				.063	5.6	3.8	-	-	-	-
10		5	4800				.063	5.1	4.1	5.7	5.7	5.6	6.5
6		10	5700				.086	5.6	3.2	-	-	-	-
9		20	5400				.108	5.5	2.0	-	-	-	-
25	8	0.6	1250	10	2/3	5.4	.077	3.0	2.4	6.1	5.3	6.0	5.8
28		5	1280				.120	2.7	1.8	-	-	-	-
26		10	1290				.170	2.6	1.4	6.1	5.5	5.8	5.7
35a		10	1220				.170	2.7	1.4	7.2	6.3	5.2	5.6
27		20	1250				.170	2.2	1.1	6.2	5.6	5.4	5.3
31	8	0.6	1220	15	2/3	5.4	.148	4.4	3.4	6.1	4.7	5.7	6.1
32		5	1240				.229	4.2	2.8	6.2	5.3	6.0	6.0
33		10	1200				.255	3.5	2.0	6.4	5.7	5.7	5.6
34		20	1280				.229	3.0	1.8	6.9	6.0	6.3	6.8

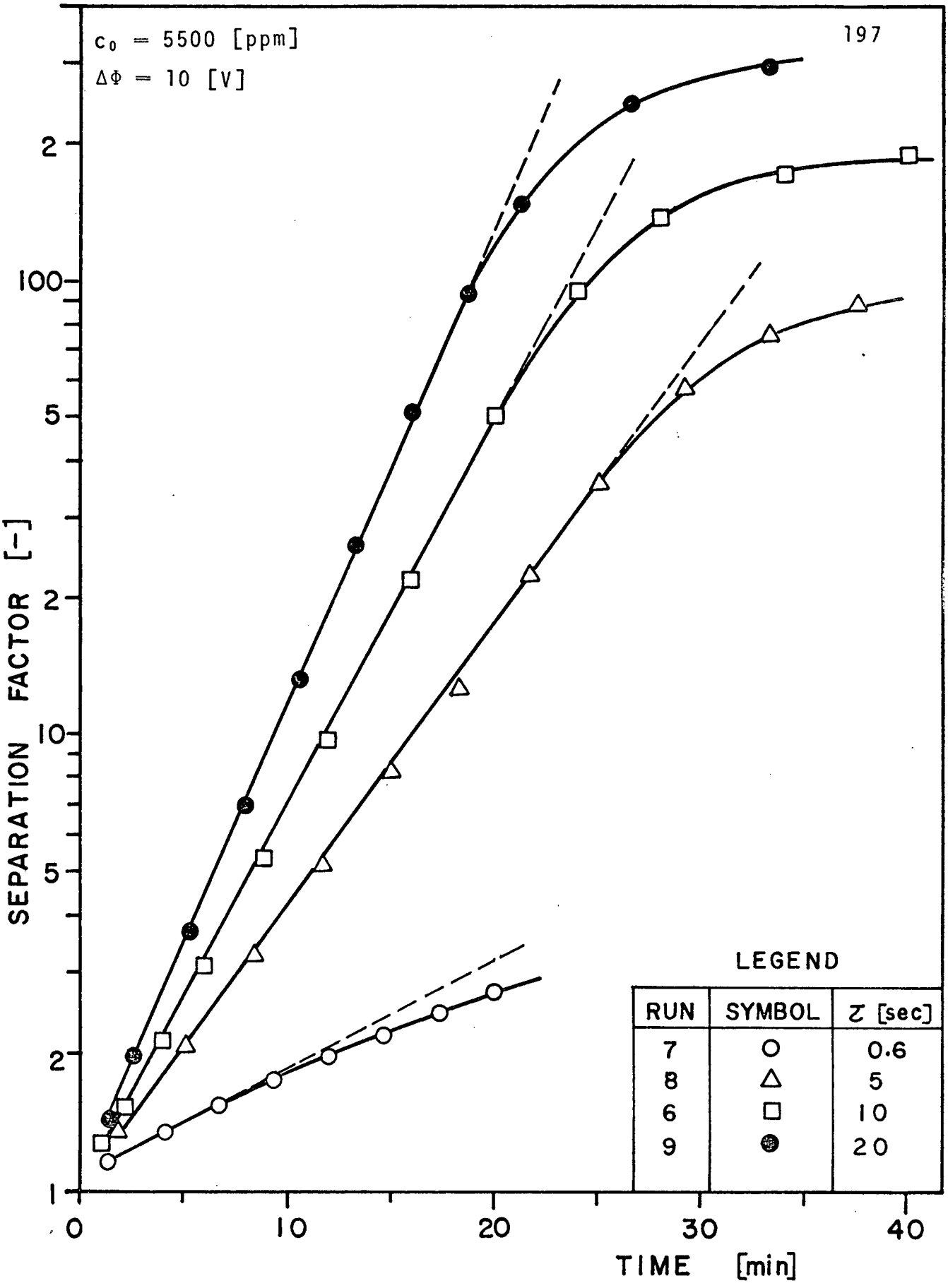

Figure 79. Effect of pause time (τ) on separation factor transients.

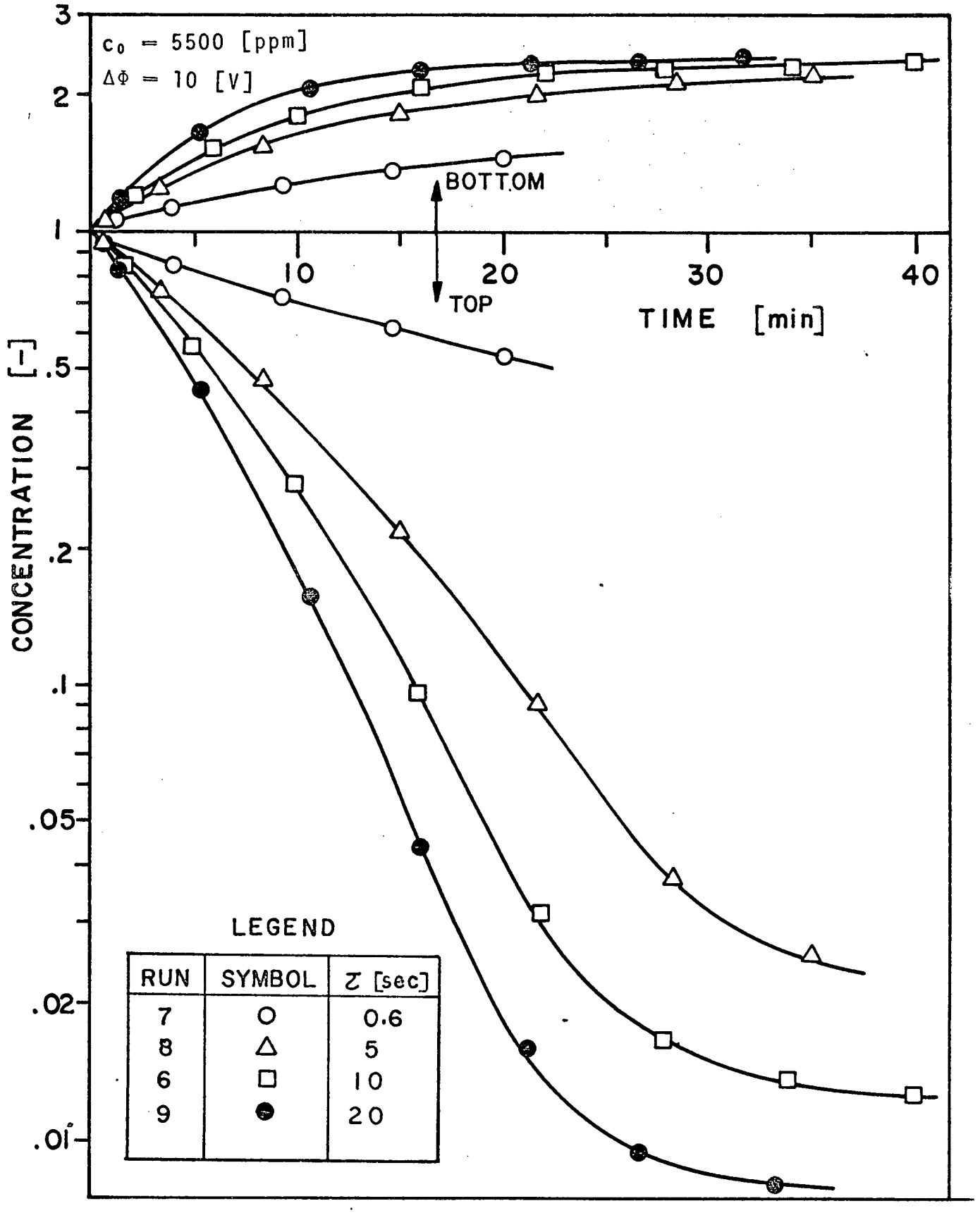

Figure 80. Effect of pause time (τ) on concentration transients.

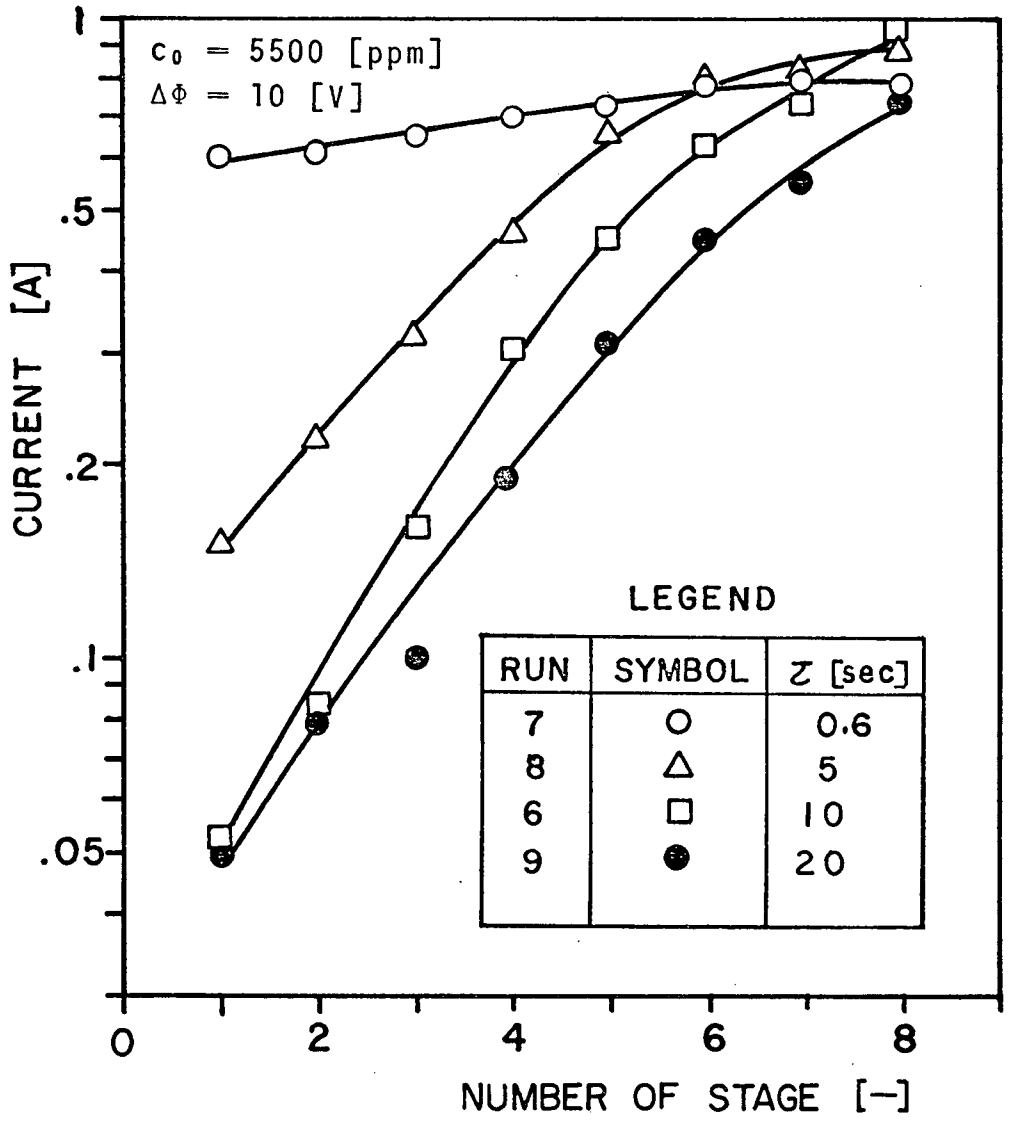

Figure 81. Effect of pause time (τ) on current distribution.

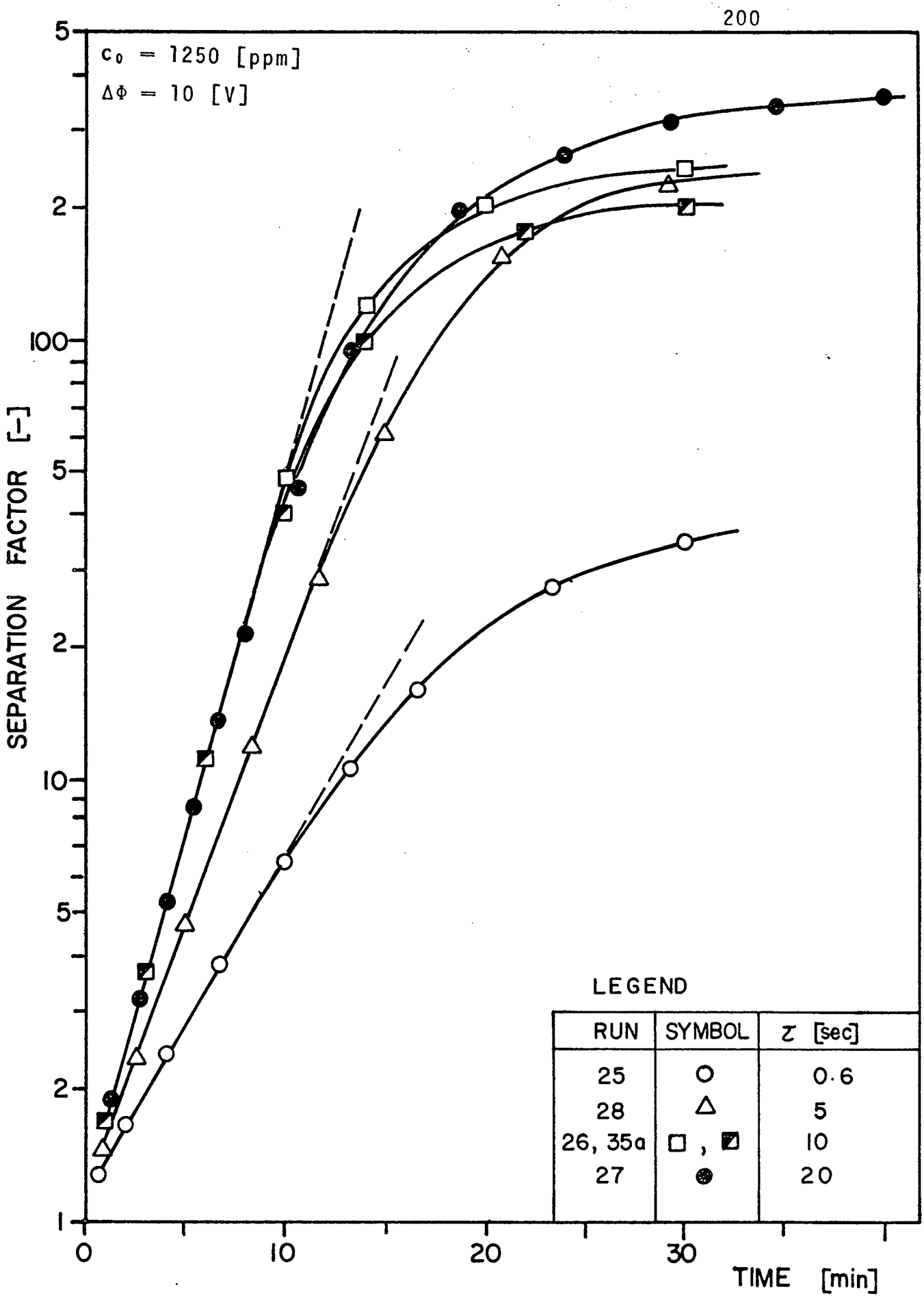

Figure 82. Effect of pause time (τ) on separation factor transients.

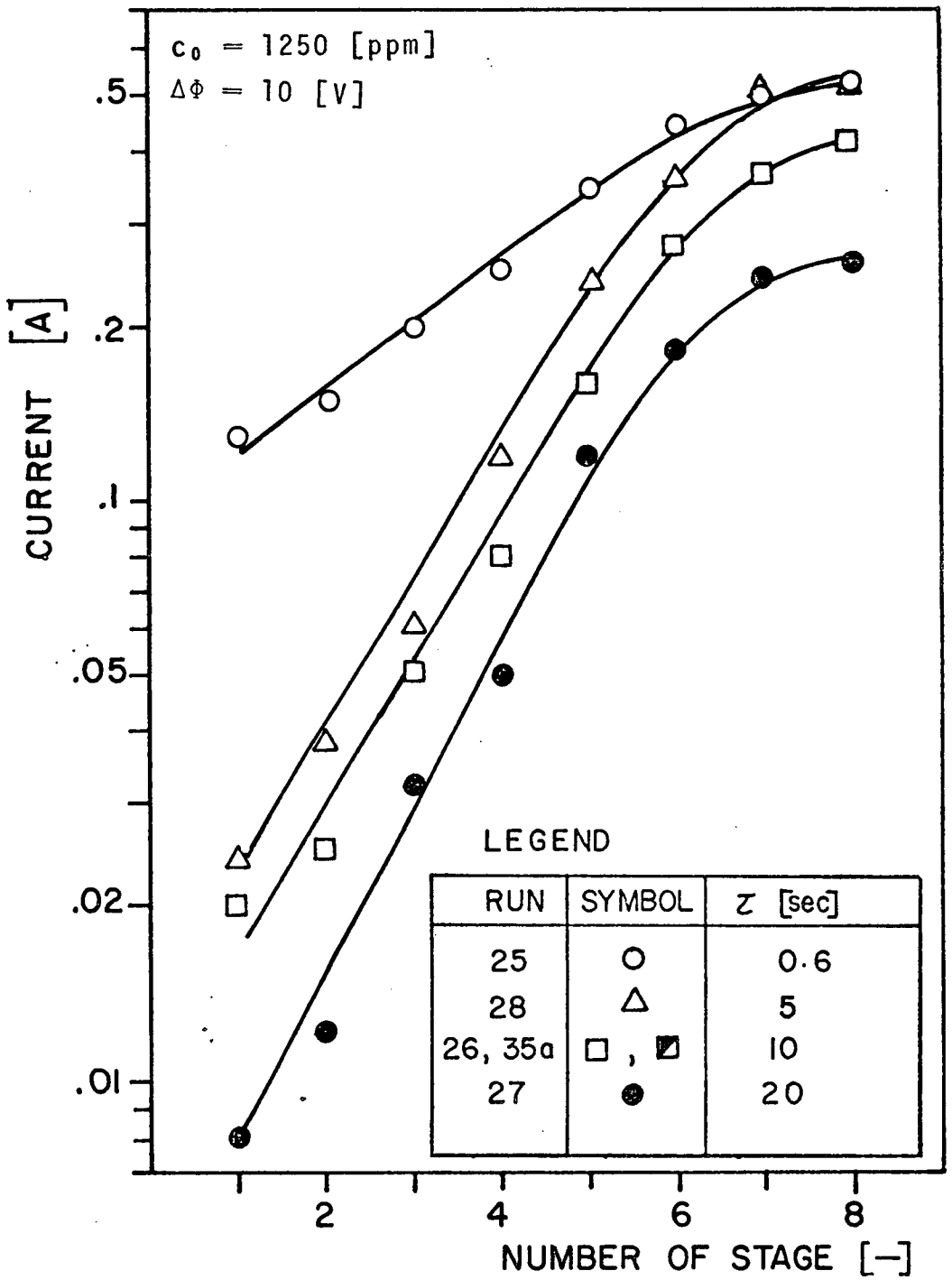

Figure 83. Effect of pause time (τ) on current distribution.

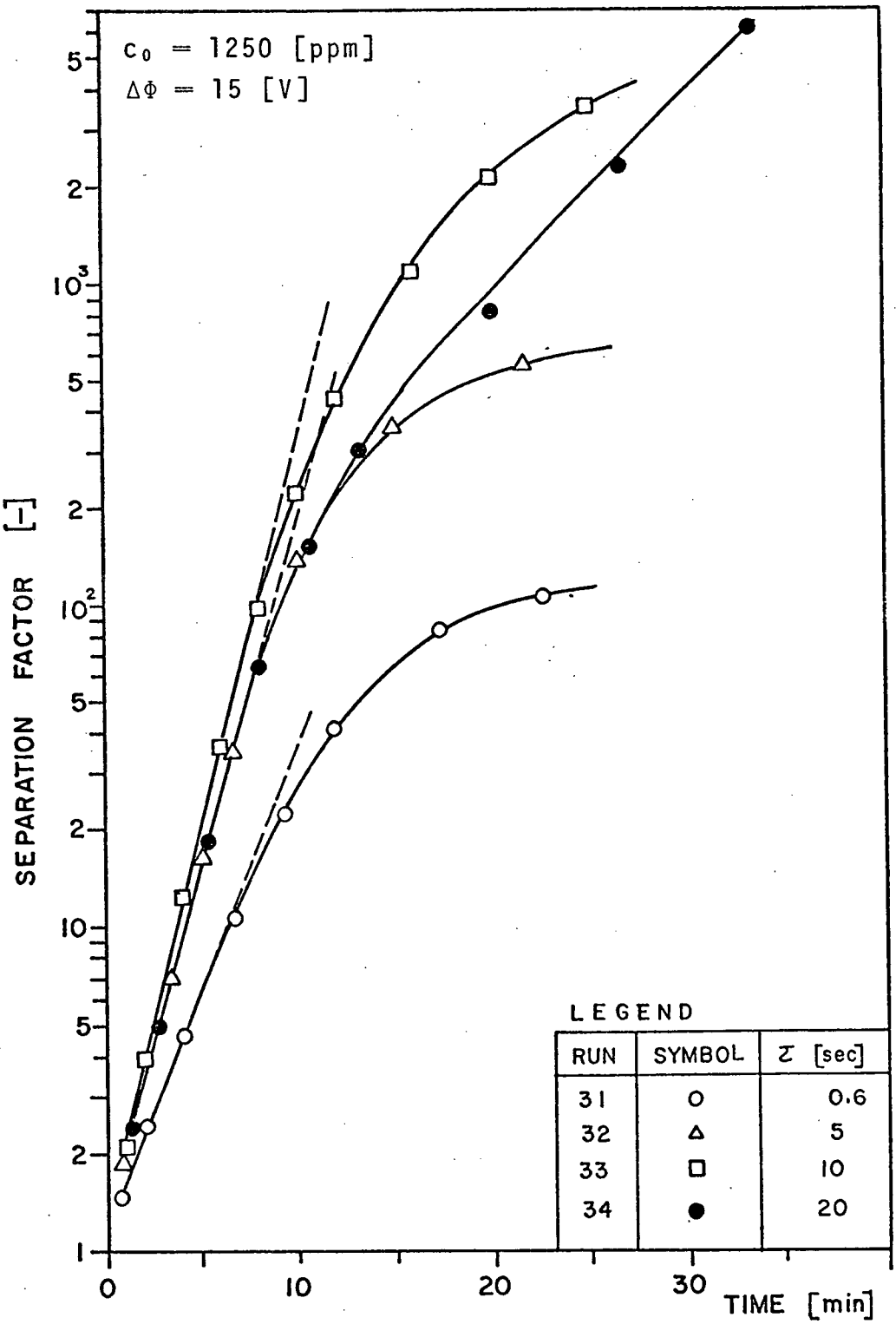

Figure 84. Effect of pause time (τ) on separation factor transients.

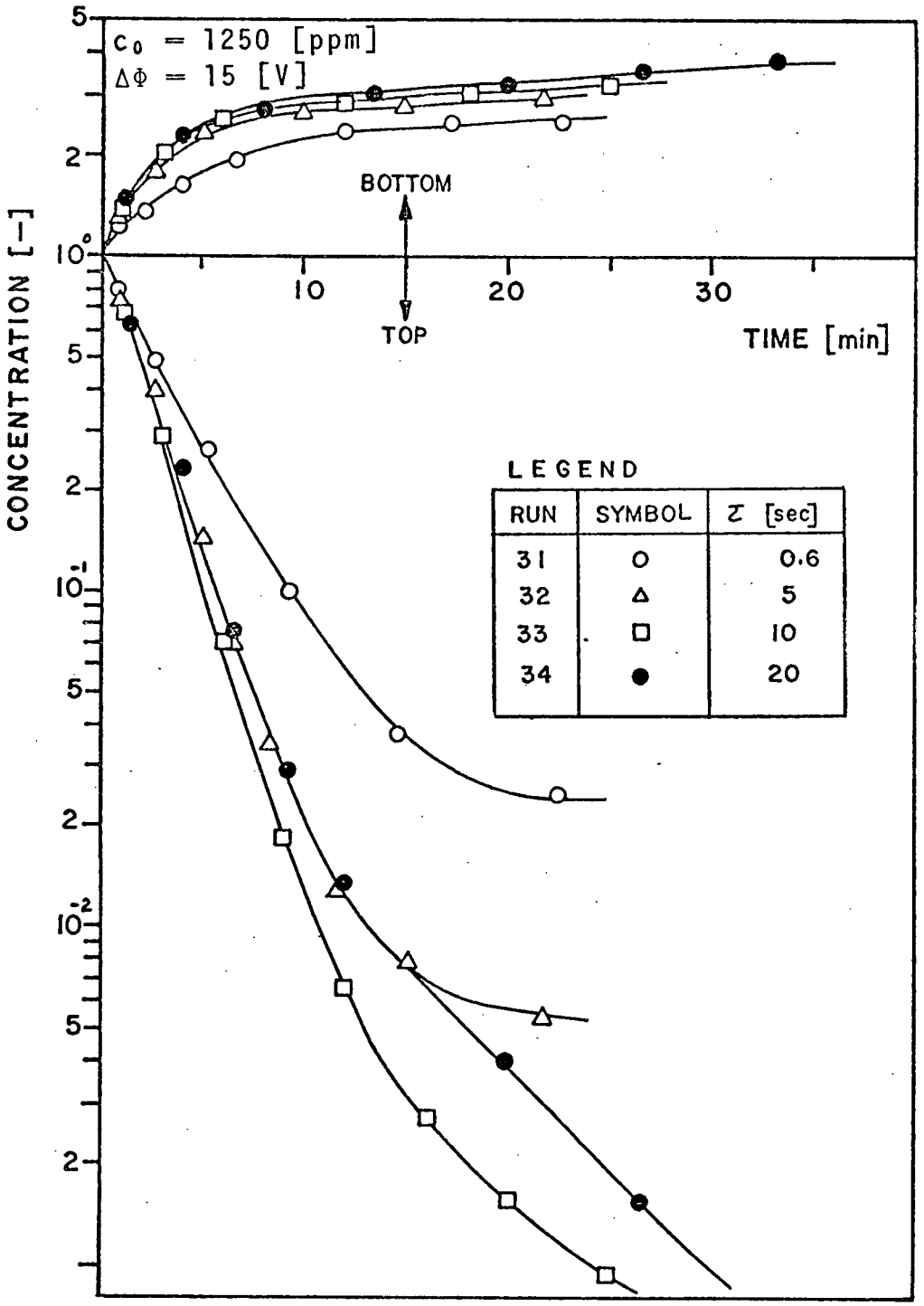

Figure 85. Effect of pause time (τ) on concentration transients.

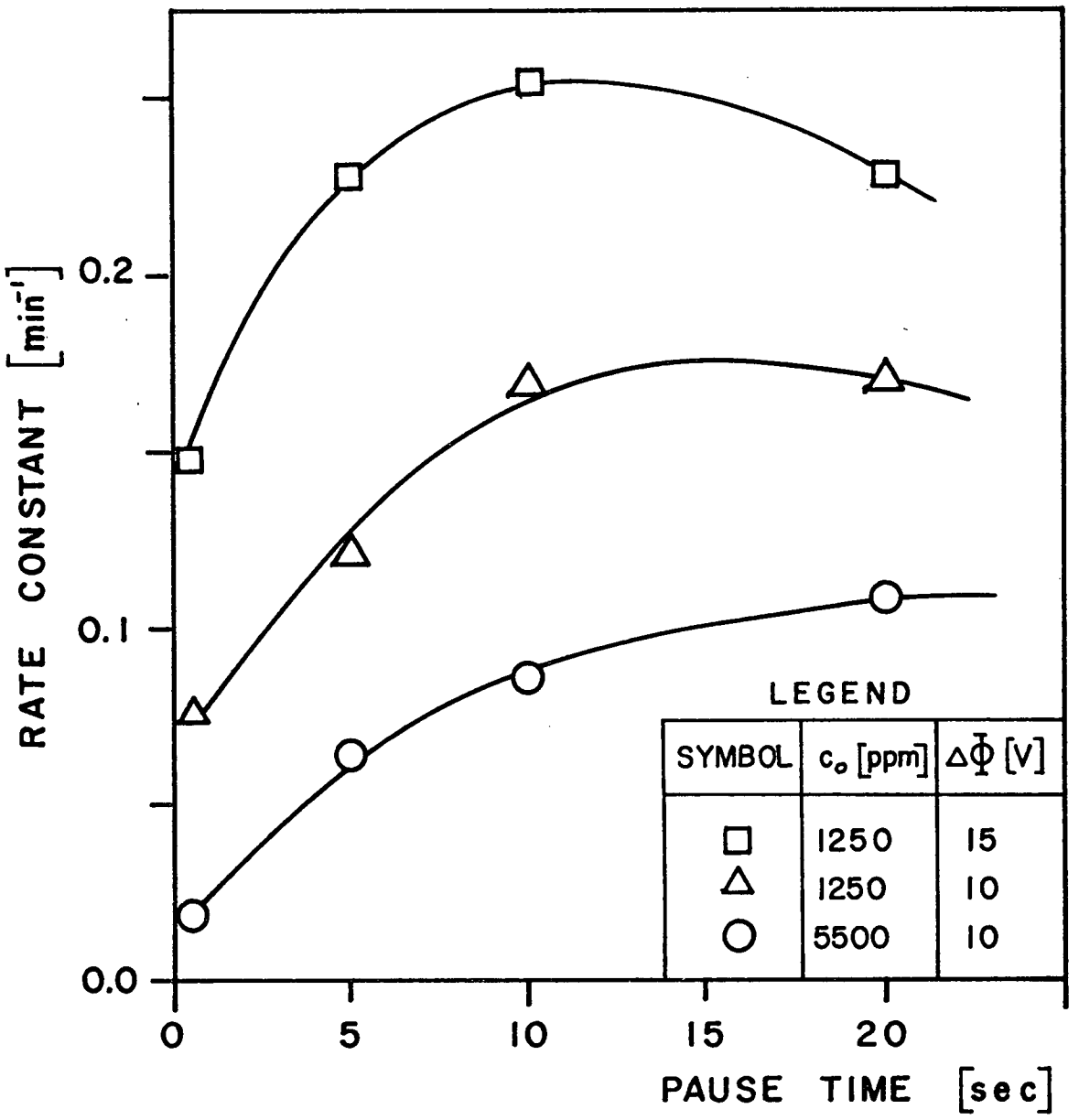

Figure 86. Effect of pause time (τ) on initial rate of separation (a).

5.5.4 Effect of applied voltage.

The applied electrode voltage ($\Delta\Phi$) was increased in three groups of experiments from 5 to 10 to 15 volts. The other system parameter values are listed in Table 36, and the transients of the separation factors are shown in Figures 87, 88, 89. The results are:

1. Initial rate and final separation are much improved by an increase of the applied potential.

2. The rate constant is approximately a linear function of $\Delta\Phi$, see Figure 90. From theoretical considerations the function has to pass through the point of origin.

3. The current consumption (both initial and final) is proportional to $\Delta\Phi$.

4. The high concentration runs show the same saturation effect which was noticed previously.

5.5.5 Effect of initial concentration.

The initial concentration (c_0) was increased for three groups of experiments from 1200 to 2500 to 5700 ppm NaCl. The rinse solution remained at 10,000 ppm NaCl. Table

Table 36

Effect of Applied Voltage ($\Delta\Phi$) on Second Electrodialyzer

RUN NO.	NO. OF STAGES	PAUSE TIME	INITIAL CONC.	APPLIED VOLTAGE	DISPL. VOLUME	SUPERF. VELOCITY	INITIAL RATE	TOTAL CURRENT		PROCESS pH		RINSE pH	
								INITIAL	FINAL	INITIAL	FINAL	INITIAL	FINAL
#	MS	τ	c_0	$\Delta\Phi$	δ	v	a						
[-]	[-]	[sec]	[ppm]	[volt]	[-]	[cm/sec]	[min^{-1}]	[ampere]	[ampere]	[-]	[-]	[-]	[-]
35	8	5	1220	5	2/3	5.4	.072	1.3	1.1	7.2	7.0	6.5	5.2
28			1280	10			.120	2.7	1.8	-	-	-	-
32			1240	15			.229	4.2	2.8	6.2	5.3	6.0	6.0
36	8	10	1250	5	2/3	5.4	.088	1.4	0.8	6.6	6.2	5.3	5.3
26			1290	10			.170	2.6	1.4	6.1	5.5	5.8	5.7
35a			1220	10			.170	2.7	1.4	7.2	6.3	5.2	5.6
33			1200	15			.255	3.5	2.0	6.4	5.7	5.7	5.6
13	8	5	5100	5	2/3	5.4	.030	2.2	2.0	5.7	5.9	5.7	6.5
8			5300	10			.063	5.6	3.8	-	-	-	-
10			4800	10			.063	5.1	4.1	5.7	5.7	5.6	6.5
16			5500	15			.116	9.5	6.9	6.0	5.5	5.4	5.4

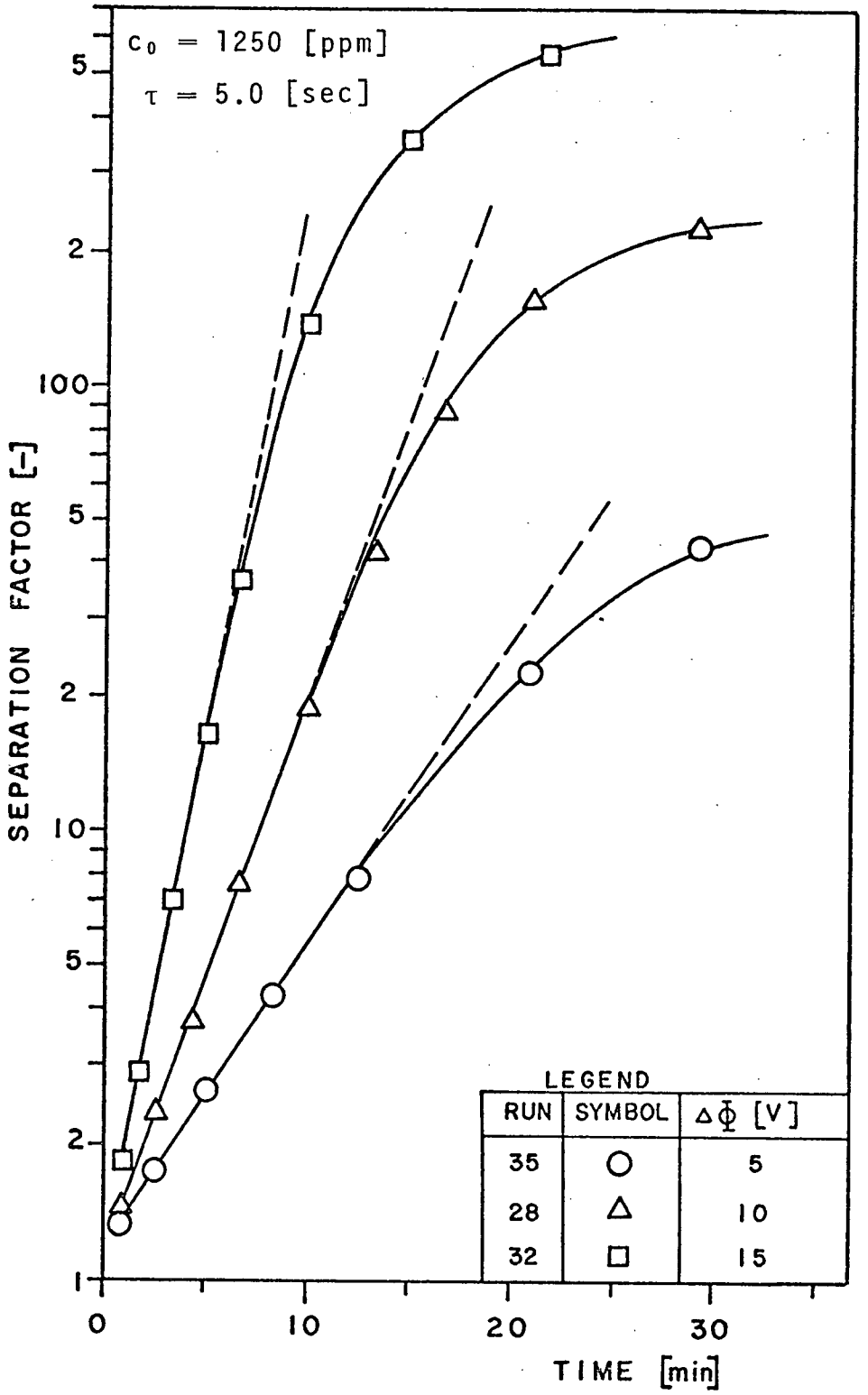

Figure 87. Effect of applied voltage (ΔΦ) on separation factor transients.

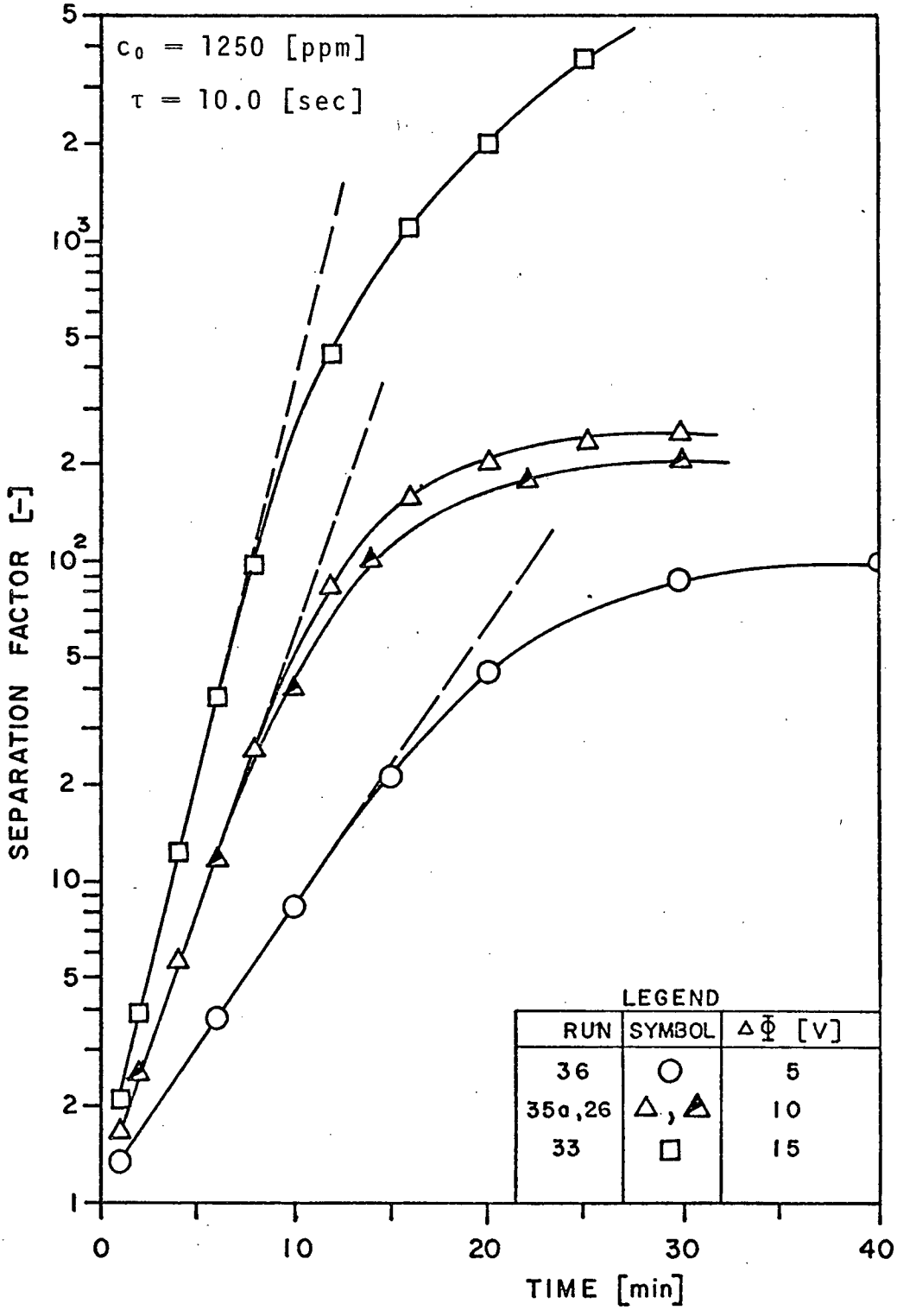

Figure 88. Effect of applied voltage ($\Delta\Phi$) on separation factor transients.

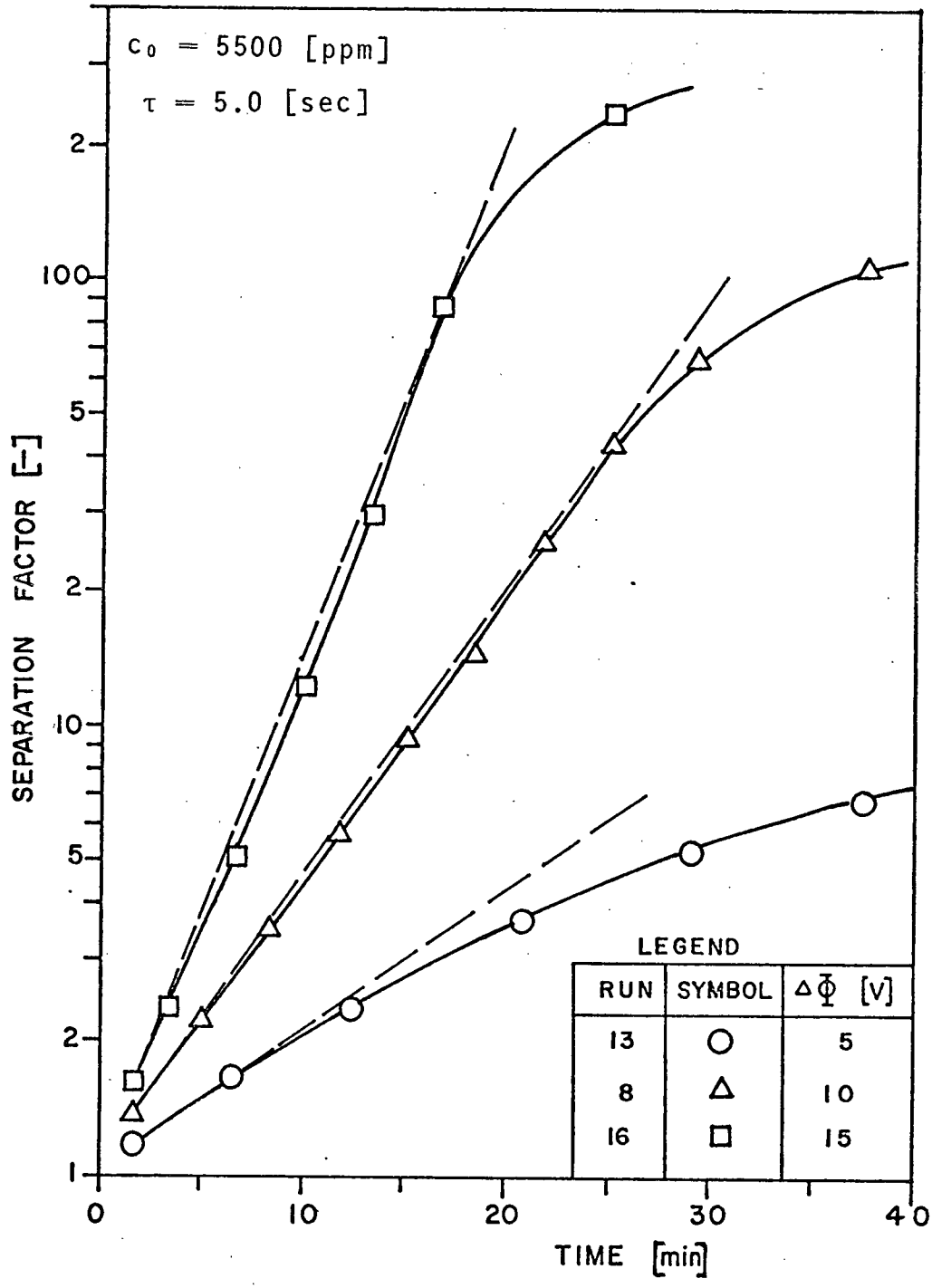

Figure 89. Effect of applied voltage (ΔΦ) on separation factor transients.

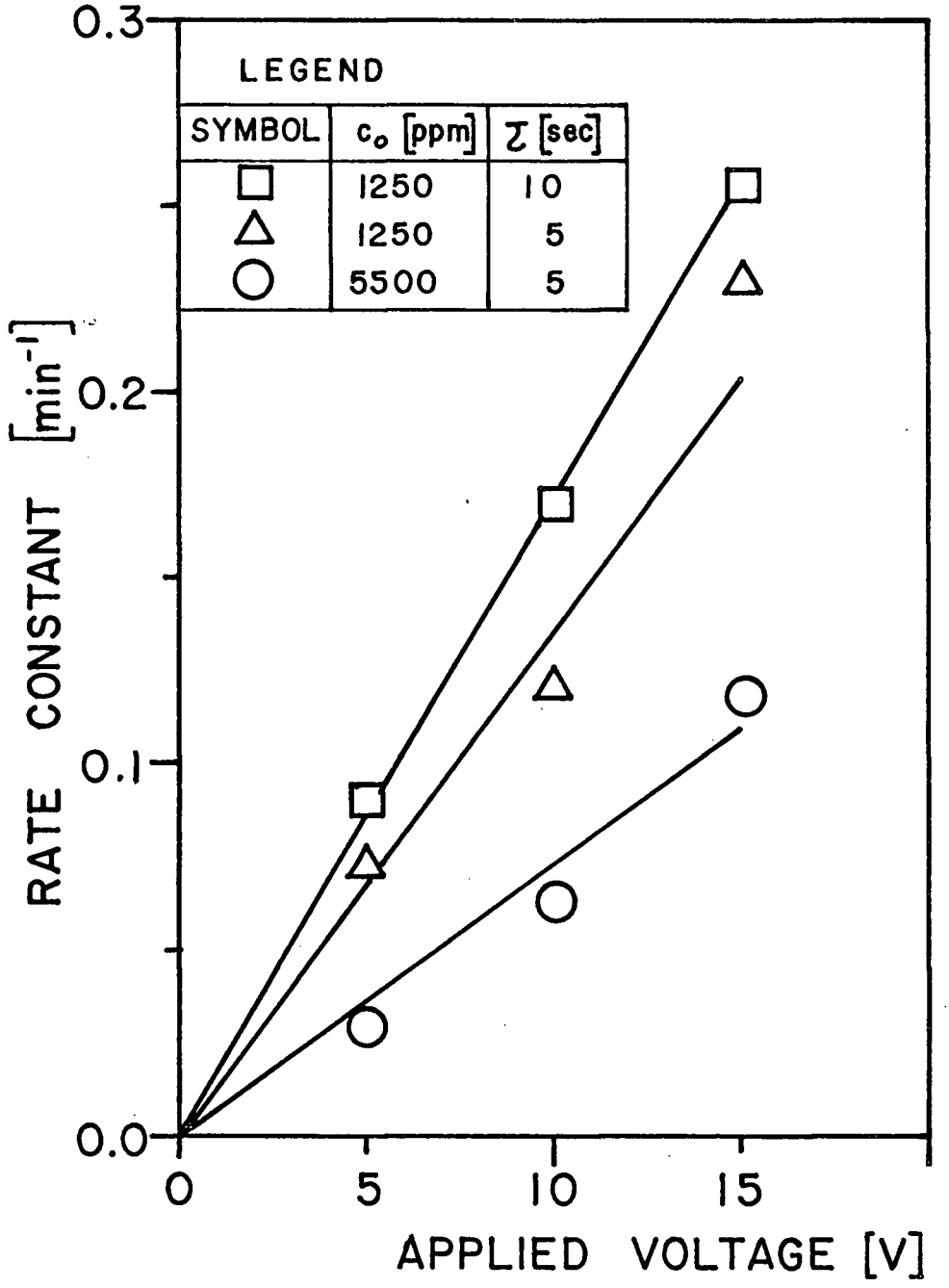

Figure 90. Effect of applied voltage ($\Delta\Phi$) on initial rate of separation (a).

37 summarizes the operating conditions and Figure 91, 92 and 93 display the separation factor transients. The results are:

1. The initial rate of separation is reduced by higher initial concentrations (see also Figure 96 and footnote on page 221).

2. The final separation factor shows no consistent results. In Figure 91 the final ns seems to be independent of c_0; the same applies for highest and lowest concentrations in Figure 92. The c_0 = 2500 ppm curve rises to a much higher level than the other two in Figure 92 but reaches a lower limiting value in Figure 93. The c_0 = 1200 ppm transient increases well beyond 10^3. It was stressed earlier that the conductivity meter is not actually capable of monitoring such large concentration changes. It is believed, however, that the accuracy of the meters is not the primary cause of this scatter.

3. Both initial and final current increase with c_0, but at a decreasing rate.

5.5.6 Effect of displaced volume.

The displaced volume (δ) was varied for three sets of experiments and increased from 1/4 to 2/3 to 1 total void

Table 37

Effect of Initial Concentration (c_0) on Second Electrodialyzer

RUN NO.	NO. OF STAGES	PAUSE TIME	INITIAL CONC.	APPLIED VOLTAGE	DISPL. VOLUME	SUPERF. VELOCITY	INITIAL RATE	TOTAL CURRENT		PROCESS pH		RINSE pH	
								INITIAL	FINAL	INITIAL	FINAL	INITIAL	FINAL
ϕ	MS	τ	c_0	$\Delta\Phi$	δ	v	a						
[-]	[-]	[sec]	[ppm]	[volt]	[-]	[cm/sec]	[min^{-1}]	[ampere]	[ampere]	[-]	[-]	[-]	[-]
27	8	20	1250	10	2/3	5.4	.150	2.2	1.1	6.2	5.6	5.4	5.3
22			2600				.150	4.0	1.5	6.2	5.3	6.1	5.5
9			5400				.108	5.5	2.0	-	-	-	-
26	8	10	1290	10	2/3	5.4	.170	2.7	1.4	6.1	5.5	5.8	5.7
35a			1220				.170	2.6	1.4	7.2	6.3	5.2	5.6
23			2650				.141	4.2	2.1	5.8	4.3	5.0	5.2
6			5700				.086	5.6	3.2	-	-	-	-
33	8	10	1200	15	2/3	5.4	.255	3.5	2.0	6.4	5.7	5.7	5.6
24			2650				.200	5.8	3.0	5.7	4.3	4.9	5.3
21			5200				.170	8.8	3.4	5.9	4.8	6.0	6.8

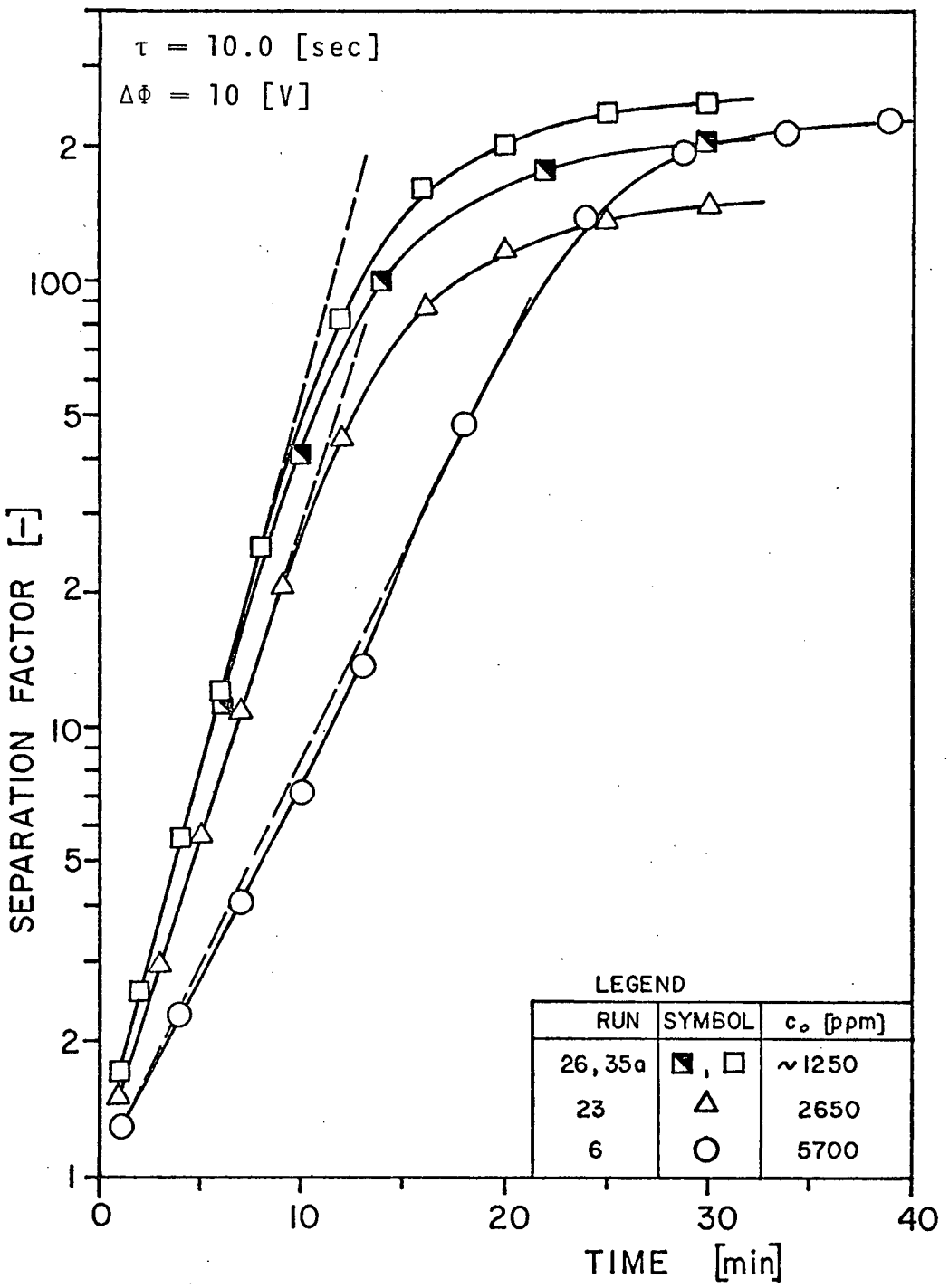

Figure 91. Effect of initial concentration (c_0) on separation factor transients.

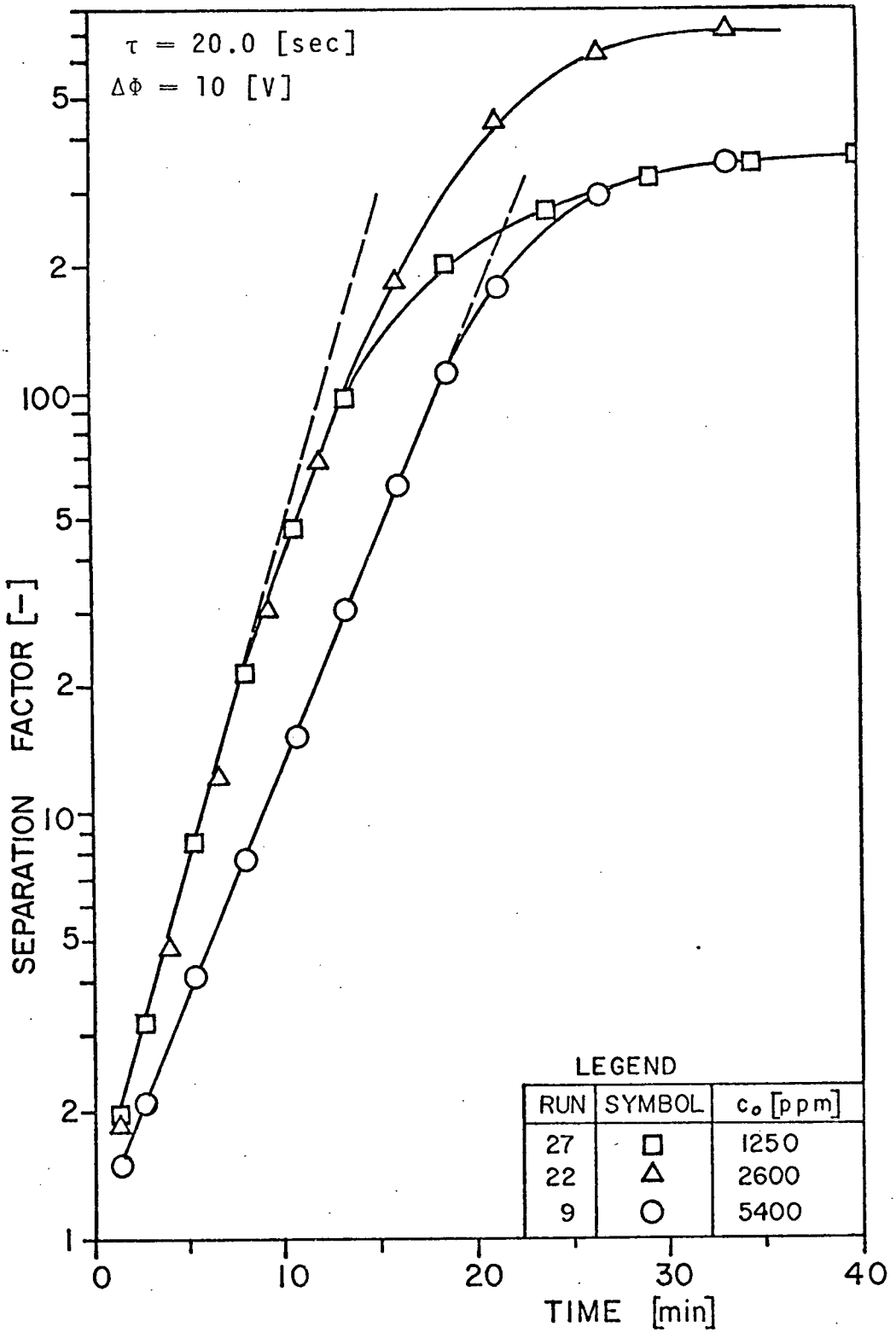

Figure 92. Effect of initial concentration (c_0) on separation factor transients.

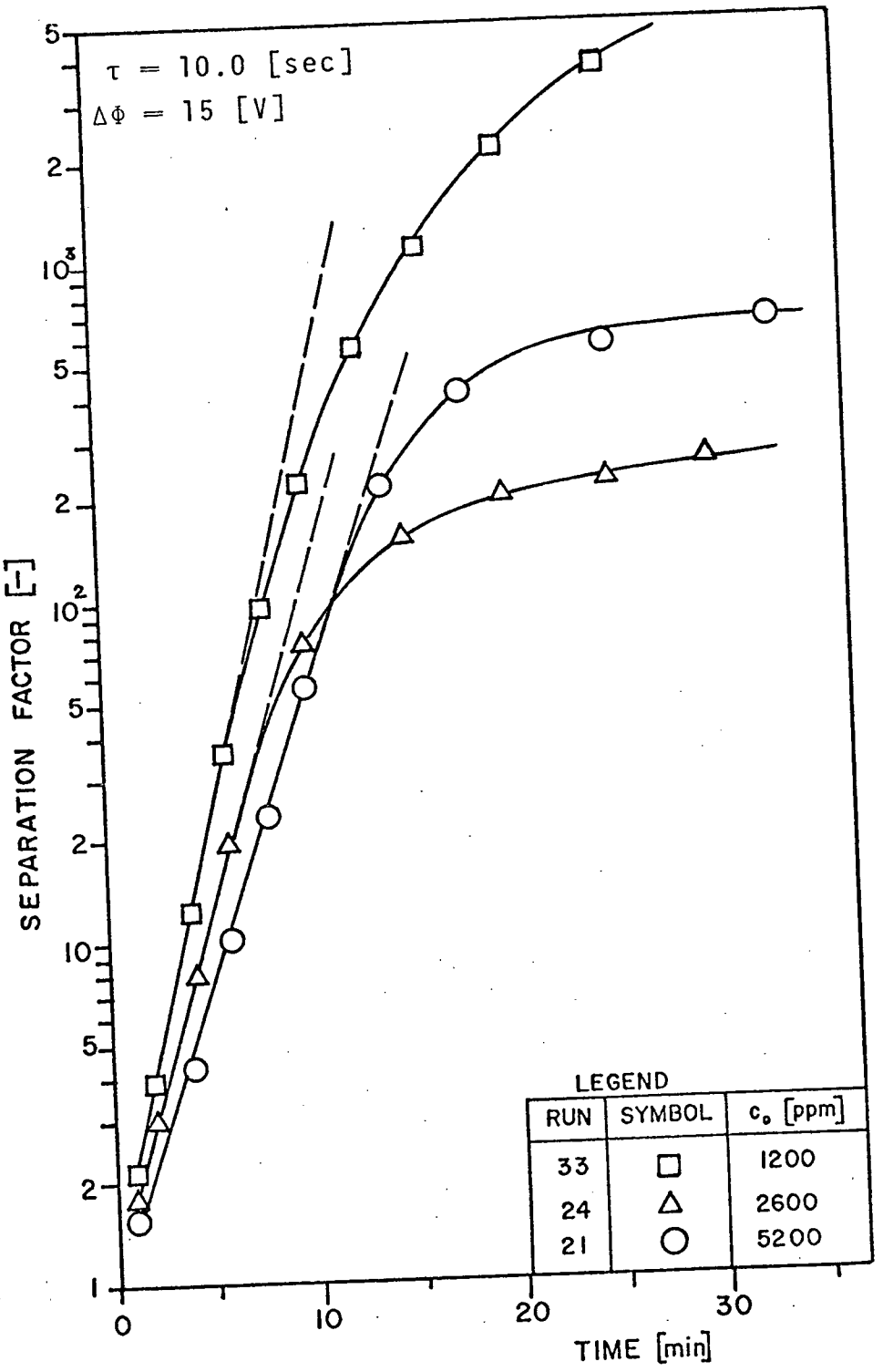

Figure 93. Effect of initial concentration (c_0) on separation factor transients.

volume, see Table 38. The separation factor transients are plotted in Figure 94, 95 and 96. The following findings have been extracted:

1. In a no-pause operation, at low concentrations, the initial rate is largest for $\delta = 1$ and decreases slightly with δ, see Figure 94. The final separation is smaller for large δ's because of the breakthrough of the concentration front (or part of it).

2. In pause operation at the same conditions this initial effect disappears more or less, see Figure 95. What remains is the continued rise of the transient for $\delta = 1/4$, beyond the bounds of accuracy of the present measuring system.

3. For high concentrations ($c_0 = 5500$ ppm) the saturation effect causes the transients to rise faster for small δ's than for large ones. The amount of salt that is redistributed between solution and sorption membranes is almost constant per cycle. The cycle period is small if δ is small. The real time transients are, therefore, accelerated. The final separation is also much smaller if δ is large, because, although the front does not break through, the system has a certain amount of internal dispersion.

Table 38

Effect of Displaced Volume (δ) on Second Electrodialyzer

RUN NO.	NO. OF STAGES	PAUSE TIME	INITIAL CONC.	APPLIED VOLTAGE	DISPL. VOLUME	SUPERF. VELOCITY	INITIAL RATE	TOTAL CURRENT		PROCESS pH		RINSE pH	
								INITIAL	FINAL	INITIAL	FINAL	INITIAL	FINAL
#	MS	τ	c_0	$\Delta\Phi$	δ	v	a						
[-]	[-]	[sec]	[ppm]	[volt]	[-]	[cm/sec]	[min^{-1}]	[ampere]	[ampere]	[-]	[-]	[-]	[-]
41	8	0.6	1300	10	1/4	5.4	.057	3.6	3.4	6.1	5.8	5.3	5.3
25			1250		2/3		.077	3.0	2.4	6.1	5.3	6.0	5.8
30			1270		1		.091	3.0	2.6	-	-	-	-
42	8	10	1175	10	1/4	5.4	.159	2.6	0.9	6.2	5.9	5.1	5.3
26			1290		2/3		.170	2.7	1.4	6.1	5.5	5.8	5.7
35a			1220		2/3		.170	2.6	1.4	7.2	6.3	5.2	5.6
29			1260		1		.170	2.7	1.8	-	-	-	-
12	8	5	4300	10	1/4	5.4	.091	5.4	2.6	5.4	5.7	5.5	6.5
8			5300		2/3		.063	5.6	3.8	-	-	-	-
10			4800		2/3		.063	5.1	4.1	5.7	5.7	5.6	6.5
11			5300		1		.046	5.5	4.6	6.2	6.3	6.8	6.7

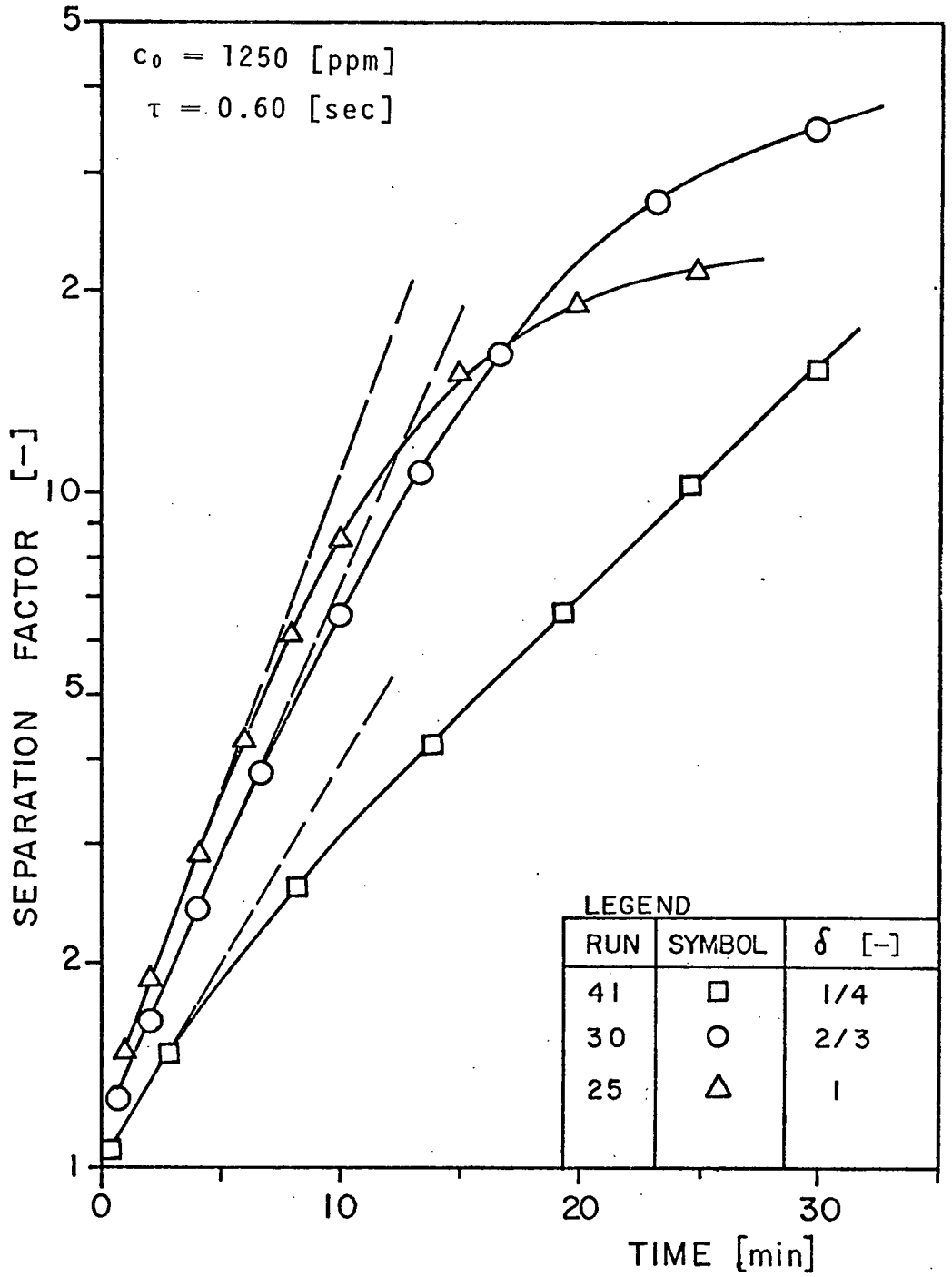

Figure 94. Effect of displaced volume (δ) on separation factor transients.

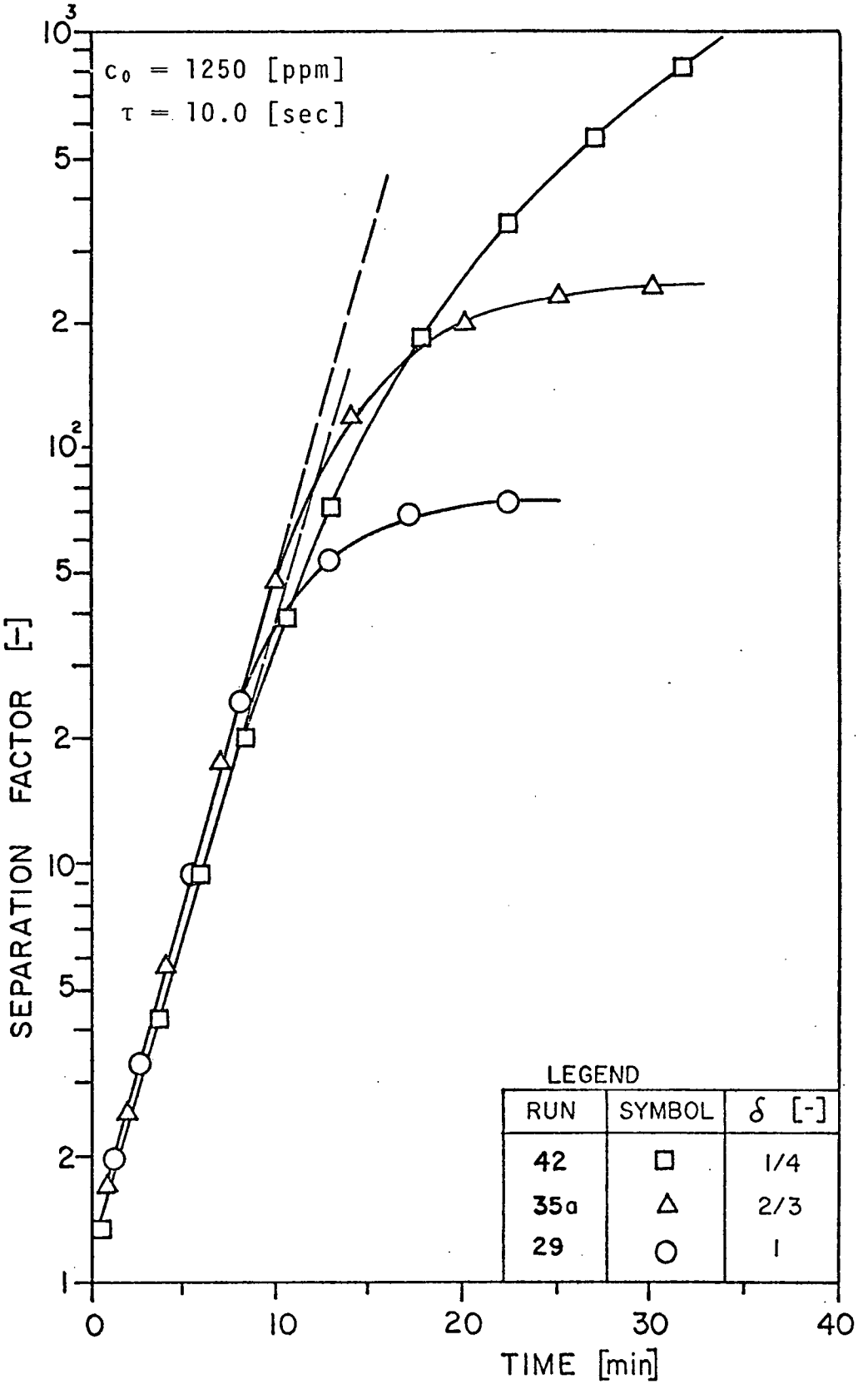

Figure 95. Effect of displaced volume (δ) on separation factor transients.

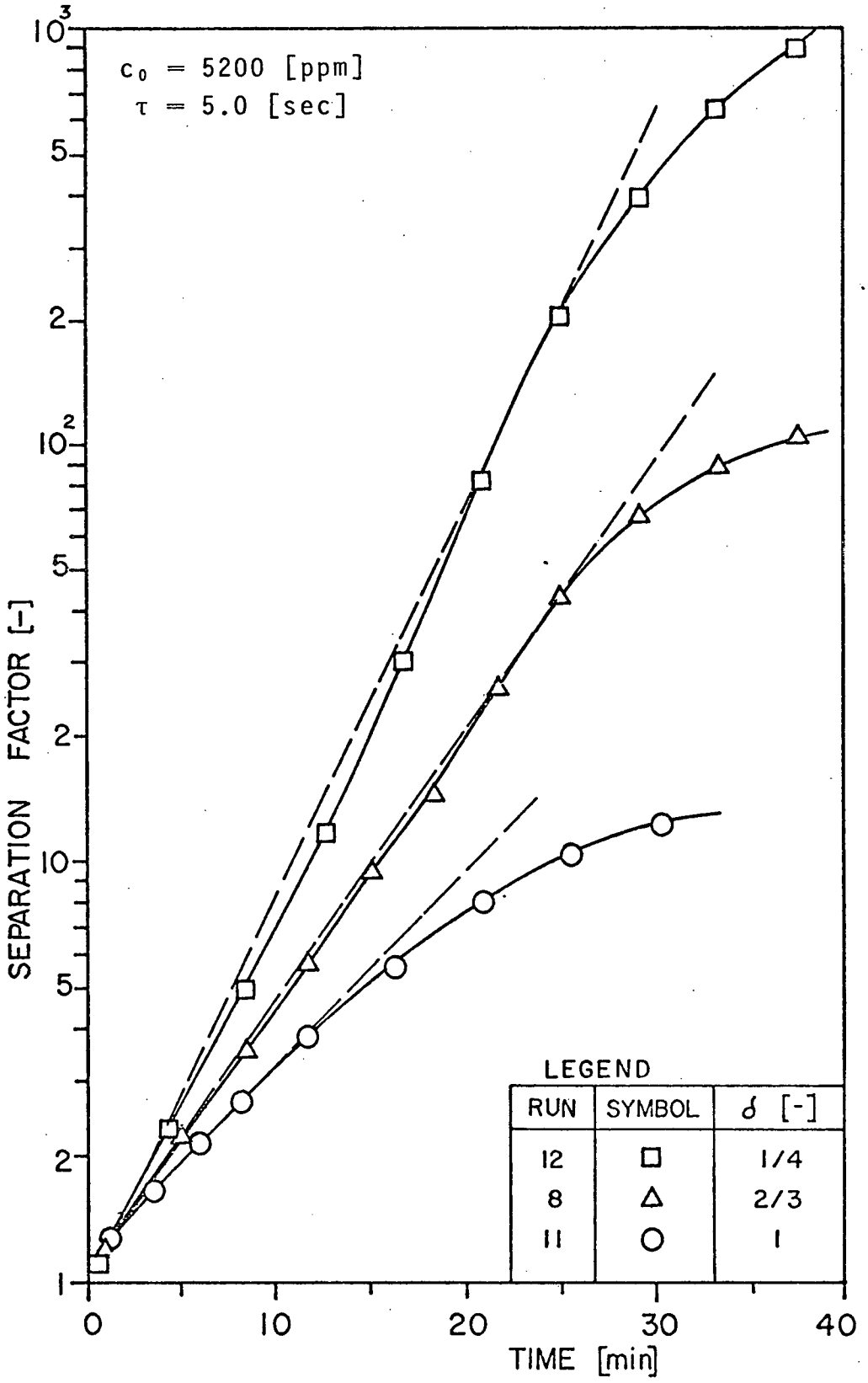

Figure 96. Effect of displaced volume (δ) on separation factor transients.

4. The initial current consumption is independent of δ except for the no-pause group. The final current reflects the amount of separation at the end of each run.

5.5.7 Effect of dead volumes.

The dead volumes[+] were increased for a single pair of runs (#45 & #52, on 4 stages) to check findings from the first ED cell. The result is shown in Figure 97 in terms of the product concentration transients. One can see that the final separation is the same for both experiments, although the presence of 1/2 void volume in each end reservoirs slows down the rate at which the limit is approached.

5.5.8 Effect of superficial velocity.

The flow rate of the process solution was altered in three groups of experiments, which are listed in Table 39 together with their operating conditions. Again, separation factor transients are diagrammatically shown in Figure 98 and 99.[*] The results are similar to those obtained on the first ED cell:

---

[*] Figure 98 contains results on no-pause experiments for high and low concentrations. The retarding influence of the initial concentration is very clear from this graph.

[+] Or excess volumes in the end reservoirs.

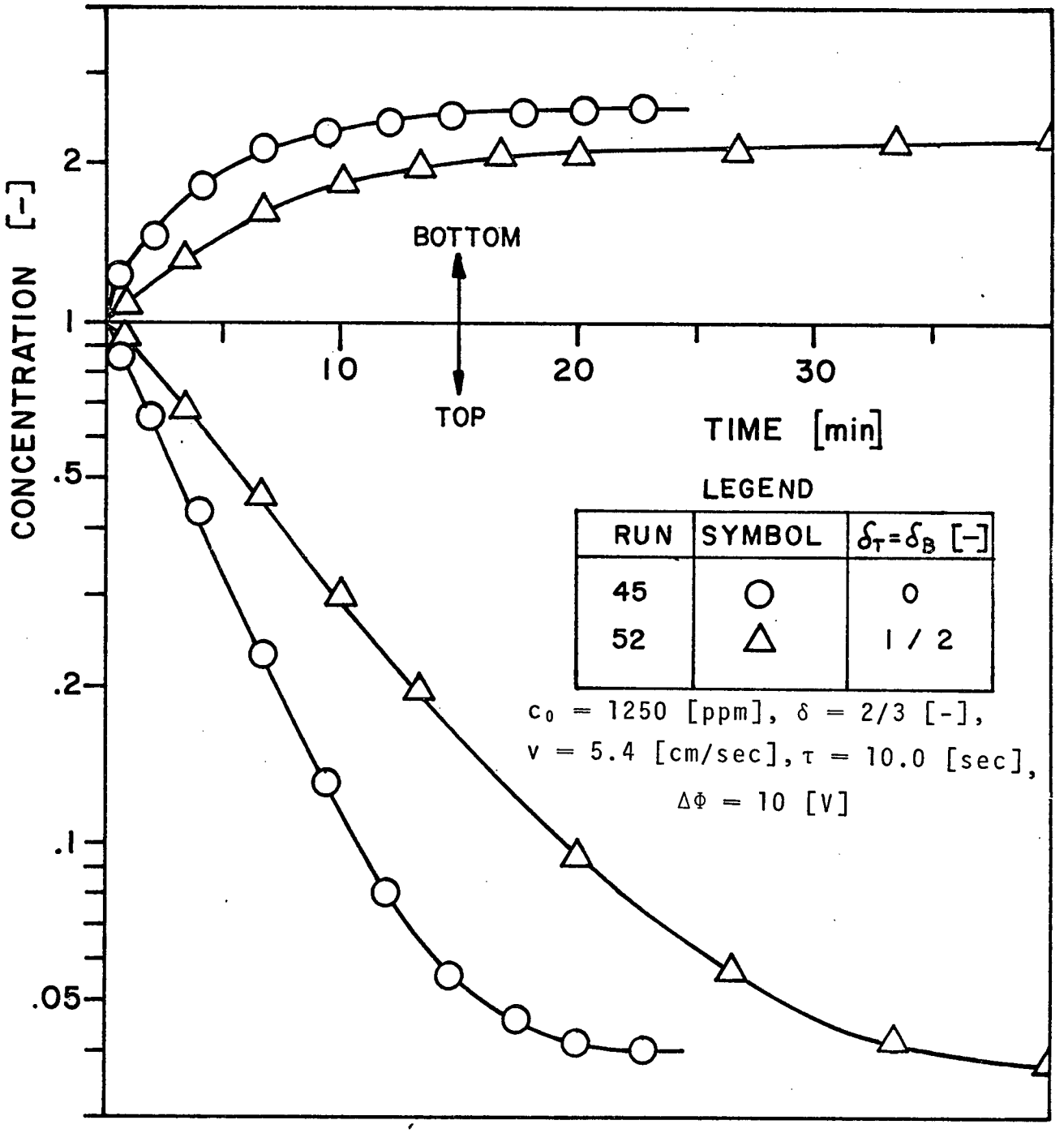

Figure 97. Effect of dead volumes (δ_B/δ_T) on concentration transients.

Table 39

Effect of Superficial Velocity (v) on Second Electrodialyzer

RUN NO.	NO. OF STAGES	PAUSE TIME	INITIAL CONC.	APPLIED VOLTAGE	DISPL. VOLUME	SUPERF. VELOCITY	INITIAL RATE	TOTAL CURRENT		PROCESS pH		RINSE pH	
								INITIAL	FINAL	INITIAL	FINAL	INITIAL	FINAL
#	MS	τ	c_0	$\Delta\Phi$	δ	v	a						
[-]	[-]	[sec]	[ppm]	[volt]	[-]	[cm/sec]	[min^{-1}]	[ampere]	[ampere]	[-]	[-]	[-]	[-]
37	8	0.6	1150	10	2/3	1.35	.100	2.0	1.6	6.6	5.6	5.4	6.0
38			1250			3.00	.091	2.7	2.2	6.4	5.4	5.8	5.6
25			1250			5.4	.077	3.0	2.4	6.1	5.3	6.0	5.8
39	8	10	1260	10	2/3	1.42	.125	2.1	1.4	6.1	5.7	5.4	6.2
40			1290			2.15	.141	2.3	1.6	6.5	5.9	5.4	5.5
26			1290			5.4	.170	2.7	1.4	6.1	5.5	5.8	5.7
35a			1220			5.4	.170	2.6	1.4	7.2	6.3	5.2	5.6
15	8	0.6	5400	10	2/3	1.6	.021	5.6	5.5	5.8	5.9	7.2	7.1
14			5050			3.0	.022	5.5	5.7	5.5	5.5	5.0	6.9
7			5700			5.4	.018	5.6	5.6	-	-	-	-

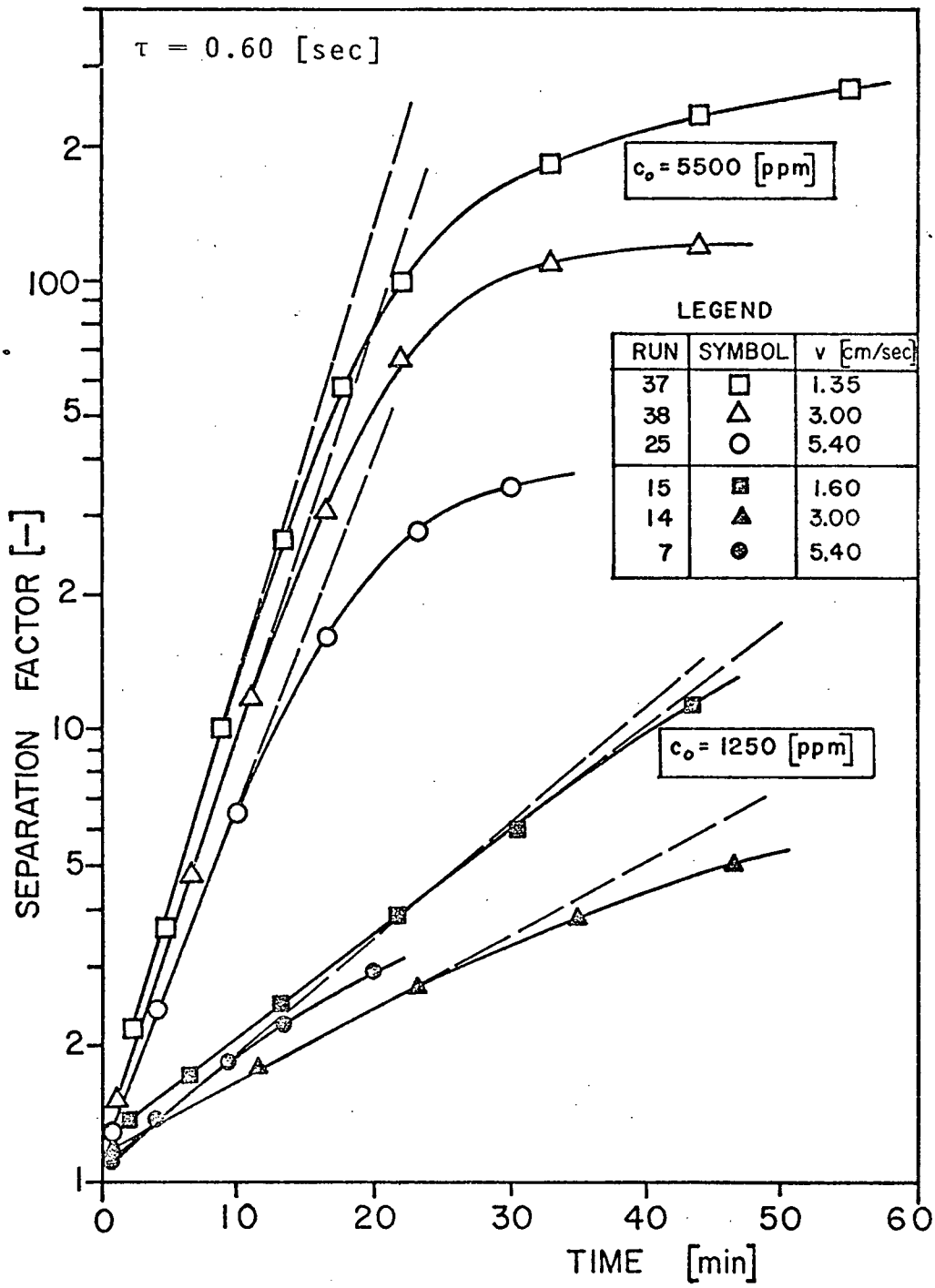

Figure 98. Effect of superficial velocity (v) on separation factor transients.

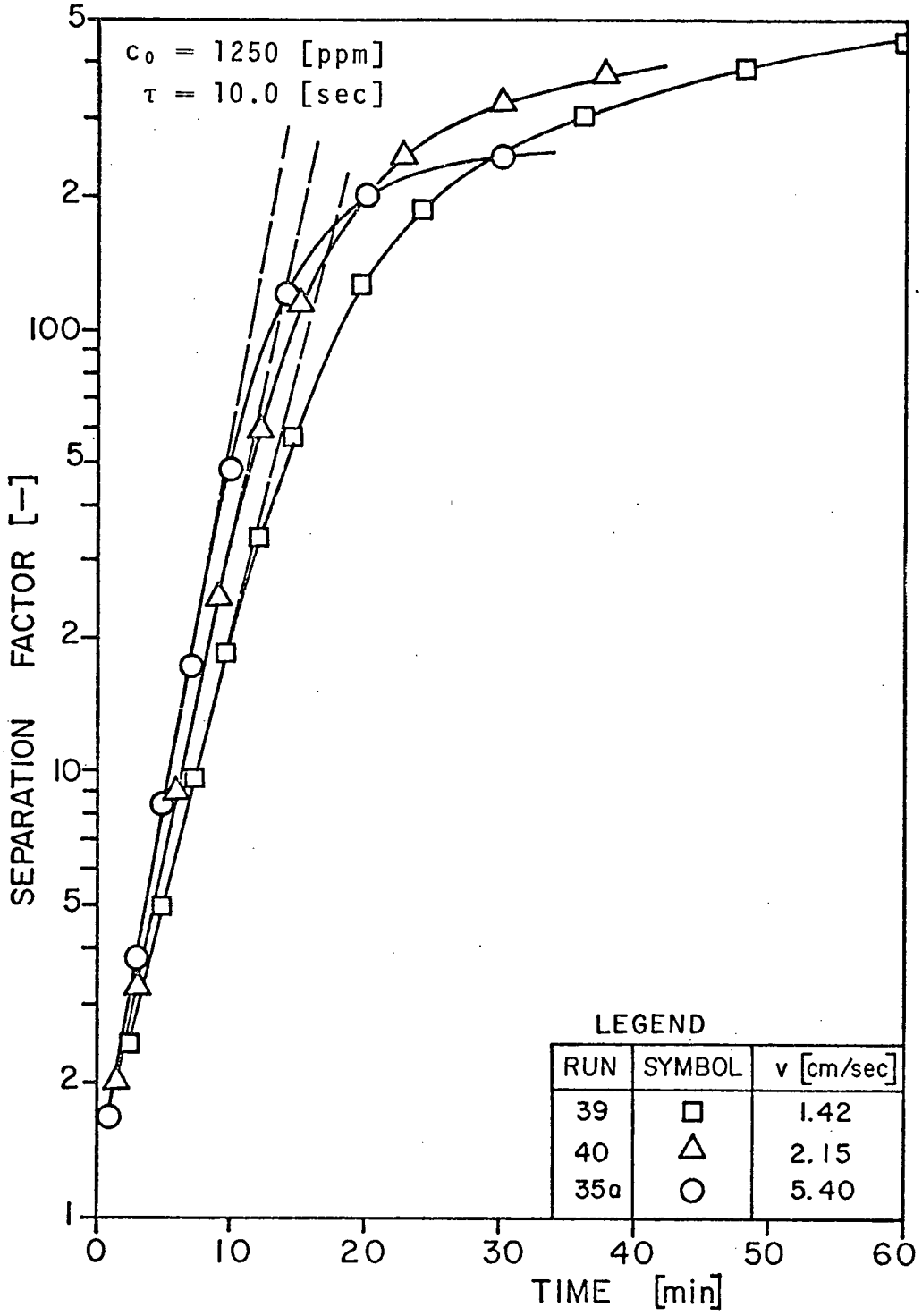

Figure 99. Effect of superficial velocity (v) on separation factor transients.

1. In continuous displacement mode (no-pause) slow displacement improves the rate as well as the final separation for low concentration, and the current consumption is smaller. At high concentrations the initial rate becomes essentially independent of the velocity v, but is also very small. The current is also independent of v.

2. In pause operation an increase of v results in a better initial performance. The final separation factor does not depend on v. The initial current consumption is smaller for the slow displacement run.

5.5.9 Reproducibility.

Several of the runs were repeated to test the reproducibility of the results. The following pairs may be compared (see Table 34, 35; Figure 82, 100, 101):

#8 & #10 , #26 & #35a ,

#27 & #49 , #40 & #50 .

The initial dialysate transient and all of the brine transient are generally extremely well reproduced. The final branch of the top product transient is subject to the limited accuracy of the conductometric measuring system. The final values of the dialysate concentrations are for most runs less than 3%

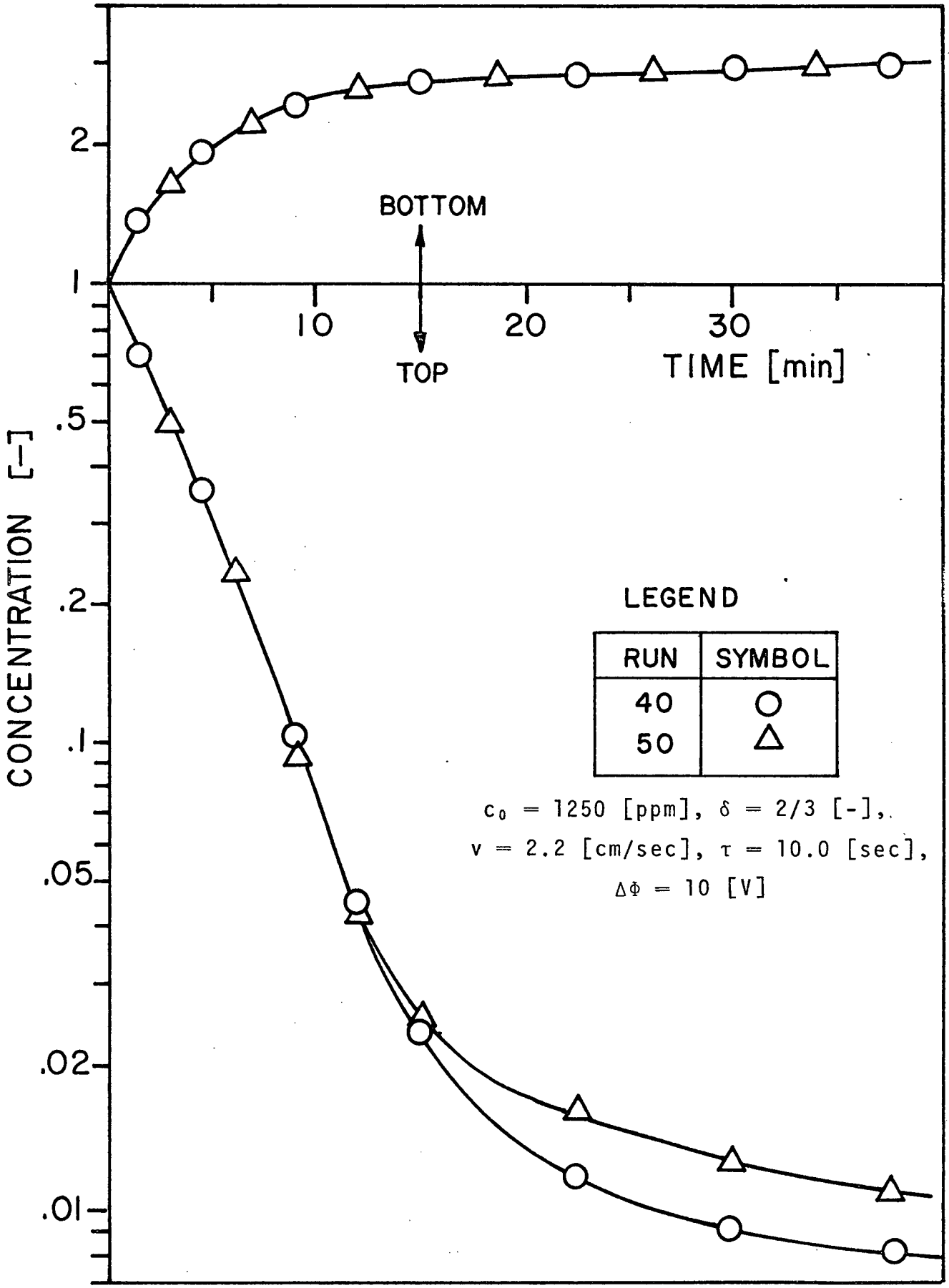

Figure 100. Reproducibility of second stack experiments.

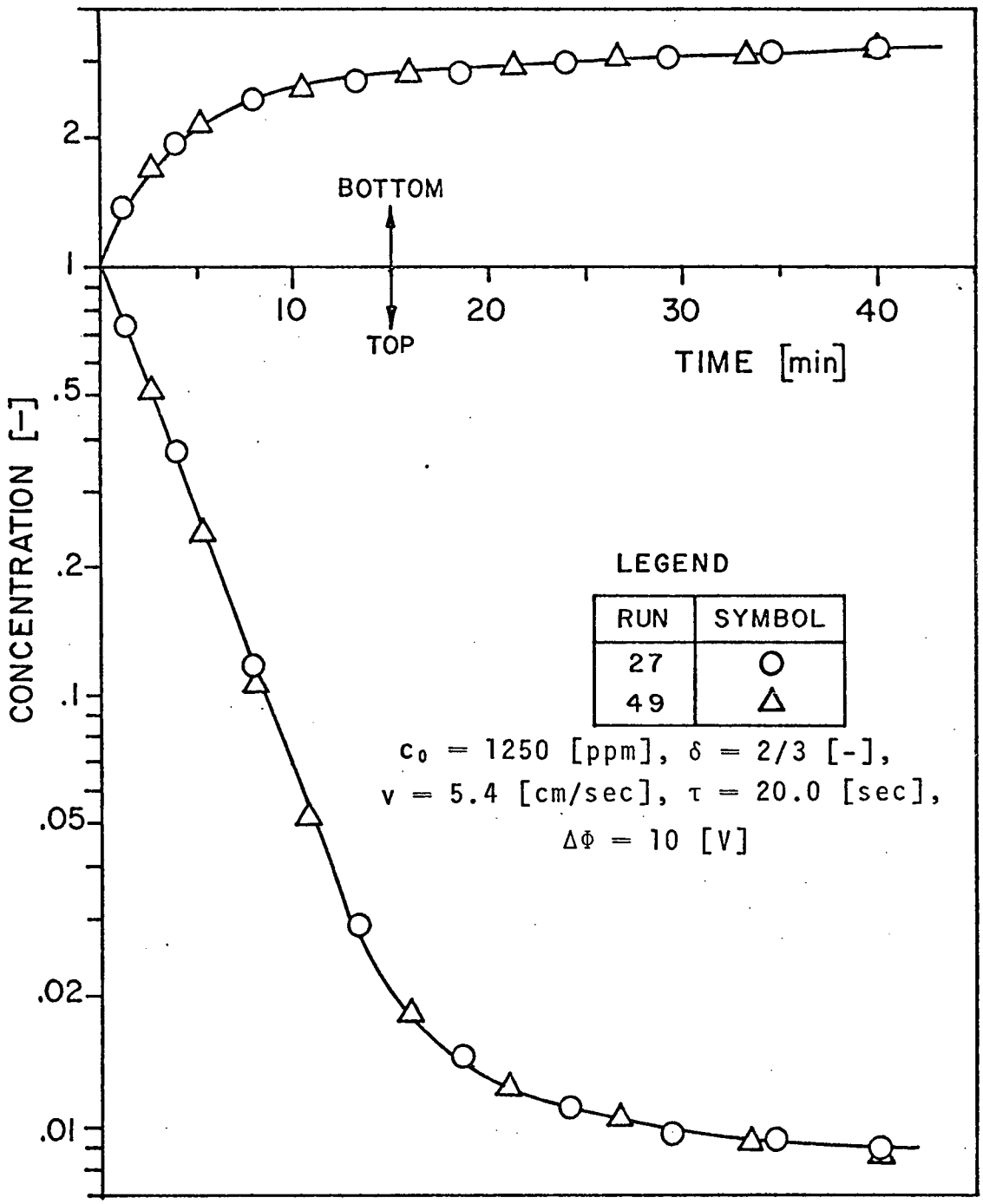

Figure 101. Reproducibility of second stack experiments.

of the initial concentration. Small variations of the operating conditions may influence the actual limit reached. The following accuracies are estimated to apply to these parameters:

Flow rate	$\dot{Q}$	: ±2 %
Applied voltage	$\Delta\Phi$	: ±1 %
Pause times	τ	: ±0.5%
Displaced volume	δ	: ±0.5%
Concentrations	c_T , c_B	: ±0.5%

5.5.10 Comment on the material balance for the solute.

A closed system requires conservation of the total mass in the system. The electrodialysis process involves two liquid streams which are separated by ion selective membranes. Solute or solvent will permeate through the membranes, and solution may seep from one stream into the other through mechanical leaks.

Any exchange of material would be detected either as volume or as concentration change of the two streams. Three situations have been considered to check the changes in the process stream.

1. The system was filled with rinse and process solutions of known volumes. The concentration of the process stream was always smaller than the concentration of the rinse

stream. The volume of the process solution decreased slightly when the system was allowed to stand for several days with no circulation or applied potential. Evaporation may have caused some volume change and osmotic water transfer was responsible for the remainder. The osmotic water transport through the separating membranes from low to high concentration was accompanied by solute flux in the opposite direction, since the process stream concentration increased more than the water removal alone would explain.

2. The system was filled with measured volumes of rinse and process solution at different concentrations, and circulated while disconnected from the power supply. After equilibration of the process solution with the sorption membranes, neither volume nor concentration of the stream changed over a period of one hour.

3. The process solution was equilibrated before and after some separation runs in which no pH samples were taken. The volumes were found to be unchanged but the concentration was usually out of balance by up to +5% for the first runs of the day. After two or three experiments, the concentrations before and after the runs were equal, however.

From these results it is concluded that no mechanical leaks existed, but that the membranes are quite permeable to solute.

The increase in solute concentration in the first daily runs may be an effect of a change in the distribution of solute between solution and sorption membranes. Since the experiments were always stopped after the completion of a full cycle, the initial distribution in the stack after some 12 hours of rest is likely to be different for that at the end of a run.

5.5.11 Comment on the performance of individual stages.

The following tests were performed to detect whether differences between individual stages of the electrodialyzer existed, and how these differences affected the separating performance.

a) Overpotential-current information.

The mean probe voltage and the mean current in each stage were evaluated and are tabulated in Appendix C.2. From these tables overpotential-current diagrams were prepared for each stage, see Figure 102. The scatter of the points, which are plotted for runs with constant applied voltage ($\Delta\Phi$ = 10 v), is considerable. Also, the bulk of the points shifts from small currents for the first stage to large currents for the eighth stage, because these constitute the dialysate and the brine end of the assembly, respectively.

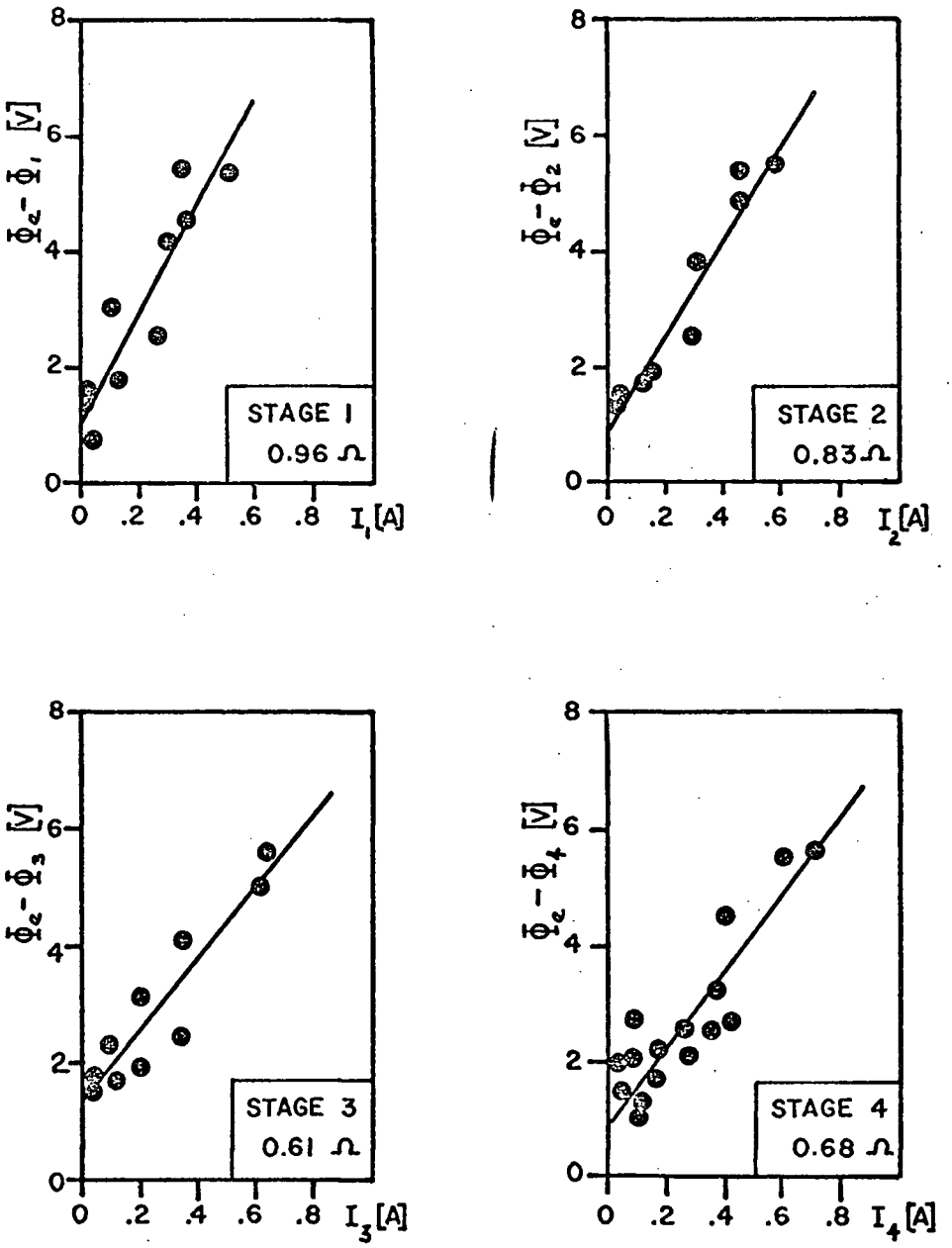

Figure 102. Overvoltage-current curves of the electrodialysis stages.

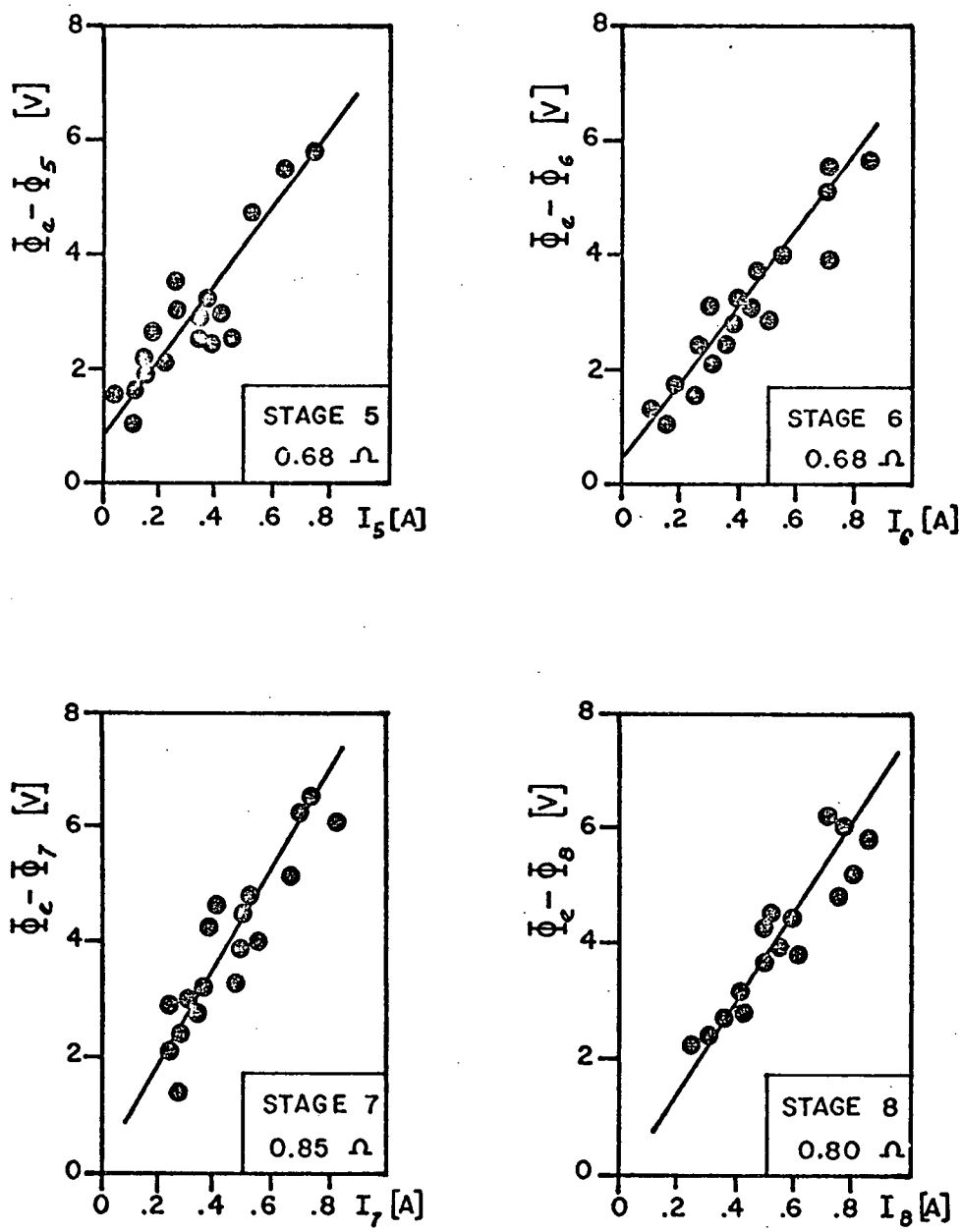

Figure 102. Overvoltage-current curves of the electrodialysis stages.

The experimental points may be approximated by straight lines in the range of currents investigated here. The slopes of the lines show a variation of 0.80 ± .16 Ω (± 20%). These slopes represent mainly the resistances of the solid connectors, the solution, and the dividing membrane in the rinse chambers. The flow rate to the various rinse chambers was almost equal, so that the hydrodynamic conditions may be assumed identical. Any difference in slope should, therefore, indicate unequal contact resistances.*

Figure 102 shows that stages 1, 2, 7, 8 have larger resistances than the others.

b) Comparison of local current and probe voltage transients during a single cycle.

The shape of the current and voltage curves traced by the multipen recorder during a complete cycle at limiting conditions is copied in Figure 103 and 104, respectively, for a typical run (#49). The numbers refer to the stage number. Each half cycle consists of a pause time followed by displacement. The first half cycle is an absorption half cycle. The general course of the transients will be described first:

---

*The graphite connectors constituted some problems in the present cells. They broke frequently and were too porous. Small amounts of rinse solution seeped through the graphite, causing corrosion of the metallic parts of the electric manifold.

The currents are relatively small during the demineralizing pause time. When the flow starts, solution of high concentration enters the eighth stage. The current through this stage increases sharply, goes through a maximum, and remains at a fairly high level. When the concentration front reaches the seventh stage the current here shows a peak, etc. Although the displacement is 2/3 void volumes, the concentration front just reaches the fourth stage by the end of the displacement period, which shows the retarded velocity of the concentration wave in the absorption stack. The highest current peak is observed in the sixth stage.

The currents increase in a step-wise manner at the start of the enriching pause time followed by rapid decays which indicate the depletion of the sorption membranes. Again the sixth stage shows a very high peak. During the displacement part of this half cycle the currents decrease further and show little influence of the hydrodynamic conditions in the flow channel.

The probe voltages are set in relation to the measured electrode voltage while the output voltage of the power supply is constant. The electrode voltage varies in time because there are several relay contacts as well as the resistances of the measuring shunts in series with the ED cell.

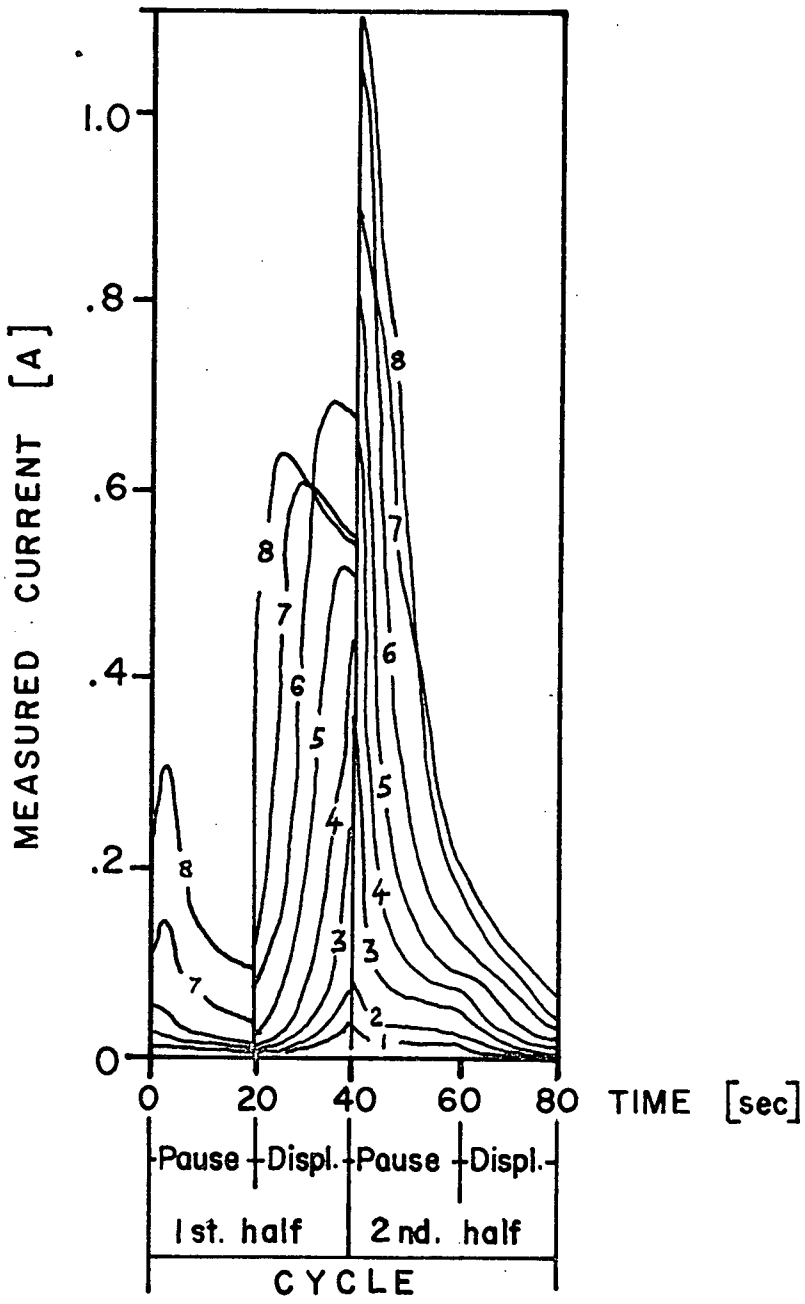

Figure 103. Time-space distribution of current at limiting conditions.

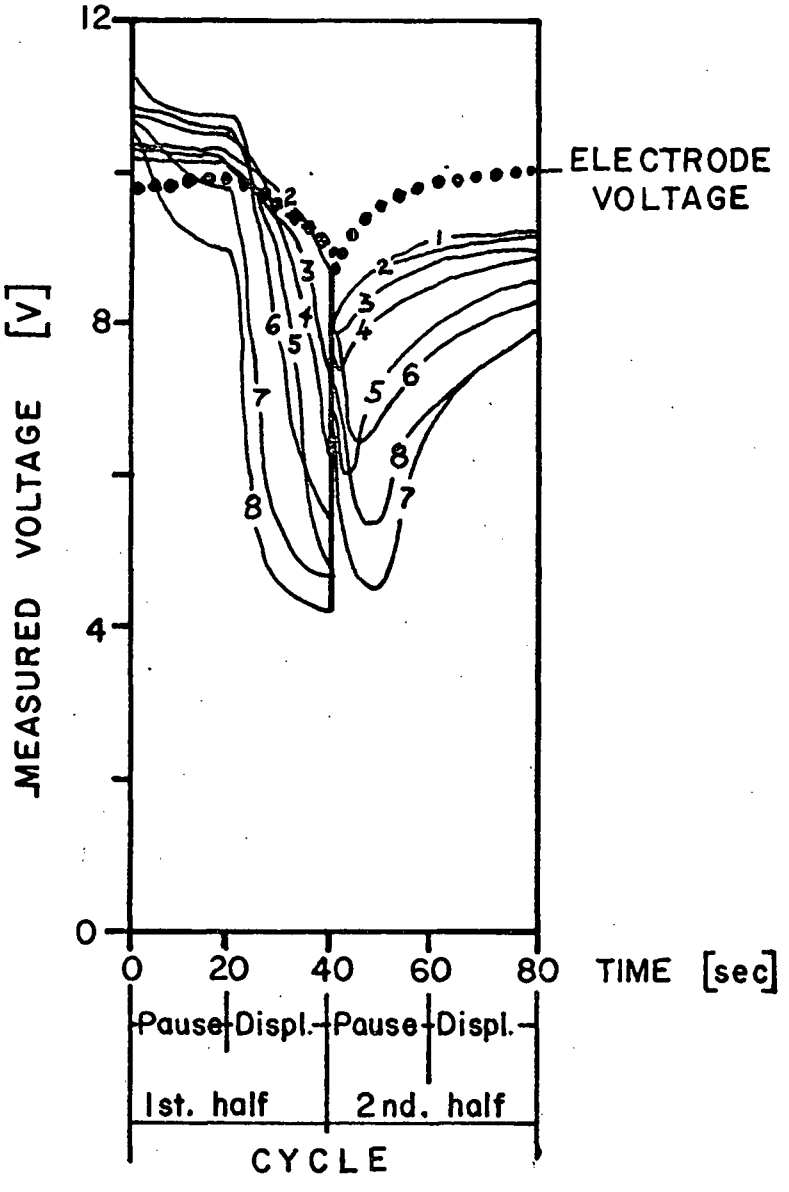

Figure 104. Time-space distribution of probe voltage at limiting conditions.

The probe voltages are higher than the applied electrode voltage during most of the first pause time. This is attributed to the membrane battery effect in unsteady-state operation. During the displacement the current increases and the probe voltage falls therefore below the applied one. When the polarity is switched the probe voltages increase. This indicates the reversed battery effect. The stack voltages pass through a minimum as the helpful concentration polarization disappears and increase subsequently toward a level distinctly below the electrode voltage.

Again, stage No. 6 seems to perform much better than No. 7 and No. 8. Its voltage level is higher despite the fact that it consumes almost as much current. The performance of No. 7 seems to be particularly poor and it shows the lowest minimum during the second part cycle.

c) Runs with selected stages.

The previous discussion shows differences between stages No. 5 & 6, and No. 7 & 8. A real life test was performed on the two pairs (see runs #19 & #20, Table 34). The separation transients coincide almost perfectly. The higher current consumption of run #20 is probably caused by the 10% higher concentration.

It is concluded that the differences between stages which are a result of the manufacturing procedure do not

seriously influence the performance of the stages with respect to their separating task. They may, however, influence the final limit of separation.

5.5.12 Experimental test of the constant rate model.

Four experiments were performed to test the constant rate model proposed in Chapter 3. The eight stages were connected in series hydraulically and electrically. The D.C. power supply was operated in constant current mode. These currents had to be fairly small, as the maximum output voltage of the D.C. supply was limited to 40 V.

In two runs the electric potential was switched in phase with the flow ($\gamma = 0$, see equations (21)). The phase shift in the other runs amounted to one quarter cycle ($\gamma = \frac{T}{4}$).

The results are shown in form of concentration transients (see Figure 105), and confirm that:

(i) the separation is virtually completed after the first cycle for in-phase switching,

(ii) the concentration transients are straight lines with equal absolute values of the slopes for equal rates when the switching is one quarter cycle out-of-phase. This holds experimentally only for the first cycles, because the power supply could not maintain constant current at a high enough voltage,

(iii) the decrease in dialysate concentration during the first cycle is larger for in-phase operation than for out-of-phase one.

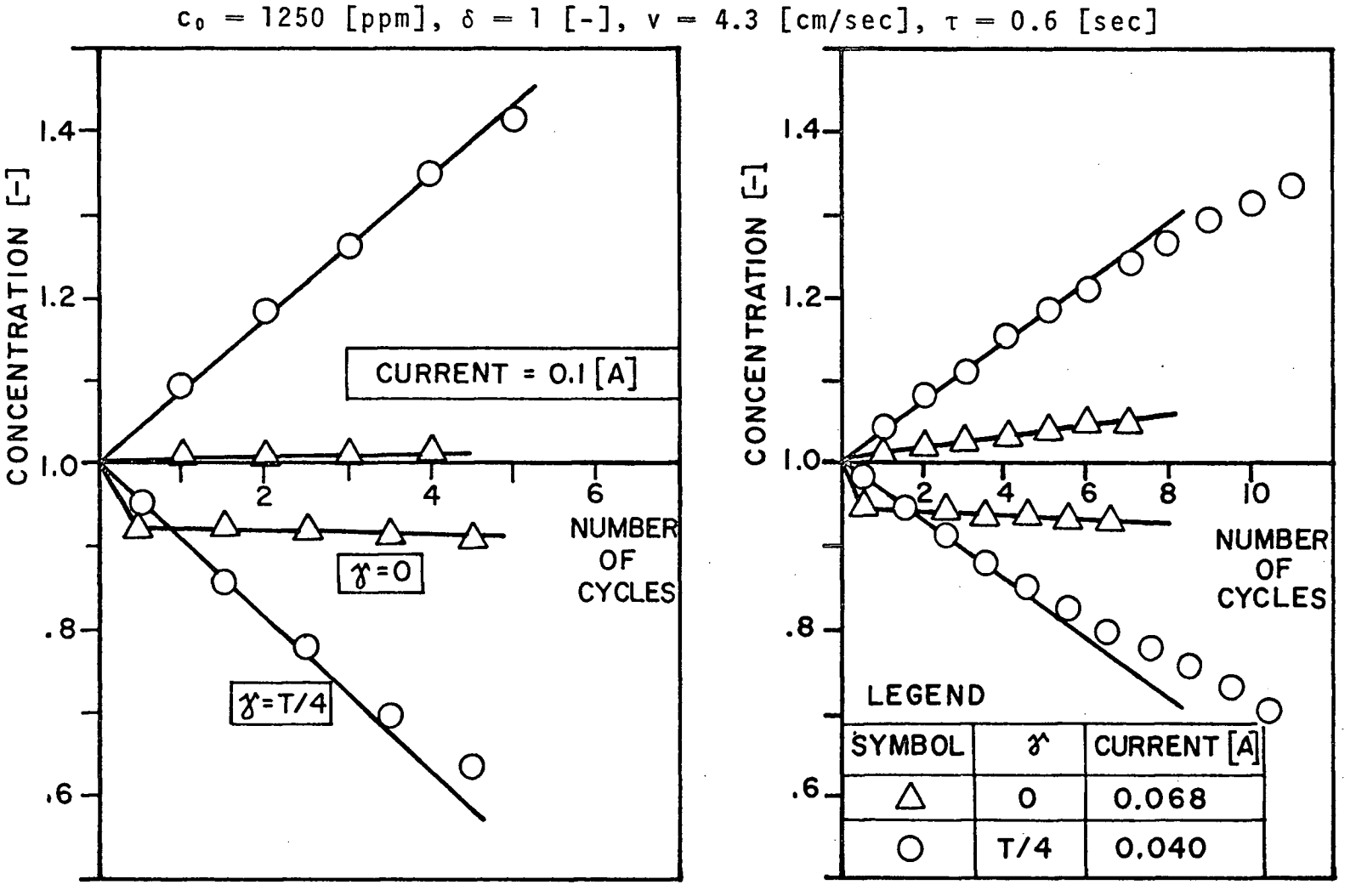

Figure 105. Influence of phase shift (γ) on transients for constant rate operation.

5.5.13 Comment on the effect of end mixing.

End mixing may be suppressed in the multiple stage ED module as follows. If less than eight stages are connected electrically the others may remain in the process flow line as inert (or idle) beds with small dispersion.

The following combination was chosen: four active stages bracketted by two idle ones on either side. Runs #51 and #53, see Table 13, were identical experiments except for the location of the conductivity cells: between the reservoirs and the last idle stages for run #51, and between the last active and the first idle stage on each side for run #53. A comparison run (#52) was performed with the same four centre stages but no idle stages. The dead volumes in the reservoirs ($\delta_B = \delta_T = 1/2$) were the same in this run as the volume of two idle stages in runs #51 and #53.

The results of the three tests are shown in Figure 106. The comparison run (#52) separates initially at a rate intermediate to those of the other experiments (#51 and #53), but reaches its final conditions before the other transients taper off. This indicates that partial suppression of the end mixing does not improve the final separation. There are two reasons that final conditions are much slower approached in runs #51 and #53 than in run #52.

1. Solute is stored in the sorption membranes when the ED stages are used as dead volumes. The brine

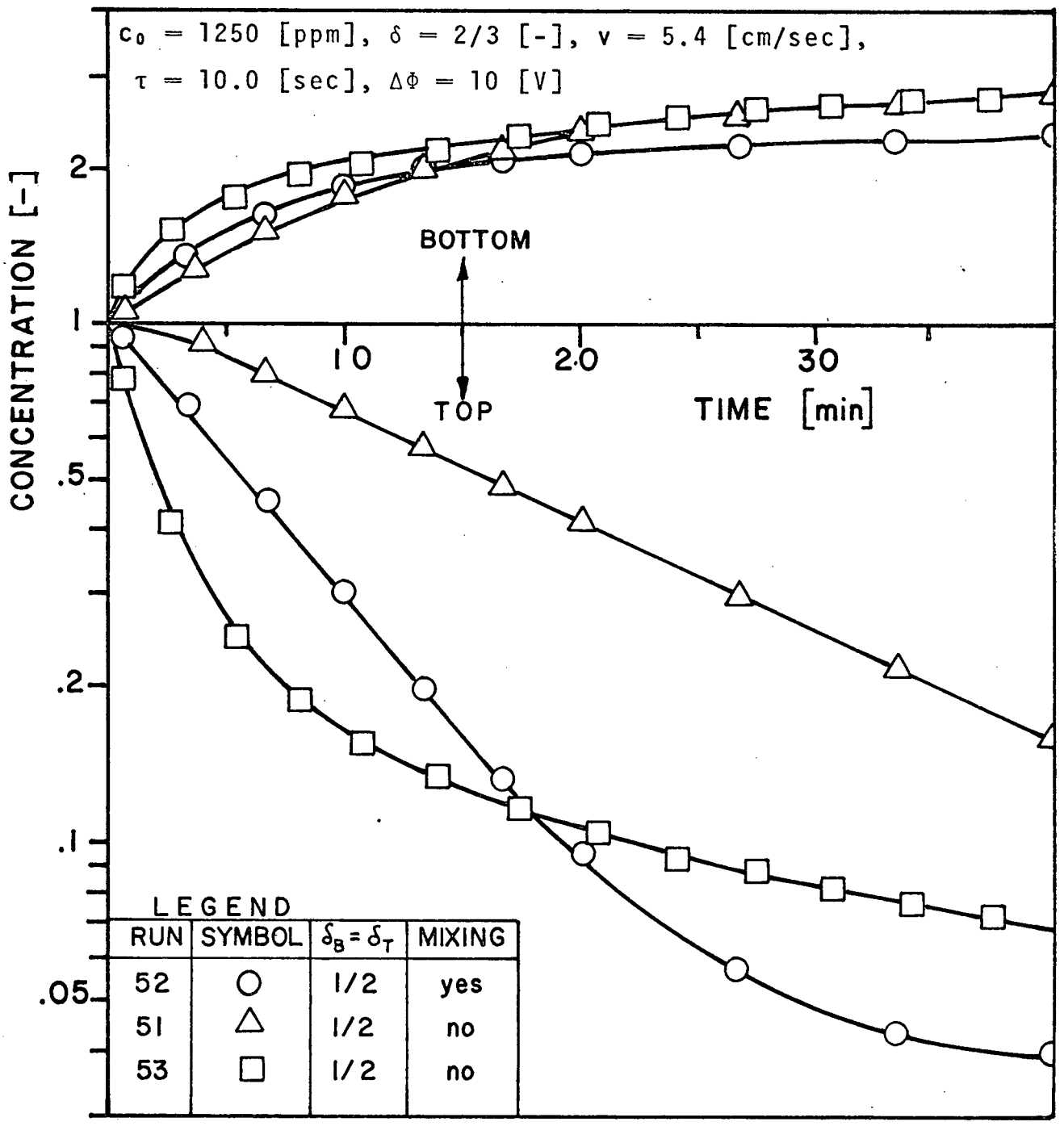

Figure 106. Effect of end mixing on concentration transients.

concentration tends toward a higher limit, therefore, and the dialysate transient is damped.

2. Suppose the internal dispersion in the ED stages may be neglected. In this case the reservoir concentrations will not experience any change whatsoever if the displaced volume is equal to the volume in the idle stages. The displaced volume in experiments #51 and #53 exceeded those of the idle stages by 1/6 void, only, and the internal dispersion is comparatively small. Hence, the concentrations of the reservoir solutions changed at a slow rate, and the concentration transients of the idle stages are damped.

5.5.14 Production of 90% demineralized solution.

The linear decay of the dialysate transients indicates the potential of the process for a continuous system. To demonstrate this, two production runs (#3 and #5) were performed in which a 90% demineralized product was intermittently replaced by fresh feed. The brine side remained closed during these expriments. Salt accumulated continuously in the brine reservoir, therefore.

Operating conditions were identical to those for batch runs #6 and #26. The concentration changes in dialysate and brine reservoirs are shown in Figures 107 and 108,

respectively for low (c_0 = 1250 ppm) and high (c_0 = 5500 ppm) concentrations.

In Figure 107 the product was removed seven times. Each demineralization lasted eight cycles. The eighth demineralization was continued until steady periodic conditions were reached. The final separation factor of ns = 322 was obtained with a final brine product concentration of close to 9000 ppm. Compared to run #26 which reproduced the initial transients of #3 fairly well, the final separation factor appears to be improved at the higher brine concentration. This is in line with the previous findings on the effect of the initial concentration, see Section 5.5.5.

In Figure 108 a similar pair of experiments, #5 and #6, is shown. The dialysate product was removed four times after every 15th cycle in run #5. The product concentration begins to increase after the second production cycle, and the final separation factor is only ns = 76, against a final brine product of almost 25,000 ppm.

The initial transients of run #5 are perfectly reproduced in run #6, which reaches a final separation factor of ns = 185 against a final brine concentration of 14,000 ppm.

The mean current consumption increases during the production runs by a small amount due to the larger brine concentration. The currents are recorded in Figures 107 and 108 for each production cycle.

$c_0 = 1250$ [ppm], $\delta = 2/3$ [-], $v = 5.4$ [cm/sec],

$\tau = 10.0$ [sec], $\Delta\Phi = 10$ [V]

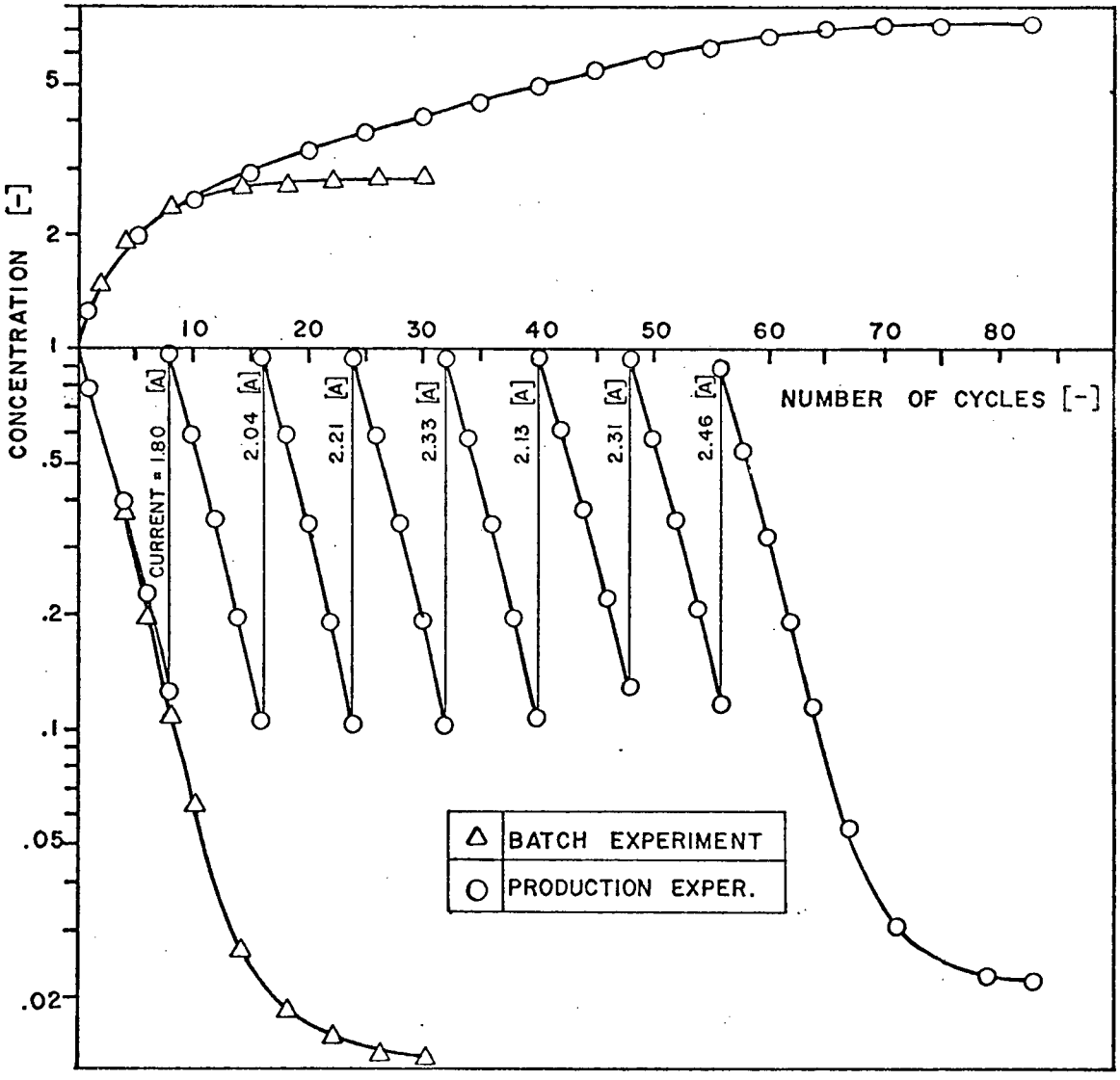

Figure 107. Concentration transients of top and bottom reservoir concentrations during production run #3 compared to batch run #26 (low concentration).

c_0 = 5600 [ppm], δ = 2/3 [-], v = 5.4 [cm/sec],

τ = 10.0 [sec], $\Delta\Phi$ = 10 [V]

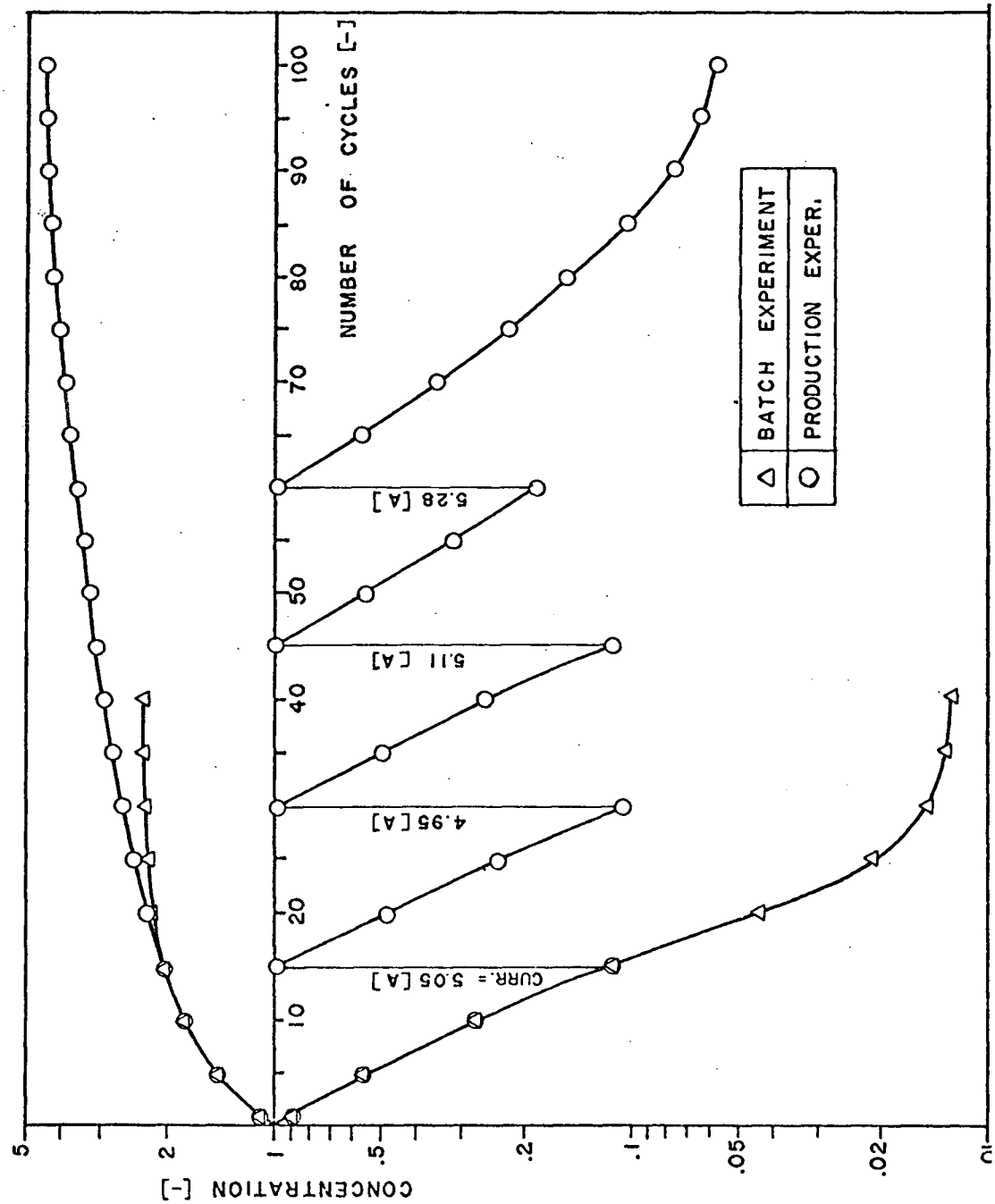

Figure 108. Concentration transients of top and bottom reservoir concentrations during production run #5 compared to batch run #6 (high concentration).

The results of the production runs confirm that cyclic electrodialysis has potential for a continuous system over a large concentration range (up to at least 10,000 ppm). The high concentrations require more recycle or longer residence times.

It should be pointed out that no attempt was made to optimize the production process. The pause time and the applied voltage were rather small, and the feed was introduced in large batches at the low concentration end, instead of in smaller portions during each cycle at a location where the averaged concentration of the travelling front coincides with the feed concentration. Similarly, one would withdraw the product intermittently during each cycle in any realistic open system.

5.6 Summary of Results and Experience on the Second ED Module

1. It was demonstrated that simple stacks may be produced on a laboratory scale. The stacks consisted of integrated frames which held the spacer screens and the absorption membranes and which distributed the flow into the channels.

2. A segmented module was built which consisted of eight individual stages. The stages seem to all perform approximately equally in separating $NaCl-H_2O$ solutions, although some problems with the electric manifold were encountered.

3. Uniform flow distribution and small internal mixing characterized the stack hydrodynamics.

4. The influence of the channel length was investigated by operating up to eight stages in series hydraulically.

   The results show improvements of the limit of separation similar to the influence of the pause time, as the residence time is increased. Also, there is less internal dispersion for longer channels. The initial rate of separation appears to be a maximum for a channel length of approximately one meter.

5. Systematic perturbations of four operating parameters and of the initial concentration were performed on the eight stage module:

Pause time	(τ)	:	$\underline{10}\ ^{+10}_{-10}$ [sec]
Applied voltage	($\Delta\Phi$)	:	$\underline{10}\ ^{+5}_{-5}$ [volt]
Displaced volume	(δ)	:	$\underline{2/3}\ ^{+1/3}_{-5/12}$ [-]
Superficial velocity	(v)	:	$\underline{5.4}\ ^{+0.0}_{-4.1}$ [cm/sec]
Initial concentr.	(c_0)	:	$\underline{1250}\ ^{+4450}_{-\ 100}$ [ppm]

6. The separation factors range from insignificant (ns = 3, for run #7) to very large (ns > 10^3 for runs #33, #34).

7. The pause times remain an essential feature of the cyclic electrodialysis process operation even for long channels, but they may be kept short (approximately 10 seconds or less) if the other conditions are favourable.

8. The initial rate of separation increases almost linearly with the applied voltage. The production may therefore be accelerated but only at the expense of additional energy because the current consumption rises in proportion to the voltage.

9. In a pause operation the velocity of displacement has little effect on the separation and may be kept as large as possible.

10. If the pause time is omitted, slow displacement is necessary to keep the residence time long, which in turn slows down the rate of separation. Usually such an operation is inefficient.

11. The displaced volume should be small enough to prevent breakthrough of the concentration front. If it is reduced the final separation increases almost without limit.

12. The initial concentration has a retarding effect on the initial rate of separation. The influence on the final separation could not be established for the conditions tested.

13. The presence of dead volumes in the end reservoirs slows down the rate of change of the concentrations. There is no effect on the limits which are eventually reached.

14. Two preliminary production runs on the module showed the potential of the cyclic electrodialysis process to separate NaCl-Water solutions up to at least 10,000 ppm. No attempt was made to optimize operating conditions.

15. A theoretical model which assumes constant and uniform rate of mass transfer through the membranes was confirmed experimentally.

16. pH changes in process and rinse solution were generally small, but there is a trend toward higher acidity of the product stream for high voltages and long pause times.

Chapter 6

MATHEMATICAL MODELS

6.1 Spacer Model

Sonin and Probstein (1968) derived general mass balance equations for mass transfer in electrodialysis channels. They made the following assumptions and simplifications:

1. The fluid consists of un-ionized (nonpolar) solvent and an infinitely dilute, fully ionized salt which is not solvated.

2. The fluid is incompressible and at constant temperature.

3. The membranes are perfectly selective, have constant electrical conductivity with respect to the gegenions, and are impermeable with respect to solvent molecules.

4. No chemical reaction takes place.

5. Nernst-Einstein equation for the ion mobilities holds.

6. Two-dimensional geometry.

7. No interphase mass transfer resistance.

8. Diffusion coefficients and valences of positive and negative ion are equal.

Under these assumptions the mass conservation equations for any volume element may be reduced to

$$\frac{\partial c'}{\partial t'} + \vec{v} \cdot \nabla c' = D \cdot \nabla^2 c' \qquad (35)$$

and

$$\nabla(c' \cdot \nabla \Phi) = 0 \qquad (36)$$

where

c'	= solution concentration	[g-mole/cm^3]
t'	= time	[sec]
$\vec{v}$	= fluid velocity vector	[cm/sec]
∇	= gradient	[cm^{-1}]
D	= solute diffusion coefficient	[cm^2/sec]
Φ	= electric potential	[volt]

Equations (35) and (36) and appropriate boundary and initial conditions have been used by Sonin and Probstein to calculate the steady-state concentration and current

distributions in channel flow assuming laminar and/or turbulent velocity profiles.

In this work different hydrodynamic conditions will be assumed based on the modified stack design. In particular, the presence of a spacer material in the flow channels suggests that the channels be divided into a series of well mixed cells. The effective number of cells is not necessarily identical to the number of spacer holes but must be determined experimentally. It will be further assumed that each mixing cell consists of a turbulent core and two stagnant sublayers across which only diffusion and electrolytic migration take place.

6.1.1 Model equations.

Figure 109 illustrates the co-ordinate systems and the dimensions of the jth mixing cell and the adjacent j^{th} section in the stagnant sorption membrane. Some of the channel volume is occupied by solid spacer material. This is indicated by shaded bars across the channel which reduce the free flow length of the mixing cell by the ratio

$$\pi = \frac{d}{\ell/m}$$

where ℓ length of flow channel
d effective length of mixing cell
m number of mixing cells.

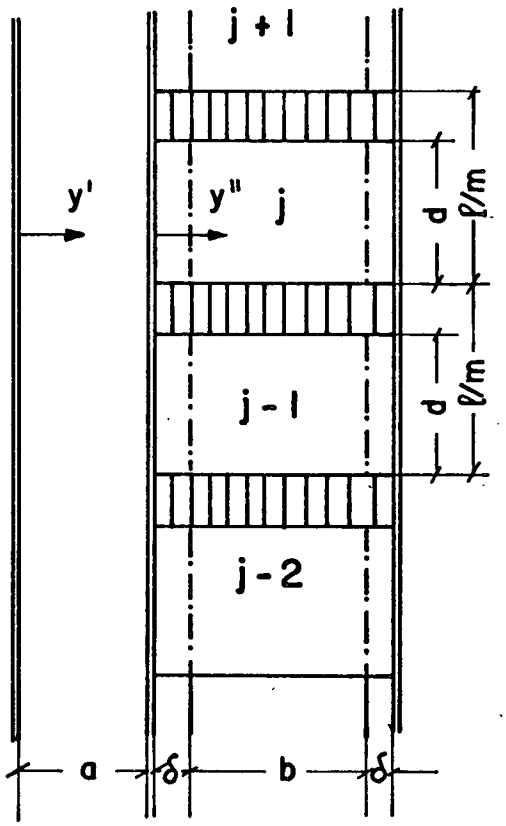

Figure 109. Derivation of the spacer model equations.

The two partial differential equations (35) and (36) will be replaced by a system of difference equations and PDEs according to the following procedure. The notation

$$c'_{j,k}$$

was chosen, where $k = 1$ for turbulent ocre

$= 2$ for stagnant sublayer

$= 3$ for stagnant inner layer

and $j = 1, 2, \cdots, m$.

For turbulent core:

$$\frac{dc'_{j,1}}{dt'} = \frac{v}{d} \cdot \left(c'_{j-1,1} - c'_{j,1}\right) - \frac{2D}{b - 2\delta} \cdot \nabla c'_{j,2}\Big|_{y''=\delta} \qquad (37)$$

with the initial condition @ $t' = 0$, $c'_{j,1} = c_0$

For stagnant sublayers: ($v = 0$)

$$\frac{\partial c'_{j,2}}{\partial t'} = D \cdot \frac{\partial^2 c'_{j,2}}{\partial y''^2} \qquad (38)$$

with initial condition $\quad @\ t' = 0\ ,\ c'_{j,2} = c_0$

boundary conditions $\quad y'' = 0\ ,\ D \cdot \frac{\partial c'_{j,2}}{\partial y''} = \frac{i'_j}{2zF}$ | anion selective membrane

$\quad j'' = \delta\ ,\ c'_{j,2} = c'_{j,1}$

For stagnant inner layer: ($v = 0$)

$$\frac{\partial c'_{j,3}}{\partial t'} = D \cdot \frac{\partial^2 c'_{j,3}}{\partial y'^2} \qquad (39)$$

with initial condition $\quad @\ t' = 0\ ,\ c'_{j,3} = c_0$

boundary conditions $\quad y' = 0\ ,\ D \cdot \frac{\partial c'_{j,3}}{\partial y'} = \frac{-i'_j}{2zF} \cdot \frac{1}{\pi}$ *) | cation selective membrane

$\quad y' = \frac{a}{2}\ ,\ \frac{\partial c'_{j,3}}{\partial y'} = 0$

*) N.B. The flux of salt due to the electric current must be corrected according to the difference in free volume between flow channel and inner layer.

The current densities (i'_j) couple equations (37), (38) and (39) over their boundary conditions. The potential drop across a flow channel and an adjacent sorption membrane has a constant value $\Delta\Phi$. Due to assumption 8 there is no

charge polarization at the membranes and the equation for the current density is simply

$$i_j' = \frac{\Delta \Phi - 2 \Delta\Phi_{Don}}{R_{tot}} \qquad (40)$$

where $\Delta\Phi_{Don}$ Donnan potential

R_{tot} total resistance

The Donnan potential and the total resistance are given by equation (26) in Section 3.3.

The following dimensionless quantities were introduced:

$$\Delta\psi = \frac{zF}{RT} \cdot \Delta\Phi$$

$$c_{j,k} = \frac{c'_{j,k}}{c_0} \qquad k = 1,2,3 \; ; \; j = 1,2,3,\cdots, m$$

$$y = \frac{y'}{b} \quad \text{and} \quad y = \frac{y''}{b}$$

$$t = \frac{t'}{\ell/v}$$

$$\rho = \frac{a}{b}$$

$$\beta = \frac{\delta}{b}$$

$$Fo = \frac{b^2}{D\ \ell/v} \qquad \text{(Fourier Number)}$$

$$i_j = \frac{i'_j \cdot b}{2\ z\ F\ D\ c_0}$$

$$\xi = \frac{2\ R_{membrane} \cdot 2\ z^2\ F^2\ D\ c_0}{b\ RT}$$

(41)

The resulting dimensionless equations and their initial and boundary conditions are

$$\frac{d\, c_{j,1}}{dt} = m \cdot \left(c_{j-1,1} - c_{j,1} \right) - \frac{1}{Fo\left(\frac{1}{2} - \beta\right)} \cdot \nabla\, c_{j,2} \Big|_{y=\beta} \tag{42}$$

$$\frac{\partial\, c_{j,2}}{\partial t} = \frac{1}{Fo} \cdot \frac{\partial^2\, c_{j,2}}{\partial\, y^2} \tag{43}$$

$$\frac{\partial\, c_{j,3}}{\partial t} = \frac{1}{Fo} \cdot \frac{\partial^2\, c_{j,3}}{\partial\, y^2} \tag{44}$$

$$\left.\begin{aligned} @\ t = 0 \quad &, \quad c_{j,1} = c_{j,2} = c_{j,3} = 1.0 \\ y = 0 \quad &, \quad \frac{\partial\, c_{j,2}}{\partial y} = i_j \\ &\qquad \frac{\partial\, c_{j,3}}{\partial y} = -\, i_j \cdot \pi \\ y = \beta \quad &, \quad c_{j,2} = c_{j,1} \\ y = \frac{\rho}{2} \quad &, \quad \frac{\partial\, c_{j,3}}{\partial y} = 0 \end{aligned}\right\} \tag{45}$$

where

$$i_j = \frac{\Delta\psi - 2\,\ell n \left.\frac{c_{j,3}}{c_{j,2}}\right|_{y=0}}{\frac{1-2\beta}{c_{j,1}} + 2\int_0^{\beta}\frac{dy}{c_{j,2}} + 2\int_0^{\rho/2}\frac{dy}{c_{j,3}} + \xi} \qquad (46)$$

At this point an additional assumption regarding the concentration profile in the stagnant sublayer is introduced. The concentration profile is linearized. This simplifies equations (42), (43), (46) and some boundary conditions in (45).

The final set of equations for the spacer model is for $j = 1,2,3,\cdots, m$.

$$\left.\begin{aligned} \frac{d\,c_{j,1}}{dt} &= m \cdot \left(c_{j-1,1} - c_{j,1}\right) \\ &- \frac{2}{Fo \cdot \beta(1-2\beta)} \cdot \left(c_{j,1} - c^{m}_{j,2}\right) \end{aligned}\right\} \qquad (47)$$

$$\left.\begin{aligned} \frac{d\, c_{j,2}}{dt} &= -\, m \cdot \left(c_{j-1,1} - c_{j,1} \right) \\ &+ \frac{2(1-\beta)}{Fo \cdot \beta^2 (1-2\beta)} \cdot \left(c_{j,1} - c^{m}_{j,2} \right) - \frac{2\, i_j}{\beta \cdot Fo} \end{aligned}\right\} \qquad (48)$$

$$\frac{\partial\, c_{j,3}}{\partial t} = \frac{1}{Fo} \cdot \frac{\partial^2 c_{j,3}}{\partial\, y^2} \qquad (49)$$

with

$$\left.\begin{aligned} t \geq 0 \quad &, \quad c_{0,1} = 1.0 \\ t = 0 \quad &, \quad c_{j,1} = c_{j,2} = c_{j,3} = 1.0 \\ y = 0 \quad &, \quad \frac{\partial\, c_{j,3}}{\partial y} = -i_j \cdot \pi \\ y = \frac{\rho}{2} \quad &, \quad \frac{\partial\, c_{j,3}}{\partial y} = 0 \end{aligned}\right\} \qquad (50)$$

and

$$i_j = \frac{\Delta\psi - 2\,\ell n\,\dfrac{c^m_{j,3}}{c^m_{j,2}}}{\dfrac{1-2\beta}{c_{j,1}} + \dfrac{2\beta\,\ell n\,\dfrac{c_{j,1}}{c^m_{j,2}}}{c_{j,1}-c^m_{j,2}} + 2\int_0^{\rho/2}\frac{dy}{c_{j,3}} + \xi} \qquad (51)$$

where the superscript (m) denotes the concentration of the solution at the interface, and $c_{0,1}$ is the feed to the first mixing cell.

The set of model equations (47) to (51) may be classified as

> *system of m directly coupled pairs of first order ordinary differential-difference equations coupled by nonlinear boundary conditions with m independent linear second order partial differential equations.*

Looking at the ODE's alone, this is an initial value problem, whereas the PDE's are of the parabolic type and constitute an initial-boundary problem.

6.1.2 Considerations related to cyclic process operations.

The system of equations (47) to (51) describes a period starting with uniformly distributed initial concentrations. In general, any concentration distribution at t = 0

may replace the initial condition in (50). This is important for cyclic operations of the electrodialysis stack. When operating parameters are changed in steps, the time axis may be transposed mathematically, because it is generally more convenient to start calculations at t = 0 for constant parameter values than to define the step changes of the parameters as functions of time.

The thickness of the stagnant sublayers (δ) is generally a function of the flow conditions and may be evaluated from mass transfer correlation data if these are available (see also Section 5.3.4). However, very little information is available on the unsteady-state mass transfer which must be considered in a cyclic operation. The thickness (δ) is, therefore, treated as an independent variable.

The concept of stagnant sublayers will break down as the velocity approaches zero, i.e. as the flow becomes more and more laminar. The model equations must, therefore, be used with caution under those conditions. In the present form they cannot be applied to pause operations.

6.1.3 Solutions.

The nonlinear form of the coupling condition (51) makes analytical solutions of the model equations very unlikely. A semi-analytical approach is, in principle, possible

if the current densities are assumed to remain stepwise constant. However, the resulting series solutions would have to be evaluated numerically in any case. It was preferred to find direct numerical solutions based on approximations of the system equations (47) to (51).

A number of standard numerical integration schemes have been considered, see e.g. McCracken and Dorn (1964), Hamming (1962):

- Fourth order Runge-Kutta (RKS)
- Milne fifth order predictor corrector using a RKS initialisation
- Common difference scheme
- Backward difference scheme
- Crank-Nicholson scheme

The first two integration schemes are suitable for first order PDEs and are offered by most computing centres as library subroutines with fixed and/or variable step length.

In the present system of equations the second order space derivative was replaced by the conventional central difference expression to test the RKS. An analytical solution of the unsteady state diffusion equation (49) was used as test case. Carslaw and Jaeger (1959) give such a solution a finite slab with constant heat influx through both boundaries.

It was found that RKS diverges in some cases when integrating with fixed step sizes, although a reduction in time step size usually led to satisfactory convergence.

The stability of the difference methods was tested using ε-schemes.

It was found that the common difference scheme is unstable for the unsteady state diffusion equation. The Crank-Nicholson scheme showed instability for equation (47). The backward difference scheme was stable in all cases.

Since RKS, as well as Milne, require difference approximations of some partial derivatives, it was finally decided to use the stable backward difference scheme in the present model. This is an implicit method which requires an iteration method as the following derivation shows.

6.1.4 Backward Difference scheme with Gauss Seidel iteration.

The backward difference scheme approximates the first time derivative by

$$\left(\frac{\partial c}{\partial t}\right)_{y,t} = \frac{c_{y,t} - c_{y,t-\Delta t}}{\Delta t} \qquad (52)$$

and the second position derivative by

$$\left(\frac{\partial^2 c}{\partial y^2}\right)_{y,t} = \frac{c_{y+\Delta y,t} - 2\, c_{y,t} + c_{y-\Delta y,t}}{\Delta y^2} \tag{53}$$

Suppose the inner layer of the sorption membrane is divided into 2n parallel slices of thickness

$$\Delta y = \frac{\rho}{2n} \tag{54}$$

This is equivalent to expanding the second subscript (k) of the concentrations to $k = 1,2,\cdots, n+3$. It is sufficient to consider half of the layer thickness only because the concentration profile is symmetric.

In addition to the two-dimensional space grid (subscripts, j,k) a time grid has been introduced by equation (52). This will be labeled by superscripts (1) and (0) for the new time value and the old one respectively.

The following abbreviations are used:

$$z_1 = \frac{2 \cdot \Delta t}{Fo \cdot \beta}$$

$$z_2 = \frac{4 \cdot n \cdot \Delta t}{\rho \cdot Fo} \cdot \pi$$

$$z_3 = \frac{4 \cdot n^2 \cdot \Delta t}{\rho^2 \cdot Fo}$$

$$z_4 = m \cdot \Delta t$$

$$z_5 = \frac{2 \cdot \Delta t}{Fo \cdot \beta \cdot (1 - 2\beta)}$$

$$z_6 = \frac{1 - \beta}{\beta} \cdot z_5$$

The system of equations (47) to (51) is transformed into the following implicit algorithm to calculate the new $c'_{j,k}$'s.

For j 1,2,$\cdots$, m

$$c'_{j,1} - c^0_{j,1} = z_4 \cdot \left(c'_{j-1,1} - c'_{j,1}\right) - z_5 \cdot \left(c'_{j,1} - c'_{j,2}\right)$$

$$c'_{j,2} - c^0_{j,2} = -z_4 \cdot \left(c'_{j-1,1} - c'_{j,1}\right) + z_6 \cdot \left(c'_{j,1} - c'_{j,2}\right) - z_1 \cdot i_j$$

$$c'_{j,3} - c^0_{j,3} = 2 \cdot z_3 \cdot \left(c'_{j,4} - c'_{j,3}\right) + z_2 \cdot i_j$$

$$c'_{j,4} - c^0_{j,4} = z_3 \cdot \left(c'_{j,5} - 2\, c'_{j,4} + c'_{j,3}\right)$$

$\cdot$
$\cdot$
$\cdot$

$$c'_{j,n+2} - c^0_{j,n+2} = z_3 \cdot \left(c'_{j,n+3} - 2\, c'_{j,n+2} + c_{j,n+1}\right)$$

$$c'_{j,n+3} - c^0_{j,n+3} = 2 \cdot z_3 \cdot \left(c'_{j,n+2} - c_{j,n+3}\right)$$

$$i_j = \frac{\Delta\psi - 2 \cdot \ell n \left(\frac{c'_{j,3}}{c'_{j,2}}\right)}{\frac{1 - 2\beta}{c'_{j,1}} + 2\beta \frac{\ell n \left(\frac{c'_{j,1}}{c'_{j,2}}\right)}{c'_{j,1} - c'_{j,2}} + \xi + S}$$

where

$$S = \frac{\rho}{3n}\left[\frac{1}{c'_{j,3}} + \frac{4}{c'_{j,4}} + \frac{2}{c'_{j,5}} + \ldots + \frac{1}{c'_{j,n+3}}\right] \quad \text{SIMPSON's rule}$$

If i_j were constant a linear matrix equation could be established and solved by standard methods. The Gauss-Seidel iteration was employed in the following way:

1. Calculate i_j for $c^0_{j,k}$ - values

2. Calculate $c'_{j,k}$ values and find

$$D = \text{Max}\left|c'_{j,k} - c^0_{j,k}\right|$$

$$k = 1,2,\cdots,n+3$$

3. If $D \geq$ iteration error go to 1.

A computer program was written which consisted of a main program and three subroutines. The main program read parameter values, initialized the concentration matrix, organized the integration, adjusted time step size and kept track of the averaged current consumption as well as of the effluent concentrations and the material balance. The periodic switching of electric polarity and direction of fluid flow was also performed automatically by the program for a given number of cycles. The printout varied according to the information that was desired.

The subroutines CURRENT, PAMPA, and GASE calculated, respectively, the current density, the values of $z_\ell (\ell=1,\cdots,6)$ according to increasing or decreasing time step size, and performed the Gauss-Seidel iteration.

A listing of the FORTRAN IV program is presented in Appendix C.3, which also details the required input data.

The integration step size was controlled by the following criterion: Each integration was performed twice with the current time step (Δt) and with $\Delta t/2$.

If

$$DD = \text{Max} \left| c'_{j,k}(\Delta t) - c'_{j,k}(\Delta t/2) \right| \geq \text{ERROR}$$

$$j = 1,2,\cdots, m$$

$$k = 1,2,\cdots, n + 3$$

the current step size was halved and the same integration step was repeated. If $DD \leq 0.05 * ERROR$ the current step size was doubled.

The two values of the new concentrations were also used to correct the actual concentrations on the basis of the estimated truncation error.

6.1.5 Results of computer simulations.

The objectives of simulation runs were:

a) To test accuracy and convergence of the integration.

b) To investigate effects of operating parameters.

c) To compare the model with experimental results.

6.1.5.1 Accuracy and convergence.

The integration was tested by

- varying the number of slices in the sorption membrane (n)
- adjusting the tolerable iteration and integration errors
- modifying the program from absolute to relative error control

The results are:

1. Between four and six slices per half sorption membrane are usually sufficient if $\rho < 1$.

2. For absolute error control both integration error and iteration error should be smaller than $5 * 10^{-3}$. If the iteration error is one order of magnitude smaller than the integration error, e.g. 10^{-4} vs. 10^{-3}, the number of iterations lies between 3 and 5 and the time step size is between 1/64 and 1/256, whereas the time step size decreases and the number of iterations becomes very small (1 to 2) in the case of comparable error limits, e.g. if both are set to 10^{-3}.

3. The material balance is generally in the order of ± 0.1%, but there are indications of systematic drifts as the number of cycles is increased.

4. Relative error control is very time consuming especially when the dialysate concentration becomes small. The results compare generally very well with results obtained under absolute error control (at least 3 significant figures).

6.1.5.2 Effect of operating parameters.

It was found that small Fourier numbers, small layer thickness, high potentials and small thickness ratios lead to

good separation. Tables 40, 41 and 42, and Figure 110 show typical results of systematic computer simulations.

6.1.5.3 Comparison with experimental results.

Figure 111 illustrates the experimental concentration transients for EDI-S1-8/#22, #23, #24 runs and computer simulations for a set of parameters which were partly calculated from the operating conditions (M, Fo, $\Delta\psi$, δ, ρ, c_0), partly estimated and adjusted for a reasonable fit (β,ξ).

The experiments were specifically performed for a test of the simulation program. As explained in Section 5.3.2 the probe voltage was subject to characteristic fluctuations, whereas the model assumed constant $\Delta\Phi$. The D.C. power supply voltage was, therefore, hand regulated in such a way as to maintain a constant probe voltage signal for the runs listed above.

Figure 112 shows a comparison of calculated (solid line) and experimental (points) concentration transients for EDI-S1-8/#36. The previously fitted parameters β and ξ were adjusted again. Although the model predicts the dialysate transient reasonably well, it fails to do so for the brine.

It was also found that the model breaks down for small membrane core thickness in combination with large applied voltages. Negative concentrations occur at some stages during

Table 40

Spacer Model No. I, Effect of Layer Thickness

Parameters

RUN NO.	M	Fo	β	ρ	ΔΦ	π	ξ	δ
3	20	2	0.05	1	16	1	3.2	1
8			0.1					

Comparison

CYCLE NO.	TOP CONCENTRATION		BOTTOM CONCENTRATION		SEPARATION FACTOR		CURRENT			
							DEPLETING		ENRICHING	
	c_T		c_B		ns		i_D		$-i_E$	
	3	8	3	8	3	8	3	8	3	8
1	1.66	1.64	.234	.246	7.1	6.7	1.47	1.42	2.29	2.25
2	1.98	1.95	.160	.193	12.4	10.1	2.01	2.08	2.12	2.12
3	2.17	2.15	.089	.122	24.4	17.6	2.04	2.04	2.08	2.12
4	2.28	2.27	.050	.075	45.7	30.1	2.03	2.00	2.02	2.05
5	2.34	2.35	.032	.050	72.6	47.2	1.98	1.95	1.97	1.99
6	2.37	2.40	.024	.037	97.9	65.6	1.94	1.92	1.94	1.95
7	2.38	2.43	.020	.030	116.8	81.6	1.92	1.89	1.92	1.92
8	2.39	2.45	.019	.026	127.5	93.4	1.91	1.88	1.91	1.89
9	2.40	2.46	.018	.024	133.2	101.1	1.90	1.87	1.91	1.88
10	2.40	2.47	.018	.023	136.1	105.8	1.90	1.86	1.91	1.87
11		2.47		.023		108.5		1.86		1.86
12		2.48		.022		110.1		1.86		1.86

Table 41

Spacer Model No. I, Effect of Fourier Number

Parameters

RUN NO.	M	Fo	β	ρ	ΔΦ	π	ξ	δ
2	20	20	0.05	1	16	1	3.2	1
3		2						

Comparison

CYCLE NO.	TOP CONCENTRATION		BOTTOM CONCENTRATION		SEPARATION FACTOR		CURRENT DEPLETING		CURRENT ENRICHING	
	c_T		c_B		ns		i_D		$-i_E$	
	2	3	2	3	2	3	2	3	2	3
1	1.00	1.66	.87	.23	1.16	7.1				
2	1.01	1.98	.87	.16	1.16	12.4				
3	1.02	2.17	.87	.089	1.17	24.4				
4	1.02	2.28	.87	.049	1.17	45.7				
5	1.03	2.34	.88	.032	1.17	72.6				
6	1.03	2.37	.88	.024	1.17	97.9				
7	1.03	2.38	.88	.020	1.17	116.8				
8	1.04	2.39	.89	.019	1.17	127.5				
9	1.04	2.40	.89	.018	1.17	133.2				
10		2.40		.018		136.1				

Table 42

Spacer Model No. I, Effect of Applied Potential

Parameters

RUN NO.	M	Fo	β	ρ	ΔΦ	π	ξ	δ
3	20	2	0.05	1	16	1	3.2	1
4			0.1		8			

Comparison

CYCLE NO.	TOP CONCENTRATION		BOTTOM CONCENTRATION		SEPARATION FACTOR		CURRENT DEPLETING		CURRENT ENRICHING	
	c_T		c_B		ns		i_D		$-i_E$	
	3	4	3	4	3	4	3	4	3	4
1	1.66	1.28	.234	.487	7.1	2.6	1.47	-	2.29	-
2	1.98	1.44	.160	.507	12.4	2.9	2.01	-	2.12	-
3	2.17	1.55	.089	.485	45.7	3.2	2.04	-	2.08	-
4	2.28	1.62	.049	.455	72.6	3.6	2.03	-	2.02	-
5	2.34	1.67	.032	.429	97.8	3.9	1.98	-	1.97	-
6	2.37	1.72	.024	.408	116.8	4.2	1.94	-	1.94	-
7	2.38		.020		127.5		1.92		1.92	
8	2.39		.019		133.0		1.91		1.91	
9	2.40		.018		136.0		1.90		1.91	
10	2.40		.018		138.0		1.90		1.91	

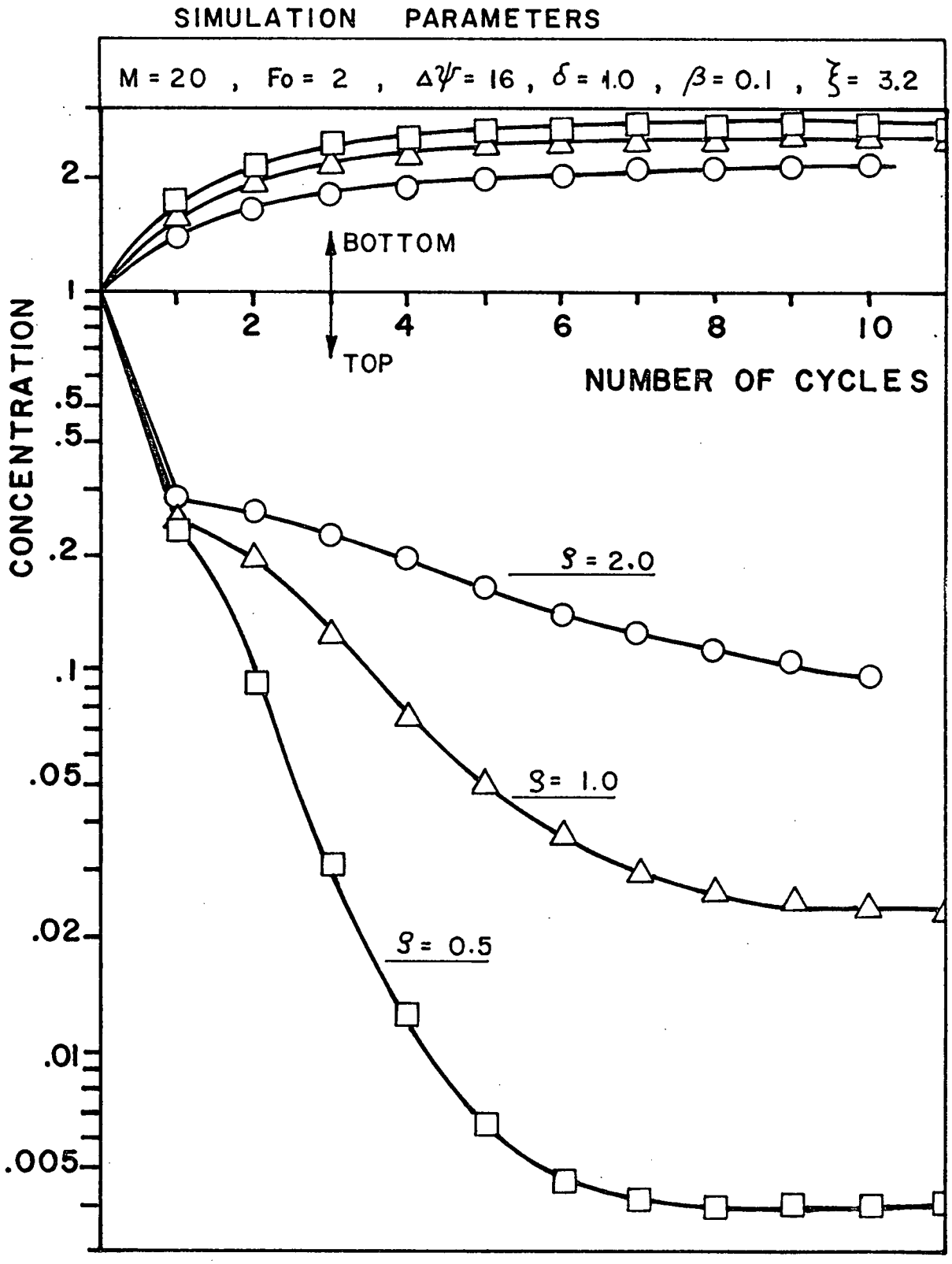

Figure 110. Effect of width ratio (ϑ) on concentration factor transients predicted by Spacer Model.

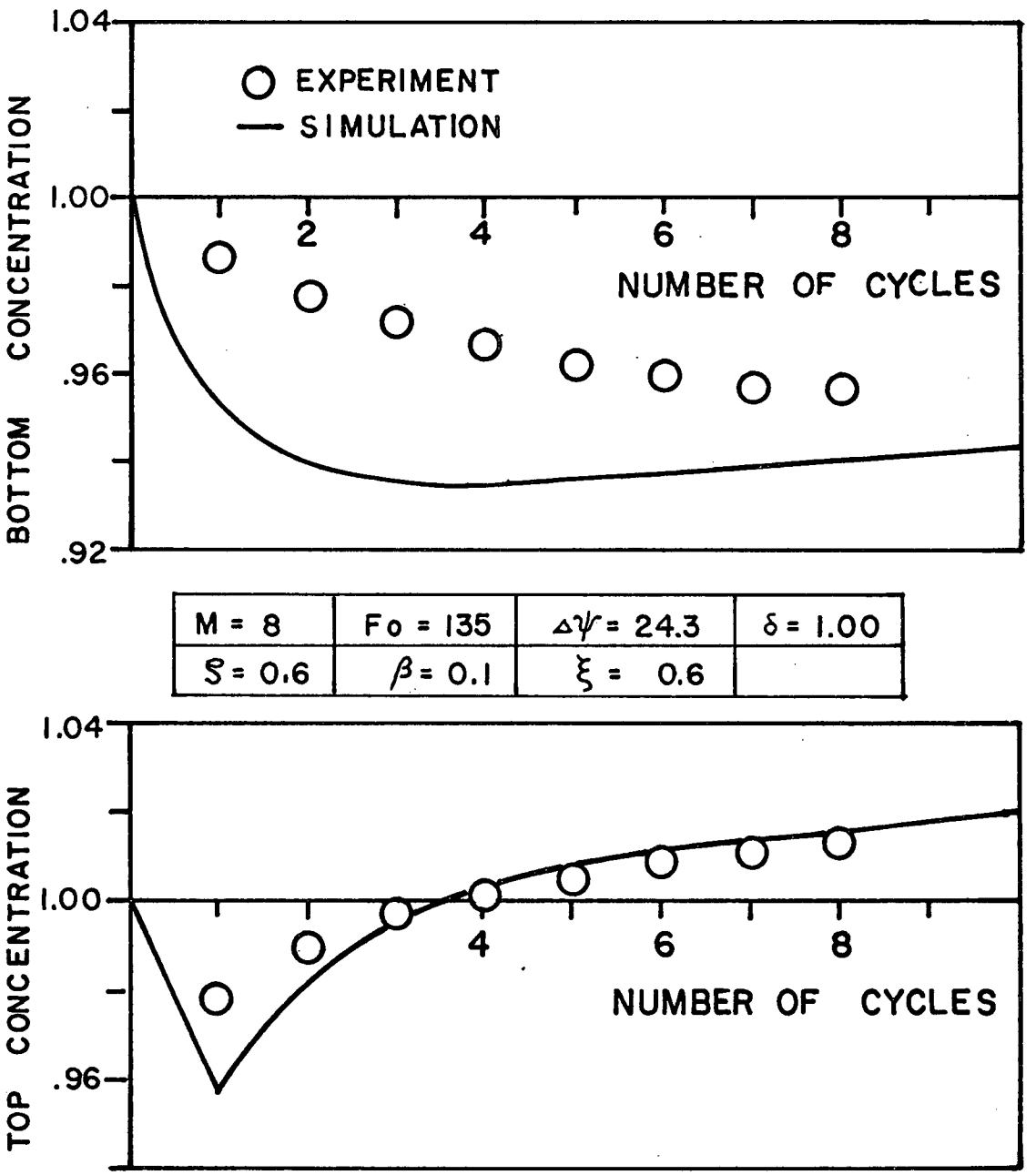

Figure III. Comparison of computer simulation with experimental results on runs #22,23,24 (first stack).

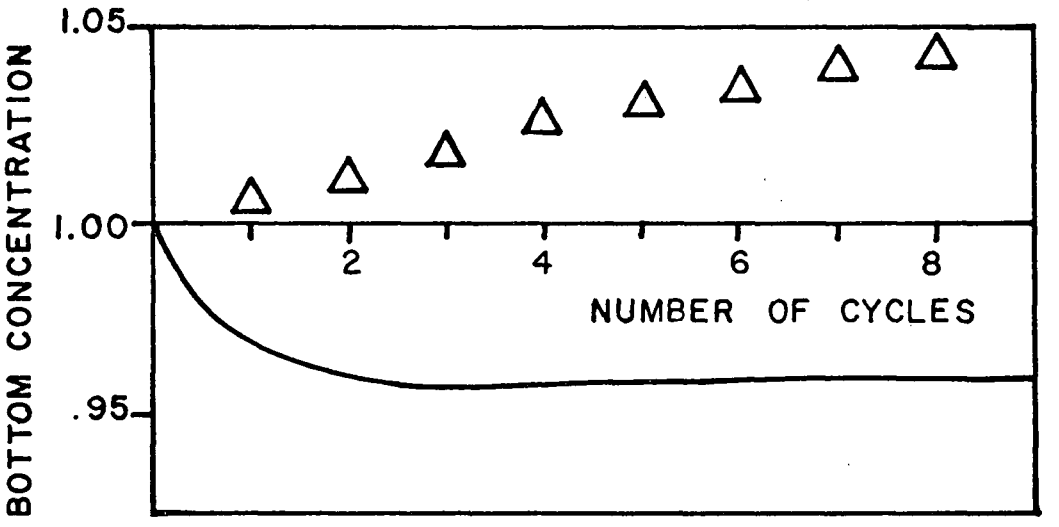

M = 8	Fo = 72.2	$\Delta\psi$ = 44.3	δ = 1.00
S = 0.6	β = 0.08	ξ = 1.0	

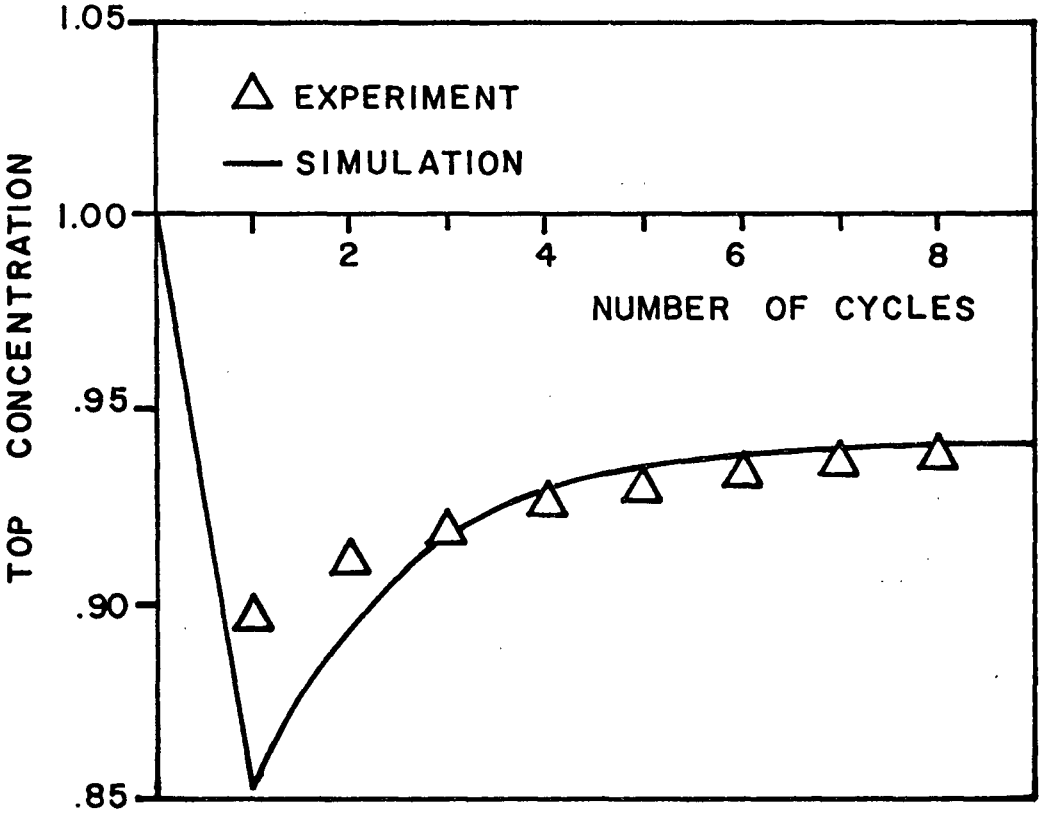

Figure 112. Comparison of computer simulation with experimental run #36 (first stack).

the Gauss-Seidel iteration loop and lead to program interrupts.

6.1.6 Concluding comments on the spacer model.

The spacer model in its present form predicts the effect of system parameters on the separation of no-pause operations qualitatively. It may be used to fit singular experiments quantitatively, but these fits do not have much practical significance. In particular, the model breaks down for very large rates of mass transfer; this is probably due to the linerization of the concentration profiles in the stagnant sublayers.

Modifications of the model may include:

1. Nonlinear concentration profiles in the sublayers, i.e. expanding the lateral concentration grid (subscript k) in the flow channels.

2. Include water transfer due to solvation of the ions.

3. Account for density induced free convection in sorption membranes.

4. Include sorption capacity of ion exchange membranes.

5. Replace concentrations by activities.

6. Modify equations to allow for flow pauses at the beginning of each half cycle.

6.2 Rate Model

The rate model presented in Section 3.3 may be improved along the following lines.

1. Combine pure pause and parametric pumping operations to a parapause operation in which the electric potential is continuously applied while the flow pauses at the beginning of each half cycle.

2. Allow for internal dispersion effects by introducing the mixing cell concept.

3. Modify the rate law by including more terms of the current density approximation (equation (27).

4. Measure rates of mass transfer experimentally as function of operating and system parameters and use these correlation data in form of semi-empirical transfer equations.

Chapter 7

CONCLUSIONS AND RECOMMENDATIONS

The purpose of this work was to investigate and to develop a cyclic electrodialysis process, both experimentally and theoretically. The results of this study lead to the following conclusions.

1. Cyclic electrodialysis can achieve very large separations ($ns > 10^3$) in a closed system.

2. The response of electrosorption stacks to periodic alternations of the polarity of the electric field and of the direction of the fluid displacement is governed by the rate of mass transfer. Equilibrium conditions have generally little influence.

3. Flow pauses at the beginning of each half cycle represent important features of the cyclic process operation. Moderate pause times (up to 10 [sec]) considerably improve both the rate of separation and the limiting separation compared to no-pause operation.

4. The effect of ten system parameters could be studied on a simple bench scale electrodialysis cell, which featured a rigid centre frame design. Final separation factors between 1 and 40 were obtained experimentally. The cyclic operation gave best separation for

moderate pause times,
high applied voltage,
small displaced volume,
small internal mixing,
uniform flow distribution,
small sorption capacity of the stack,
large flow rate.

5. Simple stacks were designed for a mini-pilot plant module and manufactured using a standardized procedure. This resulted in uniform flow distribution in the channels. Small dispersion coefficients were, thus, achieved.

6. A high final separation is obtained by increasing the channel length or the pause time. The initial rate of separation appears to be a maximum for a channel length of approximately 1 meter and pause times of about 10 seconds.

7. The separation factor (ns) during the first few cycles can be approximated by an exponential function

$$ns = 10^{a \cdot t}$$

where a is the rate constant in $[min^{-1}]$
and t is the real time in [min]

Axial dispersion limits the separation as steep concentration fronts develop.

8. The potential of the cyclic electrodialysis process for large separations in an open system over the concentration range from 1,000 to at least 10,000 [ppm] NaCl was demonstrated.

9. Modelling of the closed system has met only partial success. A qualitative model which assumes concentration dependent mass transfer rates explains most of the experimental results. A more rigorous model, which requires numerical techniques, may be fitted to some data but cannot predict experimental results a priori.

10. The experimental results are generally highly reproducible if a standardized testing procedure is followed. The conductometric concentration measuring system becomes inaccurate, however, for very small concentrations.

On the basis of the results of this study the following recommendations can be made.

1. The design of electric connectors to the electrodes should be improved.

2. Provision should be made to measure different concentration ranges, e.g. by parallel conductivity cells.

3. Other solutes should be investigated, both in binary and in multicomponent mixtures.

4. Different spacer screens may be used to analyze the influence of the hydrodynamic conditions.

5. Other operating procedures should be investigated. In particular it is proposed to disconnect the electric power from the ED stacks during displacement. This could lead to large power savings at moderately reduced separation. Also, the effect of a phase shift between electric polarity and pump reversals should be analyzed.

6. The effect of initial concentration on final separation factors should be checked. It may be desirable to close the sorption membranes along all four sides for very large concentrations (> 10,000 ppm).

7. An open system should be designed in which feed is intermittently introduced and products are drawn off.

NOMENCLATURE

			Typical Unit
a	=	thickness of inner layer of adsorption membrane	[cm]
$a_{\pm}$	=	ionic activity of cation (+) or anion (-)	[g-mole/litre]
a_1	=	rate constant during dilution half cycle	[sec^{-1}]
a_2	=	rate constant during enrichment half cycle	[sec^{-1}]
b	=	thickness of spacer screen or width of flow channel	[cm]
c	=	concentration	[g-mole/litre]
d	=	effective length of mixing cells	[cm]
D	=	diffusion coefficient	[cm^2/sec]
F	=	Faradays constant = 96.5×10^3	[A sec/g-equiv.]
Fo	=	Fourier number	
i	=	current density	[A/cm^2]
I	=	current	[A]
j	=	integer	
$\vec{j}$	=	flux vector	$\left[\frac{\text{g-mole}}{cm^2 \ sec}\right]$

			Typical Unit
k	=	integer number	
K	=	rate constant	$\left[\frac{\text{g-mole}}{\text{litre-sec}}\right]$
ℓ	=	channel length or integer	[cm]
m	=	$M(1-\varepsilon)/\varepsilon$, or number of mixing cells	
M	=	linear equilibrium constant	$\left[\frac{\text{cm}^3 \text{ of solution}}{\text{cm}^3 \text{ of solid}}\right]$
n	=	number of gram moles or integer number	[g-mole]
nc	=	number of cycles	
ns	=	separation factor	
N	=	number of segments of STOP-GO algorithm	
p	=	$\exp(-a_1 \frac{T}{2})$	
P	=	permselectivity of ion exchange membrane	
Ps or Pd	=	Salting or Desalting factor	
q	=	$\exp(-a_2 \frac{T}{2})$	
Q	=	flow rate	[cm^3/sec]
r	=	dimensionless volume ratio	
R	=	areal resistance	[Ω cm^2]
t	=	real time	[sec]

			Typical Unit
T	=	cycle time	[sec]
$\bar{u}_+$	=	ionic mobility	$\left[\frac{\text{cm}^2\ \text{g-mole}}{\text{V sec g-equiv}}\right]$
v	=	superficial velocity of fluid in packing or channels	[cm/sec]
$\vec{v}$	=	velocity vector	[cm/sec]
V	=	volume	[cm^3]
x	=	dimensionless concentration	
X	=	concentration of fixed ionic charge in membrane matrix	$\left[\frac{\text{g-mole}}{\text{g-dry membrane}}\right]$
y	=	lateral distance co-ordinate	[cm]
z	=	valence of charged species or direction of flow	[g-equiv/g-mole] [cm]
z_i	=	calculation constants ($i = 1,2,\cdots,6$)	

Greek Symbols

α	=	stoichiometric coefficient	
β	=	dimensionless layer thickness	
γ	=	phase lag	
δ	=	thickness of Nernst layer or fraction of void volume displaced	[cm] [-]
ε	=	fractional void volume of packing	
$\vec{\eta}$	=	electric field vector	$\left[\frac{\text{volt}}{\text{cm}}\right]$
Θ	=	absolute temperature	[°K]

			Typical Units
κ	=	$1 + m_1$	
λ	=	$1 + m_2$	
ν	=	transport number	
ξ	=	dimensionless membrane resistance	
π	=	length fraction	
ρ	=	$(1-\varepsilon)/\varepsilon$ = ratio of volume of packing to void volume	
τ'	=	$a_1 T/2$	
τ	=	pause time	[sec]
∇	=	finite difference symbol or divergence operator or gradient vector	$[cm^{-1}]$ $[cm^{-1}]$
$\Delta\Phi$	=	applied electric potential	[V]
$\Delta\Phi_{Don}$	=	Donnan potential	[V]
$\Delta\psi$	=	dimensionless potential	

Subscripts

+	for positively charged species (cations)
-	for negatively charged species (anions)
0	refers to initial state
lim	at limiting, steady-periodic state
s	solid or adsorbent phase

f fluid phase

T top reservoir

B bottom reservoir

Superscripts

- = refers to property in membrane

m = refers to membrane solution interface

REFERENCES

Acrivos, A., I&EC, 48, 703 (1956).

D'Alessandro, S., A. Tantillo, Desalination, 9, 225 (1971).

Alexis, R.W., Chem. Eng. Progr., 63, No. 5, p. 69 (1967).

Aris, R., I&EC fund., 8, 603 (1969).

Aris, R., N.R. Amundson, A. I. Ch. E. J., 3, 280 (1957).

Baker III, B., I&EC fund., 9, 686 (1970).

Batta, L.B., U.S. patent 3,564,816 (1971).

Belfort, G., G.A. Guter, Desalination, 5, 267 (1968).

———————————, Desalination, 10, 221 (1972).

Bier, M., "Electrophoresis: Theory, Method, and Applications," Acad. Press, N.Y. (1959).

Butts, T.J., R. Gupta, N.H. Sweed, Chem. Eng. Sci., 27, 855 (1972).

Calvit, B.W., J.J. Sloan, in Proc. First Intern. Symp. Water Desalination, Washington, D.C., Oct. 3-9, 1965, Vol. 2, p. 11.

Carslaw, H.S., J.C. Jaeger, "Conduction of Heat in Solids," 2nd ed., Clarendon Press, Oxford (1959).

Chen, H.T., F.B. Hill, Separation Sci., 6, 411 (1971).

Chen, H.T., J.L. Rak, J.D. Stokes, F.B. Hill, A. I. Ch. E. J., 18, 356 (1972).

Cohan, H.J., R.W. Kennedey, in: Proc. 1st Intern. Symp. Water Desalination, Washington, D.C., Oct. 3-9, 1965, Vol. 3, p. 389.

Cook, B.A., Electrochim. Acta., 3, 307; 4, 179; 5, 216 (1961).

————, in: Proc. 1st Intern. Symp. Water Desalination, Washington, D.C., Oct. 3-9, 1965, Vol. 2, p. 219.

Cowan, D.A., J. Brown, I&EC, 51, 1445 (1959).

Danckwerts, P.V., Chem. Eng Sci., 2, 1 (1953).

Dewey, D.R., E.R. Gilliland, U.S. Patent 2,741,591 (1956).

Eluard, R., French patent 1,601,126 (1970).

Epstein, N., Can. J. Chem. Eng., 36, 210 (1958).

Forgacs, C., N. Ishibashi, J. Leibovitz, J. Sinkovic, K.S. Spiegler, Desalination, 10, 181 (1972).

Friedlander, H.F., R.N. Rickles, Anal. Chem., 37 (8), 27 A (1965).

————————————————, Chem-Eng., 73, 111 (1966).

Frilette, V.J., J. Phys. Chem., 61, 168 (1957).

Furukawa, D.H., Chem. Eng. Progr. Symp. Ser., No. 90, Vol. 64, (1968), p. 171.

Gregory, R.A., N.H. Sweed, Chem. Eng. J., 1, 207 (1970).

Hamming, R.W., "Numerical Methods for Scientists and Engineers," McGraw-Hill (1962).

Harris, P.R., I&EC fund., 9, 684 (1970).

Helfferich, F., "Ion Exchange," McGraw-Hill, N.Y. (1962).

Hicks, R.E., W.G.B. Mandersloot, Chem. Eng. Sci., 23, 1201 (1968).

Horn, F.J.M., C.H. Lin, Berichte Bunsengesellschaft Physikalische Chemie, 73, 575 (1969).

Huffman, E.L., U.S. Off. Saline Water Res. Dev. Rep. 439 (1969).

Jenczewski, T.J., A.L. Myers, A. I. Ch. E. J., 14, 509 (1968).

———————————, I&EC fund., 9, 216 (1970).

Kitamoto, A., Y. Takashima, J. Chem. Eng. Japan, 3, 182 (1970).

———————————, Desalination, 9, 51 (1971).

Kobus, E.J.M., P.M. Heertjes, Desalination, 10, 383 (1972).

Kollsman, P., U.S. Patent 2,854,393 (1958).

————————, U.S. Patent 2,872,407 (1959).

Korngold, E., *et al.*, Desalination, 8, 195 (1970).

Kramers, H., G. Alberda, Chem. Eng. Sci., 2, 173 (1953).

Kressman, T.R.E., F.L. Tye, J. Electrochem. Soc., 116, 25 (1969).

Lacey, R.E., S. Loeb, "Industrial Membrane Technology," Wiley-Intersci., N.Y. (1972).

Lacey, R.E., "Electrosorption and Desorption, Process for Demineralization," U.S. Off. Saline Water Res. Dev. Rep. No. 398 (1968).

————————, "Desalination by Electrosorption and Desorption," U.S. Off. Saline Water Res. Dev. Rep. No. 135 (1965).

Lacey, R.E., "Demineralization by transport depletion," U.S. Off. Saline Water Res. Dev. Rep. No. 80 (1962).

Lang, E.W., E.L. Huffman, R.E. Lacey, J. Electrochem. Soc., 115, 88c (1968).

McCracken, D.D., W.S. Dorn, "Numerical Methods and FORTRAN programming," Wiley, N.Y. (1964).

McHenry, K.W. Jr., R.H. Wilhelm, A. I. Ch. E. J., 3, 83 (1957).

Mandersloot, W.G.B., R.E. Hicks, IE&C proc. des. dev., 4, 304 (1965).

Mas, L.J. *et al.*, Desalination, 7, 285 (1970).

Matz, R. in "Proc. Interregional Seminar Economic Appl. Water Desal.," N.Y., 22 Sept. to 2 Oct., 1965, p. 79.

Matz, R. *et al.*, U.S. patent 3,029,196 (1962).

Meyer, K.H., W. Strauss, Helv, chim-acta, 23, 795 (1940).

Patrick, R.R., J.T. Schrodt, R.I. Kermore, Separation Sci., 7, 331 (1972).

Pigford, R.I., E. Baker III, D.E. Blum, I&EC fund., 8, 144 (1969a).

———————————————————, I&EC fund., 8, 848 (1969b).

Placek, C., "Ion Exchange Resins," Noyes Data Corp., 1970.

Pnueli, D., G. Grossman, Desalination, 7, 297 (1970).

Popkin, R., "Desalination," F.A. Praeger, N.Y. (1968).

Rhee, H.K., N.R. Amundson, I&EC fund., 9, 303 (1970).

Rickles, R.N., "Membranes, Technology and Economics," Noyes Develop. Corp. (1967).

Rolke, R.W., R.H. Wilhelm, I&EC fund., 8, 235 (1969).

Rosenberg, N.W., C.E. Tirrell, I&EC, 49, 780 (1957).

Sata, R. *et al.*, Bull. Chem. Soc. Japan, 42, 279 (1969).

Sabadell, J.E., N.H. Sweed, Separation Sci., 5, 171 (1970).

Schlögel, R., "Stofftransport durch Membranen," Steinkopf, Darmstadt (1964).

Shaffer, L.H., M.S. Mintz, "Electrodialysis," in: "Principles of Desalination," ed. K.S. Spiegler, Acad. Press, N.Y., 1966, pp. 200-290.

Shendelman, L.H., J.E. Mitchell, Chem. Eng. Sci., 27, 1449 (1972).

Skarstrom, C.W., Ann. N.Y. Acad. Sci., 72, 751 (1959).

Solan, A., Y. Winograd, The Phys. of Fluids, 12, 1372 (1969).

Solan, A., Y. Winograd, U. Katz, Desalination, 9, 89 (1971).

Solt, G.S. in: "Proc. First Intern. Symp. Water Desal., Washington, D.C., Oct. 3-9, 1965, Vol. 2, p. 219.

Sonin, A.A., R.F. Probstein, U.S. Off. Saline Water Res. Dev. Rep. No. 375, 1968.

Spiegler, K.S. (ed), "Salt-Water Purification," John Wiley & Son, N.Y., 1962.

———————, "Principles of Desalination," Acad. Press, N.Y., 1966.

———————, Desalination, 9, 367 (1971).

———————, Adv. Chem. Ser., 38, 179 (1961).

Sporn, P., "Fresh Water from Saline Waters," Pergamon Press, Oxford, 1966.

Sweed, N.H., R.H. Wilhelm, I&EC fund., 8, 221 (1969).

Sweed, N.H., R.A. Gregory, Aichey, 17, 171 (1971b).

Sweed, N.H., F.B. Hill, "Parametric Pumping," in: "Progress in Separation and Purification," (E.S. Perry, ed.), Wiley, N.Y. (1971), Vol. 3, p. 171-240.

Tsunoda, Y. in: "Proc. 1st Intern. Symp. Water Desalination, Washington, D.C., Oct. 3-9, 1965, Vol. 2, p. 325.

Wakao, N., H. Matsumoto, K. Juzuki, A. Kawahara, Kagaku Kogaku, 32, 169 (1968).

Weiner, S.A., P.M. Rapier, W.K. Baker, I&EC proc. des. dev., 3, 126 (1964).

Wilhelm, R.H., A.W. Rice, A.R. Bendelius, I&EC fund., 5, 141 (1966).

Wilhelm, R.H., N.H. Sweed, Science, 195, 522 (1968a).

Wilhelm, R.H., A.W. Rice, R.W. Rolke, N.E. Sweed, I&EC fund., 7, 337 (1968b).

Wilson, J.R. (ed.), "Demineralization by Electrodialysis," Butterworth, London, 1960.

Yamane, R. *et al.*, I&EC proc. des. dev., 8, 159 (1969a).

———————, Bull. Chem. Soc. Japan, 42, 2741 (1969b).

Young, E.F. Jr., Chem. Eng., Feb. 1957, p. 241.

APPENDIX A

DETAIL DRAWINGS, PICTURES OF THE MODULES AND MANUFACTURING PROCEDURES

APPENDIX A.1

ELECTRODIALYZER NO. 1

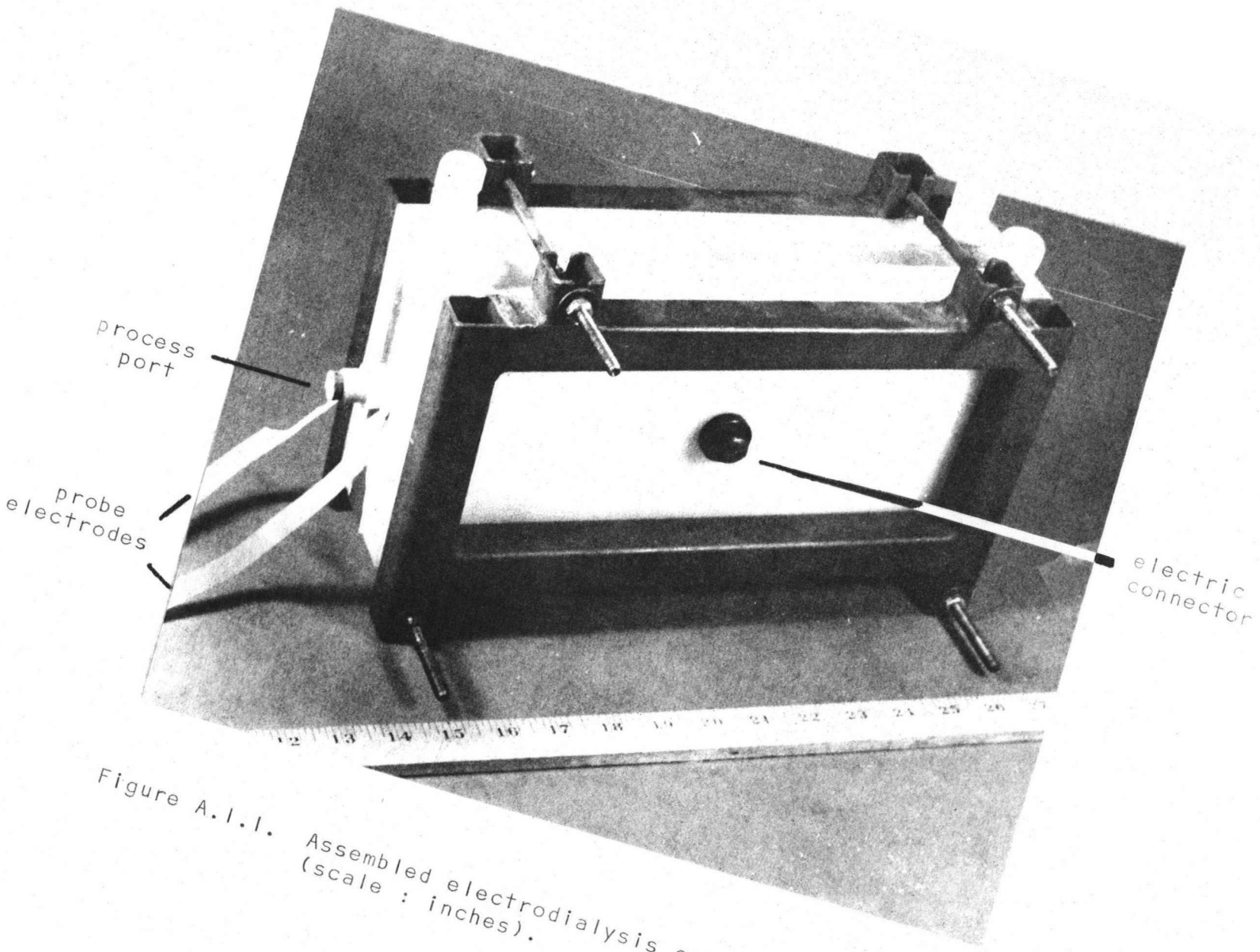

Figure A.1.1. Assembled electrodialysis cell No. 1 (scale : inches).

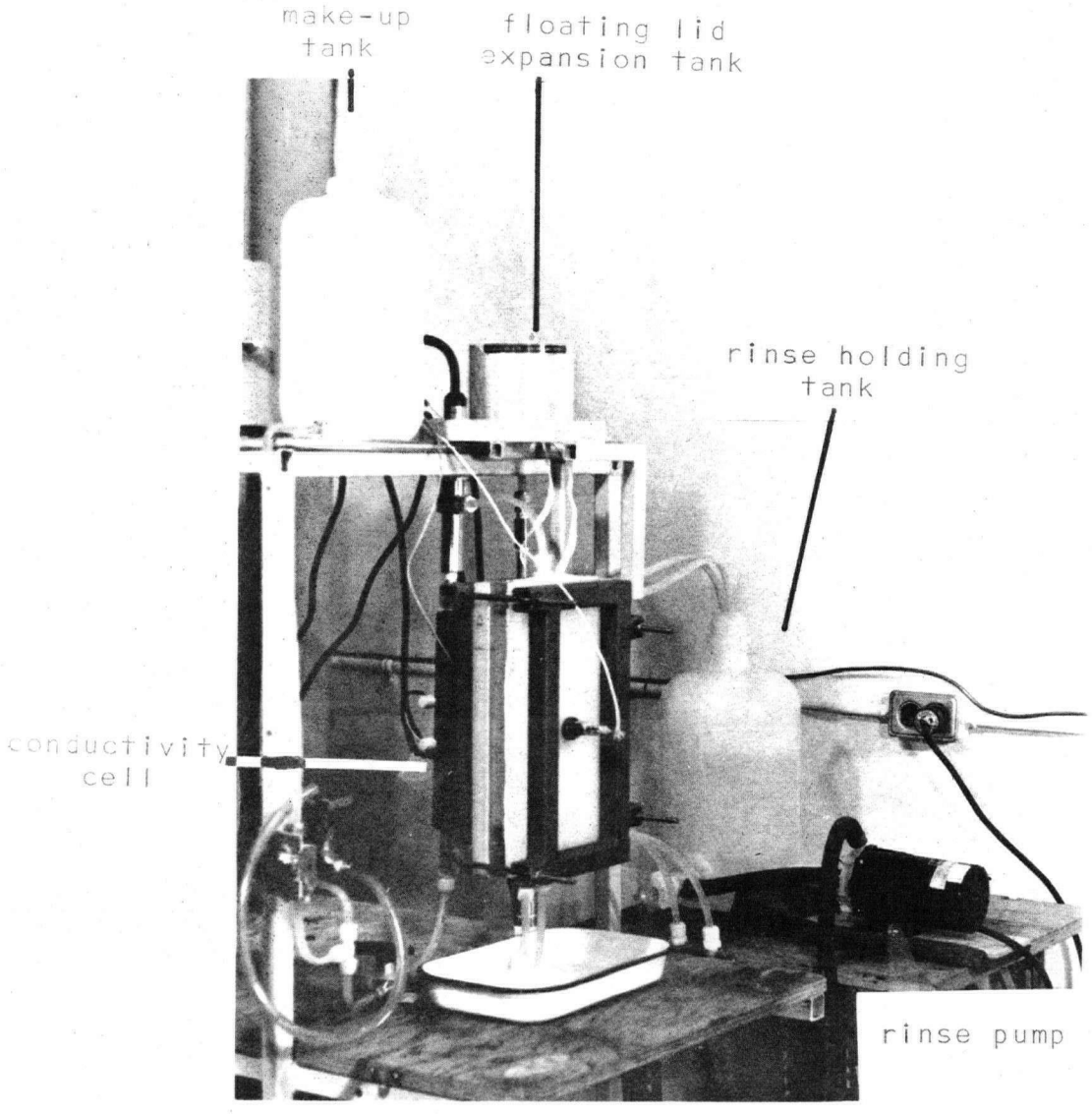

Figure A.1.2. Electrodialyzer No. 1 <in situ>.

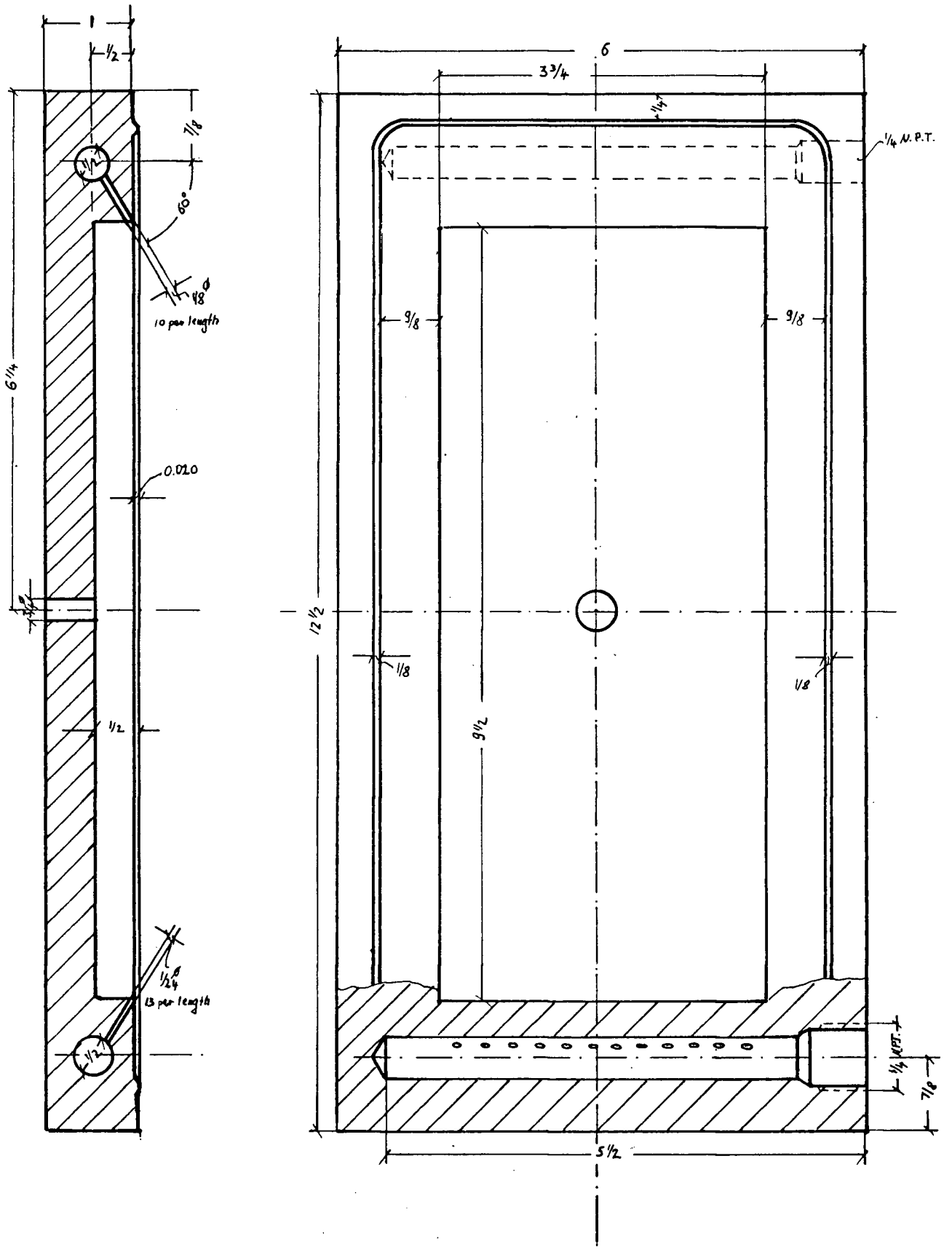

Figure A.1.3. Dimensions of EDI electrode end frame.

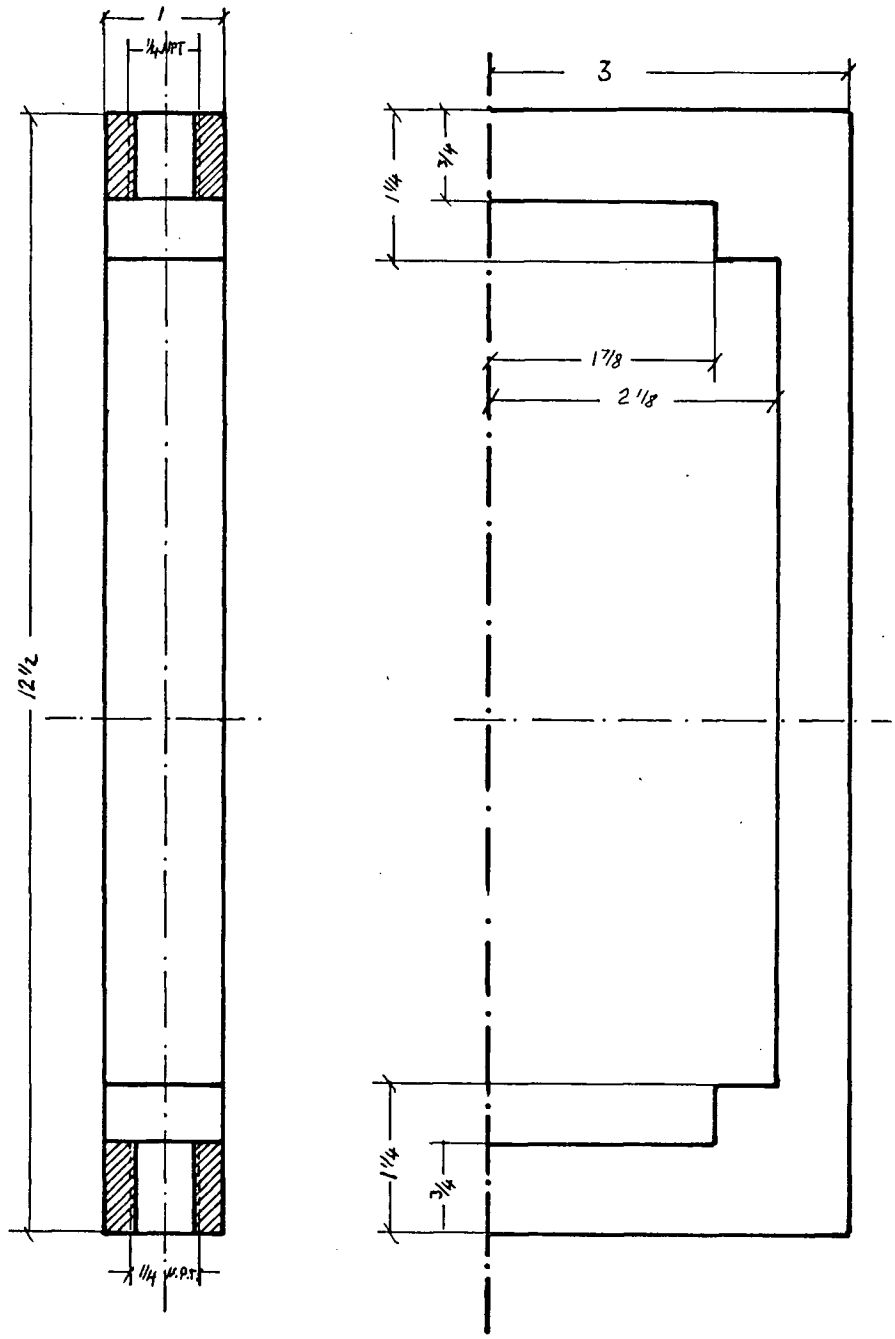

Figure A.1.4. Dimensions of EDI centre frame.

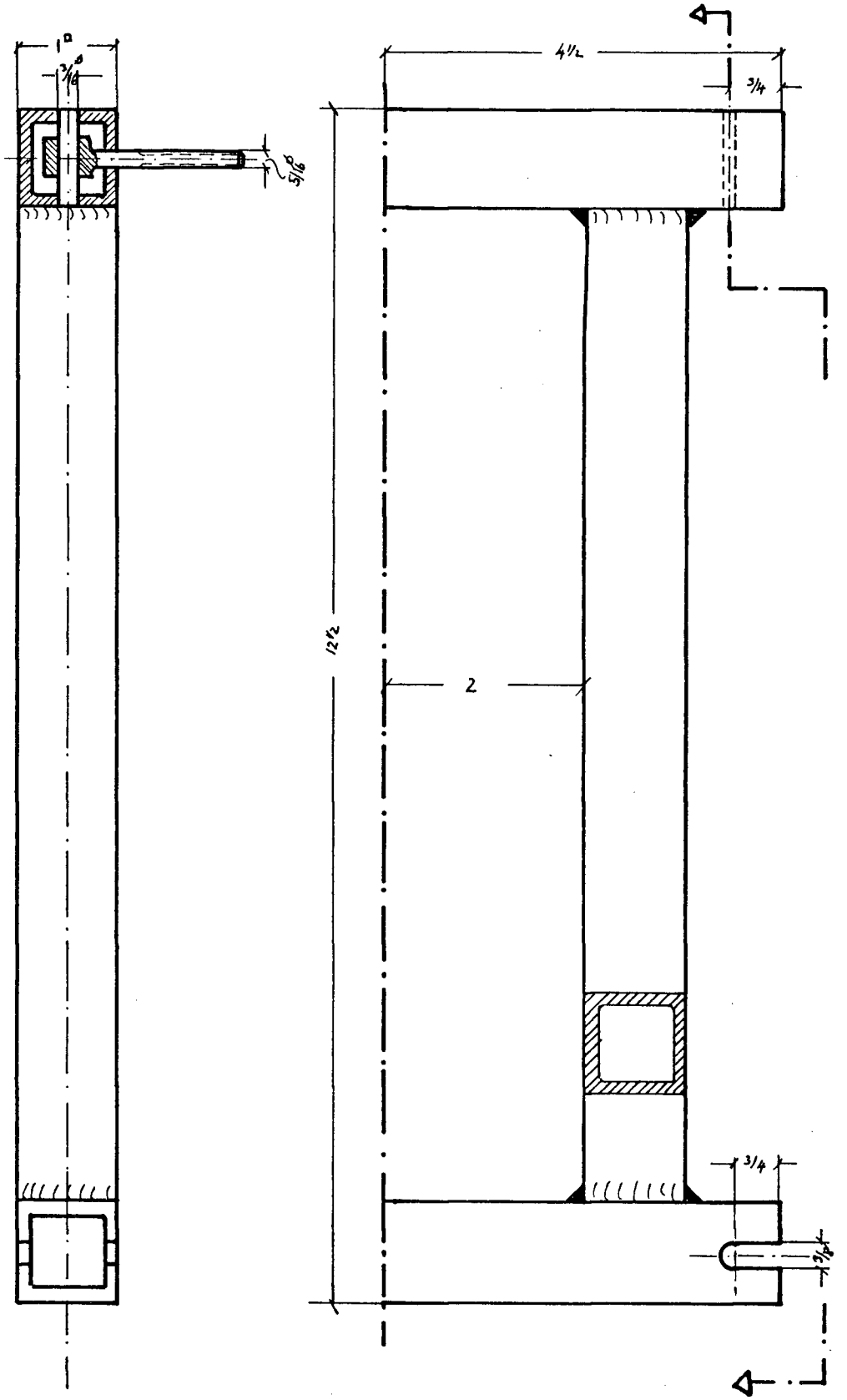

Figure A.1.5. Dimensions of EDI clamping frame.

APPENDIX A.2

ELECTRODIALYZER NO. 2

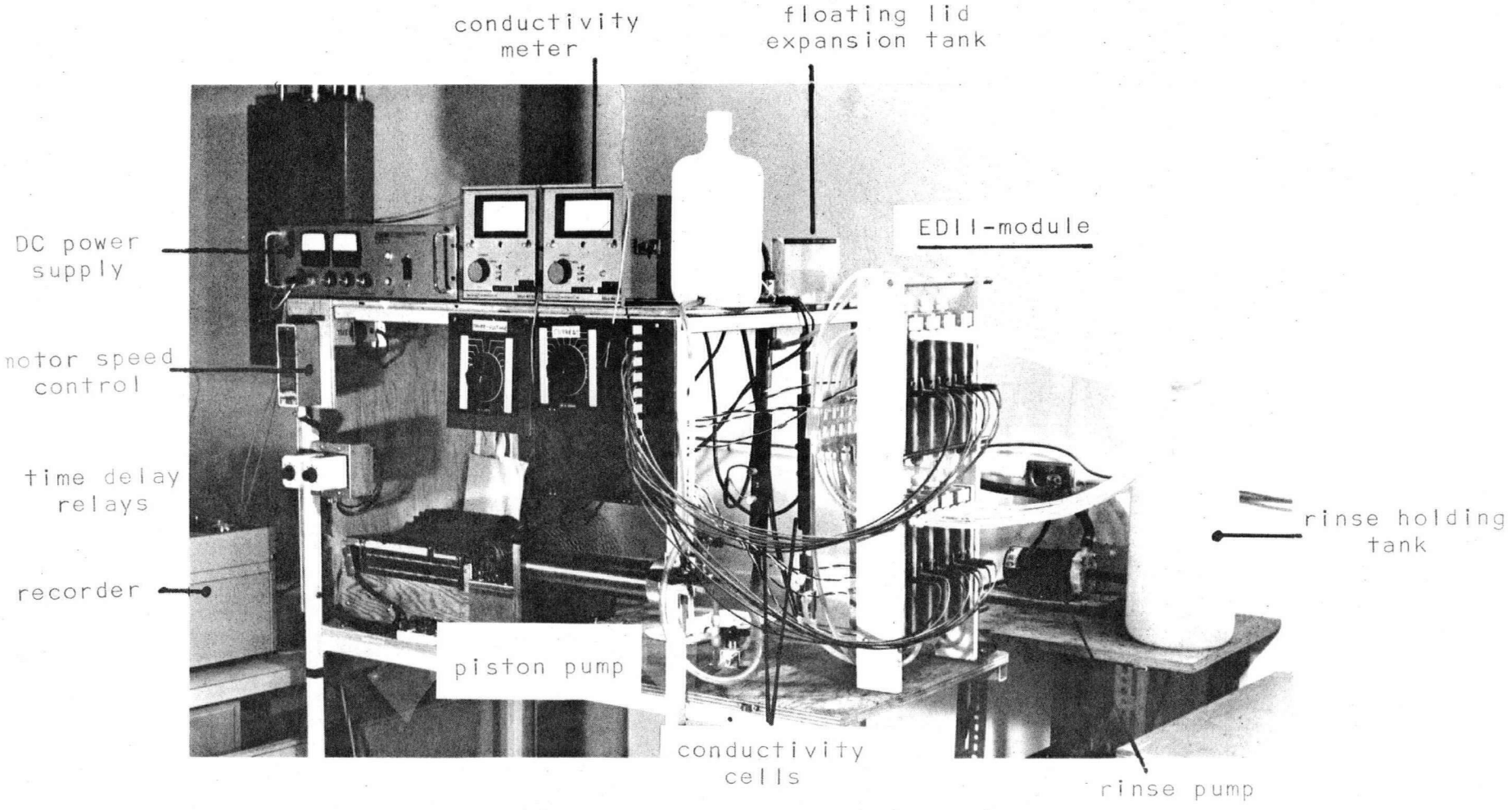

Figure A.2.1 Laboratory testing station.

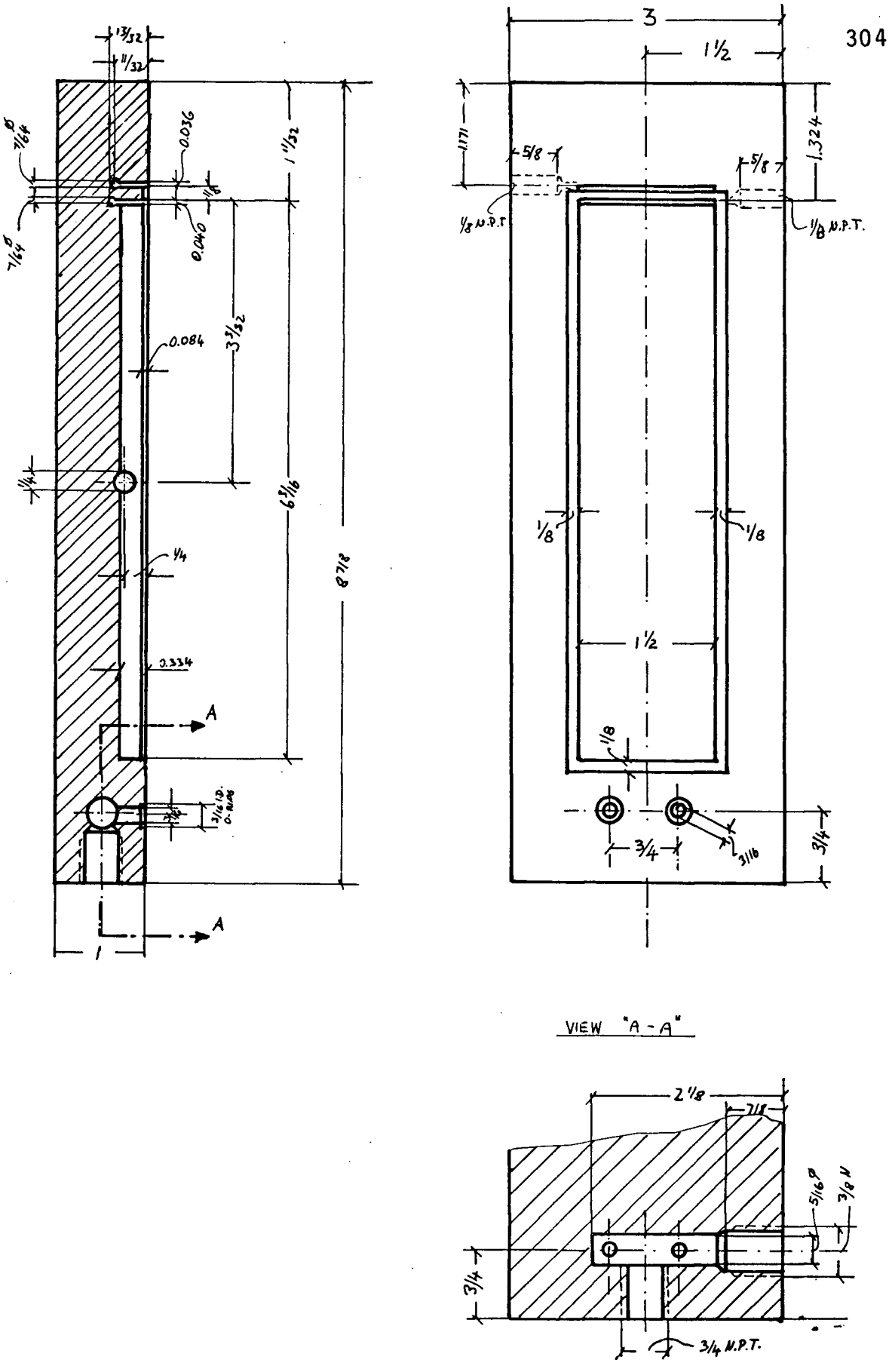

Figure A.2.2 Dimensions of EDII electrode end frame.

APPENDIX A.3

MANUFACTURING PROCEDURE FOR MEMBRANE-SPACER FRAME

Each membrane spacer frame consisted of 5 parts which were permanently joined together. Figure A-3-1 shows an exploded view of the assembly.

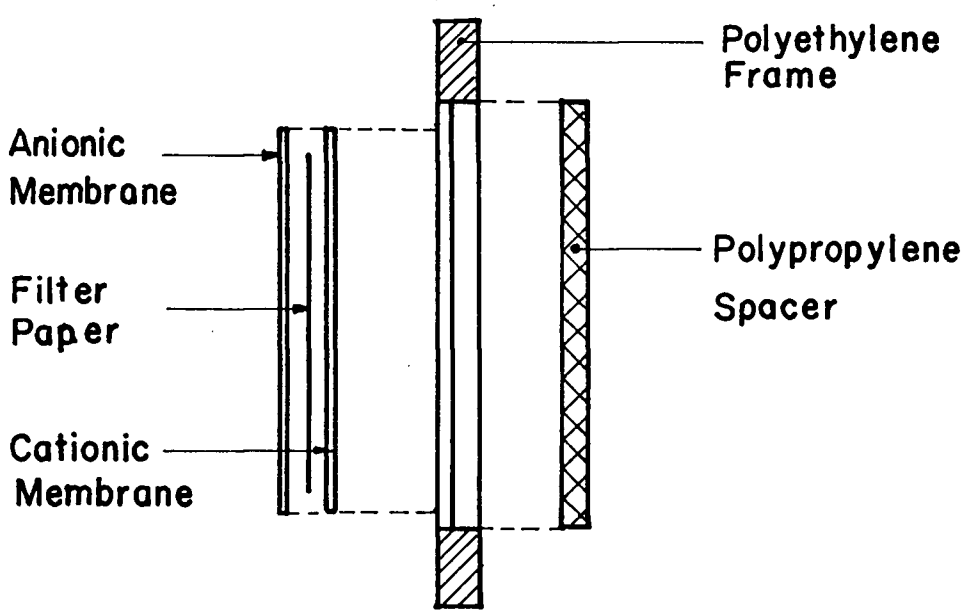

Figure A-3-1: Exploded view of membrane-spacer assembly.

CUTTING:

The supporting frame was punched out of low density polyethylene sheets (1/16" thickness) with a double-knife-edge. The outer edge cut measured 3" x 8-7/8", the inner one was 1-1/2" x 6-11/16". The frames were unsymmetric, and were therefore marked at one corner for future reference. Flow distribution slots were punched to fit the process stream holes on the electrode end plates, see Appendix A.2. Resets (1/8" wide x 0.035" deep) were milled out along both inside lengths of the frames.

Spacer screens were punched out using a single-knife-edge (1-7/8" x 6-11/16"). Spacers were then individually fitted to the resets of the frames.

Membranes were pre-cut and soaked for 24 hours in 0.5N aqueous NaCl solution and punched out using a single-knife-edge (1-3/4" x 6-3/8").

Filter paper (Whatman No. 1) was cut into 1-1/2" x 6-1/16" pieces.

ASSEMBLING:

Each membrane pair was sealed along both widths with a heated bar (seal approximately 1/8" wide). A piece of filter paper was inserted between the sealed membranes.

The spacers were welded to the frames by means of a heated jig which was mounted on a crank shaft punch. The temperature of the jig was controlled by a rheostat to approximately 240 °F. Spacer, frame, and a sheet of thin paper were positioned under the hot jig. The paper was used to aid separation of the jig after completion of the joining process of frame and spacer.

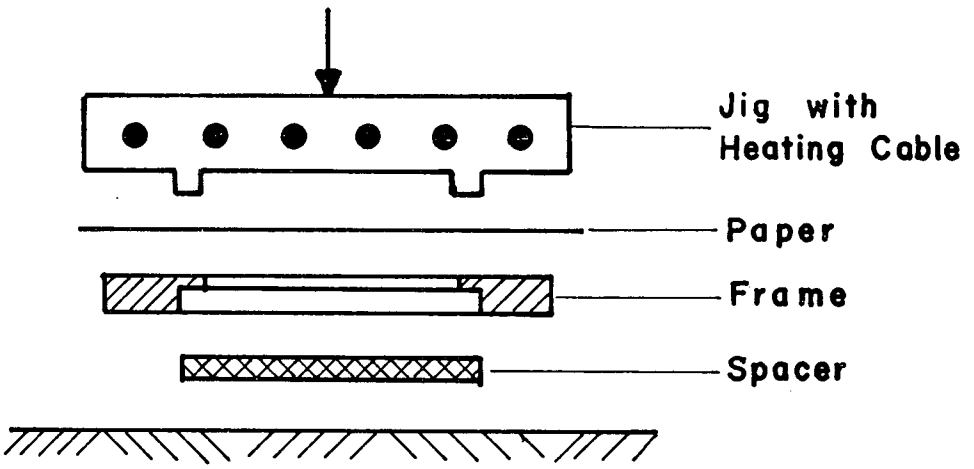

Figure A-3-2: Welding of spacer and frame.

The hot jig was lowered and pressed down with gradually increasing pressure for approximately 1 minute. The joined spacer frame was then quickly removed and quenched in a cold water bath. The paper was removed.

A sorption membrane was tagged to the frame by means of a heated bar.

APPENDIX B

MATHEMATICAL DERIVATIONS

APPENDIX B.1

DERIVATION OF CONCENTRATION TRANSIENTS FOR CONSTANT, UNIFORMLY DISTRIBUTED RATES OF MASS TRANSFER PARAMETRIC PUMPING OPERATION

Since axial dispersion is neglected it is sufficient to consider what happens to the uniform concentration of one end reservoir during any complete cycle, which starts with feeding the reservoir solution to the separator.

The brine cycle is illustrated in Figure B-1. The concentration profiles in brine tank and separator are shown at different instants during the $(k+1)^{th}$ cycle:

0 - refers to the initial concentration in the brine tank.

1 - after time $t = T/2 - \gamma$ (polarity switched to negative).

2 - after one-half cycle $t = T/2$.

3 - after time $t = T/2 + \gamma$.

4 - after time $t = T - \gamma$ (polarity back to positive).

5 - at end of cycle $t = T$.

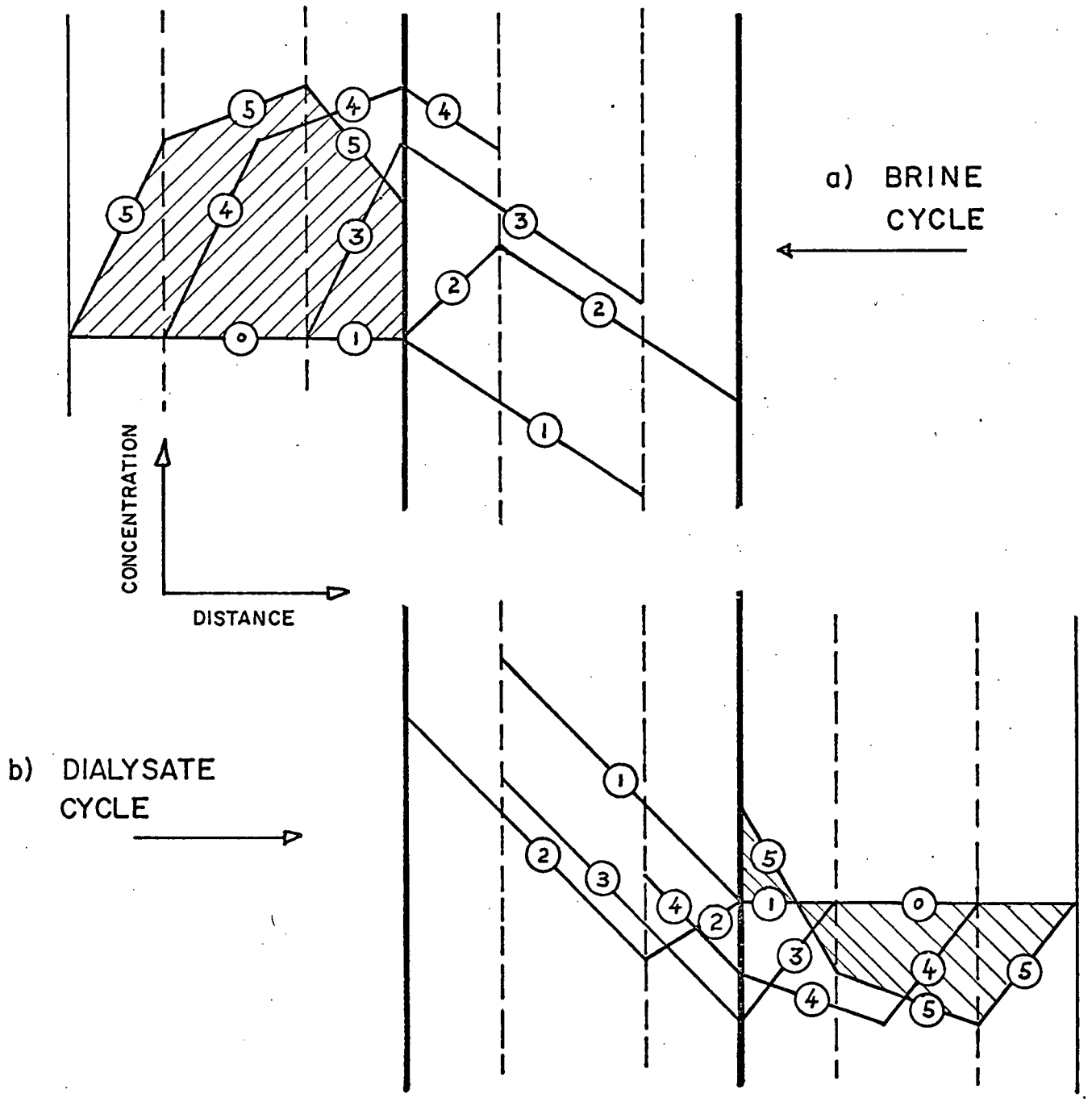

Figure B.I. Concentration changes in brine (a) and dialysate (b) reservoir during a cycle in parametric pumping operation.

The shaded area is the effluent concentration profile at the end of the cycle indicates the rise in concentration.

The calculation of the lines 5 is straightforward. The corners are listed clockwise starting from the leftmost lower one: concentrations are given first, time next, separated by a comma.

$$\left[c_{B,k} \ , \ 0\right]$$

$$\left[c_{B,k} + 2K_2\gamma \ , \ \gamma\right]$$

$$\left[c_{B,k} + (K_2-K_1)\frac{T}{2} + 2K_1\gamma \ , \ \frac{T}{2} - \gamma\right]$$

$$\left[c_{B,K} + (K_2-K_1)\frac{T}{2} \ , \ \frac{T}{2}\right]$$

$$\left[c_{B,k} \ , \ \frac{T}{2}\right]$$

The total area is simply

$$A = K_2\gamma^2 + \tfrac{1}{2}\left[(K_2-K_1)\frac{T}{2} + 2(K_1+K_2)\gamma\right](\frac{T}{2} - 2\gamma) + \tfrac{1}{2}\left[(K_2-K_1)T + 2K_1\gamma\right]$$

Thus the concentration change is given by

$$c_{B,k+1} - c_{B,k} = \frac{2}{T}A = (K_2-K_1)\frac{T}{4} + (K_1+K_2)\frac{\gamma}{2}$$

By similarity, the dialysate change during the $(\ell+1)^{th}$ cycle (see also Figure 3.1.b) is:

$$c_{T,\ell+1} - c_{T,\ell} = (K_2-K_1)\frac{T}{4} - (K_1+K_2)\frac{\gamma}{2}$$

The first dialysate producing half cycle must be calculated separately. A similar area analysis gives

$$c_{T,1} - c_{T,0} = -\frac{2}{T}\left[\left(\frac{T}{2}-\gamma\right)^2 \tfrac{1}{2} K_1 + \left\{2K_1\left(\frac{T}{2}-\gamma\right) - K_2\gamma\right\}\tfrac{1}{2}\gamma\right]$$

$$= -\frac{1}{T}\left[\left(\frac{T^2}{4}-\left(T\gamma+\gamma^2\right)K_1+2K_1\left(\frac{T\gamma}{2}-\gamma^2\right) - K_2\gamma^2\right]$$

$$= -\frac{1}{T}\left[K_1\left(\frac{T^2}{4}-\gamma^2\right) - K_2\gamma^2\right]$$

Hence

$$c_{t,1} - c_{T,0} = (k_2+K_1)\frac{\gamma^2}{T} - K_1\frac{T}{4}$$

In general, for $n \geq 1$

$$c_{T,n} = c_{T,0} - K_1\frac{T}{4} + (K_2+K_1)\frac{\gamma^2}{T} + \left[\frac{K_2-K_1}{4} - \frac{K_1+K_2}{2}\frac{\gamma}{T}\right](n-1)T$$

and

$$c_{B,n} = c_{B,0} + \left[\frac{K_2-K_1}{4} + \frac{K_1+K_2}{2}\frac{\gamma}{T}\right]n\,T$$

APPENDIX B.2

DERIVATION OF THE CONCENTRATION TRANSIENTS FOR CONCENTRATION DEPENDENT RATES OF MASS TRANSFER PURE PAUSE OPERATION

In a similar analysis to the previous section the concentrations in stationary and moving parts of the systems may be considered as blocks. One void volume displacement is assumed.

For the nth dilution half cycle one has, according to the assumed rate law

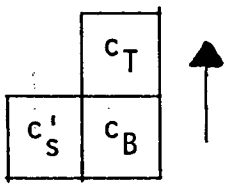

and

$$\frac{\partial \left(c_T\right)_n}{\partial t} = - a_1 \left(c_T\right)_n$$

$$\rho \frac{\partial \left(c'_S\right)_n}{\partial t} = \frac{\partial \left(c_T\right)_n}{\partial t}$$

subject to the initial conditions

for $t = 0$ $\qquad \left(c_T\right)_n = \left(c_T\right)_{n-1}$

$$\left(c'_S\right)_n = \left(c_S\right)_{n-1}$$

Hence

$$\left.\begin{aligned} \left(c_T\right)_n &= \left(c_T\right)_{n-1} \exp(-a_1 t) \\ \left(c'_s\right)_n &= \left(c_s\right)_{n-1} + \frac{1}{\rho}\left(c_T\right)_{n-1}\left[1 - \exp(-a_1 t)\right] \end{aligned}\right\} \qquad (B.2.1)$$

Similarly for the nth enrichment half cycle

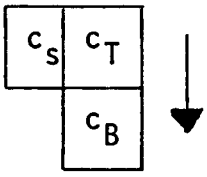

and

$$\frac{\partial\left(c_s\right)_n}{\partial t} = -a_2\left(c_s\right)_n$$

$$\frac{\partial\left(c_B\right)_n}{\partial t} = -\rho\frac{\partial\left(c_s\right)_n}{\partial t}$$

subject to the initial conditions

for $t = 0$ $\qquad \left(c_B\right)_n = \left(c_B\right)_{n-1}$

$$\left(c_s\right)_n = \left(c'_s\right)_n$$

Hence

$$\left.\begin{aligned} \left(c_s\right)_n &= \left(c_s'\right)_n \exp(-a_2\ t) \\ \left(c_B\right)_n &= \left(c_B\right)_{n-1} + \rho\left(c_s'\right)\left[1 - \exp(-a_2\ t)\right] \end{aligned}\right\} \qquad \text{(B.2.2)}$$

The systems of difference equations (B.2.1) and (B.2.2) may be solved stepwise as follows. The global starting condition is chosen to be

$$\text{for} \quad t = 0\ , \quad \left(c_T\right)_0 = \left(c_B\right)_0 = \left(c_s\right)_0 = 1$$

and the abbreviations

$$p = \exp\left(-a_1\ \frac{T}{2}\right) \quad ,$$

and

$$q = \exp\left(-a_2\ \frac{T}{2}\right)$$

are used.

$$n = 1 : \quad \left(c_T\right)_1 = p$$

$$\left(c_s'\right)_1 = 1 + \frac{1}{\rho}(1-p)$$

$$\left(c_s\right)_1 = q + \frac{q}{\rho}(1-p)$$

$$\left(c_B\right)_1 = 1 + \rho(1-q) + (1-q)(1-p)$$

$n = 2$:

$$\left(c_T\right)_2 = p^2$$

$$\left(c'_S\right)_2 = q + \frac{q}{\rho}(1-p) + \frac{1}{\rho}p\,(1-p)$$

$$\left(c_S\right)_2 = q^2 + \frac{q^2}{\rho}(1-p) + \frac{1}{\rho}pq\,(1-p)$$

$$\left(c_B\right)_2 = 1 + \rho(1-q) + (1-q)(1-p) + \rho(1-q)\left[q + \frac{q}{\rho}(1-p)\right] +$$

$$+ (1-q)(1-p)\,p$$

$$= 1 + \rho(1-q)(1+q) + (1-q)(1-p)(1+p+q)$$

$n = 3$

$$\left(c_T\right)_3 = p^3$$

$$\left(c'_S\right)_3 = q^2 + q(1-p)\frac{1}{\rho}(p+q) + \frac{1}{\rho}\,p^2(1-q)$$

$$\left(c_S\right)_3 = q^3 + q^2(1-p)\frac{1}{\rho}(p+q) + q(1-p)\,\frac{1}{\rho}\,p^2$$

$$= q\left[q^2 + \frac{1}{\rho}(1-p)(p^2 + q^2 + pq)\right]$$

$$\left(c_B\right)_3 = 1+(1-q)\left[\rho(1+q)+(1-p)(1+p+q)\right]+\rho(1-q)\left[q^2+q(1-p)\frac{1}{\rho}(p+q)\right]+$$

$$+ (1-p)(1-q)q^2 =$$

$$= 1 + (1-q)\left[\rho(1+q+q^2) + (1-p)(1+q+p+q^2+pq+p^2)\right]$$

$n = 4$

$$\left(c_T\right)_4 = p^4$$

$$\left(c_B\right)_4 = 1 + \rho(1-q)(1+q+q^2) + (1-q)(1-p)(1+p+q+q^2+pq+p^2) +$$

$$+ \rho(1-q)\left[q^3+(1-p)\frac{1}{\rho}(p^2q+q^3+pq^2)\right] + (1-q)(1-p)p^3$$

$$= 2 + \rho(1-q^4) - p^4 - q^4 + \sum_{\ell=1}^{3} p^{4-\ell}\, q^{\ell} + \sum_{\ell=1}^{4} p^{5-\ell}\, q^{\ell}$$

$$= 2 + \rho(1-q^4) - p^4 - q(1-p) \sum_{i=0}^{3} p^{3-\ell}\, q^{\ell}$$

The general recurrence scheme is clear now and the result becomes

$$\left(c_T\right)_n = p^n$$

$$\left(c_B\right)_n = 2 + \rho(1-q^n) - p^n - q(1-p)p^{n-1} \sum_{\ell=0}^{n-1} \left(\frac{q}{p}\right)^{\ell}$$

APPENDIX B.3

RATE THEORY OF PARAMETRIC PUMPING

The nth cycle consists of a dilution half cycle followed by an enrichment half cycle. After substitution of the rate laws (19) into the mass balance equation (6), one has for the first part cycle

$$\left.\begin{aligned} \frac{\partial c_f}{\partial t} + v \frac{\partial c_f}{\partial z} + a_1 c_f = 0 \quad , \\ \rho \frac{\partial c_s}{\partial t} = a_1 c_f \quad , \end{aligned}\right\} \qquad (B.3.1)$$

and for the second part cycle

$$\left.\begin{aligned} \frac{\partial c_s}{\partial t} = - a_2 c_s \quad , \\ \frac{\partial c_f}{\partial t} + v \frac{\partial c_f}{\partial z} - \frac{a_2}{\rho} c_s = 0 \quad . \end{aligned}\right\} \qquad (B.3.2)$$

The method of characteristics (Acrivos, 1956), is applied and the following sets of ordinary differential equations are obtained:

The first equation of (i) is rewritten as

$$dc_f : dt : dz = - a_1 \cdot c_f : 1 : v$$

or

$$\frac{dz}{dt} = v \ , \text{ and } \frac{d\ \ell n\ c_f}{dt} = - a_1 \qquad \text{(B.3.3)}$$

The partial differential of the second equation in (B.3.1) is identical to the total derivative

$$\frac{dc_s}{dt} = \frac{\partial c_s}{\partial t} + \frac{\partial c_s}{\partial z} \cdot \frac{dz}{dt} = \frac{\partial c_s}{\partial t}$$

since there is no flow in the stationary phase ($dz/dt = 0$).

Hence

$$\frac{dc_s}{dt} = \frac{a_1}{\rho} c_f \qquad \text{(B.3.4)}$$

Similarly, for the set of equations (B.3.2) one finds

$$\frac{dc_s}{dt} = - a_2 \; c_s \; , \qquad (B.3.5)$$

and

$$\frac{dz}{dt} = v \; , \text{ and } \frac{dc_f}{dt} = \rho \; a_2 \; c_s \qquad (B.3.6)$$

Because of (B.3.5) it is not possible to eliminate the concentration in the stationary phase, c_s, from the set of equations. The local concentration profiles in both phases have to be calculated step by step. The following equations take into account that the frames of reference for equations (B.3.3) and (B.3.6) are travelling with the fluid velocity v, whereas equations (B.3.4) and (B.3.5) are written for a stationary frame of reference. If the (z,t) plane is considered one can calculate the necessary local and average concentration profiles.

For the first part cycle:

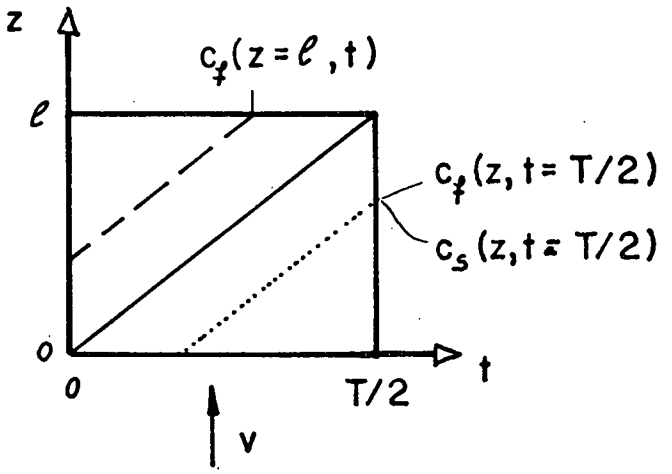

$$c_f(\ell,t) = c_f(\ell-vt,0)\ \exp(-a_1 t)$$

$$c_{t,n} = \frac{2}{T}\int_0^{T/2} c_f(\ell,t)\ dt$$

$$c_f\left(z,\frac{T}{2}\right) = c_{B,n-1}\ \exp\left(-\frac{a\ z}{v}\right)$$

$$c_s\left(z,\frac{T}{2}\right) = c_s(z\ 0) + \frac{a_1}{\rho}\int_0^{z/v} c_f(z-vt,0)\ \exp(-a_1 t)\ dt +$$

$$+ \frac{a_1}{\rho}\left(\frac{T}{2} - \frac{z}{v}\right)\ c_{B,n-1}\ \exp\left(-\frac{a_1 z}{v}\right)$$

For the second part cycle:

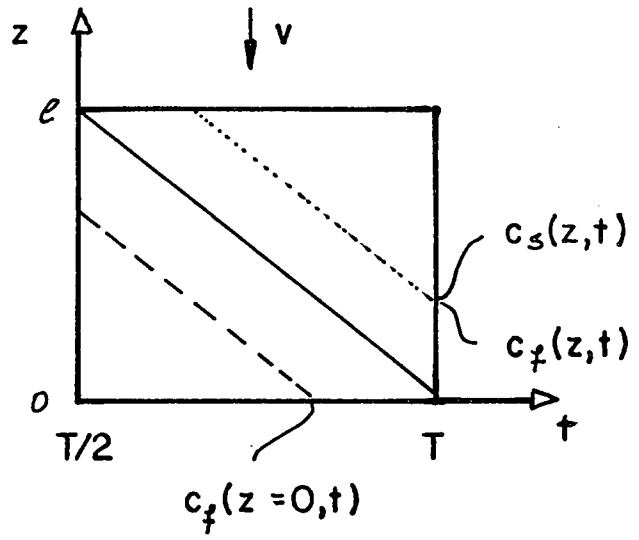

$$c_s(z,T) = c_s\left(z\,,\,\frac{T}{2}\right)\,\exp\left(-a_2\,\frac{T}{2}\right)$$

$$c_f(z,T) = c_{T,n} + \rho a_2 \int_{z/v}^{T/2} c_s\left(z+\ell-vt,\,\frac{T}{2}\right)\,\exp(-a_2 t)\,dt$$

$$c_f(0,t) = c_f\left(vt\,,\,\frac{T}{2}\right) + \rho a_2 \int_{T/2}^{T} c_s\left(vt-vs\,,\,\frac{T}{2}\right)\,\exp(-a_2 s)\,ds$$

$$c_{B,n} = \frac{2}{T}\int_{T/2}^{T} c_f(0,t)\,dt$$

In Table B-1 the concentration distributions in time and space are presented for four successive half cycles and under the restrictions, $c_f = c_s = 1.0$ at $t = 0$, $a_1 = a_2 = a$, $\rho = 1$. The time and space average concentrations are included as well. The abbreviations $\tau' = aT/2$ and $\xi = az/v$ are used.

Table B.1 :

Average and Local Concentrations During the First Two Cycles of a Parametric Pumping Operation for Concentration Dependent Rates of Mass Transfer.

CONCENTRATION \ CYCLE	1/2	1	3/2	2
AVERAGE EFFLUENT	$\frac{1}{\tau'_1}\left[1-\exp(-\tau')\right]$	$3\left(1-\frac{1}{\tau'_1}\right)+\left(1+\frac{3}{\tau'_1}-\frac{\tau'}{2}\right)\exp(-\tau')$	$\frac{1}{\tau'^2_2}+\left(2-\frac{2}{\tau'_1}-\frac{2}{\tau'^2_2}\right)\exp(-\tau')+\left(\frac{\tau'^2}{6}-\frac{\tau'}{2}+\frac{2}{\tau'_1}+\frac{1}{\tau'^2_2}\right)\exp(-2\tau')$	$3-\frac{2}{\tau'^2_2}+\left(-\frac{5\tau'}{2}-\frac{1}{2}+\frac{3}{\tau'_1}+\frac{4}{\tau'^2_2}\right)\exp(-\tau')+\left(-\frac{\tau'^3}{2}+\frac{5\tau'^2}{12}-\frac{\tau'}{2}-\frac{5}{2}-\frac{3}{\tau'_1}+\frac{2}{\tau'^2_2}\right)\exp(-2\tau')$
AVERAGE SOLUTION	$\frac{1}{\tau'_1}\left[1-\exp(-\tau')\right]$	$\frac{3}{\tau'_1}-\left(4+\frac{1}{\tau'_1}-\frac{\tau'}{2}\right)\exp(-\tau')-\frac{2}{\tau'_1}\exp(-2\tau')$	$\frac{3}{\tau'_1}-\frac{3}{\tau'^2_2}+\left(-\frac{1}{2}-\frac{2}{\tau'_1}+\frac{6}{\tau'^2_2}\right)\exp(-\tau')+\left(\frac{1}{2}-\frac{1}{\tau'_1}-\frac{3}{\tau'^2_2}\right)\exp(-2\tau')$	$\frac{2}{\tau'^2_2}+\left(\frac{5}{2}\tau'-\frac{5}{2}-\frac{6}{\tau'^2_2}\right)\exp(-\tau')+\left(\frac{\tau'^3}{8}-\frac{5\tau'^2}{12}+\frac{\tau'}{2}+4-\frac{1}{\tau'_1}+\frac{6}{\tau'^2_2}\right)\exp(-2\tau')+\left(\frac{\tau'^2}{6}-\frac{\tau'}{2}+\frac{1}{2}+\frac{1}{\tau'_1}-\frac{2}{\tau'^2_2}\right)\exp(-3\tau')$
AVERAGE ADSORBENT	$3-\frac{2}{\tau'_1}\left[1-\exp(-\tau')\right]$	$\left(3-\frac{2}{\tau'_1}\right)\exp(-\tau')+\frac{2}{\tau'_1}\exp(-2\tau')$	$3-\frac{3}{\tau'_1}+\frac{2}{\tau'^2_2}+\left(-\frac{}{}+\frac{4}{\tau'_1}-\frac{4}{\tau'^2_2}\right)\exp(-\tau')+\left(-\frac{\tau'^2}{6}+\frac{\tau'}{2}-\frac{1}{2}-\frac{1}{\tau'_1}+\frac{2}{\tau'^2_2}\right)\exp(-2\tau')$	$\left(3-\frac{3}{\tau'_1}+\frac{2}{\tau'^2_2}\right)\exp(-\tau')+\left(-\frac{3}{2}+\frac{4}{\tau'_1}-\frac{4}{\tau'^2_2}\right)\exp(-2\tau')+\left(-\frac{\tau'^2}{6}+\frac{\tau'}{2}-\frac{1}{2}-\frac{1}{\tau'_1}+\frac{2}{\tau'^2_2}\right)\exp(-3\tau')$
LOCAL SOLUTION	$\exp(-\xi)$	$\frac{1}{\tau'_1}-\left(2+\frac{1}{\tau'_1}\right)\exp(-\tau')+2\exp(-\xi)+\left[\frac{\tau'^2}{2}-\tau'-\xi\tau'+\xi^2\right]\exp(-\xi-\tau')$	$\left[3\left(1-\frac{1}{\tau'_1}\right)+\left(1+\frac{3}{\tau'_1}-\frac{\tau'}{2}\right)*\exp(-\tau')\right]\exp(-\xi)$	
LOCAL ADSORBENT	$2-(1+\xi-\tau)\exp(-\xi)$	$2\exp(-\tau)-(1+\xi-\tau')\exp(-\xi-\tau')$	$\frac{1}{\tau'_1}\left[1-\exp(-\tau')\right]+\left(-3+3\tau'-\xi-\frac{1}{\tau'_1}+\frac{3\xi}{\tau'}\right)\exp(-\xi)+\left[4+2\tau'+\frac{1}{\tau'_1}-2\xi-\frac{\tau'^2}{2}-\frac{3\xi}{\tau'}+\xi/2\left(\tau'^2-\tau'-\tau'\xi+\xi+\frac{\xi^2}{3}\right)\right]\exp(-\xi-\tau')$	

APPENDIX B.4

MULTIPLE STEP DISPLACEMENT MODEL (STOP-GO ALGORITHM)

In the conceptual model of this scheme the two phases may be represented by two-dimensional plates. The areas of the plates indicate the volumes of each of the phases. Since the frame of reference may be attached to either of the phases, it will be assumed that the adsorbent (or adsorption membrane) is displaced relative to the solution.

The displacement occurs stepwise. The plates are divided into segments of identical length $\Delta z = \ell/N$ according to the number of steps (see Figure B-2). If one void volume is displaced, there will be N segments on the moving plate and 2N segments on the stationary one. Each segment represents a separate well mixed cell.

During the STOP periods mass is transferred between adjacent cells for time intervals $\Delta t = T/2N$. During each GO step the segments are displaced by one increment without mass transfer taking place. At the end of each half cycle the

segments on the stationary plate, which have no neighbours on the moving plate, may be intermixed to satisfy the end mixing condition.

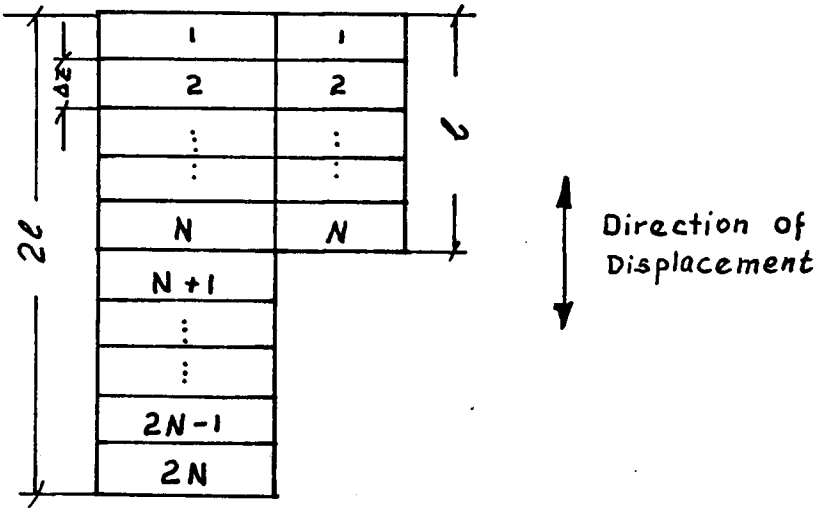

Figure B-2: Plate representation of multiple step displacement model (STOP-GO algorithm).

A FORTRAN IV program was prepared for an IBM 360/67 digital computer to simulate concentration dependent mass transfer rates according to equations (27), see Section 3.3. The program is written in double precision because round-off errors affected the overall mass balance for large N's.

The FORTRAN program is listed on the next page followed by the computer printout of a simulation run for

$N = 100$, $\delta = \frac{1}{2}$, $a_1 = 0.01[\text{sec}^{-1}]$,

$a_2 = 0.01[\text{sec}^{-1}]$, $\rho = 0.5$, $T = 10[\text{sec}]$

```
      C
      C  MULTIPLE STEP DISPLACEMENT MODEL
      C  CONCENTRATION DEPENDENT RATES OF MASS TRANSFER
      C
            DOUBLE PRECISION P,Q,P1,Q1,CEFF,S2,S1,DEXP,X(200),Y(200)
            REAL A1,A2,R,TAU,BA,BS,SEP
            READ (5,1) M,ND,N,A1,A2,R,TAU
       1    FORMAT (3I3,4F6.4)
      C
            M1=M+1
            ND1=ND+1
            M2=M+ND
            P=-A1*TAU/ND
            P=DEXP(P)
            Q=-A2*TAU/ND
            Q=DEXP(Q)
            P1=(1.D0-P)/R
            Q1=(1.D0-Q)*R
            BA=100./(M+M*R+ND)
            DO 2 I=1,M2
            X(I)=1.D0
       2    Y(I)=1.D0
      C
            WRITE (6,3) M,N,ND,M,A1,A2,R,TAU
       3    FORMAT (1H1///' DISPERSION MODEL OF RATE THEORY '//
           110X,' ENDS WELL MIXED,    EXCHANGE - DISPLACE '//
           2' NUMBER OF COMPARTMENTS                    = ', I3/
           3' NUMBER OF CYCLES                          = ',I3/
           4' DISPLACED VOLUME                          = ',I3,'/',I3/
           5' INITIAL CONCENTRATION                     = 1.0 '/
           6' DESALINATION RATE COEFFICIENT             = ',F6.4,'(1/SEC)'/
           7' CONCENTRATION RATE COEFFICIENT            = ',F6.4,'(1/SEC)'/
           8' VOLUME RATIO                              = ',F6.3/
           9' CYCLE TIME                                = ',F6.1 ,'(SEC)'///)
            WRITE (6,4)
       4    FORMAT('CYCLE NO.      BRINE    DIALYSATE    SEPARATION    BALANCE (%)
           1')
      C
      C FIRST HALF CYCLE
      C
            DO 100 J=1,N
            DO 10 L=1,ND
            I=M+L
            DO 5 K=1,M
            I=I-1
            Y(I+1)=Y(I)+X(I)*P1
       5    X(I)=X(I)*P
      10    CONTINUE
            CEFF=0.0
            DO 11 I=1,ND
      11    CEFF=CEFF+X(I)
            CEFF=CEFF/ND
            DO 12 I=1,ND
      12    X(I)=CEFF
      C
      C SECOND HALF CYCLE
      C
            DO 20 L=1,ND
            I=ND1-L
            DO 15 K=1,M
            I=I+1
            X(I)=X(I)+Y(I)*Q1
      15    Y(I-1)=Y(I)*Q
      20    CONTINUE
            S1=0.0
            S2=0.0
            S3=0.0
            DO 21 I=1,M
            S1=S1+X(I)
      21    S3=S3+Y(I)
            DO 22 I=M1,M2
      22    S2=S2+X(I)
            BS=(S1+S2+S3*R)*BA
            S2=S2/ND
            SEP=S2/CEFF
            DO 23 I=M1,M2
      23    X(I)=S2
      C
      C PRINTOUT
      C
            WRITE (6,25) J,S2,CEFF,SEP,BS
      25    FORMAT (I7,4F12.4)
      100   CONTINUE
            STOP
            END
END OF FILE
```

DISPERSION MODEL OF RATE THEORY

ENDS WELL MIXED, EXCHANGE - DISPLACE

NUMBER OF COMPARTMENTS	= 100
NUMBER OF CYCLES	= 60
DISPLACED VOLUME	= 50/100
INITIAL CONCENTRATION	= 1.0
DESALINATION RATE COEFFICIENT	= 0.0100(1/SEC)
CONCENTRATION RATE COEFFICIENT	= 0.0100(1/SEC)
VOLUME RATIO	= 0.500
CYCLE TIME	= 10.0(SEC)

CYCLE NO.	BRINE	DIALYSATE	SEPARATION	BALANCE (%)
1	0.9821	0.9507	1.0330	99.9998
2	0.9668	0.9293	1.0404	99.9998
3	0.9539	0.9105	1.0477	99.9998
4	0.9430	0.8939	1.0549	99.9998
5	0.9338	0.8793	1.0620	99.9998
6	0.9260	0.8663	1.0689	99.9998
7	0.9195	0.8548	1.0757	99.9998
8	0.9140	0.8445	1.0823	99.9998
9	0.9094	0.8352	1.0888	99.9998
10	0.9055	0.8269	1.0951	99.9998
11	0.9024	0.8194	1.1013	99.9998
12	0.8998	0.8126	1.1073	99.9998
13	0.8976	0.8063	1.1132	99.9998
14	0.8959	0.8006	1.1190	99.9998
15	0.8946	0.7954	1.1247	99.9998
16	0.8936	0.7905	1.1303	99.9998
17	0.8928	0.7861	1.1358	99.9998
18	0.8923	0.7819	1.1412	99.9998
19	0.8920	0.7780	1.1465	99.9998
20	0.8918	0.7743	1.1518	99.9998
21	0.8918	0.7708	1.1569	99.9998
22	0.8920	0.7676	1.1620	99.9998
23	0.8922	0.7645	1.1671	99.9998
24	0.8926	0.7615	1.1721	99.9998
25	0.8930	0.7587	1.1770	99.9998
26	0.8935	0.7560	1.1818	99.9998
27	0.8941	0.7535	1.1867	99.9998
28	0.8947	0.7510	1.1914	99.9998
29	0.8954	0.7486	1.1962	99.9998
30	0.8962	0.7463	1.2009	99.9998
31	0.8970	0.7440	1.2055	99.9998
32	0.8978	0.7419	1.2102	99.9998
33	0.8986	0.7398	1.2147	99.9998
34	0.8995	0.7377	1.2193	99.9998
35	0.9004	0.7357	1.2238	99.9998
36	0.9013	0.7338	1.2283	99.9998
37	0.9022	0.7319	1.2328	99.9998
38	0.9032	0.7300	1.2372	99.9998
39	0.9042	0.7282	1.2416	99.9998
40	0.9052	0.7264	1.2460	99.9998
41	0.9062	0.7247	1.2504	99.9998
42	0.9072	0.7230	1.2547	99.9998
43	0.9082	0.7213	1.2590	99.9998
44	0.9092	0.7197	1.2633	99.9998
45	0.9102	0.7181	1.2676	99.9998
46	0.9113	0.7165	1.2719	99.9998
47	0.9123	0.7149	1.2761	99.9998
48	0.9133	0.7134	1.2803	99.9998
49	0.9144	0.7119	1.2845	99.9998
50	0.9154	0.7104	1.2887	99.9998
51	0.9165	0.7089	1.2928	99.9998
52	0.9175	0.7075	1.2970	99.9998
53	0.9186	0.7060	1.3011	99.9998
54	0.9197	0.7046	1.3052	99.9998
55	0.9207	0.7032	1.3092	99.9998
56	0.9218	0.7019	1.3133	99.9998
57	0.9228	0.7005	1.3173	99.9998
58	0.9239	0.6992	1.3214	99.9998
59	0.9249	0.6979	1.3254	99.9998
60	0.9260	0.6966	1.3293	99.9998

STOP 0
EXECUTION TERMINATED

APPENDIX B.5

DERIVATION OF CONCENTRATION TRANSIENTS FOR EQUILIBRIUM CONTROLLED PURE PAUSE OPERATION

CASE A:

Initial equilibrium constant K_2. First displacement downward.

It is sufficient to consider the overall concentrations of the adsorbent (c_s) and of the solution in the end reservoirs and inside the separator (c_T and c_B).

The mass balances during the nth cycle are:

for the first half cycle

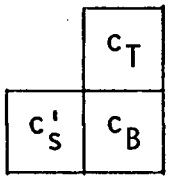

$$\left(c_B\right)_n + \rho\left(c_s'\right)_n = \left(c_B\right)_{n-1} + \rho\left(c_s\right)_{n-1}$$

and the second half cycle

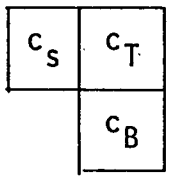

$$\left(c_T\right) + \rho\left(c_S\right)_n = \left(c_T\right)_{n-1} + \rho\left(c_S'\right)_n$$

Substitute equilibrium relations

$$\left(c_S'\right)_n = K_2\left(c_B\right)_n$$

and

$$\left(c_S\right)_n = K_1\left(c_T\right)_n$$

and let

$$\lambda = 1 + \rho K_2 \qquad \text{and} \qquad \kappa = 1 + \rho K_1$$

and use

$$\left(c_S\right)_{n-1} = K_1\left(c_T\right)_{n-1}$$

One has to solve the system of difference equations

$$\left.\begin{aligned}\left(c_B\right)_n &= \frac{\left(c_B\right)_{n-1} + \left(\kappa - 1\right)\left(c_T\right)_{n-1}}{\lambda} \\ \left(c_T\right)_n &= \frac{\left(c_T\right)_{n-1} + \left(\lambda - 1\right)\left(c_B\right)_n}{\kappa}\end{aligned}\right\} \text{ for } n \geq 1$$

subject to the initial conditions

$$\left(c_B\right)_0 = \left(c_T\right)_0 = c_0$$

E.g.

$n = 1$

$$\left(c_B\right)_1 = c_0$$

$$\left(c_T\right)_1 = \frac{c_0 + (\lambda - 1)c_0}{\kappa} = c_0 \frac{\lambda}{\kappa}$$

$n = 2$

$$\left(c_B\right)_2 = c_0 \frac{1 + (\kappa - 1)\frac{\lambda}{\kappa}}{\lambda} = c_0\left(1 + \frac{1}{\lambda} - \frac{1}{\kappa}\right)$$

$$\left(c_T\right)_2 = c_0 \frac{\lambda / + \left(\lambda - 1\right)\left(1 + \frac{1}{\lambda} - \frac{1}{\kappa}\right)}{\kappa} = c_0\left[\frac{\lambda}{\kappa} - \frac{1}{\kappa}\left(\frac{1}{\lambda} - \frac{1}{\kappa}\right)\right]$$

$n = 3$

$$\left(c_B\right)_3 = \frac{c_0}{\lambda}\left[1 + \frac{1}{\lambda} - \frac{1}{\kappa} + (\kappa - 1)\,\frac{\lambda}{\kappa} - \frac{\kappa-1}{\kappa}\left(\frac{1}{\lambda} - \frac{1}{\kappa}\right)\right]$$

$$= c_0\left[1 + \left(\frac{1}{\lambda} - \frac{1}{\kappa}\right)\left(1 + \frac{1}{\kappa\lambda}\right)\right]$$

$$\left(c_T\right)_3 = \frac{c_0}{\kappa}\left[\frac{\lambda}{\kappa} - \frac{1}{\kappa}\left(\frac{1}{\lambda} - \frac{1}{\kappa}\right) + (\lambda - 1) + (\lambda - 1)\left(\frac{1}{\lambda} - \frac{1}{\kappa}\right)\left(1 + \frac{1}{\kappa\lambda}\right)\right]$$

$$= c_0\left[\frac{\lambda}{\kappa} - \frac{1}{\kappa}\left(\frac{1}{\lambda} - \frac{1}{\kappa}\right)\left(1 + \frac{1}{\kappa\lambda}\right)\right]$$

The form of the equation is now obvious, so that in general

$$\frac{\left(c_B\right)_n}{c_0} = 1 + \left(\frac{1}{\lambda} - \frac{1}{\kappa}\right) \sum_{\ell=0}^{n-2} \left(\frac{1}{\kappa\lambda}\right)^{\ell} = 1 + \left(\frac{1}{\lambda} - \frac{1}{\kappa}\right) \frac{1 - \left(\frac{1}{\kappa\lambda}\right)^{n-1}}{1 - \frac{1}{\kappa\lambda}}$$

or

$$\left\| \begin{array}{l} \dfrac{\left(c_B\right)_n}{c_0} = 1 + \dfrac{\kappa-\lambda}{\kappa\lambda - 1}\left[1 - \dfrac{1}{(\kappa\lambda)^{n-1}}\right] \\ \\ \dfrac{\left(c_T\right)_n}{c_0} \quad \dfrac{\lambda}{\kappa} - \dfrac{1}{\kappa} \cdot \dfrac{\kappa-\lambda}{\kappa\lambda - 1}\left[1 - \dfrac{1}{(\kappa\lambda)^{n-1}}\right] \end{array} \right.$$

CASE B:

Initial equilibrium constant K_1. First displacement up.

By analogy with case A, the mass balances lead to the system of difference equations

$$\left.\begin{aligned}\left(c_T\right)_n^* &= \frac{\left(c_T\right)_{n-1}^* + (\lambda - 1)\left(c_B\right)_{n-1}^*}{\kappa} \\ \left(c_B\right)_n^* &= \frac{\left(c_B\right)_{n-1}^* + (\kappa - 1)\left(c_T\right)_n^*}{\lambda}\end{aligned}\right\} \text{ for } n \geq 1$$

Subject to the initial conditions

$$\left(c_B\right)_0^* = \left(c_T\right)_0^* = c_0$$

The solution is

$$\left\| \begin{aligned}\frac{\left(c_T\right)_n^*}{c_0} &= 1 - \frac{\kappa - \lambda}{\lambda - 1}\left[1 - \frac{1}{(\kappa\lambda)^{n-1}}\right] \\ \frac{\left(c_B\right)_n^*}{c_0} &= \frac{\kappa}{\lambda} + \frac{1}{\lambda} \cdot \frac{\kappa - \lambda}{\kappa\lambda - 1}\left[1 - \frac{1}{(\kappa\lambda)^{n-1}}\right]\end{aligned}\right.$$

APPENDIX C

COMPUTER PROGRAMS

APPENDIX C.1

EVALUATION OF EDI EXPERIMENTS

The raw data from the recorder chart was processed on a digital computer. The flow chart of the corresponding computer program is shown in Figure C.1. The printout columns involve the following calculations.

1 : Cycle number (ncyc) is part of the input data

2 : Real time (t) in seconds

$$t = 2 * \left(\tau + \frac{V_0}{Q}\right) = \quad \cdot \text{ncyc} \qquad \text{(C-1-1)}$$

3 & 4 : Average bottom (c_B) and top (c_T) reservoir concentrations in parts per million NaCl in H_2O converted from [mV] reading using calibration data for conductivity cell.

5 & 6 : Concentrations (x_B and x_T) normalized w.r.t. the initial concentrations.

7 : Separation factor (ns) as ratio of average bottom and top product concentrations

8 & 9 : Average current consumptions during enriching (I_1) and dialyzing (I_2) half cycle in amperes. Converted from [mV] reading using resistance calibration data.

10 & 11 : Current efficiencies of dialyzing (E_1) and enriching (E_2) half cycle in per cent according to the usual definition (see e.g. Wilson, 1960).

$$E = \frac{\text{actual concentration change}}{\text{theoretical concentration change}} * 100 \qquad \text{(C-1-2)}$$

The theoretical concentration change is calculated assuming perfect membranes and neglecting water transfer as well as the volume changes due to the salt transfer.

Consider a flow channel of volume V_a/n, where V_a is the active void volume of the stack and n is the number of spacer screens. The theoretical concentration change, in [ppm], of the solution in this channel is given by

$$\Delta c'_{theor.} = \frac{I \cdot t \cdot 10^6 \cdot M}{zF \cdot V_a/n} \qquad \text{(C-1-3)}$$

where

I	mean current	[A]
t	duration the current is passed	[sec]
z	valence	[g-equiv./g-mole]
F	Faraday's constant = 96,500	[A sec/g-equiv.]
M	molecular weight of solute = 58.45	[g/g-mole]

It is assumed that the displaced volume ($\delta \cdot v_0$) of concentration $c_0 + c$ is mixed with the dead volume in the reservoir which receives the efflux.

The theoretical concentration change is therefore for the enriching half cycle

$$\Delta c_{theor,1} = \frac{I_1 \cdot t_1 \cdot n}{zF} \cdot \frac{\delta \cdot V_0/V_a \cdot 10^6 \cdot M}{\delta \cdot V_0 + V_B} ,$$

for the dialyzing half cycle

$$\Delta c_{theor,2} = \frac{I_2 \cdot t_2 \cdot n}{zF} \cdot \frac{\delta \cdot V_0/V_a \cdot 10^6 \cdot M}{\delta \cdot V_0 + V_T}$$

Finally for the coulombic efficiencies in [%]

$$\left.\begin{aligned} E_1 &= \frac{c_{B,ncyc} - c_{B,ncyc-1}}{I_1 \cdot t_1 \cdot n} \cdot \frac{\delta V_0 + V_B}{\delta V_0/V_a} \cdot 0.165 \\ E_2 &= \frac{c_{T,ncyc-1} - c_{T,ncyc}}{I_2 \cdot t_2 \cdot n} \cdot \frac{\delta V_0 + V_T}{\delta V_0/V_a} \cdot 0.165 \end{aligned}\right\} \quad (C\text{-}1\text{-}4)$$

Equations (C-1-4) are reasonably accurate for dilute solutions provided water transfer is negligible.

12 : Power efficiency E_p in per cent is defined as

$$E_p = \frac{\text{theoretical minimum, reversible work of separation}}{\text{actual work performed}} * 100$$

For ideal dilute solutions the numerator is given as the reversible work of mixing per g-mole of solution

$$\left(-\Delta w_{rev}\right) = R\Theta\left[\sum_{i=1}^{n} \textcircled{2} y_i \ell n y_i - \sum_{i=1}^{n} \textcircled{1} y_i \ell n y_i\right]$$

where ① and ② refer to the state before and after mixing, and the

y_i are the mole fractions of the the components j in the state ① or ②

R universal gas constant =

$$8.317\left[\frac{\text{Wsec}}{^\circ\text{K} \quad \text{g-mole}}\right]$$

Θ absolute temperature = 298 [°K]

The actual work performed is

$$\left(\Delta w_{act}\right) = \Delta\phi \cdot \frac{T}{2} \sum_{k=1}^{ncyc} \left(i_{1,k} + i_{2,k}\right)$$

where $i_{1,k}$ = average current during k^{th} enriching half cycle

$i_{2,k}$ = average current during k^{th} dialyzing half cycle

The reversible work has to be calculated for each reservoir separately, multiplied by the number of moles in the reservoir, and the dialyzing work subtracted from the enriching work.

Thus

$$E_p = \frac{\left[\left(-\Delta w_{rev}\right)_{enr.} \cdot \left(\delta V_0 + V_B\right) - \left(-\Delta w_{rev}\right)_{dial.} \cdot \left(\delta V_0 + V_T\right)\right]}{\Delta\phi \cdot \frac{T}{2} \sum_{k=1}^{ncyc} \left(I_{1,k} + I_{2,k}\right)} \cdot 13770.0 \ [\%]$$

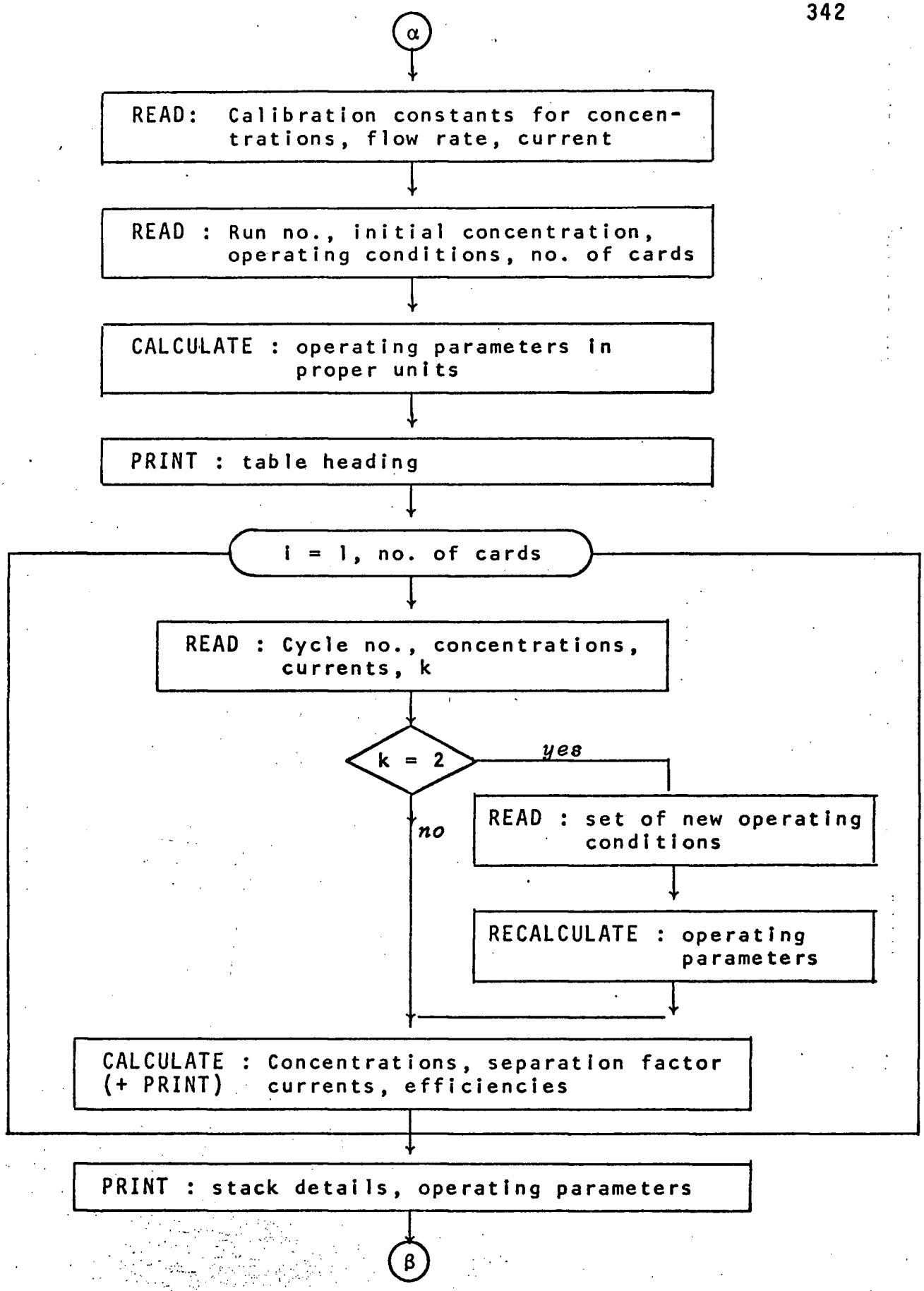

Figure C.1.: Flow chart of evaluation program for EDI runs.

```
C
C PROGRAM TO EVALUATE FIRST ED CELL EXPERIMENTS
C
      READ (5,1) NS,NC,VOL,VA
1     FORMAT (2I3,2F6.4)
      READ (5,2) AC,A1,B1,A2,B2
2     FORMAT (5F10.2)
      READ (5,3) NC,NCARD,SPE,DISP,PHI,DVB,DVT,DTF,DTS,CBV,CTV
3     FORMAT (2I3,F4.1,8F6.4)
      IF (SPE.GT.40.0) GO TO 4
      A3=0.689
      B3=0.686
      GO TO 5
4     A3=0.791
      B3=-3.43
5     V=(A3*SPE+B3)*24.1/VA
      CBO=CBV*(A1*CBV+B1)
      CTO=CTV*(A2*CTV+B2)
      YO=(CBO+CTO)/6494444.4
      X1M=YO*ALOG(YO)
      VO=2.288*DISP
      VB=2.288*DVB
      VT=2.288*DVT
      HT1=DTS+VO/V*24.1/VA
      HT2=DTF+VO/V*24.1/VA
      T=HT1+HT2
      HE1=0.165*(VO+VB)/VO*VA/NC/HT1
      HE2= 0.165*(VO+VT)/VO*VA/NC/HT2
      HEP=27540.00/PHI/T
C
C SUMMATION CONTROL VARIABLES
C
      L=0
      Z1=1.0
      Z2=100.0
      CU=0.0
      CB1=CBO
      CT1=CTO
      TIME=0.0
C
C PRINT TABLE HEAD
C
      WRITE (6,6)  (I,I=1,12)
6     FORMAT (1H1, '-----------------------------------------------------
     1-----------------------------------------------------------'/
     2I4,I7,I8,I7,I8,I7,I9,I8,I7,I8,I7,I8//
     3'CYCLE   REAL   CONCENTRATION  CONCENTRATION SEPARATION   CURRENT
     4      CURRENT      POWER'/
     5'  NO.    TIME   BOTTOM   TOP     NORMALIZED    FACTOR    ENR. DIA
     6L.    EFFICIENCY  EFFICIENCY'//
     7'NCYC     T        CB      CT       XB      XT        NS      I1      I2
     8      E1     E2       EP '/'  (-)    (SEC)   (PPM)  (PPM)     (-)     (
     9-)      (-)      (A)     (A)       (%)    (%)      (%)'/)
      WRITE (6,7)
7     FORMAT(' ---------------------------------------------------------
     1-+-----------------------------------------------------'/)
C
C PRINT INITIAL CONDITIONS
C
      WRITE (6,8) L,CU,CBO,CTO,Z1,Z1,Z1,CU,CU,Z2,Z2,Z2
8     FORMAT (I4,F9.1,F8.0,F7.0,F8.2,F7.3,F9.2,F8.3,F7.3,F8.1,F6.1,F9.3)
```

```
      C
      C READ CYCLE CONDITIONS
      C
            DO 100 I=1,NCARD
            READ (5,9) NCYC,CBV,CTV,CURF,CURS,K
    9       FORMAT (I3,4F10.1,I3)
            IF (K.EQ.1) GO TO 20
            WRITE (6,10)
   10       FORMAT (' ')
            IF (K.EQ.0) GO TO 20
            WRITE (6,7)
            READ (5,11) SPE1,PHI1,DTF1,DTS1
   11       FORMAT (4F6.2)
            IF (SPE1.GT.40.0) GO TO 12
            A3=0.689
            B3=0.686
            GO TO 13
   12       A3=0.791
            B3=-3.43
   13       V1=(A3*SPE1+B3)*24.1/VA
            HE1=HE1*HT1
            HE2=HE2*HT2
            HEP=HEP*T
            HT1=DTS1+VO/V1*24.1/VA
            HT2=DTF1+VG/V1*24.1/VA
            T=HT1+HT2
            HE1=HE1/HT1
            HE2=HE2/HT2
            HEP=HEP/T
   20       TIME=TIME+(NCYC-L)*T
            CB=CBV*(A1*CBV+B1)
            CT=CTV*(A2*CTV+B2)
            XB=CB/CBO
            XT=CT/CTO
            SEP=XB/XT
            CU1=AC*CURS
            IF (AC.LT.1.0) CU1=CU1/HT1
            CU2=AC*CURF
            IF (AC.LT.1.0) CU2=CU2/HT2
            ECU1=(CB-CB1)/CU1*HE1/(NCYC-L)
            ECU2=(CT1-CT)/CU2*HE2/(NCYC-L)
            CU=CU+(CU1+CU2)*(NCYC-L)
            Y1=CB/3247222.2
            Y2=CT/3247222.2
            EP=((VO+VB)*(X1M-Y1*ALOG(Y1))+(VO+VT)*(Y2*ALOG(Y2)-X1M))/CU*HEP
            CB1=CB
            CT1=CT
            L=NCYC
            WRITE (6,8) NCYC,TIME,CB,CT,XB,XT,SEP,CU1,CU2,ECU1,ECU2,EP
   100      CONTINUE
            WRITE (6,10)
            WRITE (6,7)
            READ (5,105) NT
    105     FORMAT (I2)
            WRITE (6,110) NT,NS,NC,NO
    110     FORMAT (//'      TABLE  C.1.',I2,'  : NUMERICAL EVALUATION OF EXPER
           1IMENT'/22X,'ECI-S',I1,'-',I2,'/#',I2//)
            WRITE (6,120) L
   120      FORMAT (1H1,I3)
            STOP
            END
END OF FILE
```

1	2	3	4	5	6	7	8	9	10	11	12
CYCLE NO.	REAL TIME	CONCENTRATION BOTTOM	TOP	CONCENTRATION NORMALIZED		SEPARATION FACTOR	CURRENT ENR.	DIAL.	CURRENT EFFICIENCY		POWER EFFICIENCY
NCYC (-)	T (SEC)	CB (PPM)	CT (PPM)	XB (-)	XT (-)	NS (-)	I1 (A)	I2 (A)	E1 (%)	E2 (%)	EP (%)
0	0.0	1032.	1013.	1.00	1.000	1.00	0.0	0.0	100.0	100.0	100.000
1	55.5	1278.	774.	1.24	0.764	1.62	1.160	1.120	32.5	32.7	2.321
2	111.1	1416.	671.	1.37	0.662	2.07	1.180	1.200	18.0	13.2	1.678
3	166.6	1497.	622.	1.45	0.614	2.36	1.200	1.180	10.3	6.4	1.303
4	222.2	1542.	593.	1.49	0.586	2.55	1.200	1.160	5.7	3.8	1.057
5	277.7	1570.	583.	1.52	0.576	2.64	1.200	1.120	3.6	1.4	0.881
6	333.2	1584.	570.	1.53	0.563	2.73	1.200	1.100	1.8	1.8	0.757
7	388.8	1589.	568.	1.54	0.561	2.75	1.200	1.100	0.7	0.4	0.655

TABLE C.1. 1 : NUMERICAL EVALUATION OF EXPERIMENT EDI-S2-15/#18

1	2	3	4	5	6	7	8	9	10	11	12
CYCLE NO.	REAL TIME	CONCENTRATION BOTTOM	TOP	CONCENTRATION NORMALIZED		SEPARATION FACTOR	CURRENT ENR.	DIAL.	CURRENT EFFICIENCY		POWER EFFICIENCY
NCYC (-)	T (SEC)	CB (PPM)	CT (PPM)	XB (-)	XT (-)	NS (-)	I1 (A)	I2 (A)	E1 (%)	E2 (%)	EP (%)
0	0.0	1013.	1019.	1.00	1.000	1.00	0.0	0.0	100.0	100.0	100.000
1	27.8	1122.	929.	1.11	0.911	1.21	1.440	1.300	23.1	21.3	0.739
2	55.5	1212.	851.	1.20	0.835	1.43	1.400	1.400	19.8	16.9	0.682
3	83.3	1303.	787.	1.29	0.772	1.67	1.400	1.400	19.9	14.1	0.648
4	111.1	1377.	735.	1.36	0.722	1.88	1.400	1.390	16.3	11.4	0.604
5	138.9	1447.	697.	1.43	0.684	2.09	1.400	1.380	15.2	8.6	0.564
6	166.6	1500.	664.	1.48	0.652	2.27	1.400	1.360	11.6	7.3	0.523
7	194.4	1564.	639.	1.54	0.627	2.46	1.400	1.360	14.1	5.8	0.497
8	222.2	1584.	626.	1.56	0.614	2.55	1.400	1.360	4.3	2.9	0.450
9	249.9	1626.	606.	1.60	0.595	2.70	1.400	1.360	9.2	4.4	0.426
10	277.7	1654.	587.	1.63	0.576	2.83	1.400	1.360	6.2	4.4	0.401
11	305.5	1679.	570.	1.66	0.559	2.96	1.400	1.360	5.6	3.8	0.379
12	333.2	1702.	559.	1.68	0.548	3.06	1.400	1.360	4.9	2.6	0.358
13	361.0	1722.	548.	1.70	0.538	3.16	1.400	1.360	4.3	2.3	0.339
14	388.8	1739.	539.	1.72	0.529	3.24	1.400	1.360	3.7	2.0	0.322

TABLE C.1. 2 : NUMERICAL EVALUATION OF EXPERIMENT EDI-S2-15/#19

1	2	3	4	5	6	7	8	9	10	11	12
CYCLE NO.	REAL TIME	CONCENTRATION BOTTOM	TOP	CONCENTRATION NORMALIZED		SEPARATION FACTOR	CURRENT ENR.	DIAL.	CURRENT EFFICIENCY		POWER EFFICIENCY
NCYC (-)	T (SEC)	CB (PPM)	CT (PPM)	XB (-)	XT (-)	NS (-)	I1 (A)	I2 (A)	E1 (%)	E2 (%)	EP (%)
0	0.0	1038.	1042.	1.00	1.000	1.00	0.0	0.0	100.0	100.0	100.000
1	27.8	1100.	942.	1.06	0.903	1.17	1.380	1.220	27.8	25.3	0.880
2	55.5	1155.	876.	1.11	0.840	1.32	1.320	1.400	25.3	14.4	0.774
4	111.1	1261.	738.	1.22	0.708	1.72	1.320	1.360	24.8	15.6	0.731
6	166.6	1347.	658.	1.30	0.631	2.06	1.320	1.320	19.9	9.3	0.653
8	222.2	1416.	599.	1.36	0.574	2.38	1.320	1.300	16.1	7.0	0.588
10	277.7	1475.	555.	1.42	0.532	2.67	1.300	1.280	13.8	5.3	0.536
12	333.2	1517.	521.	1.46	0.500	2.92	1.280	1.260	10.0	4.1	0.488
14	388.8	1547.	494.	1.49	0.474	3.15	1.280	1.260	7.4	3.3	0.446
15	416.6	1558.	482.	1.50	0.463	3.24	1.280	1.260	5.4	2.8	0.426

TABLE C.1. 3 : NUMERICAL EVALUATION OF EXPERIMENT EDI-S2-15/#20

1	2	3	4	5	6	7	8	9	10	11	12
CYCLE NO.	REAL TIME	CONCENTRATION BOTTOM	TOP	CONCENTRATION NORMALIZED		SEPARATION FACTOR	CURRENT ENR.	DIAL.	CURRENT EFFICIENCY		POWER EFFICIENCY
NCYC (-)	T (SEC)	CB (PPM)	CT (PPM)	XB (-)	XT (-)	NS (-)	I1 (A)	I2 (A)	E1 (%)	E2 (%)	EP (%)
0	0.0	978.	980.	1.00	1.000	1.00	0.0	0.0	100.0	100.0	100.000
2	55.5	1059.	890.	1.08	0.908	1.19	1.360	1.360	27.5	30.5	0.985
4	111.1	1133.	839.	1.16	0.855	1.35	1.340	1.340	25.2	17.7	0.862
6	166.6	1196.	780.	1.22	0.796	1.54	1.320	1.320	21.9	20.2	0.817
8	222.2	1250.	739.	1.28	0.754	1.70	1.320	1.320	19.1	14.4	0.757
10	277.7	1306.	699.	1.33	0.713	1.87	1.320	1.320	19.2	13.9	0.720
12	333.2	1350.	675.	1.38	0.688	2.01	1.320	1.320	15.4	8.5	0.668
14	388.8	1388.	645.	1.42	0.658	2.16	1.320	1.320	13.5	10.3	0.631
16	444.3	1425.	619.	1.46	0.632	2.31	1.320	1.320	12.6	9.0	0.599
18	499.9	1458.	596.	1.49	0.608	2.45	1.320	1.320	11.6	8.1	0.570
20	555.4	1486.	575.	1.52	0.587	2.59	1.320	1.320	9.7	7.2	0.542
22	610.9	1511.	557.	1.54	0.568	2.72	1.320	1.320	8.8	6.3	0.516

TABLE C.1. 4 : NUMERICAL EVALUATION OF EXPERIMENT EDI-S2-15/#21

1	2	3	4	5	6	7	8	9	10	11	12
CYCLE NO.	REAL TIME	CONCENTRATION BOTTOM	TOP	CONCENTRATION NORMALIZED		SEPARATION FACTOR	CURRENT ENR.	DIAL.	CURRENT EFFICIENCY		POWER EFFICIENCY
NCYC (-)	T (SEC)	CB (PPM)	CT (PPM)	XB (-)	XT (-)	NS (-)	I1 (A)	I2 (A)	E1 (%)	E2 (%)	EP (%)
0	0.0	1029.	1038.	1.00	1.000	1.00	0.0	0.0	100.0	100.0	100.000
1	50.2	1237.	805.	1.20	0.775	1.55	1.120	1.000	31.4	39.6	2.957
2	100.4	1358.	700.	1.32	0.675	1.96	1.120	1.040	18.4	17.0	2.231
3	150.6	1416.	663.	1.38	0.639	2.15	1.100	1.000	9.0	6.3	1.713
4	200.8	1430.	613.	1.39	0.590	2.35	1.060	1.000	2.2	8.5	1.410
5	251.0	1466.	596.	1.42	0.574	2.48	1.020	0.980	6.0	2.9	1.213
6	301.3	1483.	584.	1.44	0.563	2.56	1.000	0.960	2.8	2.1	1.054
7	351.5	1489.	573.	1.45	0.552	2.62	0.960	0.960	1.0	2.1	0.931
8	401.7	1494.	569.	1.45	0.548	2.65	0.960	0.960	1.0	0.7	0.829
9	451.9	1500.	564.	1.46	0.543	2.68	0.960	0.960	1.0	0.9	0.750
10	502.1	1503.	557.	1.46	0.537	2.72	0.960	0.960	0.5	1.1	0.686

TABLE C.1. 5 : NUMERICAL EVALUATION OF EXPERIMENT EDI-S2-15/#27

1	2	3	4	5	6	7	8	9	10	11	12
CYCLE NO.	REAL TIME	CONCENTRATION BOTTOM	CONCENTRATION TOP	CONCENTRATION NORMALIZED		SEPARATION FACTOR	CURRENT ENR.	CURRENT CIAL.	CURRENT EFFICIENCY		POWER EFFICIENCY
NCYC (-)	T (SEC)	CB (PPM)	CT (PPM)	XB (-)	XT (-)	NS (-)	I1 (A)	I2 (A)	E1 (%)	E2 (%)	EP (%)
0	0.0	1019.	1028.	1.00	1.000	1.00	0.0	0.0	100.0	100.0	100.000
1	30.2	1127.	885.	1.11	0.861	1.29	1.520	1.300	20.1	31.0	2.077
2	60.4	1196.	819.	1.17	0.797	1.47	1.480	1.360	13.0	13.6	1.608
3	90.6	1248.	765.	1.22	0.744	1.65	1.440	1.320	10.2	11.6	1.387
4	120.8	1272.	739.	1.25	0.719	1.74	1.440	1.320	4.8	5.5	1.154
5	151.0	1339.	684.	1.31	0.665	1.98	1.240	1.140	22.5	10.3	1.169
6	181.3	1372.	655.	1.35	0.637	2.11	1.240	1.160	11.3	5.2	1.087
7	211.5	1397.	632.	1.37	0.615	2.23	1.200	1.120	8.8	4.4	1.013
8	246.7	1441.	593.	1.41	0.577	2.45	1.080	1.000	17.3	6.6	0.866
9	281.9	1464.	571.	1.44	0.556	2.58	1.040	1.000	9.0	3.7	0.828
10	317.1	1477.	560.	1.45	0.545	2.66	1.020	1.000	5.8	2.0	0.781
11	352.3	1480.	555.	1.45	0.540	2.69	1.000	0.960	1.2	0.9	0.730
12	377.5	1419.	600.	1.39	0.583	2.39	1.280	1.200	-20.2	-10.6	0.825
13	402.7	1377.	618.	1.35	0.601	2.25	1.320	1.160	-13.3	-4.4	0.705
14	427.9	1344.	642.	1.32	0.625	2.11	1.400	1.240	-10.0	-5.6	0.601
15	453.1	1330.	654.	1.31	0.636	2.05	1.360	1.260	-4.3	-2.6	0.538
16	478.3	1317.	655.	1.29	0.637	2.03	1.320	1.280	-4.4	-0.3	0.491
17	503.6	1314.	660.	1.29	0.642	2.01	1.320	1.280	-0.9	-1.1	0.455
18	528.8	1303.	662.	1.28	0.644	1.99	1.320	1.280	-3.5	-0.3	0.420

TABLE C.1. 6 : NUMERICAL EVALUATION OF EXPERIMENT EDI-S2-15/#28

1	2	3	4	5	6	7	8	9	10	11	12
CYCLE NO.	REAL TIME	CONCENTRATION BOTTOM	CONCENTRATION TOP	CONCENTRATION NORMALIZED		SEPARATION FACTOR	CURRENT ENR.	CURRENT CIAL.	CURRENT EFFICIENCY		POWER EFFICIENCY
NCYC (-)	T (SEC)	CB (PPM)	CT (PPM)	XB (-)	XT (-)	NS (-)	I1 (A)	I2 (A)	E1 (%)	E2 (%)	EP (%)
0	0.0	1100.	1096.	1.00	1.000	1.00	0.0	0.0	100.0	100.0	100.000
1	50.2	1347.	851.	1.22	0.776	1.58	1.000	0.900	37.8	41.7	3.748
2	100.4	1480.	722.	1.35	0.659	2.04	0.960	0.920	21.3	21.5	2.885
3	150.6	1544.	639.	1.40	0.582	2.41	0.920	0.900	10.7	14.3	2.334
4	200.8	1587.	600.	1.44	0.547	2.64	0.880	0.880	7.3	6.7	1.936
5	251.0	1603.	574.	1.46	0.524	2.78	0.860	0.860	3.0	4.6	1.639
6	301.3	1617.	555.	1.47	0.506	2.91	0.840	0.840	2.6	3.5	1.429
7	351.5	1620.	548.	1.47	0.500	2.95	0.840	0.830	0.5	1.2	1.248
8	401.7	1617.	542.	1.47	0.494	2.98	0.840	0.830	-0.5	1.2	1.105
9	451.9	1617.	535.	1.47	0.488	3.01	0.840	0.830	0.0	1.2	0.994
10	502.1	1615.	530.	1.47	0.484	3.04	0.840	0.830	-0.5	1.0	0.902

TABLE C.1. 7 : NUMERICAL EVALUATION OF EXPERIMENT EDI-S2-16/# 1

1	2	3	4	5	6	7	8	9	10	11	12
CYCLE NO.	REAL TIME	CONCENTRATION BOTTOM	TOP	CONCENTRATION NORMALIZED		SEPARATION FACTOR	CURRENT ENR.	DIAL.	CURRENT EFFICIENCY		POWER EFFICIENCY
NCYC (-)	T (SEC)	CB (PPM)	CT (PPM)	XB (-)	XT (-)	NS (-)	I1 (A)	I2 (A)	E1 (%)	E2 (%)	EP (%)
0	0.0	1067.	1067.	1.00	1.000	1.00	0.0	0.0	100.0	100.0	100.000
1	83.8	1355.	784.	1.27	0.735	1.73	0.800	0.740	30.0	35.1	3.049
2	167.6	1517.	645.	1.42	0.605	2.35	0.820	0.760	18.1	16.8	2.358
3	251.3	1623.	577.	1.52	0.541	2.81	0.800	0.740	12.2	8.5	1.910
4	335.1	1643.	544.	1.54	0.510	3.02	0.780	0.720	2.3	4.1	1.525
5	418.9	1662.	526.	1.56	0.493	3.16	0.760	0.700	2.4	2.4	1.279
6	502.7	1671.	516.	1.57	0.484	3.24	0.760	0.700	1.0	1.4	1.093
7	586.4	1665.	513.	1.56	0.481	3.24	0.720	0.700	-0.7	0.3	0.945
8	670.2	1662.	510.	1.56	0.478	3.26	0.720	0.700	-0.4	0.5	0.834
9	754.0	1654.	508.	1.55	0.476	3.25	0.720	0.700	-1.1	0.2	0.742

TABLE C.1. 8 : NUMERICAL EVALUATION OF EXPERIMENT EDI-S2-16/# 2

1	2	3	4	5	6	7	8	9	10	11	12
CYCLE NO.	REAL TIME	CONCENTRATION BOTTOM	TOP	CONCENTRATION NORMALIZED		SEPARATION FACTOR	CURRENT ENR.	DIAL.	CURRENT EFFICIENCY		POWER EFFICIENCY
NCYC (-)	T (SEC)	CB (PPM)	CT (PPM)	XB (-)	XT (-)	NS (-)	I1 (A)	I2 (A)	E1 (%)	E2 (%)	EP (%)
0	0.0	1237.	1219.	1.00	1.000	1.00	0.0	0.0	100.0	100.0	100.000
1	81.6	1598.	955.	1.29	0.783	1.65	0.760	0.720	44.8	34.6	2.212
2	163.3	1867.	755.	1.51	0.619	2.44	0.750	0.700	33.8	26.9	1.930
3	244.9	2068.	619.	1.67	0.508	3.29	0.730	0.700	26.0	18.2	1.689
4	326.5	2227.	529.	1.80	0.434	4.15	0.720	0.700	20.9	12.2	1.492
5	408.2	2344.	464.	1.90	0.381	4.98	0.710	0.700	15.5	8.7	1.327
6	489.8	2418.	426.	1.96	0.349	5.60	0.700	0.700	9.9	5.2	1.177
7	571.4	2477.	393.	2.00	0.323	6.21	0.700	0.700	7.9	4.3	1.058
8	653.1	2507.	381.	2.03	0.312	6.49	0.700	0.700	4.0	1.7	0.947
9	734.7	2551.	368.	2.06	0.302	6.84	0.700	0.700	6.0	1.7	0.865
10	816.3	2566.	355.	2.07	0.291	7.13	0.700	0.700	2.0	1.7	0.790
11	898.0	2581.	348.	2.09	0.286	7.30	0.700	0.700	2.0	0.9	0.726
12	979.6	2590.	346.	2.09	0.284	7.38	0.700	0.700	1.2	0.3	0.669
13	1061.2	2599.	342.	2.10	0.280	7.49	0.700	0.700	1.2	0.5	0.622
14	1142.9	2608.	339.	2.11	0.278	7.58	0.700	0.700	1.2	0.3	0.581

TABLE C.1. 9 : NUMERICAL EVALUATION OF EXPERIMENT EDI-S2-16/# 4

1	2	3	4	5	6	7	8	9	10	11	12
CYCLE NO.	REAL TIME	CONCENTRATION BOTTOM	CONCENTRATION TOP	CONCENTRATION NORMALIZED		SEPARATION FACTOR	CURRENT ENR.	CURRENT DIAL.	CURRENT EFFICIENCY		POWER EFFICIENCY
NCYC (-)	T (SEC)	CB (PPM)	CT (PPM)	XB (-)	XT (-)	NS (-)	I1 (A)	I2 (A)	E1 (%)	E2 (%)	EP (%)
0	0.0	1264.	1249.	1.00	1.000	1.00	0.0	0.0	100.0	100.0	100.000
1	61.6	1344.	1019.	1.06	0.816	1.30	0.960	0.900	41.6	31.8	2.140
2	123.3	1408.	845.	1.11	0.677	1.65	0.950	0.920	33.5	23.6	1.851
3	184.9	1466.	710.	1.16	0.568	2.04	0.940	0.900	31.0	18.8	1.692
4	246.5	1514.	606.	1.20	0.486	2.47	0.920	0.900	25.7	14.3	1.548
5	308.2	1564.	529.	1.24	0.424	2.92	0.900	0.860	27.9	11.2	1.458
7	431.4	1626.	419.	1.29	0.336	3.83	0.820	0.800	18.8	8.6	1.275
9	554.7	1665.	361.	1.32	0.289	4.55	0.780	0.760	12.6	4.8	1.117
11	678.0	1696.	322.	1.34	0.258	5.20	0.740	0.700	10.5	3.5	1.002
13	801.2	1716.	297.	1.36	0.238	5.71	0.700	0.680	7.1	2.4	0.905
14	857.9	1730.	284.	1.37	0.227	6.02	0.500	0.480	27.5	2.5	0.964
15	914.5	1742.	270.	1.38	0.216	6.38	0.500	0.480	22.0	2.8	0.943
17	1027.8	1759.	239.	1.39	0.191	7.28	0.500	0.480	16.5	3.0	0.899
19	1141.0	1773.	228.	1.40	0.183	7.67	0.500	0.480	13.8	1.0	0.852
21	1254.3	1781.	223.	1.41	0.179	7.88	0.500	0.480	8.3	0.5	0.804
23	1347.6	1773.	243.	1.40	0.194	7.22	0.580	0.560	-7.1	-2.2	0.889
27	1534.1	1767.	252.	1.40	0.201	6.94	0.570	0.560	-2.4	-0.5	0.769
29	1627.3	1767.	259.	1.40	0.208	6.73	0.570	0.560	0.0	-0.9	0.721
30	1684.0	1776.	245.	1.40	0.196	7.16	0.490	0.440	16.9	3.0	0.589
32	1797.2	1793.	231.	1.42	0.185	7.67	0.460	0.440	18.0	1.5	0.577
36	2023.8	1798.	218.	1.42	0.175	8.15	0.450	0.440	3.1	0.7	0.537
37	2109.2	1813.	213.	1.43	0.170	8.41	0.400	0.400	18.1	0.9	0.357
39	2280.0	1827.	201.	1.45	0.161	8.97	0.400	0.400	9.1	1.0	0.351
41	2450.8	1847.	197.	1.46	0.158	9.24	0.400	0.400	12.7	0.3	0.348
43	2533.2	1824.	205.	1.44	0.164	8.78	0.480	0.450	-45.1	-1.0	0.675
45	2615.6	1818.	215.	1.44	0.173	8.34	0.460	0.440	-11.8	-1.4	0.645
47	2658.0	1815.	217.	1.44	0.174	8.27	0.450	0.440	-6.0	-0.2	0.621
51	2862.8	1815.	219.	1.44	0.176	8.18	0.450	0.440	0.0	-0.2	0.582
52	2919.4	1810.	230.	1.43	0.184	7.79	0.300	0.320	-18.5	-3.0	0.415
54	3032.7	1790.	252.	1.42	0.201	7.03	0.280	0.300	-34.6	-3.4	0.394
56	3146.0	1781.	264.	1.41	0.212	6.65	0.280	0.300	-14.8	-2.0	0.380
58	3259.2	1776.	275.	1.40	0.220	6.38	0.280	0.300	-9.9	-1.6	0.369
60	3372.5	1776.	277.	1.40	0.222	6.32	0.280	0.300	0.0	-0.4	0.362

TABLE C.1.10 : NUMERICAL EVALUATION OF EXPERIMENT
EDI-S2-16/# 5

1	2	3	4	5	6	7	8	9	10	11	12
CYCLE NO.	REAL TIME	CONCENTRATION BOTTOM	TOP	CONCENTRATION NORMALIZED		SEPARATION FACTOR	CURRENT ENR. DIAL.		CURRENT EFFICIENCY		POWER EFFICIENCY
NCYC (-)	T (SEC)	CB (PPM)	CT (PPM)	XB (-)	XT (-)	NS (-)	I1 (A)	I2 (A)	E1 (%)	E2 (%)	EP (%)
0	0.0	2435.	1225.	1.00	1.000	1.00	0.0	0.0	100.0	100.0	100.000
1	61.6	1253.	1045.	0.52	0.853	0.61	0.760	0.680	-770.3	33.2	-13.423
2	123.3	1307.	909.	0.54	0.742	0.72	0.720	0.700	31.1	24.2	-5.252
3	184.9	1347.	793.	0.55	0.647	0.85	0.720	0.680	27.5	21.3	-2.639
4	246.5	1387.	716.	0.57	0.584	0.97	0.700	0.660	28.3	14.6	-1.425
6	369.8	1448.	574.	0.59	0.468	1.27	0.600	0.600	25.4	14.8	-0.333
8	493.1	1490.	510.	0.61	0.416	1.47	0.620	0.560	17.1	7.2	0.053
10	616.3	1519.	451.	0.62	0.368	1.69	0.520	0.520	14.0	7.0	0.239
12	739.6	1535.	413.	0.63	0.337	1.87	0.500	0.500	8.0	4.8	0.305
14	862.9	1554.	390.	0.64	0.318	2.01	0.490	0.490	9.5	3.0	0.351
16	986.1	1562.	377.	0.64	0.307	2.09	0.490	0.480	4.1	1.7	0.347
17	1042.8	1575.	355.	0.65	0.289	2.23	0.380	0.400	34.1	5.2	0.422
18	1099.4	1581.	339.	0.65	0.277	2.34	0.400	0.380	13.0	3.8	0.434
20	1212.7	1599.	320.	0.66	0.261	2.52	0.400	0.370	22.7	2.5	0.468
22	1325.9	1605.	306.	0.66	0.249	2.64	0.400	0.370	6.5	1.8	0.461
23	1372.6	1605.	313.	0.66	0.256	2.58	0.420	0.420	0.0	-2.3	0.533
24	1419.2	1602.	322.	0.66	0.263	2.50	0.440	0.440	-5.9	-2.6	0.499
26	1512.4	1597.	332.	0.66	0.271	2.42	0.460	0.450	-5.6	-1.3	0.444
28	1605.7	1594.	337.	0.65	0.275	2.38	0.460	0.450	-2.8	-0.7	0.405
30	1699.0	1591.	339.	0.65	0.277	2.36	0.460	0.450	-2.8	-0.4	0.373
37	2025.4	1674.	240.	0.69	0.196	3.51	0.650	0.600	17.7	3.0	0.490
45	2478.5	1741.	174.	0.71	0.142	5.03	0.560	0.500	14.5	1.6	0.436
51	2758.3	1720.	217.	0.71	0.177	3.99	0.600	0.540	-5.8	-1.6	0.418

TABLE C.1.11 : NUMERICAL EVALUATION OF EXPERIMENT EDI-S2-16/# 6

1	2	3	4	5	6	7	8	9	10	11	12
CYCLE NO.	REAL TIME	CONCENTRATION BOTTOM	TOP	CONCENTRATION NORMALIZED		SEPARATION FACTOR	CURRENT ENR. DIAL.		CURRENT EFFICIENCY		POWER EFFICIENCY
NCYC (-)	T (SEC)	CB (PPM)	CT (PPM)	XB (-)	XT (-)	NS (-)	I1 (A)	I2 (A)	E1 (%)	E2 (%)	EP (%)
0	0.0	1242.	1251.	1.00	1.000	1.00	0.0	0.0	100.0	100.0	100.000
1	31.6	1252.	1148.	1.01	0.918	1.10	1.520	1.380	6.7	18.2	0.441
2	63.3	1263.	1099.	1.02	0.878	1.16	1.520	1.480	6.7	8.1	0.381
3	94.9	1273.	1060.	1.03	0.847	1.21	1.560	1.520	6.6	6.2	0.346
4	126.5	1278.	1027.	1.03	0.821	1.25	1.580	1.500	3.2	5.4	0.306
8	253.1	1305.	933.	1.05	0.745	1.41	1.540	1.500	4.2	3.8	0.240
12	379.6	1326.	873.	1.07	0.698	1.53	1.520	1.500	3.4	2.4	0.203
16	506.1	1337.	832.	1.08	0.665	1.62	1.500	1.500	1.7	1.7	0.171
20	632.7	1342.	804.	1.08	0.642	1.68	1.500	1.500	0.9	1.2	0.146
24	759.2	1352.	784.	1.09	0.627	1.74	1.500	1.500	1.7	0.8	0.131
28	885.7	1358.	770.	1.09	0.615	1.78	1.500	1.500	0.9	0.6	0.117
32	1012.2	1358.	761.	1.09	0.608	1.80	1.500	1.500	0.0	0.4	0.103
36	1138.8	1358.	753.	1.09	0.602	1.82	1.500	1.500	0.0	0.3	0.093
40	1265.3	1358.	743.	1.09	0.594	1.84	1.500	1.500	0.0	0.4	0.084
47	1486.7	1363.	731.	1.10	0.589	1.88	1.500	1.500	0.5	0.3	0.074

TABLE C.1.12 : NUMERICAL EVALUATION OF EXPERIMENT EDI-S2-16/# 7

1	2	3	4	5	6	7	8	9	10	11	12
CYCLE NO.	REAL TIME	CONCENTRATION BOTTOM	CONCENTRATION TOP	CONCENTRATION NORMALIZED		SEPARATION FACTOR	CURRENT ENR.	CURRENT CTAL.	CURRENT EFFICIENCY		POWER EFFICIENCY
NCYC (-)	T (SEC)	CB (PPM)	CT (PPM)	XB (-)	XT (-)	NS (-)	I1 (A)	I2 (A)	E1 (%)	E2 (%)	EP (%)
0	0.0	1226.	1238.	1.00	1.000	1.00	0.0	0.0	100.0	100.0	100.000
1	31.6	1247.	1142.	1.02	0.922	1.10	1.320	1.280	3.9	18.4	0.535
2	63.3	1263.	1104.	1.03	0.892	1.16	1.340	1.340	2.9	6.8	0.398
3	94.9	1278.	1076.	1.04	0.869	1.20	1.360	1.350	2.8	5.1	0.336
4	126.5	1294.	1050.	1.06	0.848	1.25	1.380	1.360	2.8	4.6	0.302
5	158.2	1305.	1031.	1.06	0.832	1.28	1.390	1.370	1.8	3.4	0.270
10	316.3	1347.	965.	1.10	0.779	1.41	1.420	1.400	1.4	2.3	0.184
15	474.5	1360.	931.	1.11	0.752	1.48	1.420	1.400	0.5	1.2	0.137
20	632.7	1366.	909.	1.11	0.734	1.52	1.420	1.400	0.2	0.8	0.109
25	790.8	1368.	897.	1.12	0.724	1.54	1.420	1.400	0.1	0.4	0.090
30	949.0	1344.	884.	1.10	0.714	1.54	1.420	1.400	-0.8	0.4	0.073
32	1012.2	1405.	862.	1.15	0.696	1.65	1.620	1.580	4.6	1.7	0.080
35	1107.1	1440.	835.	1.17	0.674	1.74	1.640	1.600	1.7	1.4	0.081
40	1265.3	1472.	806.	1.20	0.651	1.84	1.640	1.600	0.9	0.9	0.076
45	1423.5	1485.	791.	1.21	0.639	1.90	1.640	1.600	0.4	0.5	0.070
50	1581.6	1496.	780.	1.22	0.630	1.94	1.640	1.600	0.3	0.3	0.064
52	1702.4	1645.	686.	1.34	0.554	2.42	1.080	1.160	8.8	5.2	0.044
56	1944.0	1795.	581.	1.46	0.469	3.12	1.000	1.130	4.8	3.0	0.052
60	2185.6	1910.	537.	1.56	0.433	3.60	0.960	1.100	3.8	1.3	0.056
65	2487.7	1962.	519.	1.60	0.419	3.82	0.960	1.100	1.4	0.4	0.056
67	2550.9	1822.	581.	1.49	0.469	3.17	1.600	1.520	-10.6	-5.0	0.089
70	2645.8	1696.	658.	1.38	0.531	2.60	1.620	1.560	-6.3	-4.0	0.071
75	2804.0	1594.	722.	1.30	0.583	2.23	1.620	1.560	-3.0	-2.0	0.055
80	2962.1	1546.	742.	1.26	0.599	2.11	1.620	1.560	-1.4	-0.6	0.047

TABLE C.1.13 : NUMERICAL EVALUATION OF EXPERIMENT EC1-S2-16/8 B

1	2	3	4	5	6	7	8	9	10	11	12
CYCLE NO.	REAL TIME	CONCENTRATION BOTTOM	TOP	CONCENTRATION NORMALIZED		SEPARATION FACTOR	CURRENT ENR.	CIAL.	CURRENT EFFICIENCY		POWER EFFICIENCY
NCYC (-)	T (SEC)	CB (PPM)	CT (PPM)	XB (-)	XT (-)	NS (-)	I1 (A)	I2 (A)	E1 (%)	E2 (%)	EP (%)
0	0.0	1184.	1200.	1.00	1.000	1.00	0.0	0.0	100.0	100.0	100.000
1	51.9	1202.	993.	1.10	0.828	1.33	1.080	1.160	16.3	26.4	1.470
2	103.8	1381.	903.	1.17	0.753	1.55	1.160	1.240	10.1	10.8	1.101
3	155.6	1442.	845.	1.22	0.704	1.73	1.180	1.260	7.7	6.8	0.901
4	207.5	1488.	806.	1.26	0.672	1.87	1.200	1.280	5.6	4.5	0.761
5	259.4	1517.	777.	1.28	0.647	1.98	1.200	1.280	3.6	3.4	0.657
6	311.3	1535.	755.	1.30	0.629	2.06	1.200	1.280	2.3	2.5	0.575
7	363.1	1546.	742.	1.31	0.618	2.11	1.240	1.280	1.3	1.5	0.505
8	415.0	1551.	733.	1.31	0.611	2.15	1.240	1.280	0.6	1.0	0.448
9	466.9	1551.	725.	1.31	0.604	2.17	1.240	1.280	0.0	0.9	0.401
10	518.8	1554.	720.	1.31	0.600	2.19	1.240	1.280	0.3	0.6	0.363
11	570.7	1554.	715.	1.31	0.596	2.20	1.240	1.280	0.0	0.6	0.331
12	622.5	1551.	711.	1.31	0.592	2.21	1.240	1.280	-0.3	0.4	0.304
13	674.4	1546.	707.	1.31	0.589	2.22	1.240	1.280	-0.6	0.4	0.280
14	773.5	1634.	636.	1.38	0.530	2.60	0.760	0.900	9.0	6.1	0.166
15	872.5	1688.	593.	1.43	0.495	2.88	0.780	0.900	5.3	3.7	0.173
16	971.6	1714.	568.	1.45	0.473	3.06	0.800	0.880	2.6	2.3	0.173
17	1070.6	1741.	553.	1.47	0.461	3.19	0.800	0.880	2.6	1.3	0.172
18	1169.7	1752.	542.	1.48	0.452	3.28	0.800	0.880	1.0	1.0	0.168
19	1268.8	1754.	537.	1.48	0.447	3.31	0.800	0.880	0.3	0.5	0.162
20	1320.6	1674.	587.	1.41	0.489	2.89	1.160	1.200	-10.3	-6.2	0.262
21	1372.5	1621.	626.	1.37	0.522	2.63	1.180	1.220	-6.7	-4.7	0.228
22	1424.4	1586.	645.	1.34	0.538	2.49	1.200	1.240	-4.3	-2.3	0.205
23	1476.3	1562.	662.	1.32	0.552	2.39	1.200	1.240	-3.0	-2.0	0.187
24	1528.1	1541.	670.	1.30	0.558	2.33	1.200	1.240	-2.6	-0.9	0.173
25	1580.0	1530.	673.	1.29	0.561	2.30	1.200	1.240	-1.3	-0.5	0.162
26	1631.9	1522.	675.	1.29	0.562	2.29	1.200	1.240	-1.0	-0.2	0.154
27	1683.8	1517.	675.	1.28	0.562	2.28	1.200	1.240	-0.7	0.0	0.147
28	1735.7	1511.	676.	1.28	0.563	2.27	1.200	1.240	-0.7	-0.2	0.140
29	1787.5	1506.	677.	1.27	0.565	2.25	1.200	1.240	-0.7	-0.2	0.134

TABLE C.1.14 : NUMERICAL EVALUATION OF EXPERIMENT EDI-S2-16/# 9

1	2	3	4	5	6	7	8	9	10	11	12
CYCLE NO.	REAL TIME	CONCENTRATION BOTTOM	TOP	CONCENTRATION NORMALIZED		SEPARATION FACTOR	CURRENT ENR.	CIAL.	CURRENT EFFICIENCY		POWER EFFICIENCY
NCYC (-)	T (SEC)	CB (PPM)	CT (PPM)	XB (-)	XT (-)	NS (-)	I1 (A)	I2 (A)	E1 (%)	E2 (%)	EP (%)
0	0.0	1000.	1006.	1.00	1.000	1.00	0.0	0.0	100.0	100.0	100.000
1	46.4	1089.	886.	1.09	0.881	1.24	0.940	0.950	22.0	29.2	2.709
2	92.9	1155.	801.	1.15	0.796	1.45	1.000	0.980	15.1	20.1	2.308
3	139.3	1209.	748.	1.21	0.744	1.63	0.970	0.980	13.0	12.5	2.003
4	185.7	1239.	708.	1.24	0.704	1.76	0.930	0.970	7.5	9.5	1.742
5	232.1	1264.	681.	1.26	0.677	1.87	0.950	0.970	6.0	6.5	1.532
6	278.6	1278.	659.	1.28	0.655	1.95	0.950	0.950	3.3	5.3	1.359
7	325.0	1286.	644.	1.29	0.640	2.01	0.950	0.950	2.0	3.8	1.213
8	371.4	1292.	632.	1.29	0.628	2.06	0.950	0.950	1.3	2.8	1.092
9	417.8	1297.	623.	1.30	0.619	2.10	0.950	0.950	1.3	2.2	0.993
10	464.3	1297.	619.	1.30	0.615	2.11	0.950	0.950	0.0	0.9	0.900
12	557.1	1295.	605.	1.29	0.601	2.15	0.950	0.950	-0.3	1.7	0.765
14	650.0	1289.	602.	1.29	0.599	2.15	0.950	0.950	-0.7	0.3	0.654
16	742.8	1286.	596.	1.29	0.592	2.17	0.950	0.950	-0.3	0.8	0.576
18	835.7	1286.	591.	1.29	0.587	2.19	0.950	0.950	0.0	0.6	0.516

TABLE C.1.15 : NUMERICAL EVALUATION OF EXPERIMENT EDI-S3-17/#15

1	2	3	4	5	6	7	8	9	10	11	12
CYCLE NO.	REAL TIME	CONCENTRATION BOTTOM	TOP	CONCENTRATION NORMALIZED		SEPARATION FACTOR	CURRENT ENR. CIAL.		CURRENT EFFICIENCY		POWER EFFICIENCY
NCYC (-)	T (SEC)	CB (PPM)	CT (PPM)	XB (-)	XT (-)	NS (-)	I1 (A)	I2 (A)	E1 (%)	E2 (%)	EP (%)
0	0.0	973.	977.	1.00	1.000	1.00	0.0	0.0	100.0	100.0	100.000
1	46.4	1057.	848.	1.09	0.868	1.25	1.000	0.926	19.3	32.2	2.744
2	92.9	1122.	780.	1.15	0.799	1.44	0.982	0.999	15.3	15.5	2.213
3	139.3	1139.	730.	1.17	0.748	1.56	0.937	0.991	3.4	11.7	1.766
4	185.7	1196.	694.	1.23	0.711	1.73	0.937	0.969	14.9	8.6	1.646
5	232.1	1218.	666.	1.25	0.682	1.84	0.948	0.965	5.3	6.8	1.453
6	278.6	1234.	648.	1.27	0.663	1.91	0.905	0.948	4.2	4.4	1.296
7	325.0	1239.	632.	1.27	0.647	1.97	0.926	0.926	1.4	3.9	1.158
8	371.4	1245.	622.	1.28	0.637	2.01	0.926	0.948	1.4	2.5	1.042
9	417.8	1245.	613.	1.28	0.627	2.04	0.894	0.926	0.0	2.3	0.945
10	464.3	1245.	609.	1.28	0.624	2.05	0.926	0.905	0.0	1.0	0.859
12	557.1	1245.	596.	1.28	0.610	2.10	0.894	0.905	0.0	1.6	0.737
14	650.0	1239.	593.	1.27	0.608	2.10	0.883	0.905	-0.7	0.3	0.634
16	742.8	1234.	587.	1.27	0.601	2.11	0.894	0.894	-0.7	0.8	0.559
18	835.7	1234.	584.	1.27	0.598	2.12	0.898	0.894	0.0	0.3	0.500

TABLE C.1.16 : NUMERICAL EVALUATION OF EXPERIMENT EDI-S3-12/#16

1	2	3	4	5	6	7	8	9	10	11	12
CYCLE NO.	REAL TIME	CONCENTRATION BOTTOM	TOP	CONCENTRATION NORMALIZED		SEPARATION FACTOR	CURRENT ENR. CIAL.		CURRENT EFFICIENCY		POWER EFFICIENCY
NCYC (-)	T (SEC)	CB (PPM)	CT (PPM)	XB (-)	XT (-)	NS (-)	I1 (A)	I2 (A)	E1 (%)	E2 (%)	EP (%)
0	0.0	997.	1005.	1.00	1.000	1.00	0.0	0.0	100.0	100.0	100.000
1	63.8	1054.	916.	1.06	0.911	1.16	0.560	0.500	17.1	29.9	4.782
2	127.6	1097.	869.	1.10	0.865	1.27	0.570	0.550	12.8	14.2	3.842
3	191.3	1127.	835.	1.13	0.831	1.36	0.560	0.560	9.0	10.5	3.261
4	255.1	1152.	806.	1.16	0.802	1.44	0.520	0.550	7.9	8.7	2.909
5	318.9	1168.	784.	1.17	0.780	1.50	0.510	0.540	5.4	6.8	2.607
6	382.7	1182.	768.	1.19	0.764	1.55	0.520	0.540	4.4	5.2	2.355
7	446.4	1190.	752.	1.19	0.748	1.60	0.520	0.540	2.7	4.8	2.141
8	510.2	1196.	743.	1.20	0.739	1.62	0.520	0.540	1.8	2.8	1.940
9	574.0	1201.	735.	1.20	0.732	1.65	0.520	0.540	1.8	2.4	1.778
10	637.8	1207.	729.	1.21	0.725	1.67	0.520	0.540	1.8	2.0	1.643
12	765.3	1209.	722.	1.21	0.719	1.69	0.520	0.540	0.4	1.0	1.399
14	892.9	1207.	712.	1.21	0.709	1.71	0.520	0.540	-0.4	1.6	1.220
16	1020.4	1207.	710.	1.21	0.706	1.71	0.520	0.540	0.0	0.4	1.075
18	1148.0	1204.	704.	1.21	0.701	1.72	0.520	0.540	-0.4	0.8	0.961

TABLE C.1.17 : NUMERICAL EVALUATION OF EXPERIMENT EDI-S3-12/#17

1	2	3	4	5	6	7	8	9	10	11	12
CYCLE NO.	REAL TIME	CONCENTRATION BOTTOM	CONCENTRATION TOP	CONCENTRATION NORMALIZED		SEPARATION FACTOR	CURRENT ENR. DIAL.		CURRENT EFFICIENCY		POWER EFFICIENCY
NCYC (-)	T (SEC)	CB (PPM)	CT (PPM)	XB (-)	XT (-)	NS (-)	I1 (A)	I2 (A)	E1 (%)	E2 (%)	EP (%)
0	0.0	1081.	1081.	1.00	1.000	1.00	0.0	0.0	100.0	100.0	100.000
1	63.8	1185.	942.	1.10	0.871	1.26	0.925	0.994	19.8	26.2	2.427
2	127.6	1264.	855.	1.17	0.791	1.48	0.925	0.941	14.5	15.4	2.019
3	191.3	1322.	795.	1.22	0.735	1.66	0.878	0.879	11.1	11.6	1.765
4	255.1	1366.	749.	1.26	0.693	1.82	0.886	0.909	8.4	8.3	1.553
5	318.9	1397.	717.	1.29	0.663	1.95	0.867	0.855	5.9	6.3	1.383
6	382.7	1411.	697.	1.30	0.644	2.03	0.870	0.905	2.7	3.8	1.214
7	446.4	1422.	679.	1.32	0.628	2.10	0.862	0.878	2.2	3.5	1.088
8	510.2	1430.	666.	1.32	0.616	2.15	0.862	0.878	1.6	2.5	0.982
9	574.0	1433.	658.	1.33	0.609	2.18	0.855	0.878	0.5	1.5	0.888
10	637.8	1433.	649.	1.33	0.600	2.21	0.823	0.902	0.0	1.7	0.811
12	765.3	1433.	640.	1.33	0.592	2.24	0.855	0.870	0.0	0.9	0.687
14	892.9	1427.	633.	1.32	0.586	2.25	0.812	0.878	-0.6	0.6	0.593
16	1020.4	1427.	630.	1.32	0.582	2.27	0.839	0.878	0.0	0.4	0.523
18	1148.0	1425.	624.	1.32	0.578	2.28	0.828	0.847	-0.3	0.5	0.469

TABLE C.1.18 : NUMERICAL EVALUATION OF EXPERIMENT EDI-S3-12/#18

1	2	3	4	5	6	7	8	9	10	11	12
CYCLE NO.	REAL TIME	CONCENTRATION BOTTOM	CONCENTRATION TOP	CONCENTRATION NORMALIZED		SEPARATION FACTOR	CURRENT ENR. DIAL.		CURRENT EFFICIENCY		POWER EFFICIENCY
NCYC (-)	T (SEC)	CB (PPM)	CT (PPM)	XB (-)	XT (-)	NS (-)	I1 (A)	I2 (A)	E1 (%)	E2 (%)	EP (%)
0	0.0	1190.	1174.	1.00	1.000	1.00	0.0	0.0	100.0	100.0	100.000
1	63.8	1270.	980.	1.07	0.835	1.28	1.207	1.105	11.1	29.4	1.503
2	127.6	1366.	864.	1.15	0.736	1.56	1.192	1.184	13.6	16.5	1.290
3	191.3	1430.	780.	1.20	0.665	1.81	1.149	1.145	9.3	12.3	1.123
4	255.1	1475.	716.	1.24	0.610	2.03	1.160	1.093	6.5	9.9	0.994
5	318.9	1511.	671.	1.27	0.571	2.22	1.098	1.098	5.6	6.9	0.890
6	382.7	1539.	636.	1.29	0.542	2.39	1.098	1.082	4.3	5.4	0.804
7	446.4	1556.	609.	1.31	0.519	2.52	1.105	1.058	2.6	4.3	0.729
8	510.2	1570.	592.	1.32	0.504	2.61	1.058	1.066	2.2	2.6	0.663
9	574.0	1578.	581.	1.33	0.495	2.68	1.058	1.058	1.3	1.8	0.606
10	637.8	1587.	574.	1.33	0.489	2.73	1.058	1.058	1.3	1.0	0.556
11	701.5	1592.	570.	1.34	0.486	2.75	1.058	1.058	0.9	0.6	0.512
12	765.3	1595.	565.	1.34	0.481	2.78	1.058	1.058	0.4	0.8	0.475
13	829.1	1598.	561.	1.34	0.478	2.81	1.058	1.058	0.4	0.6	0.442
14	892.9	1598.	556.	1.34	0.474	2.83	1.058	1.058	0.0	0.8	0.414
15	956.6	1601.	555.	1.34	0.473	2.85	1.058	1.058	0.4	0.2	0.389
16	1020.4	1601.	555.	1.34	0.473	2.85	1.058	1.058	0.0	0.0	0.365

TABLE C.1.19 : NUMERICAL EVALUATION OF EXPERIMENT EDI-S3-12/#19

1	2	3	4	5	6	7	8	9	10	11	12
CYCLE NO.	REAL TIME	CONCENTRATION BOTTOM	TOP	CONCENTRATION NORMALIZED		SEPARATION FACTOR	CURRENT ENR. DIAL.		CURRENT EFFICIENCY		POWER EFFICIENCY
NCYC (-)	T (SEC)	CB (PPM)	CT (PPM)	XB (-)	XT (-)	NS (-)	I1 (A)	I2 (A)	E1 (%)	E2 (%)	EP (%)
0	0.0	1174.	1160.	1.00	1.000	1.00	0.0	C.0	100.0	100.0	100.000
1	53.4	1264.	1122.	1.08	0.968	1.11	1.067	C.706	17.0	9.6	0.272
2	106.9	1375.	1068.	1.17	C.921	1.27	1.010	C.870	21.9	12.5	0.291
3	160.3	1486.	1007.	1.27	0.869	1.46	0.992	C.861	22.5	14.1	0.303
4	213.8	1596.	951.	1.36	0.820	1.66	0.973	C.842	23.1	13.5	0.308
5	267.2	1710.	897.	1.46	C.773	1.89	0.964	C.823	23.5	13.2	0.312
6	320.7	1824.	844.	1.55	0.727	2.14	0.889	C.870	25.6	12.2	0.314
7	374.1	1910.	791.	1.63	0.682	2.39	0.889	C.851	19.3	12.5	0.309
8	427.6	2025.	746.	1.72	0.643	2.68	0.889	C.823	25.9	11.0	0.311
9	481.0	2111.	703.	1.80	0.606	2.97	0.851	C.814	20.4	10.5	0.306
10	534.4	2213.	663.	1.89	0.572	3.30	0.842	C.795	24.2	10.1	0.305
12	641.3	2389.	591.	2.03	0.509	3.99	0.814	C.777	21.7	9.3	0.299
14	748.2	2536.	533.	2.16	C.459	4.70	0.795	C.758	18.6	7.7	0.290
16	855.1	2679.	484.	2.28	0.417	5.47	0.777	C.739	18.5	6.7	0.281
18	962.0	2844.	442.	2.42	0.382	6.35	0.748	C.730	22.1	5.7	0.276
20	1068.9	2959.	406.	2.52	C.350	7.20	0.730	C.711	15.8	5.1	0.267
25	1336.1	3155.	342.	2.69	0.295	9.12	0.711	C.692	11.0	3.7	0.242
30	1603.3	3278.	303.	2.79	0.261	10.68	0.692	C.674	7.1	2.3	0.218
35	1870.5	3349.	277.	2.85	0.239	11.93	0.683	C.664	4.2	1.6	0.197
40	2137.8	3426.	262.	2.92	0.226	12.93	0.603	0.664	4.6	0.9	0.180
45	2405.0	3467.	252.	2.95	0.217	13.62	0.683	C.664	2.4	0.6	0.164
50	2672.2	3501.	245.	2.98	0.211	14.11	0.683	C.664	2.0	0.4	0.151

TABLE C.1.20 : NUMERICAL EVALUATION OF EXPERIMENT EDI-S3-12/#20

1	2	3	4	5	6	7	8	9	10	11	12
CYCLE NO.	REAL TIME	CONCENTRATION BOTTOM	TOP	CONCENTRATION NORMALIZED		SEPARATION FACTOR	CURRENT ENR. DIAL.		CURRENT EFFICIENCY		POWER EFFICIENCY
NCYC (-)	T (SEC)	CB (PPM)	CT (PPM)	XB (-)	XT (-)	NS (-)	I1 (A)	I2 (A)	E1 (%)	E2 (%)	EP (%)
0	0.0	1237.	1231.	1.00	1.000	1.00	0.0	0.0	100.0	100.0	100.000
1	73.8	1405.	1024.	1.14	0.832	1.37	0.942	C.922	26.0	32.6	3.150
2	147.6	1525.	903.	1.23	0.734	1.68	0.922	0.949	18.9	18.6	2.570
3	221.3	1606.	823.	1.30	0.669	1.94	0.895	C.930	13.2	12.5	2.176
4	295.1	1662.	768.	1.34	0.624	2.16	0.881	C.910	9.3	8.9	1.882
5	368.9	1696.	725.	1.37	0.589	2.33	0.867	0.895	5.7	6.9	1.650
6	442.7	1716.	697.	1.39	C.566	2.45	0.847	C.895	3.4	4.6	1.455
7	516.4	1759.	677.	1.42	0.550	2.58	0.849	C.881	7.3	3.2	1.330
8	590.2	1764.	664.	1.43	0.540	2.64	0.840	0.881	1.0	2.1	1.191
9	664.0	1764.	658.	1.43	0.535	2.67	0.827	0.874	0.0	1.1	1.071
10	737.8	1764.	651.	1.43	0.529	2.69	0.834	C.867	0.0	1.1	0.974
11	811.5	1761.	645.	1.42	0.524	2.72	0.834	C.861	-0.5	1.1	0.893
12	885.3	1759.	642.	1.42	0.522	2.72	0.827	0.854	-0.5	0.4	0.822
13	959.1	1753.	640.	1.42	0.520	2.73	0.827	C.854	-1.0	0.4	0.759
14	1032.9	1750.	637.	1.42	0.518	2.73	0.827	C.847	-0.5	0.4	0.707
15	1106.6	1744.	633.	1.41	0.515	2.74	0.820	C.840	-1.0	0.7	0.662
16	1180.4	1739.	631.	1.41	C.513	2.74	0.813	C.840	-1.0	0.4	0.621
17	1254.2	1733.	630.	1.40	0.512	2.74	0.813	C.834	-1.0	C.2	0.584
18	1328.0	1727.	628.	1.40	0.510	2.74	0.813	0.834	-1.0	0.2	0.551
19	1401.7	1722.	627.	1.39	0.509	2.73	0.813	C.834	-1.0	0.2	0.521
20	1475.5	1716.	626.	1.39	0.508	2.73	0.806	C.827	-1.0	0.2	0.495

TABLE C.1.21 : NUMERICAL EVALUATION OF EXPERIMENT EDI-S3-12/#21

1	2	3	4	5	6	7	8	9	10	11	12
CYCLE NO.	REAL TIME	CONCENTRATION BOTTOM	CONCENTRATION TOP	CONCENTRATION NORMALIZED		SEPARATION FACTOR	CURRENT ENR. CIAL.		CURRENT EFFICIENCY		POWER EFFICIENCY
NCYC (-)	T (SEC)	CB (PPM)	CT (PPM)	XB (-)	XT (-)	NS (-)	I1 (A)	I2 (A)	E1 (%)	E2 (%)	EP (%)
0	0.0	1201.	1197.	1.00	1.000	1.00	0.0	0.0	100.0	100.0	100.000
1	83.8	1416.	974.	1.18	0.814	1.45	0.895	0.794	30.8	36.0	3.564
2	167.6	1564.	837.	1.30	0.699	1.86	0.828	0.834	22.9	21.0	2.954
3	251.3	1657.	749.	1.38	0.626	2.20	0.797	0.809	14.9	13.9	2.495
4	335.1	1719.	689.	1.43	0.575	2.49	0.788	0.790	10.1	9.8	2.151
5	418.9	1753.	651.	1.46	0.544	2.68	0.764	0.788	5.7	6.1	1.861
6	502.7	1779.	632.	1.48	0.528	2.80	0.758	0.776	4.3	3.2	1.628
7	586.4	1787.	614.	1.49	0.513	2.90	0.752	0.764	1.5	3.0	1.440
8	670.2	1796.	604.	1.49	0.504	2.96	0.752	0.758	1.5	1.7	1.289
9	754.0	1798.	597.	1.50	0.499	3.00	0.746	0.752	0.5	1.1	1.162
10	837.8	1798.	593.	1.50	0.496	3.02	0.746	0.752	0.0	0.7	1.054
11	921.5	1798.	592.	1.50	0.495	3.03	0.740	0.746	0.0	0.2	0.964
12	1005.3	1796.	591.	1.49	0.494	3.03	0.740	0.746	-0.5	0.2	0.886
13	1089.1	1796.	590.	1.49	0.492	3.04	0.740	0.746	0.0	0.2	0.822
14	1172.9	1793.	588.	1.49	0.491	3.04	0.740	0.746	-0.5	0.2	0.764
15	1256.6	1790.	588.	1.49	0.491	3.03	0.740	0.746	-0.5	0.0	0.713
16	1340.4	1787.	587.	1.49	0.490	3.03	0.740	0.746	-0.5	0.2	0.670
17	1424.2	1784.	586.	1.49	0.489	3.04	0.740	0.746	-0.5	0.2	0.631

TABLE C.1.22 : NUMERICAL EVALUATION OF EXPERIMENT EDI-S3-12/#22

1	2	3	4	5	6	7	8	9	10	11	12
CYCLE NO.	REAL TIME	CONCENTRATION BOTTOM	CONCENTRATION TOP	CONCENTRATION NORMALIZED		SEPARATION FACTOR	CURRENT ENR. CIAL.		CURRENT EFFICIENCY		POWER EFFICIENCY
NCYC (-)	T (SEC)	CB (PPM)	CT (PPM)	XB (-)	XT (-)	NS (-)	I1 (A)	I2 (A)	E1 (%)	E2 (%)	EP (%)
0	0.0	1198.	1196.	1.00	1.000	1.00	0.0	0.0	100.0	100.0	100.000
1	93.8	1452.	955.	1.21	0.798	1.52	0.800	0.761	36.3	36.2	3.874
2	187.6	1598.	809.	1.33	0.676	1.97	0.752	0.754	22.1	22.1	3.131
3	281.3	1694.	716.	1.41	0.599	2.36	0.746	0.704	14.7	15.1	2.637
4	375.1	1750.	662.	1.46	0.553	2.64	0.704	0.714	9.2	8.7	2.237
5	468.9	1787.	622.	1.49	0.520	2.87	0.693	0.717	6.1	6.4	1.937
6	562.7	1813.	602.	1.51	0.504	3.00	0.672	0.725	4.4	3.1	1.690
7	656.4	1821.	588.	1.52	0.492	3.09	0.677	0.714	1.4	2.3	1.487
8	750.2	1830.	575.	1.53	0.481	3.17	0.682	0.698	1.4	2.1	1.332
9	844.0	1830.	571.	1.53	0.478	3.20	0.682	0.682	0.0	0.6	1.195
10	937.8	1830.	569.	1.53	0.476	3.21	0.688	0.688	0.0	0.4	1.082
11	1031.5	1830.	568.	1.53	0.475	3.22	0.688	0.688	0.0	0.2	0.988
12	1125.3	1827.	565.	1.52	0.472	3.23	0.688	0.688	-0.5	0.4	0.908
13	1219.1	1824.	564.	1.52	0.471	3.23	0.688	0.688	-0.5	0.2	0.839
14	1312.9	1821.	562.	1.52	0.470	3.23	0.688	0.688	-0.5	0.2	0.780
15	1406.6	1821.	561.	1.52	0.469	3.24	0.688	0.688	0.0	0.2	0.730
16	1500.4	1818.	561.	1.52	0.469	3.23	0.688	0.688	-0.5	0.0	0.684

TABLE C.1.23 : NUMERICAL EVALUATION OF EXPERIMENT EDI-S3-12/#23

1	2	3	4	5	6	7	8	9	10	11	12
CYCLE NO.	REAL TIME	CONCENTRATION BOTTOM	TOP	CONCENTRATION NORMALIZED		SEPARATION FACTOR	CURRENT ENR.	DIAL.	CURRENT EFFICIENCY		POWER EFFICIENCY
NCYC (-)	T (SEC)	CB (PPM)	CT (PPM)	XB (-)	XT (-)	NS (-)	I1 (A)	I2 (A)	E1 (%)	E2 (%)	EP (%)
0	0.0	1179.	1171.	1.00	1.000	1.00	0.0	0.0	100.0	100.0	100.000
1	55.0	1218.	1032.	1.03	0.881	1.17	1.091	1.091	6.9	24.9	1.777
2	110.0	1250.	980.	1.06	0.837	1.27	1.091	1.110	5.9	9.1	1.290
3	164.9	1278.	942.	1.08	0.804	1.35	1.091	1.128	4.9	6.7	1.067
4	219.9	1300.	915.	1.10	0.781	1.41	1.073	1.128	4.0	4.7	0.918
5	274.9	1314.	898.	1.11	0.767	1.45	1.073	1.119	2.5	2.9	0.793
6	329.9	1325.	886.	1.12	0.751	1.50	1.073	1.119	2.0	3.1	0.708
7	384.8	1333.	867.	1.13	0.740	1.53	1.073	1.119	1.5	2.2	0.636
8	439.8	1339.	858.	1.14	0.732	1.55	1.073	1.119	1.0	1.6	0.575
9	494.8	1344.	849.	1.14	0.725	1.57	1.073	1.119	1.0	1.6	0.527
10	549.8	1347.	841.	1.14	0.718	1.59	1.073	1.137	0.5	1.3	0.484
11	604.7	1375.	835.	1.17	0.713	1.64	1.073	1.119	5.0	1.1	0.469
12	659.7	1347.	831.	1.14	0.709	1.61	1.073	1.119	-5.0	0.7	0.412
13	714.7	1344.	828.	1.14	0.707	1.61	1.073	1.119	-0.5	0.4	0.380
14	769.7	1344.	824.	1.14	0.704	1.62	1.073	1.137	0.0	0.7	0.356
15	824.6	1344.	823.	1.14	0.703	1.62	1.073	1.119	0.0	0.2	0.333

TABLE C.1.24 : NUMERICAL EVALUATION OF EXPERIMENT EDI-S3-12/#24

1	2	3	4	5	6	7	8	9	10	11	12
CYCLE NO.	REAL TIME	CONCENTRATION BOTTOM	TOP	CONCENTRATION NORMALIZED		SEPARATION FACTOR	CURRENT ENR.	DIAL.	CURRENT EFFICIENCY		POWER EFFICIENCY
NCYC (-)	T (SEC)	CB (PPM)	CT (PPM)	XB (-)	XT (-)	NS (-)	I1 (A)	I2 (A)	E1 (%)	E2 (%)	EP (%)
0	0.0	1245.	1238.	1.00	1.000	1.00	0.0	0.0	100.0	100.0	100.000
1	93.1	1542.	943.	1.24	0.761	1.63	0.918	0.764	32.6	39.0	3.709
2	186.3	1739.	756.	1.40	0.610	2.29	0.821	0.773	24.2	24.4	3.132
3	279.4	1867.	631.	1.50	0.509	2.94	0.752	0.709	17.2	17.8	2.731
4	372.6	1953.	555.	1.57	0.448	3.50	0.735	0.719	11.8	10.7	2.366
5	465.7	2004.	507.	1.61	0.409	3.93	0.741	0.698	7.0	6.9	2.059
6	558.9	2036.	477.	1.64	0.385	4.24	0.746	0.692	4.3	4.3	1.805
7	652.0	2059.	458.	1.65	0.370	4.47	0.725	0.687	3.2	2.8	1.605
8	745.1	2076.	446.	1.67	0.360	4.63	0.735	0.676	2.4	1.7	1.440
9	838.3	2085.	444.	1.67	0.358	4.67	0.730	0.687	1.2	0.4	1.295
10	931.4	2091.	439.	1.68	0.354	4.74	0.730	0.676	0.8	0.8	1.180
11	1024.6	2097.	436.	1.68	0.352	4.78	0.725	0.676	0.8	0.4	1.082
12	1117.7	2100.	435.	1.69	0.351	4.80	0.725	0.671	0.4	0.2	0.999
13	1210.9	2100.	435.	1.69	0.351	4.80	0.725	0.671	0.0	0.0	0.925
14	1304.0	2103.	432.	1.69	0.349	4.84	0.725	0.671	0.4	0.4	0.864
15	1397.2	2105.	428.	1.69	0.346	4.89	0.725	0.671	0.4	0.6	0.812
16	1490.3	2105.	427.	1.69	0.345	4.90	0.725	0.671	0.0	0.2	0.764
17	1583.4	2108.	430.	1.69	0.347	4.88	0.725	0.671	0.4	-0.4	0.720
18	1676.6	2108.	431.	1.69	0.348	4.87	0.725	0.671	0.0	-0.2	0.681
19	1769.7	2108.	432.	1.69	0.349	4.85	0.725	0.671	0.0	-0.2	0.645

TABLE C.1.25 : NUMERICAL EVALUATION OF EXPERIMENT EDI-S3-13/# 1

1	2	3	4	5	6	7	8	9	10	11	12
CYCLE NO.	REAL TIME	CONCENTRATION BOTTOM	TOP	CONCENTRATION NORMALIZED		SEPARATION FACTOR	CURRENT ENR. CIAL.		CURRENT EFFICIENCY		POWER EFFICIENCY
NCYC (-)	T (SEC)	CB (PPM)	CT (PPM)	XB (-)	XT (-)	NS (-)	I1 (A)	I2 (A)	E1 (%)	E2 (%)	EP (%)
0	0.0	1256.	1240.	1.00	1.000	1.00	0.0	0.0	100.0	100.0	100.000
1	70.6	1475.	993.	1.17	0.801	1.47	1.017	0.946	28.6	34.6	3.373
2	141.2	1640.	839.	1.31	0.676	1.93	0.963	0.984	22.8	20.9	2.822
3	211.8	1761.	733.	1.40	0.591	2.37	0.925	0.942	17.5	14.9	2.454
4	282.4	1847.	654.	1.47	0.528	2.79	0.892	0.913	12.7	11.5	2.170
5	353.1	1901.	606.	1.51	0.489	3.09	0.892	0.892	8.1	7.1	1.908
6	423.7	1941.	568.	1.55	0.458	3.38	0.881	0.871	6.1	5.9	1.707
7	494.3	1967.	542.	1.57	0.437	3.58	0.864	0.875	4.0	3.9	1.533
8	564.9	1984.	526.	1.58	0.425	3.72	0.861	0.872	2.7	2.4	1.382
9	635.5	1993.	516.	1.59	0.416	3.81	0.857	0.864	1.3	1.6	1.253
10	706.1	1996.	510.	1.59	0.411	3.87	0.850	0.850	0.5	1.0	1.142
11	776.7	2001.	506.	1.59	0.408	3.91	0.850	0.850	0.9	0.6	1.051
12	847.3	2010.	498.	1.60	0.402	3.98	0.850	0.850	1.4	1.2	0.978
13	918.0	2013.	497.	1.60	0.401	4.00	0.950	0.850	0.5	0.2	0.909
14	988.6	2016.	495.	1.61	0.400	4.02	0.850	0.850	0.5	0.2	0.849
15	1059.2	2016.	495.	1.61	0.400	4.02	0.850	0.850	0.0	0.0	0.794
16	1129.8	2013.	491.	1.60	0.396	4.04	0.850	0.850	-0.5	0.6	0.747
17	1200.4	2010.	493.	1.60	0.398	4.03	0.850	0.850	-0.5	-0.2	0.703
18	1271.0	2010.	493.	1.60	0.398	4.03	0.850	0.850	0.0	0.0	0.665

TABLE C.1.26 : NUMERICAL EVALUATION OF EXPERIMENT EDI-S3-13/# 2

1	2	3	4	5	6	7	8	9	10	11	12
CYCLE NO.	REAL TIME	CONCENTRATION BOTTOM	TOP	CONCENTRATION NORMALIZED		SEPARATION FACTOR	CURRENT ENR. CIAL.		CURRENT EFFICIENCY		POWER EFFICIENCY
NCYC (-)	T (SEC)	CB (PPM)	CT (PPM)	XB (-)	XT (-)	NS (-)	I1 (A)	I2 (A)	E1 (%)	E2 (%)	EP (%)
0	0.0	1242.	1228.	1.00	1.000	1.00	0.0	0.0	100.0	100.0	100.000
1	45.3	1402.	1109.	1.13	0.903	1.25	1.037	0.936	32.0	26.3	1.586
2	90.6	1542.	1004.	1.24	0.817	1.52	0.971	1.015	29.7	21.6	1.450
3	135.9	1677.	908.	1.35	0.739	1.83	0.927	1.004	30.2	19.7	1.390
4	181.2	1790.	819.	1.44	0.667	2.16	0.927	0.949	25.3	19.4	1.332
5	226.5	1890.	748.	1.52	0.609	2.50	0.883	0.949	23.4	15.5	1.267
6	271.8	1981.	684.	1.60	0.557	2.86	0.872	0.927	21.8	14.4	1.213
7	317.1	2062.	635.	1.66	0.517	3.21	0.872	0.883	19.2	11.5	1.156
8	362.4	2131.	591.	1.72	0.481	3.57	0.839	0.883	17.2	10.3	1.103
9	407.8	2192.	555.	1.76	0.452	3.91	0.839	0.861	15.1	8.7	1.052
10	453.1	2248.	522.	1.81	0.425	4.25	0.817	0.850	14.1	7.9	1.007
12	543.7	2336.	471.	1.88	0.383	4.90	0.795	0.828	11.5	6.5	0.924
14	634.3	2400.	432.	1.93	0.352	5.49	0.784	0.817	8.6	4.9	0.849
16	724.9	2453.	406.	1.97	0.331	5.97	0.773	0.801	7.1	3.3	0.782
18	815.5	2483.	387.	2.00	0.315	6.34	0.766	0.790	4.0	2.5	0.721
20	906.1	2515.	377.	2.02	0.307	6.60	0.761	0.784	4.4	1.4	0.668
24	1087.3	2542.	360.	2.05	0.293	6.98	0.761	0.784	1.8	1.1	0.577
28	1268.6	2569.	352.	2.07	0.287	7.21	0.761	0.784	1.8	0.5	0.508
32	1449.8	2575.	346.	2.07	0.282	7.36	0.761	0.784	0.4	0.4	0.451
36	1631.0	2581.	342.	2.08	0.278	7.46	0.761	0.784	0.4	0.3	0.405

TABLE C.1.27 : NUMERICAL EVALUATION OF EXPERIMENT EDI-S3-13/# 3

1	2	3	4	5	6	7	8	9	10	11	12
CYCLE NO.	REAL TIME	CONCENTRATION BOTTOM	CONCENTRATION TOP	CONCENTRATION NORMALIZED		SEPARATION FACTOR	CURRENT ENR.	CURRENT DIAL.	CURRENT EFFICIENCY		POWER EFFICIENCY
NCYC (-)	T (SEC)	CB (PPM)	CT (PPM)	XB (-)	XT (-)	NS (-)	I1 (A)	I2 (A)	E1 (%)	E2 (%)	EP (%)
0	0.0	1264.	1245.	1.00	1.000	1.00	0.0	0.0	100.0	100.0	100.000
2	65.3	1391.	1184.	1.10	0.951	1.16	1.087	1.011	16.8	8.6	0.364
4	130.6	1522.	1099.	1.20	0.883	1.36	1.057	1.041	17.8	11.8	0.371
6	195.9	1657.	1013.	1.31	0.813	1.61	1.026	1.041	18.9	11.9	0.378
8	261.2	1801.	933.	1.42	0.749	1.90	0.980	1.011	21.2	11.4	0.386
10	326.5	1930.	857.	1.53	0.688	2.22	0.919	0.949	20.1	11.5	0.388
15	489.8	2216.	703.	1.75	0.565	3.10	0.857	0.903	19.2	9.8	0.380
20	653.1	2433.	587.	1.92	0.472	4.08	0.851	0.864	14.7	7.7	0.358
25	816.3	2608.	502.	2.06	0.403	5.12	0.796	0.812	12.6	6.0	0.336
30	979.6	2742.	439.	2.17	0.352	6.16	0.796	0.812	9.7	4.5	0.312
35	1142.9	2850.	395.	2.25	0.317	7.11	0.790	0.805	7.9	3.1	0.289
40	1306.1	2938.	361.	2.32	0.290	8.01	0.796	0.796	6.3	2.4	0.268
45	1469.4	2996.	338.	2.37	0.272	8.73	0.766	0.766	4.3	1.7	0.249
50	1632.7	3041.	320.	2.41	0.257	9.36	0.766	0.766	3.4	1.4	0.232
55	1795.9	3081.	308.	2.44	0.248	9.84	0.735	0.735	3.1	0.9	0.218
60	1959.2	3099.	302.	2.45	0.242	10.11	0.735	0.735	1.4	0.5	0.203
65	2122.5	3133.	294.	2.48	0.236	10.49	0.735	0.735	2.6	0.6	0.192

TABLE C.1.28 : NUMERICAL EVALUATION OF EXPERIMENT EDI-S3-13/# 4

1	2	3	4	5	6	7	8	9	10	11	12
CYCLE NO.	REAL TIME	CONCENTRATION BOTTOM	CONCENTRATION TOP	CONCENTRATION NORMALIZED		SEPARATION FACTOR	CURRENT ENR.	CURRENT DIAL.	CURRENT EFFICIENCY		POWER EFFICIENCY
NCYC (-)	T (SEC)	CB (PPM)	CT (PPM)	XB (-)	XT (-)	NS (-)	I1 (A)	I2 (A)	E1 (%)	E2 (%)	EP (%)
0	0.0	1295.	1276.	1.00	1.000	1.00	0.0	0.0	100.0	100.0	100.000
1	95.9	1517.	955.	1.17	0.748	1.57	0.975	0.964	22.3	32.6	4.402
2	191.8	1634.	823.	1.26	0.645	1.96	0.996	0.959	11.6	13.4	3.172
3	287.8	1694.	761.	1.31	0.597	2.19	0.980	0.938	5.9	6.5	2.445
4	383.7	1716.	726.	1.32	0.569	2.32	0.959	0.923	1.7	3.7	1.953
5	479.6	1725.	712.	1.33	0.558	2.39	0.949	0.917	1.5	1.5	1.617
6	575.5	1730.	703.	1.34	0.551	2.43	0.938	0.912	0.6	1.0	1.375
7	671.4	1727.	695.	1.33	0.545	2.45	0.933	0.907	-0.3	0.8	1.191
8	767.3	1725.	686.	1.33	0.538	2.48	0.928	0.907	-0.3	1.0	1.053
9	863.3	1722.	681.	1.33	0.534	2.49	0.928	0.907	-0.3	0.6	0.941
10	959.2	1716.	677.	1.33	0.531	2.50	0.917	0.897	-0.6	0.4	0.849

TABLE C.1.29 : NUMERICAL EVALUATION OF EXPERIMENT EDI-S3-13/# 5

1	2	3	4	5	6	7	8	9	10	11	12
CYCLE NO.	REAL TIME	CONCENTRATION BOTTOM	CONCENTRATION TOP	CONCENTRATION NORMALIZED		SEPARATION FACTOR	CURRENT ENR.	CIAL.	CURRENT EFFICIENCY		POWER EFFICIENCY
NCYC (-)	T (SEC)	CB (PPM)	CT (PPM)	XB (-)	XT (-)	NS (-)	I1 (A)	I2 (A)	E1 (%)	E2 (%)	EP (%)
0	0.0	1306.	1291.	1.00	1.000	1.00	0.0	0.0	100.0	100.0	100.000
1	60.6	1391.	1167.	1.07	0.904	1.18	0.668	0.610	19.9	31.4	6.133
2	121.2	1464.	1086.	1.12	0.841	1.33	0.660	0.652	17.0	19.3	5.109
3	181.8	1522.	1023.	1.17	0.792	1.47	0.643	0.660	14.1	14.8	4.499
4	242.4	1570.	971.	1.20	0.752	1.60	0.643	0.652	11.5	12.3	4.049
5	303.1	1606.	931.	1.23	0.721	1.71	0.643	0.652	8.8	9.5	3.657
6	363.7	1632.	897.	1.25	0.694	1.80	0.627	0.652	6.3	8.3	3.330
7	424.3	1654.	871.	1.27	0.674	1.88	0.627	0.652	5.6	6.1	3.048
8	484.9	1668.	850.	1.28	0.658	1.94	0.627	0.643	3.5	5.0	2.793
9	545.5	1679.	837.	1.29	0.648	1.98	0.610	0.643	2.9	3.1	2.565
10	606.1	1691.	819.	1.30	0.634	2.04	0.619	0.635	2.8	4.4	2.396
11	666.7	1699.	810.	1.30	0.627	2.07	0.610	0.627	2.2	2.2	2.229
12	727.3	1705.	804.	1.31	0.622	2.10	0.610	0.627	1.4	1.6	2.077
13	788.0	1708.	793.	1.31	0.614	2.13	0.610	0.627	0.7	2.6	1.951
14	848.6	1710.	788.	1.31	0.610	2.15	0.610	0.627	0.7	1.3	1.831
15	909.2	1713.	784.	1.31	0.607	2.16	0.610	0.627	0.7	1.0	1.724
16	969.8	1713.	780.	1.31	0.604	2.17	0.610	0.627	0.0	1.0	1.626
17	1030.4	1716.	779.	1.31	0.603	2.18	0.610	0.627	0.7	0.3	1.539

TABLE C.1.30 : NUMERICAL EVALUATION OF EXPERIMENT EDI-S3-13/# 6

1	2	3	4	5	6	7	8	9	10	11	12
CYCLE NO.	REAL TIME	CONCENTRATION BOTTOM	CONCENTRATION TOP	CONCENTRATION NORMALIZED		SEPARATION FACTOR	CURRENT ENR.	CIAL.	CURRENT EFFICIENCY		POWER EFFICIENCY
NCYC (-)	T (SEC)	CB (PPM)	CT (PPM)	XB (-)	XT (-)	NS (-)	I1 (A)	I2 (A)	E1 (%)	E2 (%)	EP (%)
0	0.0	1281.	1271.	1.00	1.000	1.00	0.0	0.0	100.0	100.0	100.000
1	60.6	1438.	1047.	1.12	0.824	1.36	1.130	1.122	21.6	30.8	2.778
2	121.2	1570.	920.	1.23	0.724	1.69	1.122	1.163	18.1	17.0	2.294
3	181.8	1674.	823.	1.31	0.648	2.02	1.114	1.138	14.5	13.2	2.008
4	242.4	1753.	751.	1.37	0.591	2.32	1.105	1.122	11.1	10.0	1.783
5	303.1	1813.	695.	1.42	0.547	2.59	1.097	1.122	8.4	7.7	1.596
6	363.7	1855.	658.	1.45	0.518	2.80	1.072	1.105	6.2	5.2	1.434
7	424.3	1887.	626.	1.47	0.492	2.99	1.072	1.089	4.5	4.6	1.301
8	484.9	1913.	606.	1.49	0.477	3.13	1.056	1.072	3.8	2.8	1.186
9	545.5	1924.	591.	1.50	0.465	3.23	1.039	1.056	1.7	2.3	1.083
10	606.1	1938.	574.	1.51	0.452	3.35	0.536	1.039	4.1	2.5	1.027
11	666.7	1947.	571.	1.52	0.450	3.38	1.031	1.023	1.3	0.4	0.945
12	727.3	1950.	564.	1.52	0.444	3.43	1.023	1.015	0.4	1.2	0.876
13	788.0	1953.	559.	1.52	0.440	3.47	0.998	1.023	0.4	0.8	0.817
14	848.6	1953.	557.	1.52	0.439	3.48	1.006	1.006	0.0	0.2	0.762
15	909.2	1956.	555.	1.53	0.437	3.50	1.006	1.023	0.4	0.4	0.715
16	969.8	1956.	552.	1.53	0.435	3.51	1.023	1.006	0.0	0.4	0.674
17	1030.4	1953.	550.	1.52	0.432	3.53	1.006	1.006	-0.4	0.4	0.636

TABLE C.1.31 : NUMERICAL EVALUATION OF EXPERIMENT EDI-S3-13/# 7

1	2	3	4	5	6	7	8	9	10	11	12
CYCLE NO.	REAL TIME	CONCENTRATION BOTTOM	TOP	CONCENTRATION NORMALIZED		SEPARATION FACTOR	CURRENT ENR.	CIAL.	CURRENT EFFICIENCY		POWER EFFICIENCY
NCYC (-)	T (SEC)	CB (PPM)	CT (PPM)	XB (-)	XT (-)	NS (-)	I1 (A)	I2 (A)	E1 (%)	E2 (%)	EP (%)
0	0.0	1270.	1262.	1.00	1.000	1.00	0.0	0.0	100.0	100.0	100.000
1	60.6	1466.	1019.	1.15	0.808	1.43	1.303	1.221	23.4	30.8	2.079
2	121.2	1626.	875.	1.28	0.693	1.85	1.303	1.254	19.0	17.9	1.736
3	181.8	1756.	764.	1.38	0.605	2.28	1.336	1.155	15.1	14.9	1.539
4	242.4	1844.	684.	1.45	0.542	2.68	1.320	1.155	10.3	10.7	1.358
5	303.1	1907.	626.	1.50	0.496	3.03	1.287	1.130	7.6	8.0	1.210
6	363.7	1953.	587.	1.54	0.465	3.31	1.213	1.163	5.9	5.2	1.084
7	424.3	1984.	557.	1.56	0.442	3.54	1.270	1.130	3.9	4.1	0.976
8	484.9	2010.	537.	1.58	0.425	3.72	1.295	1.064	3.1	3.0	0.887
9	545.5	2022.	522.	1.59	0.414	3.84	1.221	1.122	1.5	2.0	0.806
10	606.1	2033.	513.	1.60	0.407	3.93	1.229	1.122	1.5	1.2	0.738
11	666.7	2039.	506.	1.61	0.401	4.01	1.262	1.081	0.7	1.1	0.679
12	727.3	2042.	501.	1.61	0.397	4.05	1.270	1.072	0.4	0.7	0.628
13	788.0	2045.	497.	1.61	0.394	4.09	1.279	1.048	0.3	0.6	0.584
14	848.6	2045.	493.	1.61	0.391	4.12	1.237	1.204	0.0	0.5	0.543
15	909.2	2048.	490.	1.61	0.389	4.15	1.204	1.204	0.4	0.3	0.509

TABLE C.1.32 : NUMERICAL EVALUATION OF EXPERIMENT EDI-S3-13/# 8

1	2	3	4	5	6	7	8	9	10	11	12
CYCLE NO.	REAL TIME	CONCENTRATION BOTTOM	TOP	CONCENTRATION NORMALIZED		SEPARATION FACTOR	CURRENT ENR.	CIAL.	CURRENT EFFICIENCY		POWER EFFICIENCY
NCYC (-)	T (SEC)	CB (PPM)	CT (PPM)	XB (-)	XT (-)	NS (-)	I1 (A)	I2 (A)	E1 (%)	E2 (%)	EP (%)
0	0.0	1133.	1135.	1.00	1.000	1.00	0.0	0.0	100.0	100.0	100.000
1	60.6	1355.	890.	1.20	0.784	1.53	1.369	1.279	25.2	29.7	1.569
2	121.2	1533.	730.	1.35	0.643	2.10	1.361	1.328	20.3	18.7	1.346
3	181.8	1662.	617.	1.47	0.543	2.70	1.320	1.303	15.2	13.5	1.176
4	242.4	1761.	539.	1.56	0.475	3.27	1.287	1.320	11.9	9.1	1.036
5	303.1	1827.	484.	1.61	0.426	3.78	1.320	1.262	7.7	6.8	0.916
6	363.7	1875.	451.	1.66	0.398	4.16	1.312	1.270	5.7	3.9	0.812
7	424.3	1904.	424.	1.68	0.374	4.50	1.303	1.246	3.4	3.4	0.727
8	484.9	1933.	408.	1.71	0.359	4.75	1.295	1.254	3.4	2.1	0.657
9	545.5	1947.	400.	1.72	0.352	4.88	1.287	1.262	1.7	1.0	0.594
10	606.1	1961.	387.	1.73	0.341	5.08	1.270	1.287	1.8	1.6	0.545
11	666.7	1973.	384.	1.74	0.339	5.14	1.254	1.287	1.4	0.3	0.501
12	727.3	1981.	379.	1.75	0.334	5.24	1.237	1.287	1.1	0.6	0.464
14	848.6	1987.	377.	1.75	0.332	5.29	1.279	1.303	0.3	0.2	0.400
18	1091.0	1996.	372.	1.76	0.327	5.38	1.287	1.279	0.3	0.2	0.314
22	1333.5	2001.	374.	1.77	0.330	5.36	1.287	1.279	0.2	-0.1	0.258

TABLE C.1.33 : NUMERICAL EVALUATION OF EXPERIMENT EDI-S3-13/# 9

1	2	3	4	5	6	7	8	9	10	11	12
CYCLE NO.	REAL TIME	CONCENTRATION BOTTOM	TOP	CONCENTRATION NORMALIZED		SEPARATION FACTOR	CURRENT ENR.	CIAL.	CURRENT EFFICIENCY		POWER EFFICIENCY
NCYC (-)	T (SEC)	CB (PPM)	CT (PPM)	XB (-)	XT (-)	NS (-)	I1 (A)	I2 (A)	E1 (%)	E2 (%)	EP (%)
0	0.0	1057.	1045.	1.00	1.000	1.00	0.0	0.0	100.0	100.0	100.000
1	51.8	1103.	909.	1.04	0.870	1.20	0.965	0.946	8.7	26.0	1.952
2	103.6	1149.	841.	1.09	0.805	1.35	0.994	1.062	8.5	11.7	1.501
3	155.4	1190.	793.	1.13	0.759	1.48	1.042	1.013	7.1	8.5	1.274
4	207.2	1223.	756.	1.16	0.723	1.60	1.062	1.004	5.6	6.8	1.118
5	259.1	1248.	725.	1.18	0.694	1.70	1.013	1.033	4.4	5.4	0.999
6	310.9	1272.	703.	1.20	0.673	1.79	1.013	1.023	4.4	3.9	0.906
7	362.7	1289.	684.	1.22	0.654	1.86	1.013	1.052	3.0	3.3	0.824
8	414.5	1303.	668.	1.23	0.640	1.93	1.013	1.004	2.5	2.8	0.757
9	466.3	1314.	654.	1.24	0.626	1.99	1.023	1.013	2.0	2.5	0.700
10	518.1	1322.	645.	1.25	0.617	2.03	1.013	0.994	1.5	1.6	0.647
11	569.9	1330.	636.	1.26	0.609	2.07	1.033	1.004	1.5	1.6	0.603
12	621.7	1336.	628.	1.26	0.601	2.10	0.975	1.052	1.0	1.3	0.564
13	673.6	1341.	622.	1.27	0.595	2.13	1.013	0.994	1.0	1.2	0.530
14	725.4	1347.	618.	1.27	0.591	2.16	1.004	1.004	1.0	0.7	0.499
15	777.2	1350.	615.	1.28	0.589	2.17	0.994	1.004	0.5	0.5	0.470
16	829.0	1350.	611.	1.28	0.585	2.18	1.004	1.013	0.0	0.7	0.443
17	880.8	1350.	608.	1.28	0.581	2.20	0.965	1.033	0.0	0.7	0.419
18	932.6	1352.	606.	1.28	0.580	2.21	0.965	1.013	0.5	0.2	0.399
19	984.4	1352.	604.	1.28	0.578	2.22	0.994	0.994	0.0	0.5	0.379
20	1036.2	1352.	601.	1.28	0.575	2.22	1.004	0.994	0.0	0.5	0.362
21	1088.1	1352.	597.	1.28	0.572	2.24	0.984	0.984	0.0	0.7	0.347
22	1139.9	1352.	597.	1.28	0.572	2.24	0.984	0.994	0.0	0.0	0.332
23	1191.7	1352.	596.	1.28	0.570	2.24	0.994	0.984	0.0	0.2	0.318

TABLE C.1.34 : NUMERICAL EVALUATION OF EXPERIMENT EDI-S3-13/#10

1	2	3	4	5	6	7	8	9	10	11	12
CYCLE NO.	REAL TIME	CONCENTRATION BOTTOM	TOP	CONCENTRATION NORMALIZED		SEPARATION FACTOR	CURRENT ENR.	CIAL.	CURRENT EFFICIENCY		POWER EFFICIENCY
NCYC (-)	T (SEC)	CB (PPM)	CT (PPM)	XB (-)	XT (-)	NS (-)	I1 (A)	I2 (A)	E1 (%)	E2 (%)	EP (%)
0	0.0	1196.	1187.	1.00	1.000	1.00	0.0	0.0	100.0	100.0	100.000
1	60.6	1339.	984.	1.12	0.829	1.35	1.056	0.990	21.0	31.7	2.799
2	121.2	1458.	862.	1.22	0.726	1.68	1.023	1.056	18.1	18.0	2.339
3	181.8	1553.	770.	1.30	0.649	2.00	1.023	1.023	14.4	13.9	2.054
4	242.4	1629.	699.	1.36	0.589	2.31	1.015	0.990	11.6	11.1	1.843
5	303.1	1682.	648.	1.41	0.546	2.58	0.990	0.990	8.4	8.1	1.653
6	363.7	1725.	613.	1.44	0.516	2.79	0.973	0.990	6.8	5.5	1.489
7	424.3	1756.	583.	1.47	0.491	2.99	0.957	0.973	5.0	4.7	1.356
8	484.9	1779.	562.	1.49	0.474	3.14	0.932	0.957	3.8	3.3	1.240
9	545.5	1790.	548.	1.50	0.462	3.24	0.924	0.982	1.9	2.2	1.131
10	606.1	1801.	533.	1.51	0.449	3.36	0.957	0.940	1.8	2.6	1.045
11	666.7	1807.	528.	1.51	0.445	3.40	0.949	0.940	0.9	0.9	0.962
12	727.3	1813.	519.	1.52	0.437	3.47	0.949	0.949	0.9	1.5	0.895
13	788.0	1818.	515.	1.52	0.434	3.51	0.949	0.932	0.9	0.6	0.835
14	848.6	1821.	511.	1.52	0.430	3.54	0.957	0.932	0.5	0.6	0.781
15	909.2	1821.	507.	1.52	0.427	3.57	0.940	0.957	0.0	0.6	0.733
16	969.8	1821.	503.	1.52	0.424	3.59	0.924	0.957	0.0	0.6	0.691
17	1030.4	1821.	503.	1.52	0.424	3.59	0.957	0.907	0.0	0.0	0.652
18	1091.0	1821.	503.	1.52	0.424	3.59	0.957	0.957	0.0	0.0	0.616

TABLE C.1.35 : NUMERICAL EVALUATION OF EXPERIMENT EDI-S3-13/#11

1	2	3	4	5	6	7	8	9	10	11	12
CYCLE NO.	REAL TIME	CONCENTRATION BOTTOM	TOP	CONCENTRATION NORMALIZED		SEPARATION FACTOR	CURRENT ENR.	DIAL.	CURRENT EFFICIENCY		POWER EFFICIENCY
NCYC (-)	T (SEC)	CB (PPM)	CT (PPM)	XB (-)	XT (-)	NS (-)	I1 (A)	I2 (A)	E1 (%)	E2 (%)	EP (%)
0	0.0	1314.	1284.	1.00	1.000	1.00	0.0	C.0	100.0	100.0	100.000
1	70.6	1542.	1032.	1.17	C.804	1.46	1.034	C.942	29.3	35.5	3.527
2	141.2	1722.	868.	1.31	C.676	1.94	0.977	C.963	24.5	22.6	2.983
3	211.8	185C.	747.	1.41	0.582	2.42	0.921	C.977	18.5	16.5	2.599
4	282.4	1938.	660.	1.48	C.515	2.87	0.921	C.921	12.8	12.5	2.291
5	353.1	1996.	604.	1.52	C.47C	3.23	0.921	C.906	8.3	8.3	2.018
6	423.7	2042.	56C.	1.55	C.436	3.56	0.913	C.892	6.7	6.5	1.806
7	494.3	2068.	529.	1.57	C.412	3.82	0.878	C.885	3.9	4.7	1.624
8	564.9	2091.	512.	1.59	C.399	3.99	0.864	C.892	3.6	2.5	1.469
9	635.5	2103.	502.	1.60	C.391	4.09	0.871	C.892	1.8	1.5	1.331
10	706.1	2108.	498.	1.60	0.388	4.14	0.878	C.871	0.9	0.6	1.211
12	847.3	2117.	488.	1.61	C.38C	4.24	0.857	C.871	0.7	C.8	1.031
14	988.6	2117.	476.	1.61	C.371	4.34	0.864	C.871	0.0	C.9	0.897
16	1129.8	2117.	472.	1.61	0.368	4.38	0.864	C.864	0.0	C.3	0.791
18	1271.0	2117.	477.	1.61	0.372	4.33	0.871	C.850	0.0	-0.4	0.704
20	1412.2	2114.	477.	1.61	0.372	4.33	0.871	C.864	-0.2	C.0	0.634

TABLE C.1.36 : NUMERICAL EVALUATION OF EXPERIMENT EDI-S3-13/#12

1	2	3	4	5	6	7	8	9	10	11	12
CYCLE NO.	REAL TIME	CONCENTRATION BOTTOM	TOP	CONCENTRATION NORMALIZED		SEPARATION FACTOR	CURRENT ENR.	DIAL.	CURRENT EFFICIENCY		POWER EFFICIENCY
NCYC (-)	T (SEC)	CB (PPM)	CT (PPM)	XB (-)	XT (-)	NS (-)	I1 (A)	I2 (A)	E1 (%)	E2 (%)	EP (%)
0	0.0	1207.	1206.	1.00	1.000	1.00	0.0	0.0	100.0	100.0	100.000
1	90.6	1508.	924.	1.25	0.766	1.63	0.817	C.789	38.3	37.1	3.912
2	181.2	1705.	73C.	1.41	C.605	2.33	0.767	C.773	26.6	26.0	3.338
3	271.8	1833.	606.	1.52	0.503	3.02	0.734	C.745	18.0	17.2	2.863
4	362.4	1918.	528.	1.59	C.437	3.63	0.695	C.723	12.8	11.3	2.489
5	453.1	1973.	476.	1.64	C.395	4.14	0.684	C.717	8.3	7.5	2.178
6	543.7	2010.	446.	1.67	C.370	4.50	0.657	C.679	5.9	4.5	1.930
7	634.3	2033.	428.	1.69	C.355	4.75	0.690	C.712	3.5	2.6	1.709
8	724.9	2045.	413.	1.69	0.342	4.95	0.684	C.673	1.7	2.4	1.534
9	815.5	2053.	410.	1.70	0.340	5.00	0.662	C.673	1.4	C.4	1.384
10	906.1	2059.	408.	1.71	0.338	5.05	0.662	C.668	0.9	0.4	1.261
11	996.7	2062.	401.	1.71	C.333	5.14	0.662	C.706	0.5	0.9	1.157
12	1087.3	2062.	399.	1.71	0.330	5.17	0.640	C.662	0.0	0.4	1.070
13	1178.0	2062.	392.	1.71	C.325	5.26	0.673	C.662	0.0	1.0	0.996
14	1268.6	2062.	397.	1.71	C.329	5.19	0.712	C.668	0.0	-0.8	0.922
15	1359.2	2062.	393.	1.71	C.326	5.24	0.712	C.651	0.0	C.6	0.865
16	1449.8	2062.	397.	1.71	0.329	5.19	0.712	C.651	0.0	-0.6	0.810
17	1540.4	2062.	396.	1.71	C.328	5.20	0.712	C.651	0.0	C.2	0.764
18	1631.0	2062.	395.	1.71	C.327	5.22	0.712	C.640	0.0	0.2	0.723
19	1721.6	2062.	391.	1.71	0.324	5.27	0.712	C.673	0.0	C.6	0.687

TABLE C.1.37 : NUMERICAL EVALUATION OF EXPERIMENT EDI-S3-13/#13

1	2	3	4	5	6	7	8	9	10	11	12
CYCLE NO.	REAL TIME	CONCENTRATION BOTTOM	TOP	CONCENTRATION NORMALIZED		SEPARATION FACTOR	CURRENT ENR.	DIAL.	CURRENT EFFICIENCY		POWER EFFICIENCY
NCYC (-)	T (SEC)	CB (PPM)	CT (PPM)	XB (-)	XT (-)	NS (-)	I1 (A)	I2 (A)	E1 (%)	E2 (%)	EP (%)
0	0.0	1125.	1126.	1.00	1.000	1.00	0.0	C.0	100.0	100.0	100.000
1	110.6	1455.	827.	1.29	0.734	1.76	0.637	C.610	44.0	41.6	4.476
2	221.2	1660.	626.	1.48	0.556	2.66	0.610	C.592	28.5	28.9	3.763
3	331.8	1787.	511.	1.59	0.454	3.50	0.561	C.570	19.3	17.1	3.185
4	442.4	1867.	436.	1.66	C.387	4.29	0.542	C.542	12.5	11.7	2.746
5	553.1	1915.	392.	1.70	0.348	4.89	0.533	C.533	7.7	7.0	2.383
6	663.7	1950.	373.	1.73	0.331	5.24	0.506	C.524	5.8	3.1	2.091
7	774.3	1967.	359.	1.75	0.318	5.49	0.533	C.497	2.7	2.4	1.851
8	884.9	1984.	350.	1.76	C.310	5.68	0.515	C.515	2.8	1.5	1.661
9	995.5	1990.	343.	1.77	C.305	5.81	0.520	C.515	0.9	1.1	1.499
10	1106.1	1999.	344.	1.78	C.306	5.81	0.515	C.511	1.4	-C.2	1.362
11	1216.7	2001.	342.	1.78	C.304	5.86	0.520	C.506	0.5	C.4	1.249
12	1327.3	2010.	342.	1.79	C.304	5.89	0.506	C.506	1.4	C.0	1.157
13	1438.0	2016.	339.	1.79	0.301	5.95	0.497	C.502	1.0	0.4	1.079

TABLE C.1.38 : NUMERICAL EVALUATION OF EXPERIMENT EDI-S3-13/#14

1	2	3	4	5	6	7	8	9	10	11	12
CYCLE NO.	REAL TIME	CONCENTRATION BOTTOM	TOP	CONCENTRATION NORMALIZED		SEPARATION FACTOR	CURRENT ENR.	DIAL.	CURRENT EFFICIENCY		POWER EFFICIENCY
NCYC (-)	T (SEC)	CB (PPM)	CT (PPM)	XB (-)	XT (-)	NS (-)	I1 (A)	I2 (A)	E1 (%)	E2 (%)	EP (%)
0	0.0	1281.	1267.	1.00	1.000	1.00	0.0	C.0	100.0	100.0	100.000
1	68.3	1450.	1127.	1.13	0.890	1.27	0.820	C.776	28.3	24.7	1.425
2	136.6	1587.	998.	1.24	0.788	1.57	0.790	C.776	23.8	22.9	1.314
3	205.0	1725.	890.	1.35	C.703	1.92	0.790	C.790	24.0	18.8	1.242
4	273.3	1855.	792.	1.45	C.625	2.32	0.776	C.790	23.2	17.1	1.190
5	341.6	1970.	713.	1.54	0.563	2.73	0.790	C.746	19.9	14.5	1.130
6	409.9	2076.	648.	1.62	0.511	3.17	0.754	C.732	19.4	12.4	1.080
7	478.2	2166.	591.	1.69	C.466	3.63	0.739	C.732	16.7	10.7	1.028
8	546.6	2254.	553.	1.76	0.437	4.03	0.717	C.710	16.7	7.2	0.979
9	614.9	2321.	501.	1.81	0.395	4.59	0.703	C.688	13.2	10.6	0.942
10	683.2	2386.	466.	1.86	C.368	5.07	0.681	C.703	13.0	6.8	0.901
12	819.9	2480.	414.	1.94	0.327	5.92	0.673	C.659	9.6	5.4	0.823
16	1093.1	2602.	352.	2.03	0.278	7.31	0.629	C.651	6.6	3.3	0.695
20	1366.4	2688.	324.	2.10	C.256	8.21	0.651	C.622	4.6	1.6	0.596
24	1639.7	2724.	311.	2.13	0.245	8.67	0.637	C.622	1.9	0.7	0.515
28	1913.0	2736.	303.	2.14	0.239	8.93	0.629	C.615	0.7	0.4	0.451

TABLE C.1.39 : NUMERICAL EVALUATION OF EXPERIMENT EDI-S3-13/#15

1	2	3	4	5	6	7	8	9	10	11	12
CYCLE NO.	REAL TIME	CONCENTRATION BOTTOM	CONCENTRATION TOP	CONCENTRATION NORMALIZED		SEPARATION FACTOR	CURRENT ENR. CIAL.		CURRENT EFFICIENCY		POWER EFFICIENCY
NCYC (-)	T (SEC)	CB (PPM)	CT (PPM)	XB (-)	XT (-)	NS (-)	I1 (A)	I2 (A)	E1 (%)	E2 (%)	EP (%)
0	0.0	1286.	1277.	1.00	1.000	1.00	0.0	C.0	100.0	100.0	100.000
1	37.1	1450.	1152.	1.13	C.902	1.25	1.212	1.010	34.1	31.3	1.737
2	74.3	1598.	1035.	1.24	0.810	1.53	1.010	1.104	37.1	26.9	1.683
3	111.4	1733.	934.	1.35	C.731	1.84	1.050	1.037	32.6	24.5	1.611
4	148.6	1858.	844.	1.44	C.661	2.19	1.063	C.969	29.7	23.6	1.552
5	185.7	1967.	764.	1.53	0.598	2.56	0.983	1.010	28.0	20.0	1.490
6	222.9	2053.	697.	1.60	C.545	2.93	0.929	1.037	23.5	16.4	1.414
7	260.0	2140.	641.	1.66	C.502	3.31	0.969	C.929	22.6	15.1	1.355
8	297.1	2236.	588.	1.74	0.461	3.77	0.942	C.969	25.8	13.8	1.313
9	334.3	2280.	548.	1.77	0.429	4.13	0.915	C.888	12.1	11.4	1.243
10	371.4	2330.	512.	1.81	0.401	4.52	0.862	C.915	14.6	10.0	1.188
12	445.7	2424.	454.	1.88	C.356	5.30	0.902	C.862	13.2	8.5	1.093
14	520.0	2486.	414.	1.93	0.324	5.96	0.808	C.902	9.7	5.6	1.003
16	594.3	2533.	387.	1.97	C.303	6.50	0.848	C.875	7.1	3.9	0.921
18	668.6	2572.	365.	2.00	0.286	6.99	0.835	C.821	5.8	3.4	0.853
22	817.1	2628.	342.	2.04	C.268	7.63	0.821	C.808	4.4	1.8	0.740
26	965.7	2652.	326.	2.06	0.256	8.07	0.821	C.808	1.8	1.2	0.647
30	1114.3	2664.	321.	2.07	0.252	8.24	0.781	C.808	1.0	C.4	0.574
34	1262.8	2670.	317.	2.08	0.248	8.35	0.781	C.821	0.5	0.3	0.514

TABLE C.1.4C : NUMERICAL EVALUATION OF EXPERIMENT EDI-S3-13/#16

1	2	3	4	5	6	7	8	9	10	11	12
CYCLE NO.	REAL TIME	CONCENTRATION BOTTOM	CONCENTRATION TOP	CONCENTRATION NORMALIZED		SEPARATION FACTOR	CURRENT ENR. CIAL.		CURRENT EFFICIENCY		POWER EFFICIENCY
NCYC (-)	T (SEC)	CB (PPM)	CT (PPM)	XB (-)	XT (-)	NS (-)	I1 (A)	I2 (A)	E1 (%)	E2 (%)	EP (%)
0	0.0	1283.	1276.	1.00	1.000	1.00	0.0	C.0	100.0	100.0	100.000
1	33.0	1450.	1153.	1.13	C.904	1.25	1.062	1.107	44.6	31.5	1.996
2	65.9	1598.	1040.	1.24	0.815	1.53	1.138	1.092	37.1	29.6	1.851
3	98.9	1733.	933.	1.35	C.731	1.85	1.123	1.077	34.4	28.3	1.769
4	131.8	1853.	849.	1.44	0.665	2.17	1.032	C.971	33.0	24.6	1.701
5	164.8	1961.	765.	1.53	0.600	2.55	0.925	1.062	33.5	27.5	1.647
6	197.8	2056.	697.	1.60	C.546	2.93	0.971	1.016	27.9	19.2	1.576
7	230.7	2140.	641.	1.67	0.503	3.32	0.925	C.956	25.8	16.5	1.512
8	263.7	2210.	590.	1.72	0.462	3.73	0.971	C.910	20.5	16.2	1.446
9	296.6	2277.	546.	1.77	C.428	4.15	0.910	C.880	21.0	14.2	1.393
10	329.6	2323.	517.	1.82	0.401	4.53	0.880	C.910	18.0	10.5	1.333
15	494.4	2518.	397.	1.96	0.311	6.30	0.880	C.850	12.0	7.7	1.084
20	659.2	2611.	347.	2.03	0.272	7.48	0.774	C.834	6.8	3.4	0.902
25	824.0	2658.	325.	2.07	0.255	8.13	0.804	C.789	3.4	1.6	0.764
30	988.8	2682.	316.	2.09	0.248	8.44	0.758	C.774	1.8	0.7	0.661
35	1153.6	2688.	312.	2.09	0.245	8.56	0.834	C.758	0.4	0.3	0.576
40	1318.4	2694.	308.	2.10	0.242	8.69	0.789	C.758	0.4	0.3	0.512
45	1483.2	2700.	308.	2.10	0.242	8.71	0.789	C.789	0.4	0.0	0.460

TABLE C.1.4I : NUMERICAL EVALUATION OF EXPERIMENT EDI-S3-13/#17

1	2	3	4	5	6	7	8	9	10	11	12
CYCLE NO.	REAL TIME	CONCENTRATION BOTTOM	TOP	CONCENTRATION NORMALIZED		SEPARATION FACTOR	CURRENT ENR.	DIAL.	CURRENT EFFICIENCY		POWER EFFICIENCY
NCYC (-)	T (SEC)	CB (PPM)	CT (PPM)	XB (-)	XT (-)	NS (-)	I1 (A)	I2 (A)	E1 (%)	E2 (%)	EP (%)
0	0.0	1179.	1178.	1.00	1.000	1.00	0.0	0.0	100.0	100.0	100.000
1	30.1	1228.	1062.	1.13	0.901	1.25	1.112	0.946	41.6	38.3	2.091
2	60.3	1466.	960.	1.24	0.815	1.53	0.979	1.078	44.2	29.5	1.989
3	90.4	1595.	862.	1.35	0.732	1.85	0.913	1.045	43.9	29.2	1.949
4	120.5	1710.	774.	1.45	0.657	2.21	0.929	0.979	38.0	27.9	1.894
5	150.7	1807.	702.	1.53	0.596	2.57	0.913	0.929	32.9	24.2	1.816
6	180.8	1895.	637.	1.61	0.541	2.97	0.913	0.913	30.2	22.0	1.744
7	210.9	1976.	587.	1.68	0.498	3.36	0.896	0.946	27.9	18.5	1.674
8	241.1	2071.	541.	1.76	0.459	3.83	0.796	0.946	37.2	15.3	1.630
9	271.2	2103.	501.	1.78	0.425	4.20	0.879	0.780	11.3	16.0	1.540
10	301.4	2155.	467.	1.83	0.396	4.61	0.796	0.879	20.4	11.9	1.475
15	452.0	2324.	361.	1.97	0.307	6.43	0.796	0.780	13.2	8.5	1.203
20	602.7	2412.	317.	2.05	0.269	7.59	0.697	0.796	7.9	3.4	1.001
25	753.4	2456.	297.	2.08	0.252	8.27	0.763	0.697	3.6	1.8	0.848
30	904.1	2468.	288.	2.09	0.244	8.57	0.763	0.697	1.0	0.8	0.727
35	1054.7	2483.	284.	2.11	0.241	8.74	0.730	0.697	1.3	0.3	0.639
40	1205.4	2489.	283.	2.11	0.240	8.80	0.747	0.697	0.5	0.1	0.568
45	1356.1	2498.	283.	2.12	0.240	8.83	0.713	0.697	0.8	0.0	0.512

TABLE C.1.42 : NUMERICAL EVALUATION OF EXPERIMENT EDI-S3-13/#18

1	2	3	4	5	6	7	8	9	10	11	12
CYCLE NO.	REAL TIME	CONCENTRATION BOTTOM	TOP	CONCENTRATION NORMALIZED		SEPARATION FACTOR	CURRENT ENR.	DIAL.	CURRENT EFFICIENCY		POWER EFFICIENCY
NCYC (-)	T (SEC)	CB (PPM)	CT (PPM)	XB (-)	XT (-)	NS (-)	I1 (A)	I2 (A)	E1 (%)	E2 (%)	EP (%)
0	0.0	1204.	1195.	1.00	1.000	1.00	0.0	0.0	100.0	100.0	100.000
1	26.5	1226.	1143.	1.02	0.957	1.06	1.717	1.585	4.5	11.5	0.462
2	53.0	1242.	1075.	1.03	0.900	1.15	1.679	1.792	3.5	13.5	0.457
3	79.5	1259.	1036.	1.05	0.867	1.21	1.754	1.792	3.3	7.7	0.400
4	106.0	1281.	1001.	1.06	0.838	1.27	1.754	1.735	4.4	7.1	0.375
5	132.5	1297.	973.	1.08	0.814	1.32	1.717	1.735	3.4	5.8	0.349
6	159.0	1319.	944.	1.10	0.790	1.39	1.754	1.754	4.5	5.7	0.335
7	185.5	1339.	921.	1.11	0.771	1.44	1.679	1.792	4.1	4.6	0.320
8	212.0	1352.	900.	1.12	0.754	1.49	1.735	1.792	2.8	4.1	0.302
9	238.6	1372.	880.	1.14	0.737	1.55	1.717	1.698	4.0	4.3	0.293
10	265.1	1386.	862.	1.15	0.721	1.60	1.698	1.754	2.9	3.6	0.281
15	397.6	1433.	791.	1.19	0.662	1.80	1.735	1.735	1.9	2.9	0.230
20	530.1	1472.	744.	1.22	0.623	1.96	1.660	1.698	1.7	1.9	0.197
25	662.7	1494.	711.	1.24	0.595	2.09	1.622	1.679	1.0	1.4	0.171
30	795.2	1503.	688.	1.25	0.576	2.17	1.660	1.622	0.4	1.0	0.150
35	927.7	1514.	672.	1.26	0.563	2.23	1.603	1.622	0.5	0.7	0.134
40	1060.2	1517.	658.	1.26	0.551	2.29	1.622	1.660	0.1	0.6	0.120
45	1192.8	1517.	648.	1.26	0.542	2.32	1.622	1.585	0.0	0.5	0.108
50	1325.3	1517.	645.	1.26	0.540	2.33	1.641	1.603	0.0	0.1	0.098

TABLE C.1.43 : NUMERICAL EVALUATION OF EXPERIMENT EDI-S3-13/#19

1	2	3	4	5	6	7	8	9	10	11	12
CYCLE NO.	REAL TIME	CONCENTRATION BOTTOM	TOP	CONCENTRATION NORMALIZED		SEPARATION FACTOR	CURRENT ENR. DIAL.		CURRENT EFFICIENCY		POWER EFFICIENCY
NCYC (-)	T (SEC)	CB (PPM)	CT (PPM)	XB (-)	XT (-)	NS (-)	I1 (A)	I2 (A)	E1 (%)	E2 (%)	EP (%)
0	0.0	1182.	1183.	1.00	1.000	1.00	0.0	0.0	100.0	100.0	100.000
1	89.8	1264.	1071.	1.07	0.905	1.18	0.662	0.640	13.0	18.3	0.809
2	179.6	1325.	982.	1.12	0.830	1.35	0.668	0.679	9.5	13.7	0.707
3	269.5	1383.	908.	1.17	0.768	1.52	0.679	0.685	8.9	11.2	0.647
4	359.3	1450.	850.	1.23	0.719	1.71	0.685	0.679	10.2	8.9	0.609
5	449.1	1491.	797.	1.26	0.674	1.87	0.668	0.679	6.5	8.1	0.565
6	538.9	1550.	751.	1.31	0.635	2.07	0.651	0.668	9.4	7.3	0.544
7	628.7	1598.	712.	1.35	0.602	2.25	0.651	0.685	7.7	5.9	0.517
8	718.5	1646.	675.	1.39	0.570	2.44	0.646	0.685	7.7	5.7	0.496
9	808.4	1688.	644.	1.43	0.544	2.62	0.651	0.668	6.8	4.8	0.475
10	898.2	1725.	614.	1.46	0.519	2.81	0.657	0.646	5.9	4.8	0.456
12	1077.8	1787.	569.	1.51	0.481	3.14	0.657	0.646	5.0	3.7	0.419
14	1257.4	1838.	534.	1.56	0.451	3.44	0.640	0.635	4.2	2.9	0.386
16	1437.1	1887.	507.	1.60	0.429	3.72	0.623	0.635	4.1	2.2	0.360
18	1616.7	1913.	486.	1.62	0.411	3.94	0.623	0.640	2.2	1.7	0.332
20	1796.4	1944.	468.	1.64	0.396	4.16	0.623	0.612	2.6	1.5	0.311
25	2245.4	1996.	442.	1.69	0.374	4.51	0.618	0.618	1.7	0.9	0.264
30	2694.5	2019.	428.	1.71	0.362	4.72	0.601	0.612	0.8	0.5	0.228
35	3143.6	2033.	421.	1.72	0.356	4.84	0.618	0.596	0.5	0.3	0.199
40	3592.7	2033.	414.	1.72	0.350	4.91	0.562	0.629	0.0	0.2	0.176
45	4041.8	2033.	414.	1.72	0.350	4.91	0.612	0.590	0.0	0.0	0.157

TABLE C.1.44 : NUMERICAL EVALUATION OF EXPERIMENT EDI-S3-13/420

1	2	3	4	5	6	7	8	9	10	11	12
CYCLE NO.	REAL TIME	CONCENTRATION BOTTOM	TOP	CONCENTRATION NORMALIZED		SEPARATION FACTOR	CURRENT ENR. DIAL.		CURRENT EFFICIENCY		POWER EFFICIENCY
NCYC (-)	T (SEC)	CB (PPM)	CT (PPM)	XB (-)	XT (-)	NS (-)	I1 (A)	I2 (A)	E1 (%)	E2 (%)	EP (%)
0	0.0	1207.	1206.	1.00	1.000	1.00	0.0	0.0	100.0	100.0	100.000
5	70.8	1187.	1169.	0.98	0.969	1.02	1.568	1.554	-1.6	3.2	0.041
10	141.6	1168.	1165.	0.97	0.966	1.00	1.695	1.660	-1.5	0.3	0.004
15	212.4	1155.	1161.	0.96	0.963	0.99	1.589	1.660	-1.1	0.3	-0.005
20	283.2	1149.	1156.	0.95	0.958	0.99	1.624	1.624	-0.4	0.4	-0.004
25	354.0	1141.	1147.	0.95	0.951	0.99	1.624	1.695	-0.7	0.7	-0.002
30	424.8	1133.	1140.	0.94	0.945	0.99	1.695	1.660	-0.6	0.5	-0.003
40	566.4	1125.	1126.	0.93	0.934	1.00	1.554	1.660	-0.3	0.6	-0.000
50	708.0	1119.	1116.	0.93	0.925	1.00	1.695	1.638	-0.2	0.4	0.001
60	849.6	1114.	1106.	0.92	0.917	1.01	1.695	1.624	-0.2	0.4	0.001
70	991.2	1108.	1094.	0.92	0.907	1.01	1.695	1.624	-0.2	0.5	0.002
80	1132.8	1106.	1084.	0.92	0.898	1.02	1.589	1.624	-0.1	0.4	0.003
90	1274.4	1103.	1075.	0.91	0.891	1.03	1.518	1.624	-0.1	0.4	0.003
100	1416.0	1100.	1068.	0.91	0.886	1.03	1.695	1.624	-0.1	0.3	0.003
120	1699.2	1097.	1054.	0.91	0.874	1.04	1.481	1.624	-0.1	0.3	0.004
140	1982.5	1092.	1042.	0.90	0.864	1.05	1.624	1.624	-0.1	0.2	0.004
160	2265.7	1086.	1032.	0.90	0.856	1.05	1.765	1.624	-0.1	0.2	0.004

TABLE C.1.45 : NUMERICAL EVALUATION OF EXPERIMENT EDI-S3-13/421

1	2	3	4	5	6	7	8	9	10	11	12
CYCLE NO.	REAL TIME	CONCENTRATION BOTTOM	CONCENTRATION TOP	CONCENTRATION NORMALIZED		SEPARATION FACTOR	CURRENT ENR.	CURRENT DIAL.	CURRENT EFFICIENCY		POWER EFFICIENCY
NCYC (-)	T (SEC)	CB (PPM)	CT (PPM)	XB (-)	XT (-)	NS (-)	I1 (A)	I2 (A)	E1 (%)	E2 (%)	EP (%)
0	0.0	1237.	1237.	1.CO	1.CCC	1.CO	0.0	C.0	100.0	100.0	100.000
1	60.6	145C.	1004.	1.17	0.811	1.44	1.188	1.089	27.8	33.2	2.303
2	121.2	1575.	854.	1.27	0.69C	1.85	1.180	1.147	16.5	2C.2	1.848
3	181.8	1696.	743.	1.37	C.601	2.28	1.155	1.130	16.2	15.2	1.634
4	242.4	1784.	662.	1.44	0.535	2.70	1.155	1.089	11.8	11.6	1.453
5	3C3.1	1847.	604.	1.49	0.488	3.06	1.105	1.089	8.8	8.3	1.299
6	363.7	1892.	562.	1.53	0.455	3.17	1.048	1.138	6.8	5.6	1.165
7	424.3	1924.	535.	1.56	0.433	3.59	1.081	1.081	4.5	3.9	1.050
8	484.9	1947.	516.	1.57	0.417	3.77	1.031	1.097	3.4	2.7	0.953
9	545.5	1961.	501.	1.59	0.405	3.92	1.081	1.064	2.1	2.3	0.868
1C	6C6.1	197C.	484.	1.59	C.391	4.07	1.039	1.064	1.3	2.4	0.8C0
11	666.7	1981.	482.	1.60	C.390	4.11	1.072	1.039	1.7	0.2	0.736
12	727.3	1987.	48C.	1.61	C.388	4.14	1.081	1.039	0.8	C.4	0.6P0
13	788.0	1990.	472.	1.61	0.382	4.22	1.039	1.048	0.4	1.1	0.635
14	848.6	1990.	470.	1.61	0.380	4.24	1.064	1.056	0.0	0.4	0.592
15	9C9.2	199C.	467.	1.61	0.377	4.26	1.039	1.064	0.0	0.4	0.555
16	969.8	199C.	466.	1.61	0.376	4.27	1.064	1.039	0.0	0.2	0.522
17	1C30.4	199C.	464.	1.61	0.375	4.29	1.039	1.081	0.0	0.2	0.492
18	1C91.0	199C.	464.	1.61	0.375	4.29	1.056	1.039	0.0	0.0	0.466

TABLE C.1.46 : NUMERICAL EVALUATION OF EXPERIMENT
EDI-S3-13/#22

1	2	3	4	5	6	7	8	9	10	11	12
CYCLE NO.	REAL TIME	CONCENTRATION BOTTOM	CONCENTRATION TOP	CONCENTRATION NORMALIZED		SEPARATION FACTOR	CURRENT ENR.	CURRENT DIAL.	CURRENT EFFICIENCY		POWER EFFICIENCY
NCYC (-)	T (SEC)	CB (PPM)	CT (PPM)	XB (-)	XT (-)	NS (-)	I1 (A)	I2 (A)	E1 (%)	E2 (%)	EP (%)
0	0.0	1295.	1258.	1.CC	1.CCO	1.CO	0.0	C.0	100.0	100.0	100.000
1	27.1	1405.	1133.	1.C9	0.901	1.21	1.4C0	1.584	27.3	27.3	1.626
2	54.3	1511.	1032.	1.17	0.821	1.42	1.529	1.511	23.9	23.1	1.416
3	81.4	1603.	942.	1.24	C.749	1.65	1.547	1.455	20.7	21.5	1.307
4	1C8.6	1705.	86C.	1.32	0.684	1.93	1.529	1.400	23.0	2C.1	1.259
5	135.7	1796.	791.	1.39	0.629	2.21	1.474	1.455	21.3	16.6	1.203
10	271.4	2175.	533.	1.68	C.424	3.97	1.179	1.437	22.3	12.4	1.046
15	4C7.1	2400.	402.	1.85	0.32C	5.79	1.29C	1.142	12.1	7.9	0.887
20	542.8	2521.	339.	1.95	0.270	7.22	1.105	1.179	7.6	3.7	0.754
25	678.5	2578.	31C.	1.99	0.246	8.09	1.197	1.087	3.3	1.9	0.641
30	814.3	2611.	297.	2.C2	0.236	8.55	1.105	1.105	2.0	0.8	0.556
35	95C.0	2617.	288.	2.02	0.229	8.84	1.105	1.105	0.4	0.6	0.488
4C	1C85.7	2622.	286.	2.03	0.228	8.90	1.105	1.105	0.4	0.1	0.433

TABLE C.1.47 : NUMERICAL EVALUATION OF EXPERIMENT
EDI-S3-13/#24

1	2	3	4	5	6	7	8	9	10	11	12
CYCLE NO.	REAL TIME	CONCENTRATION BOTTOM	CONCENTRATION TOP	CONCENTRATION NORMALIZED		SEPARATION FACTOR	CURRENT ENR.	CIAL.	CURRENT EFFICIENCY		POWER EFFICIENCY
NCYC (-)	T (SEC)	CB (PPM)	CT (PPM)	XB (-)	XT (-)	NS (-)	I1 (A)	I2 (A)	E1 (%)	E2 (%)	EP (%)
0	0.0	1289.	1254.	1.00	1.000	1.00	0.0	0.0	100.0	100.0	100.000
1	37.1	1452.	1131.	1.13	0.902	1.25	1.230	0.996	33.4	31.1	1.865
2	74.3	1598.	1014.	1.24	0.809	1.53	1.131	1.077	32.5	27.6	1.705
3	111.4	1739.	913.	1.35	0.728	1.85	1.131	1.023	31.5	24.9	1.621
4	148.6	1858.	820.	1.44	0.654	2.20	1.037	1.050	29.1	22.4	1.548
5	185.7	1976.	746.	1.53	0.595	2.58	1.037	1.010	28.6	18.7	1.484
10	371.4	2368.	488.	1.84	0.389	4.72	0.848	0.969	23.4	13.5	1.228
15	557.1	2566.	373.	1.99	0.297	6.70	0.821	0.929	12.2	6.3	0.994
20	742.8	2667.	322.	2.07	0.257	8.05	0.700	0.969	7.3	2.6	0.822
25	928.5	2715.	301.	2.11	0.240	8.79	0.713	0.942	3.4	1.2	0.692
30	1114.3	2736.	292.	2.12	0.233	9.13	0.862	0.808	1.2	0.6	0.591
35	1300.0	2754.	286.	2.14	0.228	9.35	0.660	0.969	1.4	0.3	0.518

TABLE C.1.48 : NUMERICAL EVALUATION OF EXPERIMENT EDI-S3-13/825

1	2	3	4	5	6	7	8	9	10	11	12
CYCLE NO.	REAL TIME	CONCENTRATION BOTTOM	CONCENTRATION TOP	CONCENTRATION NORMALIZED		SEPARATION FACTOR	CURRENT ENR.	CIAL.	CURRENT EFFICIENCY		POWER EFFICIENCY
NCYC (-)	T (SEC)	CB (PPM)	CT (PPM)	XB (-)	XT (-)	NS (-)	I1 (A)	I2 (A)	E1 (%)	E2 (%)	EP (%)
0	0.0	1292.	1264.	1.00	1.000	1.00	0.0	0.0	100.0	100.0	100.000
1	37.1	1388.	1187.	1.07	0.939	1.14	0.808	0.727	30.3	26.9	3.754
2	74.3	1483.	1107.	1.15	0.876	1.31	0.808	0.862	29.6	23.5	3.352
3	111.4	1570.	1036.	1.22	0.819	1.48	0.754	0.700	29.1	25.6	3.271
4	148.6	1654.	968.	1.28	0.765	1.67	0.687	0.673	31.1	25.7	3.255
5	185.7	1727.	909.	1.34	0.719	1.86	0.673	0.619	27.6	23.7	3.193
10	371.4	2007.	690.	1.55	0.546	2.85	0.538	0.673	26.3	16.5	2.812
15	557.1	2178.	568.	1.69	0.449	3.76	0.538	0.619	16.0	10.0	2.401
20	742.8	2268.	503.	1.76	0.398	4.41	0.512	0.619	8.9	5.3	2.033
25	928.5	2318.	467.	1.79	0.369	4.86	0.565	0.565	4.5	3.2	1.737
30	1114.3	2347.	449.	1.82	0.355	5.12	0.485	0.619	3.1	1.5	1.509
35	1300.0	2365.	439.	1.83	0.347	5.28	0.512	0.592	1.7	0.9	1.327
40	1485.7	2368.	435.	1.83	0.344	5.33	0.512	0.565	0.3	0.3	1.179

TABLE C.1.49 : NUMERICAL EVALUATION OF EXPERIMENT EDI-S3-13/826

1	2	3	4	5	6	7	8	9	10	11	12
CYCLE NO.	REAL TIME	CONCENTRATION BOTTOM	CONCENTRATION TOP	CONCENTRATION NORMALIZED		SEPARATION FACTOR	CURRENT ENR. CIAL.		CURRENT EFFICIENCY		POWER EFFICIENCY
NCYC (-)	T (SEC)	CB (PPM)	CT (PPM)	XB (-)	XT (-)	NS (-)	I1 (A)	I2 (A)	E1 (%)	E2 (%)	EP (%)
0	0.0	1289.	1262.	1.00	1.000	1.00	0.0	0.0	100.0	100.0	100.000
1	32.1	1341.	1183.	1.04	0.938	1.11	0.958	0.646	18.9	30.8	3.270
2	64.3	1397.	1122.	1.08	0.890	1.22	0.866	0.673	22.1	22.8	2.892
3	96.4	1450.	1066.	1.12	0.845	1.33	0.958	0.687	19.1	20.9	2.658
4	128.6	1497.	1013.	1.16	0.803	1.45	0.847	0.687	19.3	19.5	2.540
5	160.7	1542.	968.	1.20	0.767	1.56	0.976	0.633	15.9	18.0	2.402
10	321.4	1744.	787.	1.35	0.624	2.17	0.903	0.687	15.5	13.3	2.003
15	482.1	1881.	671.	1.46	0.532	2.74	0.866	0.606	10.9	9.7	1.731
20	642.8	1978.	595.	1.53	0.471	3.26	0.829	0.633	8.1	6.1	1.507
25	803.5	2042.	548.	1.58	0.435	3.65	0.829	0.633	5.3	3.7	1.313
30	964.3	2082.	519.	1.62	0.411	3.93	0.829	0.565	3.4	2.7	1.161
35	1125.0	2105.	499.	1.63	0.396	4.13	0.755	0.592	2.1	1.7	1.037
40	1285.7	2120.	488.	1.64	0.387	4.26	0.755	0.579	1.3	1.0	0.933
45	1446.4	2126.	480.	1.65	0.380	4.34	0.718	0.592	0.6	0.7	0.846
50	1607.1	2131.	475.	1.65	0.376	4.39	0.755	0.565	0.5	0.5	0.773

TABLE C.1.5C : NUMERICAL EVALUATION OF EXPERIMENT EDI-S3-13/#27

1	2	3	4	5	6	7	8	9	10	11	12
CYCLE NO.	REAL TIME	CONCENTRATION BOTTOM	CONCENTRATION TOP	CONCENTRATION NORMALIZED		SEPARATION FACTOR	CURRENT ENR. CIAL.		CURRENT EFFICIENCY		POWER EFFICIENCY
NCYC (-)	T (SEC)	CB (PPM)	CT (PPM)	XB (-)	XT (-)	NS (-)	I1 (A)	I2 (A)	E1 (%)	E2 (%)	EP (%)
0	0.0	1237.	1214.	1.00	1.000	1.00	0.0	0.0	100.0	100.0	100.000
1	49.3	1319.	1069.	1.07	0.881	1.21	0.711	0.433	24.6	57.7	9.507
2	98.6	1400.	983.	1.13	0.810	1.40	0.677	0.663	25.1	22.5	7.304
3	147.9	1461.	913.	1.18	0.752	1.57	0.745	0.589	17.4	20.4	6.251
4	197.1	1514.	855.	1.22	0.705	1.74	0.745	0.571	15.1	17.6	5.597
5	246.4	1556.	815.	1.26	0.672	1.87	0.745	0.553	11.9	12.5	5.026
10	492.8	1674.	699.	1.35	0.576	2.35	0.666	0.534	7.5	7.5	3.429
15	739.3	1705.	660.	1.38	0.544	2.53	0.677	0.516	1.9	2.6	2.486
20	985.7	1710.	649.	1.38	0.535	2.59	0.632	0.553	0.4	0.7	1.912

TABLE C.1.5I : NUMERICAL EVALUATION OF EXPERIMENT EDI-S3-13/#28

1	2	3	4	5	6	7	8	9	10	11	12
CYCLE NO.	REAL TIME	CONCENTRATION BOTTOM	CONCENTRATION TOP	CONCENTRATION NORMALIZED		SEPARATION FACTOR	CURRENT ENR. CIAL.		CURRENT EFFICIENCY		POWER EFFICIENCY
NCYC (-)	T (SEC)	CB (PPM)	CT (PPM)	XB (-)	XT (-)	NS (-)	I1 (A)	I2 (A)	E1 (%)	E2 (%)	EP (%)
0	0.0	1295.	1267.	1.00	1.000	1.00	0.0	0.0	100.0	100.0	100.000
1	54.3	1438.	1120.	1.11	0.884	1.26	0.672	0.571	37.0	44.6	4.560
2	108.6	1550.	1009.	1.20	0.796	1.50	0.617	0.580	31.3	33.1	3.947
3	162.9	1643.	920.	1.27	0.726	1.75	0.562	0.636	28.5	24.2	3.540
4	217.1	1713.	853.	1.32	0.673	1.97	0.589	0.553	20.7	21.0	3.209
6	325.7	1801.	761.	1.39	0.601	2.32	0.562	0.589	13.5	13.4	2.622
8	434.3	1855.	712.	1.43	0.562	2.55	0.562	0.553	8.3	7.7	2.193
10	542.8	1881.	681.	1.45	0.538	2.70	0.543	0.543	4.1	4.9	1.868
12	651.4	1898.	666.	1.47	0.525	2.79	0.534	0.543	2.8	2.5	1.616
14	760.0	1904.	657.	1.47	0.518	2.84	0.534	0.543	0.9	1.4	1.413
16	868.5	1910.	652.	1.48	0.515	2.86	0.525	0.553	0.9	0.6	1.253

TABLE C.1.5J : NUMERICAL EVALUATION OF EXPERIMENT EDI-S3-13/#29

1	2	3	4	5	6	7	8	9	10	11	12
CYCLE NO.	REAL TIME	CONCENTRATION BOTTOM	TOP	CONCENTRATION NORMALIZED		SEPARATION FACTOR	CURRENT ENR.	STRIP.	CURRENT EFFICIENCY		POWER EFFICIENCY
NCYC (-)	T (SEC)	CB (PPM)	CT (PPM)	XB (-)	XT (-)	NS (-)	I1 (A)	I2 (A)	E1 (%)	E2 (%)	EP (%)
0	0.0	1297.	1276.	1.00	1.000	1.00	0.0	0.0	100.0	100.0	100.000
1	25.1	1430.	1153.	1.10	0.904	1.22	1.862	0.939	33.3	40.7	1.895
2	50.3	1536.	1046.	1.18	0.820	1.44	1.962	0.929	25.2	35.9	1.652
3	75.4	1651.	951.	1.27	0.745	1.71	1.763	0.962	30.5	30.9	1.597
4	100.5	1753.	867.	1.35	0.679	1.99	1.540	1.078	30.8	24.2	1.541
5	125.7	1853.	787.	1.43	0.617	2.32	1.415	1.078	32.8	23.1	1.512
10	251.4	2227.	526.	1.72	0.413	4.16	1.763	0.614	19.8	26.5	1.285
15	377.0	2433.	395.	1.88	0.309	6.06	1.117	0.830	17.1	9.9	1.114
20	502.7	2530.	335.	1.95	0.263	7.42	1.142	0.813	8.0	4.5	0.939
25	628.4	2578.	308.	1.99	0.242	8.22	1.018	0.846	4.4	2.0	0.805
30	754.1	2596.	297.	2.00	0.233	8.60	0.993	0.830	1.7	0.9	0.698
35	879.7	2611.	290.	2.01	0.228	8.85	1.018	0.830	1.4	0.5	0.615

TABLE C.1.53 : NUMERICAL EVALUATION OF EXPERIMENT EDI-S3-13/#3C

1	2	3	4	5	6	7	8	9	10	11	12
CYCLE NO.	REAL TIME	CONCENTRATION BOTTOM	TOP	CONCENTRATION NORMALIZED		SEPARATION FACTOR	CURRENT ENR.	STRIP.	CURRENT EFFICIENCY		POWER EFFICIENCY
NCYC (-)	T (SEC)	CB (PPM)	CT (PPM)	XB (-)	XT (-)	NS (-)	I1 (A)	I2 (A)	E1 (%)	E2 (%)	EP (%)
0	0.0	1322.	1302.	1.00	1.000	1.00	0.0	0.0	100.0	100.0	100.000
1	30.1	1491.	1169.	1.13	0.897	1.26	1.195	1.145	44.2	36.5	2.197
2	60.3	1654.	1045.	1.25	0.802	1.56	1.228	1.112	41.3	34.7	2.071
3	90.4	1796.	942.	1.36	0.723	1.88	1.029	1.095	42.9	29.4	1.995
4	120.5	1921.	842.	1.45	0.647	2.25	0.896	1.195	43.7	25.9	1.928
5	150.7	2039.	762.	1.54	0.585	2.64	0.946	1.128	38.8	22.1	1.849
10	301.4	2439.	498.	1.84	0.382	4.83	0.863	0.996	28.9	16.6	1.522
15	452.0	2637.	379.	1.99	0.291	6.85	0.730	0.962	17.0	7.7	1.250
20	602.7	2730.	329.	2.06	0.252	8.18	0.830	0.813	7.0	3.9	1.034
25	753.4	2790.	310.	2.11	0.238	8.88	0.846	0.763	4.4	1.6	0.876
30	904.1	2850.	303.	2.16	0.233	9.27	0.597	1.012	6.3	0.4	0.762

TABLE C.1.54 : NUMERICAL EVALUATION OF EXPERIMENT EDI-S3-13/#3I

1	2	3	4	5	6	7	8	9	10	11	12
CYCLE NO.	REAL TIME	CONCENTRATION BOTTOM	CONCENTRATION TOP	CONCENTRATION NORMALIZED		SEPARATION FACTOR	CURRENT ENR.	CURRENT DIAL.	CURRENT EFFICIENCY		POWER EFFICIENCY
NCYC (-)	T (SEC)	CB (PPM)	CT (PPM)	XB (-)	XT (-)	NS (-)	I1 (A)	I2 (A)	E1 (%)	E2 (%)	EP (%)
0	0.0	1317.	1290.	1.00	1.000	1.00	0.0	0.0	100.0	100.0	100.000
1	33.0	1406.	1166.	1.13	0.904	1.25	1.214	1.183	39.7	29.8	1.943
2	65.9	1637.	1049.	1.24	0.813	1.53	1.123	1.153	38.4	29.0	1.833
3	98.9	1776.	939.	1.35	0.728	1.85	1.138	1.016	34.7	30.7	1.783
4	131.8	1907.	844.	1.45	0.654	2.21	1.047	1.047	35.7	26.0	1.733
5	164.8	2022.	764.	1.54	0.592	2.59	1.077	0.971	30.4	23.5	1.667
6	197.8	2120.	694.	1.61	0.538	2.99	0.910	1.123	30.8	17.7	1.594
7	230.7	2216.	633.	1.68	0.491	3.43	1.001	0.956	27.3	18.1	1.538
8	263.7	2295.	582.	1.74	0.451	3.86	0.865	1.032	26.0	14.3	1.477
9	296.6	2368.	541.	1.80	0.419	4.29	0.986	0.880	21.2	13.4	1.418
10	329.6	2427.	501.	1.84	0.388	4.75	0.804	1.032	20.9	11.0	1.362
15	494.4	2625.	381.	1.99	0.295	6.76	0.834	0.865	13.6	7.9	1.124
20	659.2	2727.	329.	2.07	0.255	8.12	0.804	0.834	7.2	3.5	0.936
25	824.0	2802.	307.	2.13	0.238	8.94	0.789	0.834	5.4	1.5	0.799
30	988.8	2826.	297.	2.15	0.230	9.33	0.834	0.789	1.6	0.7	0.687

TABLE C.1.55 : NUMERICAL EVALUATION OF EXPERIMENT EDI-S3-13/#32

1	2	3	4	5	6	7	8	9	10	11	12
CYCLE NO.	REAL TIME	CONCENTRATION BOTTOM	CONCENTRATION TOP	CONCENTRATION NORMALIZED		SEPARATION FACTOR	CURRENT ENR.	CURRENT DIAL.	CURRENT EFFICIENCY		POWER EFFICIENCY
NCYC (-)	T (SEC)	CB (PPM)	CT (PPM)	XB (-)	XT (-)	NS (-)	I1 (A)	I2 (A)	E1 (%)	E2 (%)	EP (%)
0	0.0	1308.	1278.	1.00	1.000	1.00	0.0	0.0	100.0	100.0	100.000
1	33.0	1394.	1216.	1.07	0.952	1.12	1.168	1.092	41.8	32.3	2.294
2	65.9	1483.	1148.	1.13	0.898	1.26	1.092	1.138	46.4	34.2	2.176
3	98.9	1567.	1081.	1.20	0.846	1.42	1.062	1.107	45.0	34.5	2.128
4	131.8	1646.	1019.	1.26	0.797	1.58	1.107	1.016	40.5	34.7	2.079
5	164.8	1716.	964.	1.31	0.754	1.74	1.107	0.956	36.3	33.1	2.022
10	329.6	2019.	729.	1.54	0.570	2.71	0.910	0.986	37.9	27.1	1.850
15	494.4	2227.	570.	1.70	0.446	3.82	0.804	0.941	29.6	19.2	1.665
20	659.2	2374.	464.	1.81	0.363	4.99	0.789	0.865	21.2	13.9	1.495
25	824.0	2471.	396.	1.89	0.310	6.10	0.789	0.834	14.1	9.3	1.336
30	988.8	2542.	352.	1.94	0.275	7.05	0.758	0.789	10.7	6.3	1.205
40	1318.4	2617.	304.	2.00	0.238	8.40	0.713	0.819	5.9	3.3	0.989
50	1648.0	2658.	285.	2.03	0.223	9.11	0.774	0.774	3.1	1.4	0.828
60	1977.6	2676.	277.	2.05	0.217	9.43	0.774	0.774	1.3	0.6	0.706

TABLE C.1.56 : NUMERICAL EVALUATION OF EXPERIMENT EDI-S3-13/#33

1	2	3	4	5	6	7	8	9	10	11	12
CYCLE NO.	REAL TIME	CONCENTRATION BOTTOM	CONCENTRATION TOP	CONCENTRATION NORMALIZED		SEPARATION FACTOR	CURRENT ENR. DIAL.		CURRENT EFFICIENCY		POWER EFFICIENCY
NCYC (-)	T (SEC)	CB (PPM)	CT (PPM)	XB (-)	XT (-)	NS (-)	I1 (A)	I2 (A)	E1 (%)	E2 (%)	EP (%)
0	0.0	1215.	1196.	1.00	1.000	1.00	0.0	0.0	100.0	100.0	100.000
1	33.0	1270.	1151.	1.05	0.962	1.09	1.138	0.895	41.3	43.1	2.593
2	65.9	1325.	1096.	1.09	0.917	1.19	1.123	0.956	42.0	48.5	2.460
3	98.9	1380.	1058.	1.14	0.885	1.28	1.107	0.880	42.7	37.6	2.339
4	131.8	1436.	1023.	1.18	0.855	1.38	1.123	0.819	42.3	36.3	2.269
5	164.8	1480.	980.	1.22	0.820	1.49	1.153	0.758	33.0	48.0	2.221
10	329.6	1691.	820.	1.39	0.686	2.03	1.032	0.758	34.9	36.1	2.034
15	494.4	1853.	681.	1.52	0.570	2.68	0.834	0.895	33.2	26.6	1.881
20	659.2	1978.	587.	1.63	0.491	3.32	0.819	0.774	26.3	20.8	1.734
25	824.0	2079.	507.	1.71	0.424	4.04	0.819	0.774	21.1	17.7	1.602
30	988.8	2163.	448.	1.78	0.374	4.76	0.743	0.789	19.3	12.9	1.487
40	1318.4	2274.	368.	1.87	0.307	6.09	0.698	0.774	13.6	8.8	1.285
50	1648.0	2342.	322.	1.93	0.270	7.15	0.652	0.789	8.8	4.9	1.118
60	1977.6	2386.	295.	1.96	0.247	7.95	0.652	0.774	5.8	3.0	0.983
70	2307.2	2412.	281.	1.99	0.235	8.44	0.607	0.819	3.7	1.5	0.871

TABLE C.1.57 : NUMERICAL EVALUATION OF EXPERIMENT EDI-S3-13/#34

1	2	3	4	5	6	7	8	9	10	11	12
CYCLE NO.	REAL TIME	CONCENTRATION BOTTOM	CONCENTRATION TOP	CONCENTRATION NORMALIZED		SEPARATION FACTOR	CURRENT ENR. DIAL.		CURRENT EFFICIENCY		POWER EFFICIENCY
NCYC (-)	T (SEC)	CB (PPM)	CT (PPM)	XB (-)	XT (-)	NS (-)	I1 (A)	I2 (A)	E1 (%)	E2 (%)	EP (%)
0	0.0	1237.	1205.	1.00	1.000	1.00	0.0	0.0	100.0	100.0	100.000
1	33.0	1297.	1086.	1.05	0.901	1.16	1.168	0.986	44.3	34.3	2.492
2	65.9	1355.	970.	1.10	0.805	1.36	1.016	1.123	48.8	29.5	2.249
3	98.9	1411.	867.	1.14	0.719	1.59	1.047	0.956	45.3	30.8	2.168
4	131.8	1461.	775.	1.18	0.643	1.84	0.910	1.062	47.0	24.6	2.085
5	164.8	1511.	698.	1.22	0.579	2.11	0.925	1.001	46.4	27.0	2.023
10	329.6	1696.	440.	1.37	0.365	3.76	0.834	0.743	38.0	19.8	1.810
15	494.4	1801.	317.	1.46	0.263	5.53	0.713	0.698	25.2	10.0	1.561
20	659.2	1861.	258.	1.50	0.214	7.03	0.607	0.637	15.3	5.3	1.351
25	824.0	1895.	230.	1.53	0.191	8.04	0.652	0.637	9.0	2.5	1.174
30	988.8	1915.	215.	1.55	0.179	8.66	0.607	0.607	5.6	1.3	1.037
35	1153.6	1930.	209.	1.56	0.173	9.00	0.576	0.637	4.2	0.6	0.926
40	1318.4	1941.	206.	1.57	0.171	9.16	0.546	0.667	3.6	0.2	0.835

TABLE C.1.58 : NUMERICAL EVALUATION OF EXPERIMENT EDI-S3-13/#35

1	2	3	4	5	6	7	8	9	10	11	12
CYCLE NO.	REAL TIME	CONCENTRATION BOTTOM		CONCENTRATION NORMALIZED		SEPARATION FACTOR	CURRENT ENR.	CIAL.	CURRENT EFFICIENCY		POWER EFFICIENCY
NCYC (-)	T (SEC)	CB (PPM)	CT (PPM)	XB (-)	XT (-)	NS (-)	I1 (A)	I2 (A)	E1 (%)	E2 (%)	EP (%)
0	0.0	1292.	1263.	1.00	1.000	1.00	0.0	0.0	100.0	100.0	100.000
1	33.0	1461.	1218.	1.13	0.964	1.17	1.138	1.016	42.3	38.0	2.454
2	65.9	1606.	1166.	1.24	0.923	1.35	1.001	1.183	41.4	37.3	2.224
3	98.9	1747.	1126.	1.35	0.892	1.52	1.107	1.016	36.3	33.6	2.076
4	131.8	1881.	1081.	1.46	0.856	1.70	0.986	1.138	38.7	33.9	2.019
5	164.8	1996.	1035.	1.54	0.819	1.89	1.016	1.062	32.2	37.4	1.967
10	329.6	2456.	857.	1.90	0.686	2.77	1.047	0.986	25.1	29.1	1.674
15	494.4	2802.	748.	2.17	0.592	3.66	1.032	1.047	19.1	19.4	1.440
20	659.2	3038.	646.	2.35	0.512	4.60	0.895	1.138	15.0	15.3	1.278
25	824.0	3204.	581.	2.48	0.460	5.40	0.804	1.168	11.7	9.6	1.135
30	988.8	3346.	530.	2.59	0.420	6.17	0.986	1.047	8.2	8.2	1.017
40	1318.4	3501.	466.	2.71	0.369	7.35	0.956	1.047	4.6	5.3	0.830
50	1648.0	3601.	428.	2.79	0.339	8.22	0.941	1.062	3.0	3.0	0.698
60	1977.6	3645.	412.	2.82	0.326	8.66	0.941	1.062	1.3	1.4	0.594

TABLE C.1.59 : NUMERICAL EVALUATION OF EXPERIMENT EDI-S3-13/#36

1	2	3	4	5	6	7	8	9	10	11	12
CYCLE NO.	REAL TIME	CONCENTRATION BOTTOM		CONCENTRATION NORMALIZED		SEPARATION FACTOR	CURRENT ENR.	CIAL.	CURRENT EFFICIENCY		POWER EFFICIENCY
NCYC (-)	T (SEC)	CB (PPM)	CT (PPM)	XB (-)	XT (-)	NS (-)	I1 (A)	I2 (A)	E1 (%)	E2 (%)	EP (%)
0	0.0	4709.	4636.	1.00	1.000	1.00	0.0	0.0	100.0	100.0	100.000
1	60.6	4868.	4263.	1.03	0.920	1.12	1.708	1.683	14.4	34.4	5.089
2	121.2	4998.	4038.	1.06	0.871	1.22	1.699	1.749	11.9	20.0	4.014
3	181.8	5100.	3859.	1.08	0.832	1.30	1.650	1.782	9.5	15.5	3.457
4	242.4	5187.	3711.	1.10	0.800	1.38	1.666	1.732	8.1	13.3	3.096
5	303.1	5259.	3603.	1.12	0.777	1.44	1.666	1.724	6.8	9.7	2.787
6	363.7	5303.	3512.	1.13	0.757	1.49	1.666	1.716	4.1	8.2	2.518
7	424.3	5332.	3444.	1.13	0.743	1.52	1.658	1.699	2.7	6.2	2.282
8	484.9	5361.	3381.	1.14	0.729	1.56	1.650	1.691	2.7	5.7	2.100
9	545.5	5391.	3331.	1.14	0.718	1.59	1.650	1.691	2.7	4.7	1.946
10	606.1	5405.	3291.	1.15	0.710	1.62	1.633	1.683	1.4	3.6	1.803
11	666.7	5405.	3263.	1.15	0.704	1.63	1.625	1.683	0.0	2.6	1.665
12	727.3	5405.	3235.	1.15	0.698	1.64	1.617	1.683	0.0	2.6	1.550
13	788.0	5420.	3212.	1.15	0.693	1.66	1.617	1.683	1.4	2.1	1.458
14	848.6	5420.	3190.	1.15	0.688	1.67	1.617	1.683	0.0	2.1	1.370
15	909.2	5420.	3173.	1.15	0.684	1.68	1.617	1.683	0.0	1.6	1.290

TABLE C.1.60 : NUMERICAL EVALUATION OF EXPERIMENT EDI-S3-13/#37

1	2	3	4	5	6	7	8	9	10	11	12
CYCLE NO.	REAL TIME	CONCENTRATION BOTTOM	CONCENTRATION TOP	CONCENTRATION NORMALIZED		SEPARATION FACTOR	CURRENT ENR.	CURRENT CIAL.	CURRENT EFFICIENCY		POWER EFFICIENCY
NCYC (-)	T (SEC)	CB (PPM)	CT (PPM)	XB (-)	XT (-)	NS (-)	I1 (A)	I2 (A)	E1 (%)	E2 (%)	EP (%)
0	0.0	4537.	4502.	1.00	1.000	1.00	0.0	0.0	100.0	100.0	100.000
1	35.3	4666.	4356.	1.03	0.968	1.06	1.946	1.671	17.7	23.2	2.105
2	70.6	4753.	4246.	1.05	0.943	1.11	1.954	1.793	11.8	16.4	1.690
3	105.9	4825.	4141.	1.06	0.920	1.16	1.869	1.869	10.3	14.8	1.512
4	141.2	4911.	4043.	1.08	0.898	1.21	1.869	1.884	12.3	13.9	1.436
5	176.5	4969.	3951.	1.10	0.878	1.25	1.827	1.869	8.4	13.1	1.349
6	211.8	5042.	3865.	1.11	0.859	1.29	1.869	1.855	10.3	12.3	1.299
7	247.1	5100.	3791.	1.12	0.842	1.33	1.855	1.841	8.3	10.8	1.240
8	282.4	5158.	3722.	1.14	0.827	1.37	1.841	1.827	8.4	10.0	1.192
9	317.8	5201.	3654.	1.15	0.812	1.41	1.841	1.827	6.3	10.0	1.145
10	353.1	5245.	3597.	1.16	0.799	1.45	1.827	1.813	6.4	8.4	1.099
15	529.6	5420.	3353.	1.19	0.745	1.60	1.827	1.756	5.1	7.4	0.930
20	706.1	5537.	3196.	1.22	0.710	1.72	1.813	1.742	3.4	4.8	0.797
25	882.7	5610.	3078.	1.24	0.684	1.81	1.784	1.728	2.2	3.6	0.695
30	1059.2	5654.	3000.	1.25	0.666	1.87	1.784	1.714	1.3	2.4	0.611
35	1235.7	5683.	2944.	1.25	0.654	1.92	1.799	1.685	0.9	1.8	0.543
40	1412.2	5683.	2899.	1.25	0.644	1.95	1.799	1.685	0.0	1.4	0.485

TABLE C.1.61 : NUMERICAL EVALUATION OF EXPERIMENT.
EDI-S3-13/#38

1	2	3	4	5	6	7	8	9	10	11	12
CYCLE NO.	REAL TIME	CONCENTRATION BOTTOM	CONCENTRATION TOP	CONCENTRATION NORMALIZED		SEPARATION FACTOR	CURRENT ENR.	CURRENT CIAL.	CURRENT EFFICIENCY		POWER EFFICIENCY
NCYC (-)	T (SEC)	CB (PPM)	CT (PPM)	XB (-)	XT (-)	NS (-)	I1 (A)	I2 (A)	E1 (%)	E2 (%)	EP (%)
0	0.0	4955.	4889.	1.00	1.000	1.00	0.0	0.0	100.0	100.0	100.000
1	37.1	5230.	4648.	1.06	0.951	1.11	2.006	1.723	34.7	35.4	3.583
2	74.3	5434.	4408.	1.10	0.902	1.22	1.912	1.817	27.0	33.3	3.159
3	111.4	5669.	4199.	1.14	0.859	1.33	1.912	1.885	31.0	28.0	2.998
4	148.6	5860.	3997.	1.18	0.818	1.45	1.871	1.831	25.8	27.9	2.861
5	185.7	6037.	3825.	1.22	0.782	1.56	1.858	1.750	24.1	24.9	2.738
6	222.9	6215.	3665.	1.25	0.750	1.67	1.831	1.750	24.5	23.1	2.646
7	260.0	6348.	3517.	1.28	0.719	1.78	1.844	1.696	18.3	22.0	2.535
8	297.1	6467.	3387.	1.31	0.693	1.88	1.885	1.669	16.0	19.7	2.425
9	334.3	6602.	3263.	1.33	0.667	2.00	1.885	1.615	18.0	19.4	2.348
10	371.4	6707.	3162.	1.35	0.647	2.09	1.885	1.589	14.1	16.1	2.255
15	557.1	7097.	2766.	1.43	0.566	2.53	1.777	1.615	11.1	12.4	1.881
20	742.8	7355.	2534.	1.48	0.518	2.86	1.777	1.562	7.3	7.5	1.595
25	928.5	7491.	2386.	1.51	0.488	3.10	1.723	1.535	4.0	4.9	1.371
30	1114.3	7598.	2304.	1.53	0.471	3.25	1.696	1.535	3.2	2.7	1.198
35	1300.0	7628.	2260.	1.54	0.462	3.33	1.669	1.521	0.9	1.5	1.051

TABLE C.1.62 : NUMERICAL EVALUATION OF EXPERIMENT
EDI-S3-13/#39

1	2	3	4	5	6	7	8	9	10	11	12
CYCLE NO.	REAL TIME	CONCENTRATION BOTTOM	CONCENTRATION TOP	CONCENTRATION NORMALIZED		SEPARATION FACTOR	CURRENT ENR. DIAL.		CURRENT EFFICIENCY		POWER EFFICIENCY
NCYC (-)	T (SEC)	CB (PPM)	CT (PPM)	XB (-)	XT (-)	NS (-)	I1 (A)	I2 (A)	E1 (%)	E2 (%)	EP (%)
0	0.0	5654.	5562.	1.00	1.000	1.00	0.0	0.0	100.0	100.0	100.000
1	37.1	6066.	5132.	1.07	0.923	1.16	3.015	2.827	34.6	38.5	2.391
2	74.3	6438.	4748.	1.14	0.854	1.33	3.096	3.150	30.3	30.8	2.091
3	111.4	6766.	4397.	1.20	0.790	1.51	3.190	3.177	26.1	27.9	1.923
4	148.6	7097.	4089.	1.26	0.735	1.71	2.975	3.015	28.1	25.8	1.843
5	185.7	7400.	3814.	1.31	0.686	1.91	2.891	3.002	26.6	23.2	1.772
6	222.9	7643.	3568.	1.35	0.642	2.11	2.827	2.975	21.8	20.8	1.692
7	260.0	7873.	3410.	1.39	0.613	2.27	2.940	2.854	20.4	14.1	1.600
8	297.1	8072.	3156.	1.43	0.567	2.52	2.746	2.867	18.4	22.4	1.557
9	334.3	8272.	3000.	1.46	0.539	2.71	2.665	2.854	19.0	13.9	1.497
10	371.4	8442.	2855.	1.49	0.513	2.91	2.719	2.719	15.8	13.5	1.439
14	520.0	8955.	2430.	1.58	0.437	3.63	2.558	2.639	12.7	10.2	1.242
18	668.6	9236.	2173.	1.63	0.391	4.18	2.396	2.585	7.4	6.3	1.076
22	817.1	9409.	2026.	1.66	0.364	4.57	2.369	2.585	4.6	3.6	0.938
26	965.7	9535.	1935.	1.69	0.348	4.85	2.342	2.558	3.4	2.3	0.829
30	1114.3	9567.	1881.	1.69	0.338	5.00	2.356	2.531	0.8	1.3	0.736
34	1262.8	9614.	1854.	1.70	0.333	5.10	2.342	2.531	1.3	0.7	0.661

TABLE C.1.63 : NUMERICAL EVALUATION OF EXPERIMENT EDI-S3-13/#40

1	2	3	4	5	6	7	8	9	10	11	12
CYCLE NO.	REAL TIME	CONCENTRATION BOTTOM	CONCENTRATION TOP	CONCENTRATION NORMALIZED		SEPARATION FACTOR	CURRENT ENR. DIAL.		CURRENT EFFICIENCY		POWER EFFICIENCY
NCYC (-)	T (SEC)	CB (PPM)	CT (PPM)	XB (-)	XT (-)	NS (-)	I1 (A)	I2 (A)	E1 (%)	E2 (%)	EP (%)
0	0.0	5376.	5275.	1.00	1.000	1.00	0.0	0.0	100.0	100.0	100.000
2	74.3	6141.	4490.	1.14	0.851	1.34	3.581	2.827	27.0	35.1	1.945
4	148.6	6796.	3854.	1.26	0.731	1.73	3.285	2.881	25.2	27.9	1.769
6	222.9	7294.	3353.	1.36	0.636	2.13	3.096	2.827	20.3	22.4	1.614
8	297.1	7750.	2972.	1.44	0.563	2.56	2.800	2.692	20.6	17.9	1.510
10	371.4	8087.	2677.	1.50	0.508	2.96	2.800	2.665	15.2	14.0	1.394
15	557.1	8643.	2200.	1.61	0.417	3.85	2.773	2.531	10.1	9.5	1.148
20	742.8	8923.	1967.	1.66	0.373	4.45	2.531	2.585	5.6	4.6	0.955
25	928.5	9048.	1838.	1.68	0.348	4.83	2.531	2.477	2.5	2.6	0.809
30	1114.3	9111.	1773.	1.69	0.336	5.04	2.504	2.423	1.3	1.3	0.697
35	1300.0	9127.	1741.	1.70	0.330	5.14	2.477	2.315	0.3	0.7	0.611

TABLE C.1.64 : NUMERICAL EVALUATION OF EXPERIMENT EDI-S3-13/#00

1	2	3	4	5	6	7	8	9	10	11	12
CYCLE NO.	REAL TIME	CONCENTRATION BOTTOM	TOP	CONCENTRATION NORMALIZED		SEPARATION FACTOR	CURRENT ENR.	DIAL.	CURRENT EFFICIENCY		POWER EFFICIENCY
NCYC (-)	T (SEC)	CB (PPM)	CT (PPM)	XB (-)	XT (-)	NS (-)	I1 (A)	I2 (A)	E1 (%)	E2 (%)	EP (%)
0	0.0	5245.	5126.	1.00	1.000	1.00	0.0	0.0	100.0	100.0	100.000
1	54.3	5772.	4414.	1.10	0.861	1.28	3.150	3.003	28.9	41.0	4.593
2	108.6	6170.	3934.	1.18	0.767	1.53	3.150	2.855	21.9	29.1	3.839
3	162.9	6467.	3568.	1.23	0.696	1.77	3.058	2.763	16.8	22.9	3.373
4	217.1	6692.	3291.	1.28	0.642	1.99	3.021	2.690	12.8	17.8	3.009
5	271.4	6872.	3089.	1.31	0.603	2.17	2.984	2.653	10.4	13.2	2.707
7	380.0	7097.	2849.	1.35	0.556	2.43	2.874	2.579	6.8	8.0	2.220
9	488.6	7188.	2688.	1.37	0.524	2.61	2.837	2.579	2.8	5.4	1.856
11	597.1	7264.	2611.	1.38	0.509	2.72	2.874	2.542	2.3	2.6	1.585
13	705.7	7264.	2561.	1.38	0.500	2.77	2.837	2.395	0.0	1.8	1.371
15	814.3	7279.	2539.	1.39	0.495	2.80	2.800	2.358	0.5	0.8	1.210

TABLE C.1.65 : NUMERICAL EVALUATION OF EXPERIMENT EDI-S3-13/#41

1	2	3	4	5	6	7	8	9	10	11	12
CYCLE NO.	REAL TIME	CONCENTRATION BOTTOM	TOP	CONCENTRATION NORMALIZED		SEPARATION FACTOR	CURRENT ENR.	DIAL.	CURRENT EFFICIENCY		POWER EFFICIENCY
NCYC (-)	T (SEC)	CB (PPM)	CT (PPM)	XB (-)	XT (-)	NS (-)	I1 (A)	I2 (A)	E1 (%)	E2 (%)	EP (%)
0	0.0	5332.	5215.	1.00	1.000	1.00	0.0	0.0	100.0	100.0	100.000
1	294.3	5683.	4636.	1.07	0.889	1.20	0.574	0.605	19.5	30.6	10.206
2	588.6	5934.	4280.	1.11	0.821	1.36	0.557	0.646	14.3	17.6	7.994
3	882.9	6096.	4038.	1.14	0.774	1.48	0.557	0.637	9.3	12.2	6.643
4	1177.2	6259.	3831.	1.17	0.735	1.60	0.561	0.639	9.3	10.3	5.876
5	1471.5	6393.	3665.	1.20	0.703	1.71	0.557	0.652	7.7	8.1	5.272
7	2060.0	6542.	3421.	1.23	0.656	1.87	0.550	0.646	4.3	6.0	4.321
9	2648.6	6632.	3269.	1.24	0.627	1.98	0.554	0.652	2.6	3.7	3.621
11	3237.2	6707.	3162.	1.26	0.606	2.07	0.550	0.658	2.2	2.6	3.122
13	3825.8	6751.	3111.	1.27	0.597	2.12	0.557	0.646	1.3	1.2	2.712
15	4414.4	6766.	3055.	1.27	0.586	2.17	0.564	0.615	0.4	1.5	2.405

TABLE C.1.66 : NUMERICAL EVALUATION OF EXPERIMENT EDI-S3-13/#42

APPENDIX C.2

EVALUATION OF EDII EXPERIMENTS

(i) Numerical evaluation of second ED runs. A short computer program was written for an IBM 360/67 FORTRAN IVG compiler. The program reads the run number, initial conditions, conductivity calibration data cycle period, and the mV-readings from the recorder chart for a sequence of cycles. It prints a table for each run which displays the progress in separation for repetitive cycling. The program and the tables follow.

(ii) Tables were prepared which contain a record of current and voltage distributions for each run. The experiments are grouped together according to the parameter which was altered in each group (see Table 34 to 39). The total current is included as well as the applied voltage. The average current and voltage in each stage were measured in cycle ranges given in columns 4 and 13, respectively.

pages 379 and 380 do not exist


```
FORTRAN IV G COMPILER        MAIN            12-10-72        12:48:53       PAGE 0

            C PROGRAM TO EVALUATE SECOND ED RUNS
            C
0001              READ (5,1) M,N,CBV,CTV,A1,B1,A2,B2
0002            1 FORMAT (2I2,F6.2,5F10.4)
0003              READ (5,2) T
0004            2 FORMAT (F5.1)
0005              T=T/60.
0006              WRITE (6,5)
0007            5 FORMAT (1H1,'-----------------------------------------------
                 1----------------'/
                 2'CYCLE  REAL  CONCENTRATION   CONCENTRATION  SEPARATION'/
                 3'  NO.   TIME     BRINE   DIAL.    NORMALIZED      FACTOR'//
                 4'  NC      T        CB      CT       XB      XT       NS'/
                 5' (-)    (MIN)    (PPM)   (PPM)    (-)     (-)      (-)'/
                 6' ------------------------------------------------------------
                 7------'//)
0008              TIME=0.0
0009              P=1.0
0010              J=0
0011              CBO=CBV*(A1*CBV+B1)
0012              CTO=CTV*(A2*CTV+B2)
0013              WRITE (6,4) J,TIME,CBO,CTO,P,P,P
0014            4 FORMAT (I4,F7.2,F8.0,F7.0,F9.2,F7.4,F10.2)
0015              DO 100 I=1,N
0016              READ (5,3) K,CBV,CTV,L
0017            3 FORMAT (I2,2F6.2,I2)
0018              IF (L.NE.0) WRITE (6,6)
0019            6 FORMAT (' ')
0020              CB=CBV*(A1*CBV+B1)
0021              CT=CTV*(A2*CTV+B2)
0022              J=J+K
0023              TIME=T*J
0024              XB=CB/CBO
0025              XT=CT/CTO
0026              SE=XB/XT
0027              WRITE (6,4) J,TIME,CB,CT,XB,XT,SE
0028          100 CONTINUE
0029              READ (5,105) NT
0030          105 FORMAT (I2)
0031              WRITE (6,110) NT,M
0032          110 FORMAT (//' ----------------------------------------------
                 1----------------'//
                 2'    TABLE  C.2.',I2,'  : NUMERICAL EVALUATION OF EXPERIMENT /
                 3'                          EDII-S1-B/#',I2)
0033              WRITE (6,120) M
0034          120 FORMAT (1H1,I3)
0035           20 STOP
0036              END

 TOTAL MEMORY REQUIREMENTS 00068E BYTES

 COMPILE TIME =       1.3  SECONDS
```

CYCLE NO.	REAL TIME	CONCENTRATION BRINE DIAL.		CONCENTRATION NORMALIZED		SEPARATION FACTOR
NC (-)	T (MIN)	CB (PPM)	CT (PPM)	XB (-)	XT (-)	NS (-)
0	0.0	5742.	5641.	1.00	1.0000	1.00
1	0.67	6393.	4842.	1.11	0.8584	1.30
2	1.33	6932.	4350.	1.21	0.7712	1.57
3	2.00	7476.	3877.	1.30	0.6873	1.89
4	2.67	7980.	3438.	1.39	0.6095	2.28
5	3.33	8473.	3027.	1.48	0.5367	2.75
6	4.00	8955.	2650.	1.56	0.4698	3.32
7	4.67	9441.	2304.	1.64	0.4084	4.03
8	5.33	9867.	1989.	1.72	0.3526	4.87
9	6.00	10297.	1714.	1.79	0.3039	5.90
10	6.67	10698.	1458.	1.86	0.2585	7.21
12	8.00	11426.	1236.	1.99	0.2192	9.08
14	9.33	12064.	870.	2.10	0.1542	13.62
16	10.67	12609.	396.	2.20	0.0701	31.31
18	12.00	13075.	271.	2.28	0.0480	47.44
20	13.33	13443.	184.	2.34	0.0327	71.61
25	16.67	13983.	98.	2.44	0.0174	139.65
30	20.00	14221.	73.	2.48	0.0130	191.09
35	23.33	14357.	67.	2.50	0.0118	211.95
40	26.67	14391.	63.	2.51	0.0112	224.37

TABLE C.2. 1 : NUMERICAL EVALUATION OF EXPERIMENT EDII-S1-8/# 6

CYCLE NO.	REAL TIME	CONCENTRATION BRINE DIAL.		CONCENTRATION NORMALIZED		SEPARATION FACTOR
NC (-)	T (MIN)	CB (PPM)	CT (PPM)	XB (-)	XT (-)	NS (-)
0	0.0	5698.	5610.	1.00	1.0000	1.00
1	0.83	5904.	5233.	1.04	0.9327	1.11
2	1.67	6037.	5120.	1.06	0.9126	1.16
3	2.50	6155.	5001.	1.08	0.8914	1.21
4	3.33	6259.	4895.	1.10	0.8725	1.26
5	4.17	6378.	4777.	1.12	0.8515	1.31
6	5.00	6497.	4671.	1.14	0.8326	1.37
8	6.67	6692.	4467.	1.17	0.7961	1.48
10	8.33	6872.	4269.	1.21	0.7609	1.58
12	10.00	7067.	4084.	1.24	0.7279	1.70
14	11.67	7264.	3923.	1.27	0.6991	1.82
16	13.33	7415.	3756.	1.30	0.6695	1.94
18	15.00	7598.	3603.	1.33	0.6421	2.08
20	16.67	7750.	3455.	1.36	0.6158	2.21
22	18.33	7888.	3314.	1.38	0.5906	2.34
24	20.00	8041.	3196.	1.41	0.5696	2.48
26	21.67	8180.	3072.	1.44	0.5476	2.62
28	23.33	8318.	2955.	1.46	0.5267	2.77
30	25.00	8442.	2844.	1.48	0.5068	2.92

TABLE C.2. 2 : NUMERICAL EVALUATION OF EXPERIMENT EDII-S1-8/# 7

CYCLE NO.	REAL TIME	CONCENTRATION BRINE DIAL.		CONCENTRATION NORMALIZED		SEPARATION FACTOR
NC (-)	T (MIN)	CB (PPM)	CT (PPM)	XB (-)	XT (-)	NS (-)
0	0.0	5332.	5281.	1.00	1.0000	1.00
2	2.00	6066.	4414.	1.14	0.8359	1.36
4	4.00	6707.	3819.	1.26	0.7233	1.74
6	6.00	7294.	3280.	1.37	0.6211	2.20
8	8.00	7842.	2788.	1.47	0.5280	2.79
10	10.00	8365.	2358.	1.57	0.4466	3.51
14	14.00	9299.	1623.	1.74	0.3074	5.67
18	18.00	10090.	1079.	1.89	0.2043	9.26
22	22.00	10794.	751.	2.02	0.1421	14.24
26	26.00	11377.	437.	2.13	0.0827	25.81
30	30.00	11834.	283.	2.22	0.0537	41.35
35	35.00	12245.	182.	2.30	0.0344	66.68
40	40.00	12509.	141.	2.35	0.0268	87.65
45	45.00	12675.	121.	2.38	0.0229	103.65

TABLE C.2. 3 : NUMERICAL EVALUATION OF EXPERIMENT EDLI-S1-8/# 8

CYCLE NO.	REAL TIME	CONCENTRATION BRINE DIAL.		CONCENTRATION NORMALIZED		SEPARATION FACTOR
NC (-)	T (MIN)	CB (PPM)	CT (PPM)	XB (-)	XT (-)	NS (-)
0	0.0	5434.	5341.	1.00	1.0000	1.00
1	1.33	6542.	4338.	1.20	0.8124	1.48
2	2.67	7491.	3563.	1.38	0.6671	2.07
3	4.00	8442.	2860.	1.55	0.5356	2.90
4	5.33	9299.	2266.	1.71	0.4242	4.03
5	6.67	10090.	1768.	1.86	0.3310	5.61
6	8.00	10762.	1368.	1.98	0.2562	7.73
7	9.33	11377.	1047.	2.09	0.1961	10.68
8	10.67	11899.	776.	2.19	0.1454	15.06
9	12.00	12360.	570.	2.27	0.1067	21.31
10	13.33	12708.	416.	2.34	0.0779	30.01
12	16.00	13275.	217.	2.44	0.0407	60.02
14	18.67	13611.	121.	2.50	0.0227	110.45
16	21.33	13865.	78.	2.55	0.0146	174.35
18	24.00	14000.	58.	2.58	0.0109	237.37
20	26.67	14119.	48.	2.60	0.0090	289.84
25	33.33	14289.	40.	2.63	0.0075	348.38

TABLE C.2. 4 : NUMERICAL EVALUATION OF EXPERIMENT EDII-S1-8/# 9

CYCLE NO.	REAL TIME	CONCENTRATION BRINE DIAL.		CONCENTRATION NORMALIZED		SEPARATION FACTOR
NC (-)	T (MIN)	CB (PPM)	CT (PPM)	XB (-)	XT (-)	NS (-)
0	0.0	4781.	4765.	1.00	1.0000	1.00
1	0.83	5201.	4251.	1.09	0.8922	1.22
2	1.67	5493.	3980.	1.15	0.8352	1.38
3	2.50	5757.	3711.	1.20	0.7787	1.55
4	3.33	6022.	3455.	1.26	0.7250	1.74
6	5.00	6542.	2972.	1.37	0.6236	2.19
8	6.67	7007.	2528.	1.47	0.5306	2.76
10	8.33	7476.	2146.	1.56	0.4503	3.47
12	10.00	7918.	1795.	1.66	0.3766	4.40
14	11.67	8318.	1464.	1.74	0.3071	5.66
18	15.00	9080.	990.	1.90	0.2077	9.14
22	18.33	9740.	642.	2.04	0.1347	15.12
26	21.67	10233.	416.	2.14	0.0873	24.51
30	25.00	10601.	273.	2.22	0.0573	38.66
34	28.33	10875.	197.	2.27	0.0414	54.99
38	31.67	11036.	164.	2.31	0.0344	67.01
42	35.00	11182.	139.	2.34	0.0291	80.28
46	38.33	11231.	124.	2.35	0.0259	90.53

TABLE C.2. 5 : NUMERICAL EVALUATION OF EXPERIMENT EDII-SI-8/#10

CYCLE NO.	REAL TIME	CONCENTRATION BRINE DIAL.		CONCENTRATION NORMALIZED		SEPARATION FACTOR
NC (-)	T (MIN)	CB (PPM)	CT (PPM)	XB (-)	XT (-)	NS (-)
0	0.0	5376.	5191.	1.00	1.0000	1.00
1	1.13	5845.	4484.	1.09	0.8637	1.26
2	2.27	6244.	4165.	1.16	0.8022	1.45
3	3.40	6587.	3854.	1.23	0.7423	1.65
4	4.53	6947.	3563.	1.29	0.6863	1.88
5	5.67	7248.	3280.	1.35	0.6318	2.13
6	6.80	7552.	3016.	1.40	0.5810	2.42
7	7.93	7811.	2788.	1.45	0.5371	2.71
8	9.07	8072.	2556.	1.50	0.4923	3.05
9	10.20	8303.	2364.	1.54	0.4553	3.39
10	11.33	8519.	2157.	1.58	0.4154	3.81
12	13.60	8892.	1865.	1.65	0.3592	4.61
14	15.87	9221.	1602.	1.72	0.3086	5.56
16	18.13	9504.	1368.	1.77	0.2636	6.71
18	20.40	9725.	1184.	1.81	0.2280	7.93
20	22.67	9899.	1052.	1.84	0.2027	9.08
22	24.93	10042.	948.	1.87	0.1826	10.23
24	27.20	10185.	870.	1.89	0.1676	11.31
26	29.47	10281.	823.	1.91	0.1586	12.06

TABLE C.2. 6 : NUMERICAL EVALUATION OF EXPERIMENT EDII-SI-8/#11

CYCLE NO.	REAL TIME	CONCENTRATION BRINE DIAL.		CONCENTRATION NORMALIZED		SEPARATION FACTOR
NC (-)	T (MIN)	CB (PPM)	CT (PPM)	XB (-)	XT (-)	NS (-)
0	0.0	4380.	4280.	1.00	1.0000	1.00
1	0.42	4638.	4078.	1.06	0.9527	1.11
2	0.83	4854.	3905.	1.11	0.9124	1.21
5	2.08	5434.	3421.	1.24	0.7992	1.55
10	4.17	6274.	2672.	1.43	0.6242	2.30
15	6.25	7112.	2043.	1.62	0.4772	3.40
20	8.33	7827.	1527.	1.79	0.3568	5.01
25	10.42	8566.	1110.	1.96	0.2593	7.54
30	12.50	9315.	792.	2.13	0.1850	11.49
35	14.58	10010.	544.	2.29	0.1271	17.98
40	16.67	10698.	345.	2.44	0.0805	30.34
45	18.75	11344.	225.	2.59	0.0526	49.28
50	20.83	11981.	144.	2.74	0.0336	81.39
55	22.92	12559.	93.	2.87	0.0218	131.56
60	25.00	13142.	63.	3.00	0.0147	203.85
65	27.08	13662.	48.	3.12	0.0112	278.93
70	29.17	14102.	35.	3.22	0.0082	390.83
75	31.25	14459.	29.	3.30	0.0068	483.70
80	33.33	14801.	23.	3.38	0.0053	638.26
85	35.42	15059.	18.	3.44	0.0042	811.78
90	37.50	15317.	17.	3.50	0.0040	874.31

TABLE C.2. 7 : NUMERICAL EVALUATION OF EXPERIMENT EDII-S1-8/#12

CYCLE NO.	REAL TIME	CONCENTRATION BRINE DIAL.		CONCENTRATION NORMALIZED		SEPARATION FACTOR
NC (-)	T (MIN)	CB (PPM)	CT (PPM)	XB (-)	XT (-)	NS (-)
0	0.0	5129.	5007.	1.00	1.0000	1.00
2	1.67	5493.	4630.	1.07	0.9247	1.16
4	3.33	5816.	4321.	1.13	0.8629	1.31
6	5.00	6126.	4043.	1.19	0.8075	1.48
8	6.67	6423.	3779.	1.25	0.7548	1.66
10	8.33	6662.	3540.	1.30	0.7070	1.84
15	12.50	7264.	3016.	1.42	0.6024	2.35
20	16.67	7796.	2584.	1.52	0.5159	2.95
25	20.83	8210.	2216.	1.60	0.4426	3.62
30	25.00	8566.	1929.	1.67	0.3853	4.33
35	29.17	8861.	1688.	1.73	0.3370	5.13
40	33.33	9080.	1485.	1.77	0.2965	5.97
45	37.50	9315.	1331.	1.82	0.2659	6.83
50	41.67	9488.	1199.	1.85	0.2395	7.72
55	45.83	9598.	1094.	1.87	0.2186	8.56

TABLE C.2. 8 : NUMERICAL EVALUATION OF EXPERIMENT EDII-S1-8/#13

CYCLE NO.	REAL TIME	CONCENTRATION BRINE DIAL.		CONCENTRATION NORMALIZED		SEPARATION FACTOR
NC (-)	T (MIN)	CB (PPM)	CT (PPM)	XB (-)	XT (-)	NS (-)
0	0.0	5071.	4948.	1.00	1.0000	1.00
1	1.17	5259.	4350.	1.04	0.8791	1.18
2	2.33	5391.	4251.	1.06	0.8592	1.24
4	4.67	5610.	4020.	1.11	0.8125	1.36
6	7.00	5830.	3796.	1.15	0.7672	1.50
8	9.33	6037.	3563.	1.19	0.7200	1.65
10	11.67	6244.	3421.	1.23	0.6914	1.78
15	17.50	6692.	2927.	1.32	0.5915	2.23
20	23.33	7082.	2567.	1.40	0.5188	2.69
25	29.17	7430.	2255.	1.47	0.4556	3.22
30	35.00	7735.	1999.	1.53	0.4041	3.78
35	40.83	7980.	1773.	1.57	0.3584	4.39
40	46.67	8133.	1602.	1.60	0.3238	4.95

TABLE C.2. 9 : NUMERICAL EVALUATION OF EXPERIMENT EDII-S1-B/#14

CYCLE NO.	REAL TIME	CONCENTRATION BRINE DIAL.		CONCENTRATION NORMALIZED		SEPARATION FACTOR
NC (-)	T (MIN)	CB (PPM)	CT (PPM)	XB (-)	XT (-)	NS (-)
0	0.0	5405.	5293.	1.00	1.0000	1.00
1	2.15	5816.	4194.	1.08	0.7923	1.36
2	4.30	6111.	3934.	1.13	0.7433	1.52
3	6.45	6393.	3654.	1.18	0.6903	1.71
4	8.60	6662.	3376.	1.23	0.6378	1.93
6	12.90	7143.	2883.	1.32	0.5446	2.43
8	17.20	7446.	2446.	1.38	0.4622	2.98
10	21.50	8010.	2054.	1.48	0.3880	3.82
14	30.10	8690.	1432.	1.61	0.2705	5.94
18	38.70	9221.	1000.	1.71	0.1890	9.03
20	43.00	9472.	818.	1.75	0.1545	11.34

TABLE C.2.10 : NUMERICAL EVALUATION OF EXPERIMENT EDII-S1-B/#15

CYCLE NO.	REAL TIME	CONCENTRATION BRINE DIAL.		CONCENTRATION NORMALIZED		SEPARATION FACTOR
NC (-)	T (MIN)	CB (PPM)	CT (PPM)	XB (-)	XT (-)	NS (-)
0	0.0	5508.	5490.	1.00	1.0000	1.00
1	0.83	6126.	4601.	1.11	0.8380	1.33
2	1.67	6632.	4130.	1.20	0.7522	1.60
3	2.50	7128.	3682.	1.29	0.6707	1.93
4	3.33	7598.	3263.	1.38	0.5943	2.32
5	4.17	8057.	2871.	1.46	0.5230	2.80
6	5.00	8504.	2517.	1.54	0.4585	3.37
7	5.83	8955.	2173.	1.63	0.3958	4.11
8	6.67	9378.	1865.	1.70	0.3396	5.01
9	7.50	9788.	1581.	1.78	0.2879	6.17
10	8.33	10185.	1321.	1.85	0.2405	7.69
12	10.00	10955.	896.	1.99	0.1632	12.19
14	11.67	11638.	570.	2.11	0.1038	20.35
16	13.33	12261.	416.	2.23	0.0758	29.38
18	15.00	12791.	233.	2.32	0.0424	54.82
20	16.67	13192.	151.	2.40	0.0276	86.82
25	20.83	13780.	81.	2.50	0.0147	170.28
30	25.00	14034.	60.	2.55	0.0110	231.30

TABLE C.2.11 : NUMERICAL EVALUATION OF EXPERIMENT EDIL-S1-8/#16

CYCLE NO.	REAL TIME	CONCENTRATION BRINE DIAL.		CONCENTRATION NORMALIZED		SEPARATION FACTOR
NC (-)	T (MIN)	CB (PPM)	CT (PPM)	XB (-)	XT (-)	NS (-)
0	0.0	5143.	5061.	1.00	1.0000	1.00
1	0.83	5727.	4414.	1.11	0.8722	1.28
2	1.67	6244.	3963.	1.21	0.7830	1.55
3	2.50	6722.	3534.	1.31	0.6984	1.87
4	3.33	7173.	3128.	1.39	0.6181	2.26
5	4.17	7628.	2755.	1.48	0.5444	2.72
6	5.00	8057.	2419.	1.57	0.4779	3.28
7	5.83	8488.	2108.	1.65	0.4165	3.96
8	6.67	8861.	1838.	1.72	0.3631	4.74
9	7.50	9221.	1586.	1.79	0.3134	5.72
10	8.33	9567.	1379.	1.86	0.2725	6.83
12	10.00	10201.	1021.	1.98	0.2018	9.83
14	11.67	10714.	751.	2.08	0.1483	14.05
16	13.33	11133.	560.	2.16	0.1106	19.57
18	15.00	11458.	421.	2.23	0.0832	26.77
20	16.67	11703.	324.	2.28	0.0641	35.52
25	20.83	12113.	207.	2.36	0.0409	57.52
30	25.00	12278.	167.	2.39	0.0329	72.49
33	27.50	12327.	151.	2.40	0.0299	80.08

TABLE C.2.12 : NUMERICAL EVALUATION OF EXPERIMENT EDIL-S1-8/#17

CYCLE NO.	REAL TIME	CONCENTRATION BRINE DIAL.		CONCENTRATION NORMALIZED		SEPARATION FACTOR
NC (-)	T (MIN)	CB (PPM)	CT (PPM)	XB (-)	XT (-)	NS (-)
0	0.0	5361.	5251.	1.00	1.0000	1.00
1	0.65	5860.	4718.	1.09	0.8986	1.22
2	1.30	6289.	4338.	1.17	0.8262	1.42
4	2.60	7128.	3591.	1.33	0.6839	1.94
6	3.90	7903.	2944.	1.47	0.5606	2.63
8	5.20	8597.	2419.	1.60	0.4606	3.48
10	6.50	9268.	1972.	1.73	0.3756	4.60
15	9.75	10553.	1184.	1.97	0.2254	8.73
20	13.00	11377.	740.	2.12	0.1410	15.05
25	16.25	11883.	503.	2.22	0.0958	23.13
30	19.50	12195.	375.	2.27	0.0715	31.83

TABLE C.2.13 : NUMERICAL EVALUATION OF EXPERIMENT EDII-S1-8/#18

CYCLE NO.	REAL TIME	CONCENTRATION BRINE DIAL.		CONCENTRATION NORMALIZED		SEPARATION FACTOR
NC (-)	T (MIN)	CB (PPM)	CT (PPM)	XB (-)	XT (-)	NS (-)
0	0.0	4926.	4807.	1.00	1.0000	1.00
1	0.48	5216.	4583.	1.06	0.9536	1.11
2	0.97	5508.	4333.	1.12	0.9014	1.24
4	1.93	6126.	3837.	1.24	0.7982	1.56
6	2.90	6707.	3659.	1.36	0.7613	1.79
8	3.87	7218.	2960.	1.47	0.6159	2.38
10	4.83	7674.	2595.	1.56	0.5398	2.89
15	7.25	8643.	1886.	1.75	0.3924	4.47
20	9.67	9299.	1421.	1.89	0.2957	6.38
25	12.08	9772.	1089.	1.98	0.2266	8.76
30	14.50	10090.	870.	2.05	0.1810	11.32
35	16.92	10329.	720.	2.10	0.1497	14.01
40	19.33	10489.	627.	2.13	0.1304	16.33

TABLE C.2.14 : NUMERICAL EVALUATION OF EXPERIMENT EDII-S1-8/#19

CYCLE NO.	REAL TIME	CONCENTRATION BRINE DIAL.		CONCENTRATION NORMALIZED		SEPARATION FACTOR
NC (-)	T (MIN)	CB (PPM)	CT (PPM)	XB (-)	XT (-)	NS (-)
0	0.0	5508.	5400.	1.00	1.0000	1.00
1	0.50	5830.	5126.	1.06	0.9492	1.12
2	1.00	6244.	4865.	1.13	0.9010	1.26
4	2.00	6917.	4309.	1.26	0.7980	1.57
6	3.00	7598.	3785.	1.38	0.7009	1.97
8	4.00	8026.	3336.	1.46	0.6178	2.36
10	5.00	8365.	2955.	1.52	0.5472	2.78
15	7.50	9693.	2173.	1.76	0.4024	4.37
20	10.00	10425.	1655.	1.89	0.3065	6.17
25	12.50	10939.	1305.	1.99	0.2416	8.22
30	15.00	11296.	1079.	2.05	0.1997	10.27
35	17.50	11540.	896.	2.10	0.1659	12.63
40	20.00	11736.	797.	2.13	0.1476	14.43
45	22.50	11883.	714.	2.16	0.1323	16.31

TABLE C.2.15 : NUMERICAL EVALUATION OF EXPERIMENT EDII-SI-8/#20

CYCLE NO.	REAL TIME	CONCENTRATION BRINE DIAL.		CONCENTRATION NORMALIZED		SEPARATION FACTOR
NC (-)	T (MIN)	CB (PPM)	CT (PPM)	XB (-)	XT (-)	NS (-)
0	0.0	5216.	5102.	1.00	1.0000	1.00
1	0.98	6244.	3969.	1.20	0.7778	1.54
2	1.97	7188.	2124.	1.38	0.4163	3.31
3	2.95	8087.	3654.	1.55	0.7161	2.17
4	3.93	8986.	1940.	1.72	0.3802	4.53
5	4.92	9772.	1448.	1.87	0.2837	6.60
6	5.90	10489.	1037.	2.01	0.2032	9.90
7	6.88	11150.	725.	2.14	0.1420	15.05
8	7.87	11703.	493.	2.24	0.0966	23.23
9	8.85	12113.	329.	2.32	0.0645	35.98
10	9.83	12493.	222.	2.40	0.0436	54.94
12	11.80	12941.	106.	2.48	0.0208	119.50
14	13.77	13125.	60.	2.52	0.0119	212.28
16	15.73	13275.	40.	2.55	0.0079	322.19
18	17.70	13393.	32.	2.57	0.0062	412.82
20	19.67	13494.	28.	2.59	0.0054	476.46
25	24.58	13696.	24.	2.63	0.0047	554.16
30	29.50	13881.	22.	2.66	0.0043	612.76
34	33.43	14017.	21.	2.69	0.0041	648.22

TABLE C.2.16 : NUMERICAL EVALUATION OF EXPERIMENT EDII-SI-8/#21

CYCLE NO.	REAL TIME	CONCENTRATION BRINE DIAL.		CONCENTRATION NORMALIZED		SEPARATION FACTOR
NC (-)	T (MIN)	CB (PPM)	CT (PPM)	XB (-)	XT (-)	NS (-)
0	0.0	2654.	2501.	1.00	1.0000	1.00
1	1.33	3614.	1854.	1.36	0.7412	1.84
2	2.67	4394.	1379.	1.66	0.5513	3.00
3	4.00	5013.	979.	1.89	0.3916	4.82
4	5.33	5508.	678.	2.08	0.2712	7.65
5	6.67	5919.	462.	2.23	0.1848	12.07
6	8.00	6229.	311.	2.35	0.1245	18.85
7	9.33	6467.	205.	2.44	0.0818	29.77
8	10.67	6662.	139.	2.51	0.0555	45.22
9	12.00	6781.	93.	2.56	0.0373	68.49
10	13.33	6887.	66.	2.59	0.0262	99.03
12	16.00	7067.	37.	2.66	0.0147	181.08
14	18.67	7173.	26.	2.70	0.0103	263.13
16	21.33	7264.	16.	2.74	0.0062	438.45
18	24.00	7370.	14.	2.78	0.0056	492.53
20	26.67	7446.	11.	2.81	0.0044	633.35
25	33.33	7598.	10.	2.86	0.0040	710.93

TABLE C.2.17 : NUMERICAL EVALUATION OF EXPERIMENT EDII-S1-8/#22

CYCLE NO.	REAL TIME	CONCENTRATION BRINE DIAL.		CONCENTRATION NORMALIZED		SEPARATION FACTOR
NC (-)	T (MIN)	CB (PPM)	CT (PPM)	XB (-)	XT (-)	NS (-)
0	0.0	2668.	2611.	1.00	1.0000	1.00
1	1.02	3222.	2092.	1.21	0.8010	1.51
2	2.03	3713.	1725.	1.39	0.6606	2.11
3	3.05	4180.	1395.	1.57	0.5341	2.93
4	4.07	4609.	1110.	1.73	0.4251	4.06
5	5.08	4984.	870.	1.87	0.3332	5.61
6	6.10	5187.	668.	1.94	0.2558	7.60
7	7.12	5639.	508.	2.11	0.1947	10.86
8	8.13	5904.	391.	2.21	0.1496	14.80
9	9.15	6126.	296.	2.30	0.1134	20.24
10	10.17	6319.	228.	2.37	0.0871	27.18
12	12.20	6557.	146.	2.46	0.0561	43.83
14	14.23	6707.	101.	2.51	0.0386	65.07
16	16.27	6826.	78.	2.56	0.0297	86.05
18	18.30	6872.	66.	2.58	0.0251	102.63
20	20.33	6932.	58.	2.60	0.0222	117.05
25	25.42	7082.	51.	2.65	0.0197	134.86
30	30.50	7143.	49.	2.68	0.0187	143.02

TABLE C.2.18 : NUMERICAL EVALUATION OF EXPERIMENT EDII-S1-8/#23

CYCLE NO.	REAL TIME	CONCENTRATION BRINE DIAL.		CONCENTRATION NORMALIZED		SEPARATION FACTOR
NC (-)	T (MIN)	CB (PPM)	CT (PPM)	XB (-)	XT (-)	NS (-)
0	0.0	2668.	2606.	1.00	1.0000	1.00
1	1.00	3446.	1881.	1.29	0.7218	1.79
2	2.00	4137.	1405.	1.55	0.5393	2.88
3	3.00	4781.	1005.	1.79	0.3859	4.64
4	4.00	5318.	694.	1.99	0.2662	7.49
5	5.00	5801.	472.	2.17	0.1813	11.99
6	6.00	6170.	314.	2.31	0.1205	19.19
10	10.00	6917.	91.	2.59	0.0348	74.42
15	15.00	7233.	47.	2.71	0.0180	150.76
20	20.00	7400.	36.	2.77	0.0137	202.06
25	25.00	7598.	33.	2.85	0.0128	223.19
30	30.00	7750.	30.	2.91	0.0116	250.45

TABLE C.2.19 : NUMERICAL EVALUATION OF EXPERIMENT EDII-S1-8/#24

CYCLE NO.	REAL TIME	CONCENTRATION BRINE DIAL.		CONCENTRATION NORMALIZED		SEPARATION FACTOR
NC (-)	T (MIN)	CB (PPM)	CT (PPM)	XB (-)	XT (-)	NS (-)
0	0.0	1257.	1241.	1.00	1.0000	1.00
1	0.67	1358.	1059.	1.08	0.8534	1.27
2	1.33	1442.	986.	1.15	0.7942	1.44
3	2.00	1522.	913.	1.21	0.7360	1.64
4	2.67	1597.	845.	1.27	0.6809	1.87
6	4.00	1752.	724.	1.39	0.5832	2.39
8	5.33	1886.	618.	1.50	0.4979	3.01
10	6.67	2021.	525.	1.61	0.4231	3.80
15	10.00	2304.	348.	1.83	0.2807	6.53
20	13.33	2517.	235.	2.00	0.1892	10.58
25	16.67	2666.	165.	2.12	0.1331	15.94
30	20.00	2771.	126.	2.20	0.1019	21.64
35	23.33	2838.	103.	2.26	0.0832	27.14
40	26.67	2877.	90.	2.29	0.0728	31.45
45	30.00	2916.	84.	2.32	0.0676	34.32

TABLE C.2.20 : NUMERICAL EVALUATION OF EXPERIMENT EDII-S1-8/#25

CYCLE NO.	REAL TIME	CONCENTRATION BRINE	CONCENTRATION DIAL.	CONCENTRATION NORMALIZED		SEPARATION FACTOR
NC (-)	T (MIN)	CB (PPM)	CT (PPM)	XB (-)	XT (-)	NS (-)
0	0.0	1294.	1290.	1.00	1.0000	1.00
1	1.00	1650.	991.	1.27	0.7680	1.66
2	2.00	1940.	784.	1.50	0.6080	2.47
3	3.00	2206.	606.	1.70	0.4700	3.63
4	4.00	2452.	458.	1.89	0.3550	5.34
6	6.00	2832.	254.	2.19	0.1970	11.11
8	8.00	3089.	139.	2.39	0.1080	22.10
10	10.00	3252.	81.	2.51	0.0630	39.88
14	14.00	3415.	34.	2.64	0.0266	99.21
18	18.00	3500.	24.	2.70	0.0185	146.19
22	22.00	3563.	21.	2.75	0.0159	173.13
26	26.00	3625.	19.	2.80	0.0144	194.52
30	30.00	3671.	18.	2.84	0.0140	202.59

TABLE C.2.21 : NUMERICAL EVALUATION OF EXPERIMENT EDII-SI-8/#26

CYCLE NO.	REAL TIME	CONCENTRATION BRINE	CONCENTRATION DIAL.	CONCENTRATION NORMALIZED		SEPARATION FACTOR
NC (-)	T (MIN)	CB (PPM)	CT (PPM)	XB (-)	XT (-)	NS (-)
0	0.0	1257.	1251.	1.00	1.0000	1.00
1	1.33	1741.	915.	1.38	0.7309	1.89
2	2.67	2119.	660.	1.69	0.5278	3.19
3	4.00	2430.	464.	1.93	0.3711	5.21
4	5.33	2699.	319.	2.15	0.2546	8.43
5	6.67	2916.	215.	2.32	0.1722	13.47
6	8.00	3067.	144.	2.44	0.1155	21.12
8	10.67	3280.	71.	2.61	0.0567	46.01
10	13.33	3404.	35.	2.71	0.0284	95.50
12	16.00	3489.	23.	2.77	0.0184	151.22
14	18.67	3557.	18.	2.83	0.0143	197.43
18	24.00	3688.	14.	2.93	0.0110	265.91
22	29.33	3808.	12.	3.03	0.0096	315.89
26	34.67	3905.	11.	3.11	0.0092	338.53
30	40.00	3992.	11.	3.17	0.0088	362.28

TABLE C.2.22 : NUMERICAL EVALUATION OF EXPERIMENT EDII-SI-8/#27

CYCLE NO.	REAL TIME	CONCENTRATION BRINE DIAL.		CONCENTRATION NORMALIZED		SEPARATION FACTOR
NC (-)	T (MIN)	CB (PPM)	CT (PPM)	XB (-)	XT (-)	NS (-)
0	0.0	1284.	1277.	1.00	1.0000	1.00
1	0.83	1511.	1045.	1.18	0.8182	1.44
2	1.67	1698.	913.	1.32	0.7152	1.85
3	2.50	1865.	789.	1.45	0.6182	2.35
4	3.33	2026.	676.	1.58	0.5293	2.98
5	4.17	2178.	575.	1.70	0.4505	3.77
6	5.00	2309.	486.	1.80	0.3808	4.72
8	6.67	2561.	341.	2.00	0.2667	7.48
10	8.33	2760.	233.	2.15	0.1828	11.76
12	10.00	2921.	156.	2.28	0.1222	18.62
14	11.67	3039.	107.	2.37	0.0838	28.23
16	13.33	3128.	75.	2.44	0.0586	41.60
18	15.00	3229.	53.	2.52	0.0411	61.19
20	16.67	3291.	37.	2.56	0.0292	87.83
25	20.83	3376.	22.	2.63	0.0169	155.90
30	25.00	3427.	17.	2.67	0.0133	200.21
35	29.17	3466.	15.	2.70	0.0121	222.77

TABLE C.2.23 : NUMERICAL EVALUATION OF EXPERIMENT EDII-S1-8/#28

CYCLE NO.	REAL TIME	CONCENTRATION BRINE DIAL.		CONCENTRATION NORMALIZED		SEPARATION FACTOR
NC (-)	T (MIN)	CB (PPM)	CT (PPM)	XB (-)	XT (-)	NS (-)
0	0.0	1263.	1254.	1.00	1.0000	1.00
1	1.32	1666.	832.	1.32	0.6636	1.99
2	2.63	1983.	587.	1.57	0.4681	3.36
3	3.95	2222.	387.	1.76	0.3086	5.70
4	5.27	2397.	252.	1.90	0.2006	9.46
5	6.58	2501.	163.	1.98	0.1296	15.28
6	7.90	2584.	107.	2.05	0.0854	23.96
7	9.22	2633.	77.	2.09	0.0617	33.79
10	13.17	2694.	43.	2.13	0.0345	61.91
12	15.80	2705.	39.	2.14	0.0314	68.28
14	18.43	2738.	37.	2.17	0.0298	72.69
16	21.07	2760.	37.	2.19	0.0293	74.56

TABLE C.2.24 : NUMERICAL EVALUATION OF EXPERIMENT EDII-S1-8/#29

CYCLE NO.	REAL TIME	CONCENTRATION BRINE	CONCENTRATION DIAL.	CONCENTRATION NORMALIZED		SEPARATION FACTOR
NC (-)	T (MIN)	CB (PPM)	CT (PPM)	XB (-)	XT (-)	NS (-)
0	0.0	1289.	1267.	1.00	1.0000	1.00
1	1.00	1448.	955.	1.12	0.7536	1.49
2	2.00	1581.	826.	1.23	0.6517	1.88
3	3.00	1709.	716.	1.33	0.5652	2.35
4	4.00	1822.	619.	1.41	0.4888	2.89
6	6.00	2010.	462.	1.56	0.3646	4.28
8	8.00	2157.	347.	1.67	0.2739	6.11
10	10.00	2266.	264.	1.76	0.2088	8.42
15	15.00	2419.	159.	1.88	0.1253	14.98
20	20.00	2474.	129.	1.92	0.1018	18.84
25	25.00	2501.	116.	1.94	0.0916	21.17

TABLE C.2.25 : NUMERICAL EVALUATION OF EXPERIMENT EDII-S1-8/#30

CYCLE NO.	REAL TIME	CONCENTRATION BRINE	CONCENTRATION DIAL.	CONCENTRATION NORMALIZED		SEPARATION FACTOR
NC (-)	T (MIN)	CB (PPM)	CT (PPM)	XB (-)	XT (-)	NS (-)
0	0.0	1226.	1210.	1.00	1.0000	1.00
1	0.68	1379.	916.	1.12	0.7569	1.49
2	1.37	1506.	787.	1.23	0.6503	1.89
3	2.05	1629.	677.	1.33	0.5597	2.37
4	2.73	1757.	583.	1.43	0.4819	2.97
6	4.10	1983.	430.	1.62	0.3550	4.56
8	5.47	2184.	315.	1.78	0.2601	6.85
10	6.83	2369.	228.	1.93	0.1887	10.24
14	9.57	2650.	119.	2.16	0.0981	22.04
18	12.30	2821.	68.	2.30	0.0560	41.13
22	15.03	2927.	45.	2.39	0.0375	63.64
26	17.77	2988.	35.	2.44	0.0293	83.16
30	20.50	3027.	32.	2.47	0.0261	94.56
34	23.23	3055.	29.	2.49	0.0240	103.92

TABLE C.2.26 : NUMERICAL EVALUATION OF EXPERIMENT EDII-S1-8/#31

CYCLE NO.	REAL TIME	CONCENTRATION BRINE DIAL.		CONCENTRATION NORMALIZED		SEPARATION FACTOR
NC (-)	T (MIN)	CB (PPM)	CT (PPM)	XB (-)	XT (-)	NS (-)
0	0.0	1247.	1238.	1.00	1.0000	1.00
1	0.83	1597.	871.	1.28	0.7031	1.82
2	1.67	1902.	655.	1.53	0.5292	2.88
3	2.50	2184.	484.	1.75	0.3906	4.48
4	3.33	2435.	350.	1.95	0.2823	6.92
5	4.17	2644.	248.	2.12	0.2000	10.60
6	5.00	2827.	173.	2.27	0.1396	16.24
8	6.67	3078.	84.	2.47	0.0675	36.57
10	8.33	3224.	42.	2.59	0.0341	75.91
12	10.00	3308.	24.	2.65	0.0197	134.77
14	11.67	3370.	16.	2.70	0.0127	212.70
18	15.00	3466.	10.	2.78	0.0078	355.87
22	18.33	3546.	8.	2.84	0.0062	455.02
26	21.67	3620.	7.	2.90	0.0053	546.48

TABLE C.2.27 : NUMERICAL EVALUATION OF EXPERIMENT EDII-S1-8/#32

CYCLE NO.	REAL TIME	CONCENTRATION BRINE DIAL.		CONCENTRATION NORMALIZED		SEPARATION FACTOR
NC (-)	T (MIN)	CB (PPM)	CT (PPM)	XB (-)	XT (-)	NS (-)
0	0.0	1205.	1191.	1.00	1.0000	1.00
1	0.98	1666.	787.	1.38	0.6609	2.09
2	1.97	2064.	529.	1.71	0.4442	3.86
3	2.95	2408.	342.	2.00	0.2871	6.96
4	3.93	2677.	217.	2.22	0.1820	12.21
5	4.92	2871.	134.	2.38	0.1127	21.15
6	5.90	3027.	83.	2.51	0.0693	36.24
7	6.88	3128.	52.	2.60	0.0433	59.92
8	7.87	3201.	33.	2.66	0.0276	96.19
9	8.85	3263.	22.	2.71	0.0181	149.71
10	9.83	3314.	15.	2.75	0.0125	220.78
12	11.80	3410.	8.	2.83	0.0065	435.42
14	13.77	3478.	5.	2.89	0.0038	761.30
16	15.73	3551.	3.	2.95	0.0027	1088.42
18	17.70	3620.	2.	3.00	0.0021	1459.64
20	19.67	3677.	2.	3.05	0.0015	2012.11
25	24.58	3819.	1.	3.17	0.0009	3657.97

TABLE C.2.28 : NUMERICAL EVALUATION OF EXPERIMENT EDII-S1-8/#33

CYCLE NO.	REAL TIME	CONCENTRATION BRINE	CONCENTRATION DIAL.	CONCENTRATION NORMALIZED		SEPARATION FACTOR
NC (-)	T (MIN)	CB (PPM)	CT (PPM)	XB (-)	XT (-)	NS (-)
0	0.0	1294.	1276.	1.00	1.0000	1.00
1	1.30	1918.	806.	1.49	0.6320	2.36
2	2.60	2419.	494.	1.89	0.3873	4.87
3	3.90	2816.	294.	2.19	0.2305	9.51
4	5.20	3111.	170.	2.42	0.1335	18.16
5	6.50	3331.	98.	2.59	0.0768	33.76
6	7.80	3472.	85.	2.70	0.0667	40.53
7	9.10	3580.	37.	2.79	0.0288	96.77
8	10.40	3682.	24.	2.87	0.0190	150.90
9	11.70	3762.	17.	2.93	0.0133	219.58
10	13.00	3831.	13.	2.98	0.0100	298.12
15	19.50	4176.	5.	3.25	0.0040	804.36
20	26.00	4484.	2.	3.49	0.0015	2303.13
25	32.50	4748.	1.	3.70	0.0006	6096.32

TABLE C.2.29 : NUMERICAL EVALUATION OF EXPERIMENT EDII-S1-8/#34

CYCLE NO.	REAL TIME	CONCENTRATION BRINE	CONCENTRATION DIAL.	CONCENTRATION NORMALIZED		SEPARATION FACTOR
NC (-)	T (MIN)	CB (PPM)	CT (PPM)	XB (-)	XT (-)	NS (-)
0	0.0	1215.	1200.	1.00	1.0000	1.00
1	0.83	1342.	1013.	1.10	0.8441	1.31
2	1.67	1448.	942.	1.19	0.7849	1.52
3	2.50	1549.	871.	1.27	0.7258	1.76
4	3.33	1639.	805.	1.35	0.6710	2.01
6	5.00	1811.	684.	1.49	0.5699	2.61
8	6.67	1962.	577.	1.61	0.4806	3.36
10	8.33	2097.	485.	1.73	0.4043	4.27
15	12.50	2369.	303.	1.95	0.2527	7.72
20	16.67	2567.	186.	2.11	0.1548	13.64
25	20.83	2699.	119.	2.22	0.0989	22.46
30	25.00	2788.	81.	2.29	0.0677	33.87
35	29.17	2844.	65.	2.34	0.0538	43.53

TABLE C.2.30 : NUMERICAL EVALUATION OF EXPERIMENT EDII-S1-8/#35

CYCLE NO.	REAL TIME	CONCENTRATION BRINE	CONCENTRATION DIAL.	CONCENTRATION NORMALIZED		SEPARATION FACTOR
NC (-)	T (MIN)	CB (PPM)	CT (PPM)	XB (-)	XT (-)	NS (-)
0	0.0	1220.	1218.	1.00	1.0000	1.00
1	1.00	1575.	929.	1.29	0.7627	1.69
2	2.00	1865.	734.	1.53	0.6028	2.53
3	3.00	2129.	562.	1.74	0.4619	3.78
4	4.00	2364.	421.	1.94	0.3453	5.61
5	5.00	2561.	310.	2.10	0.2542	8.26
6	6.00	2727.	227.	2.23	0.1864	11.99
7	7.00	2860.	165.	2.34	0.1356	17.20
8	8.00	2966.	119.	2.43	0.0975	24.94
10	10.00	3111.	65.	2.55	0.0531	48.04
12	12.00	3201.	39.	2.62	0.0321	81.72
14	14.00	3257.	27.	2.67	0.0225	118.85
16	16.00	3302.	21.	2.71	0.0169	159.65
18	18.00	3342.	18.	2.74	0.0151	180.77
20	20.00	3370.	17.	2.76	0.0138	200.52
25	25.00	3444.	15.	2.82	0.0122	231.62
30	30.00	3506.	14.	2.87	0.0117	246.53

TABLE C.2.31 : NUMERICAL EVALUATION OF EXPERIMENT EDII-S1-8/#35a

CYCLE NO.	REAL TIME	CONCENTRATION BRINE	CONCENTRATION DIAL.	CONCENTRATION NORMALIZED		SEPARATION FACTOR
NC (-)	T (MIN)	CB (PPM)	CT (PPM)	XB (-)	XT (-)	NS (-)
0	0.0	1252.	1251.	1.00	1.0000	1.00
1	1.00	1448.	1099.	1.16	0.8784	1.32
2	2.00	1607.	984.	1.28	0.7866	1.63
3	3.00	1757.	869.	1.40	0.6948	2.02
4	4.00	1902.	765.	1.52	0.6113	2.49
6	6.00	2157.	578.	1.72	0.4619	3.73
8	8.00	2380.	427.	1.90	0.3412	5.57
10	10.00	2572.	311.	2.05	0.2485	8.27
15	15.00	2888.	137.	2.31	0.1093	21.11
20	20.00	3039.	68.	2.43	0.0546	44.42
25	25.00	3123.	52.	2.49	0.0412	60.48
30	30.00	3167.	37.	2.53	0.0297	85.21
35	35.00	3201.	34.	2.56	0.0269	95.02
40	40.00	3224.	32.	2.57	0.0258	99.90

TABLE C.2.32 : NUMERICAL EVALUATION OF EXPERIMENT EDII-S1-8/#36

CYCLE NO.	REAL TIME	CONCENTRATION BRINE DIAL.		CONCENTRATION NORMALIZED		SEPARATION FACTOR
NC (-)	T (MIN)	CB (PPM)	CT (PPM)	XB (-)	XT (-)	NS (-)
0	0.0	1147.	1157.	1.00	1.0000	1.00
1	2.25	1511.	703.	1.32	0.6076	2.17
2	4.50	1795.	503.	1.56	0.4348	3.60
3	6.75	2054.	348.	1.79	0.3010	5.95
4	9.00	2298.	235.	2.00	0.2029	9.88
5	11.25	2512.	156.	2.19	0.1349	16.24
6	13.50	2683.	103.	2.34	0.0892	26.23
8	18.00	2916.	52.	2.54	0.0446	57.02
10	22.50	3055.	31.	2.66	0.0270	98.75
15	33.75	3201.	18.	2.79	0.0154	181.44
20	45.00	3280.	14.	2.86	0.0123	233.22
25	56.25	3365.	13.	2.93	0.0110	265.92
30	67.50	3427.	12.	2.99	0.0105	285.13

TABLE C.2.33 : NUMERICAL EVALUATION OF EXPERIMENT EDII-S1-8/#37

CYCLE NO.	REAL TIME	CONCENTRATION BRINE DIAL.		CONCENTRATION NORMALIZED		SEPARATION FACTOR
NC (-)	T (MIN)	CB (PPM)	CT (PPM)	XB (-)	XT (-)	NS (-)
0	0.0	1252.	1242.	1.00	1.0000	1.00
1	1.18	1432.	948.	1.14	0.7632	1.50
2	2.37	1575.	819.	1.26	0.6594	1.91
3	3.55	1714.	710.	1.37	0.5711	2.40
4	4.73	1838.	606.	1.47	0.4881	3.01
5	5.92	1962.	516.	1.57	0.4154	3.77
6	7.10	2081.	436.	1.66	0.3510	4.73
8	9.47	2287.	310.	1.83	0.2492	7.33
10	11.83	2463.	213.	1.97	0.1713	11.48
15	17.75	2783.	84.	2.22	0.0675	32.93
20	23.67	2933.	44.	2.34	0.0351	66.73
25	29.58	3000.	32.	2.40	0.0254	94.17
30	35.50	3039.	28.	2.43	0.0224	108.20
35	41.42	3067.	27.	2.45	0.0214	114.50
40	47.33	3083.	26.	2.46	0.0208	118.58

TABLE C.2.34 : NUMERICAL EVALUATION OF EXPERIMENT EDII-S1-8/#38

CYCLE NO.	REAL TIME	CONCENTRATION BRINE DIAL.		CONCENTRATION NORMALIZED		SEPARATION FACTOR
NC (-)	T (MIN)	CB (PPM)	CT (PPM)	XB (-)	XT (-)	NS (-)
0	0.0	1268.	1256.	1.00	1.0000	1.00
1	2.42	1795.	729.	1.42	0.5801	2.44
2	4.83	2266.	461.	1.79	0.3665	4.88
3	7.25	2683.	280.	2.12	0.2228	9.50
4	9.67	3005.	161.	2.37	0.1283	18.47
5	12.08	3235.	95.	2.55	0.0758	33.67
6	14.50	3398.	59.	2.68	0.0467	57.38
8	19.33	3591.	29.	2.83	0.0227	124.83
10	24.17	3716.	20.	2.93	0.0156	187.83
15	36.25	3946.	13.	3.11	0.0103	303.10
20	48.33	4107.	10.	3.24	0.0083	389.50
25	60.42	4222.	9.	3.33	0.0074	450.52
30	72.50	4309.	8.	3.40	0.0062	551.77

TABLE C.2.35 : NUMERICAL EVALUATION OF EXPERIMENT EDII-S1-8/#39

CYCLE NO.	REAL TIME	CONCENTRATION BRINE DIAL.		CONCENTRATION NORMALIZED		SEPARATION FACTOR
NC (-)	T (MIN)	CB (PPM)	CT (PPM)	XB (-)	XT (-)	NS (-)
0	0.0	1289.	1286.	1.00	1.0000	1.00
1	1.53	1768.	884.	1.37	0.6871	2.00
2	3.07	2135.	658.	1.66	0.5115	3.24
3	4.60	2479.	458.	1.92	0.3561	5.40
4	6.13	2760.	310.	2.14	0.2407	8.90
5	7.67	2994.	201.	2.32	0.1565	14.84
6	9.20	3162.	130.	2.45	0.1013	24.21
8	12.27	3381.	58.	2.62	0.0451	58.12
10	15.33	3500.	30.	2.72	0.0236	115.21
15	23.00	3648.	15.	2.83	0.0115	245.37
20	30.67	3762.	12.	2.92	0.0090	323.33
25	38.33	3865.	10.	3.00	0.0080	373.71

TABLE C.2.36 : NUMERICAL EVALUATION OF EXPERIMENT EDII-S1-8/#40

CYCLE NO.	REAL TIME	CONCENTRATION BRINE DIAL.		CONCENTRATION NORMALIZED		SEPARATION FACTOR
NC (-)	T (MIN)	CB (PPM)	CT (PPM)	XB (-)	XT (-)	NS (-)
0	0.0	1305.	1300.	1.00	1.0000	1.00
1	0.27	1342.	1258.	1.03	0.9673	1.06
2	0.53	1374.	1237.	1.05	0.9514	1.11
4	1.07	1448.	1197.	1.11	0.9206	1.21
6	1.60	1501.	1158.	1.15	0.8909	1.29
8	2.13	1554.	1122.	1.19	0.8631	1.38
10	2.67	1607.	1086.	1.23	0.8353	1.47
15	4.00	1725.	1006.	1.32	0.7738	1.71
20	5.33	1848.	934.	1.42	0.7183	1.97
25	6.67	1956.	864.	1.50	0.6647	2.26
30	8.00	2064.	800.	1.58	0.6151	2.57
35	9.33	2178.	742.	1.67	0.5704	2.93
40	10.67	2271.	686.	1.74	0.5278	3.30
45	12.00	2369.	633.	1.82	0.4871	3.73
50	13.33	2463.	587.	1.89	0.4514	4.18
60	16.00	2639.	501.	2.02	0.3849	5.25
70	18.67	2805.	426.	2.15	0.3274	6.57
80	21.33	2949.	361.	2.26	0.2778	8.14
90	24.00	3100.	306.	2.38	0.2351	10.11
100	26.67	3235.	258.	2.48	0.1984	12.50
110	29.33	3336.	219.	2.56	0.1687	15.16

TABLE C.2.37 : NUMERICAL EVALUATION OF EXPERIMENT EDII-S1-8/#41

CYCLE NO.	REAL TIME	CONCENTRATION BRINE DIAL.		CONCENTRATION NORMALIZED		SEPARATION FACTOR
NC (-)	T (MIN)	CB (PPM)	CT (PPM)	XB (-)	XT (-)	NS (-)
0	0.0	1184.	1171.	1.00	1.0000	1.00
1	0.58	1421.	1045.	1.20	0.8921	1.35
2	1.17	1618.	928.	1.37	0.7919	1.73
3	1.75	1811.	823.	1.53	0.7026	2.18
4	2.33	1983.	720.	1.68	0.6145	2.73
6	3.50	2364.	555.	2.00	0.4736	4.22
8	4.67	2716.	423.	2.29	0.3612	6.35
10	5.83	3055.	322.	2.58	0.2753	9.38
14	8.17	3688.	182.	3.12	0.1553	20.07
18	10.50	4234.	108.	3.58	0.0920	38.90
22	12.83	4689.	65.	3.96	0.0557	71.09
26	15.17	5013.	42.	4.24	0.0358	118.34
30	17.50	5317.	29.	4.49	0.0246	182.90
34	19.83	5454.	21.	4.61	0.0180	256.70
38	22.17	5671.	16.	4.79	0.0138	348.02
42	24.50	5822.	13.	4.92	0.0110	446.62
46	26.83	5882.	10.	4.97	0.0089	557.12
50	29.17	6004.	9.	5.07	0.0073	697.85
54	31.50	6126.	7.	5.18	0.0064	810.23

TABLE C.2.38 : NUMERICAL EVALUATION OF EXPERIMENT EDII-S1-8/#42

CYCLE NO.	REAL TIME	CONCENTRATION BRINE DIAL.		CONCENTRATION NORMALIZED		SEPARATION FACTOR
NC (-)	T (MIN)	CB (PPM)	CT (PPM)	XB (-)	XT (-)	NS (-)
0	0.0	1226.	1204.	1.00	1.0000	1.00
1	0.52	1310.	1064.	1.07	0.8842	1.21
2	1.03	1374.	1005.	1.12	0.8349	1.34
3	1.55	1442.	942.	1.18	0.7824	1.50
4	2.07	1453.	885.	1.19	0.7353	1.61
6	3.10	1623.	780.	1.32	0.6484	2.04
8	4.13	1730.	818.	1.41	0.6795	2.08
10	5.17	1838.	738.	1.50	0.6131	2.45
15	7.75	2059.	449.	1.68	0.3730	4.50
20	10.33	2233.	335.	1.82	0.2787	6.54
25	12.92	2364.	257.	1.93	0.2133	9.04
30	15.50	2463.	204.	2.01	0.1693	11.86
35	18.08	2528.	170.	2.06	0.1415	14.58
40	20.67	2572.	148.	2.10	0.1233	17.03
45	23.25	2622.	133.	2.14	0.1104	19.38
50	25.83	2644.	125.	2.16	0.1040	20.75
55	28.42	2672.	117.	2.18	0.0975	22.35
60	31.00	2694.	115.	2.20	0.0954	23.04

TABLE C.2.39 : NUMERICAL EVALUATION OF EXPERIMENT EDII-S1-8/#43

CYCLE NO.	REAL TIME	CONCENTRATION BRINE DIAL.		CONCENTRATION NORMALIZED		SEPARATION FACTOR
NC (-)	T (MIN)	CB (PPM)	CT (PPM)	XB (-)	XT (-)	NS (-)
0	0.0	1231.	1224.	1.00	1.0000	1.00
1	0.83	1549.	987.	1.26	0.8061	1.56
2	1.67	1805.	805.	1.47	0.6575	2.23
3	2.50	2037.	648.	1.66	0.5290	3.13
4	3.33	2238.	517.	1.82	0.4225	4.30
5	4.17	2413.	406.	1.96	0.3319	5.91
6	5.00	2572.	321.	2.09	0.2624	7.96
8	6.67	2799.	196.	2.27	0.1602	14.20
10	8.33	2955.	124.	2.40	0.1012	23.73
14	11.67	3139.	58.	2.55	0.0472	54.02
18	15.00	3241.	38.	2.63	0.0307	85.85
22	18.33	3314.	30.	2.69	0.0248	108.71
26	21.67	3376.	27.	2.74	0.0223	122.76

TABLE C.2.40 : NUMERICAL EVALUATION OF EXPERIMENT EDII-S1-8/#44

CYCLE NO.	REAL TIME	CONCENTRATION BRINE	CONCENTRATION DIAL.	CONCENTRATION NORMALIZED		SEPARATION FACTOR
NC (-)	T (MIN)	CB (PPM)	CT (PPM)	XB (-)	XT (-)	NS (-)
0	0.0	1278.	1276.	1.00	1.0000	1.00
1	0.67	1506.	1103.	1.18	0.8645	1.36
2	1.33	1693.	968.	1.32	0.7583	1.75
3	2.00	1881.	842.	1.47	0.6603	2.23
4	2.67	2048.	730.	1.60	0.5723	2.80
6	4.00	2331.	542.	1.82	0.4247	4.29
8	5.33	2561.	396.	2.00	0.3104	6.45
10	6.67	2738.	293.	2.14	0.2295	9.33
14	9.33	2977.	165.	2.33	0.1294	17.99
18	12.00	3123.	103.	2.44	0.0809	30.20
22	14.67	3218.	74.	2.52	0.0576	43.68
26	17.33	3302.	61.	2.58	0.0480	53.79
30	20.00	3353.	54.	2.62	0.0425	61.76
34	22.67	3410.	51.	2.67	0.0403	66.11

TABLE C.2.41 : NUMERICAL EVALUATION OF EXPERIMENT EDII-S1-8/#45

CYCLE NO.	REAL TIME	CONCENTRATION BRINE	CONCENTRATION DIAL.	CONCENTRATION NORMALIZED		SEPARATION FACTOR
NC (-)	T (MIN)	CB (PPM)	CT (PPM)	XB (-)	XT (-)	NS (-)
0	0.0	1242.	1233.	1.00	1.0000	1.00
1	0.35	1273.	1158.	1.03	0.9393	1.09
2	0.70	1300.	1118.	1.05	0.9069	1.15
3	1.05	1331.	1080.	1.07	0.8755	1.22
4	1.40	1358.	1045.	1.09	0.8473	1.29
6	2.10	1416.	982.	1.14	0.7960	1.43
8	2.80	1464.	929.	1.18	0.7531	1.57
10	3.50	1517.	878.	1.22	0.7123	1.72
15	5.25	1634.	775.	1.32	0.6287	2.09
20	7.00	1730.	691.	1.39	0.5607	2.49
25	8.75	1816.	627.	1.46	0.5084	2.88
30	10.50	1886.	575.	1.52	0.4665	3.26
35	12.25	1940.	531.	1.56	0.4310	3.63
40	14.00	1978.	501.	1.59	0.4059	3.93
50	17.50	2059.	451.	1.66	0.3661	4.53
60	21.00	2113.	421.	1.70	0.3410	4.99
70	24.50	2146.	404.	1.73	0.3274	5.28
80	28.00	2173.	395.	1.75	0.3201	5.47

TABLE C.2.42 : NUMERICAL EVALUATION OF EXPERIMENT EDII-S1-8/#46

CYCLE NO.	REAL TIME	CONCENTRATION BRINE DIAL.		CONCENTRATION NORMALIZED		SEPARATION FACTOR
NC (-)	T (MIN)	CB (PPM)	CT (PPM)	XP (-)	XT (-)	NS (-)
0	0.0	1226.	1224.	1.00	1.0000	1.00
1	0.35	1342.	1152.	1.09	0.9410	1.16
2	0.70	1465.	1084.	1.21	0.8851	1.37
3	1.05	1618.	1011.	1.32	0.8261	1.60
4	1.40	1730.	943.	1.41	0.7703	1.83
6	2.10	1945.	815.	1.59	0.6660	2.38
8	2.80	2119.	707.	1.73	0.5774	2.99
10	3.50	2276.	606.	1.86	0.4953	3.75
15	5.25	2419.	426.	1.97	0.3477	5.67
20	7.00	2694.	308.	2.20	0.2518	8.73
25	8.75	2855.	232.	2.33	0.1897	12.28
30	10.50	2949.	187.	2.41	0.1528	15.75
35	12.25	3039.	155.	2.48	0.1264	19.61
40	14.00	3089.	137.	2.52	0.1117	22.56
45	15.75	3151.	125.	2.57	0.1022	25.15
50	17.50	3196.	116.	2.61	0.0948	27.49

TABLE C.2.43 : NUMERICAL EVALUATION OF EXPERIMENT EDII-S1-8/#47

CYCLE NO.	REAL TIME	CONCENTRATION BRINE DIAL.		CONCENTRATION NORMALIZED		SEPARATION FACTOR
NC (-)	T (MIN)	CB (PPM)	CT (PPM)	XB (-)	XT (-)	NS (-)
0	0.0	1270.	1246.	1.00	1.0000	1.00
5	0.92	1297.	1184.	1.02	0.9503	1.08
10	1.83	1333.	1126.	1.05	0.9037	1.16
15	2.75	1369.	1081.	1.08	0.8675	1.24
20	3.67	1402.	1055.	1.10	0.8468	1.30
30	5.50	1461.	984.	1.15	0.7899	1.46
40	7.33	1508.	938.	1.19	0.7526	1.58
50	9.17	1544.	903.	1.22	0.7246	1.68
60	11.00	1575.	877.	1.24	0.7039	1.76
70	12.83	1603.	855.	1.26	0.6863	1.84
80	14.67	1620.	841.	1.28	0.6749	1.89
90	16.50	1632.	829.	1.28	0.6656	1.93
100	18.33	1646.	819.	1.30	0.6573	1.97

TABLE C.2.44 : NUMERICAL EVALUATION OF EXPERIMENT EDII-S1-8/#48

CYCLE NO.	REAL TIME	CONCENTRATION BRINE DIAL.		CONCENTRATION NORMALIZED		SEPARATION FACTOR
NC (-)	T (MIN)	CB (PPM)	CT (PPM)	XB (-)	XT (-)	NS (-)
0	0.0	1289.	1264.	1.00	1.0000	1.00
1	1.33	1811.	897.	1.40	0.7092	1.98
2	2.67	2200.	640.	1.71	0.5061	3.37
3	4.00	2528.	441.	1.96	0.3490	5.62
4	5.33	2788.	301.	2.16	0.2378	9.10
5	6.67	2994.	203.	2.32	0.1602	14.50
6	8.00	3145.	133.	2.44	0.1051	23.22
7	9.33	3263.	94.	2.53	0.0740	34.22
8	10.67	3348.	65.	2.60	0.0510	50.90
9	12.00	3427.	47.	2.66	0.0372	71.38
10	13.33	3495.	35.	2.71	0.0281	96.62
12	16.00	3603.	23.	2.79	0.0184	152.17
14	18.67	3682.	18.	2.86	0.0143	199.97
16	21.33	3762.	15.	2.92	0.0122	238.36
20	26.67	3911.	13.	3.03	0.0105	288.70
25	33.33	4078.	12.	3.16	0.0092	344.49
30	40.00	4251.	11.	3.30	0.0085	389.44
35	46.67	4368.	10.	3.39	0.0081	420.34
40	53.33	4461.	10.	3.46	0.0077	452.20

TABLE C.2.45 : NUMERICAL EVALUATION OF EXPERIMENT EDII-S1-8/#49

CYCLE NO.	REAL TIME	CONCENTRATION BRINE DIAL.		CONCENTRATION NORMALIZED		SEPARATION FACTOR
NC (-)	T (MIN)	CB (PPM)	CT (PPM)	XB (-)	XT (-)	NS (-)
0	0.0	1315.	1280.	1.00	1.0000	1.00
1	1.52	1784.	922.	1.36	0.7208	1.88
2	3.03	2140.	626.	1.63	0.4889	3.33
3	4.55	2490.	458.	1.89	0.3579	5.29
4	6.07	2805.	294.	2.13	0.2298	9.28
5	7.58	3055.	184.	2.32	0.1442	16.11
6	9.10	3241.	119.	2.46	0.0927	26.56
8	12.13	3472.	54.	2.64	0.0423	62.34
10	15.17	3597.	32.	2.73	0.0252	108.50
15	22.75	3796.	21.	2.89	0.0161	178.95
20	30.33	3934.	16.	2.99	0.0126	237.35
25	37.92	4020.	14.	3.06	0.0109	280.74
30	45.50	4055.	12.	3.08	0.0094	328.82

TABLE C.2.46 : NUMERICAL EVALUATION OF EXPERIMENT EDII-S1-8/#50

CYCLE NO.	REAL TIME	CONCENTRATION BRINE DIAL.		CONCENTRATION NORMALIZED		SEPARATION FACTOR
NC (-)	T (MIN)	CB (PPM)	CT (PPM)	XB (-)	XT (-)	NS (-)
0	0.0	1294.	1271.	1.00	1.0000	1.00
1	0.67	1337.	1264.	1.03	0.9949	1.04
1	0.67	102907.	1251.	79.51	0.9848	80.74
3	2.00	1501.	1206.	1.16	0.9492	1.22
5	3.33	1650.	1148.	1.27	0.9036	1.41
9	6.00	1956.	1018.	1.51	0.8010	1.89
14	9.33	2298.	864.	1.78	0.6802	2.61
19	12.67	2572.	733.	1.99	0.5766	3.45
24	16.00	2799.	613.	2.16	0.4822	4.48
29	19.33	2988.	522.	2.31	0.4112	5.62
39	26.00	3269.	377.	2.53	0.2964	8.52
49	32.67	3466.	275.	2.68	0.2162	12.39
59	39.33	3620.	201.	2.80	0.1584	17.66
69	46.00	3762.	155.	2.91	0.1218	23.86
79	52.67	3877.	116.	3.00	0.0914	32.78
89	59.33	3974.	97.	3.07	0.0761	40.33
99	66.00	4055.	77.	3.13	0.0609	51.43
109	72.67	4124.	65.	3.19	0.0508	62.77

TABLE C.2.47 : NUMERICAL EVALUATION OF EXPERIMENT EDII-S1-8/#51

CYCLE NO.	REAL TIME	CONCENTRATION BRINE DIAL.		CONCENTRATION NORMALIZED		SEPARATION FACTOR
NC (-)	T (MIN)	CB (PPM)	CT (PPM)	XB (-)	XT (-)	NS (-)
0	0.0	1321.	1206.	1.00	1.0000	1.00
1	0.67	1395.	1138.	1.06	0.9433	1.12
2	1.33	1501.	1058.	1.14	0.8770	1.30
3	2.00	1597.	983.	1.21	0.8150	1.48
4	2.67	1671.	909.	1.27	0.7540	1.68
5	3.33	1779.	839.	1.35	0.6952	1.94
10	6.67	2146.	555.	1.62	0.4599	3.53
15	10.00	2457.	362.	1.86	0.3005	6.19
20	13.33	2584.	236.	1.96	0.1957	10.00
25	16.67	2705.	144.	2.05	0.1198	17.10
30	20.00	2794.	115.	2.12	0.0952	22.22
40	26.67	2899.	68.	2.20	0.0567	38.73
50	33.33	2977.	53.	2.25	0.0439	51.41
60	40.00	3039.	48.	2.30	0.0398	58.14

TABLE C.2.48 : NUMERICAL EVALUATION OF EXPERIMENT EDII-S1-8/#52

CYCLE NO.	REAL TIME	CONCENTRATION BRINE	CONCENTRATION DIAL.	CONCENTRATION NORMALIZED		SEPARATION FACTOR
NC (-)	T (MIN)	CB (PPM)	CT (PPM)	XB (-)	XT (-)	NS (-)
0	0.0	1278.	1262.	1.00	1.0000	1.00
1	0.67	1581.	980.	1.24	0.7771	1.59
2	1.33	1741.	800.	1.36	0.6339	2.15
3	2.00	1822.	645.	1.42	0.5112	2.79
4	2.67	1902.	516.	1.49	0.4090	3.64
5	3.33	1983.	439.	1.55	0.3476	4.46
6	4.00	2064.	387.	1.61	0.3067	5.26
8	5.33	2227.	310.	1.74	0.2454	7.10
10	6.67	2364.	271.	1.85	0.2147	8.61
12	8.00	2446.	232.	1.91	0.1840	10.40
14	9.33	2484.	210.	1.94	0.1667	11.66
16	10.67	2578.	193.	2.02	0.1534	13.15
21	14.00	2749.	168.	2.15	0.1329	16.18
26	17.33	2944.	142.	2.30	0.1125	20.47
31	20.67	3083.	132.	2.41	0.1043	23.13
36	24.00	3196.	116.	2.50	0.0920	27.16
41	27.33	3297.	110.	2.58	0.0869	29.67
46	30.67	3365.	103.	2.63	0.0818	32.17
51	34.00	3421.	97.	2.68	0.0767	34.90
56	37.33	3449.	90.	2.70	0.0716	37.70

TABLE C.2.49 : NUMERICAL EVALUATION OF EXPERIMENT EDII-S1-8/#53

Table C-2-50

Average Current and Voltage Distributions in Second ED Experiments

1	2	3	4	5	6	7	8	9	10	11	12	13	14	15	16	17	18	19	20	21	22
RUN NO.	CURRENT [ampere]		CYCLE NO.	AVERAGE CURRENT [ampere] TO STAGE NO.								CYCLE NO.	AVERAGE PROBE VOLTAGE [volt] IN STAGE NO.								VOLTAGE APPLIED
[-]	INITIAL	FINAL	[-]	1	2	3	4	5	6	7	8	[-]	1	2	3	4	5	6	7	8	[volt]
12	5.4	2.6	70-85	.02	.03	.04	.1	.26	.55	.83	.85	70-85	8.5	8.5	8.2	7.3	6.5	6.0	3.9	4.2	10
10	5.1	4.1	20-40	.3	.31	.35	.40	.52	.69	.71	.76	20-40	5.8	6.2	5.9	5.5	5.3	4.9	3.6	4.0	10
8	5.6	3.8	25-35	.15	.22	.34	.46	.65	.82	.78	.89										10
11	5.5	4.6	10-20	.36	.45	.51	.59	.64	.70	.70	.69	10-20	5.5	5.2	5.0	4.5	4.5	4.5	3.8	4.0	10
15	5.6	5.5	10-20	.30	.45	.55	.68	.73	.86	.72	.73	5-12	4.7	4.6		4.4		4.4	3.6	4.1	10
14	5.5	5.7	25-35	.5	.58	.63	.70	.74	.84	.73	.71	23-35	4.6	4.5	4.4	4.4	4.2	4.3	3.5	3.8	10
7	5.6	5.6	20-30	.6	.62	.64	.70	.71	.79	.75	.74										10
47	0.70	0.36	45-46	-	-	-	-	.1	.25	-	-	47-49	-	-	-	-	9.0	8.5	-	-	10
45	1.32	0.68	8-12	-	-	-	-	.06	.10	.25	.36	16-20	-	-	-	-	8.5	8.7	7.9	7.2	10
44	1.88	1.04	13-19	-	-	.04	.06	.11	.2	.31	.38	22-27	-	-	9.0	9.0	9.0	9.0	7.1	7.0	10
35a	2.60	1.40	16-24	.020	.025	.05	.08	.16	.275	.36	.41	5-12	8.2	8.3	8.4	8.0	7.9	7.5	6.9	7.0	10
19	1.45	0.88	37-38	-	-	-	-	-	-	.29	.61	34-35	-	-	-	-	-	-	7.6	6.2	10
20	1.75	1.00	36-37	-	-	-	-	.39	.71	-	-	42-43	-	-	-	-	7.6	6.1	-	-	10
18	3.00	1.72	22-25	-	-	-	-	.20	.33	.56	.75	27-31	-	-	-	-	8.1	7.6	5.8	5.2	10
17	4.70	2.60	19-25	-	-	.15	.20	.34	.52	.67	.80	31-33	-	-	8.3		7.5		4.9	4.8	10
6	5.60	3.20	30-40	.05	.08	.16	.30	.45	.62	.72	.95										
27	2.2	1.1	18-24	.01	.02	.04	.07	.12	.22	.28	.31	6-14	8.7	8.8	8.9	8.7	8.3	8.2	7.6	7.6	10
22	4.0	1.5	18-25	.02	.03	.05	.08	.17	.25	.38	.5	5-12	8.2	8.2	8.3	8.3	8.0	7.6	7.0	6.3	10
9	5.5	2.0	15-25	.05	.08	.10	.19	.31	.45	.55	.74										10
35a	2.6	1.4	16-24	.02	.025	.05	.08	.16	.275	.36	.41	5-12	8.2	8.3	8.4	8.0	7.9	7.5	6.9	7.0	10
23	4.2	2.1	19-27	.02	.04	.09	.15	.26	.39	.48	.59	7-15	7.3	7.6	7.7	7.5	7.0	6.8	5.6	5.6	10
6	5.6	3.2	30-40	.05	.08	.16	.30	.45	.62	.72	.95										10
33	3.5	2.0	16-24	.01	.025	.05	.1	.25	.44	.58	.70	6-14	13.8	13.8	13.6	13.6	13.2	12.8	10.8	10.8	15
24	5.8	3.0	16-24	.02	.04	.07	.13	.22	.58	.80	.94	25-34	13.2	13.3	13.0	12.4	12.5	11.6	9.7	9.4	15
21	8.8	3.4	16-24	.03	.05	.09	.16	.26	.71	.96	1.2	25-34	13.5	13.3	12.9	12.4	11.5	11.1	8.8	8.8	15
41	3.6	3.4	50-58	.26	.30	.34	.38	.42	.50	.56	.55	73-85	7.5	7.5	7.6	7.3	7.1	7.1	6.0	6.1	10
25	3.0	2.4	18-26	.13	.15	.20	.25	.35	.45	.50	.53	25-35	8.25	8.25	8.1	7.5	7.2	6.4	5.4	5.75	10
30	3.0	2.6	17-25	.10	.13	.20	.26	.37	.45	.52	.51	6-14	7.0	7.0	6.8	6.8	6.8	6.5	5.5	5.7	10

CONTINUED

Table C-2-50 (Continued)

1	2	3	4	5	6	7	8	9	10	11	12	13	14	15	16	17	18	19	20	21	22
RUN NO.	CURRENT [ampere]		CYCLE NO.	AVERAGE CURRENT [ampere] TO STAGE NO.								CYCLE NO.	AVERAGE PROBE VOLTAGE [volt] IN STAGE NO.								VOLTAGE APPLIED
[-]	INITIAL	FINAL	[-]	1	2	3	4	5	6	7	8	[-]	1	2	3	4	5	6	7	8	[volt]
42	2.56	.93	18-26	.04	.05	.05	.08	.12	.15	.28	.42	38-46	9.3	9.3	9.2	9.3	9.2	9.0	8.6	7.2	10
35a	2.6	1.4	16-24	.02	.025	.05	.08	.16	.275	.36	.41	5-12	8.2	8.3	8.4	8.0	7.9	7.5	6.9	7.0	10
29	2.65	1.8	12-15		.07		.16		.32		.39	7-11		8.5		7.8		7.3		6.3	10
35	1.3	1.05	19-27	.05	.06	.08	.10	.13	.18	.21	.23	28-36	4.3	4.3	4.2	4.0	3.8	3.6	3.0	2.9	5
28	2.7	1.8	24-32	.024	.038	.06	.12	.24	.36	.50	.51	13-22	8.4	8.5	8.3	8.0	7.75	7.45	6.25	6.25	10
32	4.2	2.75	17-25	.016	.03	.06	.13	.28	.46	.70	.82	7-15	13.4	13.4	13.2	13.0	12.5	12.0	10.0	10.0	15
36	1.4	.8	15-23	.03	.05	.06	.08	.10	.13	.18	.21	23-31	4.5	4.4	4.3	4.2	4.0	3.8	3.3	3.0	5
35a	2.6	1.4	16-24	.02	.025	.05	.08	.16	.275	.36	.41	5-12	8.2	8.3	8.4	8.0	7.9	7.5	6.9	7.0	10
33	3.5	2.0	16-24	.01	.025	.05	.1	.25	.44	.58	.70	6-14	13.8	13.8	13.6	13.6	13.2	12.8	10.8	10.8	15
13	2.2	2.0	40-50	.19	.21	.22	.24	.28	.34	.29	.28	40-50	2.4	2.5	2.2	2.0	2.1	2.0	1.6	1.5	5
8	5.6	3.8	25-35	.15	.22	.34	.46	.65	.82	.78	.89										10
16	9.5	6.9	20-30	.11	.19	.31	.50	.78	1.15	1.3	1.4	11-19	9.2	9.3	9.2	8.8	8.5	8.2	6.0	6.5	15
37	2.0	1.55	17-25	.01	.02	.03	.06	.18	.31	.42	.49	6-14	8.2	8.3	8.1	7.9	7.4	6.9	5.4	5.7	10
38	2.65	2.2	17-25	.04	.06	.11	.18	.29	.43	.52	.51	29-37	8.8	8.5	8.3	7.8	7.3	6.9	5.2	5.5	10
25	3.0	2.4	18-26	.13	.15	.20	.25	.35	.45	.50	.53	25-35	8.25	8.25	8.1	7.5	7.2	6.4	5.4	5.75	10
39	2.08	1.44	17-25	.01	.02	.03	.06	.15	.20	.39	.46	5-13	8.6	8.7	8.5	8.3	7.6	7.0	5.8	5.7	10
40	2.32	1.6	15-23	.01	.02	.03	.06	.16	.31	.40	.47	4-12	8.0	8.3	8.2	8.2	7.9	7.8	6.8	6.5	10
35a	2.6	1.4	16-24	.02	.025	.05	.08	.16	.275	.36	.41	5-12	8.2	8.3	8.4	8.0	7.9	7.5	6.9	7.0	10

APPENDIX C.3

COMPUTER PROGRAM FOR SPACER MODEL

The input data are: (in text)

M	= number of mixing cells	m
N	= number of slices in sorption membrane	n
PE	= Fourier number	Fo
R	= width ratio	ρ
CHALE	= channel length	ℓ/b
COMLE	= Cell length	d'/b
EPSILO	= layer thickness	δ/b
W	= velocity	v/b / v/ℓ
PODRO	= potential drop	Δψ
XSI	= membrane resistance	ξ
DTAU	= starting integration step length	Δt
ERROR	= maximum tolerable integration error	
TAU1	= duration of first half cycle	
TAU2	= duration of second half cycle	
OMEG	= acceleration factor for Gauss-Seidel iteration	

ERRIT = maximum tolerable iteration error

DTAUP = printing step length

ICYC = number of cycles

INIT = control digit to read in initial data or to automatically initialize.

```
C
C  SPACER MODEL      ( BACKWARD DIFFERENCE SCHEME
C                      GAUSS - SEIDEL ITERATION
C                      AUTOMATIC ADJUSTMENT OF TIME STEP SIZE )
C                      ( VERSION FOR PLOTTING )
C
      DIMENSION C(100,20),CH(100,20),CP(100,20),CPH(100,20)
      DIMENSION Z(6),ZH(6),ZZ(12),ZZH(12)
      COMMON IT,N,PODRO,SI,EPSILO,R,XSI
      READ (5,1) M,N,PE,R,CHALE,COMLE,EPSILO,W,PODRO,XSI,DTAU,ERROR
    1 FORMAT (2I3,10E6.4)
      READ(5,2) TAU1,TAU2,BALA,ERRIT,DTAUP,ICYC,INIT
    2 FORMAT (5E6.4,2I3)
C
C  SETTING OF INITIAL VALUES
C
      NCONT=0
      NINT=0
      N2=N+2
      N3=N+3
      M1=M+1
      M2=M+2
      DTAU=1.0/DTAU
      Z(1)=2./PE/EPSILO*DTAU
      Z(2)=2.*EPSILO*M*N*COMLE/R/CHALE*Z(1)
      Z(3)=4.*N*N/R/R/PE*DTAU
      Z(4)=W/COMLE*DTAU
      Z(5)=DTAU/EPSILO/(0.5-EPSILO)/PE
      Z(6)=(1.-EPSILO)/EPSILO*Z(5)
      DO 200 I=1,6
  200 ZH(I)=Z(I)*0.5
      CALL PAMPA(Z,ZH,ZZ,ZZH)
      STROH=0.0
      DH=0.5*DTAU
      IF (INIT.EQ.0) GO TO 35
      READ (3,37) C(1,1),SI
   37 FORMAT (5E15.7)
      DO 36 J=2,M1
   36 READ (3,37) (C(J,K),K=1,N3)
      GO TO 38
   35 DO 3 J=2,M1
      DO 4 K=1,N3
    4 C(J,K)=1.0
    3 CONTINUE
      SI=STROM(N,PODRO,EPSILO,R,XSI,C,2)
      C(1,1)=1.0
   38 CP(1,1)=C(1,1)
      CH(1,1)=C(1,1)
      CPH(1,1)=C(1,1)
      DO 34 J=2,M1
      DO 39 K=1,N3
      CP(J,K)=C(J,K)
   39 CH(J,K)=C(J,K)
   34 CONTINUE
      TAU=0.0
      CEFF=C(M1,1)
      CURR=SI
      TAUP=DTAUP
      L=1
      IC=1
      T1=TAU1
      XXY=0.095*ERROR
C
C  PRINTOUT OF PARAMETER VALUES
C
      WRITE (6,5)  CHALE,R,W,PE,M,COMLE,EPSILO,PODRO,XSI,N,ERROR,DTAU,
     1 ERRIT
    5 FORMAT (1H1/////20X,' FIRST SPACER MODEL'//////10X,'PARAMETER-VALU
     1ES'////'  CHANNEL-LENGTH          = ',F8.1//'  WIDTH-RATIO
     2      = ',F8.1//'  RELATED FLOW VELOCITY    = ',F8.1//'  PECLET NUMB
     3ER          = ',F8.1//'  NUMBER OF COMPARTMENTS  = ',I8//'  COMPAR
     4TMENT-LENGTH       = ',F8.1//'  ASSUMED LAYER THICKNESS = ',F11.4//
     5/'  APPLIED VOLTAGE          = ',F10.3///'  MEMBRANE RESISTANCE
     6 = ',F10.3////'  NUMBER OF SLICES          = ',I8////'  ALLOWED INTE
     7GRATION ERROR     = ',F10.5///'  INTEGRATION STEP LENGTH = ',F10.5/
     8 //'  ITERATION ERROR          = ',F10.5//)
      WRITE(6,10)
   10 FORMAT(1H1///
     1' NO. OF       CONCENTRATION        SEPARATION      CURRENT DENSITY
     2        MASS'/
     3' CYCLES      TOP        BOTTOM        FACTOR     DEPLETING     ENRICH
     4ING    BALANCE'/
     5'     N        CT          CB            NS           ID            IE
     6          (%)'/)
      WRITE(4,47) CURR
   47 FORMAT (F10.6)
```

```
      C
      C   FIRST HALF CYCLE
      C
            CCRR=(1.+3.*Z(3))/(1.+9.*Z(3))
    6       NCONT=NCONT+1
            TA=TAU+DTAU
            CC=0.00001+TA-TAUP
            DO 8 J=2,M1
            CALL GASE(C,CP,ZZ,ERRIT,J)
            CALL GASE(CH,CP,ZZH,ERRIT,J)
            DO 11 K=1,N3
   11       CPH(J,K)=CH(J,K)
    8       CONTINUE
    9       CD=0.0
            DO 12  J=2,M1
            CALL GASE(CH,CPH,ZZH,ERRIT,J)
            D=0.0
            DO 13 K=1,N3
            ET=CH(J,K)-C(J,K)
            IF (ABS(ET).GT.ERROR) GO TO 50
            C(J,K)=(1.0+CCRR*ET)*CH(J,K)
            IF (ABS(ET).GT.ABS(D)) D=ET
   13       CONTINUE
            IF (CC.GE.0.0) STROH=STROH+SI
   25       IF (ABS(D).GT.ABS(CD)) CD=D
   12       CONTINUE
            TAU=TAU+DTAU
            IF (NCONT.EQ.1) GO TO 40
            NINT=NINT+1
            IF (CC.LT.0.0) GO TO 40
            STROH=STROH/M
            WRITE (4,48) C(2,1),C(M1,1),STROH,DTAU
   48       FORMAT (3F10.6,F15.7)
            IF (TAU.GE.(T1-0.00001)) GO TO 100
            TAUP=TAUP+DTAUP
            L=L+1
            IF (L-2) 15,15,16
   15       CEFF=CEFF+4.0*C(M1,1)
            CURR=CURR+4.0*STROH
            STROH=0.0
            GO TO 40
   16       CEFF=CEFF+2.0*C(M1,1)
            CURR=CURR+2.0*STROH
            STROH=0.0
            L=1
   40       DO 17 J=2,M1
            DO 18 K=1,N3
            CH(J,K)=C(J,K)
   18       CP(J,K)=C(J,K)
   17       CONTINUE
            IF (NCONT.EQ.1) GO TO 6
            IF (ABS(CD).LE.XXY) GO TO 30
            NCONT=0
            GO TO 6
   30       IF (NINT/2-(NINT+1)/2)31,32,31
   32       NCONT=0
            GO TO 33
   31       NCONT=1
   33       NINT=NINT/2
            DH=DTAU
            DTAU=2.*DTAU
            DO 210 I=1,6
            ZH(I)=Z(I)
  210       Z(I)=2.*Z(I)
            CALL PAMPA(Z,ZH,ZZ,ZZH)
            CCRR=(1.+3.*Z(3))/(1.+9.*Z(3))
            GO TO 6
   50       DO 20 J=2,M1
            DO 21 K=1,N3
            C(J,K)=CPH(J,K)
   21       CH(J,K)=CP(J,K)
   20       CONTINUE
            DTAU=0.5*DTAU
            DH=CH*0.5
            DO 201 I=1,6
            Z(I)=ZH(I)
  201       ZH(I)=0.5*ZH(I)
            CALL PAMPA(Z,ZH,ZZ,ZZH)
            CC=0.00001+TAU+DTAU-TAUP
            NCONT=1
            NINT=2*NINT
            DO 22 J=2,M1
            CALL GASE(CH,CP,ZZH,ERRIT,J)
            DO 23 K=1,N3
   23       CPH(J,K)=CH(J,K)
   22       CONTINUE
            CCRR=(1.+3.*Z(3))/(1.+9.*Z(3))
            GO TO 9
```

```
      C
      C  SECOND HALF CYCLE
      C
  1C0 PODRO=-PODRO
      C(M2,1)=DTAUP/3.C/TAU1*(CEFF+C(M1,1))
      SF=C(M2,1)/C(1,1)
      CURR=DTAUP/3.0/TAU1*(CURR+STRCH)
      SCL=0.0
      SCT=0.0
      SC1=0.0
      SC2=0.0
      SC3=0.0
      DC 202 J=2,M1
      SCT=SCT+C(J,1)
      SCL=SCL+C(J,2)
      SC1=SC1+C(J,3)+C(J,N3)
      DC 203 K=4,N2,2
      SC2=SC2+C(J,K)
  2C3 SC3=SC3+C(J,K-1)
  2C2 SC3=SC3-C(J,3)
      SCL=0.5*(SCL+SCT)
      SCT=SCT*(1.0-2.0*EPSILC)
      SCL=SCL*2.0*EPSILO
      SC1=(SC1+4.C*SC2+2.0*SC3)*R/FLCAT(N)/3.0
      SC=(SCT+SCL+SC1)/FLOAT(M)+C(M2,1)*(1.0-2.0*EPSILO)*TAU1
      SC=(SC-BALA)*1CO.0/BALA
      IF (IC/2-(IC+1)/2) 120,122,120
  120 WRITE (6,121) IC,C(M2,1),CURR,SC
  121 FORMAT (I5,13X,F11.5,15X,F11.4,13X,F11.5)
      GC TO 124
  122 WRITE (6,123)IC,C(M2,1),SF,CURR,SC
  123 FORMAT (I5,F13.5,11X,F15.4,11X,F13.4,F11.5)
  124 J=M2
      DO 102 JR=2,M1
      J=J-1
      DO 103 K=1,N3
      CP(JR,K)=C(J,K)
  1C3 CH(JR,K)=C(J,K)
  1C2 CONTINUE
      DO 104 J=2,M1
      DO 105 K=1,N3
  1C5 C(J,K)=CP(J,K)
  1C4 CONTINUE
      C(1,1)=C(M2,1)
      CP(1,1)=C(M2,1)
      CH(1,1)=C(1,1)
      CPH(1,1)=C(1,1)
      STRCH=0.0
      DO 110 J=2,M1
  110 STROH=STROH+STROM(N,PODRO,EPSILO,R,XSI,C,J)
      STRCH=STRCH/M
      IF (IC.GE.ICYC) GO TO 1000
      CURR=STROH
      WRITE (4,47) CURR
      STRCH=0.0
      CEFF=C(M1,1)
      T1=T1+TAU2
      TAU2=TAU1
      TAU1=T1-TAUP
      TAUP=TAUP+DTAUP
      L=1
      IC=IC+1
      NINT=0
      NCONT=0
      GO TO 6
 1000 WRITE (4,37) C(1,1),STROH
      DO 300 J=2,K1
  3C0 WRITE (4,37) (C(J,K),K=1,N3)
      STOP
      END
C
      SUBROUTINE PAMPA(Z,ZH,ZZ,ZZH)
      DIMENSION Z(6),ZH(6),ZZ(12),ZZH(12)
      ZZ(1)=Z(4)*(1.0-Z(5)+Z(6))
      ZZH(1)=ZH(4)*(1.C-ZH(5)+ZH(6))
      ZZ(2)=1.0+Z(6)
      ZZH(2)=1.0+ZH(6)
      ZZ(3)=1./(ZZ(1)+ZZ(2)+Z(5))
      ZZH(3)=1./(ZZH(1)+ZZH(2)+ZH(5))
      ZZ(4)=Z(4)*Z(6)
      ZZH(4)=ZH(4)*ZH(6)
      ZZ(5)=Z(4)*(Z(6)-1.C-Z(5))
      ZZH(5)=ZH(4)*(ZH(6)-1.C-ZH(5))
      ZZ(6)=1.C+Z(4)+Z(5)
      ZZH(6)=1.C+ZH(4)+ZH(5)
      ZZ(7)=2.*Z(3)
      ZZH(7)=Z(3)
      ZZ(8)=1./(1.+ZZ(7))
      ZZH(8)=1./(1.+ZZ(7))
      ZZ(9)=Z(5)
      ZZH(9)=ZH(5)
```

```
      ZZ(10)=Z(3)
      ZZH(10)=ZH(3)
      ZZ(11)=Z(1)
      ZZH(11)=ZH(1)
      ZZ(12)=Z(2)
      ZZH(12)=ZH(2)
      RETURN
      END
C
C  SUBROUTINE FOR DIMENSIONLESS CURRENT DENSITY
C
      FUNCTION STROM(N,PODRO,EPSILO,R,XSI,C,J)
      DIMENSION C(100,20)
      N3=N+3
      A=2.0*ALOG(C(J,3)/C(J,2))
      IF (C(J,2).EQ.C(J,1)) GO TO 2
      B=(1.0-2.0*EPSILO/C(J,1)+2.0*EPSILO*ALOG(C(J,1)/C(J,2))/(C(J,1)-
     1 C(J,2))
      GO TO 3
    2 B=1.0/C(J,1)
    3 X=1.0/C(J,3)
      DO 1 K=5,N3,2
    1 X=X+4.0/C(J,K-1)+2.0/C(J,K)
      X=(X-1.0/C(J,N3))*R/(3.0*FLOAT(N))
      STROM=(PODRO-A)/(B+X+XSI)
      RETURN
      END
C
C  SUBROUTINE FOR BACKWARD DIFFERENCE SCHEME
C
      SUBROUTINE GASE(C,CP,Z,ERRIT,J)
      DIMENSION C(100,20),CP(100,20),Z(12)
      COMMON IT,N,PODRO,SI,EPSILO,R,XSI
      N2=N+2
      N3=N+3
      IT=0
    1 D=0.0
      IT=IT+1
      SI=STROM(N,PODRO,EPSILO,R,XSI,C,J)
      RHO=SI*Z(11)
      ETA=SI*Z(12)
C
      X=Z(3)*(Z(1)*C(J-1,1)+Z(2)*CP(J,1)+Z(9)*(CP(J,2)-RHO))
      IF (ABS(X-C(J,1)).GT.D) D=ABS(X-C(J,1))
      C(J,1)=X
C
      X=Z(3)*(Z(5)*C(J-1,1)+Z(4)*CP(J,1)+Z(6)*(CP(J,2)-RHO))
      IF (ABS(X-C(J,2)).GT.D) D=ABS(X-C(J,2))
      C(J,2)=X
C
      X=Z(8)*(CP(J,3)+Z(7)*C(J,4)+ETA)
      IF (ABS(X-C(J,3)).GT.D) D=ABS(X-C(J,3))
      C(J,3)=X
C
      DO 2 K=4,N2
      X=Z(8)*(CP(J,K)+Z(10)*(C(J,K+1)+C(J,K-1)))
      IF (ABS(X-C(J,K)).GT.D) D=ABS(X-C(J,K))
      C(J,K)=X
    2 CONTINUE
C
      X=Z(8)*(CP(J,N3)+Z(7)*C(J,N2))
      IF (ABS(X-C(J,N3)).GT.D) D=ABS(X-C(J,N3))
      C(J,N3)=X
C
      IF (D.LT.ERRIT) RETURN
      IF (IT.LT.40) GO TO 1
      WRITE (6,3) J
    3 FORMAT (///'NO CONVERGENCE AFTER 40 ITERATIONS'//
     1 '    OCCURED IN COMPARTMENT NO.= ',I3)
      RETURN
      END
END OF FILE
```